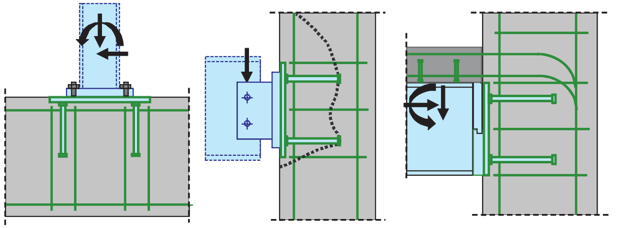

Design
of Steel-to-Concrete Joints
Design Manual II

Ulrike Kuhlmann
František Wald
Jan Hofmann
et al

Research Fund for
Coal & Steel

Deliverable of a project carried out with a financial grant
from the Research Fund for Coal and Steel of the European Community

Design
of Steel-to-Concrete Joints

Design Manual I

Prague, Stuttgart, Coimbra, and Brussels, February 2014

Deliverable of a project carried out with a financial grant
from the Research Fund for Coal and Steel of the European Community

Design of steel-to-concrete joints, Design manual I

The present document and others related to the research project INFASO RFSR-CT-2007-00051 New Market Chances for Steel Structures by Innovative Fastening Solutions between Steel and Concrete and the successive dissemination project RFS2-CT-2012-00022 Valorisation of Knowledge for Innovative Fastening Solution between Steel and Concrete, which have been co-funded by the Research Fund for Coal and Steel (RFCS) of the European Community.

ISBN 978-92-9147-119-5

František Wald, Jan Hofmann, Ulrike Kuhlmann,
Šárka Bečková, Filippo Gentili, Helena Gervásio, José Henriques, Markus Krimpmann, Ana Ožbolt, Jakob Ruopp,
Ivo Schwarz, Akanshu Sharma, Luis Simoes da Silva, and Jörg van Kann.

Printing by European Convention for Constructional Steelwork

February 2014

178 pages, 138 figures, 32 tables

Contents

SYMBOLS VI

1 INTRODUCTION 10

2 COMPONENT METHOD FOR STEEL TO CONCRETE JOINTS 12

2.1 Design method 12

2.2 Classification of joints 13

2.2.1 Global analyses 13

2.2.2 Stiffness 15

2.2.3 Strength 16

2.2.4 Deformation capacity 17

2.3 Steel-to-concrete joints 18

2.3.1 Available models 18

2.3.2 Steel and composite structures 18

2.3.3 Concrete structures 21

2.3.4 Components for joints with anchor plate 21

3 COMPONENTS IN CONCRETE 24

3.1 Component model for headed studs 24

3.1.1 Headed studs in tension, component S 24

3.1.2 Headed studs in tension, component CC 25

3.1.3 Stirrups in tension, component RS 27

3.1.4 Stirrups in tension - bond failure, component RB 28

3.1.5 Headed studs in tension, component P 29

3.1.6 Headed studs in shear, component V 30

3.2 Combination of components 31

3.2.1 Combination of concrete cone and stirrups, C1 = CC + RS/RB 31

3.2.2 Combination of steel and pullout, C2 = S + P 32

3.2.3 Combination of all components, C3 = CC + RS/RB + P +S 33

3.2.4 Design failure load 33

3.2.5 Combination of tension and shear components 34

3.3 Simplified stiffness's based on technical specifications 34

3.3.1 Headed stud in tension without supplementary reinforcement 34

3.3.2 Headed stud in shear 35

3.3.3 Concrete breakout in tension 35

3.3.4 Pull out failure of the headed studs 36

3.3.5 Interaction of components for concrete and stirrups 37

3.3.6 Determination of the failure load 38

3.3.7 Friction 38

3.4 Base plate in bending and concrete block in compression ... 38
3.4.1 Concrete 3D strength ... 38
3.4.2 Base plate flexibility ... 40
3.4.3 Component stiffness ... 41
3.5 Concrete panel ... 43
3.6 Longitudinal steel reinforcement in tension ... 45
3.7 Slip of the composite beam ... 46
4 STEEL COMPONENTS ... 47
4.1 T-stub in tension ... 47
4.1.1 Model ... 48
4.1.2 Resistance ... 50
4.1.3 Stiffness ... 57
4.2 Threaded stud in tension ... 58
4.3 Punching of the anchor plate ... 58
4.4 Anchor plate in bending and tension ... 59
4.5 Column/beam flange and web in compression ... 63
4.6 Steel contact plate ... 64
4.7 Anchor bolts in shear ... 64
5 ASSEMBLY FOR RESISTANCE ... 66
5.1 Column base ... 66
5.1.1 Column base with base plate ... 66
5.1.2 Column base with anchor plate ... 68
5.2 Simple steel to concrete joint ... 69
5.3 Moment resistant steel to concrete joint ... 75
6 ASSEMBLY FOR STIFFNESS ... 77
6.1 Column base ... 77
6.1.1 Column base with base plate ... 77
6.1.2 Column base with anchor plate ... 79
6.2 Simple steel-to-concrete joint ... 80
6.3 Moment resistant steel to concrete joint ... 84
7 GLOBAL ANALYSIS INCLUDING JOINT BEHAVIOUR ... 84
7.1 Structural analysis ... 84
7.2 Examples on the influence of joint behaviour ... 88
7.2.1 Reference building structures ... 88
7.2.2 Design ... 90
7.2.3 Structural model ... 91
7.2.4 Analysis and discussion for Service Limit State ... 97
7.2.5 Analysis and discussion for Ultimate Limit State ... 100

8 TOLERANCES ... 102
8.1 Standardized tolerances ... 102
8.2 Recommended tolerances ... 105
9 WORKED EXAMPLES ... 107
9.1 Pinned base plate ... 107
9.2 Moment resistant base plate ... 109
9.3 Stiffened base plate ... 122
9.4 Column base with anchor plate ... 126
9.5 Simple steel to concrete joint ... 145
9.6 Moment resistant steel to concrete joint ... 155
9.7 Portal frame ... 165
10 SUMMARY ... 174
REFERENCES ... 175

Symbols

Lower case

a	factor considering the shoulder width, length
b	length
c	minimum edge distance, effective width, length
$c_{cr,N}$	critical edge distance, $c_{cr,N} = 1.5\ h_{ef}$
c_w	drag coefficient
d	diameter
d_b	diameter of the bolt
d_h	diameter of the head of headed stud
d_s	diameter of the shaft of headed stud
$d_{s,re}$	diameter of the stirrup
$d_{s,nom}$	nominal diameter of the anchor shaft
d_w	diameter of the washer
$e_{x,y}$	length between the bolt axis and the edge of the plate
e	eccentricity
f_{bd}	design bond strength according to EN1992-1-1:2004
f_{cd}	design strength of concrete
f_{ck}	characteristic strength of concrete
$f_{ck,cube}$	characteristic square strength of concrete
f_u	strength of structural steel
f_{ub}	strength of the bolt
f_{uk}	characteristic strength of steel
f_y	nominal yield strength of steel
f_{ya}	average yield strength
f_{yb}	nominal value of yield strength of the bolt
f_{yd}	design yield strength of steel
$f_{yd,re}$	design yield strength of the stirrups
f_{yk}	characteristic yield strength of steel
h	height
h_{ef}	effective embedment depth according to product specifications
k	coefficient depending on the type of forming
k_1	factor for concrete cone strength in case of headed studs
k_2	factor for the headed studs for component P
k_A	factor considering the cross-section
k_a	form factor at porous edge sections
k_b	stiffness of the bolt
$k_{b,re}$	bond stiffness due to supplementary reinforcement, stirrups
k_{C1}	stiffness due to the displacement of the anchorage in case of concrete cone failure with supplementary reinforcement, combination C1
k_{C2}	stiffness due to the displacement of the head, due to the pressure under the head on the concrete, and steel elongation, combination C2
$k_{c,de}$	stiffness of the descending branch for component CC
$k_{c,soft}$	stiffness of the concrete cone in the softening branch
k_j	concentration factor
k_p	stiffness coefficient of the plate
$k_{p,de}$	stiffness of the descending branch for component P
k_s	stiffness of the anchor shaft for component S
$k_{s,re}$	steel stiffness due to supplementary reinforcement, stirrups
k_v	empirical value depending on the type of anchor
l_1	anchorage length
l_{ep}	elongated length
l_{eff}	effective length of T-stub, defined in accordance with EN1993 1-8:2006
$l_{v,eff}$	effective length of shear area
m	distance between threaded and headed studs
m_{pl}	plastic moment resistance per unit, defined as $m_{pl} = \frac{0.25 \cdot t_f^2 \cdot f_y}{\gamma_{M0}}$
n	location of the prying force, number
n_{re}	total number of legs of stirrups
p	internal pressure
r	radius of the fillet of a rolled profile
s	actual spacing of anchors

$s_{cr,N}$ critical spacing for anchors

t thickness

t_f thickness of the T-stub, flange

t_w thickness of T-stub, column

t_{p1} thickness of the anchor plate

t_{p2} thickness of the base plate

w_{fic} fictive effective width

x distance between the anchor and the crack on the concrete surface assuming a crack propagation from the stirrup of the supplementary reinforcement to the concrete surface with an angle of 35°

z distance of tension/compressed part

Upper case

A cross section area

A_{c0} loaded area

A_{c1} maximum spread area

$A_{c,N}$ actual projected area of concrete cone of the anchorage at the concrete surface, limited by overlapping concrete cones of adjacent anchors ($s < s_{cr,N}$), as well as by edges of the concrete member ($c < c_{cr,N}$)

$A^0_{c,N}$ reference area of the concrete cone of an individual anchor with large spacing and edge distance projected on the concrete surface

A_{eff} effective area

A_h area on the head of the headed stud

A_{net} net cross section area

A_s tensile stress area in the bolt

$A_{s,nom}$ nominal cross section area of all shafts

$A_{s,re}$ nominal cross section area of all legs of the stirrups

$B_{t.Rd}$ design tension resistance of a single bolt-plate assembly

$B_{t,Rd} = 0.9 \cdot f_{ub} \cdot A_s / \gamma_{Mb}$

D diameter of column

E modulus of elasticity the steel $E = 210\ 000$ MPa

F force or load

$F_{c.Rd}$ resistance of compressed part

F_d design load

F_k characteristic load

F_{memb} axial force

$F_{t.Ed}$ external tensile force

$F_{t.Rd}$ external ultimate resistance

$F_{T.Rd}$ resistance of tension part

I moment of inertia

I_t torsion constant

K general stiffness

L length

L_b length of anchor bolt

L_{cr} buckling length

L_D the elongation length of the bolt, which may be taken as the total grip length (thickness of material plus washers) plus half the sum of the height of the bolt head and the height of the nut

L_h length of the anchor shaft

$I_{p,bp}$ equivalent moment of inertia

$M_{c,Rd}$ bending moment capacity

$M_{j,Rd}$ design moment resistance of a joint

$M_{N,Rd}$ interaction resistance bending with compression

$M_{pl.Rd}$ plastic moment resistance defined as $M_{pl,Rd} = l_{eff} \cdot m_{pl}$

$M_{t,Rd}$ torsion capacity

N_{act} actual load on the anchor

$N_{b,Rd}$ design buckling resistance

N_{cr} critical buckling load

N_{Ed} tension/compression load

N_{ETA} tension load for which the displacements are derived in the product specifications

$N_{pl,Rd}$ design capacity in tension/compression

N_{Rd} design capacity

$N_{Rd,b,re}$ design tension resistance for bond failure of stirrups

$N_{Rd.C3}$ design failure load or the combined model

$N_{Rd,c}$ design tension resistance for concrete cone failure of headed stud

$N_{Rd,cs}$ design failure load for the concrete strut

$N_{Rd,p}$ design tension resistance for pull out failure of headed stud

$N_{Rd,re}$ design failure load for the supplementary reinforcement

$N_{Rd,s}$ design tension resistance for steel failure of headed stud

$N_{Rd,s,re}$ design tension resistance for steel failure of stirrups

$N^0_{Rk,c}$ characteristic resistance of a single anchor without edge and spacing effects

N_u ultimate resistance

N_y yielding resistance

Q prying force

R_d design capacity

R_k characteristic resistance

S_i elastic stiffness

$S_{j,ini}$ initial stiffness

V_{ETA} shear load for which the displacements are derived in the product specifications

$V_{pl,Rd}$ shear capacity

V_{Rd} design failure load for the anchor under shear

$V_{Rd,c}$ design shear resistance for concrete cone failure

$V_{Rd,cp}$ design shear resistance for concrete pryout

$V_{Rd,p}$ design shear resistance for pullout

$V_{Rd,s}$ design shear resistance for steel failure

W_e external work

W_{eff} section modulus of effective area

W_{el} elastic section modulus

W_i internal work

W_{pl} plastic section modulus

Greek symbols

α factor according to EN1992:2006 for hook effect and large concrete cover

α_c factor of component concrete break out in tension

α_p factor for the component head pressing

α_s factor of component stirrups

β_j material coefficient

γ_F partial safety factor for actions

γ_M material safety factor

γ_{Mb} partial safety factor for bolts γ_{Mb} = 1.25

γ_{Mc} partial safety factor for concrete γ_{Mc} = 1.5

γ_{Ms} partial safety factor for steel γ_{Ms} = 1.15

γ_{MV} partial safety factor for shear resistance of studs γ_{MV} = 1.25

γ_{Mw} partial safety factor for welds γ_{Mw} = 1.25

γ_{M0} partial safety factor for resistance of Class 1, 2 or 3 cross-sections γ_{M0} = 1.0

γ_{M1} partial safety factor for resistance of a member to buckling γ_{M1} = 1.0

γ_{M2} partial safety factor resistance of net section at bolt holes γ_{M2} = 1.25

δ deformation, displacement

δ_{act} displacement corresponding to N_{act}

δ_c displacement corresponding to N_{act} for concrete cone

δ_f corresponding displacement at failure load $N_{Rd,sre}$ or $N_{Rd,bre}$

$\delta_{N,ETA}$ displacement given in the product specifications for a corresponding tension load

$\delta_{Rd,b,re}$ deformation corresponding to design resistance for bond failure of stirrups

$\delta_{Rd,c}$ deformation corresponding to design resistance for concrete cone failure

$\delta_{Rd,p}$ deformation corresponding to design resistance for pull out failure

$\delta_{Rd,s}$ deformation corresponding to N_{Rd}

$\delta_{Rd,s}$ deformation corresponding to design resistance for steel failure

$\delta_{Rd,s,re}$ deformation corresponding to design resistance for steel failure of stirrups

$\delta_{Rd,sy}$	deformation corresponding to design yield resistance for steel failure
δ_u	elongation
$\delta_{V,ETA}$	displacement given in the product specifications for a corresponding shear load
$\varepsilon_{bu,re}$	strain limit for the stirrups due to bond
ε_{su}	ultimate design strain limit for steel
$\varepsilon_{su,re}$	strain limit for the stirrups under tension
$\varepsilon_{su,re}$	strain limit for the stirrups under tension
ε_u	ultimate strain
θ	angle
λ	slenderness of member
μ	coefficient of friction
ν	Poisson`s ratio, $\nu = 0.30$
σ	stress
c	reduction factor
$\psi_{A,N}$	factor accounting for geometric effects in anchor group, $\psi_{A,N} = A_{c,N}/A^0_{c,N}$
$\psi_{re,N}$	factor accounting for negative effect of closely spaced reinforcement in the concrete member on strength of anchors with $h_{ef} < 100$ mm
$\psi_{s,N}$	factor accounting for the influence of edges of the concrete member on the distribution of stresses in the concrete $\psi_{s,N} = 0.7 + 0.,3 \cdot c/c_{cr,N} \leq 1.0$
ψ_{supp}	support factor considering the confinement of the stirrups $\psi_{supp} = 2.5 - x/h_{ef} \geq 1.0$
Φ	rotation

Subscripts

A	area
act	actual
b	bolt, bond
bd	design bond
c	column, concrete
cb	concrete block
ck	characteristic concrete
cp	concrete pry out
cs	concrete strut
cr	critical
d	design
e	external
eff	effective
ETA	European technical approval
g	grout
h	head
i	internal
k	characteristic
lim	limit
Mc	material concrete
Ms	material steel
N	tension
nom	nominal
po	pullout
p	plate
pl	plastic
Rd	resistance design
Rk	characteristic resistance
re	failure
rec	reinforcement
Sd	internal design
s	shaft of anchor, stud
soft	softening
supp	support
T	tension part
t	tension
tot	total
p	plate
p1	anchor plate
p2	base plate
u	ultimate
uk	characteristic ultimate
V	shear
w	column web
x, y	directions
y	yield
yd	design yield
yk	characteristic yield

1 INTRODUCTION

The mixed building technology allows to utilise the best performance of all structural materials available such as steel, concrete, timber and glass. Therefore the building are nowadays seldom designed from only one structural material. Engineers of steel structures in practice are often faced with the question of economical design of steel to concrete joints, because some structural elements, such as foundations, stair cases and fire protection walls, are optimal of concrete. A gap in knowledge between the design of fastenings in concrete and steel design was abridged by standardized joint solutions developed in the INFASO project, which profit from the advantage of steel as a very flexible and applicable material and allow an intelligent connection between steel and concrete building elements. The requirements for such joint solutions are easy fabrication, quick erection, applicability in existing structures, high loading capacity and sufficient deformation capacity. One joint solution is the use of anchor plates with welded headed studs or other fasteners such as post-installed anchors. Thereby a steel beam can be connected by butt straps, cams or a beam end plate connected by threaded bolts on the steel plate encased in concrete. Examples of typical joint solutions for simple steel-to-concrete joints, column bases and composite joints are shown in Fig. 1.1.

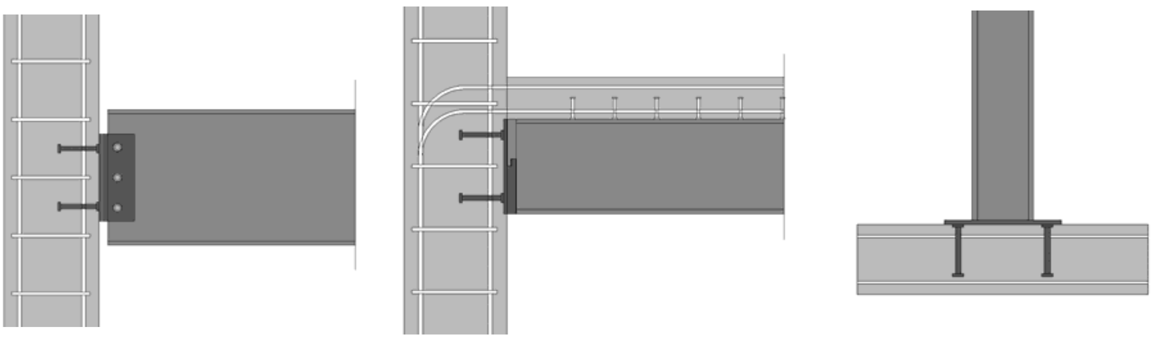

a) b) c)

Fig. 1.1 Examples for steel-to-concrete joints,
a) simple joint, b) composite joint, c) column bases

The Design Manual I gives an overview of the existing design rules and introduces components developed. To present the use of the developed design rules, worked examples are given within the Design Manual I. More detailed information about the background documents, the experiments and development of the new design rules might be found in the final report, (Kuhlman et al 2013) and in Design manual II. This manual is focused to more complex worked examples, the application of a software tool for design, sensitivity study of proposed analytical models and its boundary conditions as well as design tables of optimal solutions.

Chapter 2 gives a general overview about the component method and presents the existing models for steel-to-concrete joints. It also includes a short summary of the joint models and components developed in the project. In Chapter 3 and Chapter 4 the concrete and the steel components for the modelling of steel-to-concrete joints are described in more detail. The components already described in the codes as well as components of the newly derived models are introduced. Values for stiffness and resistance are presented. In Chapter 5 the single components are assembled to evaluate the overall joint resistance. Chapter 6 shows how the joint stiffness can be derived due to the stiffness's of the single components. For the global analysis of a structure the joint behaviour/stiffness may have an influence. The effects of the joint modelling on the global analysis are explained in Chapter 7. The tolerances for steel-to-concrete joints and their effect on the construction are discussed in Chapter 8. In the Chapter 9 worked examples for the whole range of the steel-to-concrete joints are prepared. This examples are demonstrating the possibilities of the new design rules and allow an easy access for the engineers in practice. The references are given to this Design manual I (DM I) and to Eurocodes (EN199x-1-x). Chapter 10 summarises the offered opportunity for innovations.

Chapters 1 and 2 were prepared by U. Kuhlman and J. Ruopp, Chapter 3 by J. Hofmann and A. Sharma, Chapters 4, 5 and 6 by F. Wald, Bečková Š. and Schwarz I., Chapter 7 by da Silva L. Simoes, H. Gervásio and J. Henriques and F. Gentili and Chapter 8 by M. Krimpmann. The worked examples 9.1 to 9.3 were set by Š. Bečková and I. Schwarz, 9.4 by Š. Bečková, I. Schwarz and M. Krimpmann, 9.5 by J. Ruopp, 9.6 and 9.7 by J. Henriques and F. Gentili, with help of the headed studs design models by A. Sharma.

2 COMPONENT METHOD FOR STEEL TO CONCRETE JOINTS

2.1 Design method

In the past decades, the component method has been set as a unified approach for the efficient analysis of steel and composite joints, see (Da Silva 2008). The basic principle of the component method consists of determining the complex non-linear joint response through the subdivision into basic joint components. The joint can be regarded as a set of individual basic components that contribute to its structural behaviour by means of resistance, stiffness and deformation capacity. The component method allows designers to take options more efficiently because the contribution of each component to the joint behaviour may be optimized according to the limiting components. Thus, one of the main advantages of the component method is that the analysis of an individual component can be done independently of the type of joint. In a second calculation step the single components are assembled by the designers according to the joint configuration.

Joint components may be divided by the type of loading. Accordingly, three groups of components are usually identified: components for tension, compression and shear. Additionally, a second division may be done according to their location: panel zone or connecting zone. In Fig. 2.1 these two definitions are illustrated based on a double sided composite joint.

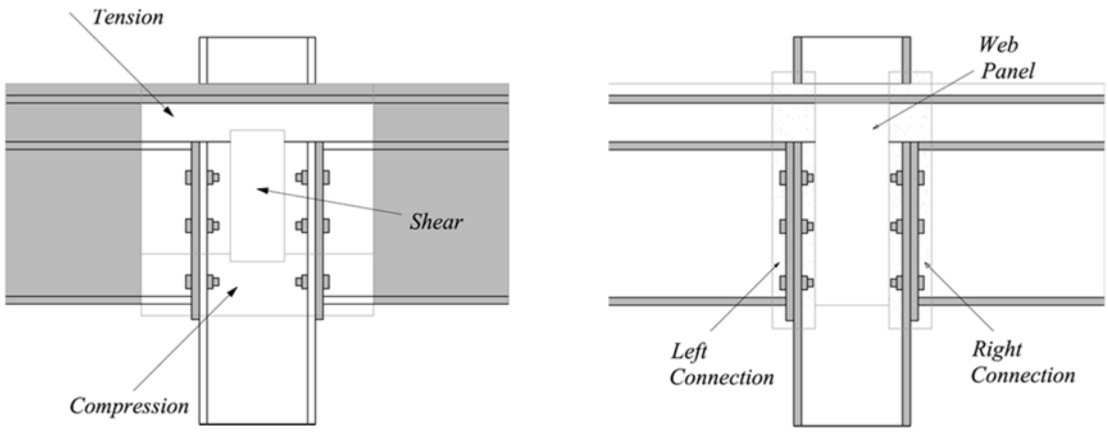

Fig. 2.1 Division of joint into groups and zones

In practice these components are modelled by translational springs with non-linear force-deformation response that are exposed to internal forces. The joint may then be represented by a spring model as illustrated in Fig. 2.2.

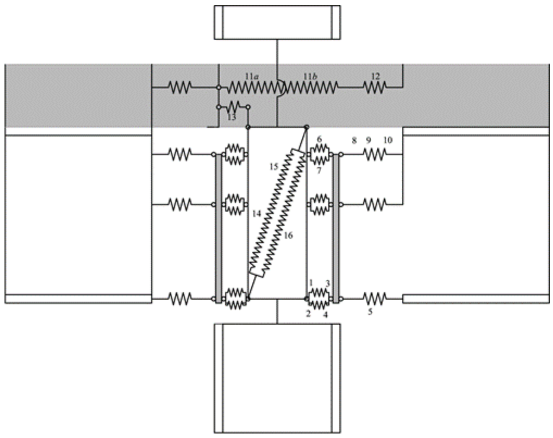

Fig. 2.2 Component model for composite joint with separated the panel zone in shear

The component method is given by EN1993-1-8:2006 and EN1994-1-1:2010 for the analysis of steel and composite joints. The application of the method requires following steps:

1. Identification of the basic joint components
2. Characterization of the structural properties of the basic joint components
3. Assembly of the component properties

In the referred codes, a list of basic joint components is provided for the most common joint configurations. Basic joint components are then characterized in terms of strength, stiffness and deformation capacity allowing to obtain the F-δ curve, see Fig. 2.3, reproducing its behaviour. Finally, through the assembly procedure the joint properties are determined. The joint behaviour may be later reproduced by an M-Φ curve, see Fig. 2.4, in the structural analysis.

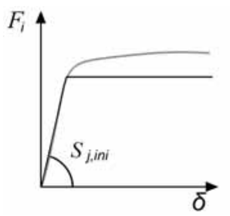

Fig. 2.3 Component force deformation, F-δ, curve, experiment in black and model in grey line

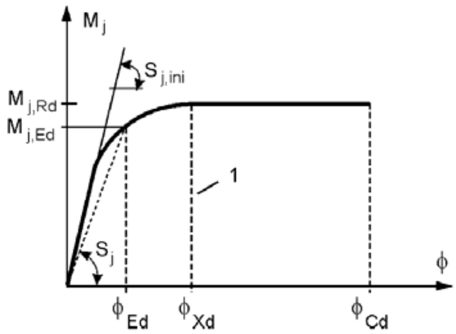

Fig. 2.4 Joint moment rotation, M-Φ, curve experiment in black and model in grey line

2.2 Classification of joints

2.2.1 Global analyses

The classification of the joints is prepared to examine the extent to which the stiffness or strength have to be considered in the calculation according the design accuracy. In total there are three different calculation methods which require different joint properties. These calculation methods and the joint properties are compared within Tab. 2.1Tab. 2.1 Relation between method of global analysis and considered joint behaviour

Method of global analysis	Considered joint behaviour
Elastic	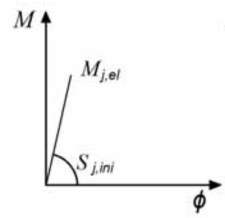 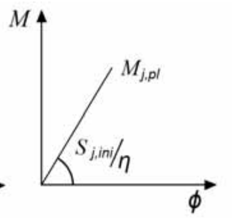
Rigid plastic	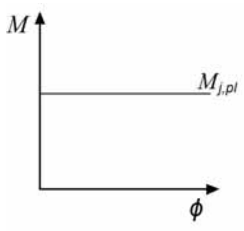
Elastic plastic	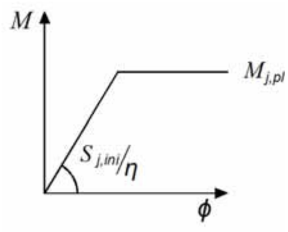

<u>Elastic method</u>

If the elastic calculation method is applied, only the joint stiffness S_j is considered. S_j is implemented in the structural calculation as spring element or one-dimensional beam element in order to determine the internal forces. If the bending moment does not exceed 2/3 of the moment resistance of the joint the initial stiffness $S_{j,ini}$ can be used to describe the elastic behaviour. For calculations, where the plastic moment capacity is reached, the joint stiffness can be calculated with the secant stiffness $S_{j,ini}/\mu$. The joints are classified for this method by taking into consideration the rotational stiffness.

<u>Rigid plastic method</u>

In the second calculation method the elastic behaviour of the joint is neglected. Internal forces of the structural calculation are calculated from 1st order plastic hinge theory only satisfying equilibrium conditions. Within this method only the plastic moment capacity is considered, but the joints must have sufficient deformation capacity to allow full plastic redistribution. In this case the joints are classified by the resistance.

<u>Elastic plastic method</u>

If the third method is applied the overall moment-rotation-relationship of the joint has to be considered. This relationship is used within the joint modelling of the structural calculation. For simplification a bilinear approach of the moment rotation curve may be used. Typically the reduced secant stiffness is applied. If the elastic plastic method is used, the joint has to be classified by stiffness and strength.

The advantages of this method are shown in the following example. In Fig. 2.5 a steel frame with horizontal and vertical loading is shown. Instead of modelling the column bases as a pinned joint as it is common in practice, the column bases may be classified as semi-rigid and modelled with a rotational spring. Thereby the column bases may stabilise the structure and reduce the bending moment in the steel-to-steel beam to column joints. So a classification of the column bases as semi-rigid instead of pinned makes the steel structure more safe and economical.

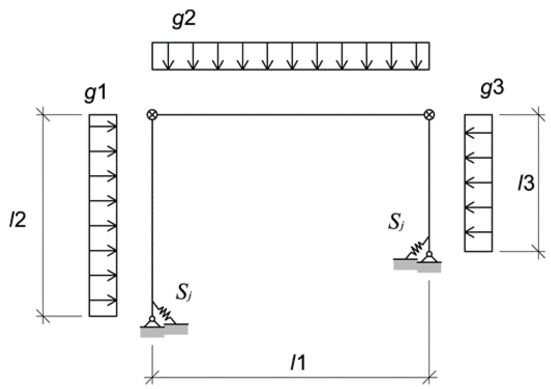

Fig. 2.5 Considering the rotation stiffness of joints with springs

It is also important not to underestimate the stiffness of the column bases, because big rotational stiffness might cause unexpected high bending moments in the joints which may lead to failure. The classification of the joints, may be found in cl 5 of EN1993-1-8:2006 and is explained in the following section.

2.2.2 Stiffness

The first part of this chapter deals with the classification of beam to column/wall and beam to beam joints, the second part with the classification of column bases. Depending on its initial rotational stiffness $S_{j,ini}$ a joint may be classified as pinned, rigid or semi-rigid. <u>Normally pinned joints</u> can transfer axial and shear force. Rotation of the joint does not cause significant bending moments. If a joint cannot be classified as normally pinned or rigid it is classified as <u>semi-rigid</u>. Rigid joints have a rotational stiffness which legitimise to treat the joint as rigid in the global analysis.

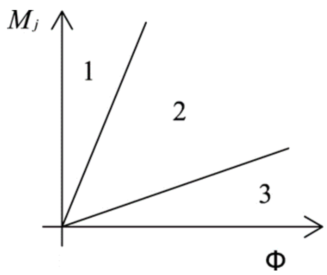

Fig. 2.6 Classification due to stiffness

<u>Joints classified according to the connecting beams</u>

<u>Rigid joints</u>, in Fig. 2.6 zone 1, is classified as rigid if

$$S_{j,ini} \geq K_b \; E \; I_b / L_b \tag{2.1}$$

If a bracing system reduces the horizontal displacement more than 80 %, then $K_b = 8$. For other frames provided that in every storey the following equation (2.2) is valid, then $K_b = 25$.

$$\frac{K_b}{K_c} \geq 0.1 \tag{2.2}$$

Semi-rigid joints, in Fig. 2.6 zone 2, are all joints which are not classified as pinned or rigid. For frames where Eq. 2.3 applies the joints should be classified as semi rigid and not as rigid.

$$\frac{K_b}{K_c} < 0.1 \tag{2.3}$$

Nominally pinned joints, in Fig. 2.6 zone 3, are expecting to have a limited bending stiffness compared to the bending stiffness of the connected beam.

$$S_{j,ini} \leq 0.5 \cdot E \cdot I_b / L_b \tag{2.4}$$

where

K_b is mean value of I_b/L_b for all the beams at the top of that storey
K_c is mean value of I_c/L_c for all columns of that storey
I_b is the second moment of area of beam
I_c is the second moment of area of column
L_b is the span of beam
L_c is the storey height of a column

Column bases classified according to the connecting column

Column bases are classified as rigid if the following conditions are satisfied. There are two possible cases which have to be considered. If there is an additional bracing in a frame and the additional bracing reduces the horizontal movement at least by 80 %, then the column base affects the accuracy of the column design, which depends on the column relative slenderness. This column base might be assumed as rigid according to EN1993-1-8:2006 cl. 5.2a, if

$$\bar{\lambda}_0 \leq 0.5 \tag{2.5}$$

for

$$0.5 < \bar{\lambda}_0 < 3.93 \text{ is } S_{j,ini} \geq 7\left(2\,\bar{\lambda}_0 - 1\right) E\, I_c/L_c \tag{2.6}$$

and for

$$\bar{\lambda}_0 \geq 3.93 \text{ and } S_{j,ini} \geq 48\, E\, I_c/L_c \tag{2.7}$$

where

$\bar{\lambda}_0$ is the relative slenderness of a column in which both ends are assumed as pinned.

For all other constructions, the cases where the storey´s sway is not prevented, the column base might be classified according to cl. 5.2d in EN1993-1-8:2006 as rigid if

$$S_{j,ini} \geq 30\, EI_c/L_c \tag{2.8}$$

2.2.3 Strength

A joint is classified for strength as pinned, full-strength or partial-strength, see Tab. 2.1 and Fig. 2.7. The classification by strength may be found in EN1993-1-8:2006 cl 5.2.3. Nominally pinned joint should have a design moment resistance less than 25 % of the design moment resistance, which would be required for a full-strength joint. They must have sufficient rotational capacity. A Partial-strength joint is a joint, which cannot be classified as pinned or full-strength.

The design moment resistance of a full-strength joint is bigger than the design moment resistance of the beam or column connected to it.

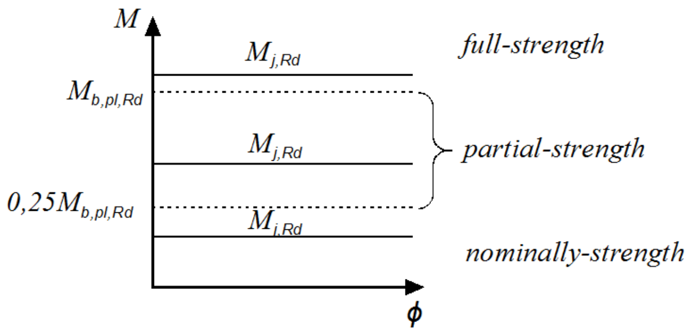

Fig. 2.7 Classification due to resistance

If the design resistance of the beam $M_{b,pl,Rd}$ is smaller than the design resistance of the column $M_{c,pl,Rd}$, $M_{b,pl,Rd}$ is replaced for connections at the top of a column by $M_{c,pl,Rd}$ see Fig. 2.7. If the design resistance of the beam $M_{b,pl,Rd}$ is smaller than the double design resistance of the column $M_{c,pl,Rd}$ than in the figure above $M_{b,pl,Rd}$ is replaced for connections within the column height by $2\ M_{c,pl,Rd}$.

2.2.4 Deformation capacity

In EN1993-1-8:2006 an explicit classification for deformation or rotational capacity of the joint is not implemented. The complexity on classification according to deformation capacity is in the lack of knowledge of the upper values of material properties by designers, which do not allow a safe prediction of the failing component. In EN 1993-1-8 cl 6.4 design rules for the rotation capacity are given based on best engineering practice. If the system is calculated with a plastic global analysis a sufficient rotation capacity is needed. No investigation of the rotation capacity of the joint is necessary, if the moment resistance of the joint $M_{j,Rd}$ is at least 20 % bigger than the plastic moment resistance $M_{pl,Rd}$ of the connected beam, see (2.9). Then the plastic hinge appears in the beam and the rotational capacity has to be satisfied by the beam section.

$$M_{j,Rd} \geq 1.2 \cdot M_{pl,Rd} \tag{2.9}$$

If the moment resistance of the joint is not 1.2 times the plastic moment resistance of the connected beam and a plastic hinge is assumed in the joint, minimum rotational capacities for bolted and welded joints have to be checked.

Bolted joints

The rules for bolted joints may be found in EN1993-1-8:2006 cl 6.4.2. A bolted joint is assumed to have a sufficient rotation capacity if following conditions can be applied:

If the failure load $M_{j,Rd}$ is determined by the resistance of the column web panel and for this panel $d/t_w \leq 69\ \varepsilon$

where

d is the nominal bolt diameter and
t_w is the thickness of the web

If the thickness of the flange of the column or the beam end plate is sufficiently thin to satisfy the following formula.

$$t \leq 0.36\, d \sqrt{f_{ub}/f_y} \quad (2.10)$$

where
f_{ub} is ultimate strength of the bolts
f_y is yield strength of the flange or the end plate

Welded joints

The rules for welded joints may also be found in EN1993-1-8:2006 cl 6.4. For a welded beam to column connection the rotation capacity $\emptyset_{Cd}$ may be calculated with the following equation. In this case the web has to be stiffened in the compression area but not in the tension are and the moment resistance is not determined by the resistance of the column web panel.

$$\emptyset_{Cd} = 0.025\, h_c/h_b \quad (2.11)$$

where
h_c is the depth of the column
h_b is the depth of the beam

For a welded beam to column connection where the compression and the tension area in the column are not stiffened, the rotation capacity may be assumed to be at least 0.015 rad.

2.3 Steel-to-concrete joints

2.3.1 Available models

Design models for steel-to-concrete joints are currently available in the three standard documents:

EN1993-1-8:2006 includes values for stiffness and resistance for all steel components and values for stiffness and resistance for concrete components in compression. There are no rules for concrete components in tension or shear.

EN1994-1-1:2010 enhancement of the rules from EN 1993-1-8 on composite joints such as the connection of composite girder to steel columns.

CEN/TS 1992-4-1:2009 summarises values for the design resistance of fasteners in concrete. But no values for stiffness and ductility are available.

2.3.2 Steel and composite structures

Design rules in the Eurocode are given for different joint configurations. The model for the column bases is described in the EN1993-1-8:2006 and the model for the composite joint in EN1994-1-1:2010.

Column bases with base plates

The analytical prediction model for column base with base plate is described in the EN1993-1-8:2006. With these design rules column bases loaded by axial force and bending moments are calculated. The model is only including concrete components for the compression forces.

For the tension force only steel components are considered. The design resistance of column bases with steel base plates is described in EN1993-1-8:2006, cl 6.2.8. First according to the eccentricity of the axial force e and the geometry of the column base one of the four loading types is chosen, and the lever arm z is calculated. For this see Tab. 2.2. Then the loading of the tension and the compression components are calculated. The failure load is determined by the weakest activated component. These components are for:

Tension

Base plate in bending under tension	cl 6.2.6.11 in EN1993-1-8
Anchor bolt in tension	cl 6.2.6.12 in EN1993-1-8
Column web in tension	cl 6.2.6.8 in EN1993-1-8

Compression

Base plate in bending under compression	cl 6.2.6.10 in EN1993-1-8
Concrete in compression	cl 6.2.6.9 in EN1993-1-8
Column web and flange in compression	cl 6.2.6.7 in EN1993-1-8

Shear

Anchor bolts in shear	cl 6.2.2.6 to 6.2.2.9 in EN1993-1-8

According to procedure in EN1993-1-8:2006 cl 6.3.4 one of the four cases of the loading and geometry is chosen, see Tab.2.2. Then the rotational stiffness is calculated. One complexity creates change of the loading type depending on the loading cases. From this different rotational stiffness values for different combinations of bending moment and axial forces are resulting. The design of the embedded column base according to Eurocodes was developed by (Pertold et al, 2000) based on set of tests and finite element modelling. This model is prepared to approve resistance to combine base plate with embedding.

Composite joints

The composite joint is described in the Section 8 in EN1994-1-1:2010. The composite joint may be used for the connection of composite beams to steel columns. The design rules are an enhancement of the rules according to EN1993-1-8:2006 and new components are added. These additional components are:

- Longitudinal steel reinforcement in tension	cl. 8.4.2.1 EN1994-1-1:2010
- Steel contact plate in compression	cl 8.4.2.2 EN1994-1-1:2010
- Column web in transverse compression	cl 8.4.3 EN1994-1-1:2010
- Reinforced components	cl 8.4.4 EN1994-1-1:2010
- Column web panel in shear	cl 8.4.4.1 EN1994-1-1:2010
- Column web in compression	cl 8.4.4.2 EN1994-1-1:2010

For all other components EN1993-1-8:2006 is applied.

Tab. 2.2 The loading situations for the definition of the lever arm

Number	Description of loading	Sketch	Explanation
1	Left side in tension Right side in compression $z = z_{T,l} + z_{C,r}$	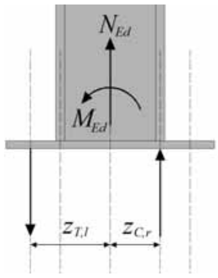	Bending moment is dominating
2	Left side in tension Right side in tension $z = z_{T,l} + z_{T,r}$	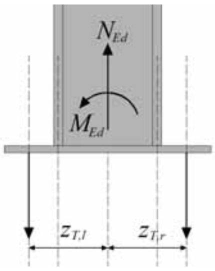	Tensile force is dominating
3	Left side in compression Right side in tension $z = z_{C,l} + z_{T,r}$	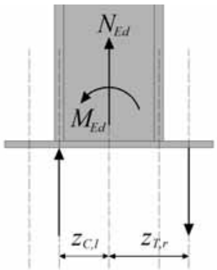	Bending moment is dominating
4	Left side in compression Right side in compression $z = z_{C,l} + z_{C,r}$	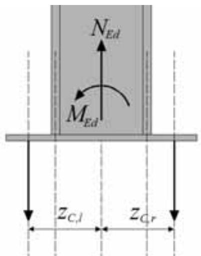	Compression force is dominating

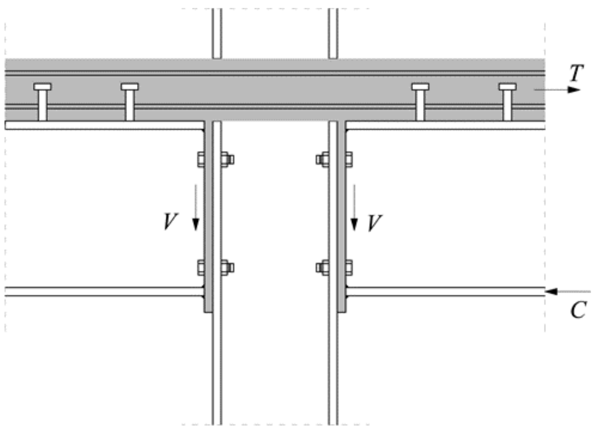

Fig. 2.8 Composite joint

Tab. 2.3 Failure modes observed for anchors in concrete

Loading	Failure modes		
Tension	Steel failure 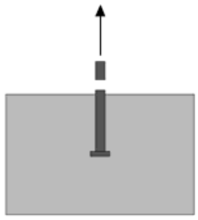	Concrete cone failure 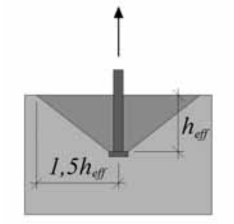	Pull-out / Pull-through 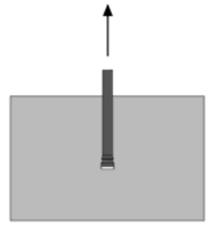
	Splitting failure 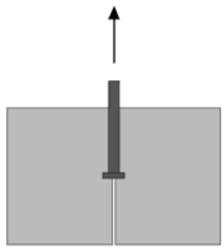	Local Blow-out failure 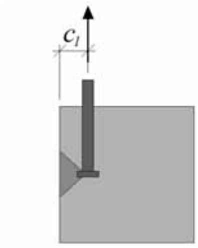	Steel failure 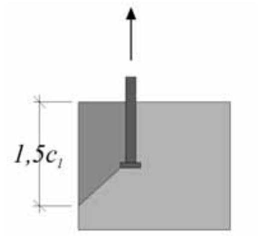
Shear	Steel failure 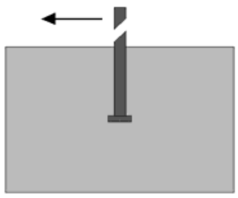	Concrete edge failure Pry-out failure 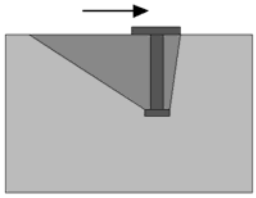	Pull-out failure 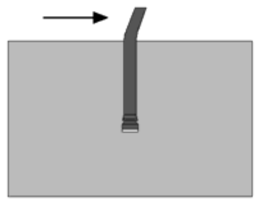

2.3.3 Concrete structures

In CEN/TS1992-4-1:2009 the design of fastenings in concrete is given. In these rules the failure modes of the fasteners and the concrete are described in a detailed way. For tension and shear loading various failure modes exist. Failure modes are given according to CEN/TS 1992-4-1:2009, see Tab. 2.3.. All possible failure modes are determined. The smallest resistance defines the design resistance of the joint. The design rules for the resistance include different types of geometries. Also edge effects, concrete with and without cracks and different kinds of fasteners are considered. However for stiffness no design rules are given and the use of additional stirrups is covered in a very conservative way.

2.3.4 Components for joints with anchor plate

<u>Headed studs in tension / Headed studs with stirrups in tension</u>

Load-displacement-curves of test specimens have shown, that in cases were additional reinforcement is used, also other components besides the reinforcement have a contribution on the overall load bearing capacity of the fixture. If, for instance, the reinforcement starts to yield, compression struts may develop and a small concrete cone failure can be the decisive component. With the design model the interaction of the concrete cone and the stirrups is considered. This allows the increase of the design resistance and the determination of the stiffness of the two combined components concrete cone and stirrups in tension in cases, where both of them are interacting. In Fig. 2.9 a headed stud with additional reinforcement and the assembly of single components is shown.

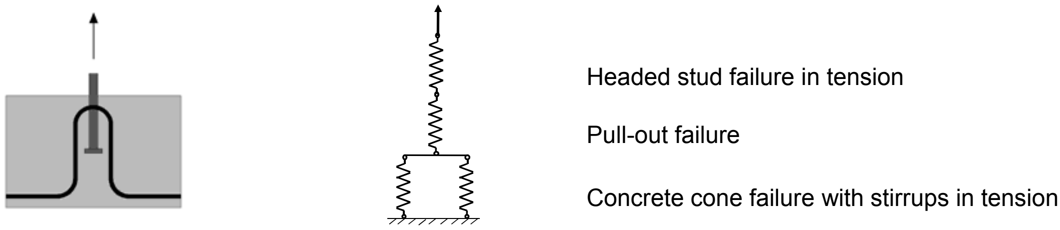

Fig. 2.9 Component headed studs with stirrups in tension

<u>Embedded plate in tension</u>

Ductile behaviour and a larger rotation capacity of column bases can be initiated with a thin anchor plate in combination with a base plate welded to the end of the column. In Fig. 2.10 three different kinds of geometries of embedded plates are shown, see Kuhlman et al, 2013.

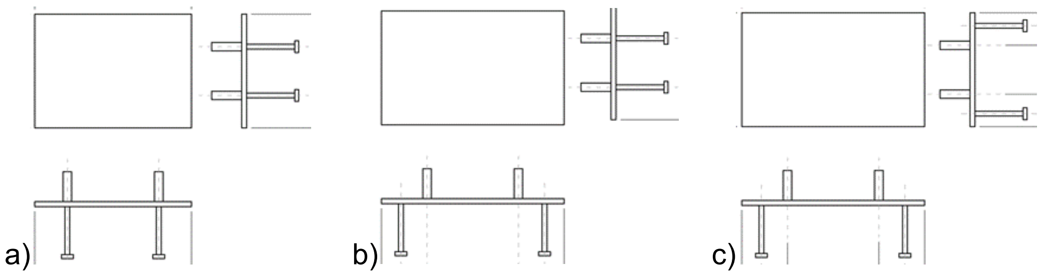

Fig. 2.10 Example of different positions of headed and treaded studs,
a) above, b) in distance in one major direction, c) in distance in general

The headed studs are welded on the bottom side of the base plate to connect the thin plate to the concrete. The column base plate is connected to the anchor plate by the threaded bolts. If the threaded bolts and the headed studs are in one line like, see Fig. 2.10, the anchor plate has no influence on the behaviour of the joint. If the threaded bolts and the headed studs are not in one line the anchor plate is activated. The model of the embedded plate represents an additional failure mode for the T-stub in tension. If the T-stub reaches its limit state, the thin base plate may still increase its capacity due to the membrane effect. The component embedded plate in tension shows a ductile behaviour as large deformations occur before failure. A detailed explanation of this component is given in Chapter 7.

The Tab. 2.4 summarises the components, which are used to model the simple and rigid steel beam to concrete column/wall joints and column bases using anchor plates.

Tab. 2.4 Components for joints with anchor plates

Component	Headed stud in tension	Concrete breakout in tension	Stirrups in tension	Pull-out failure of the headed stud	Headed stud in shear
Figure	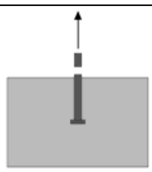	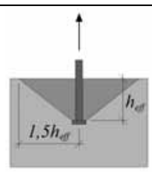	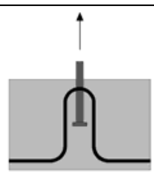	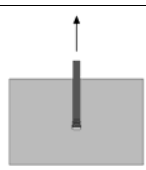	
Chapter	3.1.1	3.1.2	3.1.4	3.1.5	3.1.6

Component	Friction	Concrete in compression	Concrete panel in shear	Longitudinal steel	Slip of the composite beam

				reinforcement in tension	
Figure	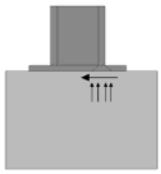	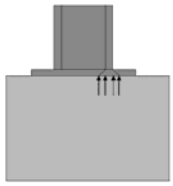	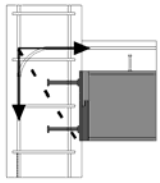	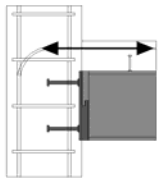	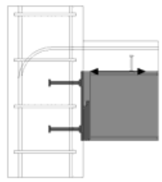
Chapter	3.3.7	3.4	3.5	3.6	3.7

Component	Threaded studs in tension/ shear	Punching of the anchor plate	Anchor plate in bending and tension	Colum/beam flange and web in compression	Steel contact plate
Figure	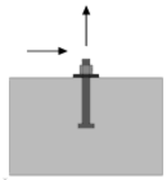	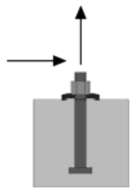	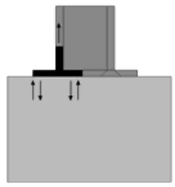	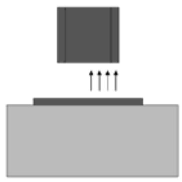	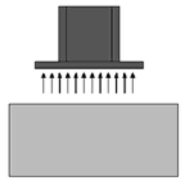
Chapter	4.7	4.3	4.4	4.5	4.6

3 COMPONENTS IN CONCRETE

3.1 Component model for headed studs

For components embedded in concrete the displacement behaviour and therefore the F-δ–curve is influenced by the concrete properties itself and the interaction between the anchorage and the concrete. The influence of concrete on the behaviour of anchorages in tension have to be considered. The scatter in concrete is much larger than that observed for the material steel, see (Pallarés and Hajjar, 2009).

For design, a material safety factor for concrete according to EN1992-1-1:2004 of $\gamma_{Mc} = 1.5$ is used. The characteristic values for the resistances are derived by assuming a normal distribution and a probability of 90 % for the 5 % fractal that corresponds to the characteristic value. The given displacements and stiffness's are mean values and can scatter with coefficient of variation up to 50 %.

The complete F-δ–curve for the design of a headed stud in tension is described by a rheological model using and combining different components for the headed stud. The individual components for anchorages with supplementary reinforcement are:

Component S	Steel failure of the headed stud ($\delta_{Rd,s}$ / $N_{Rd,s}$)
Component CC	Concrete cone failure ($\delta_{Rd,c}$ / $N_{Rd,c}$)
Component RS	Steel failure of the stirrups ($\delta_{Rd,s,re}$ / $N_{Rd,s,re}$)
Component RB	Bond failure of the stirrups ($\delta_{Rd,b,re}$ / $N_{Rd,b,re}$)
Component P	Pull out failure of the headed stud ($\delta_{Rd,p}$ / $N_{Rd,p}$)

The combination is given in Fig. 3.1.

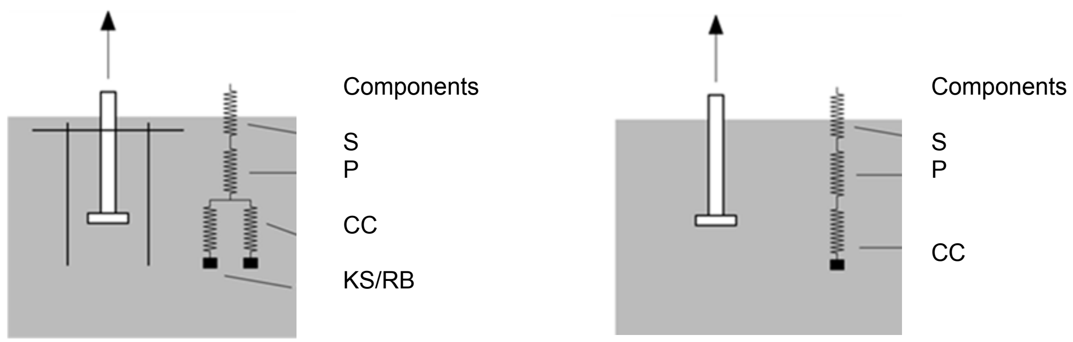

a) with supplementary reinforcement   b) without supplementary reinforcement

Fig. 3.1 Spring models for the different components of anchorages embedded in concrete

3.1.1 Headed studs in tension, component S

If a headed stud is loaded in tension, the load is first transferred from the loading point at the base plate to the bearing areas of the headed stud. Therefore the shaft will elongate up to the design yielding strength $f_{yd} = f_{yk}/\gamma_{Ms}$. For design the behaviour is assumed as linear elastic up to the yielding load of the headed stud. The corresponding elongation due to the introduced stress is calculated with the equation using the Hooke´s law. The elongation corresponding to the yield load is given by

$$\delta_{Rd,sy} = \frac{N_{Rd,s}\ L_h}{A_{s,nom}\ E_s} = \frac{\sigma_{Rd,s}\ L_h}{E_s}\ \text{[mm]} \tag{3.1}$$

where

L_h is length of the anchor shaft [mm]

$N_{Rd,s}$ is design tension resistance of the headed stud [N]

E_s is elastic modulus of the steel, $E_s = 210\ 000$ N/mm² [N/mm²]

$A_{s,nom}$ is nominal cross section area of all shafts

$$A_{s,nom} = \frac{\pi\ d_{s,nom}^2}{4}\ \text{[mm²]} \tag{3.2}$$

where

$d_{s,nom}$ is nominal diameter of the shaft [mm]

The design load at steel yielding failure is calculated as given below

$$N_{Rd,s} = A_{s,nom}\ \frac{f_{uk}}{\gamma_{Ms}} = n\ \pi \left(\frac{d_{s,nom}^2}{4}\right) \frac{f_{uk}}{\gamma_{Ms}}\ \text{[N]} \tag{3.3}$$

where

f_{uk} is characteristic ultimate strength of the shaft material of the headed stud [N/mm²]

n is number of headed studs in tension [-]

γ_{Ms} is partial safety factor for steel [-]

Exceeding the design steel yielding strength f_{yd}, the elongation will strongly increase without a significant increase in load up to a design strain limit ε_{su}. For the design, this increase of strength is neglected on the safe side and the stiffness is assumed to be zero, $k_s = 0$ N/mm. Depending on the product the failure shall be assumed at the yielding point. In general, fasteners as headed studs are deemed to have an elongation capacity of at least $\varepsilon_{su} = 0.8$ %. This limit shall be used to determine the response of the fasteners unless it is proven by means of tests that they have a higher elongation capacity.

Therefore the stiffness k_s is described as given below depending on the displacement or load

$$k_{s1} = \frac{A_{s,nom}\ E_s}{L_h}\ \text{for}\ N_{act} < N_{Rd,sy}\ \text{[N/mm]} \tag{3.4}$$

$$k_{s2} = 0\ \text{for}\ \delta \geq \delta_{Rd,sy} \leq e_{su}\ \text{and}\ N_{act} = N_{Rd,sy}\ \text{[N/mm]} \tag{3.5}$$

where

$\delta_{Rd,sy}$ is displacement at yielding of the shaft, see Eq. (3.1) [mm]

ε_{su} is maximum elongation capacity of the shaft, 0.8 % [-]

3.1.2 Headed studs in tension, component CC

The component concrete breakout in tension is described using the design load $N_{Rd,c}$ for concrete cone failure and the displacement in the softening branch after failure. Up to the design load the component can´t be assumed as absolutely rigid without any displacement. The displacement corresponding to design load is given by

$$\delta_{Rd,c1} = \frac{N_{Rd,c}}{k_{c,pp}} \text{ [mm]} \tag{3.6}$$

The design load at concrete cone failure is calculated as

$$N_{Rd,c} = N^0_{Rk,c}\ \psi_{A,N}\ \psi_{s,N}\ \frac{\psi_{re,N}}{\gamma_{Mc}} \text{ [N]} \tag{3.7}$$

where

$N^0_{Rk,c}$ is characteristic resistance of a single anchor without edge and spacing effects

$$N^0_{Rk,c} = k_1\ h_{ef}^{1.5}\ f_{ck}^{0.5} \text{ [N]} \tag{3.8}$$

where

k_1 is basic factor 8.9 for cracked concrete and 12.7 for non-cracked concrete [-]

h_{ef} is embedment depth given according to the product specifications [mm]

f_{ck} is characteristic concrete strength according to EN206-1:2000 [N/mm²]

$\psi_{A,N}$ is factor accounting for the geometric effects of spacing and edge distance [-]

$$\psi_{A,N} = \frac{A_{c,N}}{A^0_{c,N}} \text{ [-]} \tag{3.9}$$

where

$\psi_{s,N}$ is factor accounting for the influence of edges of the concrete member on the distribution of stresses in the concrete

$$\psi_{s,N} = 0.7\ +\ 0.3\ \ \frac{c}{c_{cr,N}} \le 1\ [-] \tag{3.10}$$

where

$\psi_{re,N}$ is factor accounting for the negative effect of closely spaced reinforcement in the concrete member on the strength of anchors with an embedment depth $h_{ef} < 100$ mm
$0.5 + h_{ef} / 200$ for $s < 150$ mm (for any diameter) [-]
or $s < 100$ mm (for $d_s \le 10$ mm)
1.0 for $s \ge 150$ mm (for any diameter) [-]

γ_{Mc} is 1.5 for concrete [-]

$A^0_{c,N}$ is reference area of the concrete cone of an individual anchor with large spacing and edge distance projected on the concrete surface [mm²]. The concrete cone is idealized as a pyramid with a height equal to h_{ef} and a base length equal to $s_{cr,N}$ with

$$s_{cr,N}\ =\ 3.0\ h_{ef} \text{ [mm]} \tag{3.11}$$

$$c_{cr,N}\ =\ 0.5\ s_{cr,N}\ =\ 1.5\ h_{ef} \text{ [mm]} \tag{3.12}$$

where

$A_{c,N}$ is actual projected area of concrete cone of the anchorage at the concrete surface, limited by overlapping concrete cones of adjacent anchors, $s < s_{cr,N}$, as well as by edges of the concrete member, $c < c_{cr,N}$. It may be deduced from the idealized failure cones of single anchors [mm²]

To avoid a local blow out failure the edge distance shall be larger than $0.5\ h_{ef}$. Due to sudden and brittle failure, the initial stiffness for concrete cone is considered as infinity, i.e. till the actual load, N_{act} is less than or equal to the design tension resistance for concrete cone, the displacement δ_c is zero. Once the design load is exceeded, the displacement increases with decreasing load, descending branch. Thus, the load-displacement behaviour in case of concrete cone breakout is idealized as shown in Fig. 3.2.

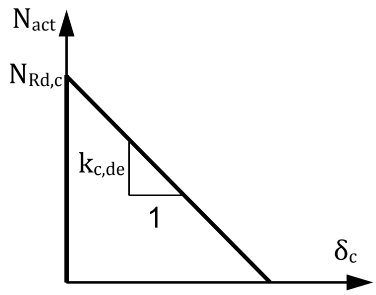

Fig. 3.2 Idealized load-displacement relationship for concrete cone breakout in tension

The stiffness of the descending branch $k_{c,de}$ for the design is described with the following function

$$k_{c,de} = \alpha_c \sqrt{f_{ck}\, h_{ef}} \cdot \psi_{A,N} \cdot \psi_{s,N} \cdot \psi_{re,N} \text{ [N/mm]} \tag{3.13}$$

where

α_c is factor of component concrete break out in tension, currently $\alpha_c = -537$
h_{ef} is embedment depth of the anchorage [mm]
f_{ck} is characteristic concrete compressive strength [N/mm²]
$A_{c,N}$ is projected surface of the concrete cone [mm²]
$A^0_{c,N}$ projected surface of the concrete cone of a single anchorage [mm²]

The displacement δ_c as a function of the acting load N_{act} is described using the design resistance and the stiffness of the descending branch.

For ascending part

$$N_{act} \leq N_{Rd,c} \text{ and } \delta_c = 0 \tag{3.14}$$

For descending branch

$$\delta_c > 0 \text{ mm and } \delta_c = \frac{N_{act} - N_{Rd,c}}{k_{c,de}} \tag{3.15}$$

3.1.3 Stirrups in tension, component RS

The component stirrups in tension was developed based on empirical studies. Therefore the tests results were evaluated to determine the displacement of the stirrups depending on the load N_{act} acting on the stirrup. The displacement is determined like given in the following equation

$$\delta_{Rd,s,re} = \frac{2\, N^2_{Rd,s,re}}{\alpha_s\, f_{ck}\, d^4_{s,re}\, n^2_{re}} \text{ [mm]} \tag{3.16}$$

where

α_s is factor of the component stirrups, currently $\alpha_s = 12\ 100$ [-]
$N_{Rd,s,re}$ is design tension resistance of the stirrups for tension failure [N]
$d_{s,re}$ is nominal diameter of thereinforcement leg [mm]
f_{ck} is characteristic concrete compressive strength [N/mm²]
n_{re} is total number of legs of stirrups [-]

The design load for yielding of the stirrups is determined as given

$$N_{Rd,s,re} = A_{s,re} f_{yd,re} = n_{re}\ \pi \left(\frac{d_{s,re}^2}{4}\right) f_{yd,re} \text{ [N]} \tag{3.17}$$

where
$A_{s,re}$ is nominal cross section area of all legs of the stirrups [mm²]
$d_{s,re}$ is nominal diameter of the stirrups [mm]
f_{yd} is design yield strength of the shaft material of the headed stud [N/mm²]
n_{re} is total number of legs of stirrups [-]

Exceeding the design steel yielding strength $f_{yd,re}$ the elongation will increase with no significant increase of the load up to a strain limit $\varepsilon_{su,re}$ of the stirrups. For the design this increase of strength is neglected on the safe side. In general reinforcement steel stirrups shall have an elongation capacity of at least $\varepsilon_{su,re}$ = 2,5 %. So the design strain limit $\varepsilon_{su,re}$ is assumed to be 2.5 %. The displacement as a function of the acting load is determined as

$$k_{s,re1} = \frac{\sqrt{n_{re}^2\ \alpha_s\ f_{ck}\ d_{s,re}^4}}{\sqrt{2\ \delta}} \quad \text{for } \delta < \delta_{Rd,s,re} \text{ [N/mm]} \tag{3.18}$$

$$k_{s,re2} = 0 \quad \text{for } \delta \geq \delta_{Rd,s,re} \leq \varepsilon_{su,re} \text{ [N/mm]} \tag{3.19}$$

3.1.4 Stirrups in tension - bond failure, component RB

The displacement of the concrete component stirrups in tension is determined under the assumption that bond failure of the stirrups will occur. This displacement is calculated with equation (3.19) as

$$\delta_{Rd,b,re} = \frac{2\ N_{Rd,b,re}^2}{\alpha_s\ f_{ck}\ d_{s,re}^4\ n_{re}^2} \text{ [mm]} \tag{3.20}$$

where
α_s is factor of the component stirrups, currently $\alpha_s = 12\ 100$ [-]
$N_{Rd,b,re}$ is design tension resistance of the stirrups for bond failure [N]
$d_{s,re}$ is nominal diameter of the stirrups [mm]
f_{ck} is characteristic concrete compressive strength [N/mm²]

The design anchorage capacity of the stirrups according CEN/TS-model [5] is determined the design tension resistance of the stirrups for bond failure

$$N_{Rd,b,re} = \sum n_{s,re} \left(\frac{l_1\ \pi\ d_{s,re}\ f_{bd}}{\alpha}\right) \text{ [N]} \tag{3.21}$$

where
$n_{s,re}$ is number of legs [-]

l_1 is anchorage length [mm]
$d_{s,re}$ is nominal diameter of the stirrups [mm]
f_{bd} is design bond strength according to EN1992-1-1:2004 [N/mm²]
α is factor according to EN1992-1-1:2004 for hook effect and large concrete cover, currently 0.7 · 0.7 = 0.49 [-]

$$k_{b,re1} = \frac{\sqrt{n_{re}^2 \ \alpha_s \ f_{ck} \ d_{s,re}^4}}{\sqrt{2\,\delta}} \quad \text{for } \delta < \delta_{Rd,b,re} \ \text{[N/mm]} \tag{3.22}$$

$$k_{b,re2} = 0 \quad \text{for } \delta \ \geq \delta_{Rd,b,re} \ \leq \ \varepsilon_{su,re} \ \text{[N/mm]} \tag{3.23}$$

3.1.5 Headed studs in tension, component P

The pull out failure of the headed studs will take place if the local stresses at the head are larger than the local design resistance. Up to this level the displacement of the headed stud will increase due to the increasing pressure under the head.

$$\delta_{Rd,p,1} = k_p \cdot \left(\frac{N_{Rd,c}}{A_h \cdot f_{ck} \cdot n}\right)^2 \text{[mm]} \tag{3.24}$$

$$\delta_{Rd,p,2} = 2\,k_p \cdot \left(\frac{\min\,(N_{Rd,p}; N_{Rd,re})}{A_h \cdot f_{ck} \cdot n}\right)^2 - \delta_{Rd,p,1} \text{[mm]} \tag{3.25}$$

$$k_p = \alpha_p \cdot \frac{k_a \cdot k_A}{k_2} \ [-] \tag{3.26}$$

where
A_h is area on the head of the headed stud [mm²]

$$A_h = \frac{\pi}{4} \cdot (d_h^2 - {d_s}^2) \tag{3.27}$$

where
k_a is form factor at porous edge sections [-]

$$k_a = \sqrt{5/a} \geq 1 \tag{3.28}$$

where
a_p is factor considering the shoulder width [mm]

$$a_p = 0.5 \cdot (d_h - d_s) \tag{3.29}$$

where
k_A is factor considering the cross section depending on factor k_a [-]

$$k_A = 0.5 \cdot \sqrt{d_s^2 + m \cdot \left(d_h^2 - d_s^2\right)} - 0.5 \cdot d_h \tag{3.30}$$

where
n is number of the headed studs [-]

α_p is factor of the component head pressing, currently is $\alpha_p = 0.25$ [-]
k_2 is factor for the headed studs in non-cracked concrete, currently 600 [-]
is factor for the headed studs in cracked concrete, currently 300 [-]
m is pressing relation, $m = 9$ for headed studs [-]
d_h is diameter of the head [mm]
d_s is diameter of the shaft [mm]
$N_{Rd,p}$ is design load at failure in cases of pull out

$$N_{Rd,p} = n\, p_{uk}\, A_h / \gamma_{Mc} \tag{3.31}$$

where
p_{uk} is characteristic ultimate bearing pressure at the headed of stud [N/mm^2]
$N_{Rd,c}$ is design load for concrete cone failure without supplementary reinforcement

$$N_{Rd,c} = N^0_{Rk,c}\, \psi_{A,N}\, \psi_{s,N} \frac{\psi_{re,N}}{\gamma_{Mc}} \text{ [N]} \tag{3.32}$$

where
$N_{Rd,re}$ design load at failure of the supplementary reinforcement minimum value of

$$N_{Rd,s,re} = A_{s,re}\, f_{yd,re} = n\, \pi\, \frac{d^2_{s,re}}{4}\, f_{yd,re} \text{ and } N_{Rd,b,re} = \sum_{n_{s,re}} \frac{l_1 \cdot \pi \cdot d_{s,re} \cdot f_{bd}}{\alpha} \text{ [N]} \tag{3.33}$$

The stiffness as a function of the displacement is determined as

$$k_{p,1} = \sqrt{\frac{(A_h\, f_{ck}\, n)^2}{\delta_{act}\, k_p}} \text{ [N/mm]} \tag{3.34}$$

$$k_{p,2} = \sqrt{\frac{(A_h\, f_{ck}\, n)^2\, (\delta + \delta_{Rd,p1})}{2\, \delta^2_{act}\, k_p}} \text{ [N/mm]} \tag{3.35}$$

$$k_{p,3} = \min(N_{Rd,p}; N_{Rd,re})/\delta + k_{p,pp}[1 - \delta_{Rd,p,2}/\delta] \text{ [N/mm]} \tag{3.36}$$

The stiffness $k_{p,de}$ depends on the failure modes. If the supplementary reinforcement fails by yielding ($N_{Rd,s,re} < N_{Rd,b,re}$ and $N_{Rd,s,re} < N_{Rd,p}$) the design stiffness $k_{p,de}$ is assumed as 10^4 N/mm², negative due to descending branch.

In all other cases (e.g. $N_{Rd,s,re} > N_{Rd,b,re}$ or $N_{Rd,s,re} > N_{Rd,p}$) $k_{p,de}$ shall be assumed as infinite due to brittle failure. The stiffness in case of pull out failure is calculated using the minimum value of the stiffness's calculated with equation (3.34) to (3.36).

$$k_{p,de} = \min(k_{p,1}; k_{p,2}; k_{p,3}) \text{ [N/mm]} \tag{3.37}$$

3.1.6 Headed studs in shear, component V

The load-displacement behaviour mainly depends on the pressure to the concrete near the surface of the concrete member. Due to concrete crushing at the surface of the concrete member, the displacement under shear loading varies very large with a coefficient of variation about 40 % to 50 %. However a semi-empirical calculation shows that the displacement at failure mainly depends on the acting loading, the diameter of the anchors and the embedment depth. Therefore the displacement under shear loading for a given load level is calculated, see (Hofmann 2005), using the following equation only as an estimation

$$\delta_{Rd,v} = k_v \frac{\sqrt{V_{Rd}}}{d} h_{ef}^{0.5} \text{ [mm]} \tag{3.38}$$

where

k_v empirical value depending on the type of anchor [-], for headed studs $k_v = 2$ to 4

V_{Rd} design failure load as the minimum of the design failure loads calculated for the different failure modes ($V_{Rd,s}$, $V_{Rd,cp}$, $V_{Rd,c}$, $V_{Rd,p}$) given according to the technical product specification CEN/TS 1992-4-1 or (FIB Bulletin 58, 2011)

The displacement at ultimate load up three times larger than the displacement at the design load level due to the assumption, that the concrete near the surface is not fully crushed at design load level.

3.2 Combination of components

To come up with the total stiffness of the connection with headed studs anchored in concrete with or without supplementary reinforcement, the stiffness's must be combined. The combination depends on whether the components are acting in parallel, equal displacements, or in serial, equal load. Three combinations are given, see (Hofmann, 2005):

Combination C1
Concrete cone failure with or without supplementary reinforcement, $k_{s,re} = 0$ and $k_{b,re} = 0$

Combination C2
Displacement due to steel elongation and head pressure, pull out

Combination C3
Total connection of headed studs anchored in concrete with supplementary reinforcement

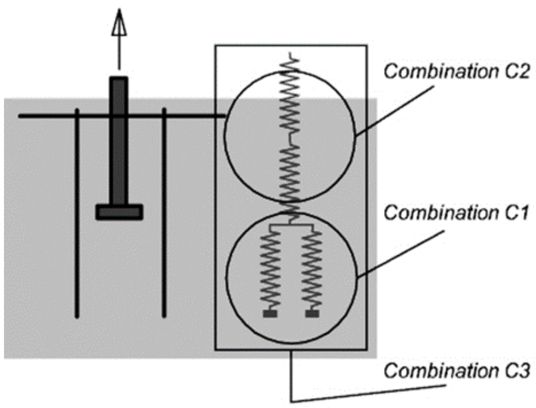

Fig. 3.3 Combinations of different single components for an anchorage with supplementary reinforcement

3.2.1 Combination of concrete cone and stirrups, C1 = CC + RS/RB

If both components are summarized, the load is calculated using the sum of the loads at the same displacement δ due to the combination of the components using a parallel connection from the rheological view. Two ranges must be considered. The first range is up to the load level at concrete failure $N_{Rd,c}$ the second up to a load level of failure of the stirrups $N_{Rd,s,re}$ or $N_{Rd,b,re}$.

$$k_{C1.1} = k_{c1} + k_{s,re} = \infty \text{ for } N_{act} \leq N_{Rd,c} \text{ [N/mm]} \tag{3.39}$$

This leads to the following equation

$$k_{C1.1} = \frac{\sqrt{n_{re}^2\ \alpha_s\ f_{ck}\ d_{s,re}^4}}{\sqrt{2\ \delta}} \text{ for } N_{act} \leq N_{Rd,c} \text{ [N/mm]} \tag{3.40}$$

In the second range the load is transferred to the stirrups and the stiffness decreases. The stiffness is calculated if N_{act} is larger than $N_{Rd,c}$ with the following equation

$$k_{C1.2} = k_{c2} + k_{s,re} \text{ for } N_{act} > N_{Rd,c} \text{ [N/mm]} \tag{3.41}$$

This leads to a relative complex equation

$$k_{C1.2} = \frac{N_{Rd,c}}{\delta} + k_{c,de} - k_{c,de}\ \frac{\delta_{Rd,c1}}{\delta} + \frac{\sqrt{n_{re}^2\ \alpha_s\ f_{ck}\ d_{s,re}^4}}{\sqrt{2\ \delta}} \tag{3.42}$$

$$\text{for } N_{act} < N_{Rd,s,re} < N_{Rd,b,re} \text{ [N/mm]}$$

If the load exceeds the ultimate load given by $N_{Rd,s,re}$ or $N_{Rd,b,re}$ the stiffness of the stirrups are negligible. Therefore the following equation applies:

$$k_{C1.3} = k_c + k_{s,re} = 0 \text{ for } N_{act} = N_{Rd,s,re} \geq N_{Rd,b,re} \text{ [N/mm]} \tag{3.43}$$

3.2.2 Combination of steel and pullout, C2 = S + P

If both components are summarized the load is calculated using the sum of the displacements at the same load N_{act} due to the combination of the components using a serial connection from the rheological view. This is done by summing up the stiffness's as given below

$$k_{C2} = \left(\frac{1}{k_s} + \frac{1}{k_p}\right)^{-1} \text{ [N/mm]} \tag{3.44}$$

This loads to the following equation

$$k_{C2} = \left(\frac{L_h}{A_{s,nom}\ E_s} + \frac{1}{k_p}\right)^{-1} = \left(\frac{L_h}{A_{s,nom}\ E_s} + \frac{1}{\min(k_{p1}; k_{p2}; k_{p3})}\right)^{-1} \text{ [N/mm]} \tag{3.45}$$

where
k_p is the minimum stiffness in case of pullout failure as the minimum of k_{p1}, k_{p2} and k_{p3}

3.2.3 Combination of all components, C3 = CC + RS/RB + P +S

To model the whole load- displacement curve of a headed stud embedded in concrete with a supplementary reinforcement the following components are combined:

concrete and stirrups in tension, components CC and RB/RS, as combination C1,
shaft of headed stud in tension, component S, and
pull-out failure of the headed stud component P as Combination 2.

The combinations C1 and C2 is added by building the sum of displacements. This is due to the serial function of both components. That means that these components are loaded with the same load but the response concerning the displacement is different. The combination of the components using a serial connection leads to the following stiffness of the whole anchorage in tension:

$$1/k_{C3} = 1/k_{C1} + 1/k_{C2} \text{ [N/mm]} \tag{3.46}$$

where
k_{C1} is the stiffness due to the displacement of the anchorage in case of concrete cone failure with supplementary reinforcement, see combination C1 [N/mm], if no supplementary reinforcement is provided k_{C1} is equal to k_c
k_{C2} is the stiffness due to the displacement of the head, due to the pressure under the head on the concrete, and steel elongation, see combination C2 [N/mm]

3.2.4 Design failure load

In principle two failure modes are possible to determine the design failure load $N_{Rd,C3}$ for the combined model. These modes are failure of

the concrete strut $N_{Rd,cs}$,

the supplementary reinforcement $N_{Rd,re}$.

The design failure load in cases of concrete strut failure is calculated using the design load in case of concrete cone failure and an increasing factor to consider the support of the supplementary reinforcement, angle of the concrete strut,

$$N_{Rd,cs} = \psi_{supp} \, N_{Rd,c} \text{ [N]} \tag{3.47}$$

where
$N_{Rd,c}$ is design failure load in case of concrete cone failure, see Eq. 3.7 [N]
$\Psi_{support}$ is support factor considering the confinement of the stirrups

$$2.5 - \frac{x}{h_{ef}} \geq 1 \text{ [−]} \tag{3.48}$$

where
x is distance between the anchor and the crack on the concrete surface assuming a crack propagation from the stirrup of the supplementary reinforcement to the concrete surface with an angle of 35° [mm]

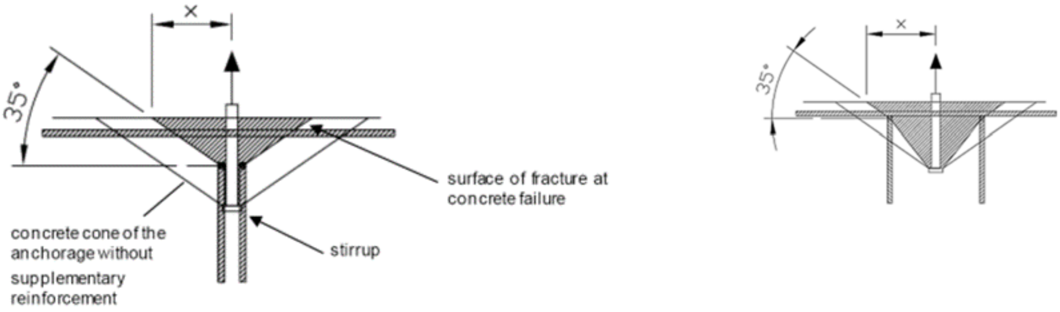

Fig. 3.4 Distance between the anchor and the crack on the concrete surface

The load is transferred to the stirrups and the concrete cone failure load is reached. Depending on the amount of supplementary reinforcement the failure of the stirrups can decisive $N_{Rd,re} < N_{Rd,cs}$. Two failure modes are possible:

steel yielding of stirrups $N_{Rd,s,re}$, see equation (3.16),

anchorage failure of stirrups $N_{Rd,b,re}$, see equation (3.20).

The corresponding failure load is calculated according to equation (3.49) summarizing the loads of the corresponding components

$$N_{Rd,re} = \min(N_{Rd,s,re}; N_{Rd,b,re}) + N_{Rd,c} + \delta_f \cdot k_{c,de} \text{ [N]} \tag{3.49}$$

where

$N_{Rd,c}$ is design failure load in case of concrete cone failure, see equation (3.7), [N]

$N_{Rd,s,re}$ is design failure load in case of yielding of the stirrups of the supplementary reinforcement, see equation (3.16) [N]

$N_{Rd,b,re}$ is design failure load in case of bond failure of the stirrups of the supplementary reinforcement, see equation (3.20) [N]

$k_{c,de}$ is stiffness of the concrete cone in the descending branch, see equation (3.13) [N/mm]

δ_f is corresponding displacement at failure load $N_{Rd,s,re}$ or $N_{Rd,b,re}$ [mm]

3.2.5 Combination of tension and shear components

The displacements in tension and shear is calculated by the sum of the displacement vectors.

3.3 Simplified stiffness's based on technical specifications

3.3.1 Headed stud in tension without supplementary reinforcement

For simplification the displacements and the stiffness of headed studs or anchorages is estimated using technical product specifications. The elongation δ_{Rd} is estimated up to the design load N_{Rd} using the displacements given in the technical product specification. The displacement is estimated by the following equation

$$\delta_{Rd,N} = \frac{\delta_{N,ETA}}{N_{ETA}} N_{Rd} \tag{3.50}$$

where

$\delta_{N,ETA}$ is displacement given in the product specifications for a corresponding load

N_{ETA} is tension load for which the displacements are derived in the product specifications

N_{Rd} is design tension resistance

The stiffness of the anchorage is calculated with the following equation

$$k_{Rd,N} = \frac{\delta_{N,ETA}}{N_{ETA}} \tag{3.51}$$

where
$\delta_{N,ETA}$ is displacement given in the product specifications for a corresponding load
N_{ETA} is tension load for which the displacements are derived in the product specifications

3.3.2 Headed stud in shear

For the design the displacement δ_v is estimated up to the design load V_{Rd} using the displacements given in the technical product specification. The displacement is estimated using the displacements far from the edge $\delta_{v,ETA}$ for short term and long term loading. The displacement is estimated by the following equation

$$\delta_{Rd,v} = \frac{\delta_{v,ETA}}{V_{ETA}}\ V_{Rd} \tag{3.52}$$

where
$\delta_{V,ETA}$ is displacement given in the product specifications for a corresponding load
V_{ETA} is shear load for which the displacements are derived in the product specifications
$V_{Rd,c}$ is design shear resistance

The stiffness of the anchorage is calculated with the following equation

$$k_{Rd,v} = \frac{\delta_{v,ETA}}{V_{ETA}} \tag{3.53}$$

where
$\delta_{V,ETA}$ is displacement given in the product specifications for a corresponding load
V_{ETA} is shear load for which the displacements are derived in the product specifications

3.3.3 Concrete breakout in tension

The characteristic load corresponding to the concrete cone breakout in tension for a single headed stud without edge influence is given by equation

$$N^0_{Rk,c} = k_1\ h_{ef}^{1.5}\ \sqrt{f_{ck}} \tag{3.54}$$

where
k_1 is basic factor for concrete cone breakout, which is equal to 8.9 for cracked concrete and 12.7 for non-cracked concrete, for headed studs, [-]
h_{ef} is effective embedment depth given according to the product specifications [mm] [-]
f_{ck} is characteristic concrete strength according to EN206-1:2000 [N/mm²]

The design load for concrete cone breakout for a single anchor, $N^0_{Rd,c}$ is obtained by applying partial safety factor of concrete γ_{Mc} to the characteristic load as

$$N^0_{Rd,c} = \frac{N^0_{Rk,c}}{\gamma_{Mc}} \tag{3.55}$$

For concrete, the recommended value of is γ_{Mc} = 1.5.

For a group of anchors, the design resistance corresponding to concrete cone breakout is given by equation (3.56), which is essentially same as equation (3.7)

$$N_{Rd,c} = N^0_{Rk,c}\ \psi_{A,N}\ \psi_{s,N}\ \psi_{re,N}/\gamma_{Mc} \tag{3.56}$$

where

$N^0_{Rk,c}$ is characteristic resistance of a single anchor without edge and spacing effects

$\psi_{A,N}$ is factor accounting for the geometric effects of spacing and edge distance given as $\psi_{A,N} = \frac{A_{c,N}}{A^0_{c,N}}$

$A^0_{c,N}$ is reference area of the concrete cone for a single anchor with large spacing and edge distance projected on the concrete surface [mm²].
The concrete cone is idealized as a pyramid with a height equal to h_{ef} and a base length equal to $s_{cr,N}$ with $s_{cr,N} = 3.0\ h_{ef}$, thus $A^0_{c,N} = 9\ h^2_{ef}$.

$A^0_{c,N}$ is reference area of the concrete cone of an individual anchor with large spacing and edge distance projected on the concrete surface [mm²].
The concrete cone is idealized as a pyramid with a height equal to h_{ef} and a base length equal to $s_{cr,N}$ with $s_{cr,N}\ =\ 3{,}0\ h_{ef}$ [mm]

$A_{c,N}$ is actual projected area of concrete cone of the anchorage at the concrete surface, limited by overlapping concrete cones of adjacent anchors $s < s_{cr,N}$,
as well as by edges of the concrete member $c < c_{cr,N}$.
It may be deduced from the idealized failure cones of single anchors [mm²]

c is minimum edge distance $c = 1.5\ h_{ef}$ [mm]

$c_{cr,N}$ is critical edge distance $c_{cr,N} = 1.5\ h_{ef}$ [mm]

$\psi_{re,N}$ is factor accounting for the negative effect of closely spaced reinforcement in the concrete member on the strength of anchors with an embedment depth h_{ef} < 100 mm
0.5 + h_{ef} / 200 for s < 150 mm, for any diameter [-]
or s < 100 mm, for $d_s \le$ 10 mm
1.0 for $s \ge$ 150 mm (for any diameter) [-]

γ_{Mc} is 1.5 for concrete [-]

3.3.4 Pull out failure of the headed studs

The design load corresponding to the pull out failure of the headed stud, $N_{Rd,p}$ is given by

$$N_{Rd,p} = p_{uk}\ A_h/\gamma_{Mc} \tag{3.57}$$

where

p_{uk} is characteristic ultimate bearing pressure at the head of stud [N/mm²]

A_h is area on the head of the headed stud [mm²]

$$A_h = \frac{\pi}{4} \cdot (d^2_h - {d_s}^2) \tag{3.57b}$$

d_h is diameter of the head [mm]

d_s is diameter of the shaft [mm]

γ_{Mc} is 1.5 for concrete [-]

3.3.5 Interaction of components for concrete and stirrups

In case of headed stud anchored in concrete with supplementary reinforcement, stirrups, the stirrups do not carry any load till the concrete breakout initiates, i.e. till N_{act} is less than or equal to $N_{Rd,c}$. Once, the concrete breakout occurs, the load shared by concrete decreases with increasing displacement as depicted in Fig. 3.4. The load shared by concrete $N_{act,c}$ corresponding to a given displacement δ is therefore given by equation

$$N_{act,c} = N_{Rd,c} + k_{c,de}\,\delta \tag{3.57}$$

where $k_{c,de}$ is the slope of descending branch of Fig. 3.4, negative value, given by Eq. (3.7). Simultaneously, in case of concrete with supplementary reinforcement, the stirrups start to carry the load. The load carried by the stirrups corresponding to a given displacement δ is given by equation

$$N_{act,re} = n_{re}\, d_{s,re}^2 \sqrt{\frac{\alpha_s\, f_{ck}\, \delta}{2}} \tag{3.58a}$$

where
α_s is factor of the component stirrups, currently is α_s = 12 100 [-]
$d_{s,nom}$ is nominal diameter of the stirrups [mm]
f_{ck} is characteristic concrete compressive strength [N/mm²]
n_{re} is total number of legs of stirrups [-]

The total load N_{act} carried by concrete cone and stirrups corresponding to any given displacement δ is therefore given as the sum of the two components:

$$N_{act} = N_{act,c} + N_{act,re} = N_{Rd,c} + k_{c,de}\,\delta + \min\left(n_{re}\, d_{s,re}^2 \sqrt{\frac{\alpha_s\, f_{ck}\, \delta}{2}};\ N_{Rd,s,re};\ N_{Rd,b,re}\right) \tag{3.59}$$

The displacement corresponding to peak load of the system is obtained by differentiating the right hand side of Eq. (3.60) and equating it to zero. If the bond failure or steel failure of stirrups is not reached at an earlier displacement then the design peak load carried by the system $N_{u,c+s}$ is given by

$$N_{u,c+s} = N_{Rd,c} + \frac{3}{8}\,\frac{n_{re}^2\, d_{s,re}^4\, \alpha_s\, f_{ck}}{k_{c,de}} \tag{3.60}$$

where
$N_{Rd,c}$ is design load at concrete cone failure given by equation (3.7)
α_s is factor of the component stirrups, currently is α_s = 12 100 [-]
$d_{s,re}$ is Nominal diameter of the stirrups [mm]
f_{ck} is characteristic concrete compressive strength [N/mm²]
n_{re} is total number of legs of stirrups [-]
$k_{c,de}$ is stiffness of descending branch for concrete cone failure, given by eq. (3.13)

In a relatively rare case of all studs loaded in tension, both the legs of the hanger reinforcement are not uniformly loaded and the distribution of forces is difficult to ascertain. Due to this reason and also to avoid the problems with serviceability requirements, it is recommended that in such a case, the contribution of hanger reinforcement is ignored.

3.3.6 Determination of the failure load

The failure load N_u is given by the minimum of the failure load corresponding to each considered failure mode

3.3.7 Friction

For base plates the friction is defined in EN1993-1-8 cl 6.2.2. For the resistance the resistance values of friction and bolts may be added as long as the bolt holes are not oversized. For the friction between a base plate and the grout underneath the plate the following calculation may be used.

$$F_{f,Rd} = C_{f,d} \, N_{c,Ed} \tag{3.61}$$

where
$C_{f,d}$ is coefficient for friction, for sand-cement mortar $C_{f,d} = 0.2$
$N_{c,Ed}$ is axial compressive force of the column

In this design manual the friction is not only applied to compression forces caused by axial forces but also for compression forces generated by bending moments. This principle is applied in EN1993-1-8:2006 for beam to the column end joints with end plates in cl 3.9.2(3).

3.4 Base plate in bending and concrete block in compression

3.4.1 Concrete 3D strength

The components concrete in compression and base plate in bending represent the behaviour of the compressed part of a steel to concrete connection. The resistance of these components depends primarily on the bearing resistance of the concrete block under the flexible base plate, see (Melchers, 1992). The resistance of concrete is influenced by flexibility of base plate. In case of loading by an axial force, the stresses in concrete are not uniformly distributed, they are concentrated around the footprint of the column under the plate according to its thickness, see (Dewolf, Sarisley, 1980). For the design the flexible base plate is replaced by reducing the effective fully rigid plate. The grout layer between the base plate and concrete block influences the resistance and stiffness of the component. That is why this layer is also included into this component, see (Penserini, Colson, 1989). Other important factors which influence the resistance are the concrete strength, the compression area, the location of the plate on the concrete foundation, the size of the concrete block and its reinforcement.

The stiffness behaviour of column base connection subjected to bending moment is influenced mostly by elongation of anchor bolts. The Component concrete in compression is mostly stiffer in comparison to the component anchor bolts in tension. The deformation of concrete block and base plate in compression is important in case of dominant axial compressive force.

The strength of the component $F_{Rd,u}$, expecting the constant distribution of the bearing stresses under the effective area, is given by

$$F_{Rd,u} = A_{c0} \, f_{jd} \tag{3.62}$$

The design value of the bearing strength f_{jd} in the joint loaded by concentrated compression, is determined as follows. The concrete resistance is calculated according to cl. 6.7(2) in EN1992-1-1:2004 see Fig. 3.6 is

$$F_{Rd,u} = A_{c0}\, f_{cd} \sqrt{\frac{A_{c1}}{A_{c0}}} \leq 3.0\, A_{c0}\; f_{cd} \tag{3.63}$$

where

$$A_{c0} = b_1\, d_1 \quad \text{and } A_{c1} = b_2\, d_2 \tag{3.64}$$

where A_{c0} is the loaded area and A_{c1} the maximum spread area. The influence of height of the concrete block to its 3D behaviour is introduced by

$$\begin{gathered} h \quad \geq b_2 - \; b_1 \text{ and } h \quad \geq d_2 - \; d_1 \\ 3\, b_1 \;\geq b_2 \text{ and } \; 3\, d_1 \;\geq d_2 \end{gathered} \tag{3.65}$$

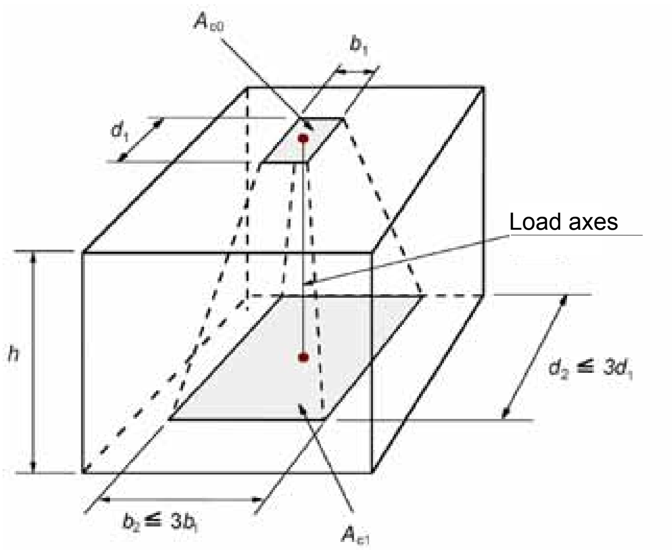

Fig. 3.5 Concrete compressive strength for calculation of 3D concentration

From this geometrical limitation the following formulation is derived

$$f_{jd} = \frac{\beta_j\, F_{Rd,u}}{b_{eff}\, l_{ef}} = \frac{\beta_j\, A_{c0}\, f_{cd}\sqrt{\frac{A_{c1}}{A_{c0}}}}{A_{c0}} = \beta_j\, f_{cd}\, k_j \leq \frac{3\, A_{c0}\, f_{cd}}{A_{c0}} = 3.0\, f_{cd} \tag{3.66}$$

The factor β_j represents the fact that the resistance under the plate might be lower due to the quality of the grout layer after filling. The value 2/3 is used in the case of the characteristic resistance of the grout layer is at least 0.2 times the characteristic resistance of concrete and thickness of this layer is smaller than 0.2 times the smallest measurement of the base plate. In different cases, it is necessary to check the grout separately. The bearing distribution under 45° is expected in these cases, see (Steenhuis et al, 2008) and Fig. 3.5 Concrete compressive strength for calculation of 3D concentration

Fig. 3. The design area A_{c0} is conservatively considered as the full area of the plate A_p.

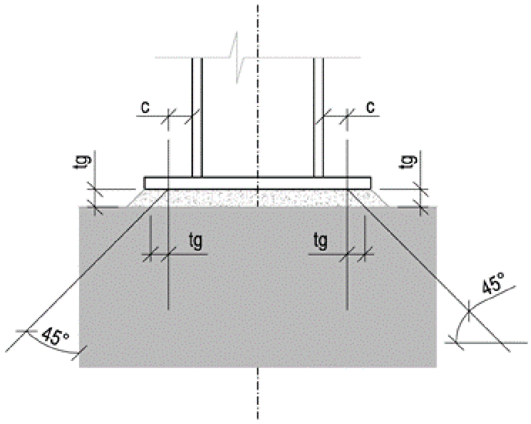

Fig. 3.6 Modelling of grout

3.4.2 Base plate flexibility

In case of the elastic deformation of the base plate is expected homogenous stress distribution in concrete block is expected under the flexible base plate based on the best engineering practice. The formula for the effective width c is derived from the equality of elastic bending moment resistance of the base plate and the bending moment acting on the base plate, see (Astaneh et al., 1992). Acting forces are shown in Fig. 3.7.

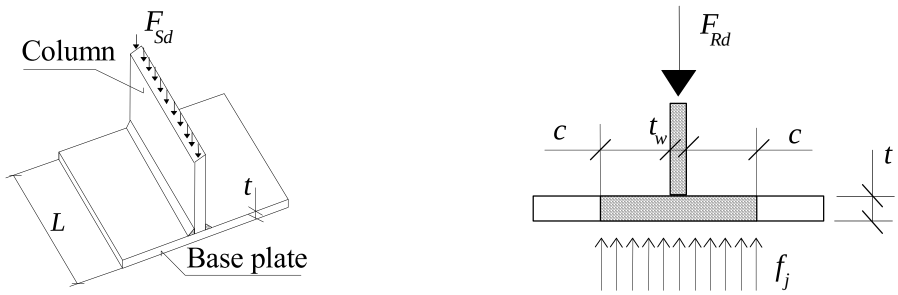

Fig. 3.7 Base plate as a cantilever for check of its elastic deformation only

Elastic bending moment of the base plate per unit length is

$$M' = \frac{1}{6}\, t^2 \frac{f_y}{\gamma_{M0}} \tag{3.69}$$

and the bending moment per unit length on the base plate of span c and loaded by distributed load is

$$M' = \frac{1}{2} f_j\, c^2 \tag{3.70}$$

where f_j is concrete bearing strength and from Eq. (3.69) and (3.70) is

$$c = t \sqrt{\frac{f_y}{3 \cdot f_{jd} \cdot \gamma_{M0}}} \tag{3.71}$$

The flexible base plate, of the area A_p, is replaced by an equivalent rigid plate with area A_{eq}, see Fig. 3.8. Then the resistance of the component, expecting the constant distribution of the bearing stresses under the effective area is given by

$$F_{Rd,u} = A_{eq} \cdot f_{jd} \tag{3.72}$$

The resistance F_{Rd} should be higher than the loading F_{Ed}

$$F_{Ed} \leq F_{Rd,u} \tag{3.73}$$

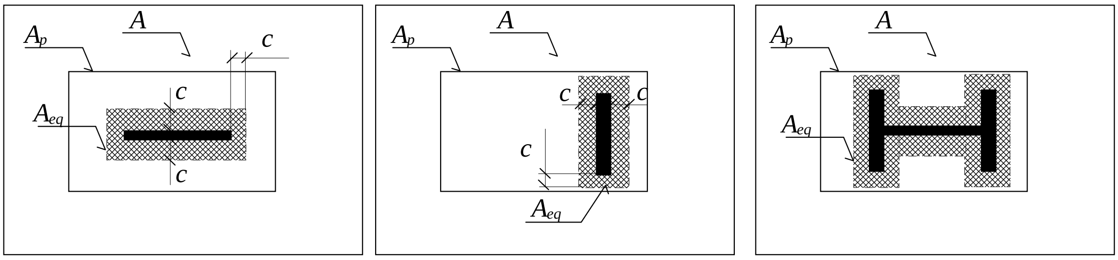

Fig. 3.8 Effective area under the base plate

3.4.3 Component stiffness

The proposed design model for stiffness of the components base plate in bending and concrete in compression is given also in (Steenhuis et al, 2008). The stiffness of the component is influenced by factors: the flexibility of the plate, the Young´s modulus of concrete, and the size of the concrete block. By loading with force, a flexible rectangular plate could be pressed down into concrete block. This flexible deformation is determined by theory of elastic semi-space

$$\delta_r = \frac{F \ \alpha \ a_r}{E_c \, A_p} \tag{3.74}$$

where
F is acting load
α is shape factor of the plate
a_r is width of equivalent rigid plate
E_c is elastic modulus of concrete
A_p is area of the plate

The factor α depends on the material characteristics. The Tab. 3.1 gives values of this factor dependent on the Poison's ratio, for concrete is $\nu \approx 0.15$. The table shows also the approximate value of factor α, that is $0.58 \cdot \sqrt{L/a_r}$.

Tab. 3.1 Factor α and its approximation for concrete

l / a_r	α	Approximation as $\alpha = 0.58 \cdot \sqrt{L/a_r}$.
1	0.90	0.85
1.5	1.10	1.04
2	1.25	1.20
3	1.47	1.47
5	1.76	1.90
10	2.17	2.69

For steel plate laid on concrete block it is

$$\delta_r = \frac{0.85\ F}{E_c\sqrt{l \cdot a_r}} \tag{3.75}$$

where

σ_r is deformation under the rigid plate

l is length of the plate

The model for the elastic stiffness behaviour of component is based on a similar interaction between concrete block and steel plate. The flexible plate is expressed as an equivalent rigid plate based on the same deformation, modelled in Fig. 3.9.

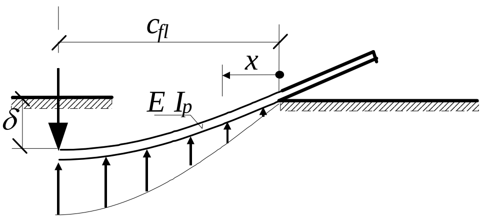

Fig. 3.9 A flange of flexible T-stub

Independent springs support the flange of a unit width. Then, the deformation of the plate is a sine function.

$$\delta_{(x)} = \delta \sin\left(½\ \pi\ x\ /\ c_{fl}\right) \tag{3.76}$$

The uniform stress on the plate is rewritten by the fourth differentiate and multiplied by $E\ I'_p$

$$\delta_{(x)} = E\ I'_p\ (½\ \pi/c_{fl})^4\ \delta \sin\left(½\ \pi\ \frac{x}{c_{fl}}\right) = E\ \frac{t^3}{12}\left(½\ \frac{\pi}{c_{fl}}\right)^4 \delta \sin\left(½\ \pi\ x\ /c_{fl}\right) \tag{3.77}$$

where

E is elastic modulus of steel

I'_p is moment of inertia per unit length of the steel plate ($I'_p = t^3\ /\ 12$)

t is thickness of the plate

$$\delta_{(x)} = \sigma_{(x)}\ h_{ef}/E_c \tag{3.78}$$

where

h_{ef} is equivalent concrete height of the portion under the steel plate

Assume that

$$h_{ef} = \xi\ c_{fl} \tag{3.79}$$

Factor ξ expresses the rotation between h_{ef} and c_{fl}. Hence

$$\delta_{(x)} = \sigma_{(x)}\ \xi\ c_{fl}/E_c \tag{3.80}$$

After substitution and using other expressing it is

$$c_{fl} = t\sqrt[3]{\frac{(\pi/2)^4}{12}\,\xi\,\frac{E}{E_c}} \qquad (3.81)$$

The flexible length c_{fl} may be replaced by an equivalent rigid length

$$c_r \;=\; c_{fl}\,2\,/\,\pi \qquad (3.82)$$

The factor ξ shows the ratio between h_{eq} and c_{fl}. The value a_r represents height h_{eq}. Factor α is approximated to $1.4 \cdot a_r = t_w + 2c_r$ and $t_w = 0.5\,c_r$. Then it is written

$$h_{eq} = 1.4 \cdot (0.5+2)\,c_r = 1.4 \cdot 2.5 \cdot c_{fl} \cdot \frac{2}{\pi} = 2.2\,c_{fl} \qquad (3.83)$$

Hence $\xi = 2.2$.

For practical joints is estimated by $E_c \cong$ 30 000 N / mm^2 and $E \cong$ 210 000 N / mm^2, what leads to

$$c_{fl} = t\sqrt[3]{\frac{(\pi/2)^4}{12}\xi\frac{E}{E_c}} = t\sqrt[3]{\frac{(\pi/2)^4}{12}2.2\frac{210000}{30000}} = 1.98\,t \qquad (3.84)$$

or

$$c_r \;=\; c_{fl}\,\frac{2}{\pi} = 1.98 \cdot \frac{2}{\pi} \cdot t = 1.25\,t \qquad (3.85)$$

The equivalent width a_r is in elastic state replace with

$$a_{eq,el} = t_w + 2.5\,t = 0.5\,c_r + t \qquad (3.86)$$

or

$$a_{eq,el} = 0.5 \cdot 1.25\,t + 2.5\,t = 3.125\,t \qquad (3.87)$$

From the deformation of the component and other necessary values which are described above, the formula to calculate the stiffness coefficient is derived

$$k_c = \frac{F}{\delta\,E} = \frac{E_c\,\sqrt{a_{eq,el}\,L}}{1.5 \cdot 0.85\,E} = \frac{E_c\,\sqrt{a_{eq,el}\,L}}{1.275\,E} = \frac{E_c \cdot \sqrt{t \cdot\,L}}{0.72 \cdot\,E} \qquad (3.88)$$

where

$a_{eq,el}$ is equivalent width of the T-stub

L is length of the T-stub

3.5 Concrete panel

The resistance and deformation of the reinforced concrete wall in the zone adjacent to the joint is hereby represented by a joint link component, see (Huber and Cermeneg, 1998). Due to the nature of this joint, reinforced concrete, the developed model is based on the strut-and-tie method, commonly implemented in the analysis of reinforced concrete joints. The problem is 3D, increasing its complexity, as the tension load is introduced with a larger width than the compression, which may be assumed concentrated within an equivalent dimension of the anchor plate, equivalent rigid plate as considered in T-stub in compression. Thus, a numerical model considering only the reinforced concrete wall and an elastic response of the material has been tested to identify the flow of principal stresses. These show that compression stresses flow from the hook of the longitudinal reinforcement bar to the anchor plate. In this way the strut-and-tie model (STM) represented in Fig. 10a is idealized. Subsequently, in order to contemplate the evaluation of the deformation of the joint, a diagonal spring is idealized to model the diagonal compression concrete strut, as illustrated in Fig. 10. The ties correspond to the longitudinal steel reinforcement bars. The properties of this diagonal spring are determined for resistance and stiffness.

The resistance is obtained based on the strut and nodes dimension and admissible stresses within these elements. The node at the anchor plate is within a tri-axial state. Therefore, high stresses are attained as confinement effect. In what concerns the strut, because of the 3D nature, stresses tend to spread between nodes. Giving the dimensions of the wall of infinite width, the strut dimensions should not be critical to the joint. Thus, the node at the hook of the bar is assumed to define the capacity of the diagonal spring. The resistance of the spring is then obtained according to the dimensions of this node and to the admissible stresses in the node and in the strut. For the latter, the numerical model indicates the presence of transverse tension stresses which have to be taken into consideration.

The deformation of the diagonal spring is obtained by assuming a non-linear stress-strain relation for the concrete under compression, as defined in (Henriques, 2012). The maximum stress is given by the limiting admissible stress as referred above. Then, deformation is calculated in function of the length of the diagonal strut and the concrete strain.

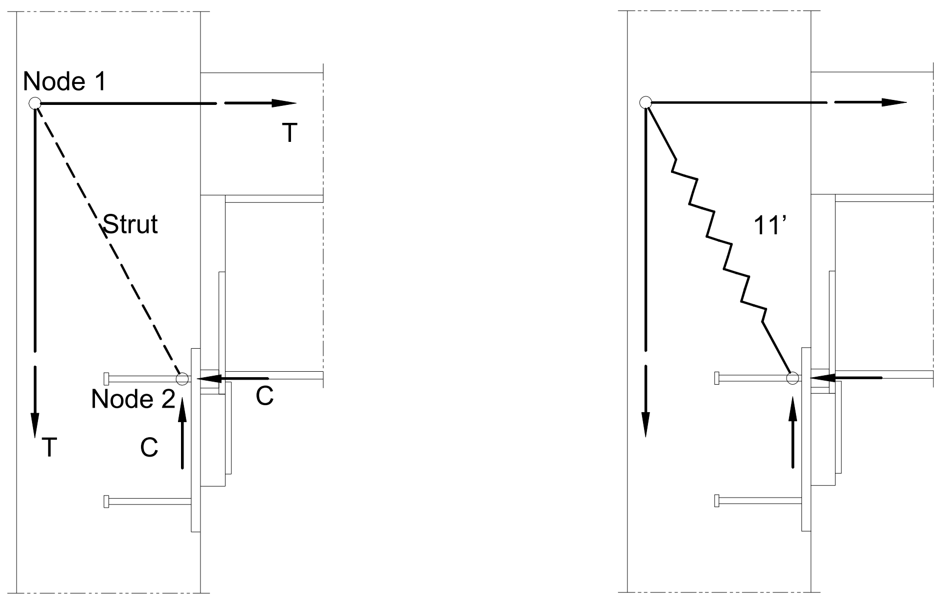

a) Strut-and-tie model

b) Single diagonal spring

Fig. 3.10 Joint link modelling

Tab. 3.2 provides the stresses for nodes and struts according to EN1992-1-1:2004. Node 1 is characterized by the hook longitudinal reinforcement bar. The represented dimension is assumed as defined in CEB-FIP Model Code 1990. In what concerns the width of the node, based on the numerical observations, it is considered to be limited by the distance between the external longitudinal reinforcement bars within the effective width of the slab. The numerical model demonstrates that the longitudinal reinforcement bars are sufficiently close, as no relevant discontinuity in the stress field is observed. Though, this is an issue under further investigation and depending on the spacing of the reinforcing bars, this assumption may or may not be correct (Henriques, 2013).

Tab. 3.2 Stresses in strut-and-tie elements according to EN1992-1-1:2004

Element	Limiting stresses
Node 1	$0.75\ \nu\ f_{cd}$
Node 2	$3\ \nu\ f_{cd}$
Strut	$0.6\ \nu\ f_{cd}$ with $\nu = 1 - f_{ck}/250$

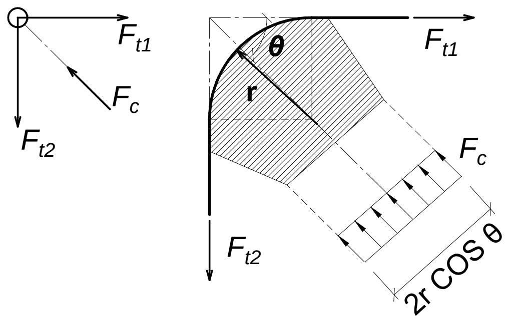

Fig. 3.11 Definition of the dimension related to the hook
of the longitudinal reinforcement bar in Node 1, according to the CEB Model Code

Finally, to simplify the assembling of the joint model, the diagonal spring representing the joint link component is converted into a horizontal spring. The properties of the horizontal spring are directly obtained from the diagonal spring determined as a function of the angle of the diagonal spring.

3.6 Longitudinal steel reinforcement in tension

In the composite joint configuration under consideration, the longitudinal reinforcement in tension is the only component able to transfer tension forces introduced by the bending moment to the supporting member e.g. a reinforced concrete wall. This component determines the behaviour of the joint. According to EN1994-1 the longitudinal steel reinforcement may be stressed to its design yield strength. It is assumed that all the reinforcement within the effective width of the concrete flange is used to transfer forces. The resistance capacity of the component may then be determined as in Eq. (3.89). Regarding the deformation of the component, the code provides stiffness coefficients for two composite joint configurations, single and double-sided joints. The stiffness coefficient for single-sided joints may be estimated as in Eq. (3.90). This stiffness coefficient depends essentially on the elongation length of the longitudinal reinforcement contributing to the deformation of the component. Analogous to the code provisions, the dimension h involved in Eq. (3.90) is assumed as shown in Fig. 3.12.

$$\mathrm{F_{s,r} = A_{s,r}\ f_{yr}} \tag{3.89}$$

$$\mathrm{k_{s,r} = \frac{A_{s,r}}{3.6\ h}} \tag{3.90}$$

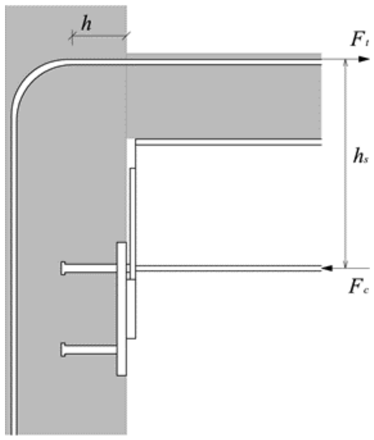

Fig. 3.12 Dimension h for elongation length

The tension component of the joint is calculated according to

$$F_t = -M_{y,Ed}/h_s \tag{3.91}$$

3.7 Slip of the composite beam

The slip of composite beam does not directly influence the resistance of the joint. However, the level of interaction between concrete slab and steel beam defines the maximum load the longitudinal reinforcement can achieve. Therefore in such joint configuration, where reinforcement is the only tension component, the level of interaction affects the joint resistance. In the EN1994-1-1:2008, the influence of the slip of composite beam is taken into account. The stiffness coefficient of the longitudinal reinforcement, see Eq. (3.92) should be multiplied with the reduction factor k_{slip} determined as follows:

$$k_{slip} = \frac{1}{1 + \frac{E_s\ k_{sr}}{k_{SC}}} \tag{3.92}$$

$$K_{SC} = \frac{N\ k_{sc}}{\vartheta - \left(\frac{\vartheta - 1}{1 + \xi}\right) \frac{h_s}{d_s}} \tag{3.93}$$

$$\vartheta = \sqrt{\frac{(1 + \xi)\ N\ k_{sc}\ l\ d_s^2}{E_a\ I_a}} \tag{3.94}$$

$$\xi = \frac{E_a\ I_a}{d_s^2\ E_s\ A_s} \tag{3.95}$$

where

h_s is the distance between the longitudinal reinforcing bars and the centre of compression of the joint, that may be assumed as the midpoint of the compression flange of the steel beam

d_s is the distance between the longitudinal reinforcing bars and the centroid of the steel beam section, see Fig. 13

I_a is the second moment area of the steel beam section

l is the length of the beam in hogging bending adjacent to the joint, in the case of the tested specimens is equal to the beam's length

N is the number of shear connectors distributed over the length l

k_{sc} is the stiffness of one shear connector

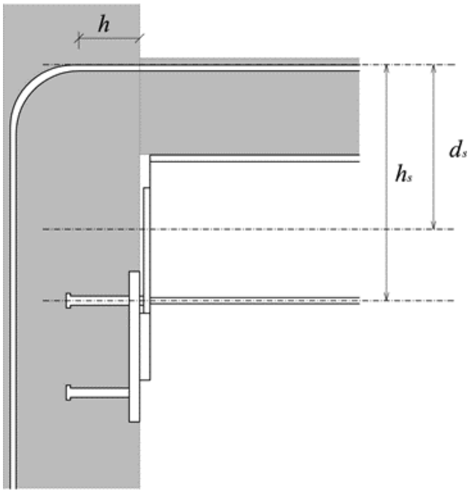

Fig. 3.13 Dimensions h_s and d_s

4 STEEL COMPONENTS

4.1 T-stub in tension

The base plate in bending and anchor bolts in tension is modelled by the help of T-stub model based on the beam to column end plate connection model. Though in its behaviour there are some differences. Thickness of the base plate is bigger to transfer compression into the concrete block. The anchor bolts are longer due to thick pad, thick base plate, significant layer of grout and flexible embedding into concrete block. The influence of a pad and a bolt head may be higher.

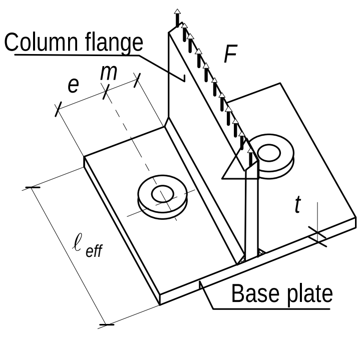

Fig. 4.1 The T stub - anchor bolts in tension and base plate in bending

Due to longer free lengths of bolts, bigger deformations could arise. The anchor bolts, compare to bolts, are expecting to behave ductile. When it is loaded by tension, the base plate is often separated from the concrete surface. This case is shown in (Wilkinson et al, 2009). By bending moment loading different behaviour should be expected. The areas of bolt head and pad change favourably distribution of forces on T-stub. This influence is not so distinctive during calculation of component stiffness. The all differences from end plate connections are involved in the component method, see EN1993-1-8:2006. The design model of this component for resistance as well for stiffness is given in (Wald et al, 2008).

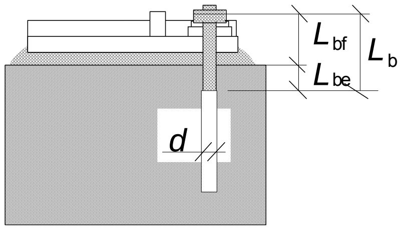

Fig. 4.2 Length of anchor bolt

4.1.1 Model

When the column base is loaded by bending moment as it is shown in Fig. 4.3, anchor bolts transfer tensile forces. This case of loading leads to elongation of anchor bolts and bending of the base plate. Deformed bolts can cause failure as well as reaching of the yield strength of the base plate. Sometimes failure in this tensile zone is caused by both, see (Di Sarno et al, 2007).

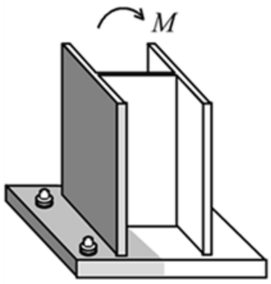

Fig. 4.3 Tensile zone and equivalent T-stub in case of loading by bending moment

Column with connected base plate taken, as it is shown in Fig. 4.4, into model of T-stub.

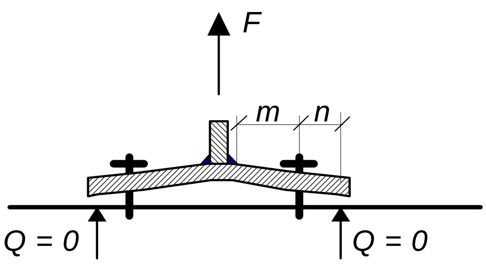

Fig. 4.4 T-stub separated from the concrete block with no prying force

There are two models of deformation of the T-stub of the base plate according to presence of prying. In the case the base plate separated from the concrete foundation, there is no prying force Q, see Fig. 4.4. In other case, the edge of the plate is in contact with concrete block, the bolts are loaded by additional prying force Q. This force is balanced just by the contact force at the edge of the T-stub, see Fig. 4.5.

When there is contact between the base plate and the concrete block, beam theory is used to describe deformed shape of the T-stub.

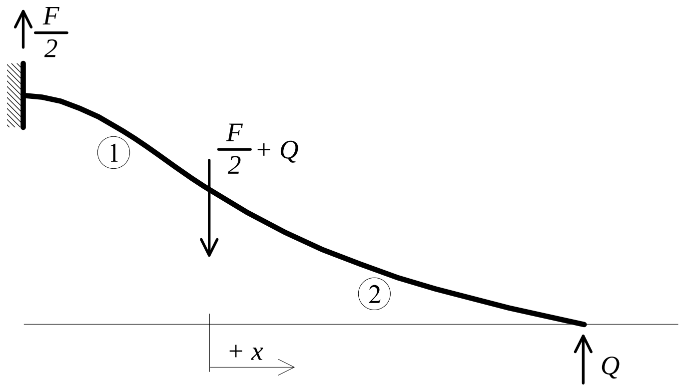

Fig. 4.5 Beam model of T-stub and prying force Q

Deformed shape of the curve is described by differential equation

$$E\,I\,\delta'' = -M \tag{4.1}$$

After writing the above equation for both parts of the beam model 1 and 2, application of suitable boundary conditions, the equations could be solved. The prying force Q is derived just from these solved equations as

$$Q = \frac{F}{2} \cdot \frac{3(m^2\, n\ A - 2\, L_b\, I)}{2\, n^2 A\, (3\, m + n) + 3\, L_b\, I} \tag{4.2}$$

When the base plate is in contact with concrete surface, the prying of bolts appears and on the contrary no prying forces occur in the case of separated base plate from the concrete block due to the deformation of long bolts. This boundary, between prying and no prying has to be determined. Providing that $n = 1.25\ m$ it may be expressed as

$$L_{b,min} = \frac{8.82\ m^3 A_s}{l_{eff} t^3} < L_b \tag{4.3}$$

where

A_s is the area of the bolt

L_b is equivalent length of anchor bolt

l_{eff} is equivalent length of T-stub determined by the help of Yield line method, presented in following part of work

For embedded bolts length L_b is determined according to Fig. 4.2 as

$$L_b = L_{bf} + L_{be} \tag{4.4}$$

where

L_{be} is $8\ d$ effective bolt length

When the length of bolt $L_b > L_{b,min}$ there is no prying. Previous formulae is expressed for boundary thickness t_{lim}, see (Wald et al, 2008), of the base plate as

$$t_{lim} = 2.066\ m \cdot \sqrt[3]{\frac{A_s}{l_{eff}\, L_b}} \tag{4.5}$$

If the base plate are loaded by compression force and by bending moment and not by tensile force it is recommended to neglect these prying forces. In other cases it needs to be checked.

4.1.2 Resistance

The design resistance of a T-stub of flange in tension of effective length ℓ_{eff} is determined as minimum resistance of three possible plastic collapse mechanisms. For each collapse mechanism there is a failure mode. Following collapse modes, shown in Fig. 4.6, is used for T-stub in contact with the concrete foundation, see in EN1993-1-8:2006.

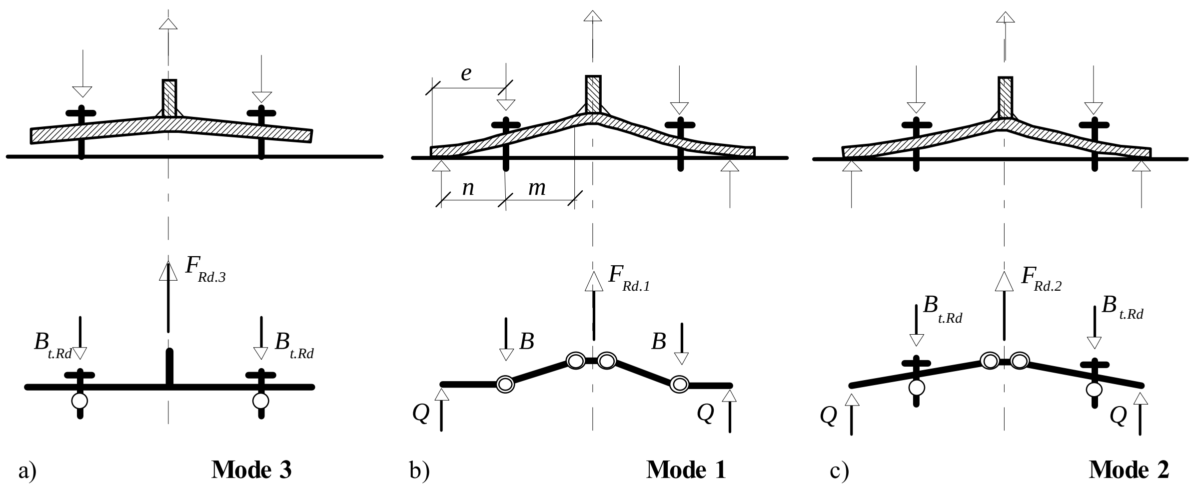

Fig. 4.6 Failure modes of the T-stub in contact with the concrete foundation

Mode 1

According to this kind of failure the T-stub with thin base plate and high strength anchor bolts is broken. In the base plate plastic hinge mechanism with four hinges is developed.

$$F_{1,Rd} = \frac{4\ l_{eff}\ m_{pl,Rd}}{m} \tag{4.6}$$

Mode 2

This mode is a transition between failure Mode 1 and 3. At the same time two plastic hinges are developed in the base plate and the limit strength of the anchor bolts is achieved.

$$F_{2,Rd} = \frac{2\ l_{eff}\ m_{pl,Rd} + \Sigma\, B_{t,Rd} \cdot n}{m + n} \tag{4.7}$$

Mode 3

Failure mode 3 occurs by the T-stub with thick base plate and weak anchor bolts. The collapse is caused by bolt fracture.

$$F_{3,Rd} = \Sigma\, B_{t,Rd} \tag{4.8}$$

The design strength F_{Rd} of the T-stub is derived as the smallest of these three possible modes:

$$F_{Rd} = \min\left(F_{1,Rd}, F_{2,Rd}, F_{3,Rd}\right) \tag{4.9}$$

Because of the long anchor bolts and thick base plate different failure mode arises compare to an end plate connection. When the T-stub is uplifted from the concrete foundation, there is no prying, new collapse mode is obtained, see Fig. 4.7. This particular failure mode is named Mode 1-2.

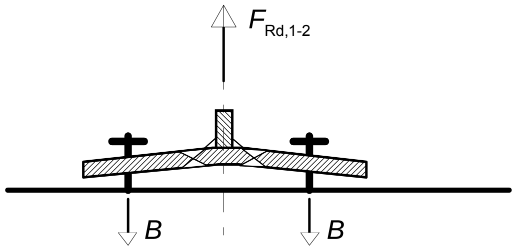

Fig. 4.7 T-stub without contact with the concrete foundation, Mode 1-2

<u>Mode 1-2</u>

The failure results either from bearing of the anchor bolts in tension or from the yielding of the plate in bending, where a two hinges mechanism develops in the T-stub flange. This failure does not appear in beam to column connection because of the small deformation of the bolts in tension, see (Wald et al, 2008).

$$F_{1-2,Rd} = \frac{2\ l_{eff}\ m_{pl,Rd}}{m} \tag{4.10}$$

The relationship between Mode 1-2 and modes of T-stub in contact with concrete is shown in Fig. 4.8.

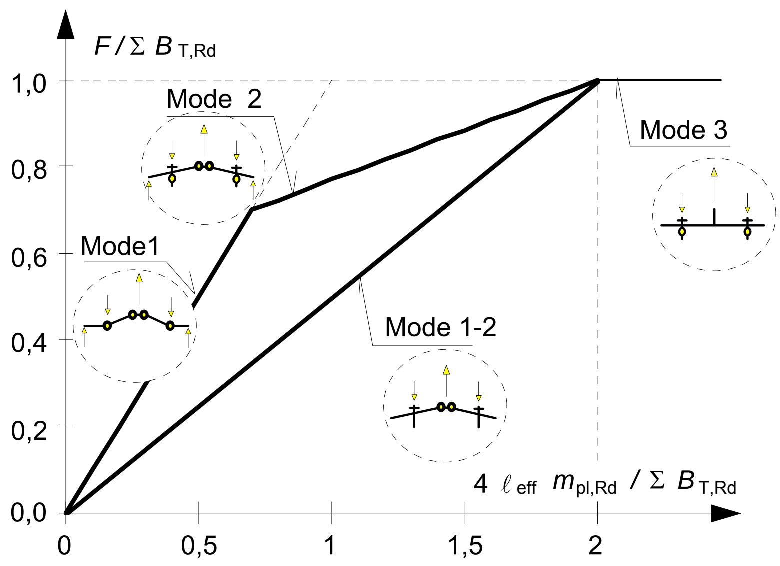

Fig. 4.8 Failure mode 1-2

The boundary between the mode 1-2 and others is given in the same way like the boundary of prying and no prying – according to the limiting bolt length $L_{b,min}$.

During the Mode 1-2 large deformations of the base plate can develop. Finally these deformations could lead to contact between the concrete block and the edge of the T-stub (prying forces can arise even in this case). After loading Modes 1 or 2 should be obtained like the first. But for reaching this level of resistance, which is necessary to obtain these modes, very large deformations are required. And so high deformations are not acceptable for design. In conclusion, in cases where no prying forces develop, the design resistance of the T-stub is taken as

$$F_{Rd} = \min\left(F_{1-2,Rd}, F_{3,Rd}\right) \tag{4.11}$$

where

$$F_{3,Rd} = \Sigma B_{t,Rd} \tag{4.12}$$

The equivalent length of T-stub l_{eff}, which is very important for the resistance determination, is calculated by the help of the yield line method, which is explained in the following part of the work.

Yield line method

Although numerical methods, based on extensive use of computers, are potentially capable of solving the most difficult plate problems, yield-line analysis is such an alternative computational technique (Thambiratnam, Paramasivam, 1986). It provides such an alternative design method for plates. This simple method, which uses concepts and techniques familiar to structural engineers, provides realistic upper bounds of collapse loads even for arbitrary shapes and loading conditions. The advantages of the yield-line method are: simplicity and economy, information is provided on the real load-carrying capacity of the slab, the basic principles used are familiar to structural engineers, the method also gives acceptable estimates for the ultimate load-carrying capacity of structural steel plates, and resulting designs are often more economical. On the other hand, the present limitations of the method are: the method fails in vibration analysis and cannot be used in the case of repeated static or dynamic loads (but is applied effectively for suddenly applied one-time loads), and theoretically, the law of superposition is not valid. The yield-line method offers, especially for the practicing engineer, certain advantages over the elastic stress analysis approaches.

Assumptions

The correct failure pattern is known, the critical load is obtained either from virtual work or from equilibrium considerations. Both approaches use the following basic assumptions: at impending collapse, yield lines are developed at the location of the maximum moments, the yield lines are straight lines, along the yield lines, constant ultimate moments m_u are developed, the elastic deformations within the slab segments are negligible in comparison with the rigid body motions, created by the large deformations along the yield lines, from the many possible collapse mechanisms, only one, pertinent to the lowest failure load, is important. In this case the yield-line pattern is optimum, when yield lines are in the optimum position, only ultimate bending moments, but no twisting moments or transverse shear forces are present along the yield lines. The location and orientation of yield lines determine the collapse mechanism. The Fig. 4.9 introduces an example of yield line.

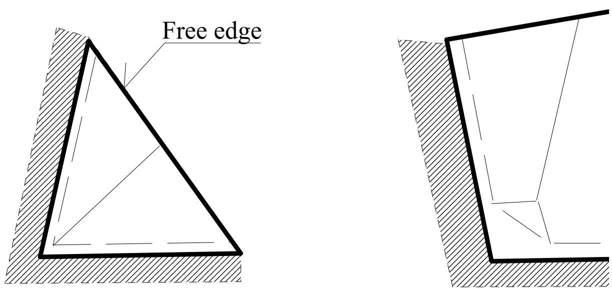

Fig. 4.9 Possible yield line patterns

The work method

The work method, see (Johansen, 1949), gives an upper-bound solution to the critical load at which the slab, with a certain ultimate resisting moment, fails. A particular configuration is searched, from a family of possible yield-line patterns which gives the lowest value of the ultimate load. The solution is based on the principle of virtual work.

The effective length of T-stub

The effective length l_{eff} of a T-stub is influenced by the failure mode of the T-stub. When there are more than one possible failure modes, it means more than one effective length, the calculation is done with the smallest (shortest) length, see EN1993-1-8:2006. The Fig. 4.10 shows, that two groups of yield line patterns can arise circular yield line and non-circular yield line. The main difference between these two types is related to contact between the T-stub and concrete foundation. By the non-circular patterns prying forces are developed. In this work there are taken into account only the modes without the contact of the edge of the base plate to the concrete foundation, it means without prying forces in bolts.

a) Circular pattern, $\ell_{eff,cp}$ b) Non-circular pattern, $\ell_{eff,np}$

Fig. 4.10 The yield line patterns

As it was written in previous paragraphs, the effective length could be determined by the yield line method. Hence the yield line of the base plate must be designed. The collapse Mode 1 of the plate, which is shown in Fig. 4.11, is expected.

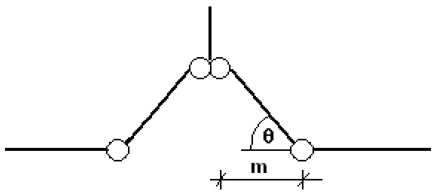

Fig. 4.11 Expected collapse mode

For this collapse mode there are following formulas:

$$m_{pl,Rd} = \frac{1}{4}\, t^2\, f_{yd} \tag{4.13}$$

$$\tan\theta = \frac{\delta}{m} \approx \theta \tag{4.14}$$

$$F_{pl} = \frac{4 l_{eff}\, m_{pl,Rd}}{m} \tag{4.15}$$

where

$m_{pl,Rd}$ is plastic bending moment resistance of the base plate per unit length

F_{pl} is force acting in the bolt position

The assumptions to determine the yield line of the base plate are following the yield line is a straight line, this line is perpendicular to a line which pass through the bolt and tangent to the column, or this line is tangent to the column and parallel to the edge of the base plate. With these assumptions are determined. Following calculation procedure of the effective length of the T-stub in plate corner is given in (Wald et al, 2000) and (Heinisuo et al, 2012).

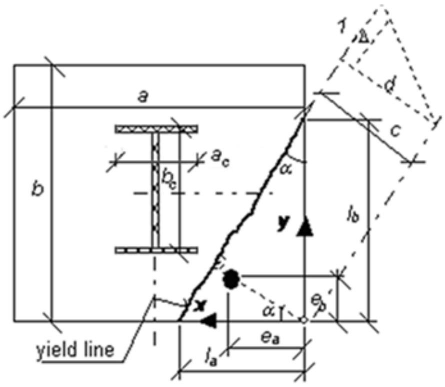

Fig. 4.12 The yield line parameters

α represents the angle between the yield line and the edge and c the minimal distance between the corner of the plate and the yield line. With the previous geometrical relation, the following relations is obtained

$$\tan \alpha = \frac{x}{y} \tag{4.16}$$

where

x, y are coordinates of the bolt, which could vary

For the design of the parameter c, the work method of the yield line theory is used. The internal work is

$$W_i = \sum_n \left[\overline{\theta_j}; \overline{m_{uj}}; 1\right] = m_{pl}\left(\frac{1}{y}x + \frac{1}{x}y\right) \tag{4.17}$$

The external work is

$$W_e = P_u\Delta = F_{pl}\Delta \tag{4.18}$$

where Δ represents the deformation of the plate in the bolt position, see Fig. 4.13.

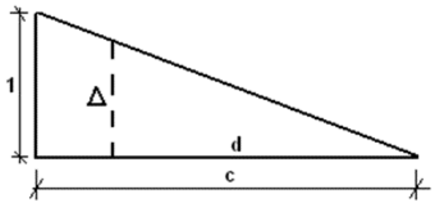

Fig. 4.13 The deformation of the plate represented by value Δ

According to previous figure is Δ replaced with

$$\frac{\Delta}{1} = \frac{d}{c} = \frac{\sqrt{x^2 + y^2}}{c} \tag{4.19}$$

After replacement Δ in the formula of the external work and putting it into equality with the internal work as

$$\frac{\sqrt{x^2 + y^2}}{c} F_{pl} = m_{pl} \left(\frac{x}{y} + \frac{y}{x} \right) \tag{4.20}$$

and then the effective length of the T-stub is

$$l_{eff} = \frac{c\, m}{4} \frac{\sqrt{x^2 + y^2}}{c} \tag{4.21}$$

The ultimate load is given by

$$F_{pl} = c\, m_{pl} \frac{\sqrt{x^2 + y^2}}{x\, y} \tag{4.22}$$

$$\frac{\partial\, F_{pl}}{\partial\, c} = m_{pl} \frac{\sqrt{x^2 + y^2}}{x\, y} = cst \tag{4.23}$$

With the yield line assumption the characteristics of the different possible failure models could be designed.

The effective length of T-stub

Two groups of yield line patterns called circular and non-circular yield lines are distinguished in EN1993-1-8:2006. The major difference between circular and non-circular patterns is related to contact between the T-stub and rigid foundation. The contact may occur only for non-circular patterns and prying force will develop only in this case. This is considered in the failure modes as follows:

Mode 1

The prying force does not have influence on the failure and development of plastic hinges in the base plate. Therefore, the formula (4.2) applies to both circular and non-circular yield line patterns.

Mode 2

First plastic hinge forms at the web of the T-stub. Plastic mechanism is developed in the base plate and its edges come into contact with the concrete foundation. As a result, prying forces develop in the anchor bolts and bolt fracture is observed. Therefore, Mode 2 occurs only for non-circular yield line patterns, which allow development of prying forces.

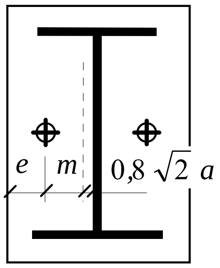

Fig. 4.14a The effective length of T-stub for bolts inside the flanges

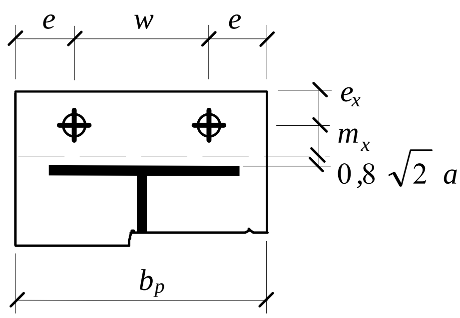

Fig. 4.14b The effective length of T-stub for bolts outside the flanges

Mode 3

This mode does not involve any yielding of the plate and applies therefore to any T-stub. In the design procedure, the appropriate effective length of the T-stub should be used for Mode 1

$$l_{eff,1} = \min\left(l_{eff,cp}; l_{eff,np}\right) \tag{4.24}$$

and for Mode 2

$$l_{eff,2} = \min\left(l_{eff,np}\right) \tag{4.25}$$

The design resistance of the T-stub is given by the formula (4.8). Tab. 4.1 and Tab. 4.2 indicate the values of l_{eff} for typical base plates in cases with and without contact. See Fig. 4.14 for the used symbols.

Tab. 4.1 The effective length l_{eff} of a T-stub with bolts inside the flanges (Wald et al, 2008)

Prying case	No prying case
$l_1 = 2\ \alpha\ m$ - (4 m - 1,25 e)	$l_1 = 2\ \alpha\ m$ - (4 m + 1,25 e)
$l_2 = 2\ \pi\ m$	$l_2 = 4\ \pi\ m$
$l_{eff,1} = \min\ (l_1; l_2)$	$l_{eff,1} = \min\ (l_1; l_2)$
$l_{eff,2} = l_1$	$l_{eff,2} = l_1$

Tab. 4.2 Effective length l_{eff} for bolts outside the flanges (Wald et al, 2008)

Prying case	No prying case
$l_1 = 4\ \alpha\ m_x + 1{,}25\ e_x$	$l_1 = 4\ \alpha\ m_x + 1.25\ e_x$
$l_2 = 2\ \pi\ m_x$	$l_2 = 2\ \pi\ m_x$
$l_3 = 0.5 b_p$	$l_3 = 0.5\ b_p$
$l_4 = 0.5\ w + 2\ m_x + 0.625\ e_x$	$l_4 = 0.5\ w + 2\ m_x + 0.625\ e_x$
$l_5 = e + 2\ m_x + 0.625\ e_x$	$l_5 = e + 2\ m_x + 0.625\ e_x$
$l_6 = \pi\ m_x + 2\ e$	$l_6 = 2\ \pi\ m_x + 4\ e$
$l_7 = \pi\ m_x + w$	$l_7 = 2\ (\pi\ m_x + w)$
$l_{eff,1} = \min\ (l_1 ; l_2 ; l_3 ; l_4 ; l_5 ; l_6 ; l_7)$	$l_{eff,1} = \min\ (l_1 ; l_2 ; l_3 ; l_4 ; l_5 ; l_6 ; l_7)$
$l_{eff,2} = \min\ (l_1 ; l_2 ; l_3 ; l_4 ; l_5)$	$l_{eff,2} = \min\ (l_1 ; l_2 ; l_3 ; l_4 ; l_5)$

4.1.3 Stiffness

The prediction of the base plate stiffness is based on (Steenhuis et al, 2008). The stiffness of the component analogous to the resistance of the T-stub is influenced by the contact of the base plate and the concrete foundation (Wald et al, 2008). The formula for deformation of the base plate loaded by the force in bolt F_b is

$$\delta_p = \frac{1}{2}\frac{F_b m^3}{3EI} = \frac{2F_b m^3}{E \cdot l_{eff} t^3} = \frac{2F_b}{E \cdot k_p} \tag{4.26}$$

and deformation of the bolt is

$$\delta_p = \frac{F_b L_b}{E_b A_b} = \frac{F_b}{E_b k_b} \tag{4.27}$$

The stiffness of the T-stub is written as

$$k_T = \frac{F_b}{E\left(\delta_p + \delta_b\right)} \tag{4.28}$$

In following conditions cases prying force are appearing in the T-stub

$$\frac{A_s}{L_b} \geq \frac{l_{eff,ini}\ t^3}{8.82\ m^3} \tag{4.29}$$

Formulas for stiffness coefficient of the base plate and of the bolt are

$$k_p = \frac{l_{eff,ini}\ t^3}{m^3} = \frac{0.85\ l_{eff} t^3}{m^3} \tag{4.30}$$

$$k_b = 1.6\frac{A_s}{L_b} \tag{4.31}$$

In case of no prying, it means when

$$\frac{A_s}{L_b} \leq \frac{l_{eff,ini}\ t^3}{8.82\ m^3} \tag{4.32}$$

Formulas are as following:

$$k_p = \frac{F_p}{E\ \delta_p} = \frac{l_{eff,ini}\ t^3}{2\ m^3} = \frac{0.425\ l_{eff}\ t^3}{m^3} \tag{4.33}$$

$$k_b = \frac{F_p}{E\delta_p} = 2.0\ \frac{A_s}{L_b} \tag{4.34}$$

The stiffness of the component of base plate in bending and bolts in tension is summarised from above simplified predictions as

$$\frac{1}{k_T} = \frac{1}{k_{b,i}} + \frac{1}{k_{p,i}} \tag{4.35}$$

For base plates are used the bolt pads under the bolt nut to help to cover the tolerances. The impact of an area of the bolt pad/nut changes the geometrical characteristics of T-stub. The influence is taken into account by the help of equivalent moment of inertia $I_{p,bp}$ and addition of stiffness k_w to the previous stiffness k_p. By practical design this influence is neglected for simplicity, see (Hofmann, 2005), even if it may be significant for resistance.

4.2 Threaded stud in tension

The threaded studs are efficient connectors welded by fabricator or on side with high level of automation, see (Metric studs 2009,2013 and Pitrakkos and Tizani, 2013) . The tension resistance of a threaded stud may be limited by

yielding resistance

$$N_{y,s} = n_a \, A_s \, f_{yk} \tag{4.36}$$

ultimate resistance

$$N_{u,s} = n_a \, A_s \, f_{uk} \tag{4.37}$$

initial stiffness

$$S_{i,s} = n_a \frac{E \, A_s}{l_{eff}} \tag{4.38}$$

where

n_a is the number of threaded studs in a row

A_s is the area in tension of one threaded stud

l_{eff} is the effective length of the threaded stud

f_{yk} is the yield stress of the threaded stud

f_{uk} is the ultimate stress of the threaded stud

This solution procedure is applied to the headed stud connection the anchor plate to concrete block.

4.3 Punching of the anchor plate

The anchor plate under the threaded stud or above the headed stud may reach its load capacity due to shear resistance

$$F_{ap,Rd} = \frac{A_{p1,eff} \cdot f_{y,k}}{\gamma_{M0}} \tag{4.39}$$

The stress area $A_{p1,eff}$ is determined from the thickness of the anchor plate t_{p1} and effective length $l_{v1,eff}$ of the sheared area

$$A_{ap,eff} = l_{v1,eff} \cdot t_{p1} \tag{4.40}$$

Due to high bending of the threaded stud under the large deformations of the thin plate is assumed the effective length of shear area as half of the circumference only

$$l_{v1,eff} = 2\pi \cdot \left(a_w + \frac{d_{ts}}{2}\right) \tag{4.41}$$

where

a_w is throat thickness of weld of threaded stud [mm]

d_{ts} is diameter of the headed/threaded stud [mm]

This failure is assumed at all places, where a stud loaded by tension force is welded directly to a steel plate. The endless stiffness of this component should be assumed in calculations as no visible significant deformation performs due to punching trough steel plate during loading.

4.4 Anchor plate in bending and tension

The anchor plate is designed as a thin steel plate located at the top of concrete block and loaded predominantly in compression and shear. By loading the column base by the bending or tension is the anchor plate exposed to the tensile force from the treaded studs. If the threaded studs are not located directly under the headed studs, which are embedded in concrete, the anchor plate is exposed to bending, see Fig. 2.15. After the plastic hinges of the T-stub are developed, the anchor plate between the plastic hinges is elongates by tensile force.

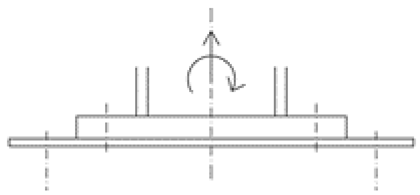

Base plate and anchor plate

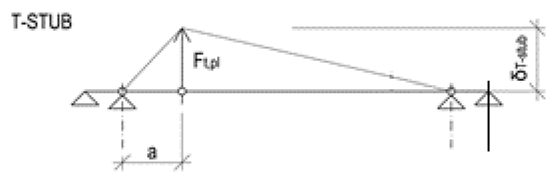

T stub plastic deformation under threaded stud

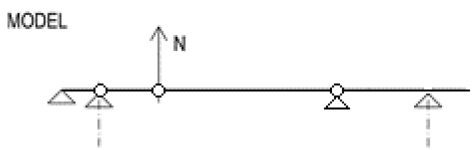

Plastic hinges at anchor plate

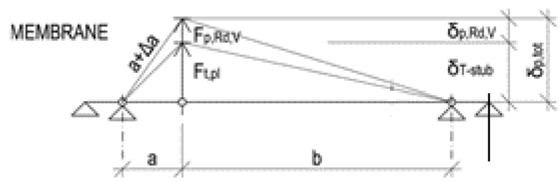

Anchor plate elongation under the threaded stud

Fig. 4.15 Model of the anchor plate in bending and tension

The resistance of the component, see (Kuhlman et al, 2012), is not restricted to plastic mechanism only. The deformed shape with the elongated anchored plate between the threaded and headed studs is caring the additional load and may be taken into account. The behaviour, till the plastic hinges are developed, is modelled as the based plate in bending with help of T stub model, see Chapter 3.4. The anchor plate in tension resistance is

$$F_{t,ap,Rd} = A_{ap,1} \cdot \frac{f_{yk}}{\gamma_{M0}} = t_{p1} \cdot b_{ap,eff} \cdot \frac{f_{yk}}{\gamma_{M0}} \tag{4.42}$$

where

t_{p1} is the thickness of the anchor plate

$b_{ap,eff} = n_1 \cdot (d_1 + 2 \cdot \sqrt{2} \cdot a_w)$ is the anchor plate effective width

a_w is throat thickness of weld of threaded stud

n_1 is the number of treaded studs

d_1 is the diameter of treaded stud

As the tensile force is developing in anchor plate the headed and threaded studs are exposed to horizontal force, see in Fig. 4.16. The elastic-plastic deformation at the stage of full plastification of the T stub is evaluated, see in Fig 4.17, by model of beam with four supports and three plastic hinges, see Fig. 4.15. The elongation of the anchor plate allows the uplift of the threaded stud. The model assumes that the supports, i.e. the headed and threaded studs, don't move in the horizontal direction and the headed stud in the vertical direction. E.g. the horizontal force depends linearly to the vertical one, see Fig. 4.18 and Fig. 4.19. The resulting horizontal force from tension in anchor plate is taken into account for evaluation of resistance of the components in shear and for the interaction of shear and tensile resistances.

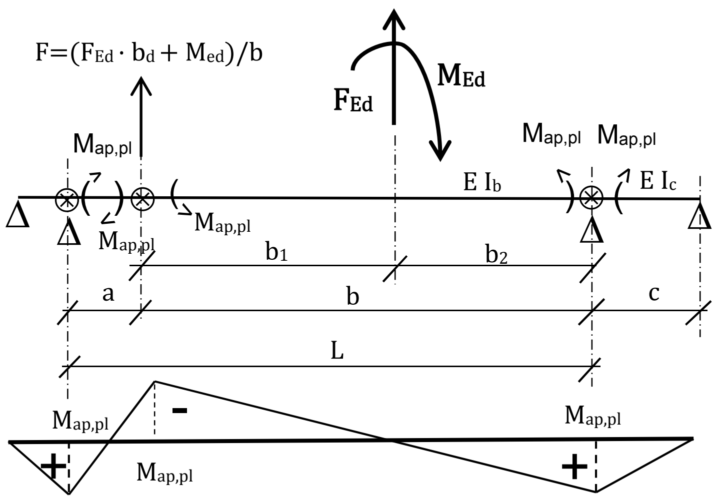

Fig. 4.16 Plastic hinges and bending moments in the anchor plate

In case of activation of the membrane action in anchor plate is verified the resistance of the related components in tension in vertical direction and in shear in horizontal direction. In the procedure is derived:

- the bending resistance of the anchor plate,
- the tensile resistance of the anchor plate,
- the bending and tensile deformation of the anchor plate.

and further is limited the resistance of the component anchor plate in bending and tension by

- the vertical resistance of the threaded stud (tensile and punching resistance) and the headed studs (tensile resistance, concrete cone failure, stirrups failure, bond failure).
- the horizontal resistance of the threaded stud (shear and bearing resistance) and the headed studs (shear and pry out resistance).

- the interaction in the threaded stud (tension and shear resistances) and the headed studs (tension and shear resistances).

The plastic resistance of the anchor plate is

$$M_{ap,pl} = \frac{l_{eff,1} \cdot t_{p1}^2}{4} \cdot \frac{f_{yk}}{\gamma_{M0}} \tag{4.43}$$

where

t_{p1} is thickness of the anchor plate [mm]

$l_{eff,1}$ is the effective width of the anchor plate [mm]

The effective width of the anchor plate is minimum of the

$$l_{eff,1} = \min \left\{ \begin{matrix} 4\ m_1 + 1.25\ e_{a1} \\ 2\,\pi\ m_1 \\ 5\ n_1\ d_1 \cdot 0.5 \\ 2\ m_1 + 0.625\ e_{a1} + 0.5\ p_1 \\ 2\ m_1\ + 0.625\ e_{a1} + e_{b1} \\ \pi\ m_1 + 2\ e_{b1} \\ \pi\ m_1 + p_1 \end{matrix} \right\} \tag{4.44}$$

where $5\ h_1\ d_1$is the effective width of the T stub between the headed and threaded studs.

The vertical deformation of the anchor plate under bending may be assumed for a beam with four supports and three plastic hinges as

$$\delta_T = \frac{1}{E\ I_b} \cdot \frac{1}{6} \cdot b^2 \cdot M_{ap,pl} + \frac{1}{E\ I_c} \cdot \frac{1}{3} \cdot b \cdot c \cdot M_{ap,pl} \tag{4.45a}$$

The elastic part of the deformation is

$$\delta_{T,el} = \frac{2}{3} \cdot \delta_T \tag{4.45b}$$

The elastic-plastic part of the deformation, see Fig. 4.17, is

$$\delta_{T,pl} = 2.22\ \delta_{T,el} \tag{4.45c}$$

The force at the bending resistance of the anchor plate is evaluated from equilibrium of internal forces

$$N_{pl} \cdot \delta_T \cdot \frac{b_2}{b} + M_{Ed} \cdot \frac{\delta_T}{b} = 2 \cdot M_{ap,pl} \cdot \frac{\delta_T}{a} + 2 \cdot M_{ap,pl} \cdot \frac{\delta_T}{b} \tag{4.45}$$

$$N_{pl} \cdot b_2 + M_{Ed} = 2 \cdot M_{ap,pl} \cdot b \cdot \left(\frac{1}{a} + \frac{1}{b}\right) \tag{4.46}$$

for $M_{Ed} = N_{Rd} \cdot e$

$$\text{is } N_{pl} \cdot b_2 + N_{Rd} \cdot e = 2 \cdot M_{ap,pl} \cdot b \cdot \left(\frac{1}{a} + \frac{1}{b}\right) \tag{4.47}$$

$$N_{pl} = 2 \cdot M_{ap,pl} \cdot b \cdot \frac{\left(\frac{1}{a} + \frac{1}{b}\right)}{(b_2 + e)} \tag{4.48}$$

The vertical resistance of the component anchor plate in tension is limited by the resistance of the components: threaded stud in tension, punching of the threaded stud and tensile resistance of the anchor plate. For the thin anchor plate is decisive the punching of the threaded stud. The deformed length of the anchor plate between the threaded and headed studs at the resistance in punching of the anchor plate under the threaded stud is

$$a_{ap} = a + \Delta a = a + \frac{a \cdot F_{ap,Rd}}{t_{p1} \cdot b_{ap,eff} \cdot E} \tag{4.49}$$

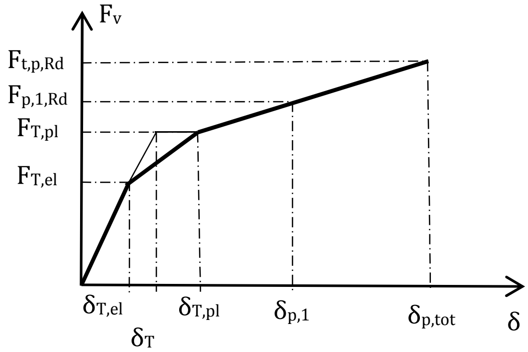

Fig. 4.17 Linear relation of acting vertical forces F_v and vertical deformation δ_v

The component of vertical deformation by the elongation of the anchor plate, see Fig. 4.14, is

$$\delta_{p,tot} = \delta_{T,pl} + \sqrt{a_{ap}^2 - a^2} \tag{4.50}$$

The component of the horizontal force at the resistance in punching of the anchor plate under the threaded stud, see Fig. 4.18, is

$$F_{p,Rd,H} = \frac{a}{\delta_{p,tot}} \cdot F_{t,p,Rd} \tag{4.51}$$

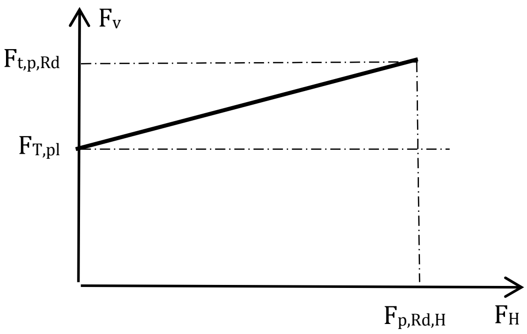

Fig. 4.18 Linear relation of vertical F_v and horizontal forces F_H

The horizontal force $F_{ap,v}$ is limited by shear resistance of the threaded and headed studs V_{Rd}, see in Figs 4.19. The resistance to vertical force is

$$F_{p,1,Rd} = F_{T,pl} + \frac{F_{t,p,Rd} - F_{T,pl}}{F_{p,Rd,H}} \cdot V_{Rd} \tag{4.52}$$

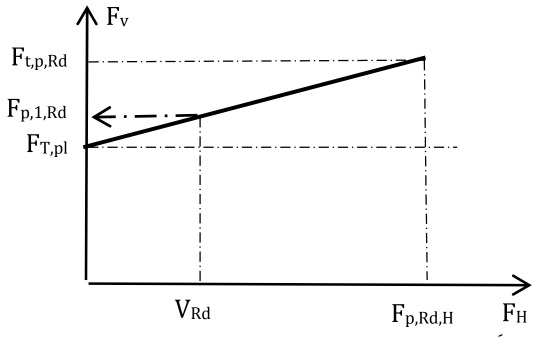

Fig. 4.19 Linear relation of vertical F_v and horizontal forces F_H at resistance

The interaction of the tensile and shear forces is verified for the threaded and headed studs, see Tab. 3.4 in EN1993-1-8:2006 by

$$\frac{F_{v,Ed}}{F_{v,Rd}} + \frac{F_{t,Ed}}{1.4 \cdot F_{t,Rd}} \leq 1 \tag{4.53}$$

The interaction of tensile and shear forces is verified for the headed stud anchoring to concrete, see Chapter 3.2.5 by

$$\left(\frac{F_{v,Ed}}{F_{v,Rd}}\right)^{\frac{3}{2}} + \left(\frac{F_{t,Ed}}{F_{t,Rd}}\right)^{\frac{3}{2}} \leq 1 \tag{4.54}$$

4.5 Column/beam flange and web in compression

The resistance of the column flange and web in compression may be expected as for the beam flange, see Chapter 6.2.6.7 in EN1993-1-8:2006. In this model the column/beam web has its full plastic resistance on the lever arm of column/beam flanges

$$F_{c,f,Rd} = \frac{M_{c,Rd}}{(h - t_f)} \tag{4.55}$$

in EN1993-1-8:2006 Eq. (4.1), where

$M_{c,Rd}$ is the design moment resistance of the beam cross-section, see EN1993-1-1:2004

h is the depth of the connected column/beam

t_f is the column/beam flange thickness

If the height of the column/beam including the haunch exceeds 600 mm the contribution of the beam web to the design compression resistance should be limited to 20%. If a beam is reinforced with haunches the proposal for design is in cl 6.2.6.7(2). The stiffness of this component in compression is expected to be negligible.

4.6 Steel contact plate

The resistance of the steel contact plate in joint may be taken as its full plastic resistance

$$F_{cp} = f_{y,cp}\, A_{cp} \tag{4.56}$$

where

$f_{y,cp}$ is the yield strength of the steel contact plate

A_{cp} is the effective area of the contact plate under compression

A height or breadth of the contact plate exceeds the corresponding dimension of the compression flange of the steel section, the effective dimension should be determined assuming dispersion at 45° through the contact plate. It should be assumed that the effective area of the contact plate in compression may be stressed to its design yield strength f_{yd}, see EN1994-1-1:2010. The stiffness of the component the steel contact plate is negligible

4.7 Anchor bolts in shear

In most cases the shear force is transmitted via friction between the base plate and the grout. The friction capacity depends on the compressive normal force between the base plate and the grout and the friction coefficient, see Chapter 3.3.7. At increasing horizontal displacement the shear force increases till it reaches the friction capacity. At that point the friction resistance stays constant with increasing displacements, while the load transfer through the anchor bolts increases further. Because the grout does not have sufficient strength to resist the bearing stresses between the bolts and the grout, considerable bending of the anchor bolts may occur, as is indicated in Fig. 4.20, see (Bouwman et al, 1989). The tests shows the bending deformation of the anchor bolts, the crumbling of the grout and the final cracking of the concrete. Based on the work (DeWolf and Sarisley, 1980) and (Nakashima,1998) and of tests (Bouwman et al, 1989) the analytical model for shear resistance of anchor bolts was derived in EN1993-1-8 cl 6.2.2, see (Gresnight at al, 2008). Also, the preload in the anchor bolts contributes to the friction resistance. However, because of its uncertainty, e.g. relaxation and interaction with the column normal force, it was decided to neglect this action in current standard.

Fig. 4.20 Test specimen loaded by shear force and tensile force

The design shear resistance $F_{v.Rd}$ may be derived as follows

$$F_{v,Rd} = F_{f,Rd} + n\, F_{vb,Rd} \tag{4.57}$$

where

$F_{f,Rd}$ is the design friction resistance between base plate and grout layer

$$F_{f.Rd} = C_{f,d}\ N_{c,Ed_{v,Rd}} \tag{4.58}$$

$C_{f,d}$ is the coefficient of friction between base plate and grout layer. The following values may be used for sand-cement mortar $C_{f,d}$ = 0.20, see Chapter 3.3.7.

$N_{c,Sd}$ is the design value of the normal compressive force in the column. If the normal force in the column is a tensile force $F_{f,Rd}$ = 0

n is the number of anchor bolts in the base plate

$F_{vb,Rd}$ is the smallest of $F_{1.vb.Rd}$ and $F_{2.vb.Rd}$

$F_{1.vb.Rd}$ is the shear resistance of the anchor bolt and

$$F_{2,vb,Rd} = \frac{\alpha_b\ f_{ub}\ A_s}{\gamma_{M2}} \tag{4.59}$$

A_s is the tensile stress area of the bolt or of the anchor bolt

α_{bc} is a coefficient depending on the yield strength f_{yb} the anchor bolt

$$\alpha_{bc} = 0.44 - 0.0003\ f_{yb} \tag{4.60}$$

f_{yb} is the nominal yield strength the anchor bolt

where 235 N/mm^2 ≤ f_{yb} ≤ 640 N/mm^2

γ_2 is the partial safety factor for anchor bolt

5 ASSEMBLY FOR RESISTANCE

5.1 Column base

5.1.1 Column base with base plate

The calculation of the column base resistance, based on the plastic force equilibrium on the base plate and applied in EN1993-1-8:2006, is described in (Wald et al, 2008). Based on the combination of acting load, see Fig. 5.1, three patterns may be distinguished:

<u>Pattern 1</u> <u>without tension in anchor bolts</u> occurs due to high normal force loading. The collapse of concrete appears before developing stresses in the tension part.

<u>Pattern 2</u> <u>with tension in one anchor bolt row</u> arises when the base plate is loaded by small normal force compared to the ultimate bearing capacity of concrete. During collapse the concrete bearing stress is not reached. The breaking down occurs because of yielding of the bolts or because of plastic mechanism in the base plate.

<u>Pattern 3</u> <u>with tension in both rows of anchor bolts</u> occurs when the base plate is loaded by tensile normal force. The stiffness is guided by yielding of the bolts or because of plastic mechanism in the base plate. This pattern occurs often in base plates designed for tensile force only and may lead to contact of baseplate to the concrete block.

The connection is loaded by axial force N_{Ed} and bending moment M_{Ed}, see Fig. 5.1. The position of the neutral axis is calculated according to the resistance of the tension part $F_{T,Rd}$. Then the bending resistance M_{Rd} is determined assuming a plastic distribution of the internal forces, see (Dewolf, Sarisley, 1980). For simplicity of the model, only the effective area is taken into account. The effective area A_{eff} under the base plate, which is taken as an active part of equivalent rigid plate, is calculated from an equivalent T-stub, with an effective width c, see Chapter 3.4.2. The compression force is assumed to act at the centre of the compressed part. The tensile force is located at the anchor bolts or in the middle when there are more rows or bolts, see (Thambiratnam, Paramasivam, 1986). Like for another cross sections of the composite structures there should be a closer look at the resistance for the ultimate limit state ULS and to the elastic behaviour under the serviceability limit state SLS. In the ultimate limit state the failure load of the system is important. Under service loads is checked the elastic behaviour and that the concrete cone will not fail. This would lead to cracks and with the time to a corrosion of the reinforcement of the concrete wall and finally to a failure of the construction.

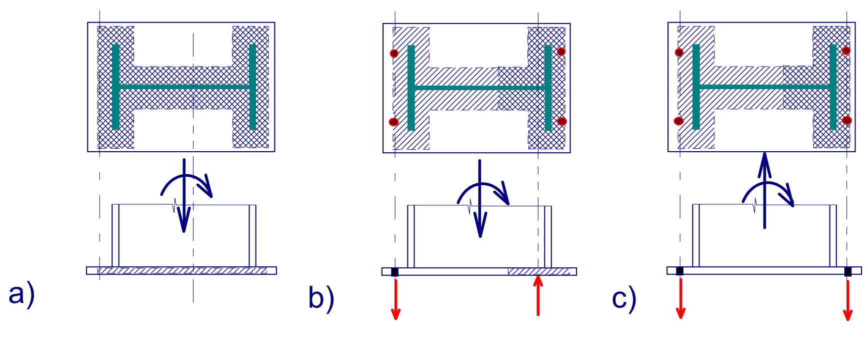

Fig. 5.1 The force equilibrium of the base plate a) no tension in anchor bolts, b) one row of the anchor bolts in tension, c) two rows of the anchor bolts in tension

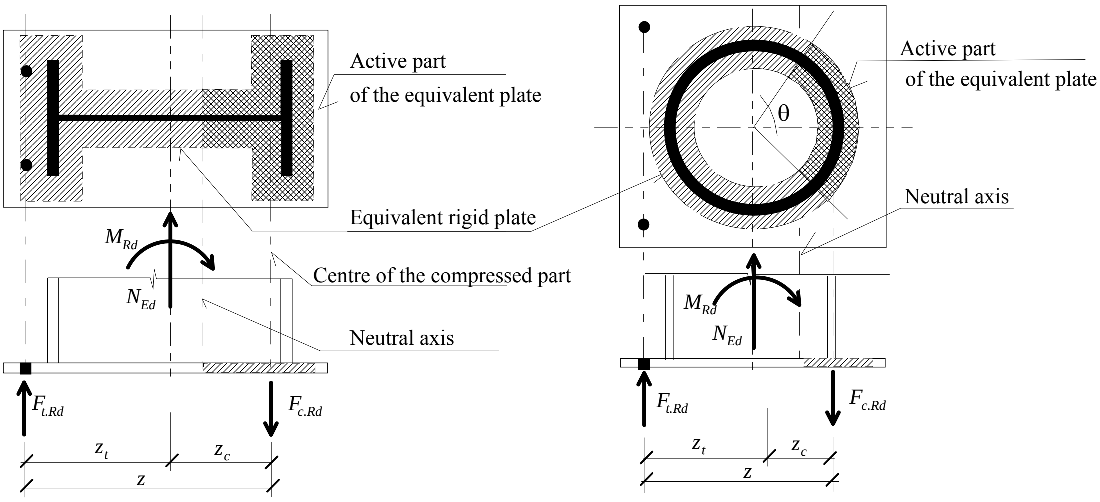

Fig. 5.2 Force equilibrium for the column base, one row of the anchor bolts in tension

The equilibrium of forces is calculated according to Fig. 5.2 as follows:

$$\mathrm{N_{Ed}} = \mathrm{F_{c,Rd}} + \mathrm{F_{t,Rd}} \tag{5.1}$$

$$\mathrm{M_{Rd}} = \mathrm{F_{c,Rd}} \cdot \mathrm{z_c} + \mathrm{F_{t,Rd}} \cdot \mathrm{z_t} \tag{5.2}$$

where

$$\mathrm{F_{c,rd}} = \mathrm{A_{eff}} \cdot \mathrm{f_{jd}} \tag{5.3}$$

$\mathrm{A_{eff}}$ is effective area under the base plate.

The resistance of the compressed part $\mathrm{F_{c,Rd}}$ and the resistance of the part in tension $\mathrm{F_{t,Rd}}$ are determined in previous Chapters. If the tensile force in the anchor bolts according to Fig. 5.2 occur for

$$\mathrm{e} = \frac{\mathrm{M_{Rd}}}{\mathrm{N_{Ed}}} \geq \mathrm{z_c} \tag{5.4}$$

formulas for tension and compressed part is derived

$$\frac{\mathrm{M_{Rd}}}{\mathrm{z}} - \frac{\mathrm{N_{Ed}} \cdot \mathrm{z_c}}{\mathrm{z}} \leq \mathrm{F_{c1,Rd}} \tag{5.5}$$

$$\frac{\mathrm{M_{Rd}}}{\mathrm{z}} + \frac{\mathrm{N_{Ed}} \cdot \mathrm{z_{c1}}}{\mathrm{z}} \leq \mathrm{F_{c,Rd}} \tag{5.6}$$

Then, the column base moment resistance $\mathrm{M_{Rd}}$ under a constant normal force $\mathrm{N_{Ed}}$ is expressed as follow:

with tension force in the anchor bolts

$$\mathrm{M_{Rd}} = \min\begin{cases}\mathrm{F_{t,Rd}} \cdot \mathrm{z} + \mathrm{N_{Ed}} \cdot \mathrm{z_c}\\ \mathrm{F_{c,Rd}} \cdot \mathrm{z} - \mathrm{N_{Ed}} \cdot \mathrm{z_t}\end{cases} \tag{5.7}$$

without tension force, both parts are compressed

$$M_{Rd} = \min \begin{cases} F_{c1,Rd} \cdot z + N_{Ed} \cdot z_c \\ F_{c,Rd} \cdot z - N_{Ed} \cdot z_{c1} \end{cases} \tag{5.8}$$

The procedure is derived for open section of I/H cross section. For rectangular hollow section RHS may be taken directly taking into account two webs. For circular/elliptical hollow sections CHS/EHS may be modified, see Fig. 5.2 and (Horová, 2011). Using sector coordinates depends the effective area $A_{eff} = 2\,\theta\,r\,c$ on the angle θ. The lever arm and the resistance of the component in compression is

$$z_c = r \cdot \cos\frac{\theta}{2} \tag{5.9}$$

$$F_{c,Rd} = F_{c1,Rd} = \pi \cdot r \cdot c \tag{5.10}$$

The resistance of the base plate connection under different loading is illustrated in M-N interaction diagram. In Fig. 5.3a there is an example of this diagram with its important points.

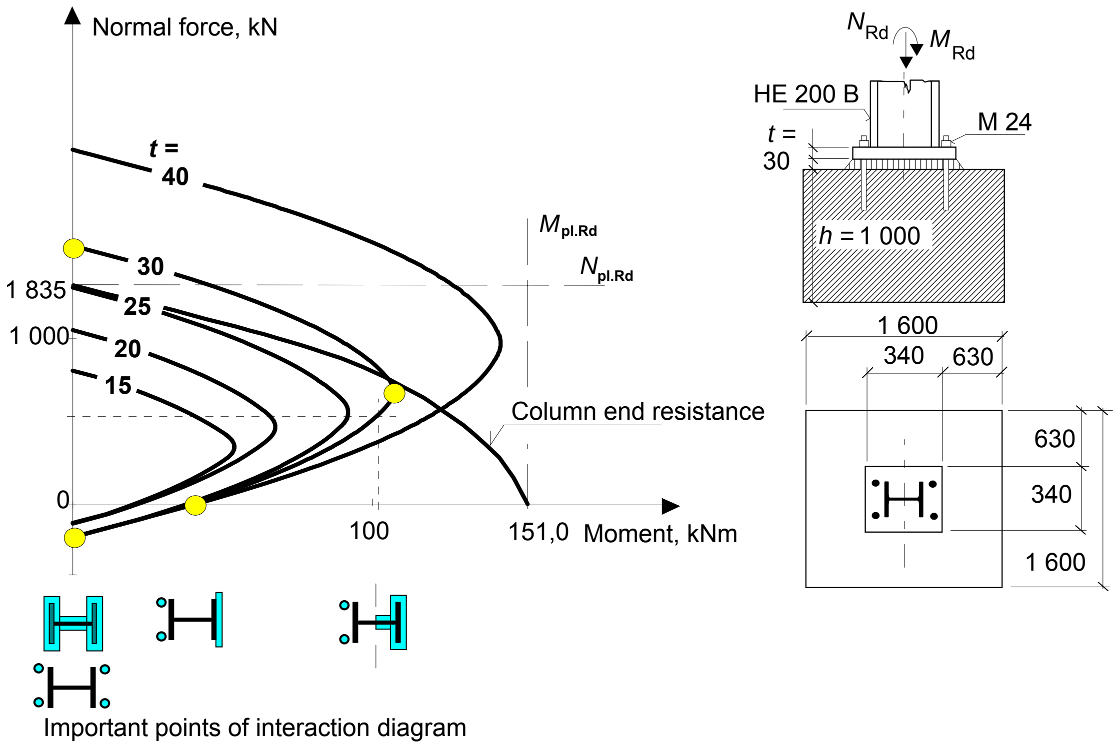

Fig. 5.3a An example of M-N interaction diagram for the base plate connection

5.1.2 Column base with anchor plate

The bending resistance of the base plate with anchor plate is assembled from the tensile/compression resistances of its component. The additional components to the column bases without the anchor plate is the anchor plate in bending and in tension. The procedure for evaluation of the resistance is the same in all connections loaded by bending moment and normal force.

First the resistance of the components in tension is evaluated: the base plate, the threaded studs, the anchor plate and the headed studs. The activated area in contact under the base and anchor plate is calculated from the equilibrium of internal forces for the tensile part resistance. From the known size of the contact area is calculated the lever arm and the bending resistance of the column base for particular acting normal force by the same procedure like for column base with the base plate only without the anchor plate.

During design of the base plate with the anchor plate is the elastic-plastic stage at serviceability limit verified separately, similar to the composite steel and concrete beam design. If the headed and threaded studs are not over each another the resistance of the base plate is influenced by the resistance of the component the anchor plate in tension and related components like punching of treated studs. The elastic-plastic resistance at Serviceability limit state is calculated based on the bending resistance of the anchor plate only. Moment rotational diagram at Fig. 5.4b sums up the behaviour of column base which is influenced by the elastic bending of the anchor plate (1), its elastic-plastic bending (2) and its tension (3).

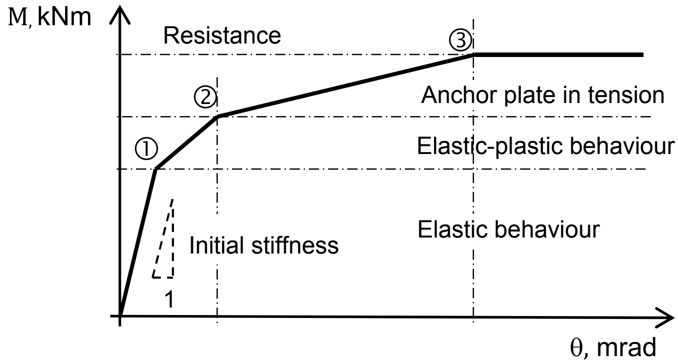

Fig. 5.3b Moment rotational diagram of column base with anchor plate

5.2 Simple steel to concrete joint

This joint typically represents a connection of a steel structure to a concrete wall. The anchor plate is loaded by shear load V_{Ed} and a bending moment$M_{y,Ed}$. The developed model assumes a stiff anchor plate and deformations due to the anchor plate are neglected. The connection between the girder and the anchor plate may be regarded as pinned, rigid or semi-rigid. For most structures the connection between the beam and the anchor plate may be assumed as pinned. In this case of a simple connection the anchor plate is only loaded by shear load and a corresponding bending moment caused by the eccentricity of the shear load. The connection between the girder and the anchor plate may be realised with butt straps or cams or any other simple connection, see Fig. 5.4.

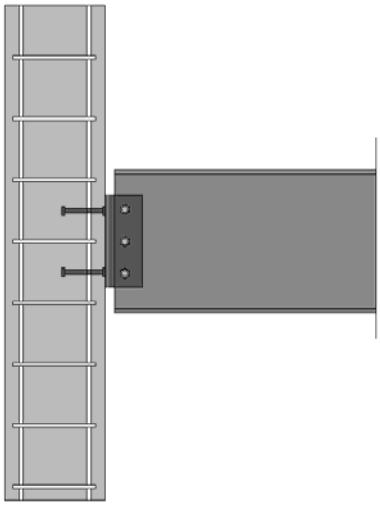

Fig. 5.4a Simple joint with butt straps

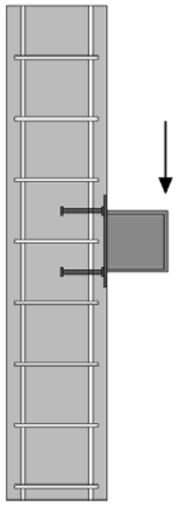

Fig. 5.4b Simple joint with cams

If the connection between the girder and the anchor plate cannot be assumed as pinned, there might be larger bending moments in the joint. In this Chapter the system described is a pinned connection between the beam and the anchor plate with an eccentricity e_v. However if there is a bending moment derived in the global analysis, the eccentricity e_v may be assumed no longer a purely geometrical value anymore but is calculated by

$$e_v = \frac{M_{y,Ed}}{V_{Ed}} \tag{5.11}$$

The developed component model describes the structural behaviour of the simple joints. The joints are consisting of an anchor plate with headed studs with and without additional reinforcement in cracked as well as non-cracked concrete. To prove a sufficient resistance for the ultimate limit state, the following steps have to be done:

- evaluation of the tension force caused by the shear load,
- verification of the geometry of the tension zone,
- evaluation of the tension resistance,
- evaluation of the shear resistance,
- verification of interaction conditions.

In the following the mechanical joint model for the simple joints is described. Due to the eccentricity of the applied shear load a moment is acting on the anchor plate. This moment causes forces, which are shown in Fig. 5.5. The anchor row on the non-loaded side of the anchor plate is in tension. This anchor row represents the tension component of the joint $N_{Ed,2}$ and forms a vertical equilibrium with the compression force C_{Ed} under the anchor plate on the loaded side. The shear forces are carried by the headed studs, $V_{Ed,1}$ and $V_{Ed,2}$, and the friction between steel and concrete V_f.

The tension component of the joint, which is represented by the headed studs in tension or headed studs with stirrups in tension, in the case of using additional reinforcement, is described in Chapter 3. If no additional reinforcement is used, the following failure modes may occur: steel failure of the shaft, pull-out failure of the headed stud due to the high compression of the stud head on the concrete and concrete cone failure of the anchorage. When using additional reinforcement however, the stirrups contribute to the deformation and the resistance of the tension component. Besides the steel failure and the pull-out failure of the headed studs, a concrete failure due to yielding of the stirrups, an anchorage failure of the stirrups and a smaller concrete cone failure may appear. A detailed description of these components is found in Chapter 3.

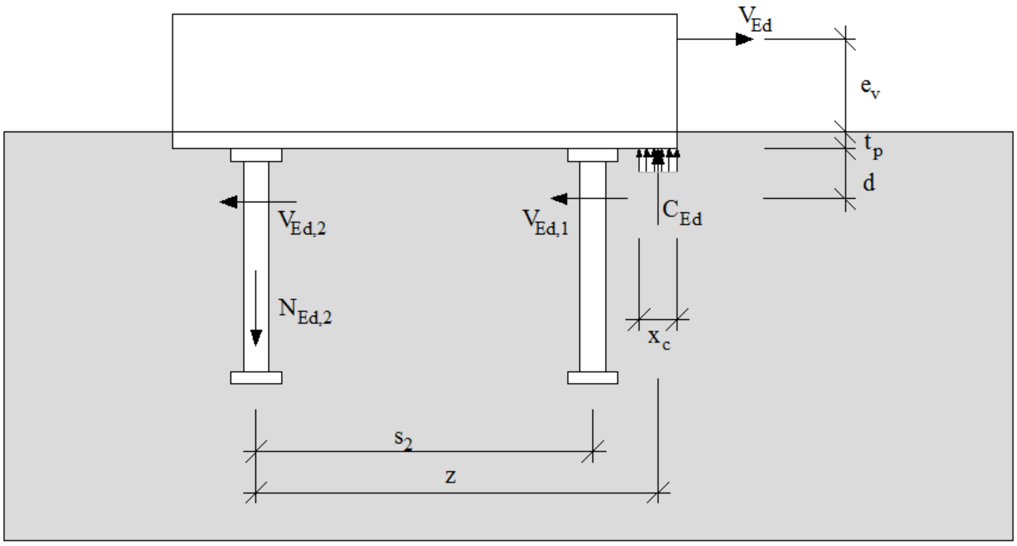

Fig. 5.5 Forces at the anchor plate caused by the shear force V_{Ed} and its eccentricity e_V

For the compression zone a rectangular stress block is assumed under the loaded side of the plate. The stresses in the concrete are limited according to EN1993 1-8 cl 6.2.5. The design bearing strength of the concrete is f_{jd}. When there is no grout and the anchor plate has a common geometry, f_{jd} may be assumed as $f_{jd} = 3f_{cd}$. The stress area A_c is given by the width of the anchor plate b and the length of the compression zone x_c perpendicular to the load, resulting from the equilibrium with the assumed tension force in the studs on the non-loaded side $N_{Ed,2}$. As the anchor plate is regarded as stiff, the compression zone starts at the edge of the plate. The stiffness of this component is assumed according to Chapter 3.

Equilibrium
$$\sum N: C_{Ed} = N_{Ed,2} \tag{5.12}$$

Compression force
$$C_{Ed} = f_{jd} \cdot x_c \cdot b \quad \text{for most cases } f_{jd} = 3\, f_{cd} \tag{5.13}$$

The position of the shear load $V_{Ed,1}$ and $V_{Ed,2}$ has been derived according to the stress distribution given by the results of numerical calculations. There it is seen that the resulting shear force is placed with a distance of about d in average from the anchor plate, when d is the diameter of the headed stud. As a simplification of the mechanical joint model it is assumed that the shear forces of both anchor rows appear in the same line, see Fig. 5.6. In case of a high tension in the first row of studs only small additional shear forces $V_{Ed,2}$ is applied the 2nd stud row. The position of the friction force V_f is assumed between the concrete surface and the anchor plate.

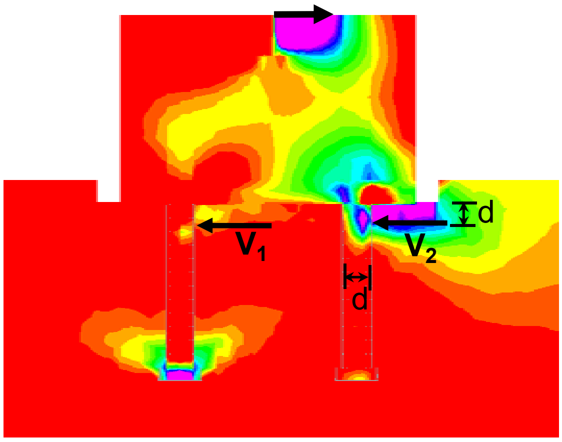

Fig. 5.6 Stress distribution σ_x in load direction

Forming the moment equilibrium according to (5.14), the size of the tension and the compression component of the joint is calculated. The rotational equilibrium is calculated for the point in the middle of the compression zone in one line with $V_{Ed,1}$ and $V_{Ed,2}$. The shear force is turning clockwise with a lever arm of $e_v + d + t_p$. The tension force $N_{Ed,2}$ is turning counter clockwise with a lever arm of z. The friction force is turning counter clockwise with a lever arm of d. The tension component carried by the second stud row $N_{Ed,2}$ is calculated with the following formula.

$$V_{Ed} \cdot (e_v + d + t_p) = N_{Ed,2} \cdot z + V_f \cdot d \tag{5.12}$$

$$N_{Ed,2} = \frac{V_{Ed} \cdot \left(e_v + d + t_p\right) - V_f \cdot d}{z} \tag{5.13}$$

If the pinned joint is loaded by diagonal pull, additional normal forces have to be considered in the moment equation, see Eq. (5.16). This equation requires, that the normal force does not lead to an uplift of the anchor plate. In this case both anchor rows would be subjected to tension forces and no shear resistance due to friction forces is carried by the pinned joint.

$$V_{Ed} \cdot \left(e_v + d + t_p\right) + N_{Ed} \cdot \left(z - \frac{s_2}{2}\right) = N_{Ed,2} \cdot z + V_f \cdot d \tag{5.14}$$

As already described above, the assumed tension load in the headed studs on the non-loaded side and the compression component form a vertical equilibrium. This approach requires an iterative process, as the area of the compression zone is dependent on the assumption for the tension load in the studs on the non-loaded side. But the shear resistance of the joint is not only limited by the acting moment. Therefore as a last step the resistance of the shear components have to be verified. The joint shear resistance is defined by the sum of the shear resistance of the studs and the friction between the concrete surface and the anchor plate, see Fig. 5.7 The resistance due to friction V_f is defined by the coefficient μ for friction between steel and concrete. In cl 6.2.2 of EN1993-1-8:2006 a friction coefficient of $\mu = 0.2$ is proposed. The stiffness is assumed as infinite, as the displacement is zero if the shear force is smaller than V_f.

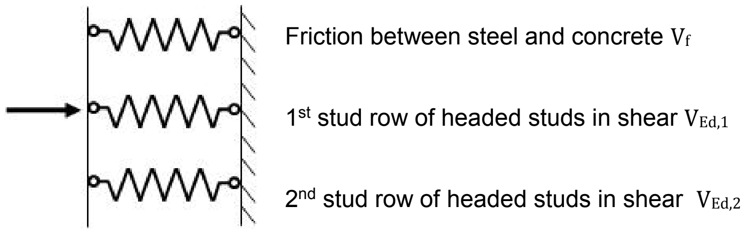

Fig. 5.7 Shear components

After subtracting the component of the friction force, the rest of the applied shear load has to be carried by the headed studs. The total shear resistance depends on two possible failure modes due to shear: Steel failure of the headed studs as well as Concrete cone failure respectively pry-out failure. Also the distribution of the shear load among the anchor rows depends on the failure mode. Furthermore interaction between tension and shear loads in the stud row on the non-loaded side of the anchor plate has to be considered resulting in a reduced resistance of these studs. In case of a steel failure of the headed studs, it is assumed that at ultimate limit state the front anchor row is subjected to 100% of its shear resistance, as there are acting no tensional forces. The remaining part of the shear load is carried by the back row of anchors, depending on the interaction conditions. In contrast when verifying the anchorage for concrete failure, the shear load is distributed half to the front and half to the back row of anchors. Thereby the interaction condition for concrete failure has to be considered. The following interaction conditions are used:

Concrete failure $$n_N^{3/2} + n_V^{3/2} \leq 1 \qquad (5.15)$$

Steel failure $$n_N^2 + n_V^2 \leq 1 \qquad (5.16)$$

where

n_N is the minimum value for $\frac{N_{Ed,i}}{N_{Rd,i}}$

n_V is the minimum value for $\frac{V_{Ed,i}}{V_{Rd,i}}$

<u>Additional verifications required</u>

In the preceding description not all verifications are covered. Additional checks, which are not described in this manual have to be done:

- Verification of the steel components connected to the anchor plate.
- Calculation of the anchor plate. The calculated tension and compression forces causes bending moments in the anchor plate. The anchor plate must be able to carry these bending moments. The anchor plate has to be stiff and therefore in the plate no yielding is allowed.
- Additional checks for the reinforcement in the concrete wall to prevent local failure of the concrete due to the compression force with have to be done, see EN19921-1:2004.
- The concrete wall must be able to carry the loads transferred by the anchor plate.

The verification of the design resistance of the joint is described in the Table 5.1 in a stepwise manner.

Tab. 5.1 Verification of the design resistance of the joint

<table>
<tr><th>Step</th><th>Description</th><th colspan="2">Formula</th></tr>
<tr><td colspan="4">The eccentricity e_v and the shear force V_{Ed} are known.</td></tr>
<tr><td>1</td><td>Evaluation of the tension force caused by the shear load
Estimation of x_c and calculation of the tension component $N_{Ed,2}$.</td><td colspan="2">z is depending on x_c
$$N_{Ed,2} = \frac{V_{Ed} \cdot (e_v + d + t_p) - V_f \cdot d}{z}$$</td></tr>
<tr><td>2</td><td>Verification of compression height.
Check if the assumption for x_c is OK.</td><td colspan="2">$$\sum N:\ C_{Ed} = N_{Ed,2} \qquad x_c = \frac{C_{Ed}}{b \cdot f_{jd}}$$
If x is estimated too small go back to Step 1 and try again.
For most cases $f_{jd} = 3\ f_{cd}$</td></tr>
<tr><td rowspan="2">3</td><td rowspan="2">Evaluation of the tension resistance
Calculation of $N_{Rd,u}$</td><td>Without Stirrups</td><td>With Stirrups</td></tr>
<tr><td>$$N_{Rd,u} = \min \begin{cases} N_{Rd,u,s} \\ N_{Rd,p} \\ N_{Rd,u,c} \end{cases}$$</td><td>$$N_{Rd,u} = \min \begin{cases} N_{Rd,u,s} \\ N_{Rd,p} \\ N_{Rd,cs} \\ N_{Rd,re,1} \\ N_{Rd,re,2} \end{cases}$$</td></tr>
<tr><td>4</td><td>Calculation of the shear resistance</td><td colspan="2">$$V_{Rd,s} = 0.7 \cdot N_{Rd,u,s}$$
$$V_{Rd,cp} = k\ \min[N_{Rd,cs}, N_{Rd,re,1}, N_{Rd,re,2}, N_{Rd,u,group}]$$</td></tr>
<tr><td rowspan="7">5</td><td rowspan="7">Verification of interaction conditions</td><td colspan="2">Possible failure modes</td></tr>
<tr><td>Steel failure
of the headed studs</td><td>Concrete failure</td></tr>
<tr><td>$$V_{Ed,2} = V_{Ed} - V_{Rd,s} - V_f$$</td><td>$$V_{Ed,2} = \frac{V_{Ed} - V_f}{2}$$</td></tr>
<tr><td>$$\left(\frac{N_{Ed,2}}{N_{Rd,u,s}}\right)^2 + \left(\frac{V_{Ed,2}}{V_{Rd,s}}\right)^2 \leq 1$$</td><td>$$\left(\frac{N_{Ed,2}}{N_{Rd,u}}\right)^{3/2} + \left(\frac{V_{Ed,2}}{V_{Rd,cp}}\right)^{3/2} \leq 1$$
$N_{Rd,u}$ is not including $N_{Rd,u,s}$</td></tr>
<tr><td colspan="2">Are both interaction equations OK?</td></tr>
<tr><td>YES</td><td>NO</td></tr>
<tr><td>Design calculation finished</td><td>The load carrying capacity of the joint is not sufficient. The joint has to be improved.</td></tr>
</table>

5.3 Moment resistant steel to concrete joint

A representative spring and rigid link model was idealized for the behaviour of composite beam to reinforced concrete wall joint, subjected to hogging bending moment, which is illustrated in Fig. 5.8. The joint components are:

- longitudinal steel reinforcement in the slab, at Fig. component 1
- slip oft he composite beam ,component 2;
- beam web and flange, component 3;
- steel contact plate, component 4;
- components activated in the anchor plate connection, components 5 to 10 and 13 to 15;
- the joint link, component 11.

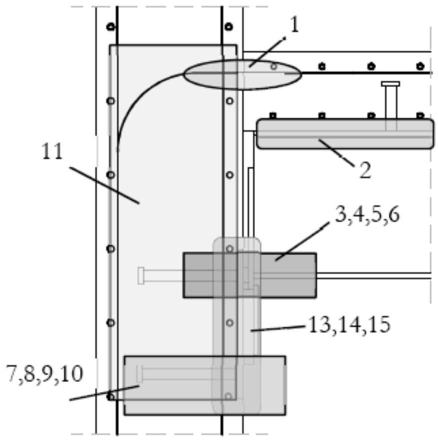

Fig. 5.8: Joint component model for the composite beam to reinforced concrete wall joint

In order to obtain the joint properties, the assembly of the components and of the joint models is described in the present section. For the joint under hogging bending moment, the assembly procedure was based on the mechanical model depicted in Fig. 5.8b. The determination of the joint properties to bending moment may be performed using a direct composition of deformations. The longitudinal steel reinforcement bar in slab, the slip of the composite beam, and the anchor plate components consider the models described in section 3. These models enable a good approximation to the real behaviour of the components, see (Henriques, 2008). The models may be described and composed also based on its stiffness coefficients as used in EN1993-1-8:2006.

The mechanical model represented in Fig. 5.9 presents only one row of components in tension and another in compression. This implies that the assembly procedure is much simpler, as no distribution of load is required amongst rows, as in steel/composite joint with two or more tension rows. Thus, the first step is the assembly of the components per row. Equivalent springs are defined per row, as represented in Fig. 5.9. The equivalent component/spring should perform as the group of components/springs it represents. The determination of its properties takes into consideration the relative position of the components: acting in series or in parallel. In the present case, either for the compression row either for the tension row, all joint components are acting in series. Thus, the determination of the properties of equivalent components/springs was performed as expressed in (5.17) for resistance $F_{eq,t}$ and $F_{eq,c}$, see (Henriques, 2008).

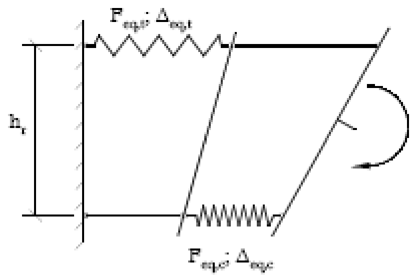

Fig. 5.9 Simplified joint model with assembly of components per row

$$F_{eq} = \min\{F_i \text{to} F_n\} \tag{5.17}$$

where, the indexes i to n represent all components to consider either in tension either in compression, depending on the row under consideration.

Then, because only one tension row and one compression row was considered, the determination of the joint properties, M_j, Φ_j, becomes relatively easy. In order to determine the joint rotation, it is important to define the lever arm h_r. According to the joint configuration, it was assumed that the lever arm is the distance between the centroid of the longitudinal steel reinforcement bar and the mid thickness of bottom flange of the steel beam. The centroid of steel contact plate is assumed to be aligned with this reference point of the steel beam. Accordingly, the joint properties are obtained as follows:

$$F_{eq} = \min\{F_{eq,t}, F_{eq,c}, F_{JL}\}\, h_r \tag{5.18}$$

where, $F_{eq,t}$and $F_{eq,c}$are the equivalent resistance of the tension and compression rows, respectively, determined using Eq. (5.17).

6 ASSEMBLY FOR STIFFNESS

6.1 Column base

6.1.1 Column base with base plate

The calculation of stiffness of the base plate, given in (Wald et al, 2008), is compatible with beam to column stiffness calculation. The difference between these two procedures is in the fact that by the base plate joint the normal force has to be introduced, see (Ermopoulos, Stamatopoulos, 1996). In Fig. 6.1 there is the stiffness model which shows a way of loading, compression area under the flange, allocating of forces under the base plate, and a position of the neutral axes.

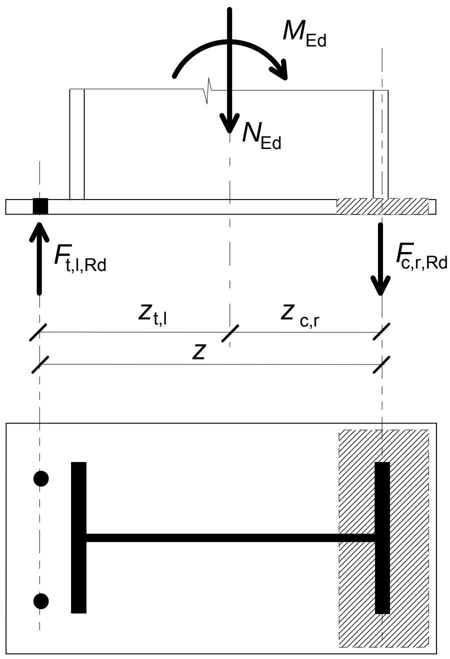

Fig. 6.1 The stiffness model of the base plate connection of the column base

By the calculation of the stiffness the effective area is only taken into account. The position of compression force $F_{c.Rd}$ is located at the centre of compression area. The tensile force $F_{t.Rd}$ is located at the anchor bolts. The rotational bending stiffness of the base plate is usually determined during proportional loading with constant eccentricity

$$e = \frac{M_{Ed}}{N_{Ed}} = \text{const.} \tag{6.1}$$

According to the eccentricity three possible basic collapse modes can arise with activation of anchor bolts, see (Wald et al, 2008). For large eccentricity with tension in one row of anchor bolts Pattern 1, see Fig. 6.2a, without tension in row of anchor bolts, small eccentricity, Pattern 2 in Fig. 6.2b, and with tension in both row of anchor bolts Pattern 3.

Pattern 1 with tension in one bolt row of anchor bolts arises when the base plate is loaded by small normal force compared to the ultimate bearing capacity of concrete. During collapse the concrete bearing stress is not reached. The breaking down occurs because of yielding of the bolts or because of plastic mechanism in the base plate.

Pattern 2 without tension in anchor bolts grows up during high normal force loading. The collapse of concrete appears before developing stresses in the tension part.

Pattern 3 with tension in one bolt row of anchor bolts arises when both bolt row of anchor bolts may be activated and column base is exposed to tension force in not so common, and the theorems may be derived similarly.

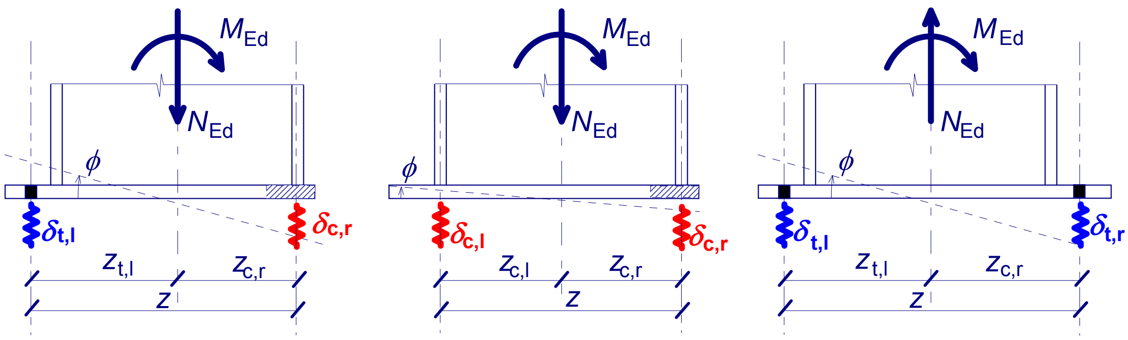

Fig. 6.2 The mechanical model of the base plate a) one anchor bolt row activated, b) no anchor bolt activated c) both anchor bolt rows activated

Deformations δ_t and δ_c of components depend on the stiffness of tension part k_t and the stiffness of the compression part k_c.

$$\delta_{t,l} = \frac{\frac{M_{Ed}}{z} - \frac{N_{Ed}\, z_t}{z}}{E\, k_t} = \frac{M_{Ed} - N_{Ed}\, z_t}{E\, z\, k_t} \tag{6.2}$$

$$\delta_{c,r} = \frac{\frac{M_{Ed}}{z} - \frac{N_{Ed}\, z_t}{z}}{E\, k_c} = \frac{M_{Ed} - N_{Ed}\, z_t}{E\, z\, k_c} \tag{6.3}$$

The rotation of the base plate could be determined from formulas above

$$\phi = \frac{\delta_{t,l} + \delta_{c,r}}{z} = \frac{1}{E\, z^2} \cdot \left(\frac{M_{Ed} - N_{Ed} \cdot z_c}{k_t} + \frac{M_{Ed} + N_{Ed} \cdot z_t}{k_c} \right) \tag{6.4}$$

From the rotation the initial stiffness is derived

$$S_{j,ini} = \frac{E\, z^2}{\frac{1}{k_c} + \frac{1}{k_t}} = \frac{E\, z^2}{\sum \frac{1}{k}} \tag{6.5}$$

Nonlinear part of the moment-rotation curve is given by coefficient μ, which express the ratio between the rotational stiffness in respect to the bending moment, see (Weynand et al, 1996) and EN1993-1-8:2006

$$\mu = \frac{S_{j,ini}}{S_j} = \left(\kappa\, \frac{M_{Ed}}{M_{Ed}} \right)^{\xi} \geq 1 \tag{6.6}$$

where

κ is coefficient introducing the beginning of non-linear part of curve, κ = 1.5

ξ is shape parameter of the curve, ξ = 2.7

The rotation stiffness is calculated as

$$S_j = \frac{E\,z^2}{\mu \sum \frac{1}{k}} \tag{6.7}$$

For above described components, the stiffness coefficients, showed in Fig. 6.3, is revised from bolt in tension k_b, base plate in bending k_p, and concrete in compression k_c.

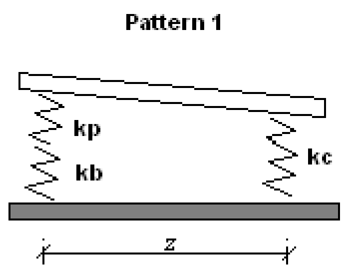

Fig. 6.3 The mechanical simulation with stiffness coefficients

As it is evident in Fig. 6.3, the stiffness of the tension part k_t consists of the stiffness of the base plate k_p and the stiffness of bolts k_b. With these parameters, S_j, μ, and M_{Rd}, we obtain the moment rotation curve, which is the best way how to describe behaviour of the base plate connection, see Fig. 6.4.

The procedure for evaluation of stiffens is derived for open section of I/H cross section. For rectangular hollow section RHS may be taken directly taking into account two webs. For circular/elliptical hollow sections CHS/EHS may be modified, see (Horová, 2011).

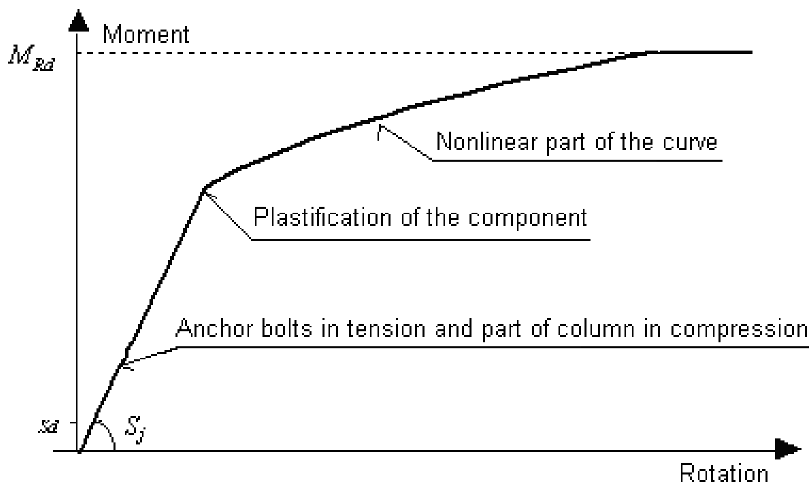

Fig. 6.4 Moment rotation curve for proportional loading

6.1.2 Column base with anchor plate

The bending stiffness of the base plate with anchor plate is assembled from the deformation stiffness's of its components, e.g. in the tensile part the base plate, the threaded studs, the anchor plate, and the headed studs and in the compressed part the concrete block in compression and base plate plus anchor plate in bending. The additional components are the anchor plate and treated studs. The deformation springs representing the individual components and its lever arms are summarized in Fig. 6.5. The effective stiffness coefficient, see Chapter 6.3 in EN1993-1-8:2005, is applied to transfer all deformational springs into the position of the threated stud.

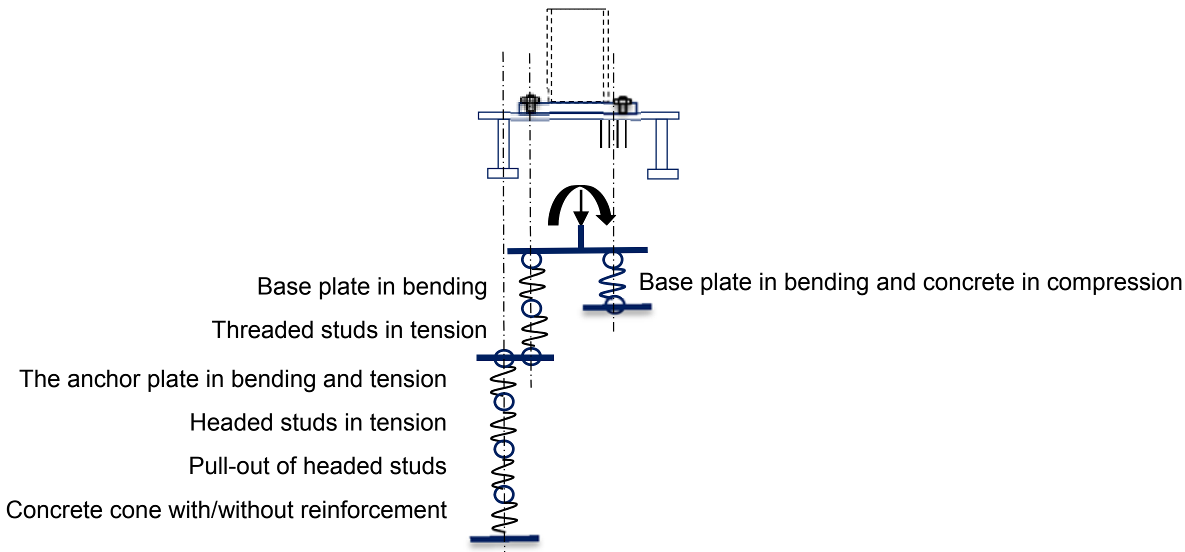

Fig. 6.5 Deformational springs representing in the model the components

6.2 Simple steel-to-concrete joint

The stiffness of the concrete components are not yet considered in the CEN/TS 1992-4-2 to calculate the deformation behaviour of the Simple joint. In the following the stiffness that have been developed within the INFASO project were applied to the Simple joint and from this the rotational stiffness of the joint is developed. A detailed description of this components may be found in Chapter 3. Thereby the rotational behaviour of the joint caused by the shear load V_{Ed} is calculated. It is assumed that in the case of a Simple joint the rotation does not influence the global analysis or the bending resistance of the joint to a high extend, see Fig. 6.6 and 6.7. The Simple joint is primarily a shear force connection and the rotation or the rotational stiffness of the joint is not relevant.

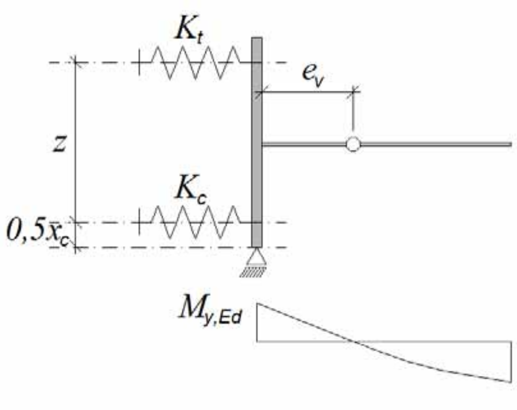

Fig. 6.6 Model for the global analysis of a simple joint between the beam and the anchor plate

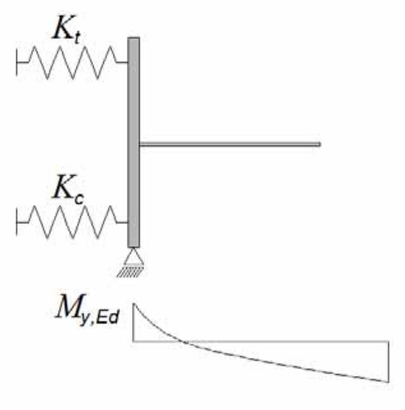

Fig. 6.7 Model for the global analysis of a rigid joint between the beam and the anchor plate

If the connection between the girder and the anchor plate cannot be assumed as pinned, there might be larger bending moments in the joint. In the following Chapters the system described is a simple connection between the beam and the anchor plate with an eccentricity e_v. However if there is a real bending moment derived in the global analysis, the eccentricity e_v may be assumed no longer a purely geometrical value anymore but is calculated by

$e_v = \frac{M_{y,Ed}}{V_{Ed}}$. In this case it is very important to determine the rotational stiffness of the joint because the rotational stiffness may influence the load distribution in the global analysis and the size of the bending moment of the joint, see Fig. 6.8. In order to model the rotational behaviour of the joint, at minimum two components are necessary, a tension component and a compression component. The tension component is represented by the headed stud in tension, see Chapter 3, and the compression component by the component concrete in compression. With these two components and the lever arm z and the rotational behaviour of the joint may be modelled.

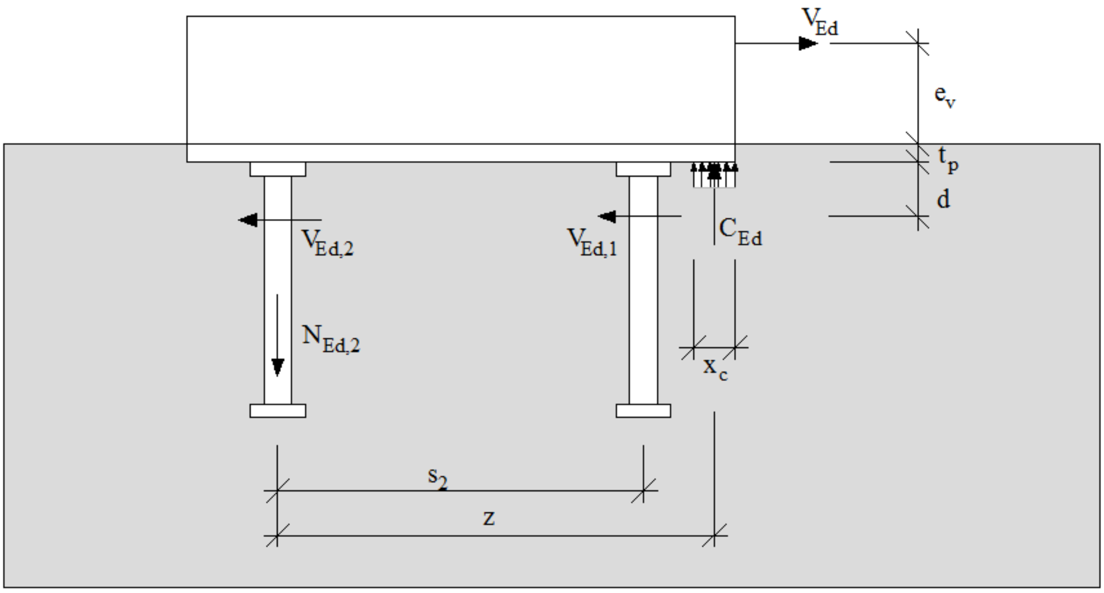

Fig. 6.8 Forces at the anchor plate caused by the shear force V_{Ed} and its eccentricity e_V

The shear load V_{Ed} causes a tension force $N_{Ed,2}$in the headed stud on the non-loaded side of the anchor plat. In equilibrium with the tension force there is a compression force C_{Ed}. For the equilibrium of moments and forces also see Chapter 3.

This forces are leading to a deformation δ_T caused by the tension force on the non-loaded side of the anchor plate and a deformation δ_C caused by the compression force on the loaded side of the anchor plate, see Fig. 6.. With these two deformation values and the lever arm z the rotation of the stiff anchor plate may be calculated according to the following formula

$$\varphi = \frac{\delta_T + \delta_C}{z} \tag{6.8}$$

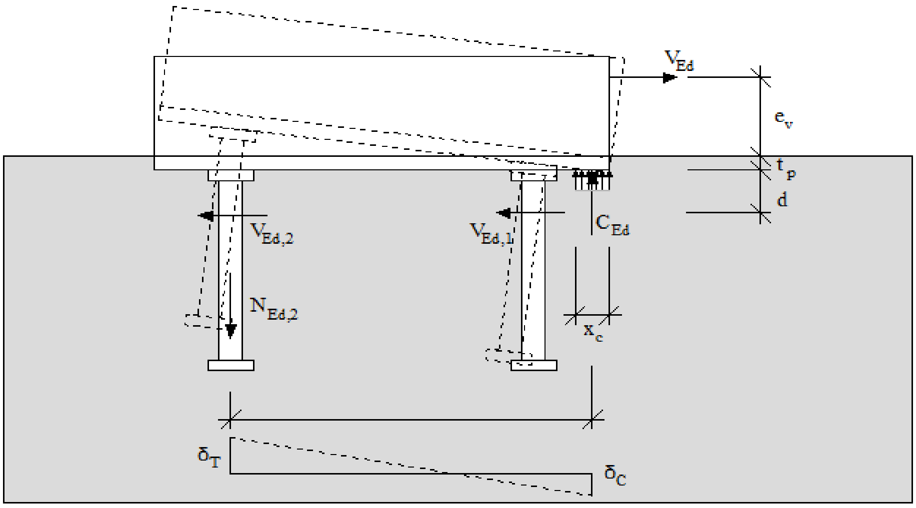

Fig. 6.9 Rotation of the anchor plate caused by the shear load V_{Ed}

In the following an overview over the tension and over the compression component is given.

<u>The tension component</u>

The tension component is described in detail in Chapter 3. For these components two alternatives exist, one with additional stirrups and one without, see Fig. 6.10. For every alternative a model including several springs has been developed.

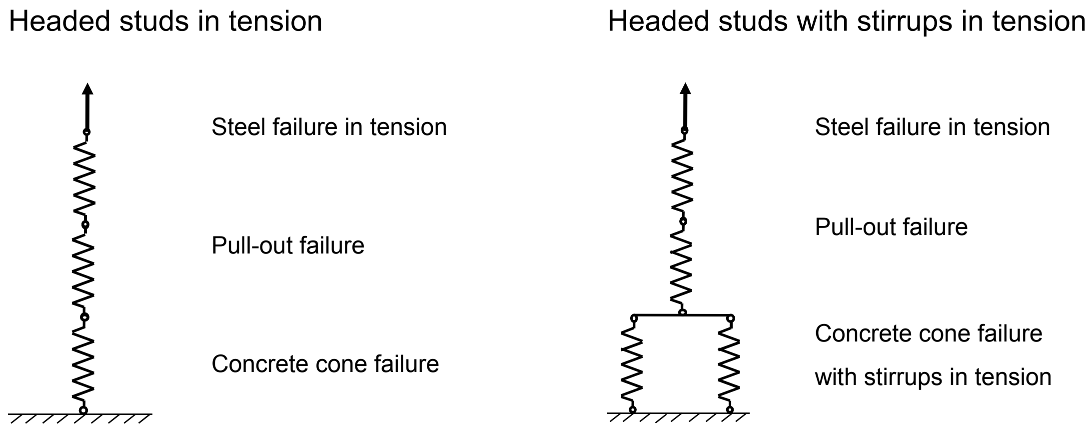

Fig. 6.10 Spring model for headed stud in tension, with and without stirrups

Depending on, whether additional reinforcement is used or not, the deformations of the headed studs are defined as follow:

Headed studs in tension

$\mathrm{N} = 0$ to $\mathrm{N} = \mathrm{N}_{u,c}$ and $\delta_1 = \delta_{p1} + \delta_h$ (6.9)

$\mathrm{N} = \mathrm{N}_{u,c}$ to $\mathrm{N} = 0$ and $\delta_2 = \delta_1(\mathrm{N}_{u,c}) + \dfrac{\mathrm{N} - \mathrm{N}_{u,c}}{k_c}$ (6.10)

Headed studs with stirrups in tension

$\mathrm{N} = 0$ to $\mathrm{N} = \mathrm{N}_{u,c}$ and $\delta_1 = \delta_{p1} + \delta_h$ (6.11)

$\mathrm{N} = \mathrm{N}_{\mathrm{u,c}}$ to $\mathrm{N} = \mathrm{N}_{\mathrm{u}}$ and $\delta_2 = \delta_{p2} + \delta_h + (\delta_c + \delta_s)$ (6.12)

$\mathrm{N} = \mathrm{N}_{\mathrm{u}}$ to $\mathrm{N} = 0$ and $\delta_3 = \delta_2(\mathrm{N_u}) + \dfrac{\mathrm{N} - \mathrm{N_u}}{\mathrm{k_c}} + \dfrac{\mathrm{N_u} - \mathrm{N}}{10\,000}$ (6.13)

In both cases it is necessary to ensure that neither yielding nor pull-out failure of the headed studs is the decisive failure mode. The load-displacement behaviour after of these failure modes are not considered in the equations above.

<u>The compression component</u>

For the compression force the spring stiffness may be calculated as follows:

$$\mathrm{K_c} = \frac{\mathrm{E_c} \cdot \sqrt{\mathrm{A_{eff}}}}{1.275} \tag{6.14}$$

The formula is taken from EN1993-1-8. The influence of the concrete stiffness is not very large on the rotational behaviour.

<u>Determination of the lever arm z</u>

Due to the equilibrium for each value of the shear load $\mathrm{V_{Ed}}$, a corresponding tension force $\mathrm{N_{Ed,2}}$ and the compression force $\mathrm{C_{Ed}}$ have to be calculated. As every value of $\mathrm{V_{Ed}}$ corresponds to a different compression force $\mathrm{C_{Ed}}$, there is also a different height of the compression area $\mathrm{x_c}$ and another corresponding lever arm z. For example if a small $\mathrm{V_{Ed}}$ causes a small $\mathrm{N_{Ed,2}}$ and $\mathrm{C_{Ed}}$, the height of the compression zone x_c is small and the lever arm z is relatively large. If the shear load is increased, the size of the compression force rises and the height of the compression area x_c also grows, whereas the lever arm z decreases.

The changing of the lever arm z is easily taken into account in a computer based calculation. For a calculation without computer a constant lever arm should be assumed. For the most structures the best solution to determine the lever arm is to calculate the maximum resistance of the tension load of the headed studs. Based on this value the maximum compression force and the minimum z may be calculated. Only if the anchor plate is extreme small and the tension resistance is extremely large the lever arm should be determined in a different way.

<u>The rotational stiffness</u>

Not only the rotation caused by the shear load, but also the rotational stiffness of the joint is calculated. With the help of the rotational stiffness it is possible to model the joint in the global analysis assuming his realistic behaviour. The initial rotational stiffness $\mathrm{S_{j,ini}}$ may be calculated according to EN1993-1-8. The following equation may be found in EN1993-1-8:2006, cl 6.3.1

$$\mathrm{S_{j,ini}} = \frac{\mathrm{z}^2}{\left(\frac{1}{\mathrm{K_T}} + \frac{1}{\mathrm{K_c}}\right)} \tag{6.15}$$

where

$\mathrm{K_T}$ is the stiffness of the tension component

$\mathrm{K_c}$ is the stiffness of the compression component

If no ductile behaviour is expected, the initial stiffness $\mathrm{S_{j,ini}}$ is assumed up to the maximum load. In the case of ductility the stiffness $\mathrm{S_j}$ of the joint is changed according to the utilization level of the joint. Therefore the behaviour of the joint is represented by a moment-rotation curve with a trilinear shape, see equation 6.17. The determination of the associated factor μ is taken from

EN1993-1-8. It has to be mentioned that in this case large cracks that are undesirable might occur.

$$S_j = S_{j,ini}/\mu \tag{6.16}$$

6.3 Moment resistant steel to concrete joint

For the joint under hogging bending moment, the assembly procedure was based on the mechanical model represented in Fig. 5.8a. The determination of the joint properties to bending moment is performed using two different approaches: the direct deformation superposition and model based on composition of stiffness coefficients by spring procedure.

The mechanical model represented in Fig. 5.8b presents only one row of components in tension and another in compression. The determination of the properties of equivalent components/springs was performed as expressed in (6.17), for deformation $\Delta_{eq,t}$ and $\Delta_{eq,c}$.

$$\Delta_{eq} = \sum_{i=1}^{n} \Delta_i \tag{6.17}$$

where, the index i to n represent all components to consider either in tension either in compression, depending on the row under consideration. In order to determine the joint rotation, it is important to define the lever arm h_r. Accordingly, the joint properties are obtained as follows

$$\phi_j = \frac{\Delta_{eq,t} + \Delta_{eq,c} + \Delta_{JL}}{h_r} \tag{6.18}$$

where

$\Delta_{eq,t}$ and $\Delta_{eq,c}$ are the equivalent deformation of the tension and compression rows, respectively, determined using (6.17).

7 GLOBAL ANALYSIS INCLUDING JOINT BEHAVIOUR

7.1 Structural analysis

The analysis of structures regarding the steel and composite joints modelling has been conventionally based on the concept of rigid, infinite rotational stiffness, or pinned, no rotational stiffness. However, it is well recognized that the real behaviour is often intermediate between these extreme situations, see (Jaspart, 2002). In these cases, the joints are designated as semi-rigid. In such joints, partial relative rotation between connected members is assumed, contrarily to the traditional concept of no or free rotation.

Consequently, the behaviour of the joint has a non-negligible influence on the structural analysis, see (Jaspart, 1997); and (Maquoi, Chabrolin, 1998) affecting: distribution of internal forces and deformations. In terms of resistance, the influence of the joint properties is obvious, as the structural capacity is limited if the joint is not fully capable of transmitting the internal forces, namely the bending moments. In such cases, the joint rotation capacity also becomes critical, defining the type of failure and the possibility to redistribute the internal forces. Thus, joints are keys parts of the structure, playing an important role in the behaviour of the structure. In what regards to the reinforced concrete joints, the structural analysis remains in the classical concept of rigid or pinned joints EN1992-1-1:2004. This is understandable due to the nature of the joints. In what concerns the steel-to-concrete joints, the joint behaviour is similar to steel joints. In this way, the effect of the steel-to-concrete joint on the structural behaviour should be considered as in steel structures.

With the component method (Jaspart, 1997), the real behaviour of the steel/composite joints may be efficiently evaluated and characterized in terms of rotational stiffness, bending moment resistance and rotation capacity. Subsequently, their behaviour is introduced in the structural analysis. This allows integrating the joint design with the structural design. Such type of analysis is recommended by the codes, EN1993-1-8:2006 and EN1994-1-1:2010, and should follow the subsequent steps:

- Characterization of the joint properties in terms of rotational stiffness, bending moment resistance and rotation capacity,
- Classification of the joint,
- Joint modelling on the structural model,
- Joint idealization.

The joint classification as already been introduced in section 2.2 and consists in determining the boundaries for the conventional type of joint modelling regarding the stiffness, see Fig. 2.6, and the resistance, see Fig. 2.7. The classification of the joint determines the type of joint modelling that should be adopted for the structural analysis. For stiffness classification, the stiffness of the connected beam is used to define the boundaries. In terms of resistance, the classification is set according to the minimum capacity of the connected members. In terms of rotation capacity, the information available is quite limited. In the code EN1993-1-8:2006 only a qualitative classification is given which consists in the following: i) ductile joints (suitable for plastic analysis) – ductile components govern the behaviour of the joint; ii) semi-ductile joints components with limited deformation capacity govern the joint response; iii) and brittle joints (do not allow redistribution of internal forces) - brittle components control the joint response.

Tab. 7.1 Criteria to define the boundaries
for classification of beam-to-column steel and composite joints

Stiffness	
Rigid/Semi-rigid	$8\ E\ I_b/L_b$
Semi-rigid/Pinned	$0.5\ E\ I_b/L_b$
Resistance	
Full-strength/Partial-strength	Top of column: min$\{M_{c,pl,Rd};\ M_{b,pl,Rd}\}$ Within column height: min$\{2M_{c,pl,Rd};\ M_{b,pl,Rd}\}$
Partial-strength/Pinned	25% of Full-strength/Partial-strength

In the structural analysis, according to the stiffness and strength classification, three types of joint modelling are possible, as listed in Tab. 7.2. In the case of continuous joint, the full rotation continuity is guaranteed between the connected members. In the case of simple joint, all rotational continuity is prevented between the connected members.

Otherwise, the joint is semi-continuous. In relation to the physical representation of the joint in the structural model, different approaches may be used, as illustrated in Tab. 7.2. In Fig. 7.1a the actual behaviour of the joint is modelled: L-springs $S_{r,L}$ representing the connecting zone and S-springs $S_{r,S}$ representing the panel zone. The infinite rigid stubs assure that the flexibility of the joint will not be taken into consideration more than once. In Fig. 7.1b is presented a model to be used in the software which does not support flexural springs. Stubs with adequate bending stiffness $E\,I$ and resistance M, maintaining the clear separation between bending and shear influences are used to replace rotational springs. Finally, the concentrated model is represented in Fig. 7.1c. In this model, L-springs and S-springs are assembled into one single spring and displaced to the column axis S_c. The overall joint behaviour is then represented by a single rotational spring, two in the case of double sided joints. This simplified modelling solution is prescribed by EN1993-1-8:2006. The simplifications adopted are compensated in the joint transformation. The joint transformation takes into account the shear force acting in the column, and the combination of the shear panel and connections in the joint spring at the beam-to-column axis intersection point, see (Huber et al, 1998).

Tab. 7.2 Criteria to define the boundaries for classification of beam-to-column steel and composite joints EN1993-1-8:2006

Joint modelling	Joint Classification
Continuous	Full-strength and Rigid
Semi-continuous	Full-strength and Semi-rigid Partial-strength and Rigid Partial-strength and Semi-rigid
Simple	Pinned and Pinned

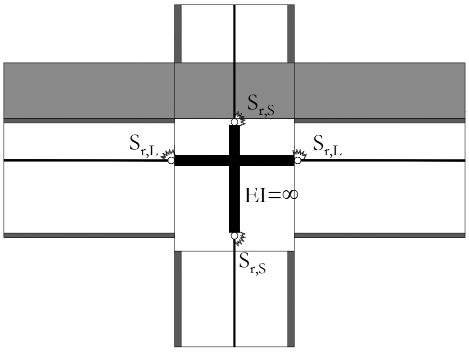

Fig. 7.1a Representation of joint by infinite rigid stubs

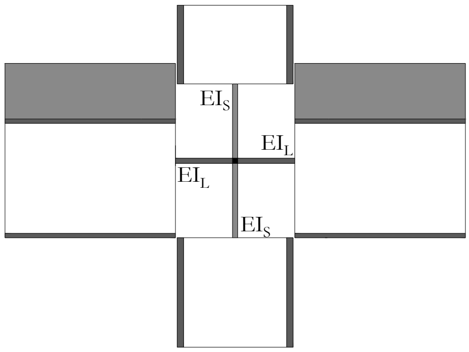

Fig. 7.1b Representation of joint by deformable stubs

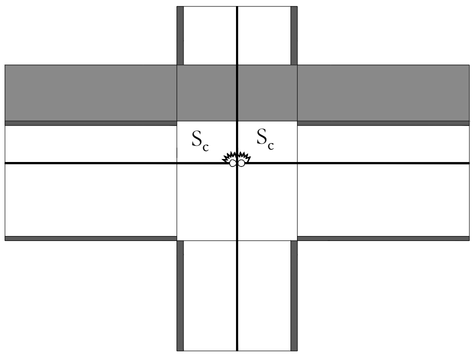

Fig. 7.1c Representation of joint by two rotational springs

The joint idealization consists in defining the type of flexural curve which will be attributed to the flexural spring representing the joint. The behaviour of the joints is typically nonlinear; however, its implementation in the flexural spring is not practical for everyday design. In this way, the behaviour of the joint may be simplified as schemed in Fig. 7.2. The selection of the appropriate curve depends on the type of analysis to perform: elastic, elastic-plastic, rigid-plastic. Accordingly the following behaviours may be assumed: i) linear elastic, Fig. 7.2a only requires rotational stiffness; ii) bi-linear or tri-linear elastic-plastic, Fig. 7.2b requires rotational stiffness, resistance and deformation capacity; iii) rigid plastic, Fig. 7.2c requires resistance and rotation capacity. In the case of semi-rigid joint, the joint rotational stiffness to be consider depends on the expected load on the joint, thus the following is considered: i) the acting bending moment is smaller than 2/3 of the joint bending moment resistance $M_{j,Rd}$ and the joint initial rotational stiffness $S_{j,ini}$ may be used; ii) in the other cases, the joint secant rotational stiffness S_j should be used. The latter is obtained dividing the joint initial stiffness $S_{j,ini}$ by the stiffness modification coefficient η. The codes EN1993-1-8:2006 and EN1994-1-1:2010 provide the stiffness modification coefficient to consider according to the type of connection.

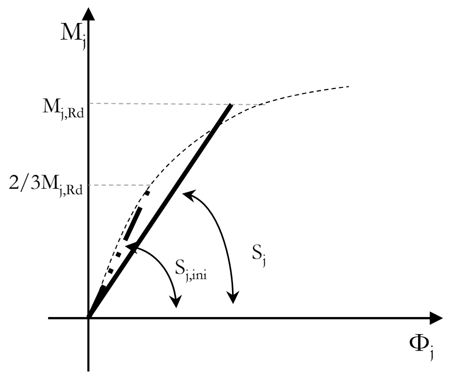

Fig. 7.2a Linear elastic M-Φ curve idealized for the joint behaviour

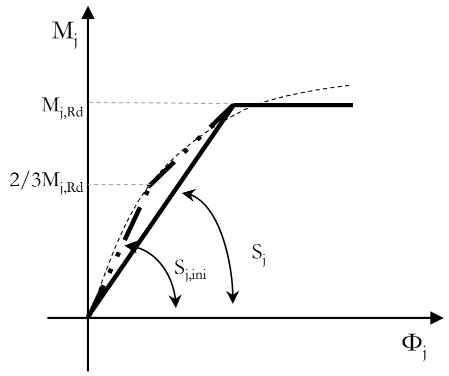

Fig. 7.2b Bi-linear and tri-linear elastic-plastic M-Φ curve idealized for the joint behaviour

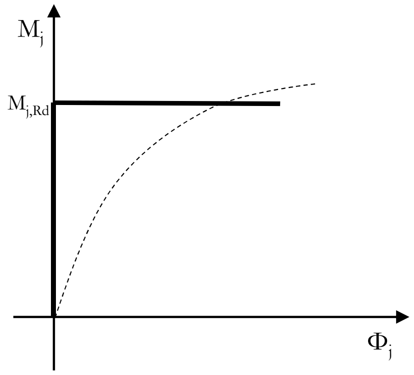

Fig. 7.2c Rigid plastic M-Φ curve idealized for the joint behaviour

The stiffness of a joint influences the deformability of the structure, which is reflected in the check for SLS. The influence of non-linear behaviour of joints in terms of ULS is more difficult to assess as it requires a non-linear analysis. The following example illustrates in a simplified way, the influence of joints in the behaviour of the structure. Considering the beam represented in Fig. 7.3, under a linear uniform load q and assuming rigid joints at both ends of the beam leads to the bending moment $M_{j,\infty}$ at both supports, and to the bending moment diagram represented by the dashed line. On the other hand, assuming at both ends of the beam a rotational stiffness of the joints S_j, then the bending diagram represented by the continuous line is obtained. This represents a bending moment re-distribution of ΔM that varies from 0 to $q\ L^2/12$. This re-distribution is also reflected in the vertical deflection of the beam, which may vary from $q\ L^4/(384\ EI)$ to $5\ q\ L^4/(384\ E\ I)$.

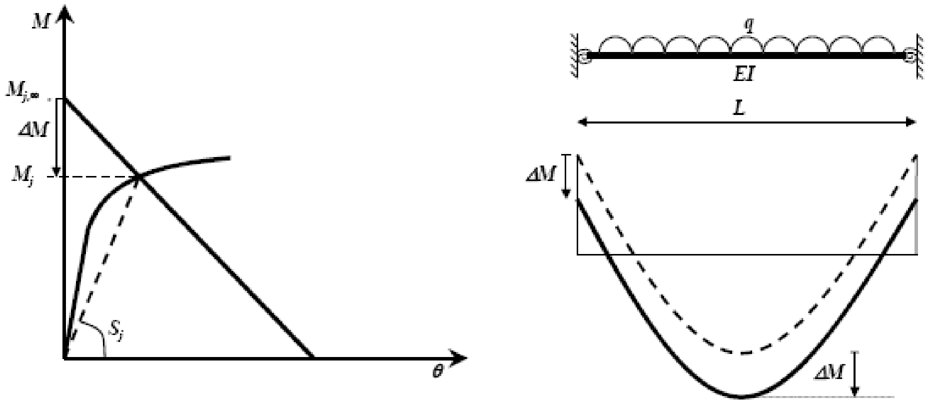

Fig. 7.3 Influence of a semi-rigid joint in the behaviour of the beam

The use of the concept of semi-rigid joints may has economic benefits, particularly in the optimization of moment connections. Possible savings due to semi-rigid design is 20 – 25 % in case of unbraced frames and 5 - 9 % in case of braced frames, see EN1990:2002.

7.2 Examples on the influence of joint behaviour

7.2.1 Reference building structures

In order to illustrate the influence of joint behaviour in the global analysis of structures, an example is provided in the following paragraphs. For complete details of the analysis see (Henriques, 2013). The building structures selected for the analysis considered two types of occupancy: office and car park. For the first type, the building structure erected in Cardington and subject to fire tests was chosen, see (Bravery 1993) and (Moore 1995). The building was designed to represent a typical multi-storey building for offices. For the car park building, the structure used in a recent RFCS project regarding Robustness in car park structures subject to a localized fire, see (Demonceau et al, 2012), was selected. Though the main characteristics of the reference building structures are used, modifications were performed whenever required to adapt the structures. Furthermore the performed calculations only considered the analysis of plane sub-structures which were extracted from the complete building structures. As higher variation of the structural system was found in the office building, two sub-structures were selected to represent this type of building while for the car park only one sub-structure was considered. The main characteristics and the adopted modifications of the referred building structures are summarized in the following paragraphs, see (Kuhlmann et al, 2012) and (Maquoi, 1998).

<u>The office building structure</u>

The main geometrical and mechanical properties of the office building are summarized in Tab. 3, together with the adopted modifications. The floor layout is illustrated in Fig. 7.4..

Tab. 7.3 The main properties and performed modifications of the reference structure representing the office building type

Reference Structure	Modifications
Nº of floors and height: 1 x 4.34 m + 7 x 4.14 m Nº of spans and length in longitudinal direction: 5 x 9 m Nº of spans in transversal direction: 2 x 6 m+1 x 9 m	No modifications
Columns: British steel profiles, grade S355, cross-section variation along height Beams: composite, British steel profiles + composite slab; grade S355 and grade S275; Lightweight concrete Bracing system: cross bracing flat steel	All British steel profiles were replaced by common European steel profiles with equivalent mechanical properties. Bracing systems were replaced by shear walls in order to introduce in the structural system, steel-to-concrete joints.
Beam-to-column joints: simple joints Column bases: continuous	The type of joint between horizontal members and vertical members was one of the key parameters of the study. The joint modelling was varied from continuous to simple. Column bases were assumed as simple joints.

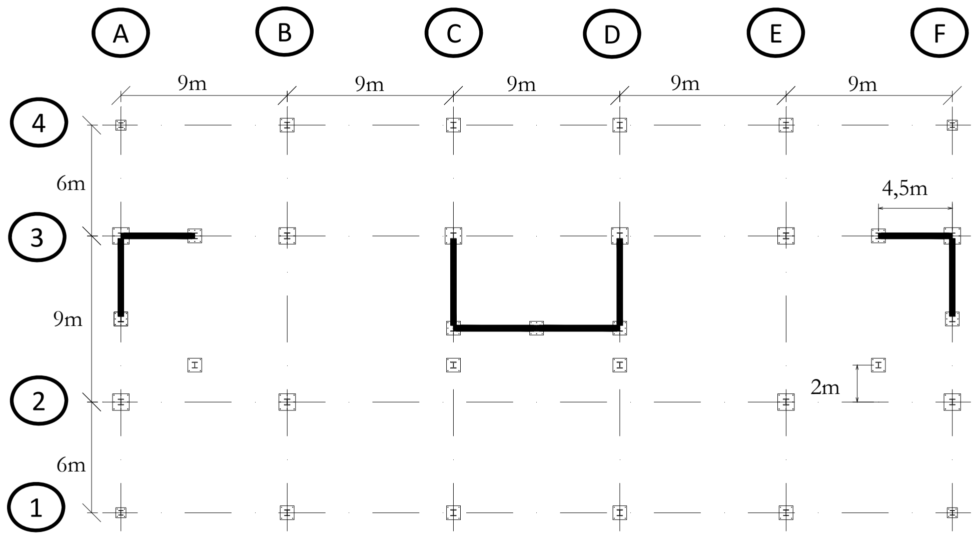

Fig. 7.4 Floor layout of the reference structure representing the office building type

The car park building structure

This type of building represents the standard configuration of a car park structure in Europe. The main geometrical and mechanical properties of this type of building are summarized in Tab. 7.4. In this case, only a few modifications were required. Fig. 7.5 illustrates the floor layout.

Tab. 7.4 The main properties and performed modifications for the car park building type

Reference structure	Modifications
Nº of floors and height: 8 x 3 m Nº of spans and length in longitudinal direction: 6 x 10 m Nº of spans in transversal direction: 10 x 16 m	No modifications
Columns: steel profiles, grade S460, cross-section variation along height Beams: composite (steel profiles + composite slab); grade S355; normal weight concrete Bracing system: concrete core (assumed but not defined)	Dimensions given to the concrete core
Beam-to-column joints: semi-continuous joints Column bases: simple joints	No modifications

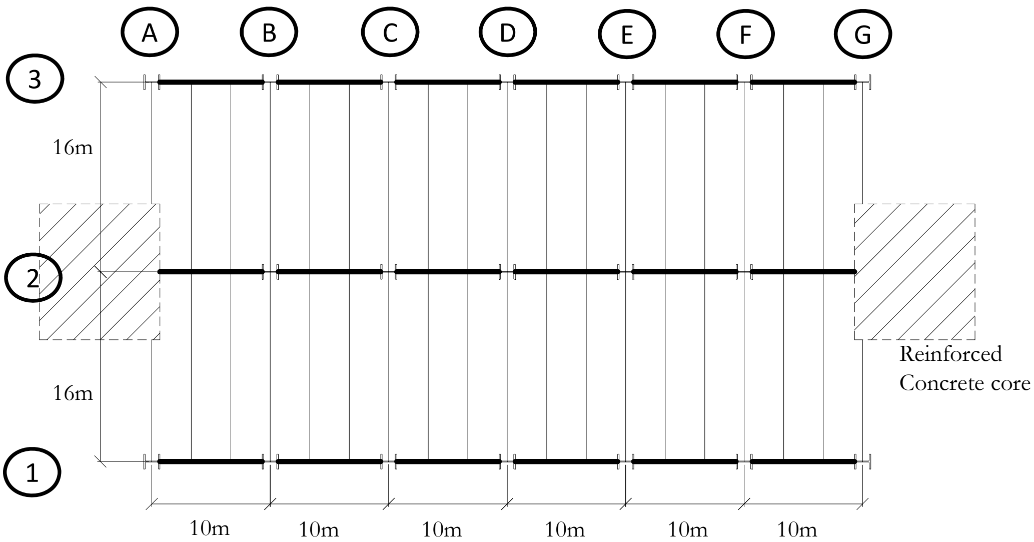

Fig. 7.5 Structural layout of the car park building type

7.2.2 Design

The structural calculations performed considered an elastic-plastic analysis. In all members and joints, except RC walls, plastic deformations were admissible. For sake of simplicity, the wall behaviour was always assumed elastic without limitation of capacity. However, it was considered that the steel-to-concrete joint includes the part of the wall surrounding the joint. Therefore, partially, hypothetic localized failure of the wall was considered. In terms of loading, two types of combinations were considered: i) Service Limit State; and ii) Ultimate Limit State.

In relation to the calculations, the strategy consisted in performing several numerical simulations where the beam-to-column and beam-to-wall joint properties were varied within the boundaries for joint classification. In addition, two cases considered the extreme situations of all joints either continuous or simple joints. For the other cases, the steel joints and steel-to-concrete joints are semi-continuous. In all calculations, the column bases joints were assumed simple. Tab. 7.5 lists the numerical simulations performed and identifies the joint properties considered in each case. Although the focus was on steel-to-concrete joints, steel joints were also considered to be semi-continuous so that the structural system was consistent.

The different cases presented in Tab. 7.5 considered the combination of different values of joint initial rotational stiffness and resistance capacity. In terms of rotation capacity, it was assumed that unlimited rotation capacity was available. A total of 10 cases were considered for each load combination.

Tab. 7.5 Definition of the cases for each load combination and each sub-structure

Case	**Initial Rotational Stiffness**			**Bending Moment Resistance**		
	Steel-to-concrete joint	**Steel joint**	**Col. bases**	**Steel-to-concrete joint**	**Steel joint**	**Col. bases**
1	R	R	P	FS	FS	P
2	R	SR: 0.5 (R/SR+SR/P)	P	FS	FS	P
3	SR: 2/3 (R/SR+SR/P)	SR: 0.5 (R/SR+SR/P)	P	FS	FS	P
4	SR: 1/3 (R/SR+SR/P)	SR: 0.5 (R/SR+SR/P)	P	FS	FS	P
5	SR: 2/3 (R/SR+SR/P)	SR: 0.5 (R/SR+SR/P)	P	PS: 2/3 (FS/PS+PS/P)	PS: 2/3 (FS/PS+PS/P)	P
6	SR: 1/3 (R/SR+SR/P)	SR: 0.5 (R/SR+SR/P)	P	PS: 2/3 (FS/PS+PS/P)	PS: 2/3 (FS/PS+PS/P)	P
7	SR: 2/3 (R/SR+SR/P)	SR: 0.5 (R/SR+SR/P)	P	PS: 1/3 (FS/PS+PS/P)	PS: 1/3(FS/PS+PS/P)	P
8	SR: 1/3 (R/SR+SR/P)	SR: 0.5 (R/SR+SR/P)	P	PS: 1/3 (FS/PS+PS/P)	PS: 1/3 (FS/PS+PS/P)	P
9	P	SR: 0.5 (R/SR+SR/P)	P	P	PS: 0.5 (FS/PS+PS/P)	P
10	P	P	P	P	P	P

R-Rigid; SR-Semi-rigid; P-Pinned; FS-Full-strength; PS-Partial-strength

7.2.3 Structural model

<u>Geometric and mechanical properties of members</u>

The three sub-structures selected for the structural calculations are illustrated in Fig. 7.6. The members' geometric dimensions and material properties are given in Tab. 7.6. For the bare steel cross-sections, the material behaviour was considered elastic-perfectly-plastic.

Tab. 7.6 Sub-structures members' geometric and material properties

Sub-structure	Members	Geometric	Material
I	Columns: AL-1 and 4	Bottom to 2nd floor: HEB320 2nd floor to Top: HEB260	S355 S355
	AL-2	Bottom to 2nd floor: HEB340 2nd floor to Top: HEB320	S355 S355
	Beams*	IPE360+Composite slab (h_{slab} = 130mm) #Φ6//200mm	S355 LC35/38
	Walls	t_w = 300mm vertical reinforcement Φ20//30cm horizontal Φ10//30cm	C30/37 S500
II	Columns	Bottom to 2nd floor: HEB 340 2nd floor to Top: HEB 320	S355 S355
	Beams*	IPE360+Composite slab (h_{slab} = 130mm) #Φ6//200mm	S355 LC35/38
	Walls	t_w = 300 mm vertical reinforcement Φ20//300 mm horizontal Φ10//300mm	C30/37 S500
III	Columns	Bottom to 2nd floor: HEB 550 2nd floor to 4th floor: HEB 400 4th floor to 6th floor: HEB 300 6th floor to 8th floor: HEB 220	S460 S460 S460 S460
	Beams*	IPE450+Composite slab (h_{slab} = 120 mm) #Φ8//200 mm	S355 C25/30
	Walls	t_w = 400 mm # Φ20//200 mm	C30/37 S500

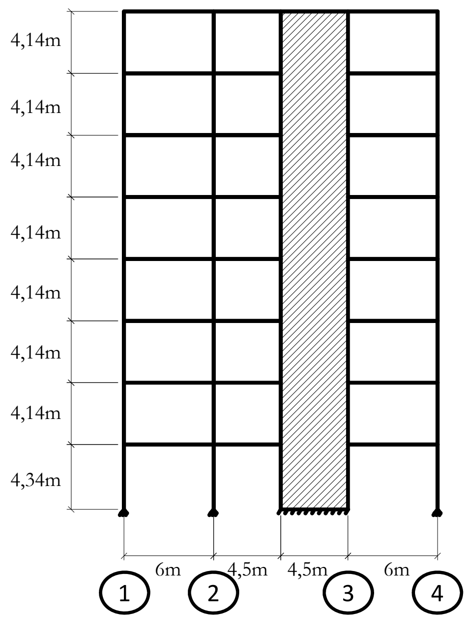

Fig. 7.6a Geometry of sub-structure I, office building alignment A

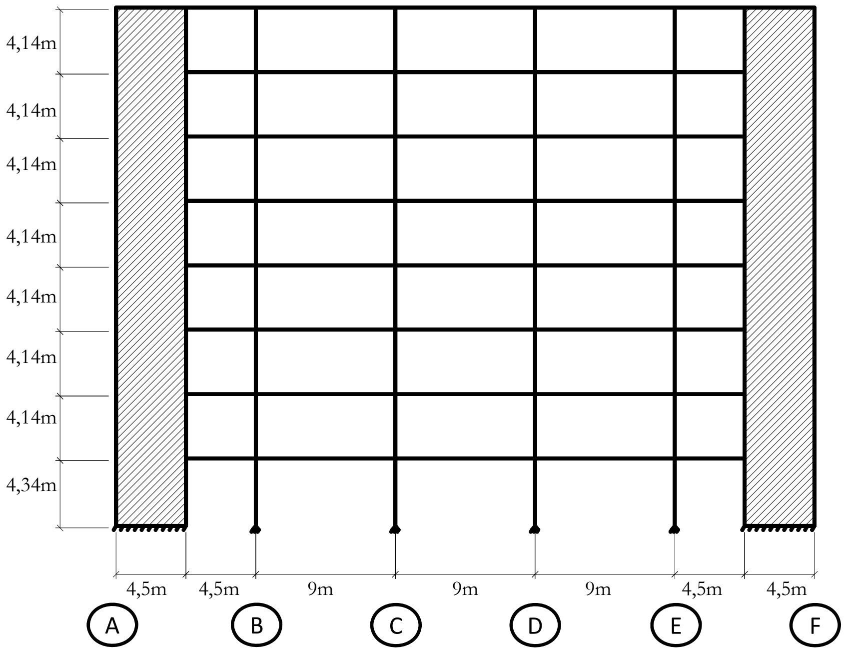

Fig. 7.6b Geometry of sub-structure II, Office building alignment 3

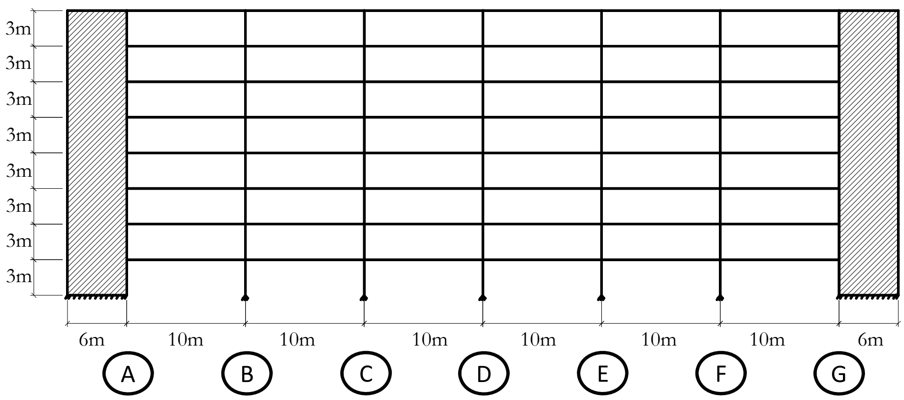

Fig. 7.6c Geometry of sub-structure III, car park building alignment 2

In order to simplify the structural modelling, the composite beams cross-section was replaced by equivalent rectangular cross-sections, see Table 7.7. Because of the different behaviour of the composite section under sagging and hogging bending moments, the equivalent beams cross-section (EqCS) varies within its length, as identified in Fig. 7.7. In terms of material properties, equivalent yield strength was also determined so that the equivalent cross-section attained a maximum bending moment equal to the resistance of the real composite cross-section.

Tab. 7.7 Properties of the equivalent cross-sections
replacing the real composite cross-sections

Sub-structure I				
Eq CS-1	Eq CS-2	Eq CS-3	Eq CS-4	Eq CS-5
$I=1.59\times10^8 mm^4$ $A=7034.56mm^2$	$I=3.885\times10^8 mm^4$ $A=14512.67mm^2$	$I=1.63\times10^8 mm^4$ $A=7087.57mm^2$	$I=5.4975\times10^8 mm^4$ $A=12633.20mm^2$	$I=1.58\times10^8 mm^4$ $A=7024.62mm^2$
Equivalent rectangular cross-section dimension				
h=520.08mm b=13.53mm	h=566.78mm b=25.61mm	h=525.23mm b=13.49mm	h=580.67mm b=21.76mm	h=519.09mm b=13.53mm
Yield strength (f_y) of the equivalent rectangular cross-section to obtain the maximum bending moment ($M_{cb.max}$) of the composite beam cross-section				
$M_{cb.max}$ =351.41kN.m f_y=576.30N/mm^2	$M_{cb.max}$ =605.00kN.m f_y=441.31N/mm^2	$M_{cb.max}$ =358.94kN.m f_y=578.52N/mm^2	$M_{cb.max}$ =565.00kN.m f_y=462.12N/mm^2	$M_{cb.max}$ =349.98kN.m f_y=575.88N/mm^2
Sub-structure II				
Eq CS-1	Eq CS-2	Eq CS-3	Eq CS-4	Eq CS-5
$I=1.14\times10^8 mm^4$ $A=6012.32mm^2$	$I=2.74\times10^8 mm^4$ $A=11207.20mm^2$	$I=1.20\times10^8 mm^4$ $A=6101.78mm^2$	$I=3.38\times10^8 mm^4$ $A=16431.90mm^2$	$I=1.23\times10^8 mm^4$ $A=6141.54mm^2$
Equivalent rectangular cross-section dimension				
h=476.37mm b=12.62mm	h= 541.42mm b= 20.70mm	h=486.39mm b= 12.54mm	h=496.74mm b= 33.08mm	h=490.57mm b= 12.52mm
f_y of the equivalent rectangular cross-section to obtain the M_{max} of the composite cross-section				
M_{max}=274.86kN.m f_y=575.81N/mm^2	M_{max}=470kN.m f_y=464.75N/mm^2	M_{max}=286.85kN.m f_y=579.90N/mm^2	M_{max}=631kN.m f_y=463.83N/mm^2	M_{max}=292.05kN.m f_y=581.62N/mm^2
Sub-structure III				
Eq CS-1	Eq CS-2	Eq CS-3		
$I=6.72\times10^8 mm^4$ $A=13192.32mm^2$	$I=1.42\times10^9 mm^4$ $A=27012.63mm^2$	$I=7.23\times10^8 mm^4$ $A=13600.91mm^2$		
Equivalent rectangular cross-section dimension				
h=781.66mm b=16.88mm	h=794.22mm b=34.01mm	h=798.44mm b=17.00mm		
f_y of the equivalent rectangular cross-section to obtain the M_{max} of the composite cross-section				
M_{max}=988.86kN.m f_y=575.37N/mm^2	M_{max}=1338.00kN.m f_y=374.20N/mm^2	M_{max}=1057.61kN.m f_y=584.00N/mm^2		

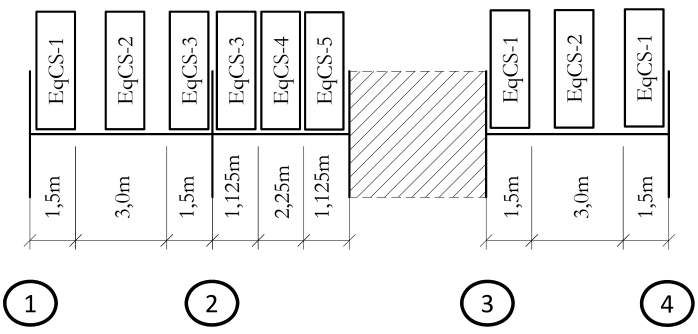

Fig. 7.7a Identification of the equivalent cross-sections of the beams in sub-structure I

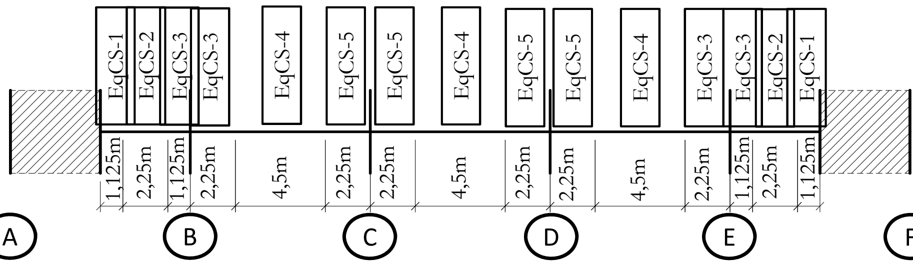

Fig. 7.7b Identification of the equivalent cross-sections of the beams in sub-structure II

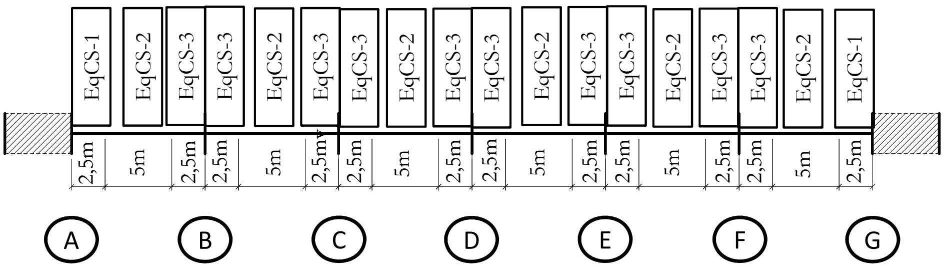

Fig. 7.7c Identification of the equivalent cross-sections of the beams in each sub-structure III

Joint properties

The boundaries values for classification of the joint in terms of rotational stiffness and resistance are listed in Tab. 7.8 for the three sub-structures. The joints were included in the structural models using concentrated flexural springs. For the partial-strength joints, a tri-linear behaviour was assigned, Fig. 7.8. The initial joint rotational stiffness is considered up to 2/3 of $M_{j,Rd}$, and then the joint rotation at $M_{j,Rd}$ is determined using the secant joint rotational stiffness. The latter is determined using a stiffness modification coefficient η equal to 2.

Tab. 7.8 The boundary values for classification of the joints in each sub-structure

	Joints	Rotational Stiffness		Bending Moment Resistance	
		R-SR [kNm/rad]	**SR-P** [kNm/rad]	**FS-PS** [kNm]	**PS-P** [kNm]
Sub-structure I	AL-1-right	108780.0	2782.5	351.4	87.9
	AL-2-left	108780.0	2782.5	358.9	89.7
	AL-2-right	205340.0	3710.0	358.9	89.7
	AL-3-left	205240.0	3710.0	345.0	87.5
	AL-3-right	108780.0	2782.5	351.4	85.9
	AL-4-left	108780.0	2782.5	351.4	87.9
Sub-structure II	AL-A-right	102293.3	2660.0	274.9	68.7
	AL-B-left	102293.3	2660.0	286.9	71.7
	AL-B-right	94640.0	2100.0	286.9	71.7
	AL-C-left to AL-D-right	94640.0	2100.0	292.1	73.0
	AL-E-left	94640.0	2100.0	286.9	71.7
	AL-E-right	102293.3	2660.0	286.9	71.7
	AL-F-left	102293.3	2660.0	274.9	68.7
Sub-structure III	AL-A-right	238560.0	7056.0	988.9	247.2
	AL-B-left	238560.0	7056.0	As below	As below
	AL-B-right to AL-F-left	238560.0	7591.5	b-6th: 1058.1 6th-T:380.4	b-6th: 264.3 6th-T: 95.1
	AL-F-right	238560.0	7056.0	As above	As above
	AL-G-left	238560.0	7056.0	988.9	247.2

R-Rigid; SR-Semi-rigid; P-Pinned; FS-Full-strength; PS-Partial-strength

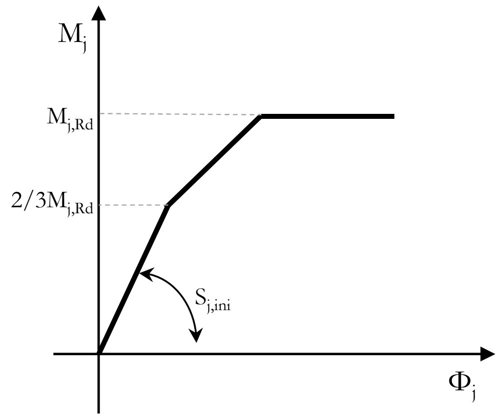

Fig. 7.8 Partial strength joint mechanical behaviour

Loading conditions

The loading considered in each sub-structure was determined for each load combination and varies with the structural conception and building occupancy. The loads and load combinations were defined according to EN1990:2002 and EN1991-1-1:2002. Note that for Sub-structure I and II, the wind action was also considered while for Sub-structure 3 no lateral action was assumed, this action was not quantified in (Demonceau et al, 2012) and it was considered that the stiffness of the wall will absorb it. In the office building structure, the slab works in the transverse direction, therefore the beams in the Sub-structure II are loaded with uniform distributed loads. For the other two sub-structures, the represented beams are the main beams so the loads are transmitted as concentrated loads, at the intersection of the secondary beams. In all cases the self-weight is considered.

Sub-structures finite element models

The structural calculations were performed in the finite element software (Abaqus 6.11, 2011). In Tab. 7.9 are listed the types of elements used to reproduce each component of the structural system (members and joints): i) beam elements for beams and columns, ii) shell/plate elements for the RC walls, and iii) spring elements to connect the structural members, in the different degrees of freedom.

Tab. 7.9 Types of finite elements attributed to each component, members and joints

Structural Model Component	**Type of finite element**	**Description**
Beams and Columns	Beam element	2-node linear beam element B31
Shear Walls	Shell element	4-node shell element S4R (general-purpose) with reduce integration and hourglass control
Beam-to-column and Beam-to-Wall Joints	Spring element	Non-linear spring element with single degree of freedom

The concentrated joint modelling was selected, where a flexural spring was used to represent the connection at each side of the column. As the parametric study was performed varying the properties of this flexural spring, it was assumed that this spring was already integrating the deformation of the column web panel and was already affected by the transformation parameter β, so that an iterative calculation was avoid. As the main goal is to analyse the influence of the joint and to obtain some structural requirements to the steel-to-concrete joints, the joint springs are located at the axis of the columns, and the eccentricity associated to the height of this member is neglected. . In what concerns the other degrees of freedom, namely axial and shear direction of the beam, translation springs are used to connect the members.

In this way, in each connection, between structural members, three springs are used, one for each relevant degree of freedom.

The use of the above described types of elements was previously validated against academic problems (Simoes da Silva et al, 2010). Simultaneously, the calibration of the required mesh refinement was performed. Tab. 7.10 summarizes the mesh refinement to consider in the different members of the structural models simulated and discussed in the next section.

Tab. 7.10 Summary of the mesh refinement for each member of the structural model

Member	Number of elements or mesh size
Beams	40
Columns	10
Shear walls	400 mm x 400 mm

The performed numerical calculations are two dimensional; therefore, no out-of-plane deformations occur. Both material and geometrical non-linearities are taken into account. Furthermore, the analysis neglects any possible in-plane buckling phenomena. The structural capacity is in this way only limited by the maximum resistance of the members and joints cross-sections. Finally, in what concerns to the simulation of the column loss, the procedure consisted in replacing the support of the relevant column by the reactions forces obtained in a previous calculation during the application of the real loading, and then to reduce them to zero.

7.2.4 Analysis and discussion for Service Limit State

The structure under service limit state (SLS) has to guarantee the comfort of the users. If in terms of loading this limit state is less demanding, in terms of deformation requirements it is often the most limiting state, and therefore, design guiding. For this load condition, the analysis of the steel-to-concrete joint properties is performed using the two following parameters: beams deflection and structure lateral deformation. For the latter, only Substructures I and II are considered, as no horizontal load (namely wind load) was considered in the analysis of Sub-structure III.

Fig. 7.10 illustrates how the beams deflection was considered. The maximum values obtained for each case are listed in Table 7.11, in a beam connected to a RC member, columns in grey, and in a beam only supported by steel columns. According to the Portuguese National Annex to EN1993-1-1:2006 the limit value $\delta_{max} = L/300$ was calculated and is included in the table. It is observed that in Sub-structures I and II, the values are distant from this limit, even if the beams deformation achieves 20 mm in the sub-structure II with simple joints, the value is still 33% below the limit. The beam deformations in sub-structure III are closer to the limit value but still, this value is not exceeded for any of the cases. In Fig. 7.11 are represented the beams deformations for the cases corresponding to the maximum and minimum deflections, for the beams implementing steel-to-concrete joints. These is seen as the envelope of the beams deformation, as these cases consider the two extreme situations in what respects the joint properties: i) continuous (Rigid + Full Strength); and ii) simple (Pinned). Using the beam deformation mode corresponding to the maximum beam deflection, the deformation corresponding to the code limit was extrapolated and is also included in the figure. The figure illustrates the above observations, confirming Substructure III closer to the limit.

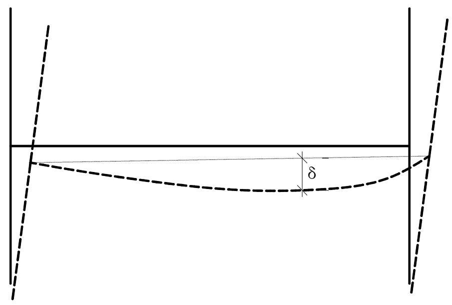

Fig. 7.9 Representation of the considered beams deflection

Tab. 7.11 Maximum beams deformation under service limit state [mm]

Case	Sub-structure I		Sub-structure II		Sub-structure III		Joint Properties	
	Beam 1-2	Beam 3-4	Beam C-D	Beam A-B	Beam C-D	Beam F-G		
1	2.6	3.0	5.5	0.3	21.7	7.7	R	FS
2	3.3	3.2	7.8	0.3	22.9	12.7		
3	3.3	3.5	7.8	0.4	23.4	12.6		
4	3.3	3.6	7.8	0.4	23.7	12.6		
5	3.3	3.5	7.8	0.4	23.7	14.1		
6	3.3	3.6	7.8	0.4	24.1	14.1	↓	↓
7	3.3	3.5	7.8	0.4	24.7	18.8		
8	3.3	3.6	7.8	0.4	25.2	18.8		
9	3.2	4.6	7.8	0.6	28.1	15.1		
10	6.1	6.1	20.5	1.5	31.8	27.1	P	P
δ_{max} [mm]	20	20	30	15	33.3	33.3		

R-Rigid; P-Pinned; FS-Full-strength

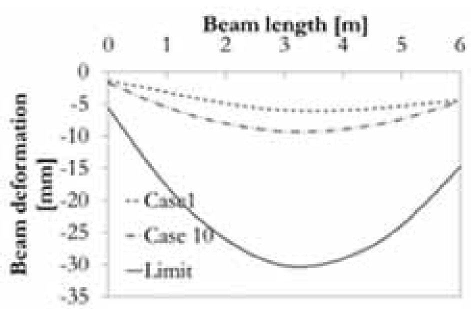

a) Sub-structure I

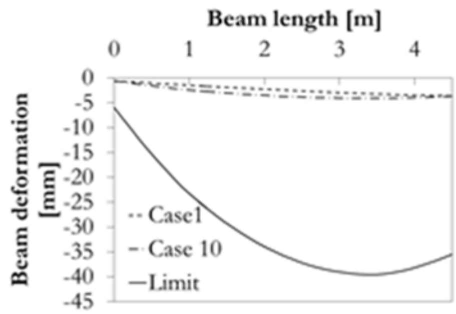

b) Sub-structure II

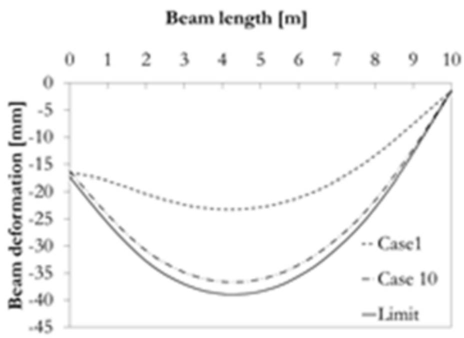

c) Sub-structure III

Fig. 7.10 Beam deformations envelop and limit according to PNA to EN1993-1-1:2006 supported by a steel-to-concrete joint

Besides the beams deformation, the lateral stiffness of the sub-structures is also affected by the joint properties. In Tab. 7.12 are listed the maximum top floor displacements obtained for each case and for Sub-structures I and II. The design limit $d_{h,top,limit}$ according to Portuguese National Annex to EN1993-1-1:2006 is also included. As for the beams deflections, it is observed that the observed values are distant from the code limit. Note that as long as the joints are continuous or semi-continuous, the top floor displacement suffers small variations. This is due to the dominant contribution of the RC wall to the lateral stiffness of the sub-structures. In Fig. 7.11 are represented the sub-structures lateral displacement envelops and the code limit. In Sub-structure II, because two RC walls contribute to the lateral stiffness of the sub-structure, the variation between minimum and maximum is quite reduced.

Tab. 7.12 Top floor lateral displacement for Sub-structures I and II [mm]

Case	Sub-structure I	Sub-structure II	Joint Properties	
1	26.7	13.5	R	FS
2	27,6	14.0		
3	28.3	14.1		
4	28.6	14.2		
5	28.3	14.1		
6	28.6	14.2	↓	↓
7	28.3	14.1		
8	28.6	14.2		
9	31.4	14.8		
10	36.0	16.2		
$d_{h.top.limit}$ [mm]	94.3	94.3	P	P

R-Rigid; P-Pinned; FS-Full-strength

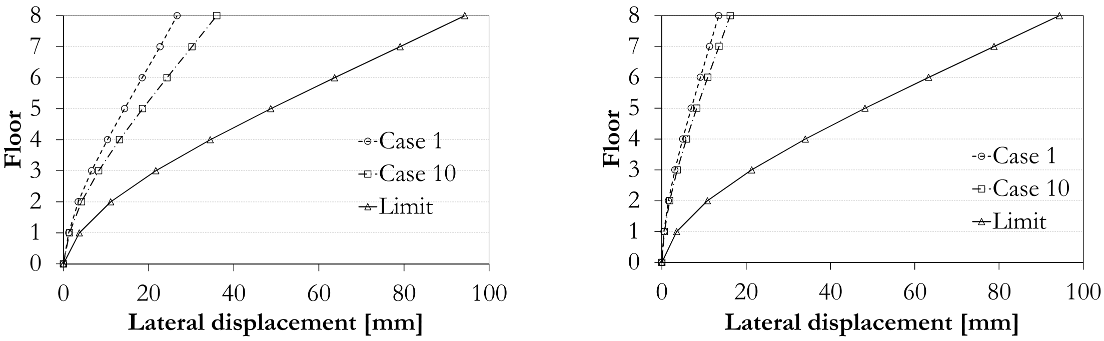

Sub-structure I Sub-structure II

Fig. 7.11 Lateral displacements envelops

In what concerns the steel-to-concrete joints, under service limit state, the bending moment developed in the joints and the required joint rotation are represented in Fig. 7.12. In Fig. 7.13 the ratio between the bending moment developed in the joints and the joint or beam bending moment capacity is represented. For none of the cases, the joints under SLS attained the maximum bending moment resistance of the joint. As for the deformations, Sub-structure III is the most demanding to the joints. In case 7, almost 70% of the joint bending moment capacity is activated. Because the assumed joint resistance is lower, in case 7 and 8 the percentage of bending moment activated is higher. In Fig. 7.13 is shown the maximum joint rotations observed for each sub-structure and for each case. For the cases where the joints are modelled as pinned, the joint rotation required is naturally higher, but never greater than 11 mrad. In the other cases, the joint rotation is quite low, below 3.2 mrad, which is expectable as not plastic deformation of the joints occurs.

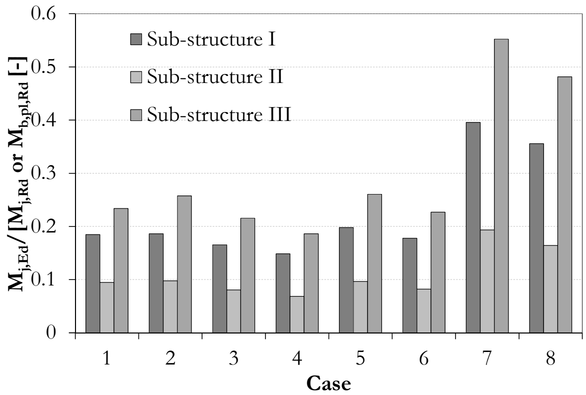

Fig. 7.12 Ratio between acting bending moment and bending moment capacity of joint/beam under SLS

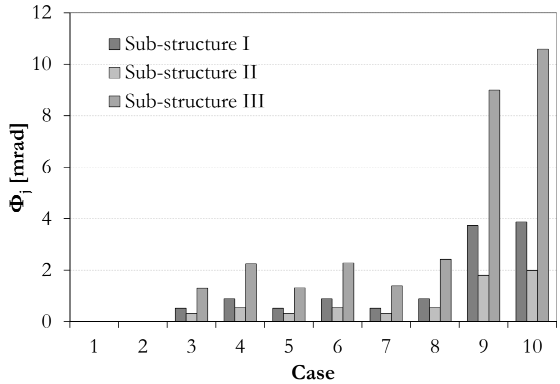

Fig. 7.13 Joint rotation under SLS

7.2.5 Analysis and discussion for Ultimate Limit State

At Ultimate Limit State (ULS), joints should perform so that the structural integrity is not lost. This requires to the joints either resistance either deformation capacity, allowing the redistribution of internal forces within the structure. In order to quantify such structural demands to the steel-to-concrete joints, calculations considering the load combinations of this limit state are performed. In Fig. 7.14 are summarized the maximum loads obtained on these joints M_j, N_j, V_j. In all cases, hogging bending moment and the axial compression are reported. Though, it should be referred that axial tension is observed in bottom floors of the sub-structures; however, in average, the maximum value does not exceed 10 kN.

Tab. 7.13 Top floor lateral displacement for Sub-structures I and II

	Sub-structure I			Sub-structure II			Sub-structure III			Joint Properties	
Joint Location	AL-3-L	AL-3-R	AL-3-L	AL-F-L	AL-A-R	AL-F-L	AL-G-L	AL-A-R	AL-A-L		
Case	M_j [kNm]	N_j [kN]	V_j [kN]	M_j [kNm]	N_j [kN]	V_j [kN]	M_j [kNm]	N_j [kN]	V_j [kN]		
1	169.0	68.5	181.1	64.7	31.8	72.9	441.1	387.6	345.8	R	FS
2	170.0	61.7	183.3	65.	33.4	73.9	539.5	406.4	371.4		
3	151.2	62.3	178.3	54.2	31.5	70.8	406.4	392.6	362.3		
4	136.2	62.8	174.3	46.2	30.1	68.7	350.4	382.1	355.6		
5	151.2	62.3	178.3	54.2	31.5	70.8	432.1	384.0	381.6		
6	136.3	62.8	174.3	46.2	30.1	68.7	376.1	372.5	376.1	↓	↓
7	138.0	62.1	174.8	54.8	33.0	71.3	401.9	381.3	394.5		
8	121.7	62.4	170.5	46.6	31.6	69.2	344.7	371.9	388.9		
9	0	65.9	138.9	0	21.0	56.5	0	282.4	346.5		
10	0	43.3	134.0	0	51.7	59.4	0	346.7	370.9	P	P

AL-Alignment; L – Left hand side; R- right hand side; R – Rigid; P – Pinned; FS – Full Strength

Fig. 7.14 shows the ratio between acting bending moment and the bending moment capacity of the steel-to-concrete joints or of the beams, in the case of full strength joints. As expected, for this limit state the ratio increases in comparison to the service limit state though, in none of the cases the full capacity of joints is activated. The higher ratios are observed in Sub-structures I and III, for the cases with lower bending moment resistance.

In Fig. 7.15 are plotted the maximum joint rotations observed in the different calculations. The maximum required joint rotation is approximately 20 mrad for the case studies where the steel-to-concrete joints are modelled as simple joints.

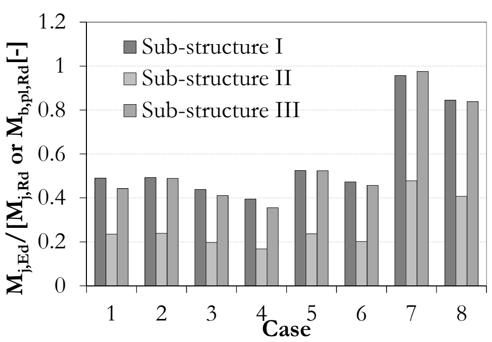

Fig. 7.14 Ratio between acting bending moment and bending moment capacity of joints, and beam at ULS

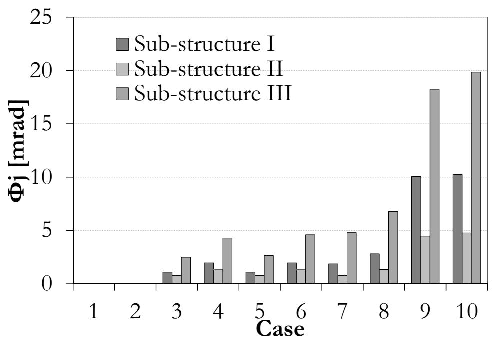

Fig. 7.15 Maximum joint rotation at ULS

8 TOLERANCES

8.1 Standardized tolerances

The European standard EN1090-2:2008 describes the geometric tolerances in Chapter 11. Limits of geometric deviations contained therein are independent from the execution classes and they are divided into two types.

Essential tolerances called those which are necessary for the mechanical resistance and stability of the completed structure.

Functional tolerances have decisive influence on other criteria such as fit-up and appearance. The permitted limits of deviations are defined for two tolerance classes in generally. Stricter limits apply to class 2. Is not a class set, tolerance class 1 applies.

The essential tolerances, as well as the functional tolerances are normative.

With regard to the connections of steel structures in concrete components, essential tolerances are limited in Chapter 11.2.3.2 for foundation bolts and other supports and in Chapter 11.2.3.3 for column bases. There, with regard to their desired location, permissible deviations of a group of anchor bolts and instructions for the required hole clearance are specified for base plates.

More interesting for connections with embedded anchor plates in concrete structures are the functional tolerances given in Annex D Tab. 2.20, see Fig. 8.1.

The European standard EN13670:2011 Execution of concrete structures contains in Chapter 10 also information to geometrical tolerances, which are for buildings of importance, such as structural safety. Two tolerance classes are defined, in which in generally the tolerance class 1 (reduced requirements) applies. The application of the tolerance class 2 is intended mainly in connection with structural design according to EN1992-1-1:2004 Appendix A. Fig. 8.2 (Fig. 2 in EN13670:2011) provides limits of permissible deviations from the vertical of walls and pillars. Deviations of these components have decisive influence on the steel structures to be connected there (if required).

No	Criterion	Parameter	Permitted deviation Δ
1	Foundation level 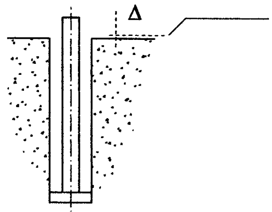	Deviation Δ from specified level	-15 mm ≤ Δ ≤ +5 mm
2	Vertical wall 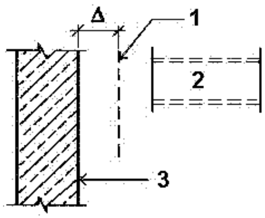 Kay 1 Specified position 2 Steel component 3 Supporting wall	Deviation Δ from specified position at support point for steel component	Δ = ± 25 mm
3	Pre-set foundation bolt where prepared for adjustment 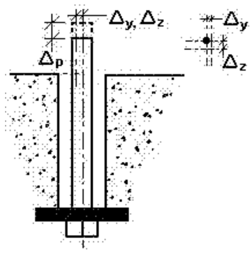	Deviation Δ from specified location and protrusion : - Location at tip - Vertical protrusion Δ_p NOTE The permitted deviation for location of the centre of a bolt group is 6 mm.	Δ_y, Δ_z = ± 10 mm -5 mm ≤ Δ_p ≤ 25 mm
4	Pre-set foundation bolt where not prepared for adjustment 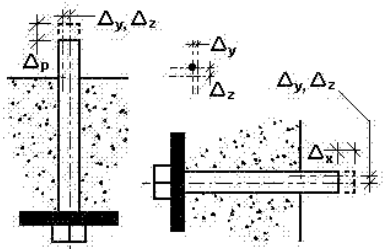	Deviation Δ from specified location, level and protrusion: - Location at tip - Vertical protrusion Δ_p - Vertical protrusion Δ_x NOTE The permitted deviation for location also applies to the centre of bolt group.	Δ_y, Δ_z = ± 3 mm -5 mm ≤ Δ_p ≤ 45 mm -5 mm ≤ Δ_x ≤ 45 mm
5	Steel anchor plate embedded in concrete 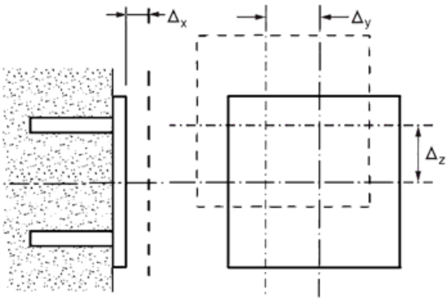	Deviations Δ_x, Δ_y, Δ_z from the specified location and level	Δ_x, Δ_y, Δ_z = ± 10 mm

Fig. 8.1 Functional tolerances – concrete foundations and support,
Tab. D.2.20 in EN1090-2:2008

No	Type of deviation	Description	Permitted deviation Δ Tolerance class 1
a	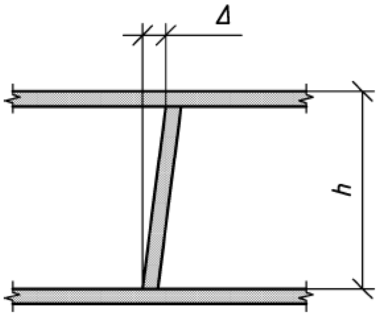 h= free height	Inclination of a column or wall at any lever in a single or a multi-storey building $h \leq 10\,m$ $h > 10\,m$	The larger of $15\,mm\ or\ h/400$ $25\,mm\ or\ h/800$
b	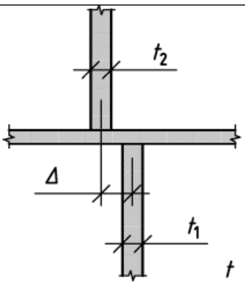	Deviation between centres	The larger of $\mathrm{t}/300$ or $15\ \mathrm{mm}$ But not more than $30\ \mathrm{mm}$
c	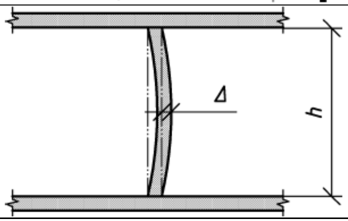	Curvature of a column or wall between adjacent storey levels	The larger of $t/30$ or $15\ \mathrm{mm}$ But not more than $30\ \mathrm{mm}$
d	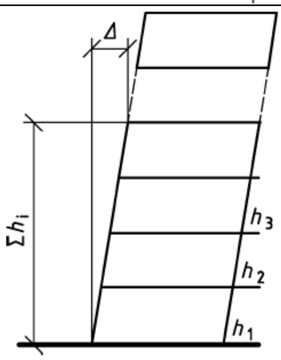 $\sum h_i$=sum of height of storeys considered	Location of a column or a wall at any storey level, from a vertical line through its intended centre at base level in a multi-storey structure n is the number of storeys where $n > 1$	The smaller of $50\ mm$ or $\frac{\sum h_i}{(200n^{\frac{1}{2}})}$

Fig. 8.2 Permissible deviations from the vertical of walls and pillars,
abridged **Fig. 2 in EN13670:2011**

Geometric tolerances, which are in terms of suitability for use and the accuracy of fit for the building of importance, are regulated in the informative Annex G, unless regulated otherwise, the tolerances of Annex G apply, see Fig. 8.3. It is assumed that tolerances contained therein relate to geometrical sizes, which have only a limited influence on the bearing capacity. Fig. 8.1 shows the permissible deviations of built in components in all directions, compare EN1090-2:2008 D. 2.20 line 5.

No	Type of deviation	Description	Permitted deviation Δ
d	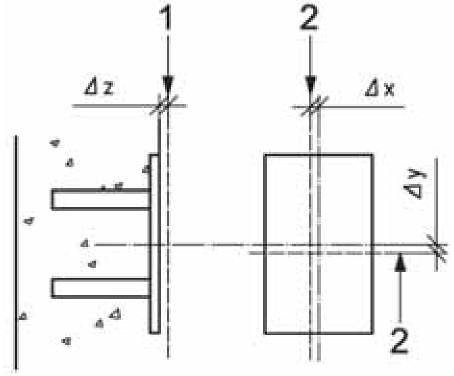 1 normal position in plane 2 normal position in depth	Anchoring plates and similar inserts Deviation in plane Deviation in depth	Δ_x, Δ_y = ±20 mm Δ_z = ±10 mm

Fig. 8.3 Permitted deviations for holes and inserts,
abridged **Fig. G.6 in EN13670:2011**

An assessment of the impact of the tabular listed permissible limits on connections with embedded anchor plates will be in the next Chapter 8.2.

8.2 Recommended tolerances

For deviations from fixtures (anchoring) of the target location, relatively low values are allowed in the previously mentioned standards, ±10 mm in each direction, see EN1090-2:2008, or ± 20 mm in the plains and ± 10 mm perpendicular to the surface, see EN13670:2011. Tolerances for angular misalignments of the anchor plates to their installation levels are not available.

However, in EN 13670 Fig. 2d for multi-story buildings clearly greater deviations of the upper floors to the vertical are allowed. For example, the permissible horizontal displacement of the top-level of a floor from the target location is for a seven-story building with a floor height of 3.50 m.

$$\sum h_i \,/\, (200 \ n^{1/2}) = 46 \text{ mm} \tag{8.1}$$

If the building is made of prefabricated concrete elements, the concrete anchor plate - even with exact location within the individual component - may exhibit the same displacement from the target location as the above shown deviations.

Therefore, the deviations defined directly for anchor plates by ± 10 mm seem to be hardly feasible. Much larger deviations have to be expected. If necessary, special tolerances for the location of the built in components have to be defined. EN13670:2011 describes another principle of tolerance definition, in which the allowable deviation of any point of construction compared to a theoretical target location over a fixed value is defined in Chapter 10.1 cl 5. A recommendation for the maximum permissible deviation is ± 20 mm.

Definitely, connecting elements between steel and concrete structures must be able to compensate tolerances. Considering the previous explanations, a development of joints for taking deviations of the anchor plate from the theoretical target location of ± 20 to 25 mm is recommended. Fig. 8.4 and 8.5 show exemplary a connections with and without the possibility to compensate geometrical derivations.

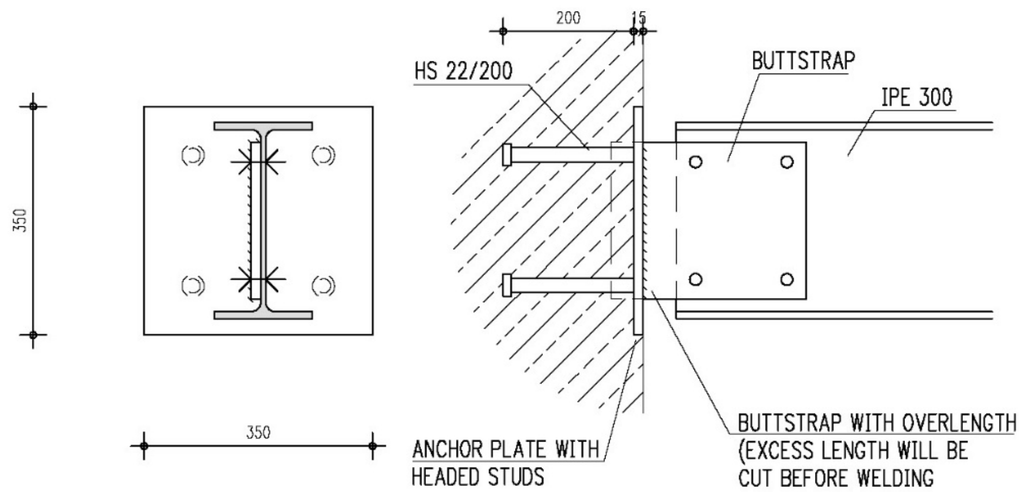

Fig. 8.4 Joint with possibility of adjustment

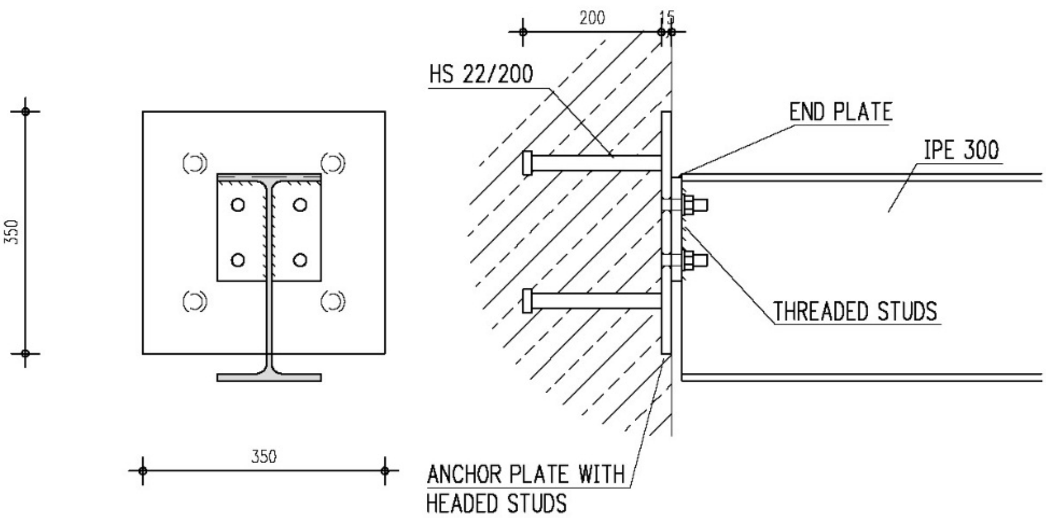

Fig. 8.5 Joint without possibility of adjustment

The following methods is used to compensate certain displacements of build in components to the target location. Depending on the loading, priority direction of the loads, the most appropriate solution has to be chosen.

Tolerance absorption in the longitudinal direction of the profile

Bolted connection with end plate and scheduled filler plates
Bolted connection with base plate and grouting
Cleat / console
Beam / pillar scheduled with overlength; adjustment and welding on site
Buttstrap with overlength; adjustment and welding on site
Buttstrap with slot holes

Tolerance absorption perpendicular to the longitudinal direction of profile:

Additional steel plate with threaded bolts; welded on site; beam / pillar with end plate
Anchor plate with threaded bolts; head plate with oversized holes
Buttstrap; welding on site

9 WORKED EXAMPLES

9.1 Pinned base plate

Check the resistance of the column base. The column of HE 200 B section, a concrete foundation size 850 x 850 x 900 mm, a base plate thickness 18 mm, steel S 235 and concrete C 12/15, γ_{Mc} = 1.50, γ_{M0} = 1.00.

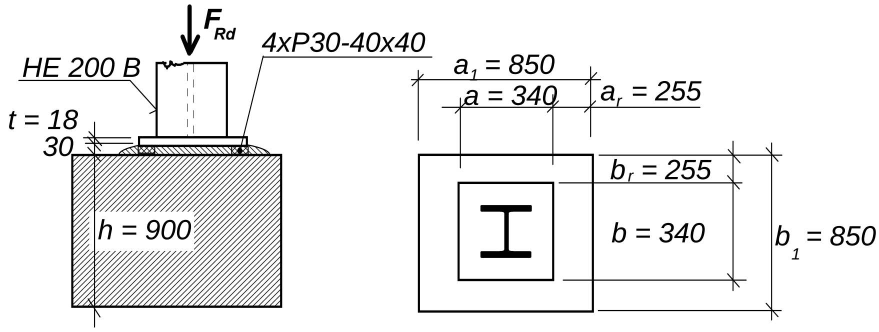

Fig. 9.1 Designed column base

Step 1 Concrete design strength

The stress concentration factor should be calculated, see Chap. 3.3. The minimum values for a_1 (or b_1) are taken into account

EN1993-1-8 cl. 6.2.5

$$a_1 = b_1 = \min\begin{Bmatrix} a + 2\,a_r = 340 + 2 \cdot 255 = 850 \\ 3\,a = 3 \cdot 340 = 1\,020 \\ a + h = 340 + 900 = 1\,240 \end{Bmatrix} = 850\ \mathrm{mm}$$

The condition $a_1 = b_1 = 850 > a = 340$ mm is satisfied, and therefore

$$k_j = \sqrt{\frac{a_1 \cdot b_1}{a \cdot b}} = \sqrt{\frac{850 \cdot 850}{340 \cdot 340}} = 2.5$$

The concrete design strength is calculated from the equation

EN1993-1-8 cl 6.2.5

$$f_{jd} = \frac{\beta_j\, F_{Rd,u}}{b_{eff}\, l_{ef}} = \frac{\beta_j\, A_{c0}\, f_{cd}\sqrt{\frac{A_{c1}}{A_{c0}}}}{A_{c0}} = \beta_j\, f_{cd}\, k_j = 0.67 \cdot \frac{12.0}{1.5} \cdot 2.5 = 13.4\ \mathrm{MPa}$$

Step 2 Flexible base plate

The flexible base plate is replaced by a rigid plate, see the following picture Fig. 9.2.

The strip width is

EN1993-1-8 cl 6.2.5

$$c = t\sqrt{\frac{f_y}{3 \cdot f_{jd} \cdot \gamma_{M0}}} = 18 \cdot \sqrt{\frac{235}{3 \cdot 13.4 \cdot 1.00}} = 43.5\ \mathrm{mm}$$

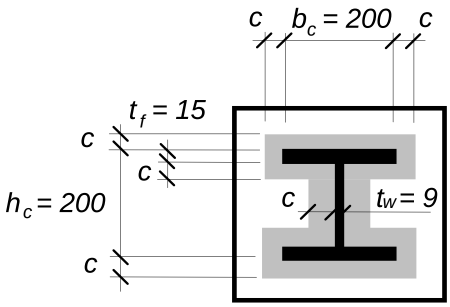

Fig. 9.2 Effective area under the base plate

The effective area of the base plate of H shape is calculated as a rectangular area minus the central areas without contact such that;

$$A_{eff} = \min(b; b_c + 2c) \cdot \min(a; h_{ef} + 2c)$$
$$- \ \max[\min(b; b_c + 2c) - t_w - 2c; 0] \cdot \max(h_c - 2t_f - 2c; 0)$$

$$A_{eff} = (200 + 2 \cdot 43.5) \cdot (200 + 2 \cdot 43.5)$$
$$- (200 + 2 \cdot 43.5 - 9 - 2 \cdot 43.5) \cdot (200 - 2 \cdot 15 - 2 \cdot 43.5)$$

EN1993-1-8
cl 6.2.5

$$A_{eff} = 82\ 369 - 15\ 853 = 66\ 516\ \text{mm}^2$$

Step 3 Design resistance

The design resistance of the column base in compression is

$$N_{Rd} = A_{eff} \cdot f_{jd} = 66\ 516 \cdot 13.4 = 891 \cdot 10^{\,3}\text{N}$$

EN1993-1-8
cl 6.2.5

Comments

The design resistance of the column footing is higher than the resistance of the column base

$$N_{pl,Rd} = \frac{A_c \cdot f_y}{\gamma_{M0}} = \frac{7808 \cdot 235}{1.00} = 1\ 835 \cdot 10^3\text{N} > \ N_{Rd}$$

EN1993-1-1
cl 6.2.4

where A_c is area of the column. The column base is usually designed for column resistance, which is determined by column buckling resistance.

It is expected, that the grout will not affect the column base resistance. The grout has to be of better quality or the thickness has to be smaller than

$$0.2 \min(a; b) = 0.2 \cdot 340 = 68\ \text{mm}$$

EN1993-1-8
cl 6.2.5

The steel packing or the levelling nuts is placed under the base plate during the erection. It is recommended to include the packing/nuts in the documentation

9.2 Moment resistant base plate

In the following example the calculation of the moment resistance and the bending stiffness of the column base at Fig. 9.3 is shown. The Column HE 200 B is loaded by a normal force F_{Sd} = 500 kN. The concrete block C25/30 of size 1 600 x 1 600x 1000 mm is designed for particular soil conditions. The base plate is of 30 mm thickness and the steel strength is S235. Safety factors are considered as γ_{Mc} = 1.50; γ_{Ms} = 1.15, γ_{M0} = 1.00; and γ_{M2} = 1.25. The connection between the base plate and the concrete is carried out through four headed studs of 22 mm diameter and an effective embedment depth of 150 mm, see Fig. 9.3. The diameter of the head of the stud is 40 mm. The supplementary reinforcement for each headed stud consists of two legged 12 mm diameter stirrups on each side of the stud. Consider f_{uk} = 470 MPa for studs and design yield strength of the supplementary reinforcement as $f_{yd,re} = \frac{f_{yk,re}}{\gamma_{Ms}} = \frac{500}{1.15} = 435\text{ MPa}$.

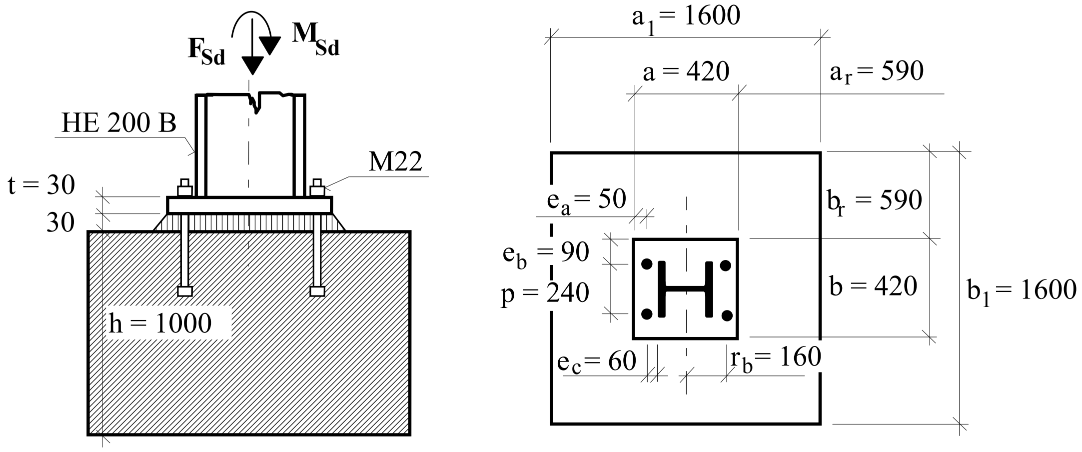

Fig. 9.3 Designed column base

<u>Step 1 Base plate resistance</u>

<u>1.1 Component base plate in bending and headed studs in tension</u>

Lever arm, for fillet weld $a_{wf} = 6$ mm is

$$m = 60 - 0.8 \cdot a_{wf} \cdot \sqrt{2} = 60 - 0.8 \cdot 6 \cdot \sqrt{2} = 53.2 \text{ mm}$$

The minimum T-stub length in base plates where the prying forces not taken into account, is

DM I
Fig. 4.4

$$l_{eff,1} = \min \left\{ \begin{array}{c} 4\text{ m} + 1.25\text{ e}_a = 4 \cdot 53.2 + 1.25 \cdot 50 = 275.3 \\ 2\,\pi\text{ m} = 2\,\pi \cdot 53.2 = 334.3 \\ b \cdot 0.5 = 420 \cdot 0.5 = 210 \\ 2\text{ m} + 0.625\text{ e}_a + 0.5\text{ p} = 2 \cdot 53{,}2 + 0.625 \cdot 50 + 0.5 \cdot 240 = 257.7 \\ 2\text{ m} + 0.625\text{ e}_a + \text{e}_b = 2 \cdot 53.2 + 0.625 \cdot 50 + 90 = 227.7 \\ 2\,\pi\text{ m} + 4\text{ e}_b = 2\,\pi \cdot 53.2 + 4 \cdot 90 = 694.3 \\ 2\,\pi\text{ m} + 2\text{ p} = 2\,\pi \cdot 53.2 + 2 \cdot 240 = 814.3 \end{array} \right\}$$

EN1993-1-8
cl 6.2.6.4

(Wald et al, 2008)

$$l_{eff,1} = 210 \text{ mm}$$

DM I
Tab. 4.2

The effective length of headed studs L_b is taken as

$$L_b = \min(h_{eff};\ 8 \cdot d) + t_g + t + \frac{t_n}{2} = 150 + 30 + 30 + \frac{19}{2} = 219.5\ \text{mm}$$

DM I
Fig. 4.1

The resistance of T - stub with two headed studs is

$$F_{T,1-2,Rd} = \frac{2\ L_{eff,1}\ t^2\ f_y}{4\ m\ \gamma_{M0}} = \frac{2 \cdot 210 \cdot 30^2 \cdot 235}{4 \cdot 53.2 \cdot 1.00} = 417.4\ \text{kN}$$

EN1993-1-8
cl 6.2.4.1

The resistance is limited by tension resistance of two headed studs M 22, the area in tension $A_s = 303\ \text{mm}$.

$$F_{T,3,Rd} = 2 \cdot B_{t,Rd} = 2 \cdot \frac{0.9 \cdot f_{uk} \cdot A_s}{\gamma_{M2}} = 2 \cdot \frac{0.9 \cdot 470 \cdot 303}{1.25} = 205.1\ \text{kN}$$

EN1993-1-8
cl 6.2.4.1

<u>1.2 Component base plate in bending and concrete block in compression</u>

To evaluate the compressed part resistance is calculated the connection factor as

$$a_1 = b_1 = \min \left\{ \begin{matrix} a + 2.a_r = 420 + 2 \cdot 590 = 1\,600 \\ 3a = 3 \cdot 420 = 1260 \\ a + h = 420 + 1\,000 = 1\,420 \end{matrix} \right\} = 1\,260\ \text{mm}$$

and $a_1 = b_1 = 1\,260 > a = b = 420$ mm

EN1993-1-8
cl 6.2.5

The above condition is fulfilled and

$$k_j = \sqrt{\frac{a_1 \cdot b_1}{a \cdot b}} = \sqrt{\frac{1\,260 \cdot 1\,260}{420 \cdot 420}} = 3.00$$

DM I
Eq. 3.65

The grout is not influencing the concrete bearing resistance because

$$0.2 \cdot \min(a; b) = 0.2 \cdot \min(420;\ 420) = 84\ \text{mm} > 30\ \text{mm} = t_g$$

The concrete bearing resistance is calculated as

EN1993-1-8
cl 6.2.5

$$f_{jd} = \frac{2}{3} \cdot \frac{k_j \cdot f_{ck}}{\gamma_{Mc}} = \frac{2}{3} \cdot \frac{3.00 \cdot 25}{1.5} = 33.3\ \text{MPa}$$

From the force equilibrium in the vertical direction $F_{Sd} = A_{eff} \cdot f_{jd} - F_{t,Rd}$, the area of concrete in compression A_{eff} in case of the full resistance of tension part is calculated

EN1993-1-8
cl 6.2.5

$$A_{eff} = \frac{F_{Sd} + F_{Rd,3}}{f_{jd}} = \frac{500 \cdot 10^3 + 205.1 \cdot 10^3}{33.3} = 21\,174\ \text{mm}^2$$

The flexible base plate is transferred into a rigid plate of equivalent area. The width of the strip c around the column cross section, see Fig. 9.4, is calculated from

EN1993-1-8
cl 6.2.5

$$c = t\sqrt{\frac{f_y}{3 \cdot f_{jd} \cdot \gamma_{M0}}} = 30 \cdot \sqrt{\frac{235}{3 \cdot 33.3 \cdot 1.00}} = 46.0\ \text{mm}$$

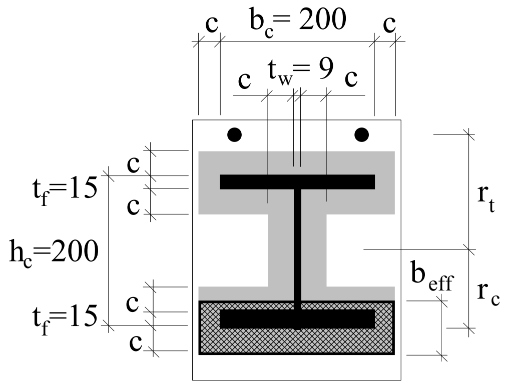

Fig. 9.4 The effective area under the base plate

1.3 Assembly for resistance

The active effective width is calculated as

$$b_{eff} = \frac{A_{eff}}{b_c + 2\,c} = \frac{21\,174}{200 + 2 \cdot 46.0} = 72.5 \text{ mm} < t_f + 2\,c = 15 + 2 \cdot 46.0 = 107.0 \text{ mm}$$

EN1993-1-8 cl 6.2.5

The lever arm of concrete to the column axes of symmetry is calculated as

$$r_c = \frac{h_c}{2} + c - \frac{b_{eff}}{2} = \frac{200}{2} + 46.0 - \frac{72.5}{2} = 109.8 \text{ mm}$$

EN1993-1-1 cl 6.2.5

The moment resistance of the column base is $M_{Rd} = F_{T,3,Rd} \cdot r_t + A_{eff} \cdot f_{jd} \cdot r_c$

EN1993-1-1 cl 6.2.4

$$M_{Rd} = 205.1 \cdot 10^3 \cdot 160 + 21\,174 \cdot 33.3 \cdot 109.8 = 110.2 \text{ kNm}$$

Under acting normal force $N_{Sd} = 500$ kN the moment resistance in bending is $M_{Rd} = 110.2$kNm.

1.4 The end of column resistance

The design resistance in poor compression is

$$N_{pl,Rd} = \frac{A \cdot f_y}{\gamma_{M0}} = \frac{7808 \cdot 235}{1.00} = 1\,835 \cdot 10^3\text{N} > N_{Rd} = 500\text{kN}$$

EN1993-1-1 cl 6.2.5

The column bending resistance

$$M_{pl,Rd} = \frac{W_{pl} \cdot f_{yk}}{\gamma_{M0}} = \frac{642.5 \cdot 10^3 \cdot 235}{1.00} = 151.0 \text{ kNm}$$

EN1993-1-1 cl 6.2.9

The interaction of normal force reduces moment resistance

$$M_{Ny,Rd} = M_{pl,Rd} \frac{1 - \frac{N_{Sd}}{N_{pl,Rd}}}{1 - 0.5\,\frac{A - 2\,b\,t_f}{A}} = 151.0 \cdot \frac{1 - \frac{500}{1\,835}}{1 - 0.5\,\frac{7\,808 - 2 \cdot 200 \cdot 15}{7\,808}} = 124.2 \text{ kNm}$$

EN1993-1-8 cl 6.3

The column base is designed on acting force only (not for column resistance).

Step 2 Base plate stiffness

2.1 Component base plate in bending and headed stud in tension

The component stiffness coefficients for headed studs and base plate are calculated

$$k_b = 2.0 \cdot \frac{A_s}{L_b} = 2.0 \cdot \frac{303}{219.5} = 2.8 \text{ mm}$$ EN1993-1-8 cl 6.3

$$k_p = \frac{0.425 \cdot L_{beff} \cdot t^3}{m^3} = \frac{0.425 \cdot 210 \cdot 30^3}{53.2^3} = 16.0 \text{ mm}$$ EN1993-1-8 cl 6.3

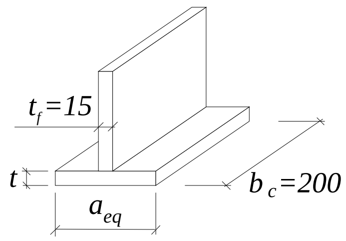

Fig. 9.5 The T stub in compression

2.2 Component base plate in bending and concrete block in compression

For the stiffness coefficient the T-stub in compression, see Fig. 9.5, is

$$a_{eq} = t_f + 2.5\,t = 15 + 2.5 \cdot 30 = 90 \text{ mm}$$

$$k_c = \frac{E_c}{1.275 \cdot E_s} \cdot \sqrt{a_{eq} \cdot b_c} = \frac{31\,000}{1.275 \cdot 210\,000} \cdot \sqrt{90 \cdot 200} = 15.5 \text{ mm}$$ EN1993-1-8 cl 6.3

2.3 Assembly of component tensile stiffness coefficient to base plate stiffness

The lever arm of component in tension z_t and in compression z_c to the column base neutral axes is

$$z_t = \frac{h_c}{2} + e_c = \frac{200}{2} + 60 = 160 \text{ mm}$$

$$z_c = \frac{h_c}{2} - \frac{t_f}{2} = \frac{200}{2} - \frac{15}{2} = 92.5 \text{ mm}$$ EN1993-1-8 cl 6.3

The stiffness coefficient of tension part, headed studs and T stub, is calculated as

$$k_t = \frac{1}{\dfrac{1}{k_b} + \dfrac{1}{k_p}} = \frac{1}{\dfrac{1}{2.8} + \dfrac{1}{16.0}} = 2.4 \text{ mm}$$ EN1993-1-1 cl 6.2.9

For the calculation of the initial stiffness of the column base the lever arm is evaluated

$z = z_t + z_c = 160 + 92.5 = 252.5$ mm and

$$a = \frac{k_c \cdot z_c - k_t \cdot z_t}{k_c + k_t} = \frac{15.5 \cdot 92.5 - 2.4 \cdot 160}{15.5 + 2.4} = 58.6 \text{ mm}$$ EN1993-1-8 cl 6.3

The bending stiffness is calculated for particular constant eccentricity

$$e = \frac{M_{Rd}}{F_{Sd}} = \frac{110.2 \cdot 10^6}{500 \cdot 10^3} = 220.4 \text{ mm}$$

EN1993-1-1
cl 6.2.9

as

$$S_{j,ini} = \frac{e}{e+a} \cdot \frac{E_S \cdot z^2}{\mu \sum_i \frac{1}{k_i}} = \frac{220.4}{220.4 + 58.6} \cdot \frac{210\,000 \cdot 252.5^2}{1 \cdot \left(\frac{1}{2.4} + \frac{1}{15.5}\right)} = 21.981 \cdot 10^9 \text{ Nmm/rad}$$

$$= 21\,981 \text{ kNm/rad}$$

EN1993-1-8
cl 6.3

Step 3 Anchorage resistance and stiffness

As discussed in Chapter 3 Concrete components, the stiffness of anchorage is determined for separate components, failure modes, and then combined together. In this case, the anchorage is considered as a group of four headed studs with nominal stud diameter of 22 mm arranged in a way displayed in Fig. 9.6. Furthermore, supplementary reinforcement with the arrangement shown in Fig. 9.6 is considered.

Due to moment loading on the anchor group generated by the lateral loads only one side studs will be subjected to tension loads. Therefore in the following example, two studs are considered while evaluating the behaviour of the anchor group. Here, diameter of the reinforcing bar is considered as 12 mm and the effective embedment depth of the stud is considered as 150 mm, distance from of the head to the concrete surface.

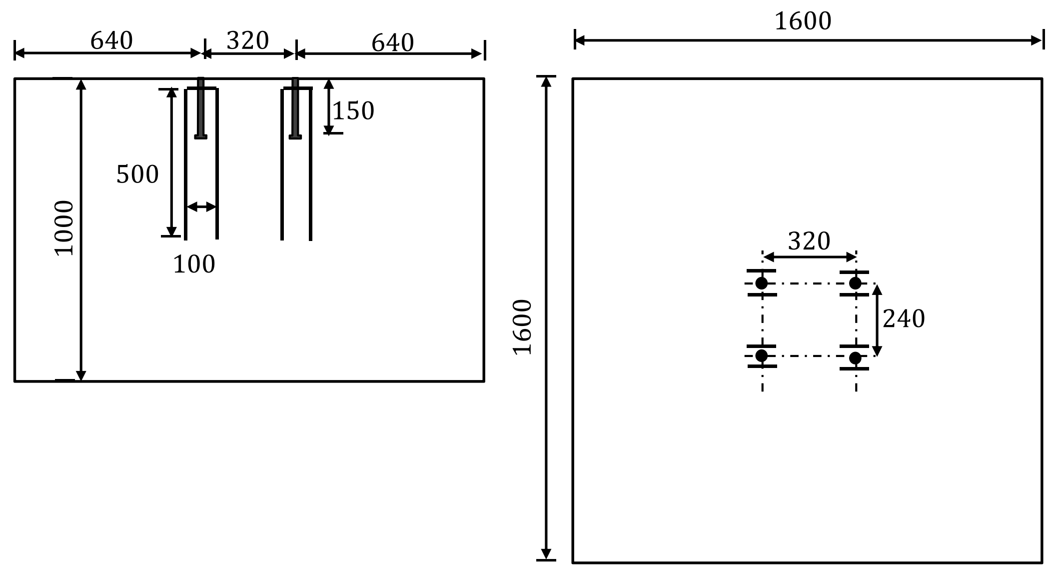

Fig. 9.6 Headed studs and supplementary reinforcement configuration

3.1 Component S – Steel failure of headed stud

Component S comprises of evaluating the design load-displacement response of the headed studs under tensile loading, when they undergo steel failure. Only two anchors will be considered in tension. From Eq. (3.3) and (3.4) is calculated the load and the stiffness as

$$N_{Rd,s} = \frac{n \cdot \pi \cdot d_{s,nom}^2 \cdot f_{uk}}{4 \cdot \gamma_{Mp}} = \frac{2 \cdot \pi \cdot 22^2 \cdot 470}{4 \cdot 1.5} = 238\,216\ \text{N} = 238.2\ \text{kN}$$ DM I Eq. (3.3)

$$k_{s1} = \frac{A_{s,nom} E_s}{L_h} = \frac{n \cdot \pi \cdot d_{s,nom}^2}{4} \frac{\cdot E_s}{L_h} = \frac{2 \cdot \pi \cdot 22^2 \cdot 210\,000}{4 \cdot 150} =$$ DM I Eq. (3.4)

$$= 1\,064\,371 \frac{\text{N}}{\text{mm}} = 1\,064.4 \frac{\text{kN}}{\text{mm}},\ \text{for } N_{act} < 238.2\ \text{kN}$$

$$k_{s2} = 0;\ N_{act} = 238.2\ \text{kN}$$ DM I Eq. (3.5)

Hence, the load-displacement curve for the spring is obtained as shown in Fig. 9.7.

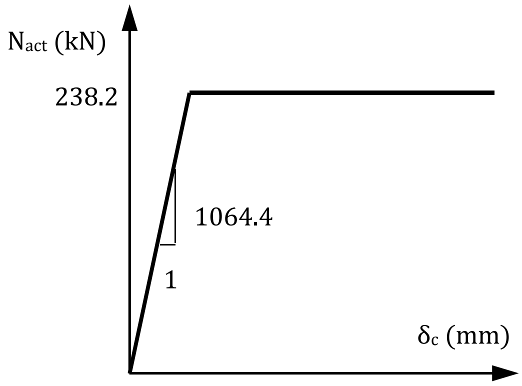

Fig. 9.7 Load-displacement behaviour of spring representing component S

3.2 Component C – Concrete cone failure

Component CC comprises of evaluating the design load-displacement response of the headed studs under tensile loading, when they undergo concrete cone failure. The critical edge distance $c_{cr,N} = 1.5\ h_{ef} = 225\ \text{mm}$. Using Eqs (3.7) through (3.9), it is

$$N_{Rd} = N_{Rk,c}^0 \cdot \psi_{A,N} \cdot \psi_{s,N} \cdot \psi_{re,N} / \gamma_{Mc}$$ DM I Eq. (3.7)

$$N_{Rk,c}^0 = k_1 \cdot h_{ef}^{1.5} \cdot f_{ck}^{0.5} = 12.7 \cdot 150^{1.5} \cdot 25^{0.5}\ \text{N} = 116{,}7\ \text{kN}$$ Eq. (3.8)

$$\psi_{A,N} = \frac{A_{c,N}}{A_{c,N}^0} = \frac{(1.5 \cdot 150 + 240 + 1.5 \cdot 150) \cdot (1.5 \cdot 150 + 1.5 \cdot 150)}{9 \cdot 150^2} = \frac{690 \cdot 450}{9 \cdot 150^2} = 1.53$$ Eq. (3.9) Eq. (3.13)

Since maximum edge distance, $c < c_{cr,N} = 225\ \text{mm}$, hence $\psi_{s,N} = 1.0$

There is no closely spaced reinforcement, hence, $\psi_{re,N} = 1.0$

Therefore, $N_{Rd,c} = 116.7 \cdot 1.53 \cdot 1.0 \cdot \frac{1.0}{1.5} = 119.0\ \text{kN}$

The stiffness of the descending branch $k_{c,de}$ for the design is described with the following function

$$k_{c,de} = \alpha_c \sqrt{f_{ck}\, h_{ef}} \cdot \psi_{A,N} \cdot \psi_{s,N} \cdot \psi_{re,N} = -537\sqrt{25 \cdot 150} \cdot 1.53 \cdot 1.0 \cdot 1.0 = -50.31 \frac{\text{kN}}{\text{mm}}$$

The displacement corresponding to zero load is $\frac{119.0}{50{,}31} = 2.37\ \text{mm}$

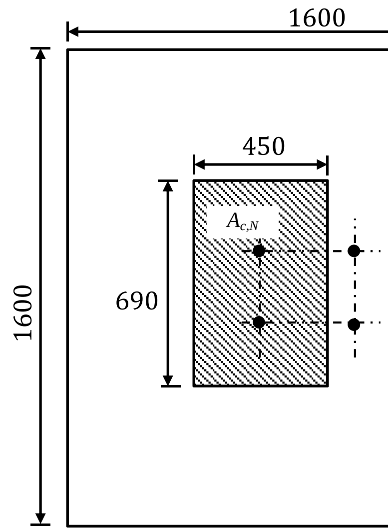

Fig. 9.8 Evaluation of group effect

The load-displacement curve for the spring is shown in Fig. 9.9.

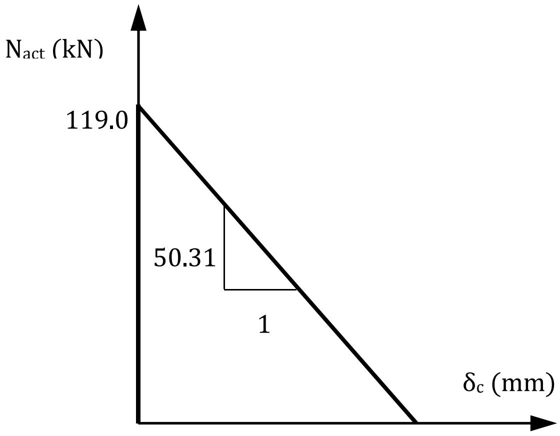

Fig. 9.9 Load-displacement behaviour of spring representing component CC

3.3 Component RS – Steel failure of stirrups

Component RS comprises of evaluating the design load-displacement response of the stirrups, when they undergo steel failure. The design load for yielding of the stirrups is given as Eq. (3.17)

DM I
Eq. (3.13)

$$\mathrm{N_{Rd,s,re}} = \mathrm{A_{s,re}} \cdot \mathrm{f_{yd,re}} = \mathrm{n_{re}} \cdot \pi \cdot \left(\mathrm{d^2_{s,re}}/4\right) \cdot \mathrm{f_{yd,re}}$$

For each stud, two stirrups with two legs on either side of the headed stud are provided. Therefore, for two headed studs in tension, the total number of the legs of the stirrups in tension is 8. Hence,

$$\mathrm{N_{Rd,s,re}} = 8 \cdot \left(\frac{\pi}{4} \cdot 12^2\right) \cdot 435 = 393.6\ \text{kN}$$

DM I
Eq. (3.17)

$$\delta_{\mathrm{Rd,s,re}} = \frac{2 \cdot \mathrm{N^2_{Rd,s,re}}}{\alpha_s \cdot \mathrm{f_{ck}} \cdot \mathrm{d^4_{s,re}} \cdot \mathrm{n^2_{re}}} = \frac{2 \cdot 393\,578^2}{12\,100 \cdot 25 \cdot 12^4 \cdot 8^2} = 0.77\ \text{mm}$$

Stiffness as a function of displacement is given as Eq. (3.18)

$$k_{s,re1} = \frac{\sqrt{n_{re}^2 \cdot \alpha_s \cdot f_{ck} \cdot d_{s,re}^4}}{\sqrt{2 \cdot \delta}} = \frac{\sqrt{8^2 \cdot 12\,100 \cdot 25 \cdot 12^4}}{\sqrt{2 \cdot \delta}} = \frac{448\,023}{\sqrt{\delta}} \text{ N/mm}$$ DM I Eq. (3.16)

for $\delta < \delta_{Rd,s,re}$ DM I eq. (3.18)

$k_{s,re2} = 0$ for $\delta \geq \delta_{Rd,s,re}$

The load-displacement curve for the spring is shown in Fig. 9.10 DM I eq. (3.19)

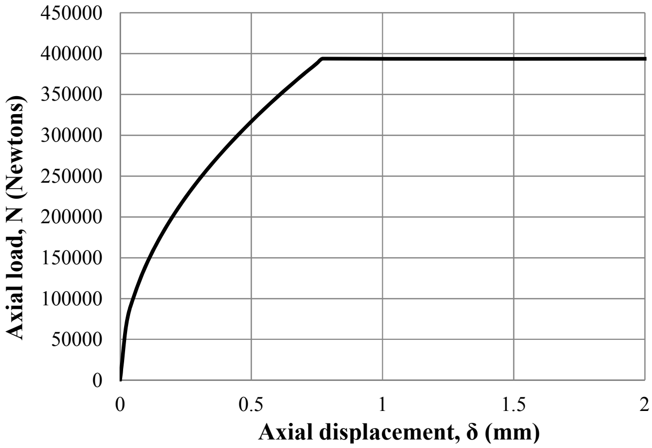

Fig. 9.10 Load-displacement behaviour of spring representing component RS

3.4 Component RB – Bond failure of stirrups

Component RB comprises of evaluating the design load-displacement response of the stirrups under tensile loading, when they undergo bond failure. The design anchorage capacity of the stirrups is given by Eq. (3.21). Assuming a cover of 25 mm to stirrups and considering the distance between the stud and the stirrup as 50 mm, l_1 is calculated as CEN/TC1992-4-1:2009

$l_1 = 150 - 25 - 0.7 \cdot 50 = 90$ mm

Considering f_{bd} for C25/30 grade concrete is $2.25 \cdot \frac{1.8}{1.5} \cdot 1.0 \cdot 1.0 = 2.7$ N/mm^2, see Eq (8.2) cl 8.4.2.(2) in EN1992:2004, it is

$$N_{Rd,b,re} = \sum n_{re} \cdot l_1 \cdot \pi \cdot d_{s,re} \cdot \frac{f_{bd}}{\alpha} = 8 \cdot 90 \cdot \pi \cdot 12 \cdot \frac{2.7}{0.49} = 149\,565 \text{ N} = 149.6 \text{ kN}$$ DM I Eq. (3.21)

The corresponding displacement is obtained using Eq. (3.20) as DM I Eq. (3.20)

$$\delta_{Rd,b,re} = \frac{2 \cdot N_{Rd,b,re}^2}{\alpha_s \cdot f_{ck} \cdot d_{s,re}^2 \cdot n_{re}^2} = \frac{2 \cdot 149\,565^2}{12100 \cdot 25 \cdot 12^4 \cdot 8^2} = 0.11 \text{ mm}$$

It may be noted that since $N_{Rd,b,re} < N_{Rd,s,re}$, bond failure of stirrups is the governing failure mode for the stirrups.

Stiffness as a function of displacement is given as

$$k_{b,re1} = \frac{\sqrt{n_{re}^2 \cdot \alpha_s \cdot f_{ck} \cdot d_{s,re}^4}}{\sqrt{2\delta}} = \frac{\sqrt{8^2 \cdot 12100 \cdot 25 \cdot 12^4}}{\sqrt{2\delta}} = \frac{448\,023}{\sqrt{\delta}} \text{ N/mm}$$ DM I Eq. (3.22)

for $\delta < \delta_{Rd,b,re}$ DM I Eq. (3.23)

$k_{b,re2} = 0$ for $\delta \geq \delta_{Rd,b,re}$

The load-displacement curve for the spring is shown in Fig. 9.11.

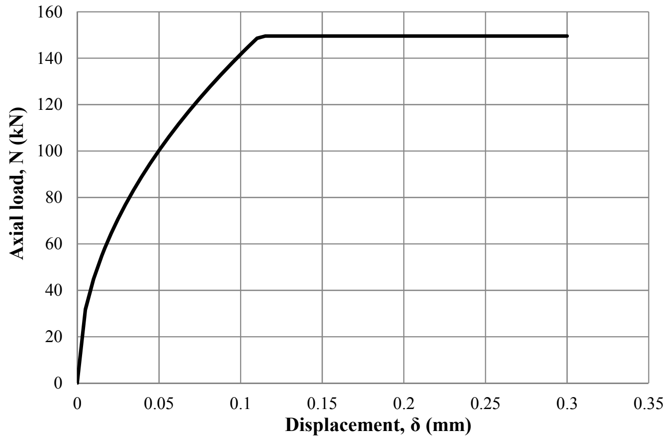

Fig. 9.11 Load-displacement relation of spring representing component RB

3.5 Component P - Pull out failure of the headed stud

For the first range, $N > N_{Rd,c}$ using Eqs (3.26) through (3.30), it is

$$k_p = \alpha_p \cdot \frac{k_a \cdot k_A}{k_2}$$

$a = 0.5 \cdot (d_h - d_s) = 0.5 \cdot (40 - 22) = 9$ mm

DM I Eq. (3.26)

$k_a = \sqrt{\frac{5}{a}} \geq 1.0$; hence, $k_a = 1.0$

DM I Eq. (3.29)

$$k_A = 0.5 \cdot \sqrt{d_s^2 + m \cdot (d_h^2 - d_s^2)} - 0.5 \cdot d_h = 0.5 \cdot \sqrt{22^2 + 9 \cdot (40^2 - 22^2)} - 0.5 \cdot 40 = \\ = 31.30$$

DM I Eq. (3.28)

k_2 = 600 (assuming uncracked concrete)

$$k_p = \alpha_p \cdot \frac{k_a \cdot k_A}{k_2} = 0.25 \cdot \frac{1.0 \cdot 31.30}{600} = 0.0130$$

DM I Eq. (3.30)

Thus, using Eq. (3.24), it is

$$\delta_{Rd,p,1} = k_p \cdot \left(\frac{N_{Rd,c}}{A_h \cdot f_{ck} \cdot n}\right)^2 = 0.0130 \cdot \left(\frac{119.0 \cdot 10^3}{\frac{\pi}{4} \cdot (40^2 - 22^2) \cdot 25 \cdot 2}\right)^2 = 0.096 \text{ mm}$$

In second range, using Eq. (3.25), it is

DM I Eq. (3.24)

$$\delta_{Rd,p,2} = 2k_p \cdot \left(\frac{\min(N_{Rd,p}; N_{Rd,re})}{A_h \cdot f_{ck} \cdot n}\right)^2 - \delta_{Rd,p,1}$$

Eq. (3.31) yields

$N_{Rd,p} = n \cdot p_{uk} \cdot A_h / \gamma_{Mc}$

DM I Eq. (3.25)

$N_{Rd,re} = \min(N_{Rd,s,re}; N_{Rd,b,re}) = \min\ (393.6; 149.6) = 149.6$ kN

The typical value of p_{uk} is considered as $12\ f_{ck} = 12 \cdot 25 = 300$ MPa. Hence, it is

$$N_{Rd,p} = 2 \cdot 300 \cdot \frac{\pi}{4} \cdot \frac{(40^2 - 22^2)}{1.5} = 350.6 \text{ kN}$$

$$\delta_{Rd,p,2} = 2 \cdot 0.0130 \cdot \left(\frac{149\,565}{\frac{\pi}{4} \cdot (40^2 - 22^2) \cdot 25 \cdot 2} \right)^2 - 0.096 = 0.21 \text{ mm}$$

The stiffness as a function of displacement is obtained using equations (3.34) and (3.35) as:

$$k_{p,1} = \sqrt{\frac{\left(\frac{\pi}{4} \cdot (40^2 - 22^2) \cdot 25 \cdot 2\right)^2}{0.0130 \cdot \delta_{act}}} = \frac{384\,373}{\sqrt{\delta_{act}}}$$ DM I Eq. (3.34)

$$k_{p,2} = \sqrt{\frac{\left(\frac{\pi}{4} \cdot (40^2 - 22^2) \cdot 25 \cdot 2\right)^2}{2 \cdot 0.0130 \cdot \delta_{act}^2} (\delta_{act} + 0.096)} = \frac{271\,792}{\delta_{act}} \cdot \sqrt{\delta_{act} + 0.096}$$ DM I Eq. (3.35)

The load-displacement curve for the spring is shown in Fig. 9.12.

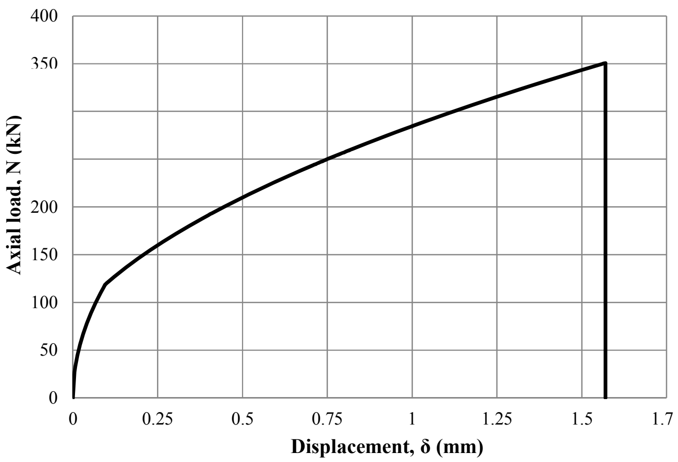

Fig. 9.12 Load-displacement behaviour of spring representing component P

<u>3.6 Interaction of components Concrete and Stirrups</u>

Once the concrete breakout occurs, the load is transferred to the stirrups and the load shared by concrete decreases with increasing displacement. The load carried by the combined component concrete + stirrups corresponding to any given displacement is given by Eq. (3.59) as

$$N_{act} = N_{Rd,c} + k_{c,de}\,\delta + \min\left(n_{re}\,d_{s,re}^2 \sqrt{\frac{\alpha_s\,f_{ck}\,\delta}{2}};\; N_{Rd,s,re};\; N_{Rd,b,re}\right)$$ DM I Eq. (3.59)

Hence, for a given displacement δ [mm] the load [kN] carried by combined concrete and stirrups is given as

$$N_{act} = 119.0 - 50.31 \cdot \delta + \min(448.023\sqrt{\delta};\; 393.6;\; 149.6)$$ DM I Eq. (3.59)

The load-displacement curve for the spring is shown in Fig. 9.13.

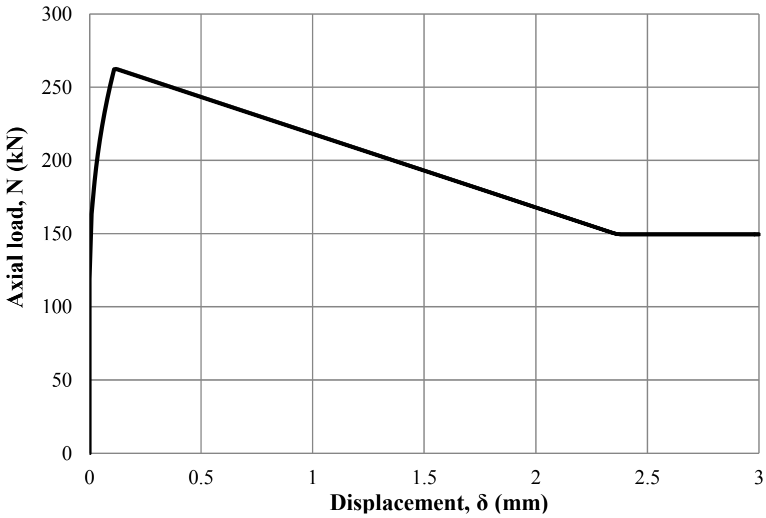

Fig. 9.13 Load-displacement behaviour of spring representing combined component concrete and stirrups

Interaction of all components:

The combined load-displacement behaviour combining all the components is displayed in Figure 9.14

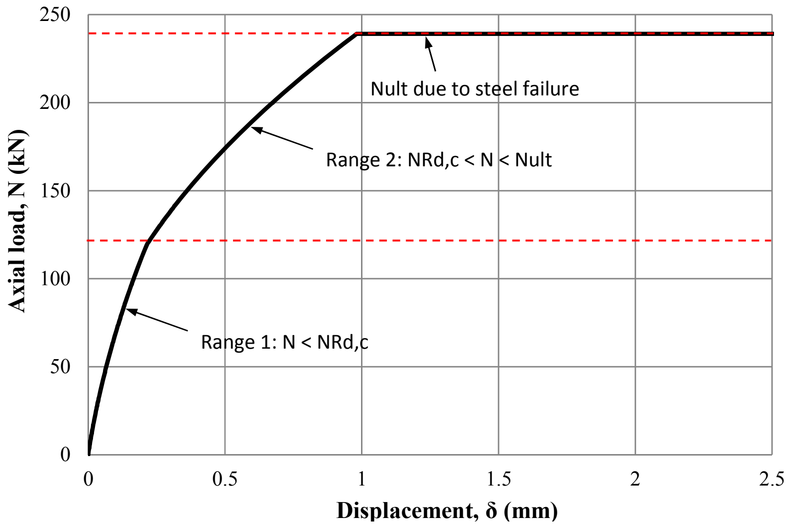

Fig. 9.144 Load-displacement behaviour obtained by combining all the components

<u>Notes</u>

- The resistance of the anchoring by the headed studs is limited by its threaded part, which represents a ductile behaviour.
- The resistance of the base plate is limited by the tension resistance of two headed studs M 22, 205.1 kN. Under the serviceability limit state SLS is required resistance of the concrete cone,119.0 kN. The elastic behaviour is expected till the 2/3 of the bending resistance of the base plate, which comply, $2/3 \cdot 417.4 = 314.3$ kN.

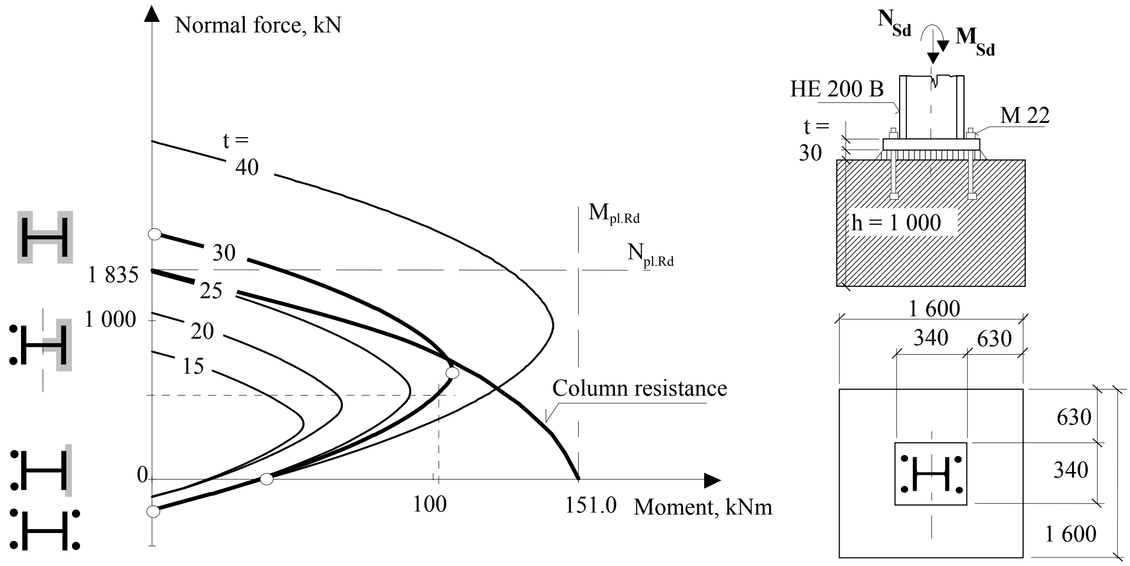

Fig. 9.155a The column base resistance is compared to the column resistance for different base plate thickness

- The column base resistance is compared to the column resistance for different base plate thickness, see Fig. 9.15a. For plate P 30 are shown the major points of the diagram, e.g. the pure compression, the highest bending resistance, in case of coincidence of the neutral axis and the axis of symmetry of cross-section, the pure bending and the pure tension.
- A conservative simplification may be applied by placing the concrete reaction on the axes of the compressed flange only see Fig. 9.15b. This model is uneconomical and not often used for prediction of resistance, but applied for stiffness prediction.

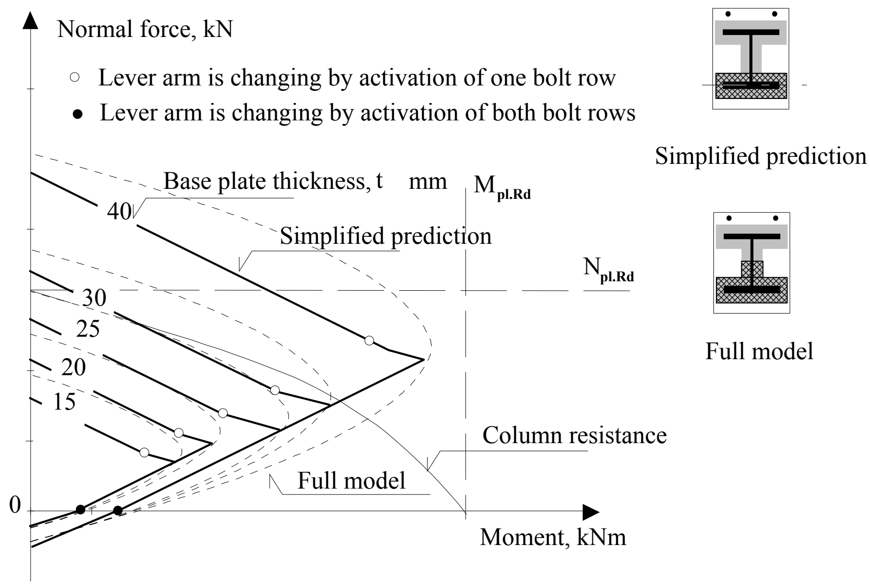

Fig. 9.16b The column base resistance calculated by the simplified prediction, the contact force under the compressed flange only, is compared to the application of the of the full contact area

- The stiffness of the anchoring by the headed studs corresponds to the expected stiffness calculated by a simplified conservative method based on the embedded effective length. The component stiffness coefficients for headed studs is estimated as

$k_b = 2.0 \cdot \frac{A_s}{L_b} = 2.0 \cdot \frac{A_s}{\min(h_{eff}; 8 \cdot d)} = 2.0 \cdot \frac{303}{150} = 4.04$ mm

and the deformation for acting force 300 kN is $\delta_{300} = \frac{F_{Ed}}{E \quad k_b} = \frac{300}{210\,000 \cdot 4.04} = 0.35$ mm.

For headed stud is predicted, see Fig. 9.13, more precise value reached 0.22 mm.

- The classification of the column base according to its bending stiffness is evaluated in comparison to column bending stiffness. For column length $L_c = 4$ m and its cross-section HE 200 B is relative bending stiffness

$$\overline{S}_{j,ini} = S_{j,ini} \cdot \frac{L_c}{E_s \cdot I_c} = 21.981 \cdot 10^9 \cdot \frac{4000}{210\,000 \cdot 56.96 \cdot 10^6} = 7.53$$

EN1993-1-8 cl 6.3

The designed column base is sway for braced as well as non-sway frames because

$\overline{S}_{j,ini} = 7.53 < 12 = \overline{S}_{j,ini,EC3,n}$; $\overline{S}_{j,ini} = 7.53 < 30 = \overline{S}_{j,ini,EC3,s}$

- The influence of tolerances and size of welds, see EN 1090-2 and Chapter 8, is not covered in above calculation.

9.3 Stiffened base plate

Calculate the moment resistance of the column base shown in Fig. 9.17. Column HE 200 B is loaded by normal force F_{Sd} = 1 100 kN. Concrete block C16/20 of size 1 600 x 1 600 x 1000 mm is design for particular soil conditions. Base plate of thickness 30 mm, steel S235, γ_{Mc} = 1.50; γ_{M0} = 1.00; and γ_{M2} = 1.25.

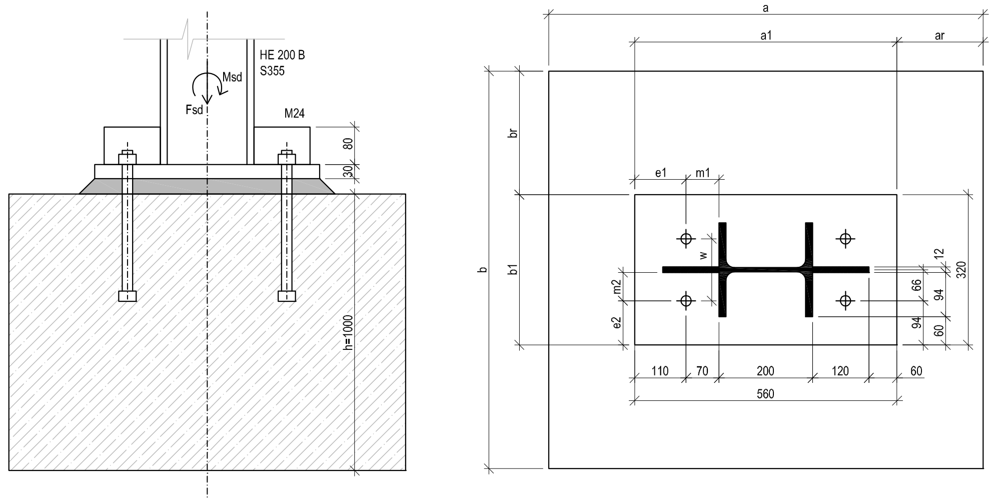

Fig. 9.17 Designed column base

<u>Step 1 Component in tension</u>

Resistance of component base plate in bending and headed studs in tension. Anchor stud lever arm, for fillet weld $a_{wf} = 6$ mm is

$$m = 70 - 0.8 \cdot a_{wf} \cdot \sqrt{2} = 70 - 0.8 \cdot 6 \cdot \sqrt{2} = 63.2 \text{ mm}$$

DM I
Fig. 4.4

The T-stub length, in base plates are the prying forces not taken into account, is:

$$l_{eff,1} = \min \left\{ \begin{array}{c} 4\,m + 1.25\,e_1 = 4 \cdot 63.2 + 1.25 \cdot 110 = 390.3 \\ 2\pi\,m = 2\,\pi \cdot 63.2 = 397.1 \\ b \cdot 0.5 = 320 \cdot 0.5 = 160 \\ 2\,m + 0.625\,e_1 + 0.5\,w = 2 \cdot 63.2 + 0.625 \cdot 110 + 0,5 \cdot 132 = 261.2 \\ 2\,m + 0.625\,e_1 + e_2 = 2 \cdot 63.2 + 0.625 \cdot 110 + 94 = 289.2 \\ 2\,\pi\,m + 4\,e_2 = 2\,\pi \cdot 63.2 + 4 \cdot 94 = 773.1 \\ 2\,\pi\,m + 2\,w = 2\,\pi \cdot 63.2 + 2 \cdot 132 = 661.1 \end{array} \right\}$$

EN1993-1-8
6.2.6.4

$l_{eff,1} = 160$ mm

The effective length of headed studs L_b is taken as

DM I
Fig. 4.1

$$L_b = 8 \cdot d + t_g + t + \frac{t_n}{2} = 8 \cdot 24 + 30 + 30 + \frac{19}{2} = 261.5 \text{ mm}$$

The resistance of T - stub with two headed studs is

$$F_{T,1-2,Rd} = \frac{2\, L_{eff,1}\, t^2 f_y}{4\, m\, \gamma_{M0}} = \frac{2 \cdot 160 \cdot 30^2 \cdot 235}{4 \cdot 63.2 \cdot 1.00} = 267.7 \text{ kN}$$ EN1993-1-8 6.2.4.1

The resistance is limited by tension resistance of two headed studs M 24 with the area in tension $A_s = 353$ mm

$$F_{T,3,Rd} = 2 \cdot B_{t,Rd} = 2 \cdot \frac{0.9 \cdot f_{ub} \cdot A_s}{\gamma_{M2}} = 2 \cdot \frac{0.9 \cdot 360 \cdot 353}{1.25} = 183.0 \text{ kN}$$ EN1993-1-8 6.2.4.1

Step 2 Component in compression

The connection concentration factor is calculated as

$$a_1 = \min \begin{Bmatrix} a_1 + 2\, a_r = 560 + 2 \cdot 520 = 1\,600 \\ 3\, a_1 = 3 \cdot 560 = 1\,680 \\ a_1 + h = 560 + 1\,000 = 1\,560 \end{Bmatrix} = 1\,560 \text{ mm}$$ EN1993-1-8 6.2.5

$$b_1 = \min \begin{Bmatrix} b_1 + 2b_r = 320 + 2 \cdot 640 = 1\,600 \\ 3\, b_1 = 3 \cdot 320 = 960 \\ b_1 + h = 320 + 1\,000 = 1\,320 \end{Bmatrix} = 960 \text{ mm}$$

and $a_1 = 1560 > a_1 = 560 \text{ mm} \quad b_1 = 960 > b_1 = 320\, a_1$

The above condition is fulfilled and

$$k_j = \sqrt{\frac{a_1 \cdot b_1}{a \cdot b}} = \sqrt{\frac{1\,560 \cdot 960}{560 \cdot 320}} = 2.89$$ DM I Eq. 3.65

The grout is not influencing the concrete bearing resistance because

$0.2 \cdot \min(a; b) = 0.2 \cdot \min(560;\ 320) = 64 \text{ mm} > 30 \text{ mm} = t_g$

The concrete bearing resistance is calculated as

$$f_{jd} = \frac{2}{3} \cdot \frac{k_j \cdot f_{ck}}{\gamma_{Mc}} = \frac{2}{3} \cdot \frac{2.89 \cdot 16}{1.5} = 20.6 \text{ MPa}$$ EN1993-1-8 6.2.5

From the force equilibrium in the vertical direction $F_{Sd} = A_{eff} \cdot f_{jd} - F_{t,Rd}$, is calculated the area of concrete in compression A_{eff} in case of the full resistance of tension part.

$$A_{eff} = \frac{F_{Sd} + F_{Rd,3}}{f_{jd}} = \frac{1\,100 \cdot 10^3 + 183 \cdot 10^3}{20.6} = 62\,282 \text{ mm}^2$$

The flexible base plate is transferred into a rigid plate of equivalent area. The width of the strip c around the column cross section, see Fig. 9.18, is calculated from EN1993-1-8 6.2.5

$$c = t \sqrt{\frac{f_y}{3 \cdot f_{jd} \cdot \gamma_{M0}}} = 30 \cdot \sqrt{\frac{235}{3 \cdot 20.6 \cdot 1.00}} = 58.5 \text{ mm}$$ EN1993-1-8 6.2.5

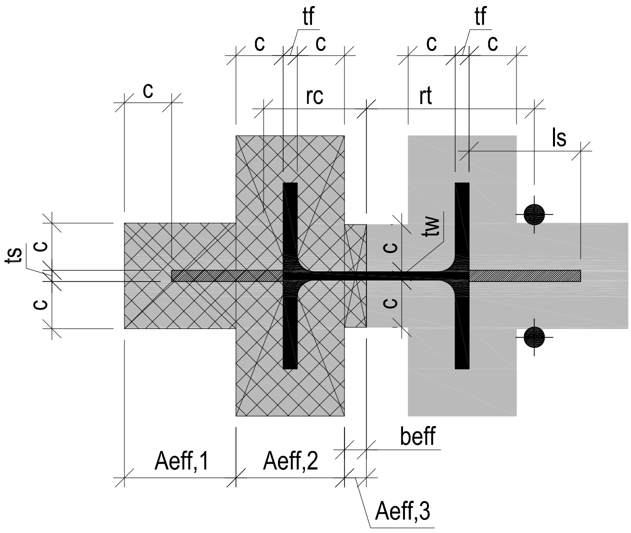

Fig. 9.18 The effective area under the base plate

The effective area is

$$A_{eff,1} = l_s \cdot (2c + t_s) = 120 \cdot (2 \cdot 58.5 + 12) = 15\,480\ \text{mm}^2$$ EN1993-1-8 6.2.5

$$A_{eff,2} = (2c + 200) \cdot (2c + t_f) = (2 \cdot 58.5 + 200) \cdot (2 \cdot 58.5 + 15) = 41\,844\ \text{mm}^2$$

$$A_{eff,3} = A_{eff} - \left(A_{eff,1} + A_{eff,2}\right) = 62\,282 - (15\,480 + 41\,844) = 4\,958\ \text{mm}^2$$

The active effective width is calculated from known area in compression

$$b_{eff} = \frac{A_{eff,3}}{2\,c + t_w} = \frac{4\,958}{2 \cdot 58.5 + 9} = 39.3\ \text{mm}$$ EN1993-1-8 6.2.5

<u>Step 3 Assembly for resistance</u>

The gravity centre of effective area

$$x_t = \frac{A_{eff,1} \cdot x_{t1} + A_{eff,2} \cdot x_{t2} + A_{eff,3} \cdot x_{t3}}{A_{eff}}$$

$$= \frac{15\,480 \cdot \frac{l_s}{2} + 41\,844 \cdot \left(l_s + \frac{2c + t_f}{2}\right) + 4\,958 \cdot \left(l_s + 2c + t_f + \frac{b_{eff}}{2}\right)}{62\,282}$$

$$= \frac{15\,480 \cdot 60 + 41\,844 \cdot \left(120 + \frac{2 \cdot 58.5 + 15}{2}\right) + 4\,958 \cdot \left(120 + 2 \cdot 58.5 + 15 + \frac{39.3}{2}\right)}{62\,282}$$

$$= 161.5\ \text{mm}$$

The lever arm of concrete to the column axes of symmetry is calculated as

$$r_c = \frac{h_c}{2} + 120 + c + \left(b_{eff} - \frac{53}{2}\right) - x_t = \frac{200}{2} + 120 + 58.5 + (39.3 - 26.5) - 161.5 =$$

$= 129.8$ mm

The lever arm of concrete to the column axes of symmetry is calculated as

$$r_t = \frac{h_c}{2} + 70 + (\frac{53}{2} - b_{eff}) = 170 + (26.5 - 39.3) = 157.2 \text{ mm}$$

EN1993-1-1 cl 6.2.5

Moment resistance of column base is

$$M_{Rd} = F_{T,3,Rd} \cdot r_t + A_{eff} \cdot f_{jd} \cdot r_c$$

$$M_{Rd} = 183 \cdot 10^3 \cdot 157.2 + 62\,282 \cdot 20.6 \cdot 129.8 = 195.3 \text{ kNm}$$

Under acting normal force $N_{Sd} = 1\,100$ kN is the moment resistance

$M_{Rd} = 195.3$ kNm

Step 4 Resistance of the end of column

The design resistance in poor compression is

EN1993-1-1 cl 6.23

$$N_{pl,Rd} = \frac{A \cdot f_y}{\gamma_{M0}} = \frac{(A_{HE200B} + 2 \cdot l_s \cdot t_s) \cdot 235}{1.00} = \frac{(7\,808 + 2 \cdot 120 \cdot 12) \cdot 235}{1.00} = 2\,511.7 \text{ kN}$$

$> N_{Rd} = 1\,100$ kN

and column bending resistance

$$M_{pl,Rd} = \frac{W_{pl} \cdot f_{yk}}{\gamma_{M0}}$$

$$W_{pl} = W_{pl,s} + W_{pl,HEB} = 2 \cdot l_s \cdot t_s \cdot z_s + 642.5 \cdot 10^3 = 2 \cdot 12 \cdot 120 \cdot 160 + 642.5 \cdot 10^3 =$$

$$= 1\,103.3 \cdot 10^3 \text{ mm}^3$$

$$M_{pl,Rd} = \frac{W_{pl} \cdot f_{yk}}{\gamma_{M0}} = \frac{1\,103.3 \cdot 10^3 \cdot 235}{1.00} = 259.3 \text{ kNm}$$

The interaction of normal force reduces moment resistance

EN1993-1-1 cl 6.29

$$M_{Ny,Rd} = M_{pl,Rd} \frac{1 - \frac{N_{Sd}}{N_{pl,Rd}}}{1 - 0.5 \frac{A - 2\,b\,t_f}{A}} = 259.3 \cdot \frac{1 - \frac{1\,100}{2\,511.7}}{1 - 0.5 \frac{7\,808 - 2 \cdot 200 \cdot 15}{7\,808}} = 164.8 \text{ kNm}$$

The column base is designed on acting force even for column resistance.

Note

The resistance of the base plate is limited by the tension resistance of two headed studs M 24; 183.0 kN. The elastic behaviour is expected till the 2/3 of the bending resistance of the base plate; 2/3 · 267.7 = 178.5 kN, which comply for the bending moment at SLS about 195.3 · 178.5/183.0 kNm.

9.4 Column base with anchor plate

Evaluate the resistance of the column base shown in Fig. 9.19 using component method. The Column HE 200 B is loaded by the normal force F_{Ed} = 45 kN and by the bending moment M_{Ed} = 20 kNm. The concrete block designed for the particular soil conditions is made out of concrete strength C30/37 and has dimensions of 1600 x 1600 x 1000 mm. The base plate thickness is 30 mm and the anchor plate 10 mm. The steel grade is S355 and the safety factors are considered as γ_{Mc} = 1.50; γ_{M0} = 1.00 and γ_{M2} = 1.25.

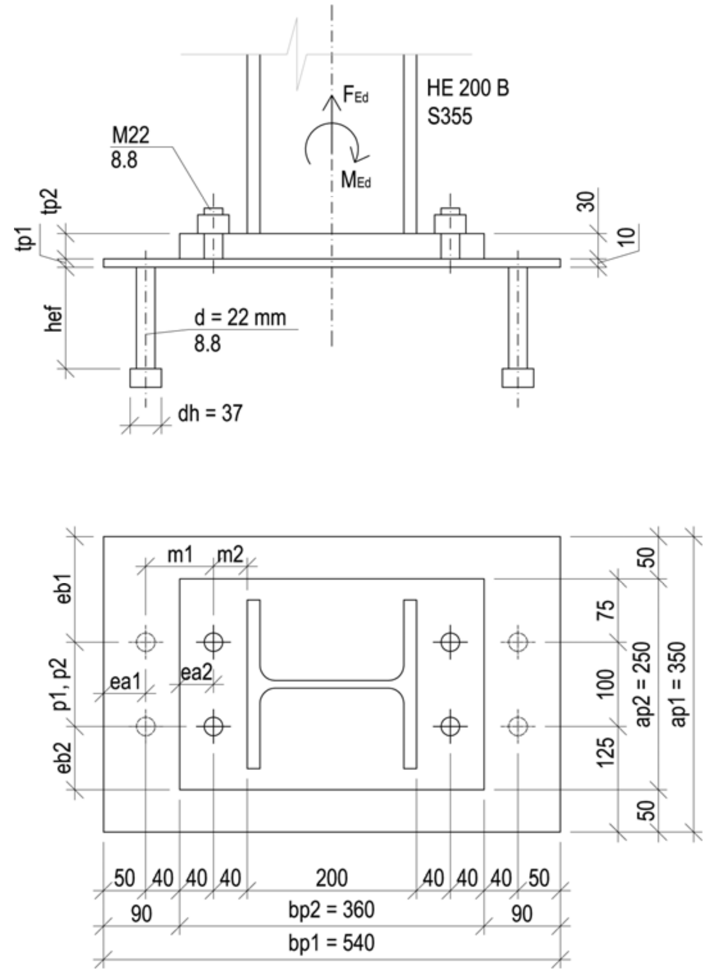

Fig. 9.19 Designed column base with anchor plate

Procedure

The calculation follows the Component method procedure for the column bases:

1 Components in tension

1.1. Threaded studs in tension

1.2. Punching of the anchor plate under threaded studs

1.3. Base plate in bending

1.4. Threaded studs in shear and bearing

1.5. Headed studs in tension

1.6. Punching of the anchor plate above the headed studs

1.7. Concrete cone failure without reinforcement
1.8. Concrete cone failure with reinforcement
1.9. Pull out failure of headed studs
1.10. T stub of the anchor plate in bending
1.11. Anchor plate in tension
1.12. Headed studs in shear
1.13. Pry-out failure of headed stud
1.14. Reduction of vertical resistance
of the threaded stud (tensile and punching resistance) and
the headed studs (tensile resistance, concrete cone failure, stirrups failure, bond failure the threaded stud)
Reduction of horizontal resistance
of the threaded stud (shear and bearing resistance) and
the headed studs (shear and pry out resistance)
1.15. Interaction in shear and tension for threaded and the headed studs
2 Component in compression
3 Assembly for resistance
3.1 Base plate resistance
3.2 End column resistance
3.3 Elastic resistance for Serviceability limit state
4 Connection stiffness
4.1 Component´s stiffness
4.2 Assembly for stiffness

Step 1 Components in tension

Step 1.1 Threaded studs in tension

The resistance of the component threaded studs in tension, with d = 22 mm, strength 8.8, f_{ub} = 800 N/mm^2, with number of studs is n = 2, area of one stud is A_s = 303 mm^2 and coefficient k_2 = 0.9, is

$$F'_{t,Rd,2} = \frac{n \cdot k_2 \cdot A_s \cdot f_{ub}}{\gamma_{M2}} = \frac{2 \cdot 0.9 \cdot 303 \cdot 800}{1.25} = 349.1 \text{ kN}$$

EN1993-1-8
Tab. 3.41

The resistance of one stud is 174.5 kN.

Step 1.2 Punching of the anchor plate under threaded studs

The resistance in punching of the anchor plate, for f_u = 510 MPa and the effective width of studs weld a_w = 1 mm, is

$$F_{p,Rd,V} = \frac{n \cdot A_v \cdot f_{uk}}{\sqrt{3} \cdot \gamma_{M2}} = \frac{n \cdot t_{p1} \cdot l_{v,eff,1} \cdot f_{uk}}{\sqrt{3} \cdot \gamma_{M2}} = \frac{n \cdot t_{p1} \cdot 2\,\pi \cdot \left(a_w + \frac{d_{stud}}{2}\right) \cdot f_{uk}}{\sqrt{3} \cdot \gamma_{M2}} =$$ DMI Ch. 4.3

$$= \frac{2 \cdot 10 \cdot 2\pi \cdot \left(1 + \frac{22}{2}\right) \cdot 510}{\sqrt{3} \cdot 1.25} = 355.2 \text{ kN}$$

The resistance of one stud is 177.6 kN.

Step 1.3 Base plate in bending

The base plate has thickness t_{p2} = 30 mm, width a_{p2} = 250 mm, yield strength f_{yk} = 355 N/mm^2, m_2 = 33.2 mm, e_{a2} = 40 mm, e_{b2} = 75 mm, and p_2 = 100 mm, see in Fig. 9.18. Headed stud lever arm for fillet weld $a_{wf} = 6$ mm is

$$m = 40 - 0.8 \cdot a_{wf} \cdot \sqrt{2} = 40 - 0.8 \cdot 6 \cdot \sqrt{2} = 33.2 \text{ mm}$$ DM I Ch. 4.1.1

The T-stub length, in base plate are the prying forces not taken into account, is

$$l_{eff,2} = \min \left\{ \begin{array}{c} 4\,m + 1.25\,e_a = 4 \cdot 33.2 + 1.25 \cdot 40 = 182.9 \\ 2\,\pi\,m = 2\,\pi \cdot 33.2 = 208.7 \\ b \cdot 0.5 = 250 \cdot 0.5 = 125.0 \\ 2\,m + 0.625\,e_a + 0.5\,p = 2 \cdot 33.2 + 0.625 \cdot 40 + 0.5 \cdot 100 = 141.4 \\ 2\,m + 0.625\,e_a + e_b = 2 \cdot 33{,}2 + 0.625 \cdot 40 + 75 = 166.4 \\ 2\,\pi\,\,m + 4\,e_b = 2\pi \cdot 33.2 + 4 \cdot 75 = 508.7 \\ 2\,\pi\,\,m + 2\,p = 2\,\pi \cdot 33.2 + 2 \cdot 100 = 408.7 \end{array} \right\}$$ EN1993-1-8 cl 6.2.6.5

$$l_{eff,2} = 125 \text{ mm}$$

Resistance of rigid plate T-stub in bending is verified for three possible failure modes

Mode 1

$$F_{T,1,Rd,2} = \frac{4 \cdot l_{eff,2} \cdot m_{pl,1,Rd,2}}{m} = \frac{4 \cdot l_{eff,2} \cdot \frac{t_{p,2}^2 \cdot f_{yk}}{4 \cdot \gamma_{M0}}}{m} = \frac{4 \cdot 125 \cdot \frac{30^2 \cdot 355}{4 \cdot 1.0}}{33.2} = 1\,202.5 \text{ kN}$$ EN1993-1-8 cl 6.2.4.1

Mode 2

$$F_{T,2,Rd,2} = \frac{2 \cdot l_{eff,2} \cdot m_{pl,2,Rd,2} + \sum F_{t,Rd}\,.\,n}{m+n} = \frac{2 \cdot l_{eff,2} \cdot \frac{t_{p,2}^2 \cdot f_{yk}}{4 \cdot \gamma_{M0}} + \sum F_{t,Rd} \cdot n}{m+n} =$$

$$= \frac{2 \cdot 125 \cdot \frac{30^2 \cdot 355}{4 \cdot 1.0} + 349 \cdot 10^3 \cdot 40}{33.2 + 40} = 463.5 \text{ kN}$$ EN1993-1-8 cl 6.2.4.1

Mode 3

$$\sum F_{t,Rd} = \min(F'_{t,Rd};\ F_{p,Rd,V}) = \min(349.1; 355.2) = 349.1\ \mathrm{kN}$$

EN1993-1-8 Tab. 3.41

$$F_{T,3,Rd,2} = \sum F_{t,Rd} = 349.1\ \mathrm{kN}$$

Decisive is Mode 3 with failure in threaded studs in tension $F_{t,3,Rd}$ = 349.1 kN.

Step 1.4 Threaded studs in shear and bearing

Threaded studs have diameter d = 22 mm, d_0 = 24 mm, base plate thickness t_{p2} = 30 mm, coefficient e_1 = 40 mm, e_2 = 75 mm, tensile strength f_u = 510 N/mm^2, f_{ub} = 800 N/mm^2, area of one stud A_s = 303 mm^2; α_v = 0.6; γ_{M2} = 1.25 see in Fig. 9.18.

EN1993-1-8 Tab. 3.41

$$F_{v,Rd} = \frac{n \cdot \alpha_v \cdot f_{ub} \cdot A_s}{\gamma_{M2}} = \frac{2 \cdot 0.6 \cdot 800 \cdot \pi \cdot \left(\frac{22}{2}\right)^2}{1.25} = 291.9\ \mathrm{kN}$$

The resistance of one stud is 146.0 kN.

EN1993-1-8 Tab. 3.41

$$F_{b,Rd,2} = \frac{n \cdot k_1 \cdot \alpha_b \cdot f_u \cdot d \cdot t}{\gamma_{M2}} = \frac{2 \cdot 2.5 \cdot 0.56 \cdot 510 \cdot 22 \cdot 30}{1.25} = 754.0\ \mathrm{kN}$$

The resistance of one stud is 377.0 kN.

where

$$k_1 = \min\left\{2.8\frac{e_2}{d_0} - 1.7; 2.5\right\} = \min\left\{2.8\frac{75}{24} - 1.7; 2.5\right\} = \min\{7.05; 2.5\} = 2.5$$

$$\alpha_b = \min\left\{\frac{f_{ub}}{f_u}; 1.0; \frac{e_1}{3d_0}\right\} = \min\left\{\frac{800}{510}; 1.0; \frac{40}{3 \cdot 24}\right\} = \min\{1.57; 1.0; 0.56\} = 0.56$$

Step 1.5 Headed studs in tension

The resistance of headed studs in tension, of diameter d = 22 mm and material 8.8, with tensile strength f_{ub} = 800 N/mm^2, two studs n = 2 and coefficient k_2 = 0.9; is

EN1993-1-8 Tab. 3.41

$$F'_{t,Rd} = \frac{n \cdot k_2 \cdot A_s \cdot f_{ub}}{\gamma_{M2}} = \frac{2 \cdot 0.9 \cdot \pi \cdot \left(\frac{22}{2}\right)^2 \cdot 800}{1.25} = 437.9\ \mathrm{kN}$$

The resistance of one stud is 219.0 kN.

Step 1.6 Punching of the anchor plate above the headed studs

The resistance in punching of the anchor plate, for f_u = 510 N/mm² and the effective width of studs weld a_w = 1 mm, is

DM I
Ch. 4.3

$$F_{p,Rd,V} = \frac{n \cdot A_v \cdot f_{uk}}{\sqrt{3} \cdot \gamma_{M2}} = \frac{n \cdot t_{p1} \cdot l_{v,eff,1} \cdot f_{uk}}{\sqrt{3} \cdot \gamma_{M2}} = \frac{n \cdot t_{p1} \cdot 2\,\pi \cdot \left(a_w + \frac{d_{stud}}{2}\right) \cdot f_{uk}}{\sqrt{3} \cdot \gamma_{M2}} =$$

$$= \frac{2 \cdot 10 \cdot 2\pi \cdot \left(1 + \frac{22}{2}\right) \cdot 510}{\sqrt{3} \cdot 1.25} = 355.2 \text{ kN}$$

The resistance of one headed stud is 177.6 kN.

Step 1.7 Concrete cone failure without reinforcement

The resistance of concrete cone failure without reinforcement, for the concrete block made out of concrete strength C30/37, f_{ck} = 30 N/mm², k_1 = 12.7; and length of headed studs h_{ef} = 200 mm, is

DM I
Chap. 3.1.2

$$N_{Rd} = N^0_{Rk,c} \cdot \psi_{A,N} \cdot \psi_{s,N} \cdot \psi_{re,N} / \gamma_{Mc}$$

$$N^0_{Rk,c} = k_1 \cdot h_{ef}^{1.5} \cdot f_{ck}^{0.5} = 12.7 \cdot 200^{1.5} \cdot 30^{0.5} \text{ N} = 196.8 \text{ kN}$$ Eq. (3.7)

$$\psi_{A,N} = \frac{A_{c,N}}{A^0_{c,N}} = \frac{420\,000}{360\,000} = 1.17$$ Eq. (3.8)

Eq. (3.9)

$$A^0_{c,N} = s^2_{cr,N} = \left(2\, c_{cr,N}\right)^2 = \left(2\,(1.5 \cdot h_{ef})\right)^2 = \left(2(1.5 \cdot 200)\right)^2 = 360\,000 \text{ mm}^2$$

$$A_{c,N} = \left((1.5 \cdot h_{ef}) \cdot 2\right) \cdot (1.5 \cdot h_{ef} + p + 1.5 \cdot h_{ef}) =$$

$$= \left((1.5 \cdot 200) \cdot 2\right) \cdot (1.5 \cdot 200 + 100 + 1.5 \cdot 200) = 420\,000 \text{ mm}^2$$

Since maximum edge distance is $c < c_{cr} = 1.5\, h_{ef} = 300$ mm and $\psi_{s,N} = 1.0$

There is no closely spaced reinforcement and $\psi_{re,N} = 1.0$

$$N_{Rk,c} = 196.8 \cdot 1.17 \cdot 1.0 \cdot 1.0 = 230.3 \text{ kN}$$

$$N_{Rd,c} = \frac{N_{Rk,c}}{\gamma_{Mc}} = \frac{230.3}{1.5} = 153.5 \text{ kN}$$

Step 1.8 Concrete cone failure with reinforcement

For concrete cone failure with reinforcement, with diameter of headed studs d = 22 mm and diameter of stirrups d_s = 8 mm, is factor for support of reinforcement

$$\psi_{supp} = 2.5 - \frac{x}{h_{ef}} = 2.5 - \frac{\frac{d}{2} + d_{s,a} + \frac{d_{s,t}}{\tan 35°}}{h_{ef}} = 2.5 - \frac{\frac{d}{2} + \left(5 \cdot \frac{d_s}{2} - \frac{d}{2}\right) + \frac{\left(\frac{d_s}{2} + 10\right)}{\tan 35°}}{h_{ef}} =$$ DM I Eq. (3.48)

$$= 2.5 - \frac{\frac{22}{2} + \left(5 \cdot \frac{8}{2} - \frac{22}{2}\right) + \frac{\left(\frac{8}{2} + 10\right)}{\tan 35°}}{200} = 2.3$$

and resistance

DM I Eq. (3.47)

$$N_{Rd,max} = \frac{\psi_{supp} \cdot N_{Rk,c}}{\gamma_{Mc}} = \frac{2.3 \cdot 230.2}{1.5} = 353.0 \text{ kN}$$

with DM I Eq. (3.13)

$$k_{c,de} = \alpha_c \cdot \sqrt{f_{ck} \cdot h_{ef}} \cdot \psi_{A,N} \cdot \psi_{s,N} \cdot \psi_{re,N} = -537 \cdot \sqrt{30 \cdot 200} \cdot 1.17 \cdot 1.0 \cdot 1.0 =$$

$$= -48.7 \text{ kN/mm}$$

where
α_c = -537 is factor of component concrete break out in tension

Yielding of reinforcement will occur for DM I Eq. (3.16)

$$N_{Rd,1} = N_{Rd,s,re} + N_{Rd,c} + \delta_{Rd,s} \cdot k_{c,de} =$$

DM I Eq. (3.16)

$$= A_{s,re} \cdot \frac{f_{yk,s}}{\gamma_{Ms}} + N_{Rd,c} + \frac{2 \cdot N_{Rd,s,re}{}^2}{\alpha_s \cdot f_{ck} \cdot d_{s,re}^4 \cdot (n \cdot n_{re})^2} \cdot k_{c,de} =$$

$$= n \cdot n_{re} \cdot \pi \cdot \left(\frac{d_{s,re}^2}{4}\right) \cdot \frac{f_{yk,s}}{\gamma_{Ms}} + N_{Rd,c} + \frac{2 \cdot \left(n \cdot n_{re} \cdot \pi \cdot \left(\frac{d_{s,re}^2}{4}\right) \cdot \frac{f_{yk,s}}{\gamma_{Ms}}\right)^2}{\alpha_s \cdot f_{ck} \cdot d_{s,re}^4 \cdot (n \cdot n_{re})^2} \cdot k_{c,de} =$$

$$= 2 \cdot 4 \cdot \pi \cdot \left(\frac{8^2}{4}\right) \cdot \frac{500}{1.15} + 153.5 + \frac{2 \cdot \left(2 \cdot 4 \cdot \pi \cdot \left(\frac{8^2}{4}\right) \cdot \frac{500}{1.15}\right)^2}{12100 \cdot 30 \cdot 8^4 \cdot (2 \cdot 4)^2} \cdot (-48.7) =$$

$$= 174.8 + 153.5 + 0.642 \cdot (-48.7) = 297.0 \text{ kN}$$

where

α_s = 12 100	is factor of the component stirrups
n_{re} = 4	is total number of legs of shafts
$N_{Rd,s,re}$	is design tension resistance of the stirrups for tension failure [N]
$d_{s,re}$ = 8 mm	is nominal diameter of the stirrup
d_p = 25 mm	is the covering
$f_{yk,s}$ = 500 N/mm²	is design yield strength of the stirrups
γ_{Ms} = 1.15	is the partial safety factor
l_1	is anchorage length [mm]

Anchorage failure resistance of the of reinforcement is

$$N_{Rd,2} = N_{Rd,b,re} + N_{Rd,c} + \delta_{Rd,b} \cdot k_{c,de} = \sum n_{re} \cdot l_1 \cdot \pi \cdot d_{s,re} \cdot \frac{f_{bd}}{\alpha} + N_{Rd,c} + \delta_{Rd,b} \cdot k_{c,de} =$$

DM I

Eq. (3.20)

DM I

Eq. (3.21)

$$= n \cdot n_{re} \cdot l_1 \cdot \pi \cdot d_s \cdot \frac{f_{bd}}{\alpha} + N_{Rd,c} + \frac{2 \cdot N_{Rd,b,re}^2}{\alpha_s \cdot f_{ck} \cdot d_{s,re}^4 \cdot n_{re}^2} \cdot k_{c,de} =$$

$$= n \cdot n_{re} \cdot \left(h_{ef} - d_p - d_{s,t} - \frac{d_{s,a}}{1.5}\right) \cdot \pi \cdot d_s \cdot \frac{2.25 \cdot \eta_1 \cdot \eta_2 \cdot f_{ctk;0,05}}{\alpha \cdot \gamma_{Mc}} + N_{Rd,c}$$

$$+ \frac{2 \cdot \left(n \cdot n_{re} \cdot l_1 \cdot \pi \cdot d_s \cdot \frac{f_{bd}}{\alpha}\right)^2}{\alpha_s \cdot f_{ck} \cdot d_{s,re}^4 \cdot n_{re}^2} k_{c,de} =$$

$$= n \cdot n_{re} \cdot \left(h_{ef} - d_p - \left(\frac{d_s}{2} + 10\right) - \frac{\left(5 \cdot \frac{d_s}{2} - \frac{d}{2}\right)}{1.5}\right) \cdot \pi \cdot d_s \cdot \frac{2.25 \cdot \eta_1 \cdot \eta_2 \cdot f_{ctk;0,05}}{\alpha \cdot \gamma_{Mc}} + N_{Rd,c} +$$

$$\frac{2 \cdot \left(n \cdot n_{re} \cdot \left(h_{ef} - d_p - \left(\frac{d_s}{2} + 10\right) - \frac{\left(5 \cdot \frac{d_s}{2} - \frac{d}{2}\right)}{1.5}\right) \cdot \pi \cdot d_s \cdot \frac{2.25 \cdot \eta_1 \cdot \eta_2 \cdot f_{ctk;0,05}}{\alpha \cdot \gamma_{Mc}}\right)^2}{\alpha_s \cdot f_{ck} \cdot d_{s,re}^4 \cdot n_{re}^2} \cdot k_{c,de} =$$

$$= 2 \cdot 4 \cdot \left(200 - 25 - \left(\frac{8}{2} + 10\right) - \frac{\left(5 \cdot \frac{8}{2} - \frac{22}{2}\right)}{1.5}\right) \cdot \pi \cdot 8 \cdot \frac{2.25 \cdot 1.0 \cdot 1.0 \cdot 2.0}{0.49 \cdot 1.5} + 153.5$$

$$+ \frac{2 \cdot \left(2 \cdot 4 \cdot \left(200 - 25 - \left(\frac{8}{2} + 10\right) - \frac{\left(5 \cdot \frac{8}{2} - \frac{22}{2}\right)}{1.5}\right) \cdot \pi \cdot 8 \cdot \frac{2.25 \cdot 1.0 \cdot 1.0 \cdot 2.0}{0.49 \cdot 1.5}\right)^2}{12100 \cdot 30 \cdot 8^4 \cdot (2 \cdot 4)^2} \cdot (-48.7)$$

$$= 190.8 + 153.5 + 0.765 \cdot (-48.7) = 307.0 \text{ kN}$$

where

EN1992-1-1

l_1 is anchorage length [mm]

d_s is diameter of stirrups [mm]

$\alpha = 0.7 \cdot 0.7 = 0.49$ is factor for hook effect and large concrete cover

f_{bd} is for C30/37 grade concrete is $2.25 \cdot \frac{2.0}{1.5} \cdot 1.0 \cdot 1.0 = 3.0$ N/mm²

$\eta_1 = 1.0$ is coefficient of bond conditions for vertical stirrups and 0.7 for horizontal stirrups

$\eta_2 = 1.0$ is coefficient of bond conditions for dimension ≤ 32 mm and $(132 - d_s)/100$ for dimension ≥ 32 mm

The resistance of concrete cone failure with reinforcement is

$$\min\left(N_{Rd,max}; N_{Rd,1}; N_{Rd,2}\right) = \min(353.0; 297.0; 307.0) = 297.0 \text{ kN}$$

Step 1.9 Pull-out failure of headed studs

The resistance of pull-out failure of headed studs, with diameter of stud d = 22 mm, diameter of stud's head d_h = 37 mm, concrete C30/37 with compressive strength f_{ck} = 30 N/mm^2 and the characteristic ultimate bearing pressure at ultimate limit state under the headed of stud $p_{uk} = 12 \cdot f_{ck}$ N/mm^2, is DM I Eq. (3.20)

DM I Eq. (3.21)

$$N_{Rk,p} = n \cdot p_{uk} \cdot A_h = n \cdot 12 \cdot f_{ck} \cdot \frac{\pi}{4} \cdot \left(d_h^2 - d^2\right) = 2 \cdot 12 \cdot 30 \cdot \frac{\pi}{4} \cdot (37^2 - 22^2) = 500.5 \text{ kN}$$

$$N_{Rd,p} = \frac{N_{Rk,p}}{\gamma_{Mc}} = \frac{500.5}{1.5} = 333.7 \text{ kN}$$

The resistance of one stud is 166.8 kN

Step 1.10 T stub of the anchor plate in bending

The resistance of component T-stub of the anchor plate in bending has thickness t_{p1} = 10 mm, yield strength f_{yk} = 355 N/mm^2, distance of threaded and headed stud m_1 = 80 mm, e_{a1} = 50 mm, e_{b1} = 125 mm and p_1 = 100 mm, see in Fig. 9.18.

Due to small thickness of the anchor plate are the prying forces for evaluation of the effective length of T stub taken into account as

Resistance of anchor plate T-stub in tension is verified for three failure modes, see in Fig. 9.19. For effective length of the T stub

DM I 3.1.5. Eq. 3.31

$$l_{eff,1} = \min \left\{ \begin{array}{c} 4\ m_1 + 1.25\ e_{a1} = 4 \cdot 80 + 1.25 \cdot 50 = 382.5 \\ 2\,\pi\ m_1 = 2\,\pi \cdot 80 = 502.7 \\ 5\ n_1\ d_1 \cdot 0.5 = 220 \cdot 0.5 = 110.0 \\ 2\ m_1 + 0.625\ e_{a1} + 0.5\ p_1 = 2 \cdot 80 + 0.625 \cdot 50 + 0.5 \cdot 100 = 241.3 \\ 2\ m_1\ + 0.625\ e_{a1} + e_{b1} = 2 \cdot 80 + 0.625 \cdot 50 + 93.8 = 285.0 \\ \pi\ m_1 + 2\ e_{b1} = \pi \cdot 80 + 2 \cdot 93.8 = 721.4 \\ \pi\ m_1 + p_1 = \pi \cdot 80 + 100 = 351.3 \end{array} \right\}$$

$$l_{eff,1} = 110.0 \text{ mm}$$

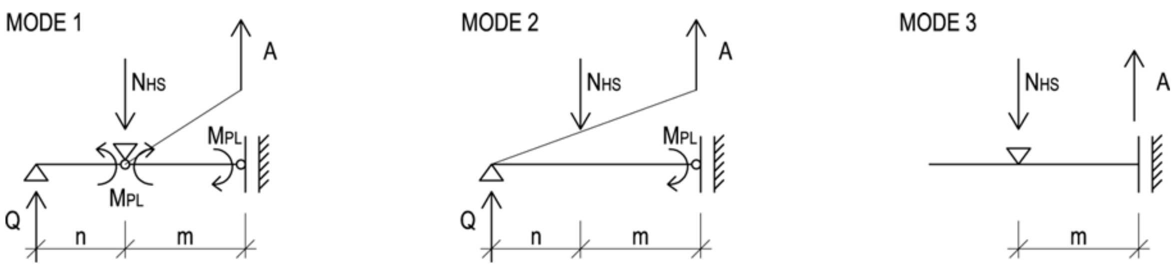

Fig. 9.19 T-stub in tension and forces in the individual failure modes

Mode 1

$$F_{T,1,Rd,ap} = \frac{4 \cdot l_{eff,1} \cdot m_{pl,Rd,1}}{m} = \frac{4 \cdot l_{eff,1} \cdot \frac{t_{p,1}^2 \cdot f_{yk}}{4 \cdot \gamma_{M0}}}{m} = \frac{4 \cdot 110.0 \cdot \frac{10^2 \cdot 355}{4 \cdot 1.0}}{80} = 48.8 \text{ kN}$$

EN1993-1-8
cl 6.2.4.1

Mode 2

$$F_{T,2,Rd,ap} = \frac{2 \cdot l_{eff,1} \cdot m_{pl,2,Rd,2} + \sum F_{t,Rd} \cdot n}{m + n} = \frac{2 \cdot l_{eff,1} \cdot \frac{t_{p,1}^2 \cdot f_{yk}}{4 \cdot \gamma_{M0}} + \sum F_{t,Rd} \cdot n}{m + n} =$$

EN1993-1-8
cl 6.2.4.1

$$= \frac{2 \cdot 110.0 \cdot \frac{10^2 \cdot 355}{4 \cdot 1.0} + 297.0 \cdot 10^3 \cdot 50}{80 + 50} = 129.1 \text{ kN}$$

Mode 3

$$\sum F_{t,Rd} = \min\left(F'_{t,Rd1};\ F_{p,Rd,V,1};\ N_{Rd,1};\ N_{Rd,p}\right) = \min(437.9;\ 355.2;\ 297.0;\ 333.7)$$
$$= 297.0 \text{ kN}$$

EN1993-1-1
cl 6.2.4.13

$$F_{T,3,Rd,ap} = \sum F_{t,Rd} = 297.0 \text{ kN}$$

Mode 1 is decisive for the thin plate, 48.8 kN, see in Fig. 9.20.

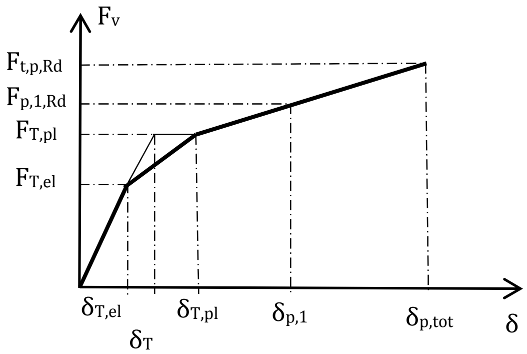

Fig. 9.20 Vertical forces F_v and vertical deformation δ of T stub

Step 1.11 Anchor plate in tension

The anchor plate in tension resistance is

$$F_{t,apRd} = A_{ap,1} \cdot \frac{f_{yk}}{\gamma_{M0}} = t_{p,1} \cdot b_{ap,eff} \cdot \frac{f_{yk}}{\gamma_{M0}} = 10 \cdot 2 \cdot \left(22 + 2 \cdot \sqrt{2} \cdot 1\right) \cdot \frac{355}{1.0} = 176.3 \text{ kN}$$

DM I
Chap. 4.4

where

$$b_{ap,eff} = n_1 \cdot \left(d_1 + 2 \cdot \sqrt{2} \cdot a_w\right)$$

studs weld effective thickness a_w = 1 mm

Step 1.12 Headed studs in shear

The shear resistance of headed studs, with material 8.8, strength f_{ub} = 800 N/mm^2, α_v = 0.6; γ_{M2} = 1.25; is

$$F_{v,Rd} = \frac{n \cdot \alpha_v \cdot f_{ub} \cdot A_s}{\gamma_{M2}} = \frac{2 \cdot 0.6 \cdot 800 \cdot \pi \cdot \left(\frac{22}{2}\right)^2}{1.25} = 291.9 \text{ kN}$$

EN1993-1-8
Tab. 3.41

The resistance of one stud is 146.0 kN.

Step 1.13 Pry-out failure of headed stud

The resistance in pry-out failure of headed studs for is

$V_{Rd,CP} = 2 \cdot N_{Rd,c} = 2 \cdot 153.5 = 307.0 \text{ kN}$

DM I
Ch. 3.2

Step 1.14 Reduction of resistance in the vertical/horizontal direction

For the calculation of plastic deformation is used model of continues beam with three plastic hinges at supports and under applied load, see in Fig. 9.21.

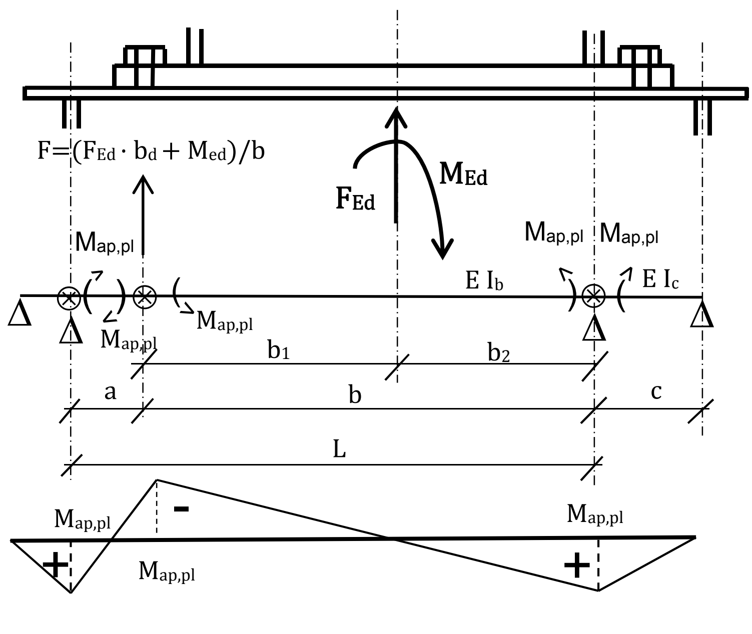

Fig. 9.21 Model of continues beam with three plastic hinges

$A = \min\left(F_{T,1,Rd,1};\ F_{T,2,Rd,1};\ F_{T,3,Rd,1}\right) = \min\ (48.8;\ 126.1; 296.7) =\ 48.8 \text{ kN}$

DM I
Ch. 4.4

$$Q = \frac{l_{eff,1} \cdot m_{pl,Rd,1}}{n} \cdot 2 = \frac{l_{eff,1} \cdot \frac{t_{p,1}^2 \cdot f_{yk}}{4 \cdot \gamma_{M0}}}{n} \cdot 2 = \frac{110.0 \cdot \frac{10^2 \cdot 355}{4 \cdot 1.0}}{50} \cdot 2 = 39.1 \text{ kN}$$

$$N_{HS,T} = A + Q = 48.8 + 39.1 = 87.9 \text{ kN}$$

Plastic deformation is calculated, see Fig. 9.21, for moment resistance

$$M_{pl} = \frac{b_{p1} \cdot t_{p1}^2}{4} \cdot \frac{f_{yk}}{\gamma_{M0}} = \frac{350 \cdot 10^2}{4} \cdot \frac{355}{1} = 3.1 \text{ kNm}$$

$$I_c = \frac{1}{12} \cdot b_{p1} \cdot t_{p1}^3 = \frac{1}{12} \cdot 350 \cdot 10^3 = 29.2 \ \cdot 10^3 \text{ mm}^4; \ I_b = \infty$$

$$\delta_T = \frac{1}{E\, I_b} \cdot \frac{1}{6} \cdot b^2 \cdot M_{pl} + \frac{1}{E\, I_c} \cdot \frac{1}{3} \cdot b \cdot c \cdot M_{pl} =$$

$$= \frac{1}{210\,000 \cdot \infty} \cdot \frac{1}{6} \cdot 232.5^2 \cdot 3106 + \frac{1}{210\,000 \cdot 29.2} \cdot \frac{1}{3} \cdot 232.5 \cdot 127.5 \cdot 3106 = 0 + 5.2$$
$$= 5.2 \text{ mm}$$

with distance between threaded stud and headed stud a = 80 mm as

$$\delta_{T,pl} = 1.48\ \delta_T = 7.8 \text{ mm}$$

$$\delta_{p,tot} = \delta_{T,pl} + \sqrt{a_{ap}^2 - a^2} = \sqrt{(a + \Delta a)^2 - a^2} = \delta_{T,pl} + \sqrt{\left(a + \frac{a \cdot F_{p,Rd}}{t_{p1} \cdot b_{ap,eff} \cdot E}\right)^2 - a^2} =$$

$$= \ \delta_{T,pl} + \sqrt{\left(a + \frac{a \cdot \frac{A \cdot f_{y,p}}{\gamma_{M0}}}{t_{p1} \cdot b_{ap,eff} \cdot E}\right)^2 - a^2} = \delta_{T,pl} + \sqrt{\left(a + \frac{a \cdot \frac{t_{p1} \cdot b_{p,eff} \cdot f_{y,p}}{\gamma_{M0}}}{t_{p1} \cdot b_{ap,eff} \cdot E}\right)^2 - a^2} =$$ DM I Eq. (4.43)

$$= 7.8 + \sqrt{\left(80 + \frac{80 \cdot 8.88 \cdot \frac{355}{1.0}}{210 \cdot 10^3}\right)^2 - 80^2} = 13.9 \text{ mm}$$

For the plastic deformation at resistance of the anchor plate punching under the threaded studs $F_{p,Rd}$ = 176.28 kN and $F_{p,Rd,V} = A + \frac{F_{p,Rd} \cdot \delta_{p,tot}}{(a+\Delta a)} = 79.0 \text{ kN}$

The acting horizontal force for this deformation is

$$F_{p,Rd,H} = \frac{F_{t,p,Rd} \cdot a}{\delta_{p,tot}} = \frac{79.0 \cdot 80}{13.9} = 454.3 \text{ kN}$$

For the resistance of headed studs in shear V_{Rd} = 291.9 kN is assumed the linear proportion between the axial and horizontal forces, see in Fig. 9.22. The resistance in tension is calculated as

$$F_{p,1,Rd} = F_{T,pl} + \frac{F_{t,p,Rd} - F_{T,pl}}{F_{p,Rd,H}} \cdot V_{Rd} = 48.8 + \frac{79.0 - 48.8}{454.3} \cdot 291.9 = 68.2 \text{ kN}$$

and deformation for $F_{p,1,Rd}$ = 68.2 kN, see in Fig. 9.20, is

$$\delta_{p,1} = \delta_{T,pl} + \frac{F_{p,1,Rd} - F_{T,pl}}{F_{t,p,Rd} - F_{T,pl}} \cdot \delta_{p,tot} = 7.8 + \frac{68.2 - 48.8}{79.0 - 48.8} \cdot 13.9 = 16.7 \text{ mm}$$

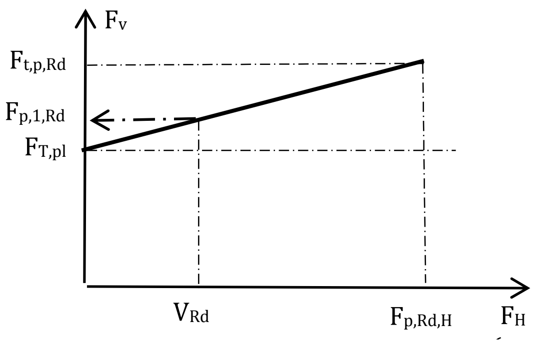

Fig. 9.22 Acting vertical F_v and horizontal F_H forces to the anchor plate

The acting force in headed studs in case of the membrane action in the anchor plate DMI Eq. (4.53)

$$N_{HS,1} = A + Q = 68.2 + 39.1 = 107.3 \text{ kN}$$

Step 1.15 Interaction in shear and tension for treaded and headed studs

For the threaded studs is the interaction in shear and tension

$$\frac{F_{v,Ed}}{F_{v,Rd}} + \frac{F_{t,Ed}}{1.4 \cdot F_{t,Rd}} \leq 1$$

DMI Eq. (4.54) EN1993-1-8 Tab.3.4

$$\frac{291.9}{291.9} + \frac{(107.3 - 48.8) \cdot \left(\frac{220 + 165.9}{140 + 165.9}\right)}{1.4 \cdot 349.1} \leq 1.00$$

1.15 is not ≤ 1

For the headed studs is the interaction in shear and tension

DMI
Eq. (4.54)
EN1993-1-8
Tab.3.4

$$\frac{F_{v,Ed}}{F_{v,Rd}}+\frac{F_{t,Ed}}{1.4\cdot F_{t,Rd}}\leq 1$$

$$\frac{291.9}{291.9}+\frac{107.3-48.8}{1.4\cdot 437.9}\leq 1$$

$1.10 \text{ is not} \leq 1$

For anchoring of headed stud in concrete is the interaction in shear and tension

DMI
Eq. (4.54)

$$\left(\frac{F_{v,Ed}}{F_{v,Rd}}\right)^{\frac{3}{2}}+\left(\frac{F_{t,Ed}}{F_{t,Rd}}\right)^{\frac{3}{2}}\leq 1$$

$$\left(\frac{291.9}{306.1}\right)^{\frac{3}{2}}+\left(\frac{107.3-48.8}{296.7}\right)^{\frac{3}{2}}\leq 1$$

$1.02 \text{ is not} \leq 1$

The full capacity in shear is not achieve due to headed stud resistance. By reducing the acting forces to 80 % it is for interaction of the threaded stud

$$\frac{233.5}{291.9}+\frac{(107.3-48.8)\cdot\left(\frac{220+165.9}{140+165.9}\right)}{1.4\cdot 349.1}\leq 1$$

$0.95 \leq 1$

and for the headed stud

$$\frac{233.5}{291.9}+\frac{107.3-48.8}{1.4\cdot 437.9}\leq 1$$

$0.86 \leq 1$

and for anchoring of headed stud in concrete

$$\left(\frac{233.5}{306.1}\right)^{\frac{3}{2}}+\left(\frac{107.3-48.8}{296.7}\right)^{\frac{3}{2}}\leq 1$$

$0.71 \leq 1$

Step 2 Component in compression

The component base plate in bending and concrete block in compression is calculated for the strength of the concrete block, C30/37, f_{ck} = 30 N/mm^2, and γ_{Mc} = 1.5.

DM I

Ch. 3.4.1

The connection concentration factor is

EN1992-1-1 cl. 6.7(2)

$$a_1 = \min\left\{\begin{matrix} a_1 + 2\,a_r = 250 + 2 \cdot 675 = 1\,600 \\ 3\,a_1 = 3 \cdot 250 = 750 \\ a_1 + h = 250 + 1\,000 = 1\,250 \end{matrix}\right\} = 750 \text{ mm}$$

$$b_1 = \min\left\{\begin{matrix} b_1 + 2b_r = 360 + 2 \cdot 620 = 1\,600 \\ 3\,b_1 = 3 \cdot 360 = 1080 \\ b_1 + h = 360 + 1\,000 = 1\,360 \end{matrix}\right\} = 1\,080 \text{ mm}$$

and $a_1 = 750 > \ a_1 = 250 \text{ mm} \quad b_1 = 1080 > \ b_1 = 360 \text{ mm}$

The above condition is fulfilled and

DM I

Eq. (3.65)

$$k_j = \sqrt{\frac{a_1 \cdot b_1}{a \cdot b}} = \sqrt{\frac{1\,080 \cdot 750}{250 \cdot 360}} = 3.00$$

The concrete bearing resistance is calculated as

$$f_{jd} = \frac{2}{3} \cdot \frac{k_j \cdot f_{ck}}{\gamma_{Mc}} = \frac{2}{3} \cdot \frac{3.00 \cdot 30}{1.5} = 40.0 \text{ N/mm}^2$$

From the force equilibrium in the vertical direction $F_{Sd} = A_{eff} \cdot f_{jd} - F_{t,Rd}$, is calculated the area of concrete in compression A_{eff} in case of the full resistance of tension part

DM I

Eq. (3.71)

$$A_{eff} = \frac{F_{Sd} + F_{Rd,3}}{f_{jd}} = \frac{-45 \cdot 10^3 + 107.3 \cdot 10^3}{40.0} = 1\,557 \text{ mm}^2$$

The flexible base plate is transferred into a rigid plate of equivalent area. The width of the strip c around the column cross section, see Fig. 9.23a, is calculated from

$$c = (t_{p1} + t_{p2})\sqrt{\frac{f_y}{3 \cdot f_{jd} \cdot \gamma_{M0}}} = (30 + 10) \cdot \sqrt{\frac{355}{3 \cdot 40.0 \cdot 1.00}} = 68.8 \text{ mm}$$

EN1993-1-8

cl 6.5.2

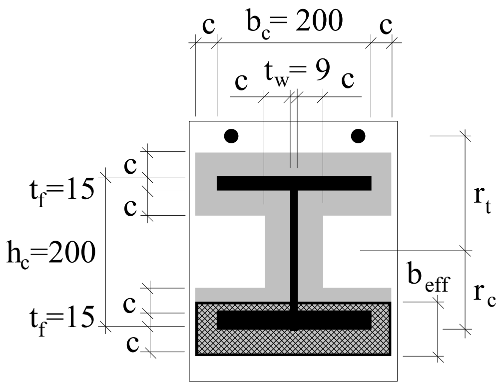

Fig. 9.23a The effective area under the base plate

Step 3 Assembly for resistance

Step 3.1 Column base resistance

The active effective width is calculated as

DM I Ch. 5.1

$$b_{eff} = \frac{A_{eff}}{a_{p2} + 2\,t_{p1}} = \frac{1\,557}{270} = 5.8\text{ mm} < \; t_f + 2\,c = 15 + 2 \cdot 68.8 = 152.6\text{ mm}$$

The lever arm of concrete to the column axes of symmetry, see Fig. 9.23b, is calculated as

$$r_c = \frac{h_c}{2} + c - \frac{b_{eff}}{2} = \frac{200}{2} + 68.8 - \frac{5.8}{2} = 165.9\text{ mm}$$

The moment resistance of the column base is $M_{Rd} = F_{T,min} \cdot r_t + A_{eff} \cdot f_{jd} \cdot r_c$

$$F_{T,min} = 107.3 \cdot \frac{220 + 165.9}{140 + 165.9} = 135.3\text{ kN}$$

$$M_{Rd} = 135.3 \cdot 10^3 \cdot 140 + 1\,557 \cdot 40 \cdot 165.9 = 29.3\text{ kNm}$$

Under acting normal force $N_{Sd} \; = \; -45$ kN the moment resistance in bending is $M_{Rd} \; = \; 29.3$ kNm.

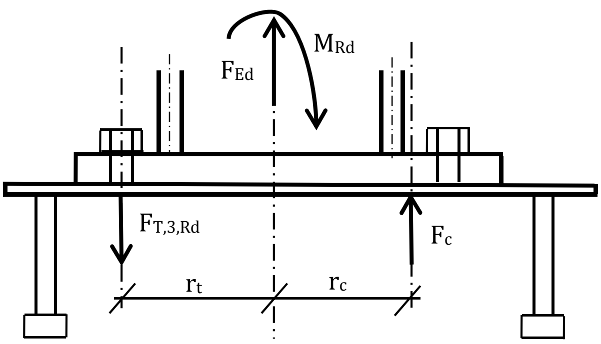

Fig. 9.23b The lever arm of concrete and threaded stud to the column axes

3.2 End of column resistance

The design resistance in poor compression is

EN1993-1-1 cl 6.2.5

$$N_{pl,Rd} = \frac{A \cdot f_y}{\gamma_{M0}} = \frac{7808 \cdot 355}{1.00} = 2\,772 \cdot 10^3 \text{N} > \; N_{Rd} = -45 \text{ kN}$$

The column bending resistance

EN1993-1-1 cl 6.2.9

$$M_{pl,Rd} = \frac{W_{pl} \cdot f_{yk}}{\gamma_{M0}} = \frac{642.5 \cdot 10^3 \cdot 355}{1.00} = 228.1 \text{ kNm}$$

The interaction of normal force reduces moment resistance (this interaction is valid for compression load only)

EN1993-1-8 cl 6.3

$$M_{Ny,Rd} = M_{pl,Rd} \frac{1 - \frac{N_{Sd}}{N_{pl,Rd}}}{1 - 0.5\, \frac{A - 2\, b\, t_f}{A}} = 228.1 \cdot \frac{1 - \frac{0}{2772}}{1 - 0.5\, \frac{7\,808 - 2 \cdot 200 \cdot 15}{7\,808}} = 258.0 \text{ kNm}$$

$$M_{Ny,Rd} = 228.1 \text{ kNm}$$

The column base is designed on acting force only not for column resistance.

Step 3.3 Elastic resistance for Serviceability limit state

DM I Ch. 5.1

The resistance of the base plate is limited by the T stub resistance, 48.8 kN. The elastic-plastic behaviour is expected by reaching the bending resistance of the anchor plate T stub; 87.9 kN, which comply for the bending moment at SLS as 22.7 kNm.

Step 4 Connection stiffness

4.1 Component´s stiffness

The component´s stiffness coefficients are calculated as in Worked example 9.2. The additional component is the anchor plate in bending and in tension and the component threaded stud. In compression are transferring the forces both plates under the column, the base and anchor plates.

The component base plate in bending and the threaded studs in tension

The stiffness coefficient for the threaded stud is assumed as

EN1993-1-8 cl. 6.3

$$k_{b2} = 2.0 \cdot \frac{A_s}{L_b} = 2.0 \cdot \frac{303}{49.5} = 12.2 \text{ mm}$$

The component stiffness coefficients for base plate is calculated as

$$k_{p2} = \frac{0.425 \cdot L_{beff} \cdot t^3}{m^3} = \frac{0.425 \cdot 125 \cdot 30^3}{33.2^3} = 39.2 \text{ mm}$$

EN1993-1-8 cl. 6.3

Component base and anchor plates and concrete block in compression

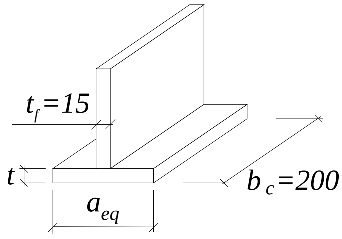

Fig. 9.23c The T stub in compression

The stiffness coefficient for concrete block in compression, see Fig. 9.23c, is calculated for $a_{eq} = t_f + 2.5\,t = 15 + 2.5 \cdot 40 = 115$ mm

where thickness $t = t_1 + t_2$ = 10 + 30 = 40 mm

$$k_c = \frac{E_c}{1.275 \cdot E_s} \cdot \sqrt{a_{eq} \cdot b_c} = \frac{33\,000}{1.275 \cdot 210\,000} \cdot \sqrt{115 \cdot 200} = 18.7 \text{ mm}$$ EN1993-1-8 Tab. 6.11

Component anchor plate in bending and in tension

The component stiffness coefficients for anchor plate is calculated from the bending of the anchor plate as

$$k_{p1} = \frac{0.85 \cdot L_{beff} \cdot t^3}{m^3} = \frac{0.85 \cdot 110.0 \cdot 10^3}{(80 - 2 \cdot \frac{22}{2})^3} = 0.5 \text{ mm}$$ EN1993-1-8 Tab. 6.11

Component headed stud in tension

The component stiffness coefficients for headed studs is calculated as

$$k_{b1} = \frac{n \cdot A_{s,nom}}{L_b} = \frac{2 \cdot \frac{\pi \cdot 22^2}{4}}{8 \cdot 22} = 4.3 \text{ mm}$$ EN1993-1-8 Tab. 6.11

4.2 Assembly for stiffness

The coefficients of the initial stiffness in elongation are assembled to rotational stiffness as in Worked example 9.2. The additional component is the anchor plate in bending and in tension only.

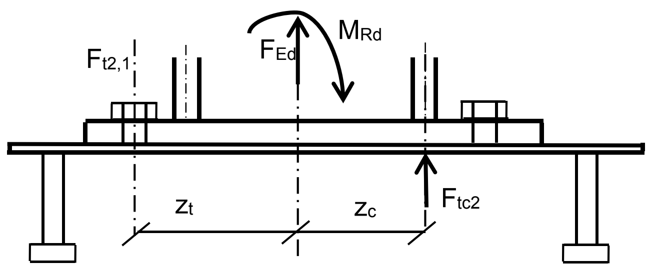

Fig. 9.23d The lever arm in tension and compression

The lever arm of components, see Fig. 9.23d, in tension z_t and in compression z_c to the column base neutral axes are

$$z_t = \frac{h_c}{2} + e_c = \frac{200}{2} + 40 = 140 \text{ mm}$$

$$z_c = \frac{h_c}{2} - \frac{t_f}{2} = \frac{200}{2} - \frac{15}{2} = 92.5 \text{ mm}$$

EN1993-1-8
cl. 6.3.3.1
DMI 6.1.2

The stiffness of tension part, studs, T stubs and concrete parts, is calculated from the stiffness coefficient for base plate and threaded studs

$$k_{t2} = \frac{1}{\frac{1}{k_{b2}} + \frac{1}{k_{p2}}} = \frac{1}{\frac{1}{12.2} + \frac{1}{39.2}} = 9.33 \text{ mm}$$

EN1993-1-8
cl. 6.3.3.1

from the stiffness coefficient for anchor plate and headed studs

$$k_{t1} = \frac{1}{\frac{1}{k_{p1}} + \frac{1}{k_{b1}}} = \frac{1}{\frac{1}{0.5} + \frac{1}{4.3}} = 0.43 \text{ mm}$$

based on eccentricity

EN1993-1-8
cl. 6.3.3.1

$$k_{t1,eff} = \frac{z}{z + 80} \cdot k_{t1} = \frac{232.5}{312.5} \cdot 0.43 = 0.32 \text{ mm}$$

where

EN1993-1-8
cl. 6.3.3.1

$$z = z_t + z_c = 140 + 92.5 = 232.5 \text{ mm}$$

with the effective stiffness coefficient in tension in position of threaded stud

$$k_t = \frac{1}{\frac{1}{k_{t1}} + \frac{1}{k_{t2}}} = \frac{1}{\frac{1}{0.32} + \frac{1}{9.33}} = 0.31 \text{ mm}$$

For the calculation of the initial stiffness of the column base the lever arm is evaluated

$z = 232.5$ mm and

$$a = \frac{k_c \cdot z_c - k_t \cdot z_t}{k_c + k_t} = \frac{18.7 \cdot 92.5 - 0.31 \cdot 140}{18.7 + 0.31} = 88.7 \text{ mm}$$

EN1993-1-8
Tab. 6.11

The bending stiffness is calculated for particular constant eccentricity

$$e = \frac{M_{Rd}}{F_{Sd}} = \frac{20 \cdot 10^6}{45 \cdot 10^3} = 444 \text{ mm}$$

as

EN1993-1-8
cl. 6.3.3.1

$$S_{j,ini} = \frac{e}{e+a} \cdot \frac{E_S \cdot z^2}{\mu \sum_i \frac{1}{k_i}} = \frac{444}{444+88.7} \cdot \frac{210\ 000 \cdot 232.5^2}{1 \cdot \left(\frac{1}{0.31} + \frac{1}{18.7}\right)} = 2\ 888 \cdot 10^6 \text{ Nmm/rad}$$

EN1993-1-8
cl. 6.3.4

$$= 2\ 888 \text{ kNm/rad}$$

Summary

Moment rotational diagram at Fig. 9.23e sums up the behaviour of column base with anchor plate for loading with constant eccentricity.

EN1993-1-8
cl. 6.3.3.1

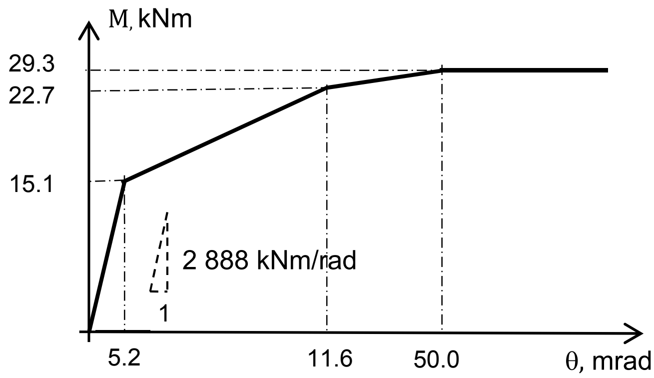

Fig. 9.23e Moment rotational diagram of column base with anchor plate for loading with constant eccentricity

9.5 Simple steel to concrete joint

In this example the calculation of a simple steel-to-concrete joint is demonstrated. A girder is connected to a concrete wall by a simple joint. The load capacity of the joint will be raised by the use of additional reinforcement. The example does only include the design calculation of the joint. The verification of the concrete wall is not included and the local failure of the concrete wall due to the tension force caused by the eccentricity of the shear load is not considered.

Overview about the system

In this example a steel platform is installed in an industrial building. The main building is made of concrete. The system consists of concrete walls and concrete girders. An extra platform is implemented in the building in order to gain supplementary storage room.

The platform consists of primary and secondary girders. The primary girders are made of HE400A and they are arranged in a grid of 4.00 m. On one side they are supported on the concrete wall, on the other side they are supported by a steel column. The concrete wall and the steel beam are connected by a pinned steel-to-concrete joint.

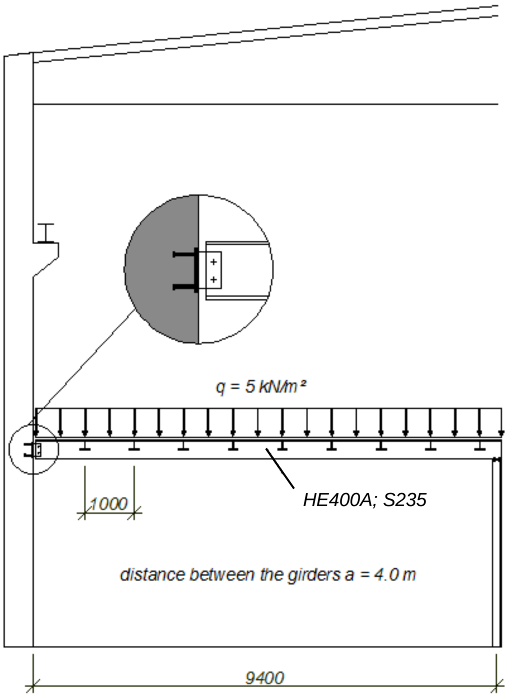

Fig. 9.24 Side view on structure

Structural system and design of the girder

The structural system of the primary girder is a simply supported beam with an effective length of 9.4 m. The cross section of the girder is HE400A. The girder carries load applied to a width a = 4.0 m which is the distance to the next girder, see Fig. 9.25

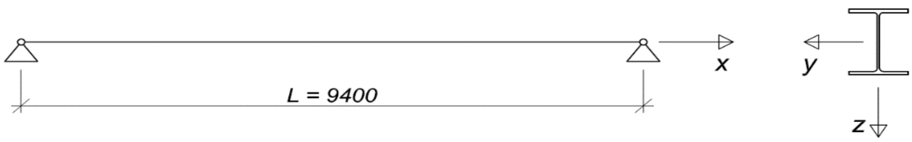

Fig. 9.25 structural system

Load on the girder

Self-weight of the girder with connection	$2.0\ \mathrm{kN/m}$
Floor and other girders	$4.0\ \mathrm{m} \cdot 1.0\,\frac{\mathrm{kN}}{\mathrm{m}^2} = 4.0\ \mathrm{kN/m}$
Dead load	$6.0\ \mathrm{kN/m}$

Live load $4.0\ \text{m} \cdot 5.0\,\frac{\text{kN}}{\text{m}^2} = 20.0\ \text{kN/m}$

Design forces

Maximum shear load

Load comb. according to EN 1990

$$V_{z,Ed} = 9.4\ \text{m}\ \cdot \frac{1.35 \cdot 6.0\,\frac{\text{kN}}{\text{m}} + 1.5 \cdot 20.0\,\frac{\text{kN}}{\text{m}}}{2} = 179\ \text{kN}\ \approx 180\ \text{kN}$$

Maximum bending moment

$$M_{y,Ed} = (9.4\ \text{m})^2\ \cdot \frac{1.35 \cdot 6.0\,\frac{\text{kN}}{\text{m}} + 1.5 \cdot 20.0\,\frac{\text{kN}}{\text{m}}}{8} = 420\ \text{kNm}$$

Verification of the girder section

Next to the joint $V_{z,Ed} = 180\ \text{kN} \leq V_{pl,z,Rd} = 777.8\ \text{kN}$

In the middle of the girder $M_{y,Ed} = 420\ \text{kNm} \leq M_{pl,y,Rd} = 602.1\ \text{kNm}$

The girder is stabilized against lateral torsional buckling by the secondary girders, which have a distance of 1.0 m. Lateral torsional buckling is not examined in this example. The example only includes the design calculation of the joint. The verification of the concrete wall is not included.

Overview of the joint

EN1993-1-1

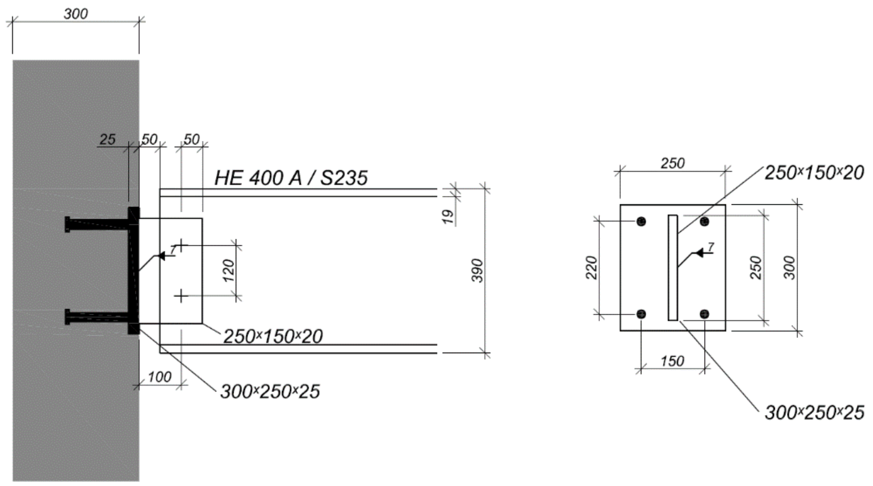

Fig. 9.26 Joint geometry

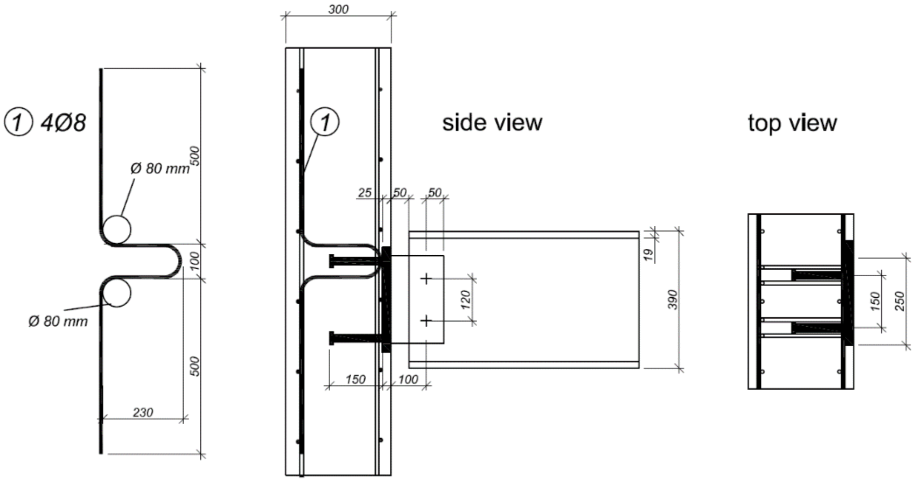

Fig. 9.27 Reinforcement

In the following an overview of the joint geometry is given.

Connected girder	HE400A, S235
Concrete	C30/37 ($f_{ck,cube}$ = 37 N/mm², cracked)
Stirrups	4 x 8 mm / B500A (two per headed stud)
Butt straps:	150 x 250 x 20 mm / S235
Anchor plate	300 x 250 x 25 mm / S235
Headed Studs	d = 22 mm
	h = 150 mm / S235J2 + C470
Bolt connection	2 x M24 10.9
Shear load of the joint	V_{Ed} =180 kN

<u>Connection between the girder HE400A and the anchor plate</u>

The small torsion moment caused by the eccentricity between the girder and the butt straps is transferred into the girder HE400A and from this primary girder to the secondary girders. The eccentric connection induces bending and shear stresses in the butt strap. In the following they are determined:

$$M_{Ed} = V_{Ed} \cdot 0.1 = 18\ \mathrm{kNm}$$

$$\tau_V = 1.5 \cdot \frac{V_{Ed}}{A_V} = 1.5 \cdot \frac{180}{5000} = 54.0 \leq 135.6\ \mathrm{N/mm^2}$$

$$\sigma = \frac{M_{Ed}}{W} = \frac{18}{\frac{250^2 \cdot 20}{6}} = 86.4 \leq 235.0\ \mathrm{N/mm^2}$$

The maximum forces don`t appear at the same place.

EN 3-1-8 Table 3.3

Edge distances: $e_1 = \ 65\ \mathrm{mm} > 1.2 \cdot d_0 = 1.2\ \cdot 26 = 31.2\ \mathrm{mm}$

$e_2 = \ 50\ \mathrm{mm} > 1.2 \cdot d_0 = 1.2\ \cdot 26 = 31.2\ \mathrm{mm}$

$p_1 = 120\ \mathrm{mm} > 2.2 \cdot d_0 = 2.2\ \cdot 26 = 57.2\ \mathrm{mm}$

Shear resistance of the bolts:

$$F_{v,Rd} = \alpha_V \cdot A_S \cdot \frac{f_{ub}}{\gamma_{M2}} = 0.6 \cdot 353 \cdot \frac{1000}{1.25} = 169.4\ \text{kN}$$ EN 3-1-8 Table 3.4

$$V_{Rd,1} = n_V \cdot F_{v,Rd} = 2 \cdot 169.4 = 338.8\ \text{kN}$$

Bearing resistance of the butt strap:

$$V_{Rd,2} = 286.8\ \text{kN}$$

$$F_{b,Rd} = \frac{k_1 \cdot \alpha_b \cdot f_u \cdot d \cdot t}{\gamma_{M2}} = \frac{2.5 \cdot 0.83 \cdot 360 \cdot 24 \cdot 20}{1.25} = 286.8\ \text{kN}$$ EN 3-1-8 Table 3.4

$$k_1 = \min\left[2.8\frac{e_2}{d_0} - 1.7; 1.4\frac{p_2}{d_0} - 1.7; 2.5\right] = \min[3.68; -; 2.5]$$

$$\alpha_b = \min\left[\frac{e_1}{3 \cdot d_0}; \frac{f_{ub}}{f_u}; 1.0\right] = \min[0.83; 2.78; 1.0]$$

Bearing resistance of the beam web:

$$V_{Rd,3} = 190.1\ \text{kN}$$ EN 3-1-8 Table 3.4

$$F_{b,Rd} = \frac{k_1 \cdot \alpha_b \cdot f_u \cdot d \cdot t}{\gamma_{M2}} = \frac{2.5 \cdot 1.0 \cdot 360 \cdot 24 \cdot 11}{1.25} = 190.1\ \text{kN}$$

$$k_1 = \min\left[2.8\frac{e_2}{d_0} - 1.7; 1.4\frac{p_2}{d_0} - 1.7; 2.5\right] = \min[3.68; -; 2.5]$$ EN 3-1-8 4.5.3.2

$$\alpha_b = \min\left[\frac{e_1}{3 \cdot d_0}; \frac{f_{ub}}{f_u}; 1.0\right] = \min[-; 2.78; 1.0]$$

$$V_{Rd} = \min\left[V_{Rd,1}; V_{Rd,2}; V_{Rd,3}\right] = 190.1\ \text{kN} \geq V_{Ed} = 180\ \text{kN}$$

<u>Welding of the butt straps to the anchor plate</u>

A welding seam all around with $a_w = 7$ mm is assumed. Following stresses in the welding seam can be determined:

$$a_w = 2 \cdot 7 = 14\ \text{mm}$$

$$l_{eff} = 250\ \text{mm}$$

$$W_{el,w} = \frac{a_w \cdot l_{w,eff}^2}{6} = \frac{14 \cdot 250^2}{6} = 145.8 \cdot 10^3\ \text{mm}^2$$

$$\sigma_{w,Rd} = \frac{f_u}{\beta_w \cdot \gamma_{M2}} = \frac{360}{0.8 \cdot 1.25} = 360\ \text{N/mm}^2$$

Shear stresses caused by shear load and eccentricity:

$$\tau_{II} = \frac{V_{ED}}{2 \cdot a_w \cdot l_{w,eff}} = \frac{180}{2 \cdot 7 \cdot 250} = 51.4\ \text{N/mm}^2$$

$$\sigma_w = \frac{M_{Ed}}{W} = \frac{1\ 8}{145.8} = 123.5\ \text{N/mm}^2$$

$$\sigma_\perp = \tau_\perp = \sigma_w \cdot \sin 45° = 123.5 \cdot \sin 45° = 87.3 \leq \frac{0.9 \cdot f_u}{\gamma_{M2}} = 259.2\ \text{N/mm}^2$$

Interaction caused by bending and shear stresses:

$$\sigma_{w,Ed} = \sqrt{\sigma_\perp^2 + 3(\tau_\perp^2 + \tau_{II}^2)} = \sqrt{87.3^2 + 3(87.3^2 + 51.4^2)} = 195.0 \leq \sigma_{w,Rd} = 360\ \text{N/mm}^2$$

Additional condition Eq. (4.1) EN 3-1-8

Design of the connection to the concrete

The anchor plate has the geometry	$300 \text{ x } 250 \text{ x } 25$ mm S235
Headed studs	$d = 22$ mm
	$h = 150$ mm S350 C470
Stirrups (for each headed stud)	$4 \cdot 8$ mm B 500 A

The verification of the design resistance of the joint is described in a stepwise manner. The eccentricity e_v and the shear force V_{Ed} are known.

Step 1 Evaluation of the tension force caused by the shear load

If the joint is loaded in shear the anchor row on the non-loaded side of the anchor plate is subjected to tension. In a first step the tension load has to be calculated. Therefore the height of the compression area has to be assumed.

Shear load of the connection	$V_{Ed} = 180$ kN
Resistance due to friction	$V_f = C_{Ed} \cdot 0.2 = N_{Ed,2} \cdot 0.2$
Thickness plate	$t_p = 25$ mm
Diameter anchor	$d = 22$ mm
Eccentricity	$e_v = 100$ mm

Calculation of $N_{Ed,2}$

$$N_{Ed,2} = \frac{V_{Ed} \cdot \left(e_v + d + t_p\right) - V_f \cdot d}{z}$$

$$N_{Ed,2} \cdot (1 + \frac{0.2 \cdot d}{z}) = \frac{V_{Ed} \cdot \left(e_v + d + t_p\right)}{z}$$

The height of the compression zone is estimated to $x_c = 20$ mm

With x_c the lever arm

$$z = 40 + 220 - \frac{x}{2} = 40 + 220 - \frac{20}{2} = 250 \text{ mm}$$

DM I Eq. (5.12)

and

$$N_{Ed,2}(1 + \frac{0.2 \cdot 22}{250}) = \frac{V_{Ed} \cdot (100 + 22 + 25)}{250}$$

From this the tension force result $N_{Ed,2} = 104.0$ kN

Step 2 Verification of the geometry of the compression zone

The tension component of the joint $N_{Ed,2}$ forms a vertical equilibrium with the compression force C_{Ed} under the anchor plate on the loaded side. The next step of the calculation is to prove that the concrete resistance is sufficient for the compression force and that the assumption of the compression area was correct.

Calculation of the compression force

$$\sum N: C_{Ed} = N_{Ed,2} = 104.0 \text{ kN}$$

Height of the compression zone is

$f_{cd} = f_{ck} \cdot \frac{\alpha}{\gamma_{Mc}} = 17$ N/mm²

where $\alpha = 0.85$

The compression forces are causing a bending moment in the anchor plate. To make sure that the anchor plate is still elastic, only the part of the anchor plate is activated which is activated with elastic bending only.

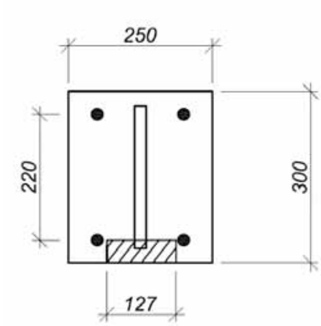

Fig. 9.28 Effective with

$$b_{eff} = t_{bs} + 2 \cdot t_p \cdot \sqrt{\frac{f_y}{3 \cdot f_{jd} \cdot \gamma_{M0}}}$$

$$= 20 + 2 \cdot 25 \cdot \sqrt{\frac{235}{3 \cdot 17 \cdot 1.0}} = 127 \text{ mm}$$

EN 3-1-8 6.2.5

$$x_c = \frac{C_{Ed}}{b \cdot 3 \cdot f_{cd}} = \frac{104.0}{127 \cdot 3 \cdot 17} = 16 \text{ mm}$$

Instead of the regular width b of the anchor plate the effective width b_{eff} is used. The calculated $x_c = 16$ mm is smaller than the predicted value of $x_c = 20$ mm. That means that the lever arm was estimated slightly too small. This is on the safe side, so the calculation may be continued.

Step 3 Evaluation of the tension resistance

3.1 Steel failure of the fasteners

Calculation of the characteristic failure load of the headed studs on the non-loaded side:

$$N_{Rd,s} = n_a \cdot A_s \cdot \frac{f_{uk}}{\gamma_{Mp}} = 2 \cdot 380 \, \frac{470}{1.5} \cdot 10^{-3} = 238.1 \text{ kN}$$

DM I Eq. (3.3)

where

Characteristic ultimate strength	$f_{uk} = 470$ N/mm²
Characteristic yield strength	$f_{yk} = 350$ N/mm²
Number of headed studs in tension	$n_a = 2$
Cross section area of one shaft	$A_s = \pi \cdot \frac{d^2}{4} = 380$ mm²
Partial safety factor	$\gamma_{Mp} = 1.2 \cdot \frac{f_{uk}}{f_{yk}} = 1.5$

3.2 Pull-out failure

If the concrete strength is too low or the load bearing area of the headed stud is too small, pull-out failure might occur.

$$N_{Rd,p} = n \cdot \frac{p_{uk}}{\gamma_{Mc}} \cdot A_h = n \cdot \frac{p_k \cdot f_{ck}}{\gamma_{Mc}} \cdot \frac{\pi}{4} \cdot \left(d_h^2 - d_{s,nom}^2\right) = 2 \cdot \frac{12 \cdot 30}{1.5} \cdot \frac{\pi}{4} \cdot (35^2 - 22^2) = 279.4 \text{ kN}$$

DM I Eq. (3.31)

where

Factor considering the head pressing	$p_k = 12 \cdot f_{ck}$
Partial safety factor	$\gamma_{Mc} = 1.5$

3.3 Concrete cone failure

A pure concrete cone failure should not occur because of the reinforcement, but this failure load has to be calculated so that the resistance may be combined with the resistance of the stirrups.

$$N_{Rd,c} = N^0_{Rk,c} \cdot \psi_{A,N} \cdot \psi_{s,N} \cdot \psi_{re,N}/\gamma_{Mc}$$

$$N^0_{Rk,c} = k_1 \cdot h_{ef}^{1.5} \cdot f_{ck}^{0.5} = 12.7 \cdot 165^{1.5} \cdot 30^{0.5} = 147.4 \text{ kN}$$

$$\psi_{A,N} = \frac{A_{c,N}}{A^0_{c,N}} = \frac{319\ 275}{245\ 025} = 1.3$$

DM I
Ch. 3.1.2

$$A^0_{c,N} = s^2_{cr,N} = \left(2\ c_{cr,N}\right)^2 = \left(2\ (1.5 \cdot h_{ef})\right)^2 = \left(2(1.5 \cdot 165)\right)^2 = 245\ 025 \text{ mm}^2$$

$$N_{Rk,c} = 147.4 \cdot 1.3 \cdot 1.0 \cdot 1.0 = 191.6 \text{ kN}$$

$$N_{Rd,c} = \frac{N_{Rk,c}}{\gamma_{Mc}} = \frac{191.6}{1.5} = 127.7 \text{ kN}$$

DM I
Eq. (3.7)
Eq. (3.8)
Eq. (3.9)
Eq. (3.11)
Eq. (3.12)

where
Effective anchorage depth $h_{ef} = h_n + t_{AP} - k = 165$ mm
Factor for close edge $\Psi_{s,N} = 1.0$
Factor for small reinforcement spacing $\Psi_{re,N} = 1.0$
Actual projected area $A_{c,N} = (2 \cdot 1.5 \cdot h_{ef}) \cdot (2 \cdot 1.5 \cdot h_{ef} + s_1) =$
$= (2 \cdot 1.5 \cdot 165) \cdot (2 \cdot 1.5 \cdot 165 + 150) = 319\ 275$ mm^2
Partial safety factor $\gamma_{Mc} = 1.5$

3.4 Concrete cone failure with reinforcement

With reinforcement one of the three below described failure modes will occur.

3.5 Concrete failure

$$N_{Rk,cs} = \Psi_{supp} \cdot N_{Rk,u,c} = 2.26 \cdot 191.6 = 433.0 \text{ kN}$$

$$N_{Rd,cs} = \frac{N_{Rk,cs}}{\gamma_{Mc}} = \frac{433.0}{1.5} = 288.7 \text{ kN}$$

where
Factor for support of reinforcement $\Psi_{supp} = 2.5 - \frac{x}{h_{ef}} = 2.26$

DM I
Ch. 3.2.4

Distance between the anchor axis and the crack on the surface

$$x = \frac{d_{nom}}{2} + d_{s,a} + \frac{d_{s,t}}{\tan 35°} = 40 \text{ mm}$$

DM I
Eq. (3.47)

Distance of hanger reinforcement to the face of the anchor shaft

$$d_{s,a} = 5 \cdot \frac{d_s}{2} - \frac{d}{2} = 9 \text{ mm}$$

Distance axis of the reinforcement to the concrete surface

$$d_{s,t} = \frac{d_s}{2} + 10 = 14 \text{ mm}$$

Partial safety factor $\gamma_{Mc} = 1.5$

3.6 Yielding of reinforcement

$$N_{Rd,re,1} = N_{Rd,s,re} + N_{Rd,c} + \delta_{Rd,s,re} \cdot k_{c,de}$$
$$N_{Rd,re,1} = 174.8 + 127.7 + 0.642 \cdot -49.1 = 271.0 \text{ kN}$$

DM I
Ch. 3.2.4

where
Normal force of hanger reinforcement

$$N_{Rd,s,re} = A_{s,y} \cdot \frac{f_{s,y,k}}{\gamma_{Ms}} = n_{re} \cdot \pi \cdot \left(\frac{d_{s,re}^2}{4}\right) \cdot \frac{f_{yk}}{\gamma_{Ms}} = 8 \cdot \pi \cdot \left(\frac{8^2}{4}\right) \cdot \frac{500}{1.15} = 174.8 \text{ kN}$$

DM I Eq. (3.17)

Deformation of reinforcement at yielding

$$\delta_{Rds,re} = \frac{2 \cdot \left(A_{s,y} \cdot f_{s,yd}\right)^2}{\alpha_s \cdot f_{ck} \cdot d_{s,re}^4 \cdot (n \cdot n_{re})^2} = \frac{2 \cdot (174.8 \cdot 10^3)^2}{12100 \cdot 30 \cdot 8^4 \cdot (2 \cdot 4)^2} = 0.642 \text{ mm}$$

DM I Eq. (3.16)

Stiffness concrete break out

$k_{c,de} = \alpha_c \cdot \sqrt{f_{ck} \cdot h_{ef}} \cdot \psi_{A,N} \cdot \psi_{s,N} \cdot \psi_{re,N} = -537 \cdot \sqrt{30 \cdot 165} \cdot 1.3 \cdot 1.0 \cdot 1.0 = -49.1$ kN/mm

Partial safety factor $\gamma_{Ms} = 1.15$

DM I Eq. (3.13)

3.7 Anchorage failure of the reinforcement

$N_{Rd,re,2} = N_{Rd,b,re} + N_{Rd,c} + \delta_{Rd,b,re} \cdot k_{c,de}$

$N_{Rd,re,2} = 147.7 + 127.7 + 0.459 \cdot -49.1 = 252.8$ kN

where

DM I Eq. (3.49)

Anchorage force of all hanger legs $N_{Rd,b,re} = n \cdot n_{re} \cdot l_1 \cdot \pi \cdot d_s \cdot \frac{f_{bd}}{\alpha}$

$N_{Rd,b,re} = 2 \cdot 4 \cdot 120 \cdot \pi \cdot 8 \cdot \frac{3.0}{0.49} \cdot 10^{-3}$

$= 147.7$ kN

Anchorage length of the hanger $l_1 = h_{ef} - d_p - d_{s,t} - \frac{d_{s,a}}{1.5} = 165 - 25 - 14 - \frac{9}{1{,}5} =$

$= 120$ mm

Dist. hanger reinforcement to the face of the anchor shaft: $d_{s,a} = 5 \cdot \frac{d_s}{2} - \frac{d}{2} = 5 \cdot \frac{8}{2} - \frac{22}{2} = 9$ mm

DM I Eq.(3.21)

Dist. axis of the reinforcement to the concrete surface $d_{s,t} = \frac{d_s}{2} + 10 = 14$ mm

Bond strength $f_{bd} = 2.25 \cdot \eta_1 \cdot \eta_2 \cdot \frac{f_{ctk}}{\gamma_{Mc}} = 2.25 \cdot 1 \cdot 1 \cdot \frac{2}{1.5} = 3.0 \text{ N/mm}^2$

where η_1 is coefficient of bond conditions, $\eta_1 = 1.0$ for vertical stirrups and 0.7 for horizontal stirrups, $\eta_2 = 1.0$ for dimension ≤ 32 mm and (132 - dimension)/100 for dimension ≥ 32 mm

Hook $\alpha = 0.49$

Def. of the reinforcement at bond failure

$$\delta_{Rd,b,re} = \frac{2 \cdot \left(N_{Rd,b,re}\right)^2}{\alpha_s \cdot f_{ck} \cdot {d_{s,re}}^4 (n \cdot n_{re})^2} = \frac{2 \cdot (147.7 \cdot 10^3)^2}{(12100 \cdot 30 \cdot 8^4 \cdot (2 \cdot 4)^2)} = 0.459 \text{ mm}$$

Partial safety factor $\gamma_{Mc} = 1.5$

The decisive component of the three failure modes of the concrete cone failure with reinforcement is the anchorage failure of the reinforcement. The anchors have a tension resistance of $N_{Rd,u} = N_{Rd,re,2} = 252.8$ kN

Step 4 Evaluation of the shear resistance

EN1992-1-1

4.1 Steel failure of the fasteners

$$F_{v,Rd} = \frac{n_{a,v} \cdot 0.6 \cdot f_{uk} \cdot A_s}{\gamma_{M2}} = \frac{2 \cdot 0.6 \cdot 470 \cdot \pi \cdot \left(\frac{22}{2}\right)^2}{1.25} = 171.5 \text{ kN}$$ DM I Eq.(3.20)

4.2 Pry-out failure

$$V_{Rd,CP} = k_3 \cdot N_{Rd,u,cc+group} = 2 \cdot 184.9 = 369.9 \text{ kN}$$

where

Min. component concrete failure	$N_{Rd+group} =$ $\min[N_{Rd,cs}; N_{Rd,s,re}; N_{Rd,b,re}; N_{Rd,u,c,group}]$ $\min[288.7 \text{ kN}; 271.0 \text{ kN}; 252.8 \text{ kN}, 184.9 \text{ kN}]$
Partial safety factor	$\gamma_{Mc} = 1.5$

According to the Technical Specifications the factor k_3 is taken as 2.0. There are not yet made examinations how the resistance $V_{Rd,CP}$ may be calculated taking account of the reinforcement. Therefore $N_{Rd,u,cc+hr}$ is determined as the minimum value of the concrete cone failure with reinforcement ($N_{Rk,u,max}$, $N_{Rd,u,1}$, $N_{Rd,u2}$) and the concrete cone failure of the whole anchor group without considering additional reinforcement ($N_{Rd,u,c}$). $N_{Rd,u,c}$ is calculated in the following.

$$N_{Rk,u,c,group} = N^0{}_{u,c} \cdot \frac{A_{c,N}}{A^0{}_{c,N}} \cdot \Psi_{s,N} \cdot \Psi_{re,N} \cdot \Psi_{ec,N}$$

$$N_{Rk,u,c,group} = 147.4 \cdot \frac{461175}{245025} \cdot 1.0 \cdot 1.0 \cdot 1.0 = 277.4 \text{ kN}$$ N1993-1-8 Cl 3.6.1

$$N_{Rd,u,c,group} = \frac{N_{Rk,u,c}}{\gamma_{Mc}} = \frac{277.4 \text{ kN}}{1.5} = 184.9 \text{ kN}$$

where

$$N^0{}_{u,c} = k_1 \cdot f_{ck}{}^{0.5} \cdot h_{ef}{}^{1.5} = 12.7 \cdot 30^{0.5} \cdot 165^{1.5} \cdot 10^{-3} = 147.4 \text{ kN}$$

Effective anchorage depth	$h_{ef} = h_n - t_{AP} = 150 - 10 + 25 = 165\text{mm}$
Factor for close edge	$\Psi_{s,N} = 1.0$
Factor for small reinforcement spacing	$\Psi_{re,N} = 1.0$
Factor for eccentricity of loading	$\Psi_{ec,N} = 1.0$
Reference projected area	$A^0{}_{c,N} = s_{crN}{}^2 = 495^2 = 245025 \text{ mm}^2$
Actual projected area	$A_{c,N} = (s_{crN} + s_2) \cdot (s_{crN} + s_1)$ $= (495 + 220) \cdot (495 + 150) =$ 461175 mm^2

Step 5 Verification of interaction conditions

5.1 Interaction of tension and shear for steel failure

Shear load in the headed studs on the non-loaded side is

$$V_{Ed,2} = V_{Ed} - V_{Rd,s} - V_f = 180 - 190.1 - 20.8 = -31.0 \text{ kN}$$

All loads is taken by the front anchor. No load for the back anchor and

$$\left(\frac{N_{Ed,2}}{N_{Rd,s}}\right)^2 + \left(\frac{V_{Ed,2}}{V_{Rd}}\right)^2 \leq 1$$ DM I Eq.(3.54)

$$\left(\frac{104.0}{238.1}\right)^2 + \left(\frac{0}{171.5}\right)^2 = 0.19 \leq 1$$ DM I (5.16)

5.2 Interaction of tension and shear for concrete failure

Shear load in the headed studs on the non-loaded side is

$$V_{Ed,2} = \frac{V_{Ed} - V_f}{2} = \frac{180 - 20}{2} = 80\ \text{kN}$$

$$\left(\frac{N_{Ed,2}}{N_{Rd,u}}\right)^{3/2} + \left(\frac{V_{Ed,2}}{V_{Rd}}\right)^{3/2} \leq 1$$ DM I (5.15)

$$\left(\frac{104.0}{252.8}\right)^{3/2} + \left(\frac{80}{184.9}\right)^{3/2} = 0.57 \leq 1$$

Note

Without the additional reinforcement there would be a brittle failure of the anchor in tension in concrete. The resistance of pure concrete cone failure with reinforcement is nearly two times the size of the resistance without reinforcement. With the additional reinforcement there is a ductile failure mode with reserve capacity.

9.6 Moment resistant steel to concrete joint

The steel-to-concrete connection is illustrated in Fig. 9.27. It represents the moment-resistant support of a steel-concrete-composite beam system consisting of a hot rolled or welded steel profile and a concrete slab, which can either be added in situ or by casting semi-finished precast elements. Beam and slab are connected by studs and are designed to act together. Whereas the advantage of the combined section is mostly seen for positive moments, where compression is concentrated in the slab and tension in the steel beam, it may be useful to use the hogging moment capacity of the negative moment range either as a continuous beam, or as a moment resistant connection. In this case, the reinforcement of the slab is used to raise the inner lever arm of the joint. The composite beam is made of a steel profile IPE 300 and a reinforced concrete slab with a thickness of 160 mm and a width of 700 mm. The concrete wall has a thickness of 300 mm and a width of 1 450 mm. The system is subjected to a hogging bending moment $M_{E,d}$ = 150 kNm. Tabs 9.1 and 9.2 summarize data for the steel-to-concrete joint.

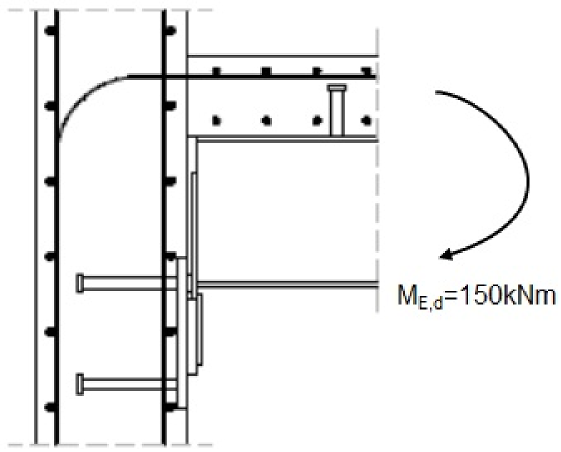

Fig. 9.27: Geometry of the moment resisting joint

Tab. 9.1 Geometry for the steel-to-concrete joint

Geometry					
RC wall		**RC Slab**		**Anchors**	
t [mm]	300	t [mm]	160	d [mm]	22
b [mm]	1450	b [mm]	700	d_h [mm]	35
h [mm]	1600	l [mm]	1550	l_a [mm]	200
Reinforcement		**Reinforcement**		h_{ef} [mm]	215
Φ_v [mm]	12	Φ_l [mm]	16	n_v	2
n_v	15	n_l	6	e_1 [mm]	50
s_v [mm]	150	s_l [mm]	120	p_1 [mm]	200
Φ_h [mm]	12	Φ_t [mm]	10	n_h	2
n_h	21	nt	14	e_2 [mm]	50
s_h [mm]	150	s_t [mm]	100	p_2 [mm]	200
		$c_{tens,bars}$ [mm]	30		
		r_{hook} [mm]	160		
Console 1		**Console 2**		**Anchor plate**	
t [mm]	20	t [mm]	10	t_{ap} [mm]	15
b [mm]	200	b [mm]	170	b_{ap} [mm]	300
h [mm]	150	h [mm]	140	l_{ap} [mm]	300
Shear Studs		**Steel beam**	**IPE 300**	**Contact Plate**	
d [mm]	22	h [mm]	300	t [mm]	10
h_{cs} [mm]	100	b [mm]	150	b_{cp} [mm]	200
N_f	9	t_f [mm]	10.7	l_{cp} [mm]	30
s [mm]	140	t_w [mm]	7.1	$e_{1,cp}$ [mm]	35
a [mm]	270	As [mm^2]	5381	$e_{b,cp}$ [mm]	235
h_c [mm]	90			b_{ap} [mm]	300

The part of the semi-continuous joint configuration, within the reinforced concrete wall, adjacent to the connection, is analyzed in this example. This has been denominated as “Joint Link”. The main objective is to introduce the behaviour of this component in the global analysis of the joint which is commonly disregarded.

Tab. 9.2 Material of the steel-to-concrete joint

Concrete wall		**Concrete slab**		**Rebars wall**	
$f_{ck,cube}$ [Mpa]	50	$f_{ck,cube}$ [Mpa]	37	f_{syk} [MPa]	500
$f_{ck,cyl}$ [Mpa]	40	$f_{ck,cyl}$ [Mpa]	30	f_u [Mpa]	650
E [GPa]	36	E [GPa]	33		
f_{ctm} [Mpa]	3.51	f_{ctm} [Mpa]	2.87		
Rebars Slab		**Steel Plates**		**Anchors**	
f_{syk} [Mpa]	400	f_{syk} [Mpa]	440	f_{syk} [Mpa]	440
f_u [Mpa]	540	f_u [Mpa]	550	f_u [Mpa]	550
ε_{sry} [‰]	2	**Steel Profile**		**Shear Studs**	
ε_{sru}	75	f_{syk} [Mpa]	355	f_{syk} [Mpa]	440
		f_u [Mpa]	540	f_u [Mpa]	550

The design value of the modulus of elasticity of steel E_s may be assumed to be 200 GPa.

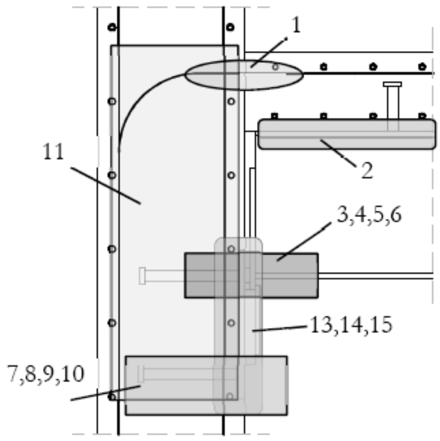

Fig. 9.28 Activated joint components

In order to evaluate the joint behaviour, the following basic components are identified, as shown in Fig. 9.28:

- longitudinal steel reinforcement in the slab, component 1
- slip of the composite beam, component 2;
- beam web and flange, component 3;
- steel contact plate, component 4;
- components activated in the anchor plate connection, components 5 to 10 and 13 to 15;
- the joint link, component 11.

<u>Step 1 Component longitudinal reinforcement in tension</u>

In this semi-continuous joint configuration, the longitudinal steel reinforcement bar is the only component that is able to transfer tension forces from the beam to the wall. In addition, the experimental investigations carried (Kuhlmann et al., 2012) revealed the importance of this component on the joint response. For this reason, the accuracy of the model to predict the joint response will much depend on the level of accuracy introduced in the modelling of this component. According to ECCS Publication Nº 109 (1999), the behaviour of the longitudinal steel reinforcement in tension is illustrated in Fig. 9.29.

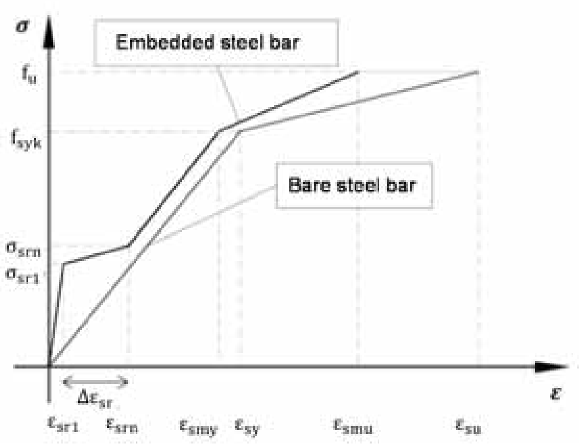

σ_{sr1}	stress of the embedded steel at the first crack
ε_{sr1}	strain of the embedded steel at the first crack
σ_{srn}	stress of the embedded steel at the last crack
ε_{srn}	strain of the embedded steel at the last crack
f_{syk}	yielding stress of the bare bar
ε_{sy}	strain at yield strength of the bare bar
ε_{smy}	strain at yield strength of the embedded bar
f_u	ultimate stress of the bare steel
ε_{su}	strain of the bare bar at ultimate strength
ε_{smu}	strain at ultimate strength of the embedded bar

Fig. 9.29 Stress-strain curve for steel reinforcement in tension

The resistance of the component may then be determined as follows

$$F_{s,r} = A_{s,r}\, f_{yr}$$

Since concrete grades of wall and slab are different it is possible to evaluate separately the stress-strain curve of the two elements. While the concrete is uncracked, the stiffness of the longitudinal reinforcement is considerably higher when compared with bare steel. Cracks form in the concrete when mean tensile strength of the concrete f_{ctm} is achieved. The stress in the reinforcement at the beginning of cracking (σ_{sr1}) is determined as follows.

$$\sigma_{sr1,d,SLAB} = \frac{\sigma_{sr1,SLAB}}{\gamma_{Ms}} = \frac{f_{ctm,SLAB} \cdot k_c}{\gamma_{Ms} \cdot \rho}\left[1 + \rho\frac{E_s}{E_c}\right] = \frac{2.87 \cdot 0.39}{1.15 \cdot 0.010}[1 + 0.010 \cdot 6.06] = 97.1 \text{ Nmm}^{-2}$$ ECCS (1999)

$$\sigma_{sr1,d,WALL} = \frac{\sigma_{sr1,WALL}}{\gamma_{Ms}} = \frac{f_{ctm,WALL} \cdot k_c}{\gamma_{Ms} \cdot \rho}\left[1 + \rho\frac{E_s}{E_c}\right] = \frac{3.51 \cdot 0.39}{1.15 \cdot 0.010}[1 + 0.010 \cdot 6.06] = 118.7 \text{ Nmm}^{-2}$$

where: f_{ctm} is the tensile strength of the concrete; E_s and E_c are the elastic modulus of the steel reinforcement bar and concrete, k_c is a factor which allows using the properties of the steel beam section and ρ is the ratio between the area of steel reinforcement and the area of concrete flange expressed as follows:

$$k_c = \frac{1}{1 + \frac{t_{slab}}{2 \cdot z_0}} = \frac{1}{1 + \frac{160}{2 \cdot 51.8}} = 0.39$$

$$\rho = \frac{A_{s,r}}{A_{c,slab}} = \frac{n_l \cdot \pi \cdot \Phi_l^2/4}{b_{eff,slab} \cdot t_{slab}} = \frac{1\,206.4}{700 \cdot 160} = 0.010$$ ECCS (1999)

where: $A_{c,slab}$ is the area of the effective concrete slab; $A_{s,r}$ is the area of the longitudinal reinforcement within the effective slab width (in this example the width of the slab is fully effective); t_{slab} is the thickness of the concrete flange and z_0 is the vertical distance between the centroid of the uncracked concrete flange and uncracked unreinforced composite section, calculated using the modular ration for short-term effects, E_s/E_c.

$$z_0 = x_{c,h} - \frac{t_{slab}}{2} = \left[\frac{b_{eff} \cdot \frac{E_c}{E_s} \cdot t_{slab} \cdot \frac{t_{slab}}{2} + \left(t_{slab} + \frac{h_{IPE300}}{2}\right) \cdot A_{IPE300}}{b_{eff} \cdot t_{slab} \cdot \frac{E_c}{E_s} + A_{IPE300}}\right] - \frac{t_{slab}}{2} = 51.8 \text{ mm}$$ CEB-FIB Model Code (1990)

where

$x_{c,h}$ is the dimension of the component concrete block in compression.

According to CEB-FIB Model Code (1990), the stress $\sigma_{srn,d}$ and the increment of the reinforcement strain $\Delta\varepsilon_{sr}$ are given by

$$\Delta\varepsilon_{sr,SL} = \frac{f_{ctm,SL} \cdot k_c}{\gamma_S \cdot E_s \cdot \rho} = 0.00045 \qquad \Delta\varepsilon_{sr,WA} = \frac{f_{ctm,WA} \cdot k_c}{\gamma_S \cdot E_s \cdot \rho} = 0.00056$$

$$\varepsilon_{sr1,SL} = \frac{\sigma_{sr1,d,SL}}{E_s} - \Delta\varepsilon_{sr,SL} = 3.0 \cdot 10^{-5} \qquad \varepsilon_{sr1,WA} = \frac{\sigma_{sr1,d,WA}}{E_s} - \Delta\varepsilon_{sr,WA} = 3.6 \cdot 10^{-5}$$

ECCS (1999)

$$\sigma_{srn,d,SL} = 1.3 \cdot \sigma_{sr1,d,SL} = 126.2\text{Nmm}^{-2} \qquad \sigma_{srn,d,WA} = 1.3 \cdot \sigma_{sr1,d,WA} = 154.3\text{Nmm}^{-2}$$

$$\varepsilon_{srn,SL} = \varepsilon_{sr1,SL} + \Delta\varepsilon_{sr,SL} = 4.9 \cdot 10^{-4} \qquad \varepsilon_{srn,WA} = \varepsilon_{sr1,WA} + \Delta\varepsilon_{sr,WA} = 5.9 \cdot 10^{-4}$$

The yield stress and strain, f_{syk} and ε_{smy} are given by

$$f_{syk,d} = \frac{f_{syk}}{\gamma_S} = \frac{400}{1.15} = 347.8\text{Nmm}^{-2}$$

$$\varepsilon_{smy,SL} = \frac{f_{syk,d} - \sigma_{srn,d,SL}}{E_s} + \varepsilon_{sr1,SL} + \Delta\varepsilon_{sr,SL} = 1.6 \cdot 10^{-3}$$

$$\varepsilon_{smy,WA} = \frac{f_{syk,d} - \sigma_{srn,d,WA}}{E_s} + \varepsilon_{sr1,WA} + \Delta\varepsilon_{sr,WA} = 1.6 \cdot 10^{-3}$$

ECCS (1999)

The ultimate strain ε_{srmu} is determined as follows, where the tension stiffening is also taken into account. The factor $\beta_t = 0.4$ takes into account the short-term loading; and for high-ductility bars, δ is taken equal to 0.8.

$$\varepsilon_{smu,SL} = \varepsilon_{sy} - \beta_t\, \Delta\varepsilon_{sr,SL} + \delta\left(1 - \frac{\sigma_{sr1,d,SL}}{f_{syk,d}}\right)(\varepsilon_{su} - \varepsilon_{sy}) = 4.4 \cdot 10^{-2}$$

$$\varepsilon_{smu,WA} = \varepsilon_{sy} - \beta_t\, \Delta\varepsilon_{sr,WA} + \delta\left(1 - \frac{\sigma_{sr1,d,WA}}{f_{syk,d}}\right)(\varepsilon_{su} - \varepsilon_{sy}) = 4.0 \cdot 10^{-2}$$

CEB-FIB Model Code (1990)

where: ε_{sy} and $f_{syk,d}$ are the yield strain and stress of the bare steel reinforcement bars, respectively; ε_{su} is the ultimate strain of the bare steel reinforcement bars.

Assuming the area of reinforcement constant, the force-deformation curve is derived from the stress-strain curve, where the reinforcement deformation should be evaluated as described above.

$$\Delta = \varepsilon \cdot l$$

The elongation length (l) to consider is equal to sum of the L_t (related to the slab) with h_c (related to the wall). Only in the determination of the ultimate deformation capacity, the length of the reinforcement bar is considered higher than this value, as expressed in the following:

$\rho < 0.8\,\%$	$\Delta_{sru} = 2\, L_t\, \varepsilon_{srmu}$
$\rho \geq 0.8\,\%$ and $a \leq L_t$	$\Delta_{sru} = (h_c + L_t)\, \varepsilon_{srmu}$
$\rho \geq 0.8\,\%$ and $a > L_t$	$\Delta_{sru} = (h_c + L_t)\varepsilon_{srmu} + (a - L_t)\, \varepsilon_{srmu}$

where is

$$L_t = \frac{k_c \cdot f_{ctm} \cdot \Phi}{4 \cdot \tau_{sm} \cdot \rho} = \frac{0.39 \cdot 2.87 \cdot 16}{4 \cdot 5.16 \cdot 0.01} = 81 \text{ mm}$$

In the above expression, L_t is defined as the transmission length and represents the length of the reinforcement from the wall face up to the first crack zone which should form close to the joint. The parameter a is the distance of the first shear connector to the joint and h_c

is the length of the reinforcement up to the beginning of the bend. τ_{sm} is the average bond stress, given by

$$\tau_{sm} = 1.8 \cdot f_{ctm}$$

Forces can be evaluated considering minimum values of tensions found for slab and wall. Table 9.3 summarizes the results for the stress-strain and force-displacement curves.

Tab. 9.3 Force-displacement relation for longitudinal reinforcement in tension

σ_{SL} [N/mm²]	ε_{SL} [-]	σ_{WA} [N/mm²]	ε_{WA} [-]	F [kN]	Δ_r [mm]
97.1	$3.0 \cdot 10^{-5}$	118.7	$3.6 \cdot 10^{-5}$	117.1	0.0
126.2	$4.9 \cdot 10^{-4}$	154.3	$5.9 \cdot 10^{-4}$	152.3	0.1
347.8	$1.6 \cdot 10^{-3}$	347.8	$1.6 \cdot 10^{-3}$	419.6	0.3
469.5	$4.4 \cdot 10^{-2}$	469.5	$4.0 \cdot 10^{-2}$	566.5	5.7

Step 2 Component slip of composite beam

The slip of composite beam is not directly related to the resistance of the joint; however, the level of interaction between the concrete slab and the steel beam defines the maximum load acting on the longitudinal reinforcement bar. In EN 1994-1-1: 2010, the slip of composite beam component is not evaluated in terms of resistance of the joint, but the level of interaction is considered on the resistance of the composite beam. However, the influence of the slip of the composite beam is taken into account on the evaluation of the stiffness and rotation capacity of the joint. The stiffness coefficient of the longitudinal reinforcement should be affected by a reduction factor k_{slip} determined according to Chap. 3.7.

According to (Aribert, 1995) the slip resistance may be obtained from the level of interaction as expressed in the following. Note that the shear connectors were assumed to be ductile allowing redistribution of the slab-beam interaction load.

$$F_{slip} = N \cdot P_{RK}$$

Where: *N* is the real number of shear connectors; and P_{RK} is characteristic resistance of the shear connectors that can be determined according to EN1994-1-1:2010 as follows EN1994-1-1:2010

$$P_{RK} = \min\left(\frac{0.8 \cdot f_u \cdot \pi \cdot d^2}{\gamma_{MV} \cdot 4}; \frac{0.29 \cdot \alpha \cdot d^2 \sqrt{f_{ck} \cdot E_{cm}}}{\gamma_{MV}}\right)$$

with

$3 \le \frac{h_{sc}}{d} \le 4$ $\qquad\qquad$ $\alpha = 0.2\left(\frac{h_{sc}}{d} + 1\right)$

$\frac{h_{sc}}{d} > 4$ $\qquad\qquad$ $\alpha = 1$

where f_u is the ultimate strength of the steel shear stud; d is the diameter of the shear stud; f_{ck} is the characteristic concrete cylinder resistance; E_{cm} is the secant modulus of elasticity of the concrete; h_{sc} is the height of the shear connector including the head; γ_V is the partial factor for design shear resistance of a headed stud.

$$P_{RK} = \min(\frac{0.8 \cdot 540 \cdot \pi \cdot 22^2}{1.25 \cdot 4}; \frac{0.29 \cdot 1 \cdot 22^2 \cdot \sqrt{30 \cdot 33)}}{1.25} = \min(486.5;\ 111.0) = 111.0 \text{ kN}$$

$$F_{slip} = 9 \cdot 111.0 = 999.0 \text{ kN}$$

Concerning the deformation of the component, assuming an uniform shear load distribution along the beam, an equal distribution of the load amongst the shear studs is expected.

The stiffness of the component is obtained as a function of the number of shear studs and of the stiffness of a single row of shear studs, as follows

$k_{slip} = N \cdot k_{sc} = 900$ kN/mm

where the stiffness of one shear connector k_{sc} may be considered equal to 100 kN/mm, see cl A.3(4) in EN 1994-1-1:2010.

Step 3 Component beam web and flange in compression

According to EN1993-1-8:2006, the resistance can be evaluated as follows

$$M_{c,Rd} = \frac{W_{pl} \cdot f_{syk}}{\gamma_{M0}} = \frac{628\ 400 \cdot 355}{1.0} = 223.0 \text{ kN}$$

$$F_{c,fb,Rd} = \frac{223\ 000}{(300 - 10.7)} = 771.1 \text{ kN}$$

The stiffness of this component may be neglected.

Step 4 Component steel contact plate in compression

According to EN1994-1-1:2010, the resistance can be evaluated as follows and the stiffness is infinitely rigid compared to rest of the connection.

$$F_{cp} = f_{y,cp}\, A_{eff,cp} = 440 \cdot 200 \cdot 30 = 2\ 640 \text{ kN}$$

Step 5 Component T-stub in compression

According to EC 1993-1-8:2006, the bearing width c can be calculated using the hypothesis of cantilever beam for all directions. It is an iterative process as the bearing width and the concrete bearing strength f_j are mutually dependent.

$$c = t_{ap} \cdot \sqrt{\frac{f_y}{3 \cdot f_{jd} \cdot \gamma_{M0}}} \qquad f_{jd} = \frac{\beta_j\, F_{Rd,u}}{b_{eff}\, l_{eff}} = \frac{\beta_j\, A_{c0}\, f_{cd} \sqrt{\frac{A_{c1}}{A_{c0}}}}{A_{c0}} = \beta_j\, f_{cd}\, k_j$$

where β_j is the foundation joint material coefficient and F_{Rdu} is the concentrated design resistance force. Assuming an uniform distribution of stresses under the equivalent rigid plate and equal to the bearing strength of the concrete, the design compression resistance of a T-stub should be determined as follows

$$F_{C,Rd} = f_{jd} \cdot b_{eff} \cdot l_{eff}$$

where b_{eff} and l_{eff} are the effective width and length of the T-stub flange, given by

$$A_{eff} = \min(2c + b_{cp}; b_{ap}) \cdot (c + l_{cp} + \min(c;\ e_{1,cp})) = 69.4 \cdot 239.4 = 16625.9 \text{ mm}^2$$

and f_{jd} is the design bearing strength of the joint.

Thus, c = 19.7 mm; f_{jd} = 84.9 MPa; l_{eff} = 69.4mm; b_{eff} = 239.4 mm; F_c = 1411.0 kN

The initial stiffness $S_{ini,j}$ may be evaluated as follows

$$S_{ini,j} = \frac{E_c \sqrt{A_{eff}}}{1.275}$$

c is given by $c = 1.25 \cdot t_{ap}$ and b_{eff} and l_{eff} are given by

$$A_{eff} = \min(2.5\ t_{ap} + b_{cp}; b_{ap}) \cdot (1.25\ t_{ap} + l_{cp} + \min(1.25\ t_{ap}, e_{1,cp})) = 67.5 \cdot 237.5 = 16\ 031 \text{ mm}^2$$

Thus, $c = 18.7$ mm; $l_{eff} = 67.5$ mm; $b_{eff} = 237.5$ mm and $S_{ini,j} = 3\ 575.0$ kN/mm

This value of the initial stiffness could be used for the calculation of the component of displacement related to the T-stub in compression.

Step 6 Joint Link

In the proposed model based on the STM principles, the properties of this diagonal spring are determined as follows:

- The resistance is obtained based on the strut and nodes dimension and admissible stresses within these elements, given in Tab. 3.2.
- The deformation of the diagonal spring is obtained by assuming a non-linear stress-strain relation for the concrete under compression, as defined in (Henriques, 2013).

In terms of resistance, the model is characterized by the resistance of the nodes at the edge of the diagonal strut. Accordingly, the maximum admissible stresses, see Tab. 3.2, and the geometry of these nodes define the joint link load capacity. It is recalled that failure is governed by the nodal regions and disregarded within the strut. Hence, the resistance of the nodes is obtained as follows.

6a) Node N1

The geometry of the node is defined in one direction by the bend radius of the longitudinal reinforcement and by the strut angle θ with the dimension a Fig. 9.30. In the other direction (along the width of the wall), assuming the distance between the outer longitudinal overestimates the resistance of this node, since the analytical approach assumes that the stresses are constant within the dimension brb and the stress field “under” the hook and along this dimension is non-uniform.

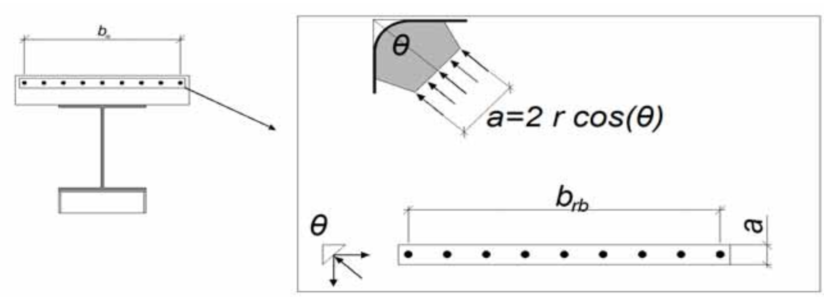

Fig. 9.30 Definition of the width of node N1

According to Henriques (2013), in order to obtain a more accurate approach, an analytical expression was derived to estimate an effective width “under” each reinforcement bar where constant stresses can be assumed. The basis of this analytical expression was a parametrical study performed by means of numerical calculations.
In order to obtain an expression which could approximate the effective width with sufficient accuracy, a regression analysis, using the data produced in the parametric study, was performed The effective width $b_{eff,rb}$ of the reinforcement is calculated as a function of the reinforcement bar diameter d_{rb}, the spacing of bars s_{rb} and strut angle θ as follows Henriques (2013)

$s_{rb} \geq 80$ mm $\qquad b_{eff,rb} = n \cdot 2.62 \cdot d_{rb}^{0.96} \cdot (\cos\theta)^{-1.05}$

$s_{rb} < 80$ mm $\qquad b_{eff,rb} = n \cdot 2.62 \cdot d_{rb}^{0.96} \cdot (\cos\theta)^{-1.05} \cdot \left(\frac{s_{rb}}{80}\right)^{0.61}$

As in this case s_{rb}>80 mm

$$\theta = \arctan\left(\frac{z}{b}\right) = \arctan\left(\frac{406.65}{300 - \frac{16}{2} - \frac{10}{2} - 30 \cdot 2}\right) = 1.06 \text{ rad}$$

$$a = 2 \cdot r_{hook} \cdot \mathrm{Cos}(\theta) = 2 \cdot 160 \cdot \mathrm{Cos}(1.06) = 155.97 \text{ mm}$$

$$b_{eff,rb} = 6 \cdot 2.62 \cdot d_{rb}^{0.96} \cdot (\cos\theta)^{-1.05} = 478.054 \text{ mm}$$

The node dimensions are determined from

$$A_{N1} = b_{eff,rb} \cdot 2 \cdot r \cdot \cos\theta$$

where A_{N1} is the cross-section area of the diagonal concrete strut at node N1. Finally, the resistance of the node is given by

$$F_{r,N1} = A_{N1} \cdot 0.75 \cdot \nu \cdot f_{cd} = 1\,252.7\text{kN} \qquad \nu = 1 - \frac{f_{ck,cyl}}{250} = 0.84$$

6b) Node N2

The geometry of the node, on the concrete strut edge, is defined by the projection of the dimensions of the equivalent rigid plate, representing the anchor plate subjected to compression, in the direction of the concrete strut, see Fig. 9.31.
The node dimensions are determined from

$$A_{N2} = \frac{l_{eff}}{\cos\theta} \cdot b_{eff} = 35\,041.3 \text{ mm}^2$$

where: A_{N2} is the cross-section area of the diagonal concrete strut at node N2 where the admissible stresses have to be verified; l_{eff} and b_{eff} are the dimensions of the equivalent rigid plate determined according to the effective T-stub in compression. Considering the admissible stresses and the node dimensions, the resistance of the node is obtained

$$F_{r,N2} = A_{N2} \cdot 3 \cdot \nu \cdot f_{cd} = 2\,354 \text{ kN}$$

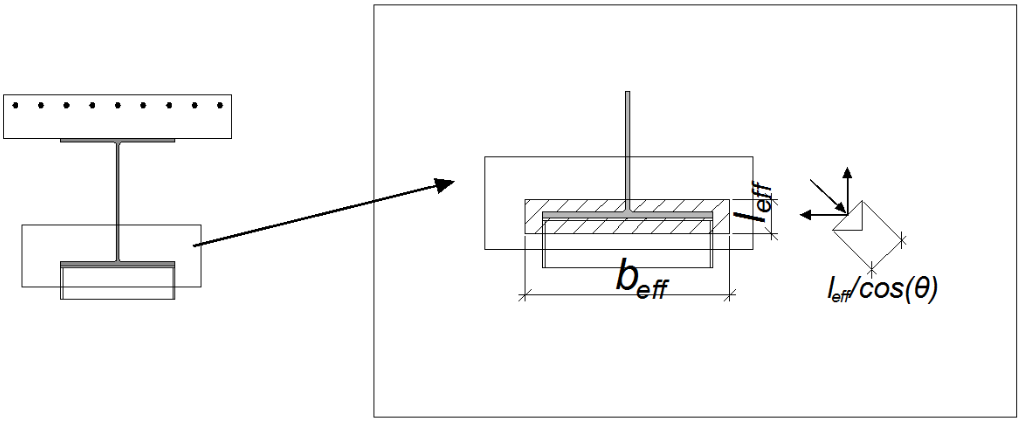

Fig. 9.31 Definition of the width of node N2

6c) Joint link properties

The minimum resistance of the two nodes, N1 and N2, gives the resistance of the joint link in the direction of the binary force generated by the bending moment applied to the joint. Projecting the resistance in the horizontal direction, yields

$$F_{C-T,JL} = F_{r,N1} \cdot \cos\theta = 610.6 \text{ kN}$$

According to (Henriques 2013), the deformation of the joint link is given by

$$\Delta_{JL} = \left(6.48 \cdot 10^{-8} \cdot F^2{}_{C-T,JL} + 7.47 \cdot 10^{-5} \cdot F_{C-T,JL}\right) \cdot \cos\theta$$

Thus, considering 10 load steps, Tab. 9.4 summarizes the force-displacement curve.

Tab. 9.4 Force-displacement for the Joint Link component

F_h [kN]	Δ_h [mm]
0.0	0.00
61.1	0.00
122.1	0.00
183.2	0.01
244.2	0.01
305.3	0.01
366.3	0.02
427.4	0.02
488.5	0.03
549.5	0.03
610.6	0.03

Step 7 Assembly of joint

The simplified mechanical model represented in Fig. 9.32 consists of two rows, one row for the tensile components and another for the compression components. It combines the tension and compression components into a single equivalent spring per row.

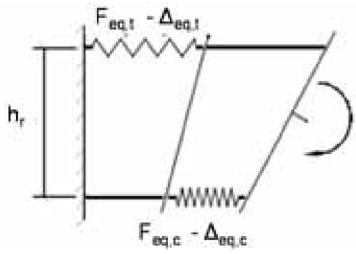

Fig. 9.32: Simplified joint model with assembly of components per row

The properties of the equivalent components/springs are calculated, for resistance, $F_{eq,t}$ and $F_{eq,c}$, and deformation, $\Delta_{eq,t}$ and $\Delta_{eq,c}$, as follows

$$F_{eq} = \min(F_i \text{ to } F_n)$$

$$\Delta_{eq} = \sum_{i=1}^{N} \Delta_i$$

where index i to n represents all relevant components, either in tension or in compression, depending on the row under consideration.

According to the joint configuration, it is assumed that the lever arm is the distance between the centroid of the longitudinal steel reinforcement bar and the middle plane of the bottom flange of the steel beam. The centroid of the steel contact plate is assumed aligned with this reference point of the steel beam. Hence, the bending moment and the corresponding rotation follow from

$$M_j = \min(F_{eq,T}; F_{eq,C}; F_{JL}) \cdot h_r \qquad \Phi_j = \frac{\Delta_{eq,T} + \Delta_{eq,C} + \Delta_{JL}}{h_r}$$

Thus

$F_{t,max}$ =	566.5 kN	Longitudinal rebar
$F_{c,max}$ =	610.6 kN	Joint link

F_{eq} = 566.5 kN
h_r = 406.65 mm
M_j = 230.36 KNm

Table 9.5 summarizes the main results in order to calculate the moment rotation curve, where Δ_r is the displacement of the longitudinal steel reinforcement, Δ_{slip} is related to the slip of composite beam through to the coefficient k_{slip}, $\Delta_{T\text{-}stub}$ is the displacement of the T-stub in compression and ΔJL is the displacement of the joint link.

Tab. 9.5 Synthesis of results

F [kN]	Δ_r [mm]	Δ_{slip} [mm]	$\Delta_{T\text{-}stub}$ [mm]	Δ_{JL} [mm]	Δ_t [mm]	Φ [mrad]	M_j [kNm]
0.0	0.00	0.00	0.00	0.00	0.00	0.00	0.00
117.1	0.01	0.13	0.03	0.00	0.17	0.40	47.64
152.3	0.09	0.17	0.04	0.01	0.30	0.73	61.93
419.6	0.27	0.47	0.12	0.02	0.88	2.06	170.63
566.5	5.68	0.63	0.16	0.03	6.36	15.53	230.36

<u>Note</u>

The resulting moment-rotation behaviour is shown in Fig. 9.33. The system is able to resist the applied load.

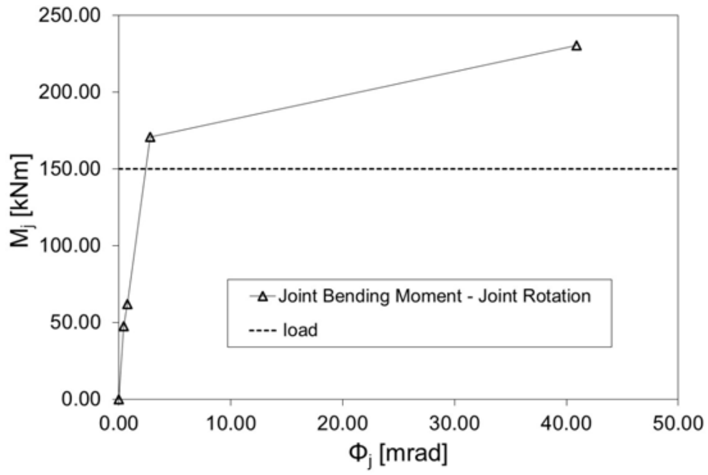

Fig. 9.33 Joint bending moment-rotation curve M_j - Φ_j

9.7 Portal frame

This example illustrates the design of a portal frame designed of columns with cross section HEB 180 and of a rafter with cross section IPE 270, as illustrated in Fig. 9.33. The stiffness of the connections and column bases is considered under design. The steel grade is S235JR, f_y = 235 N/mm² and the profiles are class 1 sections. Safety factors are considered as γ_{M0} = 1.0 and γ_{M1} = 1.1.

Fig. 9.34 highlights position of loads and Tab. 9.2 synthetizes the loads values, while load case combinations are summarized in Tab. 9.3.

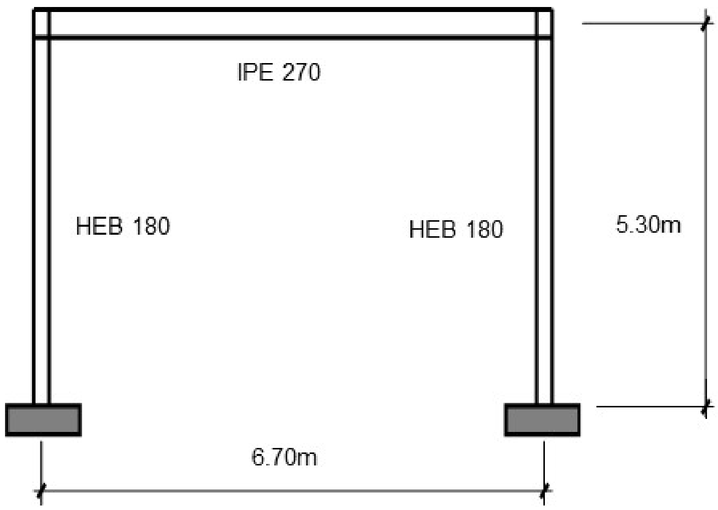

Fig. 9.33 Designed portal frame

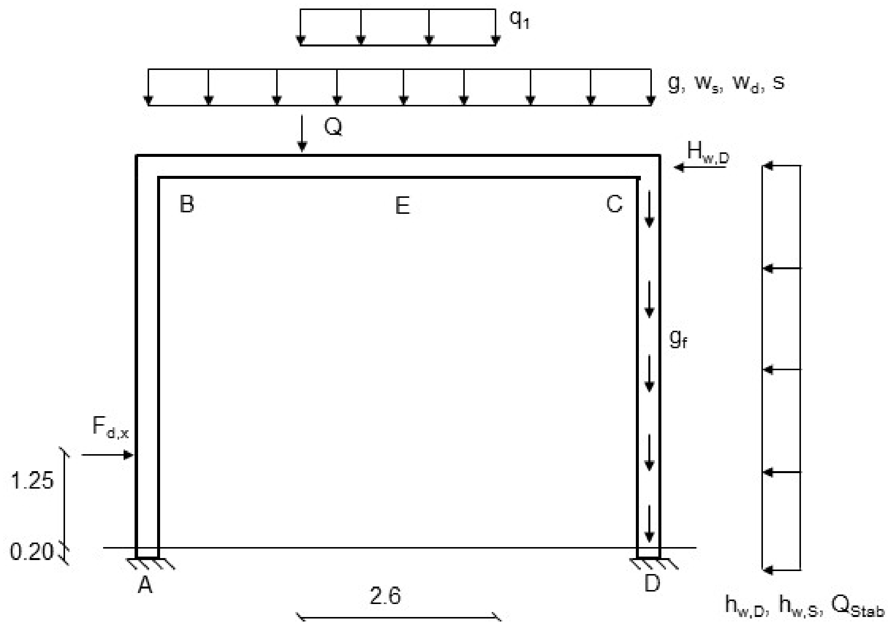

Fig. 9.34 Acting loads

Tab. 9.2 Applied loads

Self-weight + dead loads	Wind
$g_F = 0.5 \cdot 5.3 \approx 2.7$ kN/m	$h_{w.D} = 0.8 \cdot 0.65 \cdot 5.3 = 2.7$ kN/m
$g = 4.8$ kN/m	$H_{w.D} = 0.4 \cdot 0.8 \cdot 0.65 \cdot 5.3 = 1.1$ kN
$s = 5.0$ kN/m	$h_{w.S} = 0.5 \cdot 0.65 \cdot 5.3 = 1.7$ kN/m
$q_1 = 3.0$ kN/m. $b = 2.6$m (equipment)	
$Q_1 = 9.8$ kN	Impact load (EN1991-1-7:2006)
$w_D = 0.8$ kN/m	$F_{d.x} = 100$ kN ($h=1.45$m)
$w_S = -3.9$ kN/m	
	max $Q_{Stab} \approx (48+58)\ 0.85/200 < 0.5$ kN
Imperfection $r_2 = 0.85$, $n = 2$	(added in the wind load case)

Tab. 9.3 Load case combinations

LC 1	$(g+g_f) \cdot 1.35$
LC 2	$(g+g_f) \cdot 1.35 + s \cdot 1.5$
LC 3	$(g+g_f) \cdot 1.35 + s \cdot 1.5 + q_1 \cdot 1.5 \cdot 0.7$
LC 4	$(g+g_f) \cdot 1.35 + s \cdot 1.5 + (w+w_D) \cdot 1.5 \cdot 0.6 + q_1 \cdot 1.5 \cdot 0.7$
LC 5	$(g+g_f) \cdot 1.35 + s \cdot 1.5 \cdot 0.5 + (w+w_D) \cdot 1.5 + q_1 \cdot 1.5 \cdot 0.7$
LC 6	$(g+g_f) \cdot 1.35 + s \cdot 1.5 - (w+w_D) \cdot 1.5 \cdot 0.6 + q_1 \cdot 1.5 \cdot 0.7$
LC 7	$(g+g_f) \cdot 1.35 + s \cdot 1.5 \cdot 0.5 - (w+w_D) \cdot 1.5 + q_1 \cdot 1.5 \cdot 0.7$
LC 8	$(g+g_f) \cdot 1.0 + (w+w_S) \cdot 1.5$
LC 9	$(g+g_f) \cdot 1.0 + q_1 \cdot 1.0 +$ truck $+ s \cdot 0.2$ (exceptional combination – impact load)

The main steps in order to verify a steel portal frame are the following:

Step 1	Global analysis of the steel structure, with fully restrained column bases. Provide internal forces and moments and the corresponding displacements under several loading condition.
Step 2	Verification of single elements
Step 3	Verification of the column-beam joint, in terms of stiffness and resistance.
Step 4	Verification of column base joint, taking into account an impact load
Step 5	Updating of internal forces and moments of the system considering the effective stiffness of the restraints

Step 1 Global analysis

From a 1st order elastic analysis the internal force diagrams envelope due to vertical and horizontal loads, Fig. 9.35 to 9.36 are obtained. Fig. 9.37 illustrates the structural displacement in case di wind load, in direction x. For each combination is necessary to check whether 2nd order effects should be taken into account in the structural analysis by the following simplified expression for beam-and-column type plane frames

$$\alpha_{cr} = \left(\frac{H_{Ed}}{V_{Ed}}\right) \cdot \left(\frac{h_i}{\delta_{H,Ed}}\right)$$

EN 1993-1-1 cl 5.2.1

where:

H_{Ed} is the total horizontal reaction at the of the storey
V_{Ed} is the total vertical reaction at the bottom of the storey
$\delta_{H,Ed}$ is the relative horizontal displacement of the top storey
h_i is the height of the storey

In this case, α_{cr} is always greater than 10 and thus the first order analysis is enough.

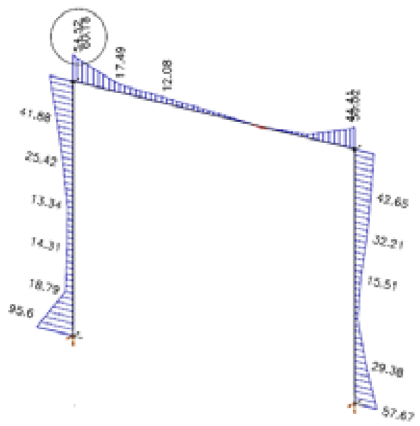

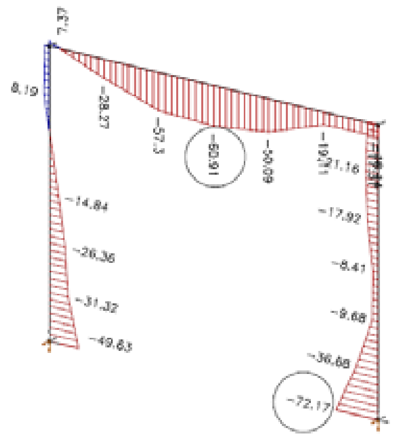

Fig. 9.35 System with max bending moment from all combinations [kNm]

Fig. 9.36 System with min bending moment from all combinations [kNm]

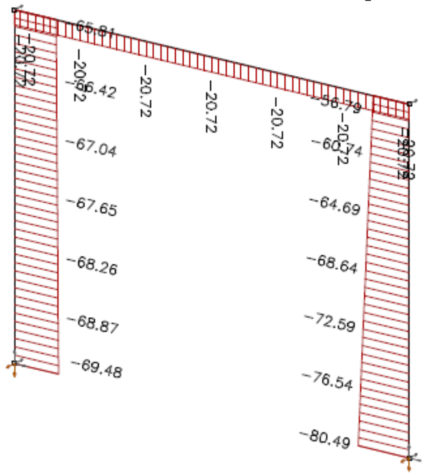

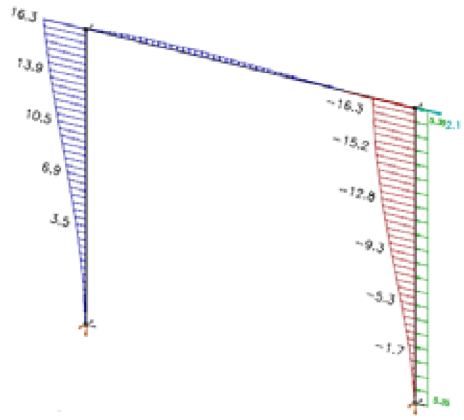

Fig. 9.37 System with min axial force from all combinations [kN]

Fig. 9.38 Deformation for wind in x-direction [mm]

Maximal deformation under variable load is 17 mm at the top.

<u>Step 2 Verification of elements</u>

Verifications are performed using the EC3 Steel Member Calculator for iPhone.

Column HEB 180 is verified as

Acting forces from LC 6	Critical section resistance	Buckling resistance	Verification
$N_{min,d}$ = -80 kN	$N_{c,Rd}$ = -1533 kN	$N_{b,y,Rd}$ = -1394 kN	ε (N+My+V) ≤ 1 0.477
$M_{Ay,d}$ = 51 kNm $M_{B'y,d}$ = 45 kNm	$M_{yAy,c,Rd}$ = 113.1 kNm $V_{c,Rd}$ = 274 kN	$N_{b,z,Rd}$ = 581 kN $M_{b,Rd}$ = 102.8 kNm	ε (M_b + N_{by} (6.61)) ≤ 1 **0.265**

Beam IPE 270 is verified as

Acting force from LC 4	Critical cection resistance	Buckling resistance	Verification
$N_{min,d}$ = -19 kN	$N_{c,Rd}$ = 1079.7 kN	$M_{b,Rd}$ = 103,4 kNm	ε (N+My+V) ≤ 1 **0.536**
$M_{Ey,d}$ = 61 kNm $M_{B''y,d}$ = -51 kNm	$M_{y,c,Rd}$ = 113.7 kNm $V_{c,Rd}$ = 300.4 kN		ε (M_b)+ N_{by} (6,61)) ≤ 1 **0.265**

Step 3 Design of beam to column joint

The connection is illustrated in Fig. Fig. 9.39. The end plate has a height of 310 mm, a thickness of 30 mm and a width of 150 mm with 4 bolts M20 10.9.

Design Values

$M_{y,Rd}$ = -70.7 kNm > -54.5 kNm (at x = 0.09 of supports axis)

$V_{z,Rd}$ = 194 kN

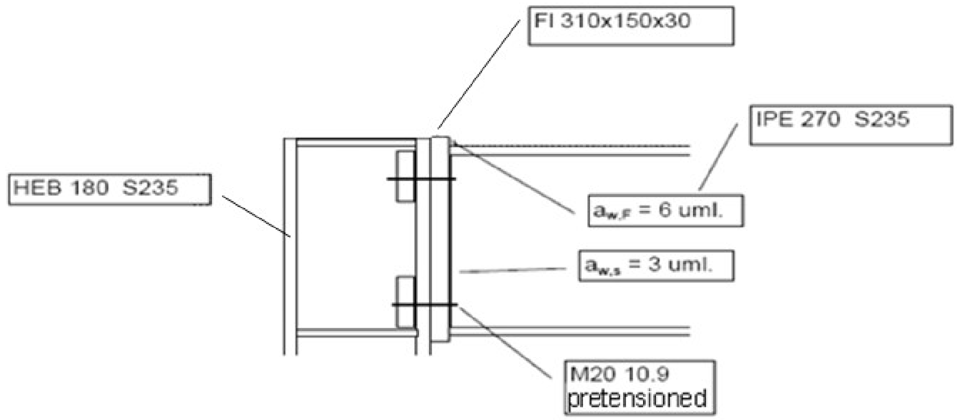

Fig. 9.39 Design of beam-to-column joint

The verification is performed using the ACOP software. The resulting bending moment – rotation curve is represented in Fig. 9.40.

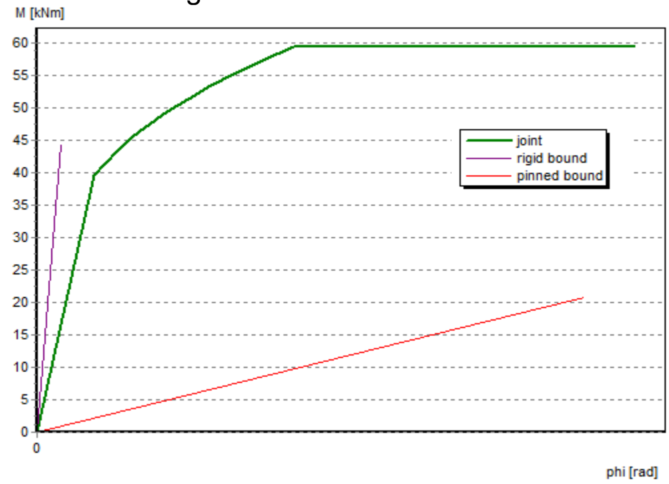

Fig. 9.40 The bending moment to rotation curve M_j - Φ_j

Step 4 Verification of the column base joint

Main Data

- Base plate of 360 x 360 x 30 mm, S235
- Concrete block of size 600 x 600 x 800 mm, C30/37
- Welds $a_{w,Fl}$ = 7 mm, $a_{w,St}$ = 5 mm
- The support with base plate is in a 200 mm deep of the foundation.

Design Values

Characteristic	LC	$N_{x,d}$ [kN]	$M_{y,d}$ [kNm]
N_{min}	6	-80	51
M_{max}	9	-31.6	95.6

Fig. 9.41 represents the designed column base. In the verification procedure, the following step are accomplished:

a) calculation of the resistance of component base plate in bending and anchor bolts in tension;
b) evaluation of the area of concrete in compression,
c) calculation of the strip *c* around the column cross section,
d) calculation of moment resistant of column base,
e) check of the end of column,
f) evaluation of the bending stiffness component stiffness;,
g) evaluation of the stiffness of tension part, bolts and T stub,
h) evaluation of the bending stiffness.

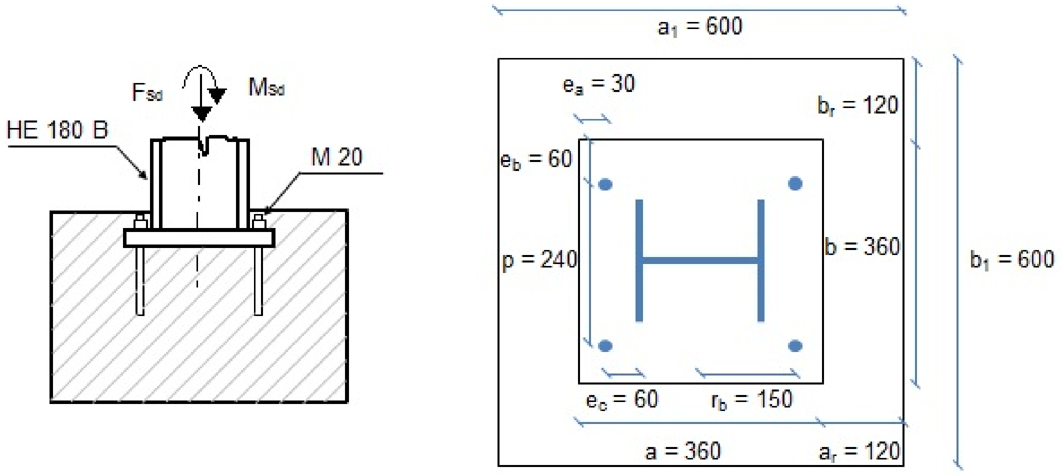

Fig. 9.41 Designed column base

4a) <u>Resistance of component base plate in bending and anchor bolts in tension</u>

For anchor bolt lever arm, for fillet weld a_{wf} = 7 mm, it is

$m = 60 - 0.8 \cdot a_{wf} \cdot \sqrt{2} = 60 - 0.8 \cdot 7 \cdot \sqrt{2} = 52.1$ mm DM I Fig. 4.4

The T - stub length, in base plates are the prying forces not taken into account, is

$$l_{eff,1} = \min \left\{ \begin{array}{l} 4 \cdot m + 1.25 \cdot e_a = 4 \cdot 52.1 + 1.25 \cdot 30 = 245.9 \\ 4 \cdot \pi \cdot m = 4 \cdot \pi \cdot 52.1 = 654.7 \\ 0.5\, b = 0.5 \cdot 360 = 180 \\ 2 \cdot m + 0.625 \cdot e_a + 0.5 \cdot p = 2 \cdot 52.1 + 0.625 \cdot 30 + 0.5 \cdot 240 = 243 \\ 2 \cdot m + 0.625 \cdot e_a + e_b = 2 \cdot 52.1 + 0.625 \cdot 30 + 60 = 183 \\ 2 \cdot \pi \cdot m + 4 \cdot e_b = 2 \cdot \pi \cdot 52.1 + 4 \cdot 60 = 567.4 \\ 2 \cdot \pi \cdot m + 2 \cdot p = 2 \cdot \pi \cdot 52.1 + 2 \cdot 240 = 807.4 \end{array} \right\} =$$

EN1993-1-8 6.4.6.5

$l_{eff,1} = 180$ mm

The effective length of anchor bolt L_b is taken as

$L_b = 8 \cdot d + t = 8 \cdot 20 + 30 = 190$ mm DM I Fig. 4.1

The resistance of T - stub with two anchor bolts is

$$F_{T,1-2,Rd} = \frac{2 \cdot L_{eff,1} \cdot t^2 \cdot f_y}{4 \cdot m \cdot \gamma_{M0}} = \frac{2 \cdot 180 \cdot 30^2 \cdot 235}{4 \cdot 52.1 \cdot 1} = 365.4 \cdot 10^3 \text{N}$$

EN1993-1-8 cl 6.2.4.1

while the tension resistance of two anchor bolts M 20 for the area of threaded part of bolt $A_s = 314$ mm

$$F_{T,3,Rd} = 2 \cdot B_{t,Rd} = 2 \cdot \frac{0.9 \cdot f_{ub} \cdot A_s}{\gamma_{M2}} = \frac{0.9 \cdot 360 \cdot 314}{1.25} = 162.8 \cdot 10^3 \text{N}$$

4b)To evaluate the <u>compressed part resistance</u> is calculated the connection concentration factor as

$$a_1 = b_1 = \min \begin{Bmatrix} a + 2 \cdot a_r = 360 + 2 \cdot 120 = 600 \\ 3 \cdot a = 3 \cdot 360 = 1\,080 \\ a + h = 360 + 800 = 116 \end{Bmatrix} = 600 \text{ mm}$$ EN1992-1-1 Fig. 3.6

and

$a_1 = b_1 = 600 \text{ mm} > \max(a, b)$

The above condition is fulfilled and EN1993-1-8 Eq. (3.65)

$$k_j = \sqrt{\frac{a_1 \cdot b_1}{a \cdot b}} = \sqrt{\frac{600 \cdot 600}{360 \cdot 360}} = 1.67$$

The grout is not influencing the concrete bearing resistance because

$0.2 \min\ (a; b) = 0.2 \cdot \min(360; 360) = 72 \text{ mm} > 30 \text{ mm} = t$ EN1991-1-8 cl 6.2.5

The concrete bearing resistance is calculated as

$$f_{j,d} = \frac{2}{3} \cdot \frac{k_j \cdot f_{ck}}{\gamma_{Mc}} = \frac{2}{3} \cdot \frac{1.67 \cdot 30}{1.5} = 22.3 \text{ MPa}$$

for each load case, from the force equilibrium in the vertical direction $F_{Sd} = A_{eff}\, f_j - F_{t,Rd}$, is calculated the area of concrete in compression A_{eff} in case of the full resistance of tension part.

$$A_{eff-LC6} = \frac{F_{Sd-LC6} + F_{Rd,1}}{f_{jd}} = \frac{80 \cdot 10^3 + 365.4 \cdot 10^3}{22.3} = 19\,973.1 \text{ mm}^2$$

$$A_{eff-LC9} = \frac{F_{Sd-LC9} + F_{Rd,1}}{f_{jd}} = \frac{31.6 \cdot 10^3 + 365.4 \cdot 10^3}{22.3} = 17\,802.7 \text{ mm}^2$$

4c) The flexible base plate is transferred into a <u>rigid plate of equivalent area</u>.

The width of the strip *c* around the column cross section, see Fig. 9.40, is calculated from

$$c = t \cdot \sqrt{\frac{f_y}{3 \cdot f_{jd} \cdot \gamma_{M0}}} = 30 \cdot \sqrt{\frac{235}{3 \cdot 22.3 \cdot 1}} = 56.2 \text{ mm}$$ EN1991-1-8 cl 6.2.5

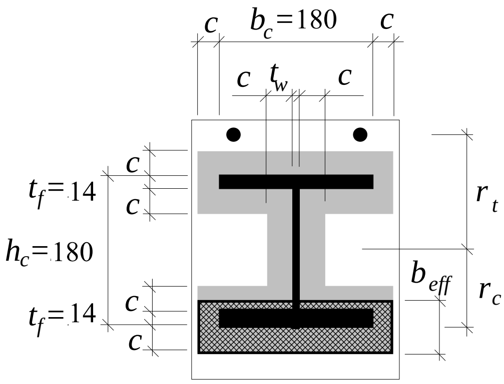

Fig. 9.42 The effective area under the base plate

4d) The active effective width is calculated from known area in compression

$$b_{eff-LC6} = \frac{A_{eff-LC6}}{b_c + 2 \cdot c} = \frac{19\,937.1}{180 + 2 \cdot 57.2} = 68.3 \text{ mm} < t_f + 2 \cdot c = 14 + 2 \cdot 56.2 = 126.4 \text{ mm}$$ EN1993-1-8 cl 6.2.5

$$b_{eff-LC9} = \frac{A_{eff-LC9}}{b_c + 2 \cdot c} = \frac{17\,802.7}{180 + 2 \cdot 57.2} = 60.9 \text{ mm} < t_f + 2 \cdot c = 14 + 2 \cdot 56.2 = 126.4 \text{ mm}$$

The lever arms of concrete to the column axes of symmetry is calculated as

$$r_{c-LC6} = \frac{h_c}{2} + c - \frac{b_{eff-LC6}}{2} = \frac{180}{2} + 56.2 - \frac{68.3}{2} = 112.1 \text{ mm}$$

$$r_{c-LC9} = \frac{h_c}{2} + c - \frac{b_{eff-LC9}}{2} = \frac{180}{2} + 56.2 - \frac{60.9}{2} = 115.8 \text{ mm}$$

Moment resistances of column base are

$M_{Rd-LC6} = F_{T,1,Rd} \cdot r_t + A_{eff-LC6} \cdot f_{jd} \cdot r_{c-LC6} = 104.7 \text{ kNm}$

$M_{Rd-LC9} = F_{T,1,Rd} \cdot r_b + A_{eff-LC9} \cdot f_{jd} \cdot r_{c-LC9} = 100.8$ kNm

4e)The end of column needs to be checked. The design resistance in pure compression is

$$N_{pl,Rd} = \frac{A \cdot f_y}{\gamma_{M0}} = \frac{6\,525 \cdot 235}{1.0} = 1\,533.4 \text{ kN}$$ EN1993-1-8 cl 6.2.4

and column bending resistance

$$M_{pl,Rd} = \frac{W_{pl} \cdot f_y}{\gamma_{M0}} = \frac{481 \cdot 10^3 \cdot 235}{1.0} = 113.1 \text{ kNm}$$ EN1993-1-8 cl 6.2.5

The interaction of normal force changes moment resistance

$$M_{Ny,Rd} = M_{pl,Rd} \cdot \frac{1 - \frac{N_{Sd}}{N_{pl,Rd}}}{1 - 0.5 \cdot \frac{A - 2 \cdot b \cdot t_f}{A}} = 113.0 \cdot \frac{1 - \frac{80}{1\,533.4}}{1 - 0.5 \cdot \frac{6\,525 - 2 \cdot 180 \cdot 14}{6\,525}} = 120.9 \text{ kNm}$$ EN1993-1-8 cl 6.2.9

4f) To evaluate the bending stiffness the particular component stiffness is calculated

$$k_b = 2.0 \cdot \frac{A_s}{L_b} = 2.0 \cdot \frac{314}{190} = 3.3 \text{ mm}$$ EN1993-1-8 cl 6.3

$$k_p = \frac{0.425 \cdot L_{beff} \cdot t^3}{m^3} = \frac{0.425 \cdot 180 \cdot 30^3}{52.1^3} = 14.6 \text{ mm}$$

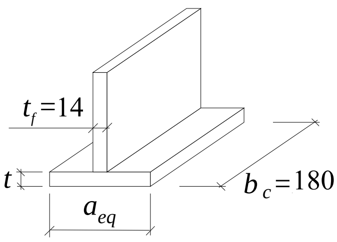

Fig. 9.43 The T stub in compression

The concrete block stiffness is evaluated based on T-stub in compression, see Fig. 9.43

$$a_{eq} = t_f + 2.5 \cdot t = 14 \cdot 2.5 \cdot 30 = 89 \text{ mm}$$

$$k_c = \frac{E_c}{1.275 \cdot E_s} \cdot \sqrt{a_{eq} \cdot b_c} = \frac{33\,000}{1.275 \cdot 210000} \cdot \sqrt{89 \cdot 180} = 15.6 \text{ mm}$$ EN1993-1-8 6.3

4g) The lever arm of component in tension z_t and in compression z_c to the column base neutral axes is

$$r_t = \frac{h_c}{2} + e_c = \frac{180}{2} + 60 = 150 \text{ mm}$$

$$z_c = \frac{h_c}{2} - \frac{t_f}{2} = \frac{180}{2} + \frac{14}{2} = 83 \text{ mm}$$

The stiffness of tension part, bolts and T stub, is calculated as

$$k_t = \frac{1}{\frac{1}{k_b} + \frac{1}{k_p}} = \frac{1}{\frac{1}{3.3} + \frac{1}{14.6}} = 2.7 \text{ mm}$$ EN1993-1-8 6.3

4h) For the calculation of the initial stiffness of column base is evaluated the lever arm

$$r = r_t + z_c = 150 + 83 = 233 \text{ mm}$$

and EN1993-1-8 cl 6.2.9

$$a = \frac{k_c \cdot r_{c1} - k_t \cdot r_t}{k_c + k_t} = \frac{15.6 \cdot 83 - 2.7 \cdot 150}{15.6 + 2.7} = 43.26 \text{ mm}$$

The bending stiffness is calculated for particular constant eccentricity

$$e_{LC-6} = \frac{M_{Rd-LC6}}{F_{Sd-LC6}} = \frac{104.7 \cdot 10^6}{80.0 \cdot 10^3} = 1\,308.8 \text{ mm}$$

$$e_{LC-9} = \frac{M_{Rd-LC9}}{F_{Sd-LC9}} = \frac{100.8 \cdot 10^6}{31.6 \cdot 10^3} = 3\,189.9 \text{ mm}$$

as

$$S_{j,ini-LC6} = \frac{e_{LC-6}}{e_{LC-6} + a} \cdot \frac{E_s \cdot r^2}{\mu \sum_i \frac{1}{k_i}} = \frac{1\,308.8}{1\,308.8 + 3\,189.9} \cdot \frac{210\,000 \cdot 233^2}{1 \cdot \left(\frac{1}{2.7} + \frac{1}{15.6}\right)} = 25\,301 \text{ kNm/rad}$$ EN1993-1-8 cl 6.3

$$S_{j,ini-LC9} = \frac{e_{LC-9}}{e_{LC-9} + a} \cdot \frac{E_s \cdot r^2}{\mu \sum_i \frac{1}{k_i}} = \frac{3\,189.9}{3\,189.9 + 3\,189.9} \cdot \frac{210\,000 \cdot 233^2}{1 \cdot \left(\frac{1}{2.7} + \frac{1}{15.6}\right)} = 25\,846 \text{ kNm/rad}$$

These values of stiffness do not satisfy the condition about the rigid base

$S_{j,ini} \geq 30\, E \cdot I_b / L_b = 45\,538$ kNm/rad

EN1993-1-8 cl 5.2

Step 5 Updating of internal forces and moments

Steps 1 to 4 should be evaluated again considering internal forces obtained from a structural analysis taking into account the stiffness of column base, see Fig. 9.44. Tab. 9.4 summarizes results of the structural analysis of the two meaning full combinations N_{min} and M_{max}.

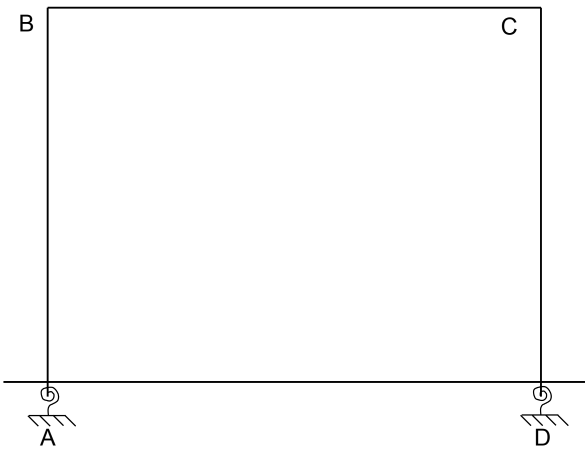

Fig. 9.44 Structural system with rotational springs

Tab. 9.4 Comparison of internal forces between the model with rigid column base joint and the model with the actual stiffness

Load case	Column base stiffness	Point A		Point B		Point C		Point D	
		N [kN]	M [kNm]	N [kN]	M [kNm]	N [kN]	M [kNm]	N [kN]	M [kNm]
6	Rigid	-57.0	1.6	-54.0	27.7	-56.0	49.3	-80.0	51.0
	Semi-rigid	-56.9	3.1	-53.3	24.3	-57.1	-40.7	-80.8	48.4
9	Rigid	-31.6	95.6	-29	-18.7	-29.0	-36.0	-47.0	32.6
	Semi-rigid	-30.5	87.3	-27.9	-17.7	-30.9	-40.6	-48.4	34.7

For the LC6 has been implemented a structural model with two rotational springs equal to 25 301 kNm/rad. For the LC9 the adopted rotational stiffness was equal to 25 846 kNm/rad. Due to the proximity of the stiffness value calculated in Step 4. it was reasonable to assumed in a simplified manner. The lower value of the stiffness in order to update the internal forces of the system.

As shown in the above table, the differences in terms of internal forces are negligible and therefore the single elements and the beam to column joint is considered verified. Tab. 9.4 synthetizes the updated properties of the column base joint.

Tab. 9.4 Updated properties of the column base joint

Load case	Column base stiffness	A_{eff} [mm^2]	b_{eff} [mm]	r_c [mm]	M_{rd} [kNm]	$S_{j.ini}$ [kNm/rad]
6	Rigid	19 973.1	68.3	112.1	104.7	25 301
	Semi-rigid	20 008.0	68.4	112.0	104.8	25 268
9	Rigid	17 802.7	60.9	115.8	100.8	25 846
	Semi-rigid	17 757.0	60.7	115.8	100.7	25 344

The designed column base fulfils the asked requirements as shown in the Tab. 9.4.

10 SUMMARY

This design manual summarises the reached knowledge in the RFCS Project RFSR-CT-2007-00051 New Market Chances for Steel Structures by Innovative Fastening Solutions between Steel and Concrete (INFASO). The material was prepared in cooperation of two teams of researchers one targeting on fastening technique modelling and others focusing to steel joint design from Institute of Structural Design and Institute of Construction Materials, Universität Stuttgart, Department of Steel and Timber Structures, Czech Technical University in Prague, and practitioners Gabinete de Informática e Projecto Assistido Computador Lda., Coimbra, Goldbeck West GmbH, Bielefeld, stahl+verbundbau GmbH, Dreieich and European Convention for Constructional Steelwork, Bruxelles.

The model of three types of steel to concrete connections with the headed studs on anchor plate are introduced. There are based on component method and enable the design of steel to concrete joints in vertical position, e.g. beam to column or to wall connections, and horizontal ones, base plates. The behaviour of components in terms of resistance, stiffness, and deformation capacity is summed up for components in concrete and steel parts: header studs, stirrups, concrete in compression, concrete panel in shear, steel reinforcement, steel plate in bending, threaded studs, anchor plate in tension, beam web and flange in compression and steel contact plate.

In the Chapters 5 and 6 are described the possibility of assembly of components behaviour into the whole joint behaviour for resistance and stiffness separately. The presented assembly enables the interaction of normal forces, bending moments and shear forces acting in the joint. The global analyses in Chapter 7 is taken into account the joint behaviour. The connection design is sensitive to tolerances, which are recapitulated for beam to column connections and base plates in Chapter 8. The worked examples in Chapter 9 demonstrates the application of theory to design of pinned and moment resistant base plates, pinned and moment resistance beam to column connections and the use of predicted values into the global analyses.

References

Standards and guidelines

CEB-FIP Model Code 1990, Comité Euro-International du Béton, Lausanne, 1993.

CEN/TS1992-4-1, *Design of fastenings for use in concrete – Part 4-2, Headed fasteners* Technical Specification, CEN, Brussels, 2009.

EN1090-2, *Execution of steel structures and aluminium structures, Part 2, Technical requirements for steel structures.* CEN, Brussels, 2008.

EN13670, *Execution of concrete structures*, CEN, Brussels, 2011.

EN1990, Eurocode 0: *Basis of structural design*, CEN, Brussels, 2002.

EN1991-1-1, *Eurocode 1: Actions on structures, Part 1.1, General actions, Densities, self-weight, imposed load for buildings*, CEN, Brussels, 2002.

EN1991-1-1, *Eurocode 1: Actions on structures, Part 1.7, General actions, Densities, self-weight, imposed load for buildings*, CEN, Brussels, 2006.

EN1992-1-1, Eurocode 2, Design of concrete structures, Part 1-7, *General actions - Accidental actions*, CEN, Brussels, 2004.

EN1993-1-1, Eurocode 3, Design of steel structures, Part 1-1, *General rules and rules for buildings*, CEN, Brussels, 2010.

EN1993-1-8, Eurocode 3, Design of steel structures, Part 1-8, *Design of joints*, CEN, Brussels, 2006.

EN1994-1-1, Eurocode 4, Design of composite steel and concrete structures, Part 1-1, *General rules and rules for buildings*, CEN, 2010.

EN206-1, Concrete - Part 1, *Specification, performance, production and conformity*, CEN, Brussels, 2000.

FIB Bulletin 58, *Design of anchorages in concrete,* Guide to good practice, International federation for structural concrete, Lausanne, 2011.

Textbooks and publications

Aribert, J. M., *Influence of Slip on Joint Behaviour*, Connections in Steel Structures III, Behaviour, Strength and Design, Third International Workshop, Trento, 1995.

Astaneh A. et al., *Behaviour and design of base plates for gravity, wind and seismic loads,* In AISC, National Steel Construction Conference, Las Vegas, 1992.

Bouwman L.P., Gresnigt A.M., Romeijn A., *Research into the connection of steel base plates to concrete foundations*, TU-Delft Stevin Laboratory report 25.6.89.05/c6, Delft.

Bravery P.N.R., *Cardington Large Building Test Facility*, Construction details for the first building. Building Research Establishment, Internal paper, Watford (1993) 158.

British Steel plc, *The behaviour of multi-storey steel framed buildings in fire*, European Joint Research Programme, Swinden Technology Centre, South Yorkshire, 1999.

Demonceau J., *Steel and composite building frames: Sway-response under conventional loading and development of membrane effects in beam further to an exceptional actions.* PhD Thesis, University of Liege, Liege, 2008.

Demonceau J.F., Huvelle C., Comeliau L., Hoang L.V., Jaspart J.P., Fang C. et al, *Robustness of car parks against localised fire,*European Comission, Final Report RFSR-CT-2008-00036, Brussels, 2012.

Da Silva L. Simoes, Towards a consistent design approach for steel joints undergeneralized

loading, *Journal of Constructional Steel Research*, 64 (2008) 1059–1075.
De Wolf J. T., Sarisle, E. F., Column base plates with axial loads and moments, *Journal of Structural Division ASCE,* 106 (1980) 2167-2184.
Di Sarno L, Pecce M.R., Fabbrocino G., Inelastic response of composite steel and concrete base column connections, *Journal of Constructional Steel Research* 63 (2007) 819–832.
ECCS, European Convention for Constructional Steelwork, *Design of Composite Joints for Buildings*. Publication 109, TC11, Composite Structures, Belgium, 1999.
Ermopoulos J. Ch., Stamatopoulos G. N., Mathematical Modelling of Column Base Plate Connections, *Journal of Constructional Steel Research,* 36 (1996) 79-100.
Gresnigt N., Romeijn A., Wald F., Steenhuis M., Column Bases in Shear and Normal Force*, Heron* (2008) 87-108.
Heinisuo M., Perttola H., Ronni H., Joints between circular tubes, *Steel Construction*, 5(2) (2012) 101-107.
Henriques J., Behaviour of joints: simple and efficient steel-to-concrete joints, PhD Thesis, University of Coimbra, 2013.
Hofmann J. Behaviour *and design of anchorages under arbitrary shear load direction in uncracked concrete*, (Tragverhalten und Bemessung von Befestigungen unter beliebiger Querbelastung in ungerissenem Beton), PhD Thesis, IWB, University of Stuttgart, 2005.
Horová K., Wald F., Sokol Z., *Design of Circular Hollow Section Base Plates,* in Eurosteel 2011 6th European Conference on Steel and Composite Structures. Brussels, 2011 (1) 249-254.
Huber G., Tschemmernegg F., Modeling of Beam-to- Column Joints: Test evaluation and practical application, *Journal of Constructional Steel Research* 45 (1998) 119-216.
Jaspart J.P., Design of structural joints in building frames, *Prog. Struct. Engng Mater*., 4 (2002) 18–34.
Jaspart J.P., *Recent advances in the field of steel joints - column bases and further configurations for beam-to-column joints and beam splices,* Professorship Thesis, Department MSM, University of Liege, Belgium, 1997.
Johansen K. W., *Pladeformler*, Kobenhavn, Pol. Forening, 1949.
Kuhlmann U. , Hofman J., Wald F., da Silva L., Krimpmann M., Sauerborn N. et al, *New market chances for steel structures by innovative fastening solutions between steel and concrete INFASO,* Final report EUR 25100 EN, European Commission, 2012.
Mallée R., Silva J. F., *Anchorage in Concrete Construction*, Ernst and Sohn Verlag, Darmstadt, 2006, ISBN 978-433-01143-0.
Maquoi R., Chabrolin B., *Frame Design Including Joint Behaviour*, ECSC, Report 18563. Luxembourg. Office for Official Publications of the European Communities, 1998.
Melchers R. E., Column-base response under applied moment, J*ournal of Constructional Steel Research* 23 (1992) 127-143.
Metric studs, Nelson stud welding specification, 2009, http://www.nelsonstud.com.
Metric studs, Nelson stud welding stud and ferrule catalog, 2013, http://www.nelsonstud.com.
Moore D.B. *Steel fire tests on a building framed. Building Research Establishment*, No. PD220/95, Watford (1995) 13.
Nakashima S., *Experimental behaviour of steel column-base connections*, Report, Osaka Institute of Technology, 1996.

Nakashima S., Mechanical Characteristics of Exposed Portions of Anchor Bolts in Steel Column Bases under Combined Tension and Shear. *Journal of Constructional Steel Research,* 46, (1998) 206-277.

Pallarés I., Hajjar J. F., Headed Steel Stud Anchors in Composite Structures: Part I – Shear, Part II – Tension and Interaction, The Newmark Structural Engineering Laboratory, NSEL-013, April 2009.

Penserini P., Colson A., Ultimate limit strength of column-base connections, *Journal of Constructional Steel Research* 14 (1989) 301-320.

Pertold J, Xiao R.Y, Wald F, Embedded steel column bases: I. Experiments and numerical simulation, *Journal of Constructional Steel Research*, *56 (3) 2000*, *253-270.*

Pertold J, Xiao R.Y, Wald F, Embedded steel column bases: II. Design model proposal, *Journal of Constructional Steel Research*, *56 (3) 2000*, *271-286.*

Pitrakkos T., Tizani W., Experimental behaviour of a novel anchored blind-bolt in tension Engineering Structures, 49, 2013, 905-919.

Romeijn A., The fatigue behaviour of multiplanar tubular joints*, Heron* 39 (1994) 3-14.

Simoes da Silva L., Simoes R., Gervasio H., *Design of Steel Structures*, *Eurocode 3: Design of steel structures, Part 1-1 General rules and rules for buildings*. ECCS Eurocode Design Manuals, 2010.

Steenhuis M., Wald F., Sokol Z., Stark J.W.B., Concrete in Compression and Base Plate in Bending*, Heron* 53 (2008) 51-68.

Thambiratnam, D. P., Paramasivam P., Base plates under axial load and moment, *Journal of Structural Engineering* 112 (1986) 1166-1181.

Wald F., Bouguin V., Sokol Z., Muzeau J.P., Component Method for Base Plate of RHS, Proceedings of the Conference Connections in Steel Structures IV: Steel Connections in the New Millenium, October 22-25, Roanoke 2000, s. IV/8- IV/816.

Wald F., Sokol Z., Jaspart J.P., Base Plate in Bending and Anchor Bolts in Tension, *Heron* 53 (2008) 21-50.

Wald F., Sokol Z., Steenhuis M. and Jaspart, J.P., Component Method for Steel Column Bases, *Heron* 53 (2008) 3-20.

Weynand K., Jaspart J.-P. Steenhuis M., *The stiffness model of revised Annex J of Eurocode 3*, in Connections in Steel Structures III, Pergamon, New York, 1996, 441-452.

Wilkinson T., Ranzi G., Williams P., Edwards M. Bolt prying in hollow section base plate connections*,* in *Sixth International Conference on Advances in Steel Structures and Progress in Structural Stability and Dynamics*, Hong Kong, 2009, ISBN 978-988-99140-5-9.

Software

Abaqus 6.11, *Theory Manual and Users Manuals*. Dassault Systemes Simulia Corp., 2011.

ACOP software, http://amsections.arcelormittal.com.

EC3 Steel Member Calculator for iPhone, CMM, Associacao Portuguesa de Construcao Metalica e Mista, https://itunes.apple.com/us/app/ec3-steel-member-calculator.

Sources

This Design manual I was prepared based on Final report (Kuhlmann et al, 2012). The following Figs were worked up according the Eurocodes and its background materials: EN1090-2:2008 Figs 8.1-8.3, EN1992-1-1:2004 Fig. 3.5, CEB-FIP:1990 Fig. 4.11, (Gresnight et al, 2008) Fig. 4.20, (Steenhuis et al, 2008) Figs 3.6-3.9, (Wald et al, 2008) Figs 4.1-4.8.

List of partners working on the dissemination project RFS2-CT-2012-00022 Valorisation of knowledge for innovative fastening solution between steel and concrete:

Ulrike Kuhlmann, Jakob Ruopp
Institute of Structural Design
University Stuttgart
Pfaffenwaldring 7
70569 Stuttgart
Germany
Jan Hofmann, Akanshu Sharma
Institute of Construction Materials
University Stuttgart
Pfaffenwaldring 4
70569 Stuttgart
Germany
František Wald, Šárka Bečková, Ivo Schwarz
Czech Technical University in Prague
Department of Steel and Timber Structures
Thákurova 7
16629 Praha
Czech Republic
Luis Simões da Silva, Helena Gervásio, Filippo Gentili
GIPAC – Gabinete de Informática e Projecto Assistido Computador Lda.
Trav. Padre Manuel da Nóbrega 17
3000-323 Coimbra
Portugal
Markus Krimpmann
Goldbeck West GmbH
Ummelner Str. 4-6
33649 Bielefeld
Germany
Jörg van Kann
stahl+verbundbau GmbH
Im Steingrund 8
63303 Dreieich
Germany
Véronique Dehan
ECCS - European Convention for Constructional Steel work
AVENUE DES OMBRAGES 32
1200 Bruxelles
Belgium

ISBN 978-92-9147-119-5

František Wald, Jan Hofmann, Ulrike Kuhlmann,
Šárka Bečková, Filippo Gentili, Helena Gervásio, José Henriques,
Markus Krimpmann, Ana Ožbolt, Jakob Ruopp, Ivo Schwarz,
Akanshu Sharma, Luis Simoes da Silva, and Jörg van Kann
Design of steel-to-concrete joints, Design manual I

Printing by European Convention for Constructional Steelwork
February 2014
178 pages, 138 figures, 32 tables

Deliverable of a project carried out with a financial grant from the Research Fund for Coal and Steel (RFCS) of the European Community

Design of Steel-to-Concrete Joints

Design Manual II

Deliverable of a project carried out with a financial grant
from the Research Fund for Coal and Steel of the European Community_

Design of Steel-to-Concrete Joints

Universität Stuttgart, Institut für Konstruktion und Entwurf / Institute for Structural Design

Pfaffenwaldring 7

70569 Stuttgart

Germany

Phone: +49-(0)711-685-66245

Fax: +49-(0)711-685-66236

E-mail: sekretariat@ke.uni-stuttgart.de

The present document and others related to the research project INFASO RFSR-CT-2007-00051 "New Market Chances for Steel Structures by Innovative Fastening Solutions between Steel and Concrete and the successive dissemination project RFS2-CT-2012-00022 "Valorisation of Knowledge for Innovative Fastening Solution between Steel and Concrete, which have been co-funded by the Research Fund for Coal and Steel (RFCS) of the European Community, can be accessed for free on the following project partners' web sites:

Czech: steel.fsv.cvut.cz/infaso

Germany: www.uni-stuttgart.de/ke/

Germany: www.iwb.uni-stuttgart.de/

Portugal: www.steelconstruct.com/site/

List of Partners

List of partners working on the dissemination project RFS2-CT-2012-00022 Valorization of knowledge for innovative fastening solution between steel and concrete:

Ulrike Kuhlmann, Jakob Ruopp
Institute of Structural Design
University Stuttgart
Pfaffenwaldring 7
70569 Stuttgart
Germany

Jan Hofmann, Akanshu Sharma
Institute of Construction Materials
University Stuttgart
Pfaffenwaldring 4
70569 Stuttgart
Germany

František Wald, Šárka Bečková, Ivo Schwarz
Czech Technical University in Prague
Department of Steel and Timber Structures
Thákurova 7
16629 Praha
Czech Republic

Luis Simões da Silva, Helena Gervásio, Filippo Gentili
GIPAC – Gabinete de Informática e Projecto Assistido Computador Lda.
Trav. Padre Manuel da Nóbrega 17
3000-323 Coimbra
Portugal

Markus Krimpmann
Goldbeck West GmbH
Ummelner Str. 4-6
33649 Bielefeld
Germany

Jörg van Kann
stahl+verbundbau GmbH
Im Steingrund 8
63303 Dreieich
Germany

Véronique Dehan
ECCS - European Convention for Constructional Steel work
AVENUE DES OMBRAGES 32
1200 Bruxelles
Belgium

Contents

LIST OF PARTNERS 3

CONTENTS 5

1 INTRODUCTION 9

1.1 Introduction and structure of the document 9

2 PROGRAM DESCRIPTION 11

2.1 Restrained connection of composite beams 11

2.1.1 General 11

2.1.2 Program structure 11

2.1.3 Input and output data and input data cells 12

2.1.4 Calculation 14

2.1.5 Output mask 14

2.1.6 Results of evaluation of individual components 17

2.1.7 Global Results 21

2.2 Slim anchor plate with headed studs – bending joints 22

2.2.1 General 22

2.2.2 Program structure and static model 22

2.2.3 EXCEL-Worksheets / VBA-Program 27

2.2.4 Components 28

2.2.5 Safety factors 28

2.2.6 Boundary conditions 28

2.2.7 Input mask 31

2.2.8 Output mask 33

2.2.9 Optimization of the joint 36

2.3 Rigid anchor plate with headed studs – simple joint 37

2.3.1 General 37

2.3.2 Program structure and static model 37

2.3.3 EXCEL Worksheets / VBA program 37

2.3.4 Components 38

2.3.5 Safety factors 38

2.3.6 Boundary condition 39

2.3.7 Input mask 39

2.3.8 Output mask 40

2.3.9 Optimization of the joint 40

3 DESIGN EXAMPLES 42

3.1 Composite beam of a standard office structure connected to reinforced concrete wall 42

3.1.1 General 42

3.1.2 Execution options 43

3.1.3 Structural analysis of the joint 44

3.1.4 Conducting 49

3.2 Column base as connection of a safety fence on a car parking deck to a reinforced concrete slab 50

3.2.1 General 50

3.2.2 Execution options 50

3.2.3 Conducting and assessment 55

3.3 Connection of a balcony construction on an insulated exterior reinforced concrete wall as simple connection 56

3.3.1 General 56

3.3.2 Execution options 57

3.3.3 Conducting and Assessment 60

4 PARAMETER STUDIES 62

4.1 General 62

4.2 Parameter study on concrete components 62

4.2.1 General 62

4.2.2 Example considered 62

4.2.3 Parameter studied and methodology followed 62

4.2.4 Sensitivity to Concrete Strength, f_{ck} 63

4.2.5 Sensitivity to parameter α_c 64

4.2.6 Sensitivity to effective embedment depth h_{ef} 65

4.2.7 Sensitivity to shoulder with a 66

4.2.8 Sensitivity to pressing relation m 66

4.2.9 Sensitivity to design bond strength f_{bd} 67

4.2.10 Sensitivity to diameter of supplementary reinforcement $d_{s,re}$ 67

4.2.11 Sensitivity to descending anchor stiffness due to concrete, $k_{p,de}$ 68

4.2.12 Summary of sensitivity of anchorage stiffness to various parameters 68

4.3 Parameter study on simple steel-to-concrete joints 70

4.3.1 General 70

4.3.2 Validation of the model 70

4.3.3 Sensitivity study of major parameters 72

4.3.4 Limits of the model and recommendations 78

4.4 Parameter study on column bases 81

4.4.1 Validation of the model 81

4.4.2 Sensitivity study of major parameters 83
4.4.3 Limits of the model 89
4.4.4 Recommendation for design values 90
4.5 Parameter study on composite joints 99
4.5.1 General 99
4.5.2 Parameters Studied and methodology followed 99
4.5.3 Failure Mechanism 100
4.5.4 Valorization of slab reinforcement properties 100
4.5.5 Variation of angle θ 102
4.5.6 Variation of wall concrete grade 104
4.5.7 Interaction between wall thickness and concrete grade 105
4.5.8 Summary, Predesign charts for ductile behaviour 107
5 SUMMARY 111
6 REFERENCES 112

1 Introduction

1.1 Introduction and structure of the document

The mixed building technology allows to utilise the best performance of all structural materials available such as steel, concrete, timber and glass. Therefore the building are nowadays seldom designed from only one structural material. Engineers of steel structures in practice are often faced with the question of economical design of steel-to-concrete joints, because some structural elements, such as foundations, stair cases and fire protection walls, are optimal of concrete. A gap in knowledge between the design of fastenings in concrete and steel design was abridged by standardized joint solutions developed in the INFASO project, which profit from the advantage of steel as a very flexible and applicable material and allow an intelligent connection between steel and concrete building elements. The requirements for such joint solutions are easy fabrication, quick erection, applicability in existing structures, high loading capacity and sufficient deformation capacity. One joint solution is the use of anchor plates with welded headed studs or other fasteners such as post-installed anchors. Thereby a steel beam can be connected by butt straps, cams or a beam end plate connected by threaded bolts on the steel plate encased in concrete. Examples of typical joint solutions for simple steel-to-concrete joints, column bases and composite joints are shown in Fig. 1.1.

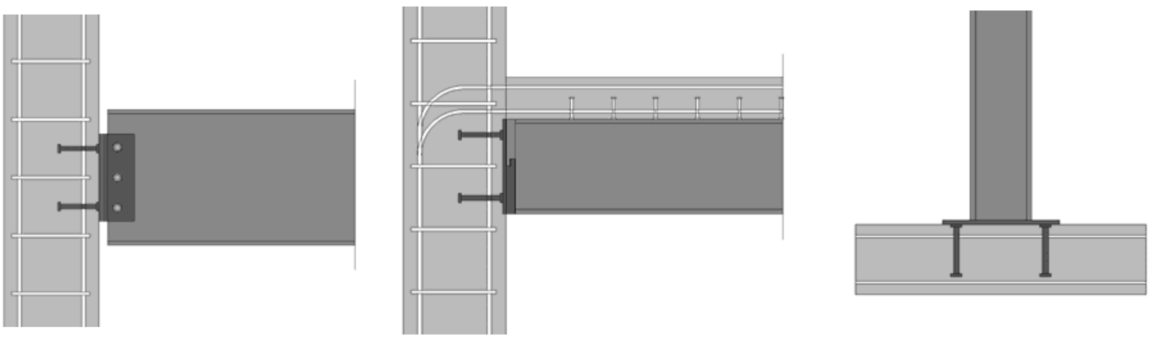

a) b) c)

Fig. 1.1: Examples for steel-to-concrete joints: a) simple joint, b) composite joint, c) column bases

The Design Manual II "Application in practice" shows, how the results of the INFASO projects can be simply applied with the help of the developed design programs. For this purpose the possibility of joint design with new components will be pointed out by using practical examples and compared with the previous realizations. A parametric study also indicates the effects of the change of individual components on the bearing capacity of the entire group of components. A detailed technical description of the newly developed components, including the explanation of their theory, can be found in the Design Manual I "Design of steel-to-concrete joints"[13].

Chapter 2 includes a description of the three design programs that have been developed for the connection types shown in Fig. 1.1. Explanations for the application in practice, the handling of results and informations on the program structure will be given as well as application limits and explanations of the selected static system and the components. Practical examples, which have been calculated by using the newly developed programs, are included in Chapter 3. These connections are compared in terms of handling, tolerances and the behaviour under fire conditions to joints calculated by common design rules. The significant increase of the bearing capacity of the "new" connections under tensile and / or bending stress result from the newly developed components "pull-out" and "concrete cone failure with additional reinforcement". Chapter 4 contains parameter studies in order to show the influence of the change of a single component on the entire group of components, and hence to highlight their effectiveness.

2 Program description

2.1 Restrained connection of composite beams

2.1.1 General

In the following the Excel sheet "Restrained connection of composite beams" (Version 2.0 Draft) [21] is presented. With this program the load bearing capacity (moment and shear) of a fully defined joint, composed of tensional reinforcement in slab and cast-in steel plate with headed studs and additional reinforcement at the lower flange of the steel section can be determined. The shear and the compression component, derived from given bending moment, are acting on a welded steel bracket with a contact plate in-between, as the loading position on the anchor plate is exactly given. The tensional component derived from given bending moment is transferred by the slab reinforcement, which is bent downwards into the adjacent wall. Attention should be paid to this issue as at this state of modelling the influence of reduced distances to edges is not considered. The wall with the cast-in steel plate is assumed to be infinite in elevation. In this program only headed studs are considered. Post installed anchors or similar have to be taken in further consideration.

2.1.2 Program structure

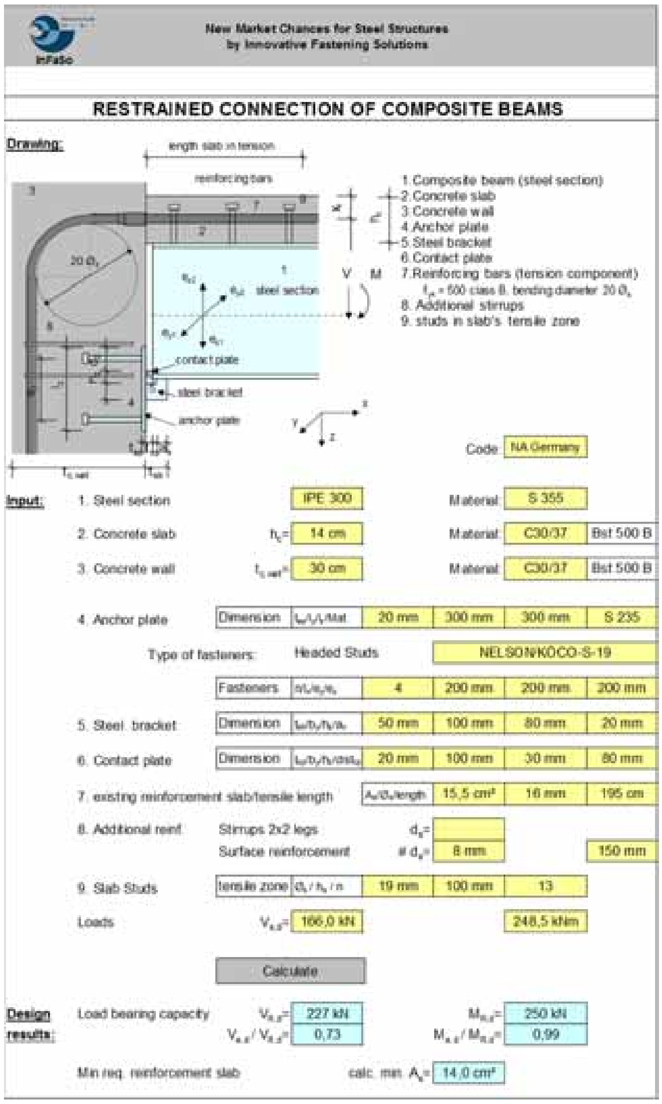

Fig. 2.1: EXCEL input file

The Excel file is composed of two visible sheets. The top sheet contains full input, a calculation button and the resulting load bearing capacity of the joint with utilization of bending moment and shear (see Fig. 2.1). The second sheet gives the input data echo, with some additional calculated geometry parameters and the characteristic material properties. Subsequently it returns calculation values to allow checking the calculation flow and intermediate data. Other sheets are not accessible to the user. One contains data for cross sections (only hot rolled sections are considered), for headed studs and concrete. The three other sheets are used to calculate tension in studs, shear resistance, anchor plate assessment and stiffness values. Parameter and results are given in output echo (sheet 2). The user introduces data in cells coloured in light yellow. All drawings presented are used to illustrate the considered dimensions and theory used behind. They do neither change with input nor are drawn to scale. A check for plausibility will be executed for some input parameters, with warning but without abortion. The user has to interpret results on own responsibility and risk. The majority of the calculations are performed introducing formulae in the cells. However, when more complex calculation and iterative procedure is required, a macro is used to perform these calculation. The user has to press the corresponding 'Calculation' button. If any changes in the parameters are made the macro calculation should be repeated. By opening the worksheet the accessible input cells (in yellow) are preset with reasonable default values. They must be changed by the user. Hot rolled steel sections, steel and concrete grades, type and length of studs/reinforcement are implemented with the help of a dropdown menu to choose one of the given parameters. To model the stiffness according to the developed theory some additional information must be given in the top (input) sheet. The effective width and length of slab in tension, the reinforcement actually built in and the number and type of studs connection slab and steel beam. These information do not influence the load capacity calculations.

2.1.3 Input and output data and input data cells

The user inserts data only into cells coloured in light yellow. The accessible input cells are not empty but preset per default with reasonable values. They can be changed by the user. The units given in the input cells must not be entered, they appear automatically to remind the correct input unit.

Choice of appropriate code – whereas Eurocode EN 1992-1-1 [7] for design of reinforced concrete, EN 1993-1-1 [8] for design of steel and EN 1994-1-1 [10] for steel-concrete composite structures are the obligatory base for all users, the national annexes must be additionally considered. For purpose of design of connections to concrete it can be chosen between EN 1992-1-1 [7] in its original version and the appropriate (and possibly altered) values according to national annex for Germany, Czech Republic, Portugal, the UK, France and Finland. The input procedure should be self-explaining, in context with the model sketch on top of first visible sheet. According to this principal sketch of the moment resisting joint there are nine components and their input parameters necessary to define characteristics and geometry.

1. + 2. Composite beam of a hot rolled section of any steel grade acc. to EN 1993-1-1 [8] and a reinforced concrete slab of any concrete grade acc. to EN 1992-1-1 [7]. They are connected by studs and working as a composite structure according to EN 1994-1-1 [10]. This composite behaviour is only subject of this calculation because it's flexibility due to slip influences the connection stiffness. Following selections can be made:

- Type of sections: Hot rolled sections IPE, HEA, HEB, HEM of any height
- Steel grades: S 235, S275, S355 acc. to EN 1993-1-1 [8] (EN-10025)
- Concrete grades: C20/25 until C50/60 acc. to EN 1992-1-1 [7]
- Reinforcement grade: BSt 500 ductility class B acc. to EN 1992-1-1 [7]

3. Concrete wall – the shear and bending moment are to be transferred into the infinite concrete wall with limited thickness. Per definition reinforcement and a cast-in steel plate are used. It can be chosen between:

- Concrete grades: C20/25 until C50/60 acc. to EN 1992-1-1 [7]
- Reinforcement grade: Bst 500 ductility class B acc. to EN 1992-1-1 [7]

4. Anchor plate with studs – at the bottom flange of the steel section an anchor plate is inserted into the concrete wall. Welded studs on the rear side transfer tensional (if any) and/or shear forces from top of anchor plate into the concrete. The compression components are transferred directly by contact between the steel plate and the concrete.

- Geometry of plate: [mm], Thickness and 2D-dimensions and steel grade, single input values in input check: thickness ≥ 8mm is deemed to be ok.
- Type of studs: Köco resp. Nelson d19, d22, d25 regular or d19, d22 stainless steel, Peikko d19, d20 regular or d20, d25 reinforcement bar with head all data including steel grades from ETA-approval (e.g. the steel grades are considered automatically according to approval).
- Length of studs: 75 until 525 mm (from ETA-approval), input check: length less than wall thickness less coverage and plate thickness is deemed to be ok.
- Distribution studs: Number of studs (4,6,8) and inner distances, input check: distances to lay within plate are deemed to be ok

5. Steel bracket is welded on top of the anchor plate and takes the shear force with small eccentricity and transfers it into the anchor plate /concrete wall.

- Geometry of plate: Thickness and 2D-dimensions, 'nose' thickness, input check: width and height less than anchor plate is deemed to be ok. Position/eccentricity is required in 6. Contact plate.

6. Contact plate – the contact plate is inserted force-fit between the end of the steel section and the anchor plate at lower flange level. The compression force component from negative (closing) bending moment is transferred on top of anchor plate.

- Geometry of plate: Thickness and 2D-dimensions, eccentricity of plate position in relation to anchor plate centre. Input check: width less than anchor plate and position within anchor plate is deemed to be ok.

7. Reinforcement bars – in the slab of the composite section. The tensional force component from negative (closing) bending moment is transferred into the wall and bent down on the rear face of the wall and anchored there. Whereas the necessary design reinforcement is calculated by the work sheet, for later use of stiffness calculation, the existing reinforcement in the slab of the composite beam is required. The bar diameter should be chosen in a way that reasonable spacings within the effective width result and that the bend can be installed within the wall. The length of tension zone is crucial for the stiffness evaluation and depends on the structural system. It must be chosen in accordance with codes or independent calculation results of the underlying model (Example: in case of beam simply supported and other side restrained it is ≈ 0,25 *length, in case of cantilever beam it is 1,0*length)

- Bars: steel area [cm^2], diameter and length of tension zone [cm], input check: reinforcement must be ≥ minimum design reinf. area, spacing of bars should be within interval 5-25 cm, bar curvature Ø*20 must fit into wall.

8. Additional stirrups – these optional stirrups are proposed as an effective means to improve the joint in case of tension forces (if any, only in case of small moments and large shear force with large eccentricity) in the stud. They are useful only in the upper row, and only under certain circumstances of the complete assemblage. Further information can be found in the parameter study in Chapter 4. Generally there is always a surface reinforcement in the front face of the wall. This may be optionally taken into account and will improve the capacity of the joint under certain circumstances of the complete assemblage.

- Reinforcement: bar-diameter of stirrups with legs each very close to studs (default: no stirrup, input range Ø8-14 mm), and surface reinforcement bar-diameter (Ø6-14 mm) and spacing (75-250 mm)

9. Slab studs – these studs are welded at the upper flange of the steel cross section and are the connection medium in the joint between steel and concrete sections to work as a composite structure according to EN 1994-1-1 [10]. Only the composite behaviour is subject of the calculation because it's flexibility due to slip influences the connection stiffness.

- Studs: Diameter (Ø16 -25 mm) and length of studs (75-525 mm) of any kind, input check: length less than slab thickness less coverage.
- Distribution studs: Number of studs < 27 within length of tension zone, input check: spacing of studs should be within limits of EN 1994-1-1 [10].

10. Loads - a combination of shear force and bending moment must be given by overwriting the preset starting values. Design Forces with partial safety factors according to current codes are required. An evaluation of capacity of composite beam section is not executed at that point and must be done separately by the user!

- Loading: Shear force V_{ed} [kN] and bending moment M_{ed} [kNm] from external member calculation.

2.1.4 Calculation

As it is the characteristic of worksheet programming the calculation has to be updated any time if the user changes input parameters. This program does the same, starting with the preset values and recalculates any time the content of a cell (if necessary for the mechanical model) is changed, so any result is up to date. Due to the nonlinear characteristic of the compressed anchor plate on the top of the wall concrete at bottom of top sheet a calculation button is placed, which starts the complex update of the effective geometry (via Macro-programming). After any change of input parameters this button must be pushed for updating the complex evaluation of anchor plate behaviour. Even if differences often can be small, only the calculation starting with the calculation button yields the correct result regarding the presented model. Detailed results are given on second sheet. If the anchor plate is assumed to be rigid, the original dimensions can be used for further calculation. In case of a thin and flexible anchor plate reduced dimensions are returned and used for further calculation.

2.1.5 Output mask

The user inserts data only into cells coloured in light yellow. Any other cell is automatically (or by using the 'Calculate' button) updated with result data. At the bottom of top sheet (see Fig. 2.2) the load bearing capacity and utilization of the joint assemblage for tension and shear is given in terms of $V_{R,d}$ and $M_{R,d}$, resp. $V_{S,d}/V_{R,d}$ and $M_{S,d}/M_{R,d}$. The minimum tensional reinforcement (design) in the slab is given as information. On top of the second sheet (see Fig. 2.2) the input data from page one together with some additionally calculated geometry parameters and characteristic material properties are given. These are:

- Steel section of the composite beam, with characteristics geometric and steel grade values. The section is restricted to common hot rolled sections as available in Europe. Three predefined steel grades are available according to EN 1993-1-1 [8]. Attention should be paid, that these steel grades are only used for assessment of the composite beam and not for the anchoring of the joint.
- Contact plate – the contact plate is an interface between lower flange of the steel section and the anchor plate. Per definition the gravity centre is in one line with the centroid axis of the flange. By input of distance between upper edge of the anchor plate to upper edge of the contact plate the loading position is defined.
- Steel bracket – this bracket is the interface to carry the shear load. The position is defined exactly by input of contact plate because of direct contact. The eccentricity of shear loading, i.e. the position of vertical support of section flange is defined by subtracting half contact area (t_{sb2} or a_x) from total thickness (t_{sb}) of the bracket.
- The rectangular steel plate is defined by three parameters. It is assumed to be flush with surface of concrete wall, where it is embedded. Three predefined steel grades are available according to EN 1993-1-1 [8]. The given steel grade applies for contact plate and steel bracket as well.

The parameters of headed studs are:

- The thickness and the steel grade with characteristic tensional resp. yield strength acc. to the European approvals of the stud types, the number of rows and columns with their corresponding distances of axis.

The parameters of the concrete parts are:

- Slab section – concrete grade with characteristic (cylindrical) strength according to EN 1992-1-1 [7], thickness together with distance of reinforcement (fixed to 40 mm), width of slab and area of reinforcement (given) are returned from input.
- Wall section – concrete grade with characteristic (cylindrical) strength according to EN 1992-1-1, wall thickness together with the distance of the reinforcement (fixed to 40 mm at both sides) are returned from input. The wall is assumed to be infinite, as close to edge anchoring is not considered. Two possible types can be built in as supplementary reinforcement. The orthogonal surface reinforcement of given diameter and spacing (distance to surface 40mm) and the supplementary reinforcement close to the stud in tension to clearly enhance the capacity of the stud in concrete. These stirrups may be defined by arbitrary diameter, whereas the number of legs in that case is fixed to four in this program (i.e. two stirrups very close to each stud, positioned orthogonal to the wall surface).

Joint loading echo:

- Beneath the given external moment and shear loading (design forces) the resulting external design components tension in slab reinforcement (T_d) and compression on contact plate (C_d) are returned – these forces are equal in absence of external axial forces, as it is assumed in that model.
- The eccentricity of the shear force is calculated with geometric components of bracket, anchor plate thickness and - following common practice - the stud diameter. This yields a local moment acting on the anchor plate which is returned.

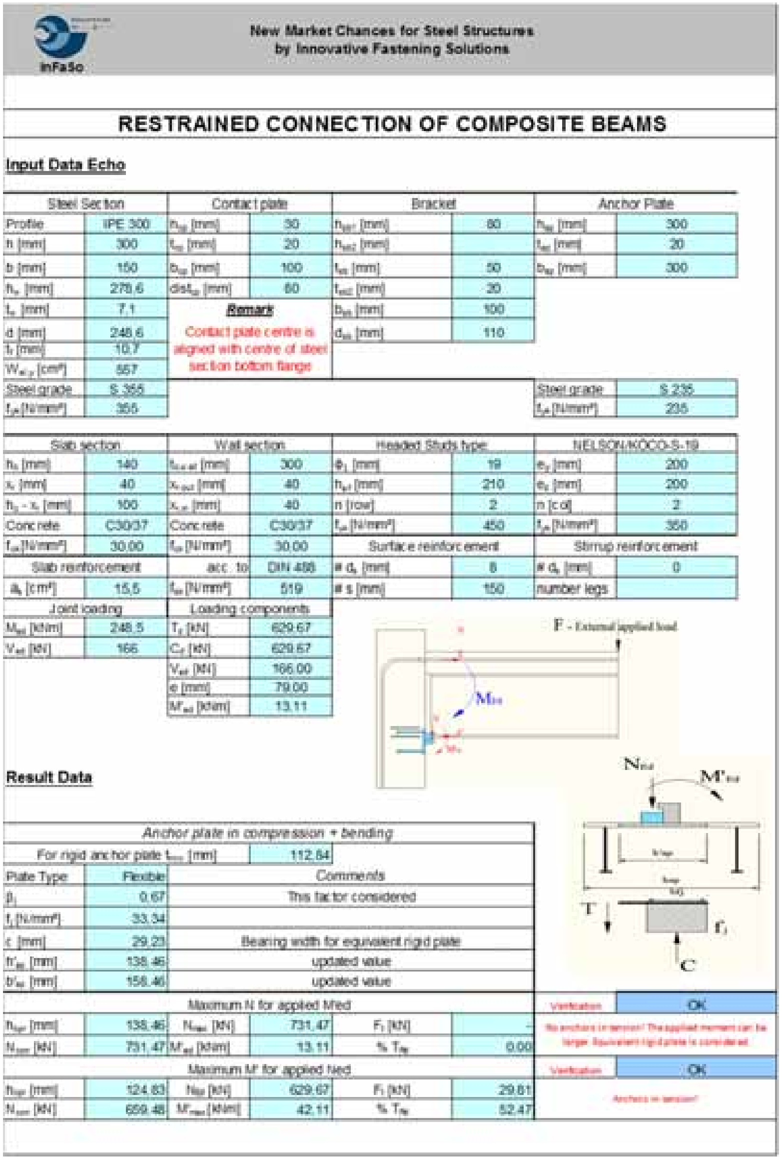

InFaSo

New Market Chances for Steel Structures
by Innovative Fastening Solutions

RESTRAINED CONNECTION OF COMPOSITE BEAMS

Input Data Echo

Steel Section		Contact plate		Bracket		Anchor Plate	
Profile	IPE 300	h_{cp} [mm]	30	h_{bs1} [mm]	80	h_{ap} [mm]	300
h [mm]	300	t_{cp} [mm]	20	h_{bs2} [mm]		t_{ap} [mm]	20
b [mm]	150	b_{cp} [mm]	100	t_{bs} [mm]	50	b_{ap} [mm]	300
h_w [mm]	278,6	$dist_{cp}$ [mm]	60	t_{bs2} [mm]	20		
t_w [mm]	7,1	**Remark**		b_{bs} [mm]	100		
d [mm]	248,6	Contact plate centre is aligned with centre of steel section bottom flange		d_{bs} [mm]	110		
t_f [mm]	10,7						
$W_{el,y}$ [cm³]	557						
Steel grade	S 355					Steel grade	S 235
f_{yk} [N/mm²]	355					f_{yk} [N/mm²]	235

Slab section		Wall section		Headed Studs type		NELSON/KÖCO-S-19	
h_c [mm]	140	t_{wall} [mm]	300	ϕ_1 [mm]	19	e_y [mm]	200
x_r [mm]	40	$x_{r,out}$ [mm]	40	h_{ef} [mm]	210	e_z [mm]	200
$h_c - x_r$ [mm]	100	$x_{r,in}$ [mm]	40	n [row]	2	n [col]	2
Concrete	C30/37	Concrete	C30/37	f_{uk} [N/mm²]	450	f_{yk} [N/mm²]	350
f_{ck} [N/mm²]	30,00	f_{ck} [N/mm²]	30,00	Surface reinforcement		Stirrup reinforcement	
Slab reinforcement		acc. to	DIN 488	# d_s [mm]	8	# d_s [mm]	0
a_s [cm²]	15,5	f_{sk} [N/mm²]	519	# s [mm]	150	number legs	
Joint loading		Loading components					
M_{Ed} [kNm]	248,5	T_s [kN]	629,67				
V_{Ed} [kN]	166	C_s [kN]	629,67				
		V_{Ed} [kN]	166,00				
		e [mm]	79,00				
		M'_{Ed} [kNm]	13,11				

Result Data

Anchor plate in compression + bending							
For rigid anchor plate t_{min} [mm]			112,84				
Plate Type	Flexible	Comments					
β_j	0,67	This factor considered					
f_j [N/mm²]	33,34						
c [mm]	29,23	Bearing width for equivalent rigid plate					
h'_{ap} [mm]	138,46	updated value					
b'_{ap} [mm]	158,46	updated value					
Maximum N for applied Med						Verification	OK
h_{spr} [mm]	138,46	N_{max} [kN]	731,47	F_1 [kN]	-	No anchors in tension! The applied moment can be larger. Equivalent rigid plate is considered.	
N_{con} [kN]	731,47	M'_{Ed} [kNm]	13,11	% T_{Rd}	0,00		
Maximum M' for applied Ned						Verification	OK
h_{spr} [mm]	124,83	N_{Ed} [kN]	629,67	F_1 [kN]	29,81	Anchors in tension!	
N_{con} [kN]	659,48	M'_{max} [kNm]	42,11	% T_{Rd}	52,47		

Fig. 2.2: EXCEL output file 1

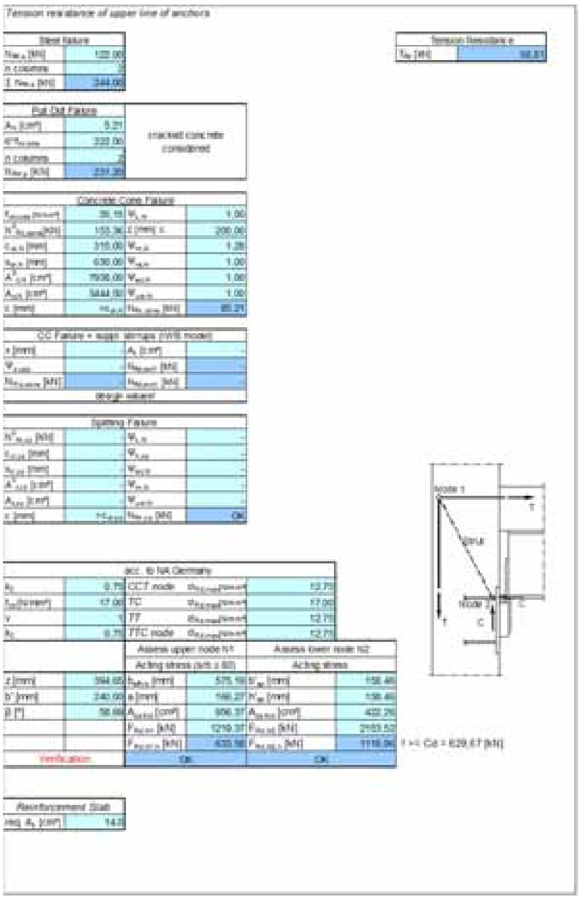

Fig. 2.3: EXCEL output file 2

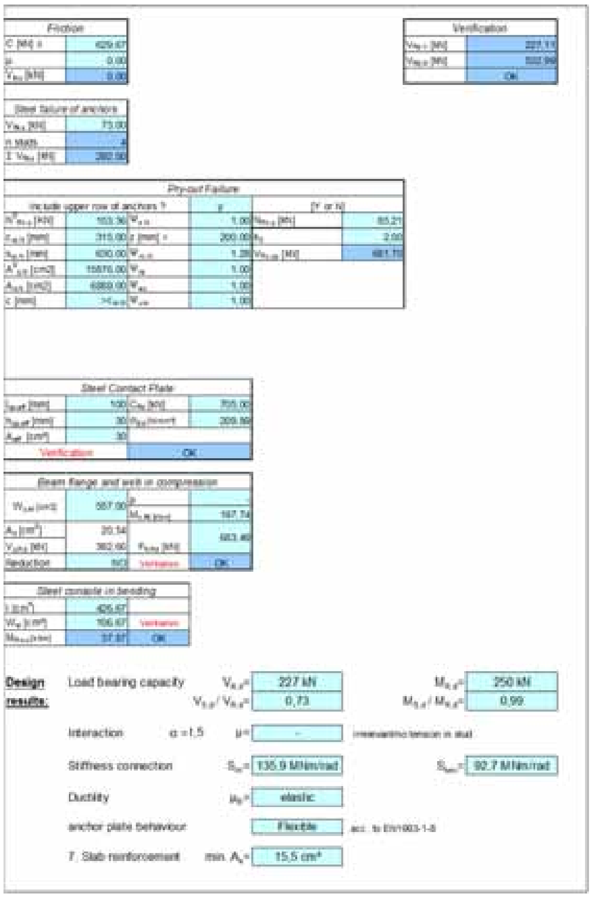

Fig. 2.4: EXCEL output file 3

2.1.6 Results of evaluation of individual components

2.1.6.1 General

In the following the results of evaluation of individual components are presented. In this specific joint constellation of moment resisting composite joint with closing, negative bending moment, generally concrete is in compression and the anchor plate is in bending. The calculation model relies on consideration of the activated components illustrated in the following Fig. 2.5. The Excel sheet evaluates the following components.

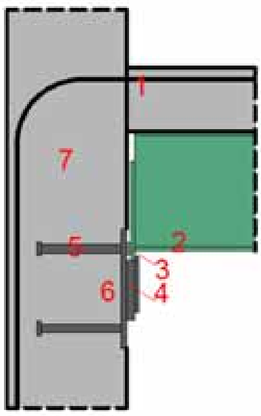

Number	Component
1	Slab reinforcement in tension
2	Beam web and flange in compression
3	Contact plate in compression
4	Bracket in bending (rotational spring)
5	Anchor in tension
6	Concrete in compression with anchor plate in bending
7	Concrete strut in compression.

Fig. 2.5: Components for joints with negative bending moment

2.1.6.2 Anchor plate in compression and bending

Any result of this component is derived from the nonlinear evaluation of combined compression force from negative bending moment and moment due to the eccentricity of shear force at the anchor plate. First the minimum thickness required to consider the anchor plate as rigid is determined. By comparing the minimum thickness previously calculated with the actual thickness of the anchor plate, the type of the plate under consideration is determined. If the plate is rigid, the real dimensions of the plate are used in the following calculations. If flexible, an equivalent rigid and smaller plate is determined. An iterative procedure using a macro is implemented. This macro will be started by pushing the 'CALCULATE' button at top sheet. Subsequently two extreme cases are considered:

- Maximum axial load under compression together with a given eccentricity moment from shear force X eccentricity.
- Maximum bending moment together with a given axial load under compression.

The given values are the same as in cells D/36 and D/33 respectively, the calculated values define the corresponding forces the anchor plate configuration can bear additionally. The fictive effective size of the plate is returned as well.

2.1.6.3 Tensional resistance of the upper row of anchors

In this part the resistance of the upper row of anchors, which possibly may be in tension, is evaluated. Different failure modes are possible. Tension resistance of studs is equal to the minimum resistance value of the five following components:

Steel failure

Steel failure is calculated according to EN 1992-4-2, Cl. 6.2.3 [2].

Pull-out failure

Pull out failure is calculated according to EN 1992-4-2, Cl. 6.2.4 [2]. Cracked concrete is assumed, though uncracked concrete of the wall is possible due to vertical loading in the wall; this must be separately assessed – in case the parameter may be 1,4 for uncracked concrete.

Concrete cone failure without supplementary reinforcement (modified standard model)

Cracked concrete is assumed, though uncracked concrete of the wall is possible due to vertical loading in the wall; this must be separately assessed – in case the parameter may be 1,4 for uncracked concrete.

Concrete cone failure with supplementary hanger reinforcement

If supplementary stirrups are used with a diameter according to the input on the top sheet and per definition with 2+2 legs, an additional resistance component can be evaluated, assuming the stirrup bar axis being 40 mm below the surface (see Fig. 2.6).This concrete cone failure mode depends fully on the behaviour of the stirrups. If steel yielding or steel bond failure occurs before reaching the concrete cone resistance, the resistance force will be the yielding or anchorage force instead.

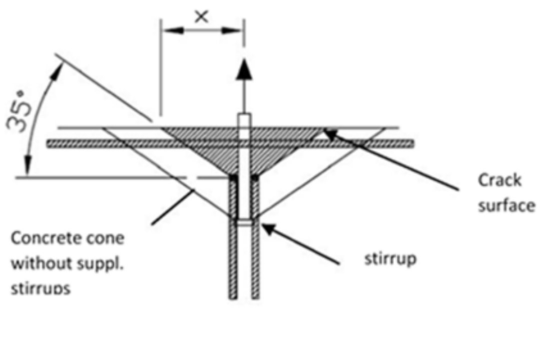

Fig. 2.6: Definition of distance x

- Yielding of stirrups
- Anchoring failure of stirrups

Splitting failure

Due to the fact, that the wall per definition is indefinite only the minimum wall thickness must be checked. For long studs with large cones splitting is generally possible and must be assessed. The existence of a minimum surface reinforcement is sufficient to avoid splitting failure. This reinforcement should be determined in each orthogonal direction according to Eq. (2.1). The material safety factor used with reinforcement bars is γ_s = 1,15. If this conditions is not fulfilled, the resistance force for splitting failure will be calculated.

$$A_s = 0{,}5 \cdot \sum \frac{N_{Ed}}{(f_{yk}/\gamma_{s,reinf})} \tag{2.1}$$

2.1.6.4 Diagonal concrete strut

Regarding the concrete part of the wall, for the bending moment a simple single diagonal compression strut has been assumed. In Fig. 2.7this strut is represented by a dashed line.

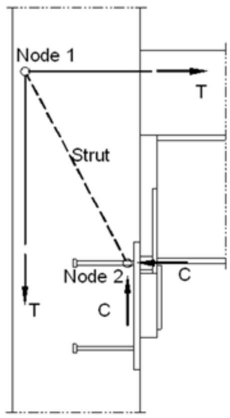

Fig. 2.7: Strut and tie model

2.1.6.5 Longitudinal steel reinforcement in tension

The longitudinal reinforcement of the concrete slab is the only element considered in the tension zone. Concrete is ignored. The tension force is calculated using a two-point-section with reinforcement in slab and compression point in the middle of lower flange, fulfilling equilibrium. The resistance of this first component is evaluated according to EN 1994-1-1, Cl. 4.4 [10] and is restricted to reinforcement within the effective width according to Cl. 4.2.

2.1.6.6 Shear components

In this part the shear resistance of the anchors is evaluated. Three resistance components can be determined for shear: friction, steel failure of the anchors and pry-out failure. Shear resistance of studs is equal to the minimum resistance value of the three components mentioned above.

Friction

In the compressed area a friction component acting opposite to the shear force is possible. Nevertheless the coefficient at that stage is set to zero, i.e. no friction.

Steel failure

Steel failure is calculated according to EN 1992-4-2, Cl. 6.3.3 [2].

Pry-out failure

Pry-out failure is calculated according to EN 1992-4-2, Cl. 6.3.4 [2].

Resulting shear resistance

The shear force which can be applied to the concrete wall is restricted by two mechanism – the minimum of these two will be the relevant design force under given geometrical circumstances.

- Pure shear: the shear resistance is derived from the fore mentioned considerations. This value is governed under usual circumstances, as found in real structures. This force is called $V_{Rd,V}$.
- Shear force with small eccentricity: the shear force can be limited as well by the resistance of the anchor plate. The maximum moment derived from eccentricity under a given compression force is evaluated in 2.1.6.2 cell D/36. Divided by the lever arm of the bracket the shear force called $V_{Rd,M}$ is defined.

2.1.6.7 Other steel components

In this part other steel components on top of the anchor plate might be assessed that should not fail even if they are not part of the model "anchor plate with headed studs". Under consideration are: steel contact plate, beam web and flange in compression and steel bracket. The first two are calculated using EN 1994-1-1 [10] and EN 1993-1-8 [9], respectively. The steel bracket is analysed comparing the acting bending moment with resisting bending moment, at the cross-section in contact with the anchor plate. Additionally one must assess the welding seams of the bracket as well. The assessment of these components is returning 'OK' or 'NOT OK'. The user has to decide what actions to be taken (e.g. changing geometry or material grades) to fulfil the requirements.

2.1.7 Global Results

2.1.7.1 Utilisation in terms of overall bending moment and shear

At the bottom of second sheet the load bearing capacity and utilization of the joint assemblage for tension and shear is given in terms of $V_{R,d}$ and $M_{R,d}$, resp $V_{S,d}/V_{R,d}$ and $M_{S,d}/M_{R,d}$. These values are transferred to bottom of top sheet (see 2.1.5).

2.1.7.2 Interaction

In case of tension and shear in the stud additionally the combined action of both components must be assessed. As it is a rare situation due the governing compression force from closing moments, usually there is no limitation. If tension and shear forces have to be considered, Eq (2.2) can be applied according to EN 1992-4-2, Cl. 6.4.1 [10].

$$\mu = \left(\frac{V_{S,d}}{V_{R,d}}\right)^{\alpha} + \left(\frac{T_{S,d}}{T_{R,d}}\right)^{\alpha} \leq 1 \qquad (2.2)$$

As Exponent α = 2,0 is taken in case of <u>steel</u> failure acc. to Cl. 6.4.1.1 or α = 1,5 in case of <u>other</u> failure modes acc. to Cl. 6.4.1.2. In case of supplementary reinforcement which is designed for both failure modes tension and shear, the same α can be applied. For simplification, and according to the current status of European approvals for headed studs, the value α = 1,5 is used.

2.1.7.3 Stiffness and ductility

Due to the character of the joint, the stiffness of the moment resisting joint (i.e. relation of overall bending moment to rotation) depends mainly on the nonlinear flexibility of steel/concrete bond, the slip of studs in slab and the behaviour of concrete shear panel in the wall which is activated by the bend of reinforcement, whereas the compression strain in the anchor plate is inferior. This approximate joint stiffness by M*lever arm/horizontal displacement in axis of reinforcement is given with two parameters:

- S_{ini} = initial stiffness in unit [MNm/rad] gives the relation between bending moment and rotation of the connection in the very beginning. The incline represents the maximum elastic behaviour.
- S_{sec} = Secant stiffness in unit [MNm/rad] gives the relation between the effective bending moment and the according, possibly nonlinear rotation of the connection. The incline is always equal (in case of small bending moment and elastic behaviour) or typically smaller than S_{ini}.

The term ductility is usually used in connections with energy consuming behaviour due to plasticity, if there is displacement which will not reset but will remain in case of load removal. So even if the descent of stiffness S_{sec} points to nonlinearity it mostly will be a nonlinear elastic effect, which yields no ductility factor. In that case the cell will give the information 'elastic'.

2.1.7.4 Anchor plate and minimum tensional reinforcement

The type of anchor plate behaviour is given as information (rigid/flexible) and represents cell B45 of this sheet and the minimum tensional reinforcement (design) in the slab is given as information.

2.2 Slim anchor plate with headed studs – bending joints

2.2.1 General

With the program “slim anchor plates with headed studs - bending joints” (Version 2.0) [22] load carrying capacities of joints with minimum four and maximum six headed studs can be proved. The headed studs therefore have to be placed in two rows and the loading only can be considered in one direction (see Fig. 2.8). In the progress of the calculation the deformation behaviour of the anchor plate up to a kinematic chain is taken into consideration. At the end a moment-rotation curve can be obtained. The load carrying capacity of the tensional component can be increased by taking the supplementary reinforcement which is placed next to the headed studs into account. Compared to pure concrete cone failure the capacity of this component can be highly increased due to supplementary reinforcement. Within anchor plates, where the load carrying capacity of the tensional-, bending- or combined components is not governed due to failure of the steel components (anchor plate in bending, headed studs in tension) high increases in loading of the joint are possible. Additional the knowledge of the deformation behaviour of the joint can be used in the global analysis.

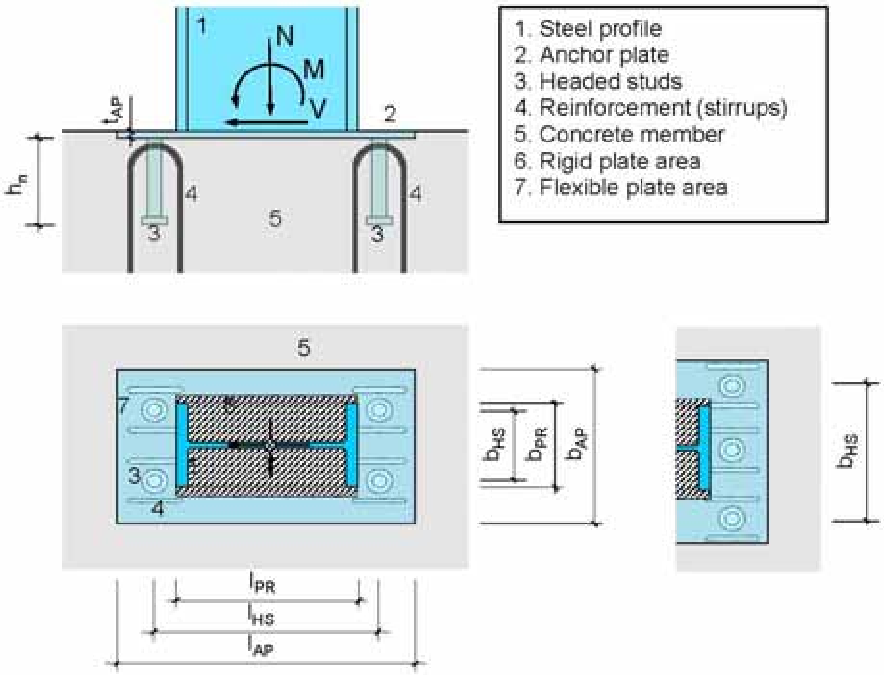

Fig. 2.8: Geometry of the joint with slim anchor plate

2.2.2 Program structure and static model

2.2.2.1 General

The design software is based on the EXCEL table calculation program with the integrated programming language VBA. Within the EXCEL file ten different spreadsheets for the in- and output, for the design of the different components, for the consideration of the joint in the global analysis and for a summary of the joint properties. Due to physical non-linear behaviour of the anchor plate under bending forces and the geometric non-linear effects based on the development of cinematic chains, the design approach is done iteratively with consideration of changes in the system. The geometric non-linear effect occurs due to the activation of the anchor plate due to tension forces and additional non-linear load-deformation behaviour of the single components. This is implemented in the VBA-program, which is accessing the input data from the different spreadsheets.

2.2.2.2 Load-transfer of the vertical loads N and the bending moment M – static model at the beginning of the calculation process

The first model for the load transfer of the vertical loads N and the bending moments M is a continuous beam supported on single springs. The anchor plate is therefore modeled as a two-dimensional system. As the connected profile stiffens the anchor plate, this sections is modeled with rigid members. Springs for compression are placed at the nodes 1 to 8 to reflect the behaviour of the concrete under compression. If the anchor plate is not in contact with the concrete surface and no compression forces in this place might occur, the springs can be neglected. Non-linear tensional springs are reflecting the load carrying behaviour of the headed stud with the supplementary reinforcement. Depending on the geometry of the anchor plate the tensional springs can be only placed on the nodes 2 and 7, 3 and 6 or 4 and 5. They are only activated if the distance between the anchor plate and the concrete surfaces increases. If not a spring which is simulating the compression forces of the concrete is placed at the same node. There are no hinges in the continuous beam at the beginning of the calculation, but within the calculation process plastic hinges might occur at the nodes 2, 3, 6 and 7. After each load step the boundary conditions of the supporting springs are adopted. The prying forces of the anchor plate are considered by the compression springs in the external nodes 1 and 8 (see Fig. 2.9).

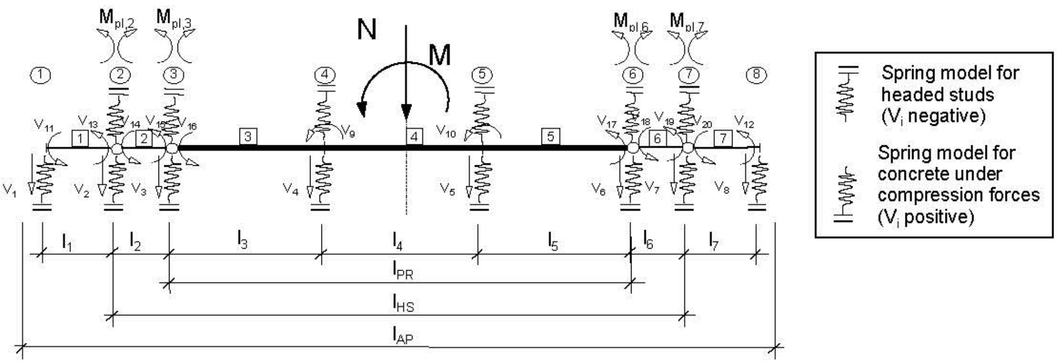

Fig. 2.9: Design model for vertical loads and bending moments

The calculation will be done by displacement method. Non-linear (physical) effects will be considered by an iterative calculation with continuous increase of load steps. For every load step the support conditions and the appearance of plastic hinges will be checked. In case of changing support conditions or appearance of plastic hinges the corresponding elements of the total stiffness matrix **K**, the kinematic transformation matrix **a** and the vector of the external nodal forces **P** will be manipulated. In case of bending loads without tension forces (N ≥ 0) the row of headed studs near to the compression zone is not considered as support spring for tension loads (c_s=0). Internal forces and global node deformations caused by bending moments and normal forces will be determined by using the displacement method, (Krätzig [18]).

$$v = a \cdot V \tag{2.3}$$

$$s = k \cdot v + \dot{s} \tag{2.4}$$

$$P = a^T \cdot s \tag{2.5}$$

$$P = a^T \cdot k \cdot aV + a^T \cdot \dot{s} = K \cdot V + a^T \cdot \dot{s} \tag{2.6}$$

$$V = K^{-1} \cdot P - K^{-1} \cdot a^T \cdot \dot{s} \tag{2.7}$$

$$s = k \cdot a \cdot V + \dot{s} \tag{2.8}$$

With:

s	Vector of internal element end forces;
v	Vector of internal element end displacements;
P	Vector of external nodal forces;
V	Vector of external nodal displacements;
k	Reduced stiffness matrix of all elements;
a	Kinematic transformation matrix;
$\dot{s}$	Vector of internal rigid-boundary element forces.

Non-linear material effects will be considered by manipulating the total stiffness matrix **K**, the kinematic transformation Matrix **a** and the vector of the external nodal forces **P.**

$$K = K_{sing} + K_{bound} \tag{2.9}$$

With:

K_{sing}	Stiffness matrix without boundary conditions and hinges at node 2, 3, 6 and 7;
K_{bound}	Stiffness matrix considering boundary conditions and reducing 0-Elements at the main diagonal caused by reducing hinges.

$$P = P' + \Delta P \tag{2.10}$$

With:

P´	Nodal forces caused by external loads;
ΔP	Nodal forces caused by non-linear support springs and plastic hinges;
a	Varying some values to reduce the number of degrees of freedom at the nodes 2, 3, 6 and 7 in case of no plastic hinges.

The bearing reactions will be determined by multiplying the diagonal elements of $\mathbf{K}_{\mathrm{bound}}$ by the corresponding deformations of **V** plus the nodal forces of **P'**.

$$C = K_{bound}^{88} \cdot V^{8} + \Delta P^{8} \tag{2.11}$$

$$C_1 = K_{bound,11} \cdot V_1 + \Delta P_1; \ldots; C_8 = K_{bound,88} \cdot V_8 + \Delta P_8 \tag{2.12}$$

$$P = \begin{bmatrix} P_1 \\ P_2 \\ \vdots \\ P_{20} \end{bmatrix} (20x1) \qquad V = \begin{bmatrix} V_1 \\ V_2 \\ \vdots \\ V_{20} \end{bmatrix} (20x1) \qquad s = \begin{bmatrix} M_l^1 \\ M_r^1 \\ \vdots \\ M_l^7 \\ M_r^7 \end{bmatrix} (14x1) \qquad \dot{s} = \begin{bmatrix} \dot{M}_l^1 \\ \dot{M}_r^1 \\ \vdots \\ \dot{M}_l^7 \\ \dot{M}_r^7 \end{bmatrix} (14x1)$$

$$k^2 = \begin{bmatrix} \frac{4EI}{l} & \frac{2EI}{l} \\ \frac{2EI}{l} & \frac{4EI}{l} \end{bmatrix}^e (2x2) \qquad k = \begin{bmatrix} \frac{4EI_1}{l_1} & \frac{2EI_1}{l_1} & \cdots & 0 & 0 \\ \frac{2EI_1}{l_1} & \frac{4EI_1}{l_1} & & 0 & 0 \\ \vdots & & \ddots & & \vdots \\ 0 & 0 & \cdots & \frac{4EI_7}{l_7} & \frac{2EI_7}{l_7} \\ 0 & 0 & & \frac{2EI_7}{l_7} & \frac{4EI_7}{l_7} \end{bmatrix} (14x14)$$

$$\mathbf{a}=\begin{bmatrix}
-\frac{1}{l_1} & \frac{1}{l_1} & 0 & 0 & 0 & 0 & 0 & 0 & 0 & 0 & 1 & 0 & 0 & 0 & 0 & 0 & 0 & 0 & 0 & 0\\
-\frac{1}{l_1} & \frac{1}{l_1} & 0 & 0 & 0 & 0 & 0 & 0 & 0 & 0 & 0 & 0 & 1 & 0 & 0 & 0 & 0 & 0 & 0 & 0\\
0 & -\frac{1}{l_2} & \frac{1}{l_2} & 0 & 0 & 0 & 0 & 0 & 0 & 0 & 0 & 0 & \boxed{0} & \boxed{1} & 0 & 0 & 0 & 0 & 0 & 0\\
0 & -\frac{1}{l_2} & \frac{1}{l_2} & 0 & 0 & 0 & 0 & 0 & 0 & 0 & 0 & 0 & 0 & 0 & 1 & 0 & 0 & 0 & 0 & 0\\
0 & 0 & -\frac{1}{l_3} & \frac{1}{l_3} & 0 & 0 & 0 & 0 & 0 & 0 & 0 & 0 & 0 & 0 & \boxed{0} & \boxed{1} & 0 & 0 & 0 & 0\\
0 & 0 & -\frac{1}{l_3} & \frac{1}{l_3} & 0 & 0 & 0 & 0 & 1 & 0 & 0 & 0 & 0 & 0 & 0 & 0 & 0 & 0 & 0 & 0\\
0 & 0 & 0 & -\frac{1}{l_4} & \frac{1}{l_4} & 0 & 0 & 0 & 1 & 0 & 0 & 0 & 0 & 0 & 0 & 0 & 0 & 0 & 0 & 0\\
0 & 0 & 0 & -\frac{1}{l_4} & \frac{1}{l_4} & 0 & 0 & 0 & 0 & 1 & 0 & 0 & 0 & 0 & 0 & 0 & 0 & 0 & 0 & 0\\
0 & 0 & 0 & 0 & -\frac{1}{l_5} & \frac{1}{l_5} & 0 & 0 & 0 & 1 & 0 & 0 & 0 & 0 & 0 & 0 & 0 & 0 & 0 & 0\\
0 & 0 & 0 & 0 & -\frac{1}{l_5} & \frac{1}{l_5} & 0 & 0 & 0 & 0 & 0 & 0 & 0 & 0 & 0 & 0 & 1 & 0 & 0 & 0\\
0 & 0 & 0 & 0 & 0 & -\frac{1}{l_6} & \frac{1}{l_6} & 0 & 0 & 0 & 0 & 0 & 0 & 0 & 0 & 0 & \boxed{0} & \boxed{1} & 0 & 0\\
0 & 0 & 0 & 0 & 0 & -\frac{1}{l_6} & \frac{1}{l_6} & 0 & 0 & 0 & 0 & 0 & 0 & 0 & 0 & 0 & 0 & 0 & 1 & 0\\
0 & 0 & 0 & 0 & 0 & 0 & -\frac{1}{l_7} & -\frac{1}{l_7} & 0 & 0 & 0 & 0 & 0 & 0 & 0 & 0 & 0 & 0 & \boxed{0} & \boxed{1}\\
0 & 0 & 0 & 0 & 0 & 0 & -\frac{1}{l_7} & -\frac{1}{l_7} & 0 & 0 & 0 & 1 & 0 & 0 & 0 & 0 & 0 & 0 & 0 & 0
\end{bmatrix} \quad (14\text{x}20)$$

In case of no hinge at node 2, 3, 6 or 7 the marked values of the corresponding lines will be changed.

$$\mathrm{K_{sing}} = \mathrm{a^T \cdot k \cdot a}\ (20\text{x}20) \tag{2.13}$$

$$\mathrm{K_{Bound}} = \begin{bmatrix} \mathrm{K_{11}} & 0 & \cdots & 0 & 0 \\ 0 & 0 & & 0 & 0 \\ \vdots & & \ddots & & \vdots \\ 0 & 0 & \cdots & 0 & 0 \\ 0 & 0 & & 0 & \mathrm{K_{2020}} \end{bmatrix} (20\text{x}20) \tag{2.14}$$

$$\mathrm{K} = \mathrm{K_{sing}} + \mathrm{K_{Bound}}\ (20\text{x}20) \tag{2.15}$$

The loading that has been implemented by the engineer in the input worksheet is subdivided into 100 load steps and applied gradually to the system. After 100 load steps the entire load is applied to the statical system. It might happen, that a kinematic chain due to plastic hinges will occur and the beam series will fail before reaching the last sub step (singular stiffness matrix). In this cases the iteration will continue with a different system, which is described in the following.

2.2.2.3 Load-transfer of the vertical loads N and the bending moment M – static model after formation of a plastic chain

The anchor plate can be considered as a tension member after the formation of a plastic chain (see Fig. 2.10.) As a simplification the whole resultant tension force is assigned to the bar with the higher inclination. For each new load step the increase in loading of the normal force in the deformed system is determined. In the next step the elongation of the tensional bar and the entire deformation of the anchor plate is calculated. In general the load carrying capacity is limited due to the component resistance of the supports (headed studs). Due to the relatively low deformation of the anchor plate extreme horizontal forces will act at the supports of the membrane system.

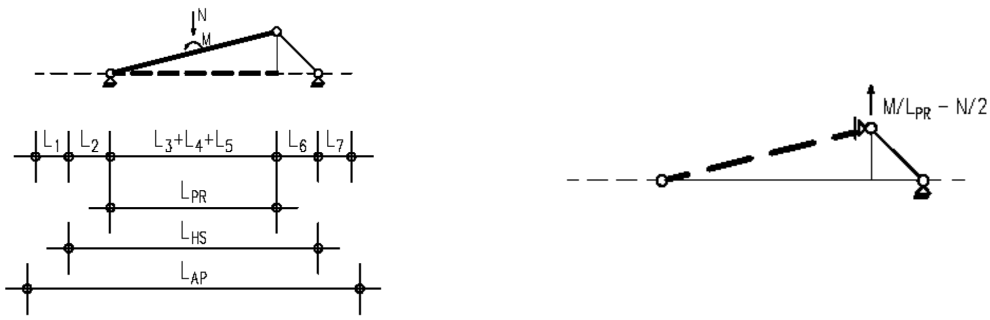

Fig. 2.10: Model of the baseplate under tension and simplified calculation model

For the load transfer of the horizontal forces V the friction forces between concrete and the anchor plate are considered on all joints with compression springs (see Fig. 2.11). The remaining forces as difference between friction part and applied shear load will be distributed among the headed studs according to the stiffness of the spring.

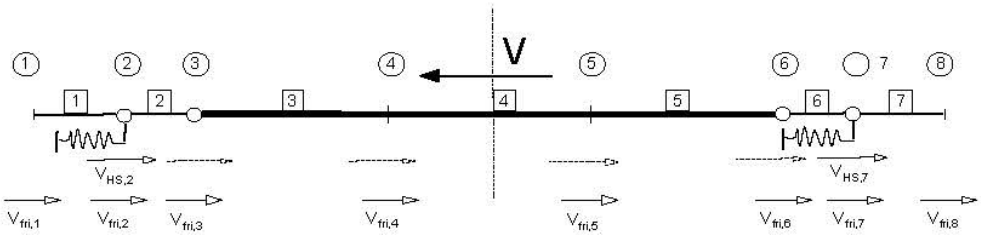

Fig. 2.11: Design model for horizontal (shear) loads

2.2.3 EXCEL-Worksheets / VBA-Program

The whole design tool contains ten Microsoft Excel worksheets and one Microsoft Visual Basic program part. Visible for the user are only the worksheets "Input + Output" and "Design output". The following schedule gives a short overview about the function of the different worksheets (see Tab. 2.1 and Tab. 2.2).

Tab. 2.1: Overview of all worksheets

Name (Worksheet)	**Function**
"Input + Output"	Chapter 2.2.7
"Design output"	Chapter 2.2.8
"Headed studs tension"	Determination of the deformation behaviour and the load bearing capacity of the component "headed studs in tension (considering additional reinforcement)"
"Headed studs shear"	Determination of the deformation behaviour and the load bearing capacity of the component "headed studs in shear"
"HS interaction tension-shear"	Determination of the load bearing capacity of headed studs under tension and shear loads
"Concrete member compression"	Determination of the deformation behaviour and the load bearing capacity of the component "Concrete member under compression loads"
"Steel plate bending"	Determination of the deformation behaviour and the load bearing capacity of the component "Steel plate under bending moments"
"Calculation core anchor plate"	Calculation of internal forces and bearing reactions by displacement method for every load step
"Data"	Data schedule for fixed values (materials, dimensions, partial factors, internal control parameters)
"Data temp"	Data schedule for temporary values (nodal displacements of every load step); nodal displacements are used to create the moment-rotation curve in "Design output"

Tab. 2.2: VBA-Subroutine

Program (Subroutine)	**Function**

"NL_Berechnung"	Iterative calculation of internal forces and bearing reactions by using the worksheet "Calculation core anchor plate" for 100 load steps; change of support conditions or introducing plastic hinges depending of the bearing reactions or the internal forces for the current load step; system change after reaching a kinematic structure

2.2.4 Components

The following components are implemented in the program. Detailed explanations of this components can be found in Handbook I in the specific sections. The load deformation behaviour of the anchor plate is considered within the iterative calculation of the load steps.

Tab. 2.3: Components implemented in the calculation program for slim anchor plate

Component	Headed stud in tension	Concrete breakout in tension	Stirrups in tension	Pull-out failure of the headed stud	Headed stud in shear
Figure	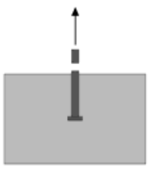	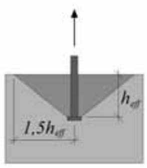	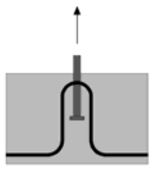	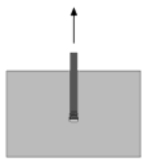	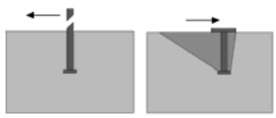

Component	Friction	Concrete in compression	Threaded studs in tension/ shear
Figure	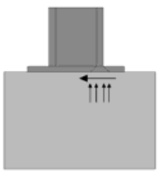	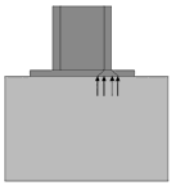	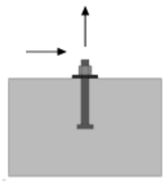

2.2.5 Safety factors

Tab. 2.4: Ultimate limit state (CEN/TS 1992-4-1:2009 4.4.3.1.1 [1])

Steel		
Anchors tension	Anchors shear	Reinforcement
γ_{Ms}	γ_{Ms}	$\gamma_{Ms,re}$
$\gamma_{Ms}=1,2*f_{uk}/f_{yk}$ ($\gamma_{Ms}\geq 1,4$)	$\gamma_{Ms}=1,0*f_{uk}/f_{yk}$ ($\gamma_{Ms}\geq 1,25$ ($f_{uk}\leq 800$ N/mm^2 and $f_{yk}/f_{uk}\leq 0,8$))	1,15
	$\gamma_{Ms}=1,25$ ($f_{uk}>800$ N/mm^2 or $f_{yk}/f_{uk}>0,8$)	

Tab. 2.5: Ultimate limit state (EN 1993-1-8 [9])

Steel
Steelplate
γ_{Ma}
1,00
(no stability failure)

Tab. 2.6: Ultimate limit state (CEN/TS 1992-4-1:2009 4.4.3.1.2 [1])

Concrete			
Cone failure	Pry-out failure	Pull out failure	Anchor. failure
γ_{Mc}	γ_{Mc}	γ_{Mp}	γ_{Mc}
1,5	1,5	1,5	1,5

2.2.6 Boundary conditions

Anchor plates with headed studs at the concrete side and a welded steel profile at the airside do have complex three dimensional load transfer. Under compression forces all sections of the anchor plate are supported in places, where a gap might occur (except in the area of the headed studs) under tensional forces. The web and the flange of the welded steel sections do have a stiffening effect on the anchor plate. Independently from the thickness of the anchor plat the anchor plate is assumed in the stiffened sections as almost completely rigid. Due to this reason the system is assumed as two dimensional continuous beam. In the midsection of the beam the normal and shear forces and the bending moments are acting. Between line 2 and line 3 (see Fig. 2.12) the anchor plate is assumed to be rigid and discretized by a rigid bar. The geometrical cross section of all other bars is formed by the effective width b_m and the thickness of the anchor plate t_{AP}. As lower limit the effective width b_m is assumed with b_{PR} + 5 * t_{AP}, as upper limit the entire width of the anchor plate is possible. If plastic hinges in the anchor plate occur the yielding lines are assumed as continuous and perpendicular to the axis of the discretized bar (see Fig. 2.12). If this plastic resistance of the anchor plate is larger as if the yielding lines would be locally limited due to a triangular shape of the yielding lines (see Fig. 2.13). The effective width of the anchor plate is reduced accordingly without falling below the resistance of the lower limit.

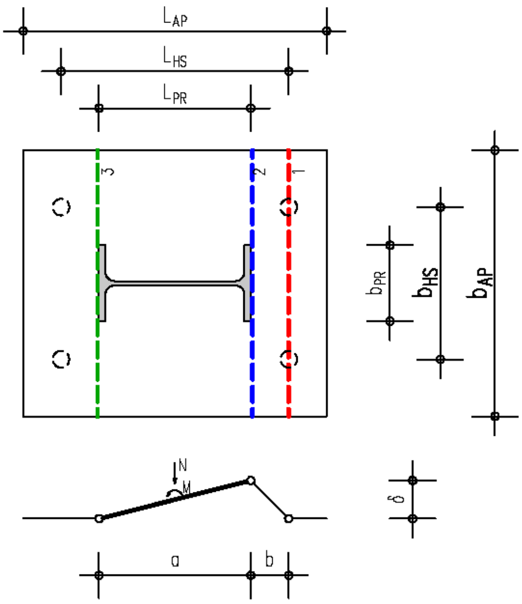

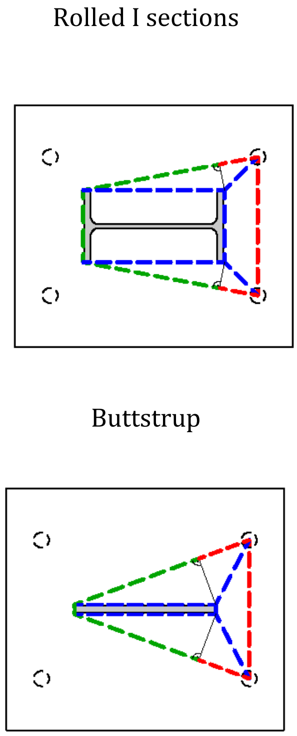

Fig. 2.12: Static model of the anchor plate yielding lines with yielding lines over the whole width

Fig. 2.13: Local rotating yielding lines for cases where $b_{HS} > b_{PR}$

The tensional resistance in cases of straight yielding lines (see Fig. 2.12) can be calculated with Equations (2.16) to (2.18).

$$Z_{Rd} \cdot \delta = m_{pl,Rd} \cdot b_{AP} \cdot \left(\frac{2 \cdot \delta}{a} + \frac{2 \cdot \delta}{b}\right) \tag{2.16}$$

$$Z_{Rd} = m_{pl,Rd} \cdot f_{bar} \tag{2.17}$$

$$f_{bar} = \frac{b_{AP} \cdot \left(\frac{2}{a} + \frac{2}{b}\right)}{\delta} \tag{2.18}$$

The tensional resistance for local rotating yielding lines (see Fig. 2.14) can be calculated with Equations (2.19) to (2.22).

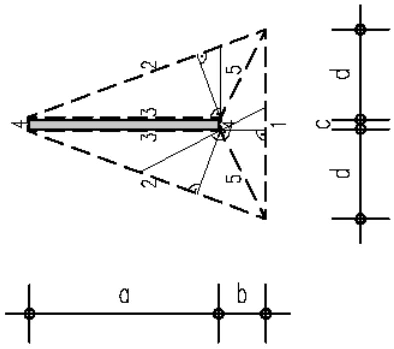

Fig. 2.14: Geometry for local rotating yielding lines

$$\begin{aligned} l_1 &= c + 2 \cdot d \\ l_2 &= ((a+b)^2 + d^2)^{1/2} \\ l_3 &= a \\ l_4 &= c \\ l_5 &= (b^2 + d^2)^{1/2} \end{aligned} \tag{2.19}$$

$$\begin{aligned} s_1 &= b \\ s_2 &= l_3 \cdot \sin \alpha_{23} \text{ with } \sin \alpha_{23} = d \,/\, l_2 \\ s_3 &= l_3 / \tan \alpha_{23} \text{ with } \tan \alpha_{23} = d \,/(a+b) \\ s_4 &= s_1 \\ s_{5-1} &= l_5 \cdot \tan \alpha_{15} \text{ with } \tan \alpha_{15} = b \,/d \\ s_{5-2} &= l_5 \cdot \tan \alpha_{25} \text{ with } \sin \alpha_{25} = s_2 \,/l_5 \end{aligned} \tag{2.20}$$

$$\begin{aligned} \tan \psi_1 &= \delta \,/s_1 \approx \psi_1 \\ \tan \psi_2 &= \delta \,/s_2 \approx \psi_2 \\ \tan \psi_3 &= \delta \,/s_3 \approx \psi_3 \\ \tan \psi_{4,0} &= \delta \,/l_3 + \delta \,/s_4 \approx \psi_{4,0} \\ \tan \psi_{4,u} &= \delta \,/l_3 \approx \psi_{4,u} \\ \tan \psi_5 &= \delta \,/s_{51} + \delta \,/s_{52} \approx \psi_5 \end{aligned} \tag{2.21}$$

$$\begin{aligned} Z_{Rd} \cdot \delta &= m_{pl,Rd} \cdot (l_1 \cdot \psi_1 + 2 \cdot l_2 \cdot \psi_2 + 2 \cdot l_3 \cdot \psi_3 + l_4 \cdot (\psi_{4,0} + \psi_{4,u}) + 2 \cdot l_5 \cdot \psi_5) \\ Z_{Rd} &= m_{pl,Rd} \cdot f_{local} \\ f_{local} &= (l_1 \cdot \psi_1 + 2 \cdot l_2 \cdot \psi_2 + 2 \cdot l_3 \cdot \psi_3 + l_4 \cdot (\psi_{4,0} + \psi_{4,u}) + 2 \cdot l_5 \cdot \psi_5)/\delta \end{aligned} \tag{2.22}$$

If $f_{local} < f_{bar}$ the effective width of the bar is calculated with Eq. (2.23).

$$b_m = b_{AP} \cdot f_{local}/f_{bar} \tag{2.23}$$

The design calculations for the connection between the steel profile and the anchor plate are not covered by the design program and have to be done in spate calculations. If steel profiles are not directly welded to the anchor plate and connected by threaded studs and an endplate the dimensions l_{AP} and b_{AP} have to be defined analogous independent from the actual dimensions of the steel profile (for example with the distances of the threaded studs l_{AP} and b_{AP}). The new components that are used in the program are based on test with large edge distances of the headed studs. Due to this reason the edge distances of Fig. 4.22 are required (see Chapter 4.3.4.2).

If the supplementary reinforcement is located with too large distance from the headed stud or from the concrete surface the anchorage length of the reinforcement within the concrete cone can be too small (see Fig. 2.15). In the worst case the contribution due to the supplementary reinforcement can be neglected. The distances X and Y in Fig. 2.15 have to be minimized.

Values X and Y as small as possible

Fig. 2.15: Arrangement of the hanger reinforcement

2.2.7 Input mask

The input sheet "Input + Output" shows on top a sketch of the connection labeling the most important input parameters. In the second part of the worksheet the dimensions, materials and loads on the anchor plate can be entered into the program. With the "Calculation-Button" on the right bottom of the worksheet the non-linear determination of internal forces and the component design will be started. Left beside the "Calculation-Button" the degree of utilization of the main components is shown. In the following the input data is described in particular.

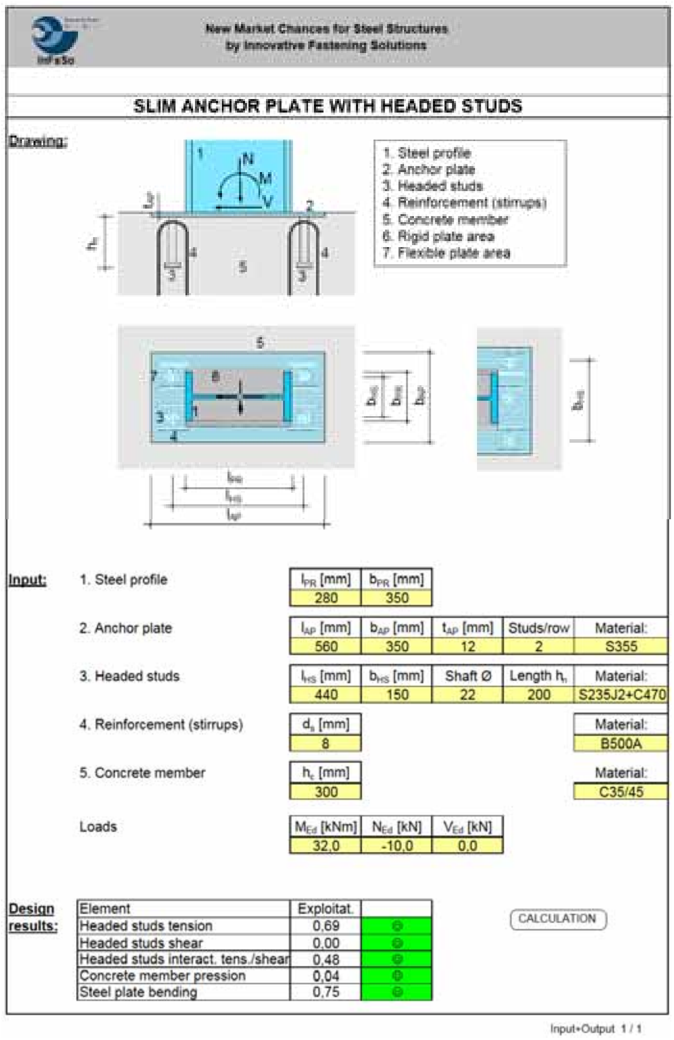

	l_{PR} [mm]	b_{PR} [mm]			Material:
1. Steel profile	280	350			

	l_{AP} [mm]	b_{AP} [mm]	t_{AP} [mm]	Studs/row	Material:
2. Anchor plate	560	350	12	2	S355

	l_{HS} [mm]	b_{HS} [mm]	Shaft Ø	Length h_n	Material:
3. Headed studs	440	150	22	200	S235J2+C470

	d_s [mm]	Material:
4. Reinforcement (stirrups)	8	B500A

	h_c [mm]	Material:
5. Concrete member	300	C35/45

	M_{Ed} [kNm]	N_{Ed} [kN]	V_{Ed} [kN]
Loads	32,0	-10,0	0,0

Element	Exploitat.
Headed studs tension	0,69
Headed studs shear	0,00
Headed studs interact. tens./shear	0,48
Concrete member pression	0,04
Steel plate bending	0,75

Fig. 2.16: Excel worksheet "Input + Output" page 1/1

Steel profile (1. line): Input of the length l_{PR} [mm] and the width b_{PR} [mm] of the connected profile or steel element to determine the rigid plate area. In case of connections of steel profiles with head plates by threaded studs welded on the anchor plate directly the outer distances of the threaded studs in both directions have to be used for l_{PR} and b_{PR}.

Anchor plate (2. line): Input of the length l_{AP} [mm], the width b_{AP} [mm] and the thickness t_{AP} [mm] of the anchor plate; the number of headed studs per row (2 or 3); the material of the steel plate (acc. to EN 1993-1-1 **Chyba! Nenalezen zdroj odkazů.** and EN 10025 [4]).

Headed studs (3. line): Input of the distances of the headed studs in longitudinal direction l_{HS} [mm], in cross direction b_{HS} [mm]; the shaft diameter [mm]; the length of the studs h_n [mm]; the material of the headed studs (acc. to EN 10025 and EN 10088). In case of $l_{HS} \leq l_{PR}$ the distance b_{HS} of the headed studs has to be equal or smaller than the width b_{PR} plus five times t_{AP} ($b_{HS} \leq b_{PR} + 5 * t_{AP}$).

Reinforcement (4. line): Input of the diameter d_S [mm] and the material (acc. to DIN 488 [3]) of the reinforcement stirrups. The reinforcement stirrups have to be formed as loops with the smallest admissible bending role diameter. They have to be grouped in pairs close to the shafts of the headed studs with minimum distance to the bottom side of the anchor plate (maximum possible overlapping length of stirrup leg and headed stud).

Concrete member (5. line): Input of the thickness h_C [mm] and the material type (acc. to EN 1992-1-1 [7]) of the concrete member.

Loads (last line): Input of the bending moment M_{Ed} [kNm], the normal force N_{Ed} [kN] and the shear force V_{Ed} [kN] as design loads (ultimate limit state). Design loads have to be determined by the user. Partial factors will not be considered at the load side by the program!

2.2.8 Output mask

The output sheet "Design output" is divided into four parts. The first part gives information about the structural system and the non-linear support conditions (spring models). Results of the non-linear determination of internal forces are shown in the second part. In part 3 the main verifications of the components are given. The last part shows the moment-rotation behaviour of the joint.

Structural analysis

System: **Design model for vertical loads and bending moments**

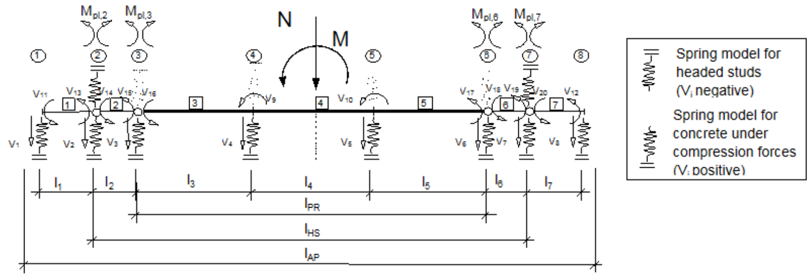

[mm]	pojektion1	beam 1	beam 2	beam 3	beam 4	beam 5	beam 6	beam 7	pojekt.7
l_i	15	45	80	93,33333	93,33333	93,33333	80	45	15
$b_{p,i}$	350	350	350	350	350	350	350	350	350
t_i	12	12	12	50	50	50	12	12	12

E-Modulus steel plate [N/mm²]: 210000 Headed studs at node 2+7.

[kN/cm]	spring 1	spring 2	spring 3	spring 4	spring 5	spring 6	spring 7	spring 8
$c_{c,i}$ (co.)	14875	24792	34378	37022	37022	34378	24792	14875
$c_{s1,i}$ (h.s.)	0	3174	0	0	0	0	3174	0
$c_{s2,i}$ (h.s.)	0	373	0	0	0	0	373	0

Spring model concrete

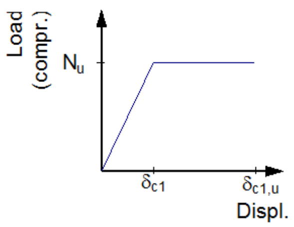

Spring model headed studs (tension)

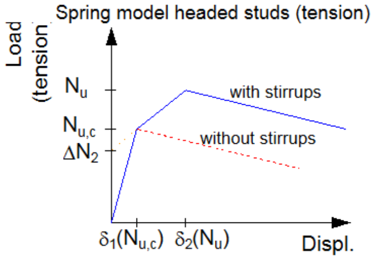

$c_{ci}=E_{ci}*A_{ci}/D_p$ and $A_{ci}=(L_{i-1}+L_i)/2*B_p$

$D_p=B_p/2$ (Participating compression depth)

$E_c=$ 34000 N/mm²

$c_{s1}=N_{u,c}/\delta_1(N_{u,c})$

$\delta_1=\delta_{p1}+\delta_h$

$c_{s2}=(N_u-N_{u,c})/(\delta_2(N_u)-\delta_1(N_{u,c}))$

$\delta_2=\delta_{p2}+\delta_h+(\delta_s+\delta_c)$

Design model for horizontal (shear) loads

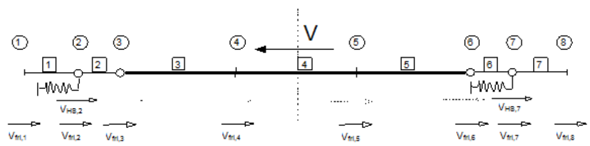

$V_E=V_{HS,1}+V_{HS,2}+\Sigma V_{fri}$ $V_{fri,i}=B_i*\mu$ $\mu=0,2$ $EA=\infty$

$V_{HS,1}=(V_E-\Sigma V_{fri})/(1+c_{V,HS56}/c_{V,HS23})$ $V_{HS,2}=(V_E-\Sigma V_{fri})/(1+c_{V,HS23}/c_{V,HS56})$ $c_{V,HS23}=c_{V,HS56}$

Design output 1/3

Fig. 2.17: Excel worksheet "Design output" page 1/3

Loads:

M_{Ed}	N_{Ed}	V_{Ed}
[kNm]	[kN]	[kN]
32,0	-10,0	0,0

$\Delta M_{Ed}=V_{Ed}*(t_P+d)$

Internal forces: **Bearing reactions and bending moments caused by M_{Ed} and N_{Ed}**

	node 1	node 2	node 3	node 4	node 5	node 6	node 7	node 8	
B_i	0,00	33,31	50,48	0,00	0,00	0,00	-161,14	67,34	[kN]
M_i	0,00	0,00	2,66	10,49	-13,23	-4,47	3,03	0,00	[kNm]

Bearing reactions caused by V_{Ed} used for concrete design

	node 1	node 2	node 3	node 4	node 5	node 6	node 7	node 8	
V_i	-	-15,11	0,00	0,00	0,00	0,00	-15,11	-	[kN]
$V_{fri,i}$	0,00	6,66	10,10	0,00	0,00	0,00	0,00	13,47	[kN]

Bearing reactions caused by V_{Ed} used for steel design

$V_{Ed,max}=MIN[((1-n_{N2}^2)*V_{Rd,s}^2)^{0,5};\ V_{Ed,tot}]$ = 0 N Statement: $n_N^2+n_V^2=1$ -> V_{Ed}

$V_{Ed,min}=V_{Ed,tot}-V_{Ed,max}$ = 0 N

Verifications: **Headed studs under tension loads**

Steel failure of fasteners

Yielding resistance $N_{Rk,y,s}=$ $n_a*A_s*f_{yk}$ = 326914 N

$\mathbf{N_{Ed}\leq N_{Rd,y,s}=N_{Rk,y,s}/\gamma_{Ms}=}$ **233510 N** $\mathbf{N_{Ed}/N_{Rd,y,s}=}$ **0,69** ☺

Ultimate resistance $N_{Rk,u,s}=$ $n_a*A_s*f_{uk}$ = 357325 N

$\mathbf{N_{Ed}\leq N_{Rd,u,s}=N_{Rk,u,s}/\gamma_{Ms}=}$ **255232 N** $\mathbf{N_{Ed}/N_{Rd,u,s}=}$ **0,63** ☺

Concrete cone failure

$N_{Rk,u,c}=N^\circ_{u,c}*A_{c,N}/A^\circ_{c,N}*\Psi_{s,N}*\Psi_{re,N}*\Psi_{ec,N}*\Psi_{m,N}*\Psi_{ucr,N}$ = 234945

$\mathbf{N_{Ed}\leq N_{Rd,u,c}=N_{Rk,u,c}/\gamma_{Mc}=}$ **156630 N** $\mathbf{N_{Ed}/N_{Rd,u,c}=}$ **1,03** ☺

Concrete cone failure with reinforcement

Concrete failure $N_{Rk,u,max}=$ $\Psi_{supp}*N_{Rk,u,c}$ = 539177 N

Yielding of reinforcement $N_{Rk,u,1}=$ $A_{s,y}*f_{s,y}+N_{u,c}+\delta_{s,y}*k_c$ = 403972 N

Anchorage failure $N_{Rk,u,2}=$ $N_{sbu}+N_{u,c}+\delta_{sbu}*k_c$ = 536688 N

$\mathbf{N_{Ed}\leq N_{Rd,u,cc+hr}=}$ **351280 N** $\mathbf{N_{Ed}/N_{Rd,u,cc+hr}=}$ **0,46** ☺

$N_{Rd,u,cc+hr}=MIN[N_{Rk,u,max}/\gamma_{Mc};N_{Rk,u1}/\gamma_{Ms};\ N_{Rk,u2}/\gamma_{Mc}]$

Pull-out failure

$N_{Rk,p}=$ $n*p_k*A_h$ = 746389 N

$\mathbf{N_{Ed}\leq N_{Rd,p}=N_{Rk,p}/\gamma_{Mp}=}$ **497593 N** $\mathbf{N_{Ed}/N_{Rd,p}=}$ **0,32** ☺

Design output 2/ 3

Fig. 2.18: Excel worksheet “Design output” page 2/3

Headed studs under shear loads

Steel failure of fasteners

$V_{Rk,S}=n_{a,V}*0{,}6*A_s*f_{usk}$ = 500255 N

$V_{Ed}\leq V_{Rd,S}=V_{Rk,S}/\gamma_{Ms}=$ **333503 N** $V_{Ed}/V_{Rd,S}=$ **0,00** ☺

Pry-out failure

$V_{Rk,CP}=K_3*N_{Rk,u,c}$ = 1615888 N

$V_{Ed}\leq V_{Rd,CP}=V_{Rk,CP}/\gamma_{Mc}=$ **1077259 N** $V_{Ed}/V_{Rd,CP}=$ **0,00** ☺

Headed studs interaction tension / shear Index 1/2 = row 1/2

Steel failure

$N_{Rd,s}$	$V_{Rd,s}$	n_{N1}	n_{N2}	n_{V1}	n_{V2}
233510 N	166752 N	0,69	0,14	0,00	0,00

$n_{N1}^2+n_{V1}^2$ **= 0,48** $n_{N2}^2+n_{V2}^2$ **= 0,02** ☺

Concrete failure

$N_{Rd,c}$	$V_{Rd,c}$	n_{N1}	n_{N2}	n_{V1}	n_{V2}
351280 N	538629 N	0,46	0,09	0,00	0,00

$n_{N1}^2+n_{V1}^2$ **= 0,27** $n_{N2}^2+n_{V2}^2$ **= 0,02** ☺

Concrete member under pression loads

$\sigma_{ck}=\alpha_{cc}*f_{ck}$ = 105,0 N/mm²

$\sigma_{cd}=\sigma_{ck}/\gamma_{Mc}=$ **70,0 N/mm²** (considered by non linear material behaviour)

ε_c=MAX[V1, V2, …,V8]/D_p = 0,00015

$\varepsilon_c\leq\varepsilon_{c,u}=$ 0,00350 $\varepsilon_c/\varepsilon_{c,u}=$ **0,04** ☺

Steel plate under bending moments

(i=1,3,6 and 7) $M_{pl,i,Rk}$ = 447,3 kNcm

$M_{pl,i,Rd}=M_{pl,i,Rk}/\gamma_{Ma}=$ **447,3 kNcm** (considered by non linear material behaviour)

Stiffness: **Deformation behaviour (element 4)**

Moment-Rotation

Rotation ϕ_4=arctan((V_4-V_5)/l_4)*1000 [mrad]

Displacement u_4=(V_4+V_5)/2

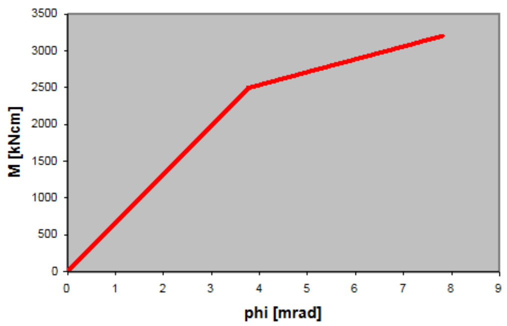

Design output 3/ 3

Fig. 2.19: Excel worksheet "Design output" page 2/3

2.2.9 Optimization of the joint

Following methods can be applied for increase in loading capacity of the joint. Which one of the following changes should be taken is linked to the individual properties of the joint. Additionally the different methods are interdependent and the optimization of the joint is an iterative process. Within this process the specific component has to be changed until sufficient load carrying capacity is reached, see Chapter 4.4.

For large bending moments M and / or large tensional forces N:

- (M1) Arrangement of supplementary reinforcement next to the tensional loaded headed stud row.
- (M2) Enlargement of the distance between the headed studs l_{HS} in the transversal direction.
- (M3) Enlargement of the distance between the headed studs up to $b_{HS} = 3 * h_{ef}$.
- (M4) Enlargement of the effective height of the headed studs.
- (M5) Enlargement of the diameter of the headed studs.
- (M6) Enlargement of the number of headed suds per row.
- (M7) Choice of different steel properties for the headed studs.
- (M8) Choice of higher concrete strength.
- (M9) Enlargement of the thickness of the anchor plate.
- (M10) Choice of different steel properties for the anchor plate.

For large shear forces V:

- (M2a) Enlargement of the distance between the headed studs $l_{HS} = 3 * h_{ef}$.
- (M3) Enlargement of the distance between the headed studs $b_{HS} = 3 * h_{ef}$.
- (M4) Enlargement of the effective height of the headed studs.
- (M5) Enlargement of the diameter of the headed studs.
- (M6) Enlargement of the number of headed suds per row.
- (M7) Choice of different steel properties for the headed studs.
- (M8) Choice of higher concrete strength.

For bending- and shear forces the methods as described above might be combined. The following table shows possibilities for optimization of joints for different objectives (see Tab. 2.7).

Tab. 2.7: Optimization of the slim anchor plate with headed studs

Objectives	**Method**
Small thickness of the anchor plate	For bending: Arrangement of the headed studs at the edges of the connected steel profile
High ductility	For bending: Configuration of the components of the joint in a way that the plastic chain becomes the decisive component of the anchor plate. Choice of a ductile steel material of the anchor plate.
Small length of the headed studs	For bending: Methods M1, M2, M3, M5, M6, (M7), M8, M9, M10; For shear: Methods M2a, M3, M5, M6, (M7), M8
No supplementary reinforcement	For bending: Methods M2 till M8, (M9), (M10)

2.3 Rigid anchor plate with headed studs – simple joint

2.3.1 General

With the program “Rigid anchor plate with headed studs – simple joint” (Version 2.0) [23] the load carrying capacities of anchor plates with minimum four and maximum six headed studs in two rows under loading in one direction can be calculated (see Fig. 2.20). It is required, that the point of load transfer into the simple joint is defined in the static system as hinged. As this point can`t be assumed directly located at the concrete surface, the eccentricity has to be taken into consideration. As the shear load is applied with some eccentricity also bending moments in the anchor plate have to be considered beside normal and shear forces. In order to increase the tensional resistance of the component of the headed stud, supplementary reinforcement can be used next to the studs. With the supplementary reinforcement high increases in loading of the joint are possible as the load carrying capacity of pure concrete cone failure can be increased by taking the reinforcement into account. The anchor plate is assumed to be rigid without any plastic reserves.

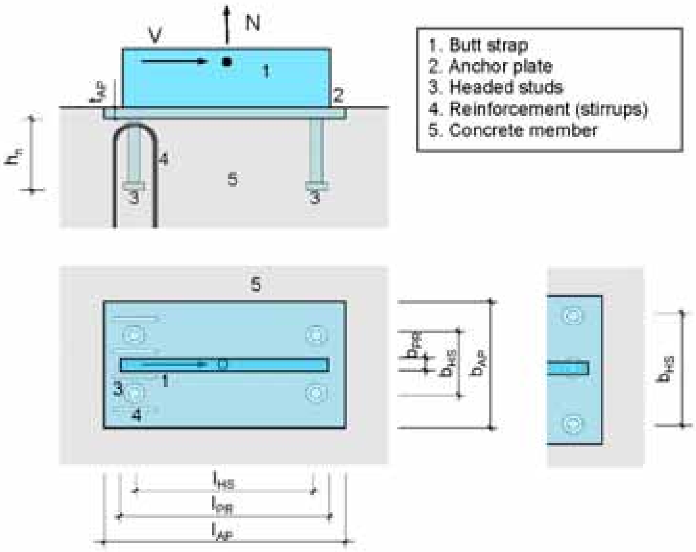

Fig. 2.20: Geometry of the joint with rigid anchor plate

2.3.2 Program structure and static model

The design software is based on the EXCEL table calculation program with the integrated programming language VBA. Within the EXCEL file ten different spreadsheets for the in- and output, for the design of the different components, for the consideration of the joint in the global analysis and for a summary of the joint properties. In a first step the height of the compression zone is assumed. Based on this assumption all unknown forces in Fig. 4.11 can be calculated. Based on moment equilibrium and equilibrium in the vertical direction the assumption can be verified. The shear force V_{Ed} is carried by a frictional part and the two shear components of the headed studs, see Eq. (2.24) .

$$V_{Ed} = V_{Ed,2} + V_{Ed,2} + V_f \tag{2.24}$$

With the equilibrium of moments at the intersection point of the action lines of the concrete force C_{Ed} and the shear components of the headed studs $V_{Ed,2}$ and $V_{Ed,1}$ the formulations in Eq. (2.25) can be obtained for the calculation of the applied normal force in the second stud row. By a vertical equilibrium of forces the assumed height of the compression zone can be verified. In the program the effective compressive height is determined iteratively. For further information see Design Manual I "Design of steel-to-concrete joints", Chapter 5.2.2 [13] and for the calculation of the deformations see Chapter 4.2 and Chapter 4.3.

$$V_{Ed} = V_{Ed,2} \cdot \frac{(e + t + d)}{(z + \mu \cdot d)} \tag{2.25}$$

2.3.3 EXCEL Worksheets / VBA program

The whole design tool contains 10 Microsoft Excel worksheets. Visible for the user are only the worksheets “Input + Output CM” and “Design output CM”. The following schedule gives a short overview about the function of the different worksheets (see Tab. 2.8).

Tab. 2.8: Overview about the different worksheets

Name (Worksheet)	Function
"Input + Output CM"	Chapter 2.3.7
"Design output CM"	Chapter 2.3.8
"Headed studs tension"	Determination of the deformation behaviour and the load bearing capacity of the component "headed studs in tension (considering additional reinforcement)"
"Headed studs shear"	Determination of the deformation behaviour and the load bearing capacity of the component "headed studs in shear"
"Headed studs interaction tension-shear"	Determination of the load bearing capacity of headed studs under tension and shear loads
"Concrete member under compression"	Determination of the deformation behaviour and the load bearing capacity of the component "Concrete member under compression loads"
"Steel plate bending CM"	Design of the anchor plate under bending moments
"Calculation core CM"	Calculation of internal forces by equilibrium of forces and moments; iterative determination of the compression zones length
"Data"	Data schedule for fixed values (materials, dimensions, partial factors, internal control parameters)
"Data temp"	Data schedule for temporary values (nodal displacements of every load step); nodal displacements are used to create the moment-rotation curve in "Design output"

2.3.4 Components

The following components are implemented in the program (see Tab. 2.9). Detailed explanations of this components can be found in Handbook I in the specific sections. The load deformation behaviour of the anchor plate is considered within the iterative calculation of the load steps.

Tab. 2.9: Components implemented in the calculation program for a rigid anchor plate

Component	Headed stud in tension	Concrete breakout in tension	Stirrups in tension	Pull-out failure of the headed stud	Headed stud in shear
Figure	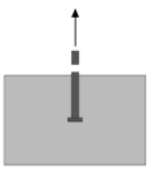	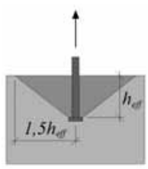	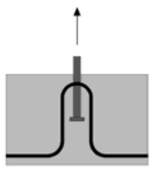	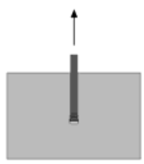	

Component	Friction	Concrete in compression	Threaded studs in tension/ shear	Anchor plate in bending and tension
Figure	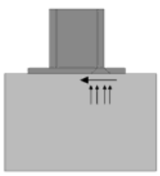	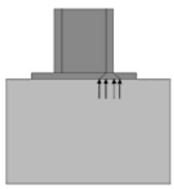	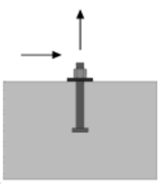	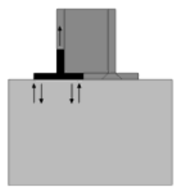

2.3.5 Safety factors

See Chapter 2.2.5

2.3.6 Boundary condition

The calculation of the design resistance of the connection between the steel element and the anchor plate is not covered by the program and has to be done separately by the engineer. If the steel elements or the steel profiles are not directly welded to the anchor plate and connected by threaded studs and an endplate the dimensions l_{AP} and b_{AP} have to be defined analogous independent from the actual dimensions of the steel profile (for example with the distances of the threaded studs l_{AP} and b_{AP}). The new components that are used in the program are based on test with large edge distances of the headed studs. Due to this reason the edge distances described in Chapter 2.2.6 are required. Also requirements for the exact location of the supplementary reinforcement are given there.

2.3.7 Input mask

The input sheet “Input + Output” shows on top a sketch of the connection labeling the most important input parameters (see Fig. 2.21). In the second part of the worksheet the dimensions, materials and loads on the anchor plate can be fed into the program. With the “Calculation-Button” on the right bottom of the worksheet the determination of internal forces and the component design will be started. Left beside the “Calculation-Button” the degree of utilization of the main components is shown. In the following the input data is described in particular.

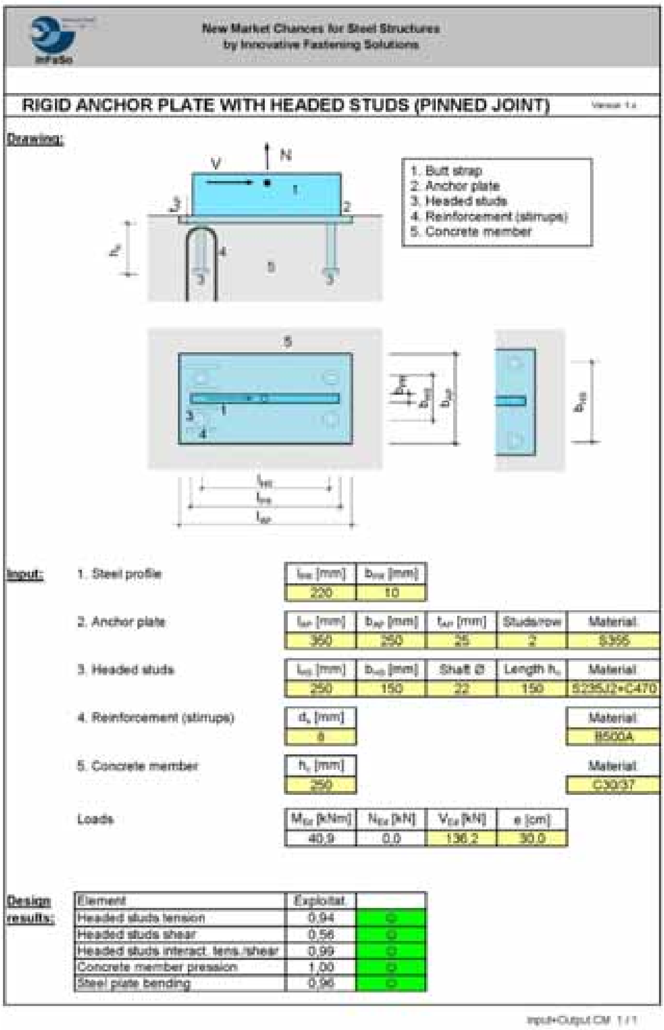

Fig. 2.21: Excel worksheet “Input + Output CM” page 1/1

Steel profile (1. line): Input of the length l_{PR} [mm] and the width b_{PR} [mm] of the connected butt strap.

Anchor plate (2. line): Input of the length l_{AP} [mm], the width b_{AP} [mm] and the thickness t_{AP} [mm] of the anchor plate; the number of headed studs per row (2 or 3); the material of the steel plate (acc. to EN 1993-1-1 [8] and EN 10025 [4]).

Headed studs (3. line): Input of the distances of the headed studs in longitudinal direction l_{HS} [mm], in cross direction b_{HS} [mm]; the shaft diameter [mm]; the length of the studs h_n [mm]; the material of the headed studs (acc. to EN 10025 [4]).

Reinforcement (4. line): Input of the diameter d_S [mm] and the material (acc. to DIN 488 [3]) of the reinforcement stirrups. The reinforcement stirrups have to be formed as loops with the smallest admissible bending role diameter. They have to be grouped in pairs close to the shafts of the headed studs with minimum distance to the bottom side of the anchor plate (maximum possible overlapping length of stirrup leg and headed stud).

Concrete member (5. line): Input of the thickness h_C [mm] and the material type (acc. to EN 1992-1-1 [7]) of the concrete member.

Loads (last line): Input of the shear force V_{Ed} [kN] and their eccentricity to the anchor plates surface in [cm]. Design loads have to be determined by the user. Partial factors will not be considered at the load side by the program!

2.3.8 Output mask

The output sheet "Design output" is divided into three parts. The first part gives information about the structural system (see Fig. 2.21). Results of the static calculation of internal forces are shown in the second part (see Fig. 2.23). In part 3 the main verifications of the components are given (see Fig. 2.23).

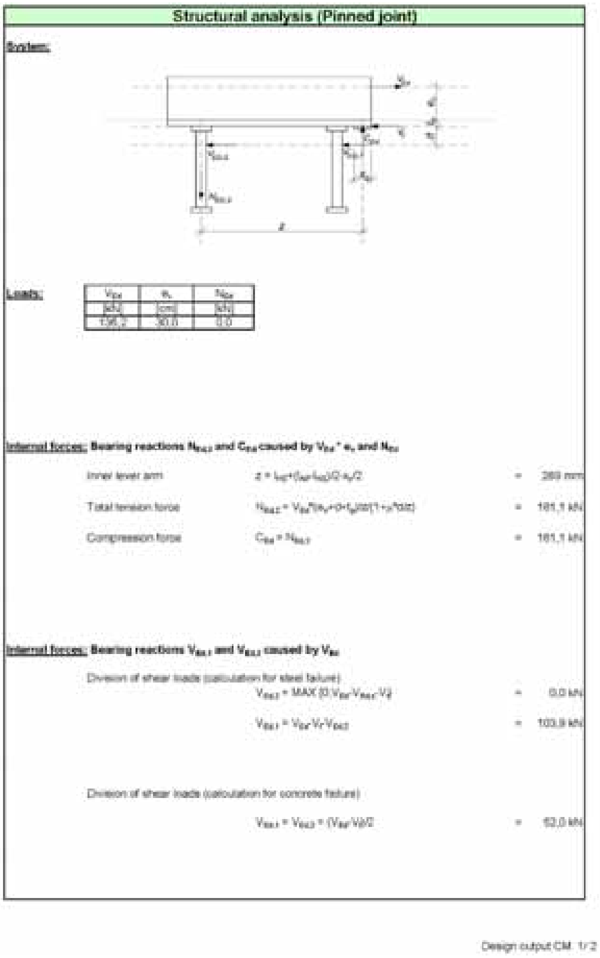

Fig. 2.22: Excel worksheet "Design output CM" page 1/2

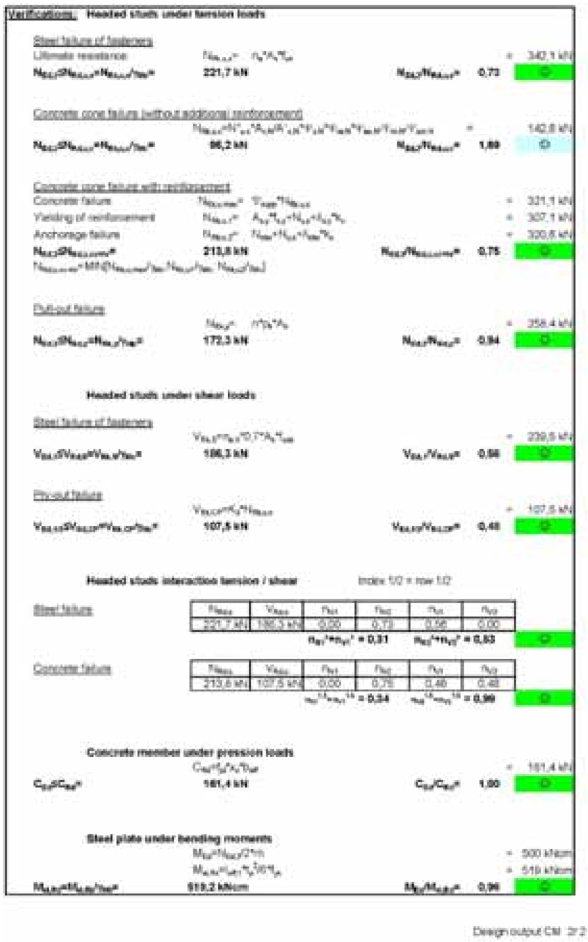

Fig. 2.23: Excel worksheet "Design output CM" page 2/2

2.3.9 Optimization of the joint

The optimization of the joint can be done according to the optimization of the connection of the slim anchor plate (see Chapter 2.2.9) more information about optimization of simple joints is given in the parameter study for simple joints in Chapter 4.3.

3 Design examples

3.1 Composite beam of a standard office structure connected to reinforced concrete wall

3.1.1 General

3.1.1.1 Depiction of the situation

Multistory office building structures often have a floor modulus of n · 1,35 m by approx. 7,8 m, which results from the room depth plus corridor. Beneath several variation of concrete slabs with or without beams concrete steel composite beams made of a hot rolled cross section IPE 300 with a semi-finished concrete slab connected by studs can be used to reduce the height of the construction and by this means the total height of each floor. One possibility to design a construction of minimum height properly can be the moment resistant constraint in the wall. The knowledge of rotational behaviour of the connection allows to optimize the connection on behalf of reinforcement and to evaluate the redistribution of forces.

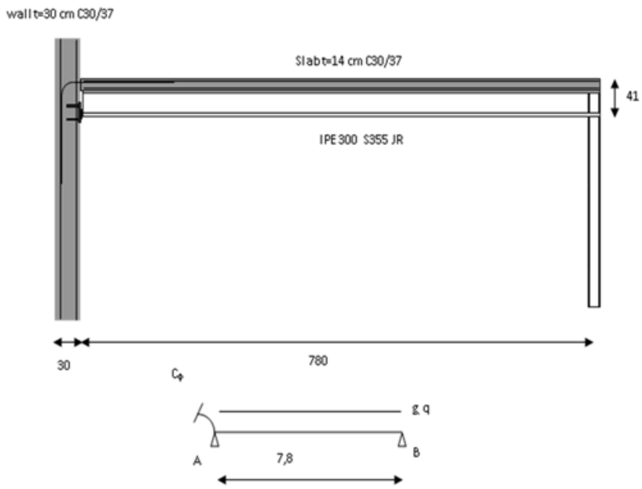

Fig. 3.1: Structural system

3.1.1.2 Overall structural system

The example shows a concrete steel composite beam made of a hot rolled cross section IPE 300 with a semi-finished concrete slab (total 14 cm) connected by studs. The lateral distance of the beams is 2 · 1,35 m = 2,70m, the span is 7,8 m. The inner support can be at a reinforced concrete (RC) wall of the building core, the outer support is a façade column (see Fig. 3.1).

- Semi-finished slab (6cm precast concrete) + cast in-situ of altogether 14 cm, continuous system, span 2,70 m each.
- Hot rolled beam IPE 300 S355 JR, L = 7,8 m; uniformly distributed loading with headed studs.
- Support façade: Steel column spaced 2,7 m.
- Support inner core: Reinforced concrete wall with fully restraint connection by reinforcement and steel/concrete compression contact.

3.1.1.3 Loads

Own weight slab	g'	=	1,6 kN/m
Own weight slab	g_1	=	3,5 kN/m^2
Dead load screed	g_2	=	1,6 kN/m
Dead load suspended ceiling + installation	g_3	=	0,4 kN/m^2
Dead load (total)	$\mathbf{g}$	=	**5,50 kN/m^2**
Live load (B2,C1 acc. DIN 1991-1-1 NA [5])	$\mathbf{q}$	=	**3,00 kN/m^2**

3.1.2 Execution options

3.1.2.1 Previous realization

To provide a moment resistant connection of composite structures to a concrete wall is not new at all, as it isn't the separation of tensile forces into the slab's reinforcement and compression into lower beam flange resp. anchor plate. Nevertheless there have been bolted solutions with fin plates for the shear forces or endplates as an adaption of common steel constructions, which were more costly in terms of manufacturing costs. These solutions with their more complex mechanisms were as well difficult to design effectively and to predict their rotational behaviour. Therefore a larger range of maximum and minimum forces has to be covered, as the redistribution of forces is unknown.

3.1.2.2 Improved implementation

The presented connection of a moment resistant connection of composite structures to a concrete wall provides a solution that is simple feasible on site, because the vertical and horizontal tolerances are relatively high, and the necessary parts are minimized. Forces are strictly separated and transferred by easy mechanisms. Due to this reason the knowledge of the connection behaviour has grown since any of these single shares have been explored further on and the characteristics have been put in a simple component (spring) model. The component method is implemented in Eurocodes, but has been improved by detail research throughout this project. So the stress-strain model of the slab's reinforcement has been developed with additive tensile stresses in concrete, the displacement of the anchor plate, the slip of the slab studs can now be considered and the contribution of the nonlinear behaviour of the shear panel in the connecting concrete wall has been added.

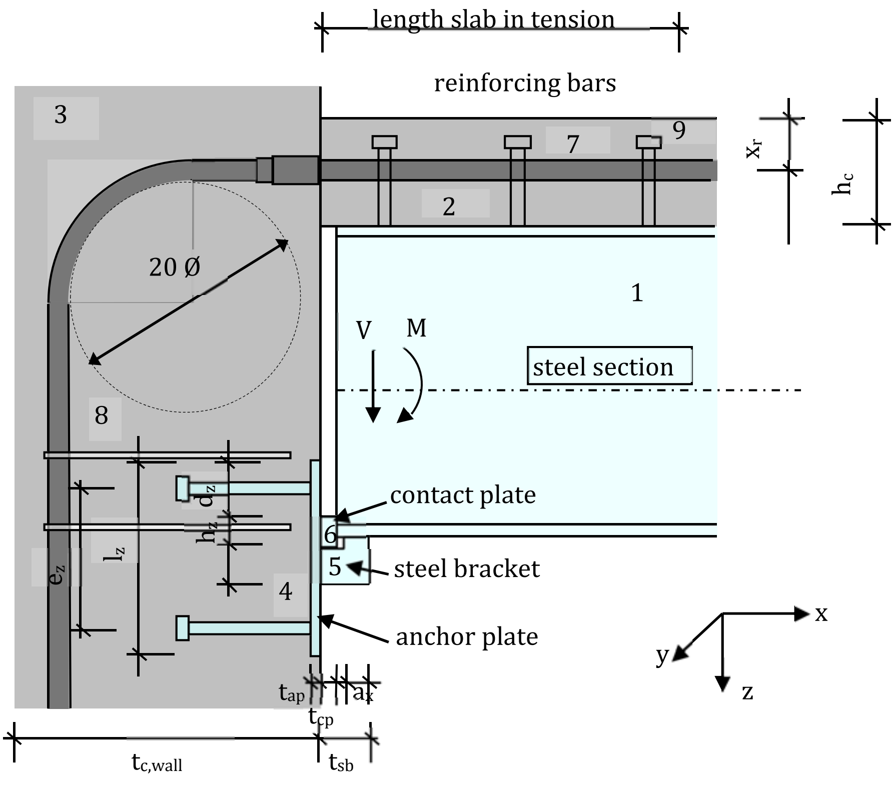

1. Composite beam (steel section)
2. Concrete slab
3. Concrete wall
4. Anchor plate
5. Steel bracket
6. Contact plate
7. Reinforcing bars (tension component)
8. Additional stirrups
9. Studs in slab's tensile zone

Fig. 3.2: Geometry of the composite joint

3.1.3 Structural analysis of the joint

3.1.3.1 Modelling

The member forces of the structure generally can be calculated with any software which is able to consider ranges of different beam stiffness and rotational springs. As the structure is statically indeterminate the different stiffness of the positive and negative moment range must be taken into account to properly calculate the member and support forces. For this example the software KRASTA [21] for spatial frame analysis has been used. Prior to any calculation we can do a reliable prediction concerning the quality of moment distribution. There will be a maximum negative moment at the moment resistant support, the moment will then be reduced and will cross the zero-line. Afterwards it will drop down to its positive maximum at approx. 5/8 of the span and ending at zero at the hinged support at the end of the beam. The negative range is assumed for the first quarter of span, the positive is set for the rest of span. According to EN 1994-1-1 Cl. 5.4.1.2 [10] the effective width can be calculated with Eq. (3.1).

$$b_{eff} = b_0 + \sum b_{e,i} \tag{3.1}$$

In case of equally spaced beams these equation can be calculated in the negative range with Eq. (3.2) and in the positive range with Eq. (3.3) each of them less as the spacing between adjacent beams (270 cm). This means that necessary reinforcement bars in the negative range of the slab must be arranged within the effective width.

$$b_{eff,2} = 15 + 2 \cdot 780 \cdot 0{,}25/8 = 63{,}8 \text{ cm} \tag{3.2}$$

$$b_{eff,1} = 15 + 2 \cdot 780 \cdot 0{,}75/8 = 161{,}25 \text{ cm} \tag{3.3}$$

The different moments of inertia I_{pos} are calculated in accordance to common values of creep influence (see Eq. (3.4) to (3.5). In this example the relation between stiffness shortly after erection and after 1-2 years (means T=∞) is approximately ¾. The effect of shrinking (eccentricity of tensional force in slab) is not considered. The moment of inertia for T=∞ will be used with dead load and value for T=0 will be used with life load. This will yield the maximum restraint moment and force at support A.

Negative range: $$I_{neg} \approx 18360 + 15{,}5 \cdot (30/2 + 15 - 4)^2 \approx 18000 \text{ cm}^4 \tag{3.4}$$

Positive range: $$I_{pos,\,t=0} \approx 30200 \text{ cm}^4 \qquad I_{pos,\,t=\infty} \approx 22500 \text{ cm}^4 \tag{3.5}$$

3.1.3.2 Calculation of forces

Using the previous mentioned characteristics in the first iteration of forces, the rotation stiffness of the connection is set to infinite, i.e. complete moment resistant restraint. The resultant internal forces for characteristic points of the beam are shown in Fig. 3.3.

The next step will be an assessment of the moment restraint connection and the evaluation of rotation to define a rotational spring characteristic.

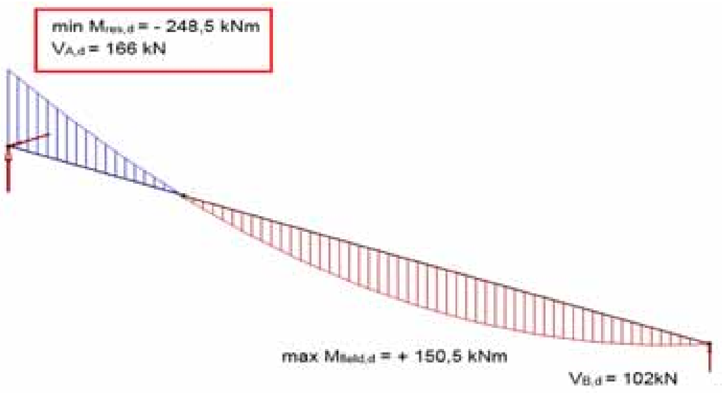

Fig. 3.3: Mind: these are independently calculated input values for

The structural design and the evaluation of the connection stiffness will be done by using the program "Restrained connection of composite beams ".The model data of the parts which contribute to the connection must be defined in detail. These are geometric data like size, position and thickness of plates with headed studs, the beams cross section, reinforcement in the slab and in the wall. As the rotational characteristics are largely dependent of the slab reinforcement, a contribution of stud slip, the concrete shear panel behaviour and the compressed anchor plate is considered as well. Therefore the user is asked for parameters, which are not important for the connection design but might have influence on the horizontal displacement of the slab. By starting the Excel worksheet all parameters are set by default with a valid set of input data, where an obviously rational result is obtained. It will never the less be a duty for the user to ensure, that all parameters are reasonable, at least under geometrical aspects (spacing of reinforcement and slab studs, enough reinforcement, studs inside plate etc.). These validation results will show up on the right of the input mask.

The slab reinforcement is set to a value a little higher than the minimum – that is due to the assessment of the shear panel resistance, which is amongst others affected by the amount of reinforcement. This area must be built in within the effective width of the negative moment range of 64 cm. The number of studs over the length of tensile action in the slab is chosen as 13, spacing approx. 15 cm.

Though the calculation is executed with an Excel sheet and is therefore directly updating most of the values upon any changed cell input value, there is a Visual-Basic-Macro implemented to iterate depending on the used model. To update all of these characteristics the calculation must be started with pushing the 'calculate' – button in the lower region of the page. Any changes connected with the anchor plate, beginning with wall concrete and reinforcement parameters and the geometry of plate and studs need the use of this updated macro.

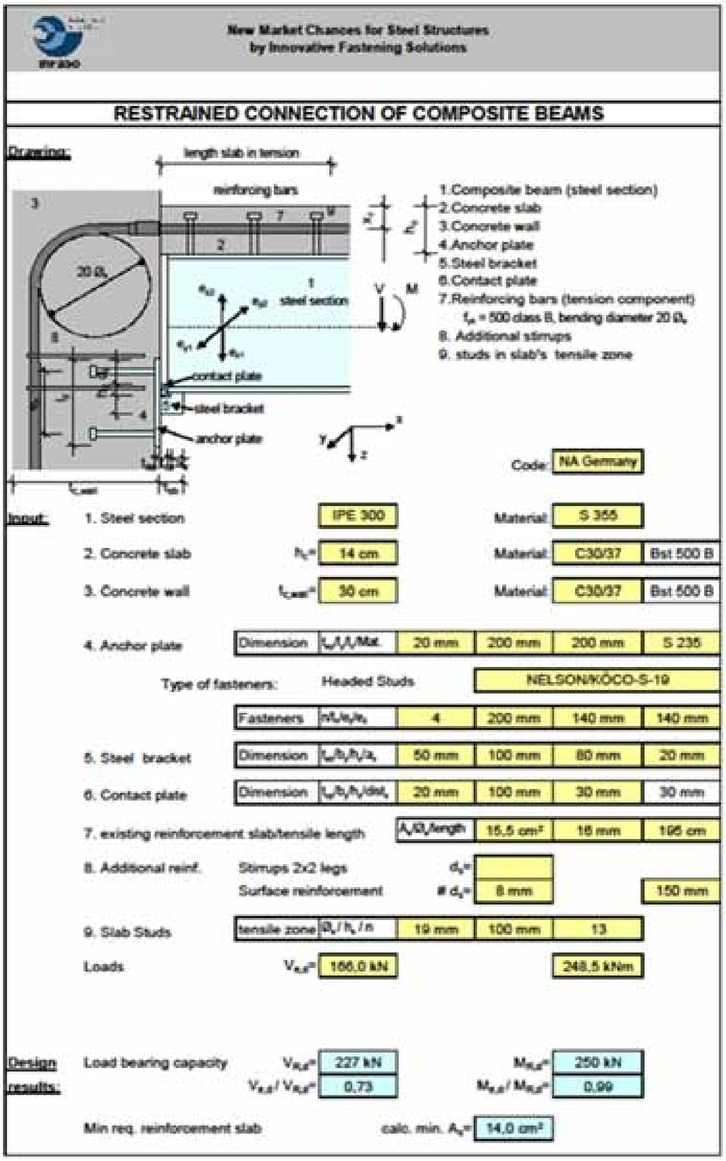

Fig. 3.4: Excel sheet, "Input+Short Output"-Mask

After all geometry data and forces have been inserted into the mask, the two main results will be the utilization of the connection, the relation between given force and the resistance of the connection, and secondly the stiffness of the restrained cross section at the edge of wall to generate a new, updated rotational spring. In the Fig. 3.4 see the completely filled input mask and resulting utilization of the connection. In the following figures (see Fig. 3.5 to Fig. 3.7) the complete detailed output with intermediate results of components and the resulting stiffness of the actual constellation is shown.

New Market Chances for Steel Structures
by Innovative Fastening Solutions

InFaSo

RESTRAINED CONNECTION OF COMPOSITE BEAMS

Input Data Echo

Steel Section		Contact plate		Bracket		Anchor Plate	
Profile	IPE 300	h_{cp} [mm]	30	h_{ws1} [mm]	80	h_{ap} [mm]	200
h [mm]	300	t_{cp} [mm]	20	h_{ws2} [mm]		t_{ap} [mm]	20
b [mm]	150	b_{cp} [mm]	100	t_{ws} [mm]	50	b_{ap} [mm]	200
h_w [mm]	278,6	d_{cp} [mm]	30	t_{ws2} [mm]	20		
t_w [mm]	7,1	*Remark*		b_{ws} [mm]	100		
d [mm]	248,6	Contact plate centre is aligned with centre of steel section bottom flange		d_{ws} [mm]	60		
t_f [mm]	10,7						
$W_{el,y}$ [cm³]	557						
Steel grade	S 355					Steel grade	S 235
f_{yk} [N/mm²]	355					f_{yk} [N/mm²]	235

Slab section		Wall section		Headed Studs type:		NELSON/KOCO-S-19	
h_c [mm]	140	$t_{c,wall}$ [mm]	300	ϕ_1 [mm]	19	e_1 [mm]	140
x_r [mm]	40	$x_{r,out}$ [mm]	40	h_{ef} [mm]	210	e_2 [mm]	140
h_c - x_r [mm]	100	$x_{r,in}$ [mm]	40	n [row]	2	n [col]	2
Concrete	C30/37	Concrete	C30/37	f_{uk} [N/mm²]	450	f_{yk} [N/mm²]	350
f_{ck} [N/mm²]	30,00	f_{ck} [N/mm²]	30,00	Surface reinforcement		Stirrup reinforcement	
Slab reinforcement		acc. to	DIN 488	# d_s [mm]	8	# d_s [mm]	0
a_s [cm²]	15,5	f_{sk} [N/mm²]	519	# s [mm]	150	number legs	
Joint loading		Loading components					
M_{ed} [kNm]	248,5	T_d [kN]	629,67				
V_{ed} [kN]	166	C_d [kN]	629,67				
		V_{ed} [kN]	166,00				
		e [mm]	79,00				
		M'_{ed} [kNm]	13,11				

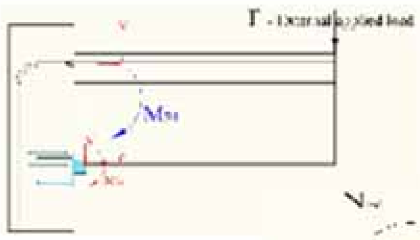

Result Data

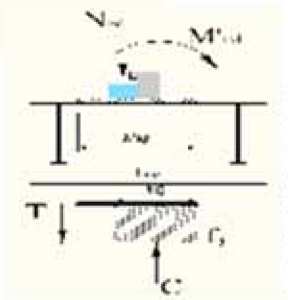

Anchor plate in compression + bending					
For rigid anchor plate t_{min} [mm]		63,08			
Plate Type	Flexible	Comments			
β_j	0,67	This factor considered			
f_j [N/mm²]	33,37				
c [mm]	29,22	Bearing width for equivalent rigid plate			
h'_{ap} [mm]	138,43	updated value			
b'_{ap} [mm]	158,43	updated value			
Maximum N for applied M'ed					
h_{cp} [mm]	138,43	N_{max} [kN]	731,91	F_t [kN]	-
N_{con} [kN]	731,91	M'_{ed} [kNm]	13,11	% T_{Rd}	0,00
Maximum M' for applied Ned					
h_{cp} [mm]	121,80	N_{Ed} [kN]	629,67	F_t [kN]	14,33
N_{con} [kN]	644,00	M'_{max} [kNm]	40,99	% T_{Rd}	25,01

Verification	OK
No anchors in tension! The applied moment can be larger. Equivalent rigid plate is considered.	
Verification	OK
Anchors in tension!	

Fig. 3.5: Output file with intermediate results (1)

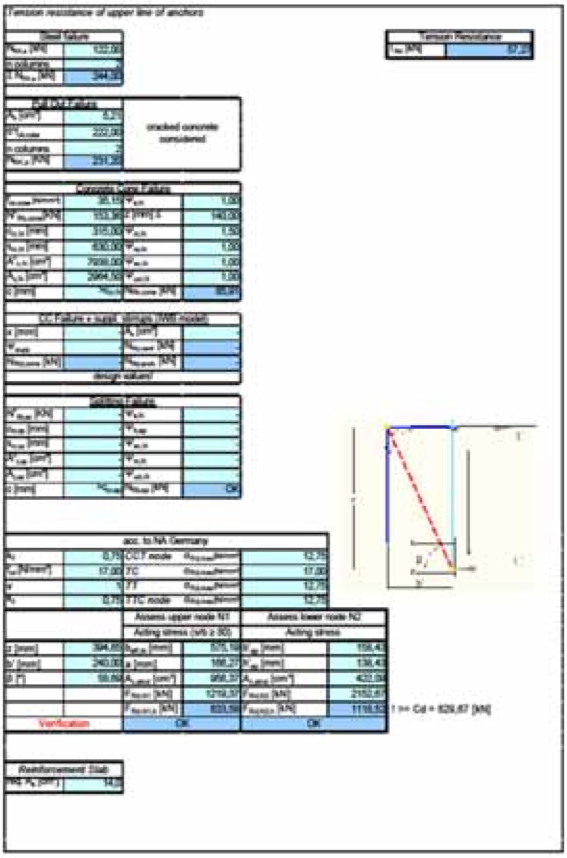

Fig. 3.6: Output file with intermediate results (2)

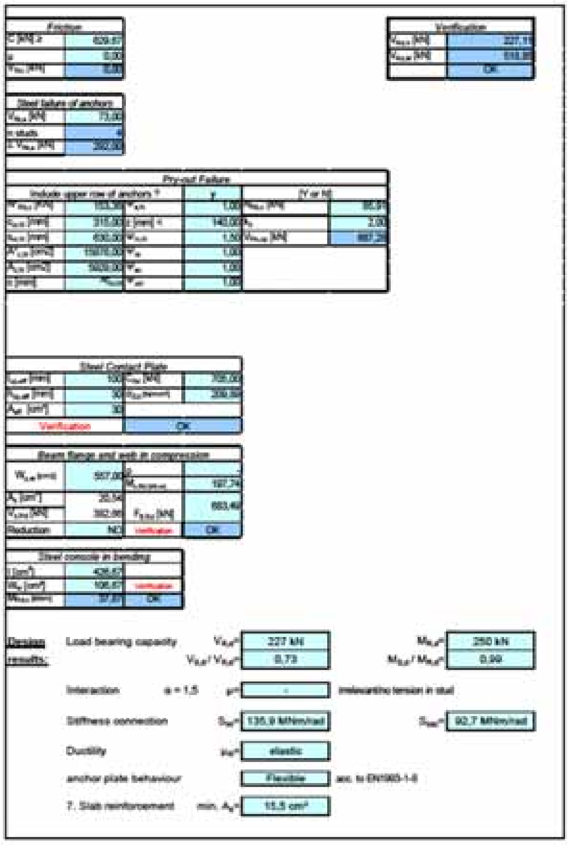

Fig. 3.7: Output file with intermediate results (3)

The rotational stiffness of the connection will be given as a result of the connection assessment, with a secant stiffness of $C_\varphi \approx 93$ MNm/rad. If the secant stiffness of C_φ is taken as a rotational stiffness of the support internal forces can be obtained (see Fig. 3.8).

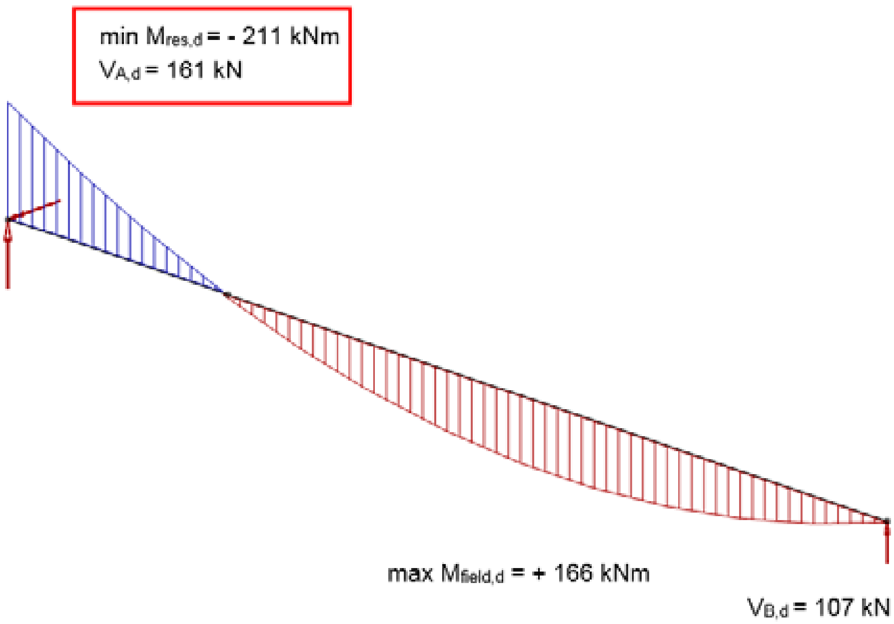

Fig. 3.8: Internal forces by taking into account the secant stiffness C_φ at the support A

These values will be approximately very close to convergence and are those values to be assessed finally, and in this case of statically indeterminant systems. The reduced moment and shear force acting in the connection will increase the resulting stiffness output to approximately $C_{\varphi} \approx 94$ MNm/rad, which is no remarkable difference to the value considered. Generally with decreasing moments the stiffness value converges to a maximum, the so called initial stiffness, which is 135 MN/rad and cannot be exceeded. This limit is connected to steel strain with uncracked concrete contribution. Due to the a possible reduction of the reinforcement grade the resulting stiffness will decrease to 89 MNm/rad. As there is no underestimation of stiffness, higher forces don`t have to be expected in the connection and the connection can be considered safe.

3.1.3.3 Structural analysis

The structural analysis will be done by using the program "Restrained connection of composite beams "(see Fig. 3.9). As mentioned above, the reinforcement grade is possibly reduced according to the moment reduction.

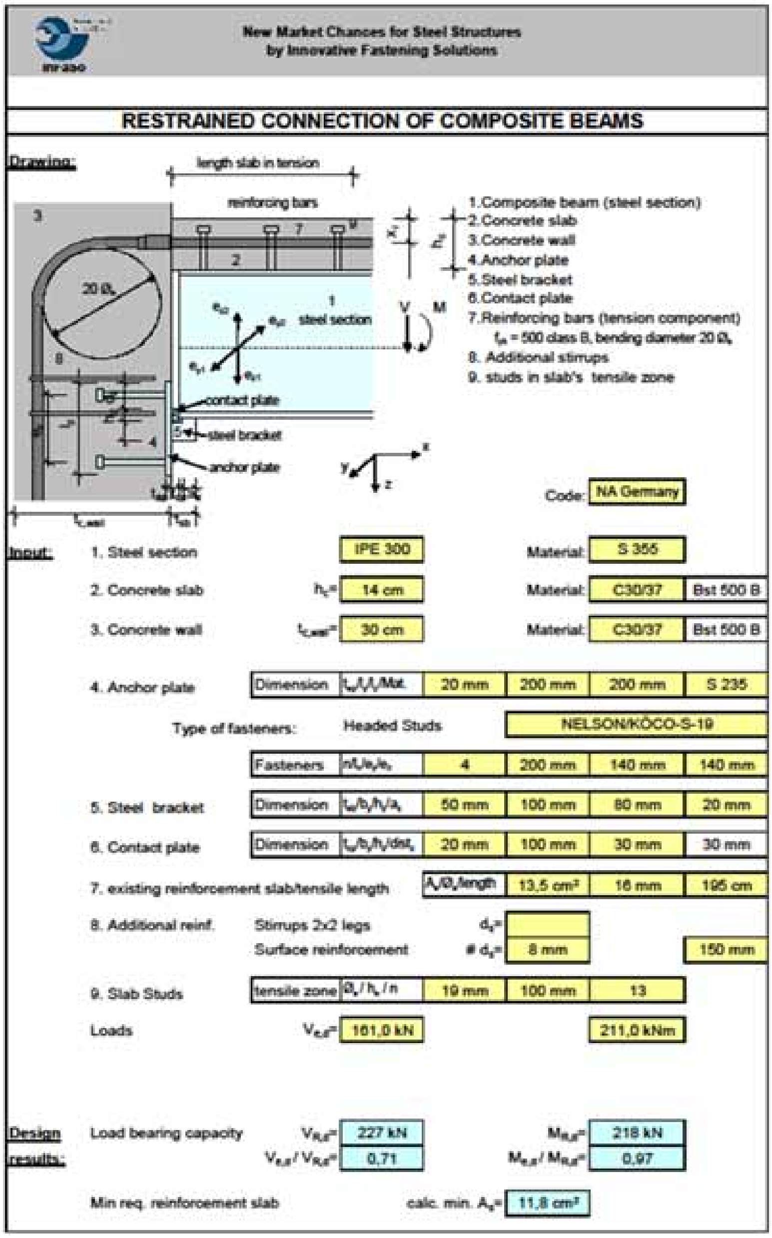

Fig. 3.9: Structural analysis of the restrained connection

The bending diameter of the reinforcement in the wall has a significant influence on the model. Even generally allowed with a value of minimum 10 $Ø_s$ (with higher edge distances) it is strongly recommended to take a value of 20 $Ø_s$, because the curvature influences the diagonal concrete strut in size. The larger the diameter of bending is, the larger is the effective concrete area which resists the tensile force within the slab's reinforcement bars. Definitely this can be the component which limits the resistance of the entire joint. Using the minimum bending diameter one will experience a limitation in the concrete shear panel behaviour which is not appropriate. The increase in the amount of reinforcement or the concrete grade is not a useful option as consequence. In case of statically determined systems the iteration step can obviously be skipped, as the internal forces are not related to the changes of the stiffness in the model.

3.1.4 Conducting

3.1.4.1 Installation

The anchor plate can be installed easily at the inner surface of the formwork because the relatively small headed studs can easily installed on-site within the crosswise placed external reinforcement layer of the concrete wall. The loop-shaped hanger reinforcement will be fixed at the inner reinforcement layer. These must be adjusted after installing the anchor plate, if the distance to the headed studs are too large. The reinforcement in the slab transferring the tensile forces into the wall will be easily mounted by using a rebar splicing system. The screwed joint will be fixed at the formwork. The bar has to have a large bending diameter of 20 $Ø_s$ as a recommendation to optimize the transfer of the diagonal compression force in the shear panel zone. After removal of formwork the steel bracket will be welded on the anchor plate. In a next step the steel profiles can be mounted, adjusted and the contact element of the formwork for the slab (or semi-finished panels) will be placed and the reinforcement can be screwed into the couplers. After having all reinforcement placed properly the concrete slab can be poured.

3.1.4.2 Tolerances

Deviations of the anchor plate regarding to the longitudinal axis of the beam in horizontal and vertical direction can easily be compensated, because the steel bracket is welded to the anchor plate on-site. If larger tolerances in longitudinal direction of the beam have to be taken into consideration, the beam has to be produced after measurement of the exact distances between supports. Small deviations can be bridged by adapting the steel contact element. The reinforcement connectors placed in the concrete wall may have vertical or horizontal deviations, as far they can be cast in the slab with the necessary concrete cover. The concrete cover should be taken into account sufficiently large not to overrate the inner lever arm of forces.

3.1.4.3 Fire protection

For the structure shown in this example usually the fire resistance R90 has to be fulfilled. The steel structure including its connections must be protected with approved coating systems or plate-shaped panels. As there is no required space for installation within the cross section chambers during erection, the chamber can be filled with concrete as a fire protection. The open bracket at lower flange must nevertheless be protected additionally. This can be assessed by a fire protection expertise. The reinforcement is protected by concrete covert and can be assessed by considering codes.

3.1.4.4 Costs

The ability to calculate the stiffness of the connection with deeper understanding and less uncertainties and therefore getting a more realistic force distribution helps to reduce overall costs of the steel construction. The connection itself can be easily installed by placing the beam on the steel bracket without using any bolts. The use of screwed reinforcement connectors is nevertheless necessary.

3.2 Column base as connection of a safety fence on a car parking deck to a reinforced concrete slab

3.2.1 General

3.2.1.1 Depiction of the situation

A safety fence, consisting of a horizontal beam barrier of two connected hollow sections on vertical columns of rolled sections, is connected at the column bases to a 300 mm thick reinforced concrete slab. Embedded anchor plates with headed studs and welded threaded studs are used to connect the columns base plates with the concrete deck. The distance between the steel columns varies from 1,50 m up to 2,00 m and the centre of the beam barrier is 0,50 m above the concrete surface. The whole construction has to be protected against corrosion, for example by galvanization.

3.2.1.2 Overall structural system

Horizontal beam barrier:
Single span beam L = 1,50 m up to 2,00 m; loaded by a horizontal vehicle impact force.
Vertical column:
Cantilever beam (vertical) L = 0,50 m; loaded by a horizontal vehicle impact force (directly or indirectly by the beam barrier)

3.2.1.3 Loads

Impact passenger car (EN 1991-1-7, Cl. 4.3.1 [6]) (Load application 0,50 m above street surface)	F_{dx}	=	50,00 kN

3.2.1.4 Joint loads

Design load	$V_{Ed} = F_{dx}$	=	50,00 kN
	$M_{Ed} = 50{,}00 * 0{,}50$	=	25,00 kNm

3.2.2 Execution options

3.2.2.1 Previous realization

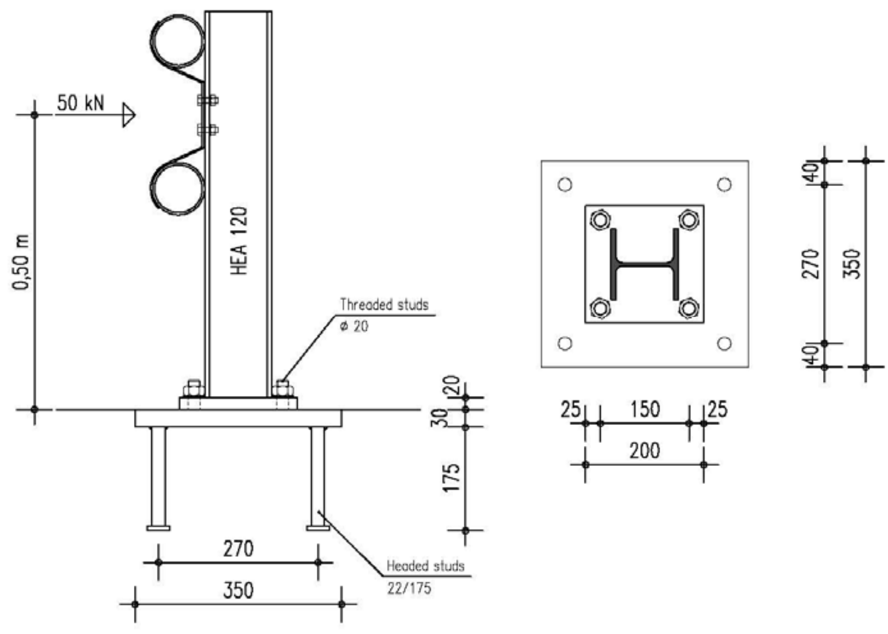

Fig. 3.10: Conventional joint solution of the safety fence

In the conventional joint solution the columns base plate is directly bolted to the anchor plate by threaded studs which are welded on the embedded steel plate (see Fig. 3.10). In order to reduce the headed studs tension forces caused by bending, the distance of the studs in load direction and therewith the length of the embedded steel plate have to be large. For this reason the distance between the threaded bolts and headed studs is quite large and high bending moments in the anchor plate are resulting. The anchor plates is designed as thick and rigid in order to consider an elastic approach in the calculation. The dimensions of the anchor plate are given in the following.

Base plate	200 / 200 / 20 mm S 235
Threaded bolts	ø 20 mm f_{ub} = 500 N/mm²
Distance threaded bolts	150 / 150 mm
Anchor plate	350 / 350 / 30 mm
Headed studs	22 / 175 mm S 235
Distance headed studs	270 / 270 mm

3.2.2.2 Improved realization Version 1

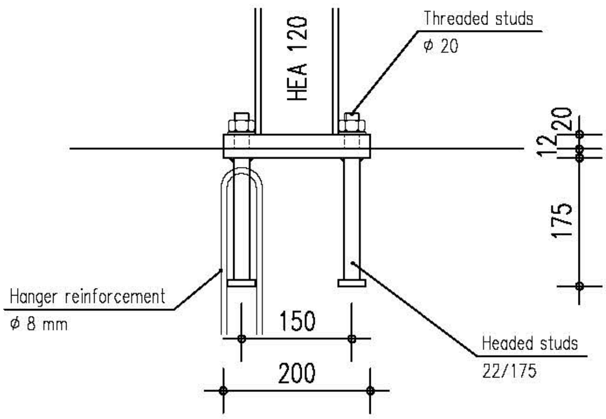

Fig. 3.11: Improved realization Version 1

Within this modified joint solution the new components of the INFASO [12] project are considered. In this solution the columns base plate is directly bolted to the anchor plate by threaded studs which are welded on the embedded steel plate (see Fig. 3.11). The choice of a quite small anchor plate generates high tension forces in the headed studs caused by external bending moment. So additional hanger reinforcement is fixed very close to the headed studs loaded by tension forces. The distance of the headed studs in load direction is small. Due to the fact that the headed studs and the threaded studs are spaced very close, low bending moments in the anchor plate are resulting. A plastic design of the anchor plate is possible. Thin steel plates can be used. The complete embedded plate is covered by the columns base plate. The dimensions of the anchor plate are given in the following.

Base plate	200 / 200 / 20 mm S 235
Threaded bolts	ø 20 mm f_{ub} = 500 N/mm²
Distance threaded bolts	150 / 150 mm
Anchor plate	200 / 200 / 12 mm
Headed studs	22 / 175 mm S 235
Distance headed studs	150 / 150 mm

The structural design will be done by using the program "Slim anchor plate with headed studs"(see Fig. 3.12 and Fig. 3.13).

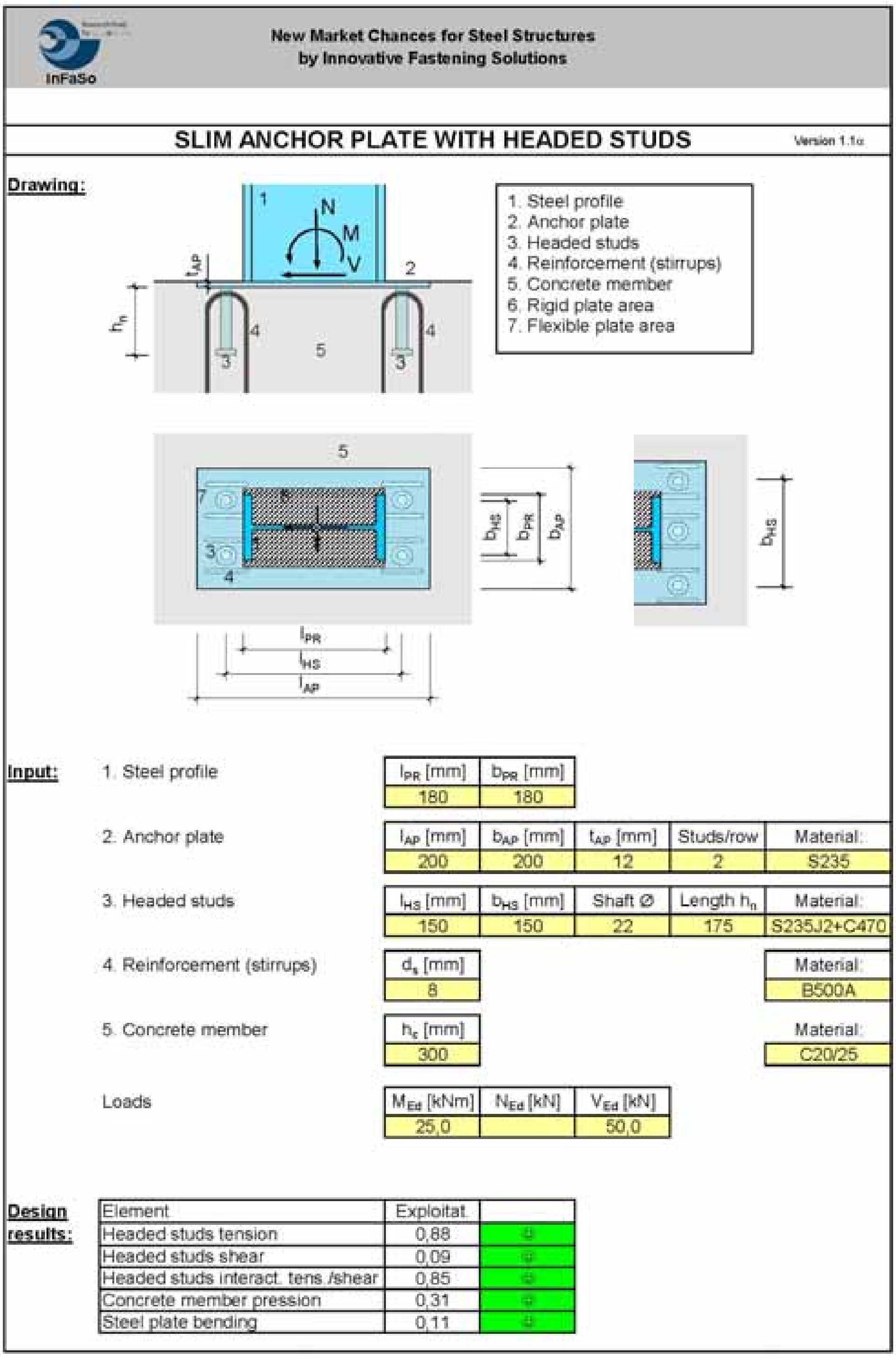
New Market Chances for Steel Structures
by Innovative Fastening Solutions

InFaSo

SLIM ANCHOR PLATE WITH HEADED STUDS Version 1.1α

Drawing:

1. Steel profile
2. Anchor plate
3. Headed studs
4. Reinforcement (stirrups)
5. Concrete member
6. Rigid plate area
7. Flexible plate area

Input:

1. Steel profile

l_{PR} [mm]	b_{PR} [mm]
180	180

2. Anchor plate

l_{AP} [mm]	b_{AP} [mm]	t_{AP} [mm]	Studs/row	Material:
200	200	12	2	S235

3. Headed studs

l_{HS} [mm]	b_{HS} [mm]	Shaft Ø	Length h_n	Material:
150	150	22	175	S235J2+C470

4. Reinforcement (stirrups)

d_s [mm]	Material:
8	B500A

5. Concrete member

h_c [mm]	Material:
300	C20/25

Loads

M_{Ed} [kNm]	N_{Ed} [kN]	V_{Ed} [kN]
25,0		50,0

Design results:

Element	Exploitat.	
Headed studs tension	0,88	☺
Headed studs shear	0,09	☺
Headed studs interact. tens./shear	0,85	☺
Concrete member pression	0,31	☺
Steel plate bending	0,11	☺

Fig. 3.12: Excel sheet, “Input+Output”-mask for version 1

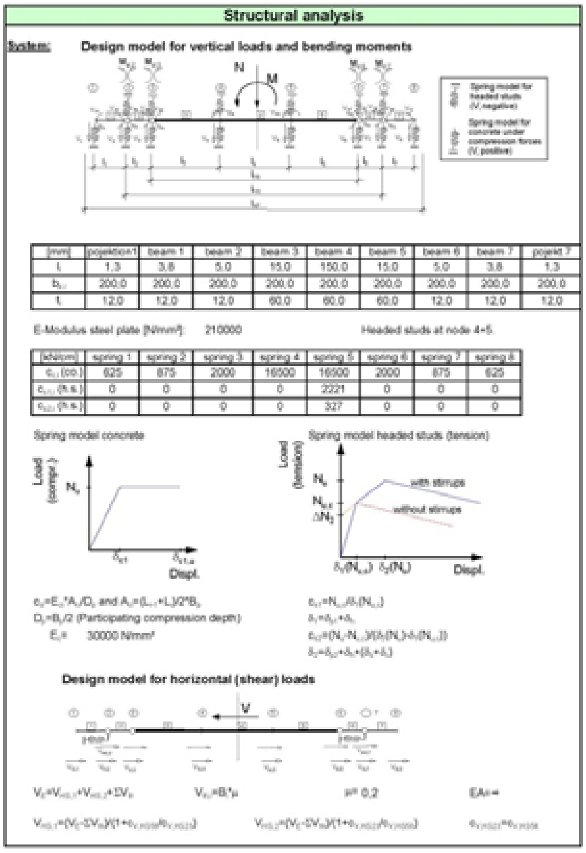
Structural analysis
System:
Design model for vertical loads and bending moments
Spring model concrete
Spring model headed studs (tension)
Design model for horizontal (shear) loads

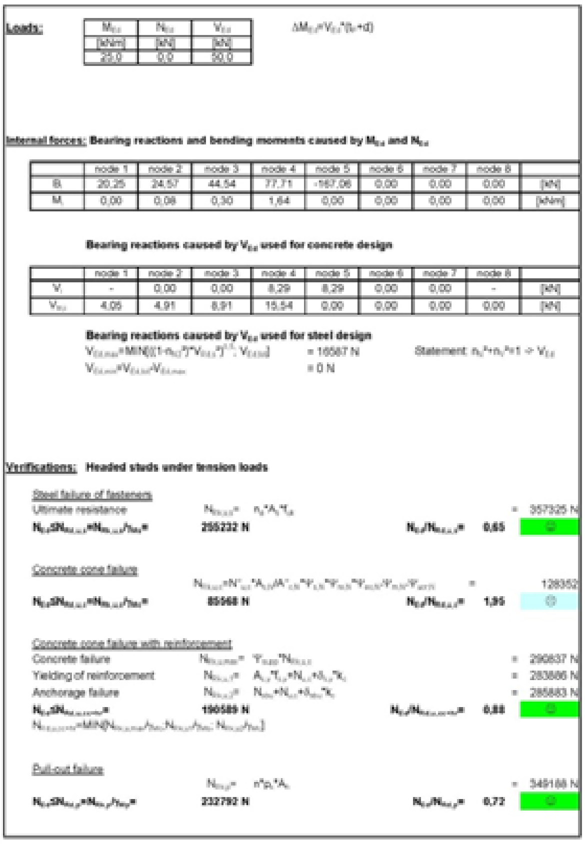
Loads:
Internal forces:
Verifications:
Headed studs under tension loads
Steel failure of fasteners
Concrete cone failure
Concrete cone failure with reinforcement
Pull-out failure

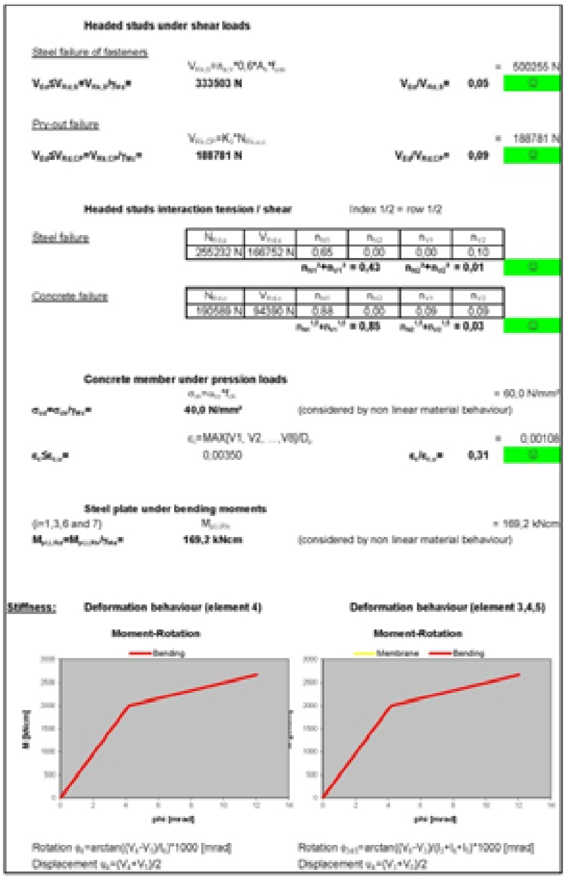
Headed studs under shear loads
Steel failure of fasteners
Pry-out failure
Headed studs interaction tension / shear
Steel failure
Concrete failure
Concrete member under pression loads
Steel plate under bending moments
Stiffness:
Deformation behaviour (element 4)
Deformation behaviour (element 3,4,5)
Moment-Rotation

Fig. 3.13: Excel sheet, “Design output” for version 1

3.2.2.3 Improved realization-Version 2

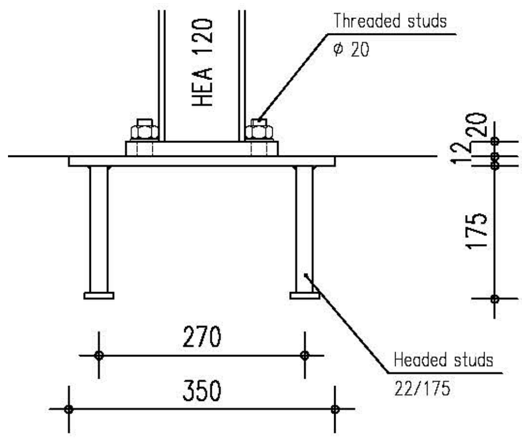

Fig. 3.14: Improved Version 2

Description of a modified joint solution considering the new components of WP 1

Within this modified joint solution the new components of the INFASO [12] project are considered. The columns base plate is directly bolted to the anchor plate by threaded studs which are welded on the embedded steel plate. Except that the anchor plate has only a thickness of 12 mm the construction is the same as shown by structure of the previous realization. The embedded steel plate cannot take the total bending moment. The behaviour of the joint is comparable with a kind of plastic hinge. The joint will be designed by transformation of kinetic energy into plastic deformation energy. The dimensions of the anchor plate are given in the following.

Base plate	200 / 200 / 20 mm S 235
Threaded bolts	ø 20 mm f_{ub} = 500 N/mm²
Distance threaded bolts	150 / 150 mm
Anchor plate	350 / 350 / 12 mm
Headed studs	22 / 175 mm S 235
Distance headed studs	270 / 270 mm

For structural design information about the bending moment resistance and the deformation behaviour of the joint is needed. The bending moment resistance will be obtained by using the program “Slim anchor plate with headed studs” with stepwise increase of the external forces (see Chapter 2.3). After the last step the moment-rotation curve of the sheet “Design output” can be used (see Fig. 3.15). The verification will be done according to EN 1991-1-7 Annex C 2.2 [6].

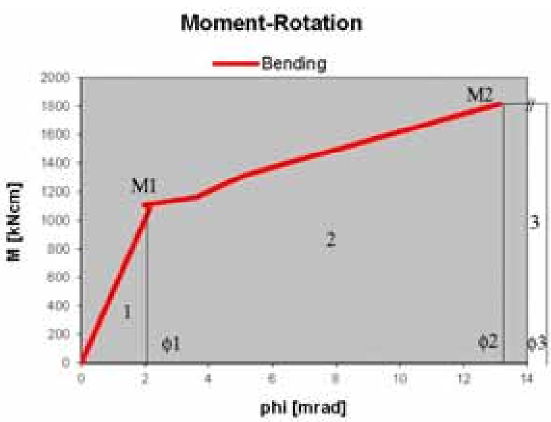

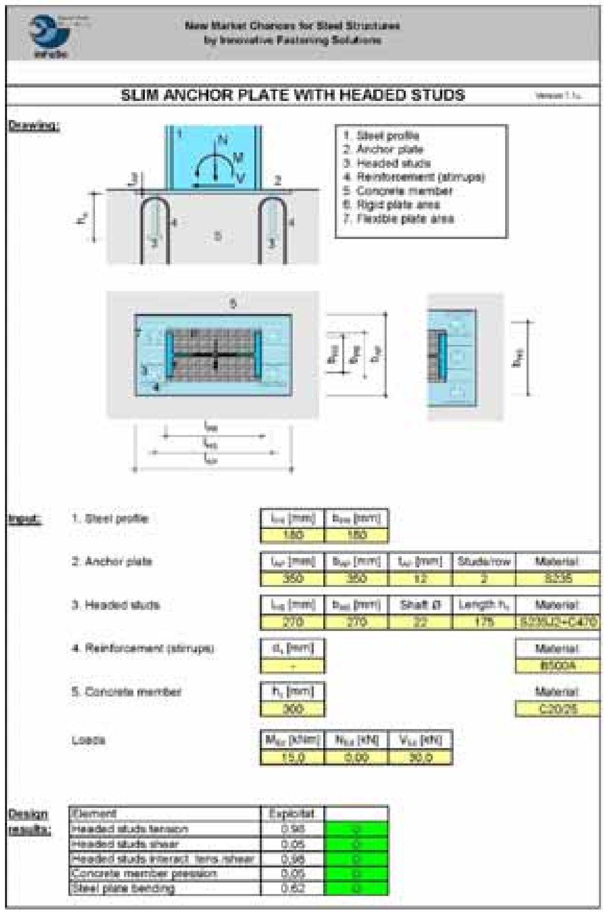

Fig. 3.15: Moment-rotation curve of the joint

Fig. 3.16: Excel sheet, “Input+Output”-mask for version 2

The moment resistance, the kinetic energy the deformation energy and the deformation of the joint can be calculated with the Equations (3.6) to (3.9)

$$\begin{gathered} M_{Ed} = 17{,}0\ kNm = M_2 \\ V_{Ed} = 34{,}0\ kN \\ M_{Ed} + V_{Ed} \cdot (t_{AP} + d_{HS}) = 18{,}0\ kNm \\ \rightarrow M_1 = 11{,}0\ kNm \cdot 17/18 = 10{,}40\ kNm \end{gathered} \tag{3.6}$$

$$E_{kin} = 1/2 \cdot m \cdot v^2 = 1/2 \cdot 1500\ kg \cdot (10/3{,}6\ m/s)^2 = 5787\ Nm = 5{,}787 KNm \tag{3.7}$$

$$\begin{gathered} E_{def,1} = 10{,}4/2 \cdot 2{,}1/1000 = 0{,}011\ KNm \\ E_{def,2} = (10{,}4 + (17 - 10{,}4)/2) \cdot (13{,}2 - 2{,}1)/1000 = 0{,}152\ KNm \\ E_{def,2} = 17 \cdot \Delta\Phi_{23} = 17 \cdot (\Phi_3 - \Phi_2) \end{gathered} \tag{3.8}$$

$$\begin{gathered} \Delta\Phi_{23} = (5{,}787 - 0{,}011 - 0{,}152)/17 = 0{,}33\ rad \\ \Delta\Phi_{03} \approx 0{,}33\ rad = 18{,}9° \end{gathered} \tag{3.9}$$

Note 1 The required rotation of 18,9° induces extremely large stretching at the locations with plastic hinges. It has to be checked that the admissible elongation is not exceeded.

Note 2 The component ‘Headed studs in tension’ is high exploited. So the installation of additional hanger reinforcement is advised to ensure that the component ‘Anchor plate in bending’ is the decisive component.

<u>Due to the extremly deviation of the necessary rotation from the calutated diagram range, the execution of this version can not be recommended!</u>

3.2.3 Conducting and assessment

3.2.3.1 Installation

In each of both cases the embedded plates can be installed easily. The anchor plate of the previous realization is large and heavy and thus it is not so easy to handle during installation. Much more compact and light is the solution of the improved realization, but additional reinforcement is needed.

3.2.3.2 Tolerances

Deviations of the anchor plate’s centre in any horizontal direction could only be settled by oversized holes, in vertical direction by using filler plates. Normally for more or less rude constructions like guide boards low tolerances are needed.

3.2.3.3 Fire protection

For the structure shown in this example, no requirements relating to fire protection have to be fulfilled. If the classification in a particular fire resistance class should be required in other cases, the steel structure including its connections shall be protected with approved coating systems or plate-shaped panels.

3.2.3.4 Costs

For the improved construction lower material costs can be expected. The advantage of the smallest weight of the anchor plate of the improved realization is a bit compensated by the installation costs of the needed additional reinforcement.

3.3 Connection of a balcony construction on an insulated exterior reinforced concrete wall as simple connection

3.3.1 General

3.3.1.1 Depiction of the situation

Continuous, 3.00 m wide balconies are connected to a thermally insulated reinforced concrete wall, supported at their outer edge at a distance of 6.50 m (see Fig. 3.17). The walk-in area is realized as a 14 cm thick precast concrete slab with surrounding up stand. Paving slabs laid in a gravel bed are laid on top. The load-bearing reinforced concrete plates are supported at their ends and arranged parallel to steel girders of 6,50 meters length. These are connected to interception beams running perpendicular to the wall plane and which are connected to the external wall and the steel columns. Embedded anchor plates are used to fasten the steel girders on the concrete wall. Due to the 22 cm thick thermal insulation composite system of the buildings external wall a joint eccentricity of 30 cm between steel beam and anchor plate has to be considered. Within the insulation, a thermal separation is provided. In order to fulfil the plastering practical and professionally, the intersection of the plaster layer should be done only by simple steel plate. All weathered external components must be galvanized.

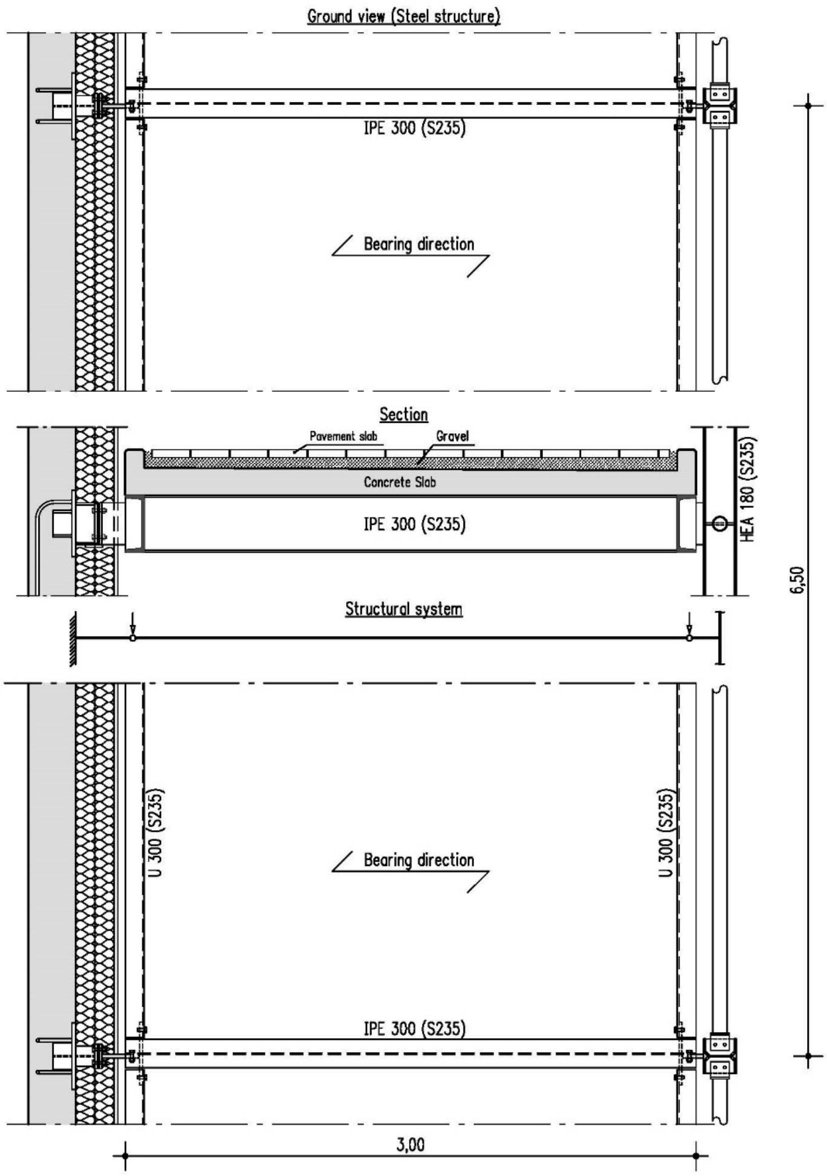

Fig. 3.17: Conventional solution and structural system

3.3.1.2 Overall structural system

Precast concrete slab:
Single span slab L = 3,00 m (uniaxial load transfer) with uniformly distributed load
Ceiling beams:
Single span beams L = 6,50 m with uniformly distributed loading
Interception beams:
Single span beams L = 3,00 m (connection eccentricity to the steel column and the anchor plate); single loads F close to the supports (see figure))
Connection adapter anchor plate to interception beam:
Cantilevers L = 0,30 m

3.3.1.3 Loads

Dead load beam construction	g1	=	0,40 kN/m²
Dead load flooring (gravel and paving slabs)	g2	=	2,00 kN/m²
Dead load precast concrete slab	g3	=	3,50 kN/m²
Dead load (total)	**g**	**=**	**5,90 kN/m²**
Live load	**q**	**=**	**4,00 kN/m²**

3.3.1.4 Joint loads

Dead load	$F_{g,k}$ = 5,90 kN/m² * 3,00 m / 2 * 6,50 m	=	57,53 kN
Dead load	$F_{q,k}$ = 4,00 kN/m² * 3,00 m / 2 * 6,50 m	=	39,00 kN
Design load	F_{Ed} = 1,35 * 57,53 + 1,50 * 39,00	=	**136,17 kN**

3.3.2 Execution options

3.3.2.1 Previous realization

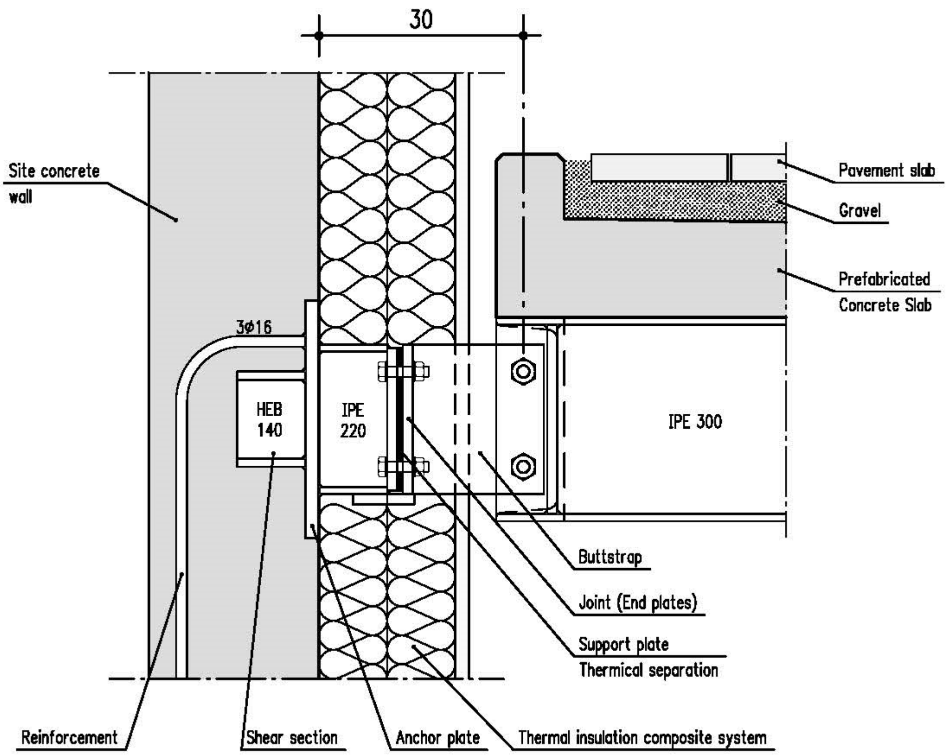

Fig. 3.18: Conventional joint solution of the balcony construction

The conventional joint solution consists of two parts with an end plate connection, where the inner part made of a rolled profile segment (IPE 220) is welded directly to the anchor plate. At the other end of the profile, a welded end plate for a rigid joint to the end plate of the outer connector part is located. This outer part consists of a vertical butt strap for a hinged connection to the web of the interception beam. A compression-proof bearing plate for the thermal separation of the two parts will be placed between the two end plates. Depending on the type and thickness of the separating layer a projecting plate to transfer the shear force without bolts in bending must be welded under the connectors' internal part. The weathered external adapter segment is galvanized. As just the inner part to the anchor plate is welded only coating is planned.

The concrete-casted part of the joint consists of an anchor plate with welded reinforcement and a welded on rolled section. The centrally arranged steel profile is designed to carry the vertical shear force. The location of the load resultant can be assumed approximately in the middle of the shear section. Bending moments caused by outer eccentricity (30 cm) and inner eccentricity (outer edge of the anchor plate up to the mid of the shear section) are taken by a couple of horizontal forces. The pressure force is transferred by contact, the tension force is taken by the welded on reinforcement bars. Due to the relatively low wall thickness, the tensile reinforcement is turned down with large bending roll diameter and overlapping with the vertical reinforcement layer of the walls inner side. The horizontal part of the diagonal, from the point of deflection to the anchor plate's lower pressure point leading strut is at equilibrium with the lower pressure force transferred by contact. The location and size of welded steel profiles have decisive influence on the stiffness of the anchor plate. As the end plate is stiffened by the welded steel profiles, pure bending has to be taken into consideration only in the external sections.

3.3.2.2 Improved realization

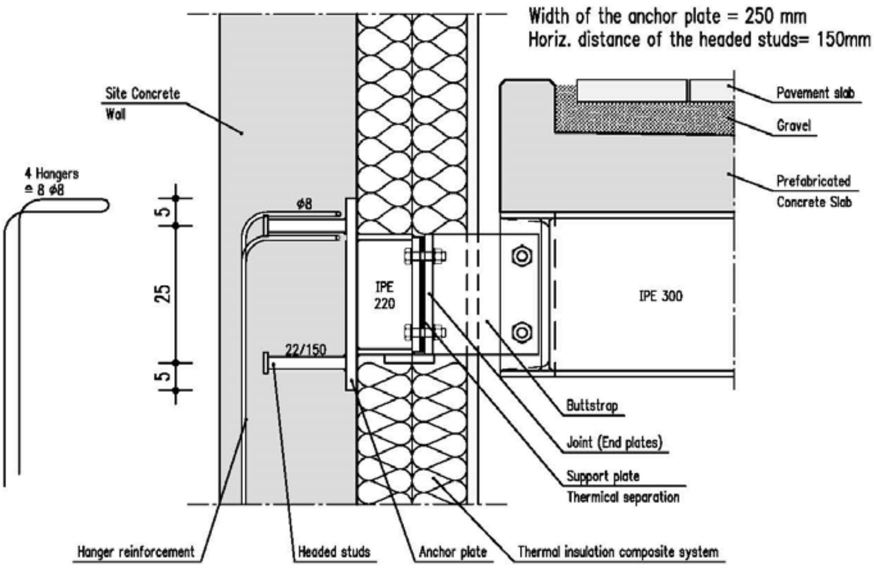

Fig. 3.19: Improved joint solution of the balcony construction

The steel connection of this version is identical to the previously described solution. The concrete-casted part consists of a 25 mm thick anchor plate with four headed studs 22/150 mm (see Fig. 3.9). Closed to the tensional loaded headed studs two reinforcing loops ø 8 mm are installed. A welding of reinforcement to the anchor plate is not required. The hanger reinforcement is placed next to the reinforcement at the inner side of the wall. The supplementary reinforcement has a large bending roll diameter and overlaps with the vertical reinforcement on the inside of the wall. All four studs are involved in the load transfer of the vertically acting shear force, where only the top couple of headed studs will also be used for carrying the horizontal tensile force resulting from the eccentricity moment. The "concrete cone failure mode" is positively influenced by the slope reinforcement arranged directly parallel to the headed studs. The anchor plate is also stiffened in this connection by the welded steel profile of the docking adapter. The structural design will be done by using the program "Rigid anchor plate with headed studs"(see Fig. 3.20 to Fig. 3.21).

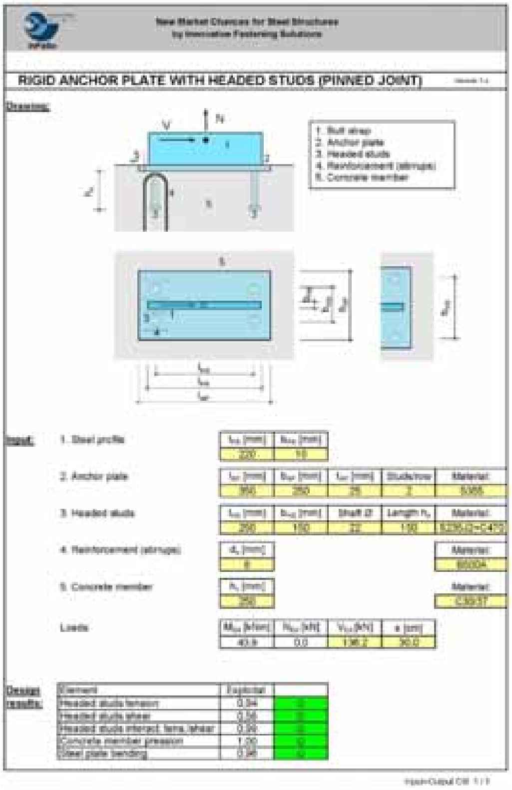

Fig. 3.20: Excel sheet, “Input+Output”-mask of the improved realization of the balcony construction

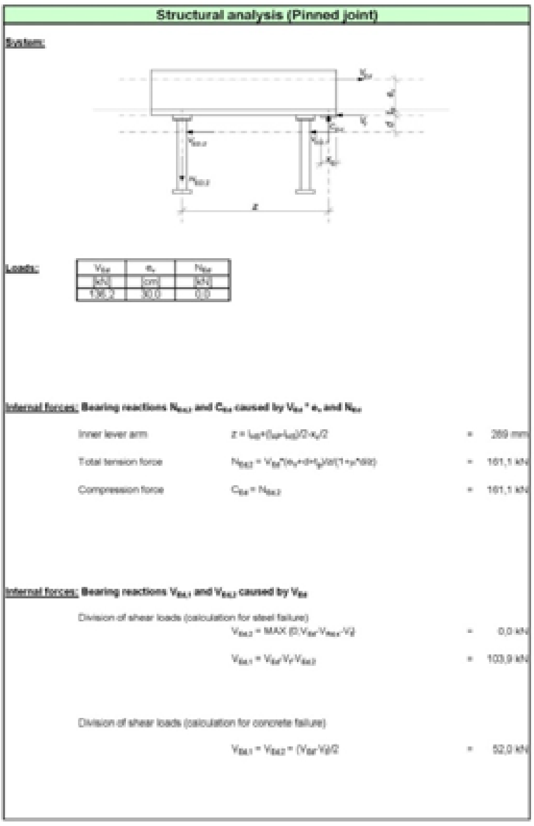

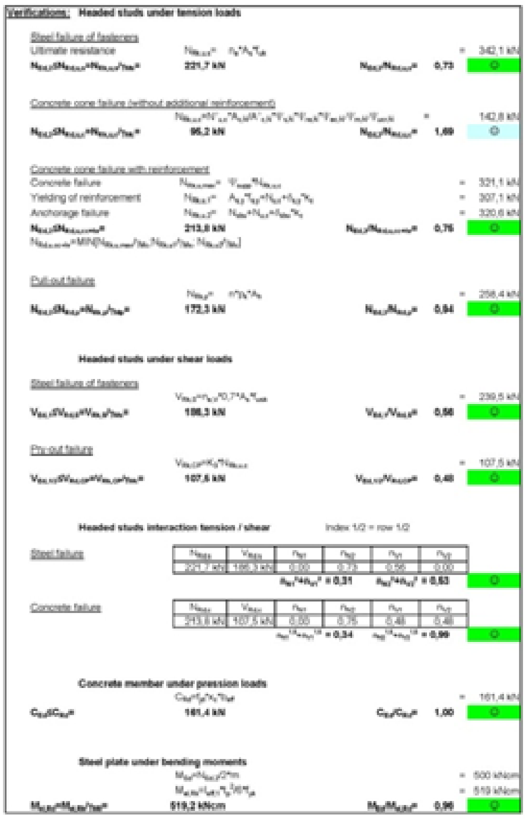

Fig. 3.21: Excel sheet, “Design output” of the improved realization of the balcony construction

3.3.3 Conducting and Assessment

3.3.3.1 Installation

In the improved realization the anchor plate can be installed easily because the relatively small headed studs have a minimal impact on the crosswise running external reinforcement layer of the concrete wall. The loop-shaped hanger reinforcement can be fixed first on the inner reinforcement layer. These must be adjusted yet after installing the anchor plate, if the distance to the headed studs is too large. Due to welded bars on shear connection in the previous realization and reinforcement the anchor plate is unhandy and the walls reinforcement and their order of installation have to be coordinated to the plate's anchors.

3.3.3.2 Tolerances

Deviations of the anchor plate's centre to the longitudinal axis of the docking adapter in horizontal and vertical direction inside the walls plane can easily be absorbed, because the adapter is welded to the anchor plate on-site. If tolerances in longitudinal direction of the adapter have to be taken, the port adapters have to be either manufactured extra-long to be cut to the appropriate size on-site or produced after measurement of the exact location of the anchor plates.

3.3.3.3 Fire protection

For the structure shown in this example, no requirements relating to fire protection have to be fulfilled. If the classification in a particular fire resistance class should be required in other cases, the steel structure including its connections shall be protected with approved coating systems or plate-shaped panels.

3.3.3.4 Costs

The cost advantage of the "improved realization" to the anchor plate with shear section and welded reinforcement mainly results by the simpler manufacturing and installation. The studs are fixed by drawn arc stud welding on the fitting steel plate. This process takes a very short time. Concerning the shear section variant, the steel and the rebar in their position must be fixed first and then circumferential welded by hand. This process takes considerably more time. The same applies also for the installation of the anchor plate, because the relatively large shear section and the welded reinforcement have influence on the assembly of the walls reinforcement and some reinforcing bars can be inserted only after the installation of the anchor plate.

4 Parameter studies

4.1 General

In this parameter studies the three steel-to-concrete connections of the Design Manual I "Design of steel-to-concrete joints" [13] are under examination (see Fig. 1.1). In the parameter study for concrete components in Chapter 4.2 experimentally determined pre-factors are taken into consideration. Their influence on the stiffness of the concrete component is shown. In Chapter 4.3 parameters for geometry and material are changed in order to show their influence on the load-deformation and moment rotational behavior of the simple steel-to-concrete joints. Changes in the thickness of the anchor plate and in steel grade for column bases are explained in Chapter 4.4 where especially this two parameters have a high influence on the structural behavior for this type of connection. Also recommendations for design values are given in this Chapter. In the last parameter study the focus is on composite joints in Chapter 4.5.

4.2 Parameter study on concrete components

4.2.1 General

As discussed in Chapter 3 on concrete components in the Design Manual I "Design of steel-to-concrete joints" [13], the stiffness of an anchorage group is determined by several parameters. Out of these parameters, certain parameters are known with high degree of confidence at the time of analysis such as dimensions of studs, dimensions of reinforcement and further parameters. Certain other parameters, such as concrete material properties, bond strength etc. are known within the statistical range of distribution normally occurring in practice. Certain parameters are used to define the stiffness and are based on empirical studies, which are not known with a high certainty. In this chapter, the sensitivity of the stiffness values towards different parameters has been investigated.

4.2.2 Example considered

A basic example of a single headed stud with supplementary reinforcement subjected to tensile loads is considered in this parameter study. The stud is considered to be far from the edges. All the components are considered while evaluating the stiffness of the anchor. The variation of secant stiffness as a function of anchor displacement is evaluated and plotted. Though the plots are given in terms of absolute values for the anchor stiffness and displacement, the objective of this study is to relatively compare the stiffness variation and verify, principally, the influence of different parameters.

4.2.3 Parameter studied and methodology followed

The stiffness of the anchorage system as a function of anchor displacement was evaluated using the formulations given in Chapter 3 of the Design Manual I "Design of steel-to-concrete joints" [13] and a parameter study was performed to investigate the influence of various parameters on the stiffness of the system. While evaluating the influence of a given parameter, all other parameters were kept constant. These parameters are considered as independent and uncorrelated for this study. The parameters considered for the parameter study along with the range of study are tabulated in Tab. 4.1. This assumption of no correlation between the parameters is valid for all the parameters except the concrete compressive strength and the bond strength between concrete and reinforcement. Therefore, for these two parameters, the dependence of bond strength on concrete compressive strength is considered in this study. As can be seen from Tab. 4.1, a sufficiently wide range is considered for the parameter studies.

Tab. 4.1: Parameters considered for the parameter study

Parameter	Symbol	Units	Recommended value in DM	Range of study
Concrete Strength	f_{ck}	N/mm² (MPa)	-	25 – 65
Factor for concrete breakout in tension	α_c	-	- 537	250 – 1000 (negative)
Embedment depth	h_{ef}	mm	-	50 – 400
Shoulder width	a	mm	-	0.25 – 4.0
Pressing relation	m	-	9	7 – 12
Design bond strength	f_{bd}	N/mm² (MPa)	-	0 – 5
Diameter of supplementary reinforcement	$d_{s,re}$	mm	-	6 – 20
Descending anchor stiffness for component P	$k_{p,de}$	N/mm	-10000	5000 – 20000 (negative)

4.2.4 Sensitivity to Concrete Strength, f_{ck}

The concrete strength influences the concrete cone failure and the pull out failure. The influence of concrete strength, f_{ck} is studied for the cases if supplementary reinforcement is considered or not. In case of plain concrete (no supplementary reinforcement), the concrete strength governs the failure load corresponding to concrete cone failure through Eq. (4.1):

$$N^0_{Rk,c} = k_1 \cdot h_{ef}^{1.5} \cdot f_{ck}^{0.5} \; [N] \qquad (4.1)$$

The stiffness of the ascending branch of the load-deflection curve is considered as infinite and the failure load is assumed to occur at zero displacement. After the peak load is reached, a linearly degrading softening branch is considered. The concrete strength, f_{ck}, governs the stiffness of this descending branch, $k_{c,de}$ through Eq. (4.2) for a single anchor far from edge influences.

$$k_{c,de} = \alpha_c \cdot [f_{ck} \cdot h_{ef}]^{0,5} \; [N/mm] \qquad (4.2)$$

No particular value of f_{ck} is recommended in the design manual. Considering the concrete class in normal strength range, in this study, the sensitivity of stiffness to concrete strength is evaluated for cylindrical concrete strength, f_{ck} within the range of 25 MPa to 65 MPa. Fig. 4.1 shows the influence of concrete strength on the stiffness of the anchorage system in concrete without supplementary reinforcement as a function of displacement. It may be noted that the secant stiffness plotted in Fig. 4.1 is the overall stiffness of the system considering all components and not only the concrete cone component.

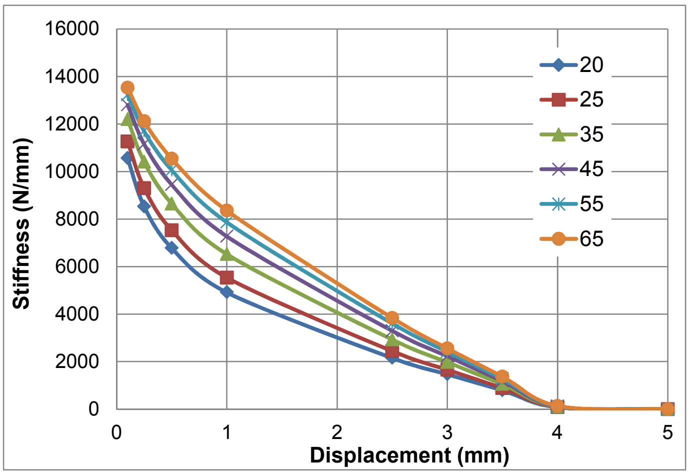

Fig. 4.1: Influence of Concrete Strength f_{ck} on stiffness of anchorage without supplementary reinforcement

The secant stiffness gradually reduces with increasing displacement. As expected, a clear but reasonable sensitivity is obtained to concrete strength. At higher displacements, the band of stiffness values gets narrower. For the given range of concrete strength that can be expected in practice from the same concrete mix, the sensitivity to concrete strength can be considered through material safety factor. Therefore, the sensitivity of stiffness on concrete strength can be reasonably considered in the analysis. In case of anchorage with supplementary reinforcement, the ascending stiffness of the component stirrups in tension depends on the concrete strength through Eq. (4.3) up to the failure load:

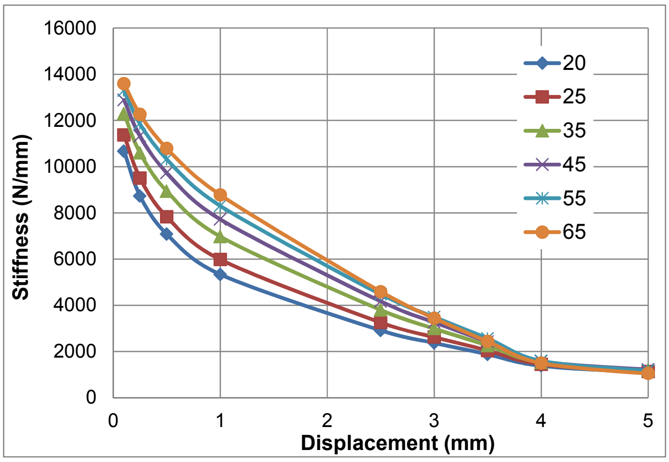

Fig. 4.2: Influence of Concrete Strength, f_{ck} on stiffness of anchorage with supplementary reinforcement

$$k_{re} = \frac{\sqrt{n_{re}^2 \cdot \alpha_s \cdot f_{ck} \cdot d_{re}^4}}{\sqrt{2\delta}} \; [\mathrm{N/mm}] \tag{4.3}$$

Thus, the stiffness of both concrete component and the stirrup component are dependent on concrete strength, f_{ck}. Fig. 4.2 shows the influence of concrete strength on the stiffness of anchorage system with supplementary reinforcement. Again, a similar shaped curve as that obtained for anchorage in plain concrete is obtained. The secant stiffness gradually reduces with increasing displacement and at higher displacements the band of stiffness values gets narrower. Based on the results of calculations, it can be said that the sensitivity of the evaluated stiffness of the anchorage to the concrete compressive strength is reasonable. For the given range of concrete strength that can be expected in practice from the same concrete mix, the sensitivity to concrete strength can be considered through material safety factor. Therefore, the sensitivity of stiffness on concrete strength can be reasonably considered in the analysis.

4.2.5 Sensitivity to parameter α_c

The parameter, α_c, is used to determine the stiffness of the linear descending branch in case of concrete breakout in tension (see Eq. (4.2)). Currently, a value of -537 is assigned to the factor α_c. In this study, the influence of variation of this parameter on the secant stiffness of the anchor is considered for α_c in the range of -250 to -1000. The influence of the factor α_c on stiffness of the anchorage is displayed in Fig. 4.3. During initial displacement range, the secant stiffness is almost independent of α_c. This is because the stiffness during initial displacements is governed by components other than component C and the factor α_c governs only the descending stiffness of the component C.

However, at higher displacements, the descending stiffness of the concrete breakout in tension becomes dominating and as seen in Fig. 4.3, the stiffness of the anchorage system becomes sensitive to the parameter α_c. The sensitivity is highest in the range of displacements between 2 to 4 mm. On further increasing of the displacements, the stiffness of the system again becomes less sensitive to the parameter a_c (Fig. 4.3). This is because after certain value of displacement equal to the concrete cone failure load, $N_{Rk,c}$ divided by descending stiffness, $k_{c,de}$, the component C does not contribute anymore to the anchorage. However, the stiffness variation in the middle range of displacements (2 – 4 mm) is not very high and can be considered through material safety factors.

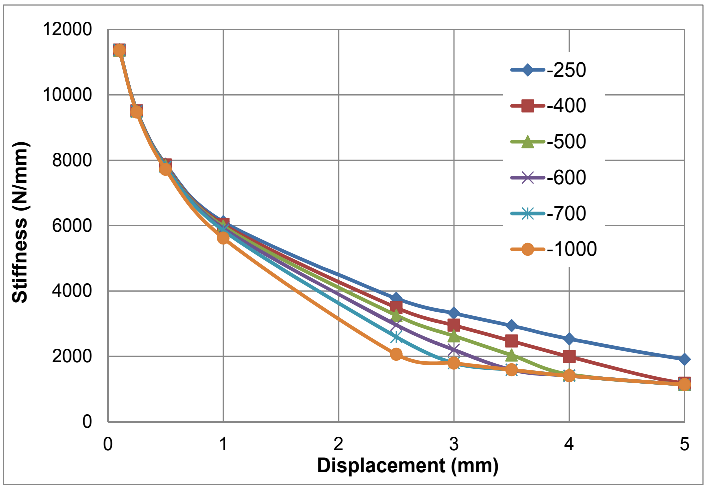

Fig. 4.3: Influence of parameter, α_c on stiffness of anchorage

4.2.6 Sensitivity to effective embedment depth h_{ef}

For concrete component (component C), the effective embedment depth, h_{ef}, is the most important factor, which significantly affects the peak failure load (see Eq. (4.1)) as well as the stiffness (see Eq. (4.2)) of the anchorage system. Further, the effective embedment depth also influences the component RB (bond failure of the stirrups) since the effective bond length, l_1 of the stirrups is dependent on h_{ef} (see Fig. 4.4). The failure load corresponding to the bond failure of stirrups is given as

$$N_{Rd,b,re} = \sum_{n_{s,re}} \left(\frac{l_1 \cdot \pi \cdot d_{s,re} \cdot f_{bd}}{\alpha} \right) \text{ [N]} \tag{4.4}$$

There is no recommended value of h_{ef} given in the design manual, however considering the most used sizes in practice, in this study, a range of h_{ef} from 50 mm to 400 mm is considered. As expected, the stiffness of the anchorage system is strongly influenced by the effective embedment depth, h_{ef} for low displacement levels (see Fig. 4.5).

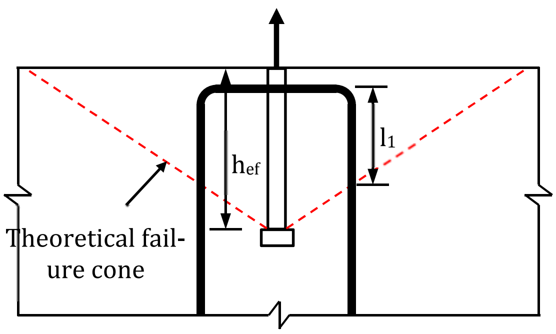

Fig. 4.4: Definition of effective bond length, l_1 of stirrups and its dependence on the effective embedment depth, h_{ef}

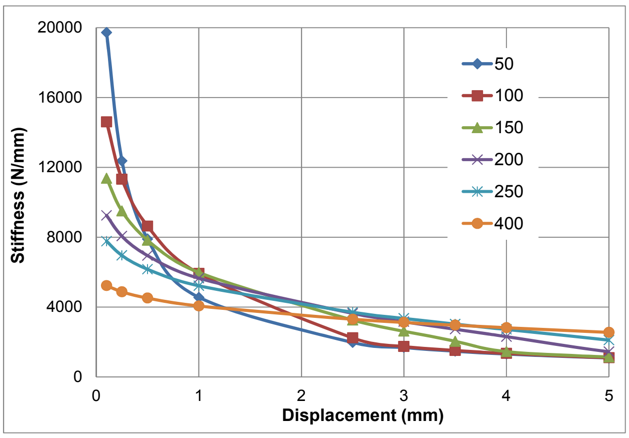

Fig. 4.5: Influence of effective embedment depth, h_{ef} on stiffness of anchorage

However, as the displacement level increases and concrete cone breakout occurs and the influence of h_{ef} reduces. Nevertheless, in reality, the effective embedment depth of the headed stud is known a priori almost accurately and therefore, the stiffness can also be estimated with reasonable confidence.

4.2.7 Sensitivity to shoulder with a

The shoulder width of the headed stud given as "a = 0.5(d_h – d_s)", where d_h is the head diameter and d_s is the shaft diameter, is an important parameter influencing the stiffness of the anchorage. The stud dimensions and hence the shoulder width is normally well known at the time of the analysis. As the bearing area of the headed stud is proportional to the square of the shoulder width, this factor dominates the stiffness of the component P. The load-deflection response for the component P is given by Eq. (4.5) up to the point of failure load corresponding to concrete cone failure and Eq. (4.6) beyond that:

$$\delta_{Rd,p,1} = k_p \cdot \left(\frac{N_{Rd,c}}{A_h \cdot f_{ck} \cdot n_{re}}\right)^2 \text{ [mm]} \tag{4.5}$$

$$\delta_{Rd,p,2} = 2k_p \cdot \left(\frac{N_{Rd,p}}{A_h \cdot f_{ck} \cdot n_{re}}\right)^2 - \delta_{Rd,p,1} \text{ [mm]} \tag{4.6}$$

In expressions (4.5) and (4.6), the shoulder width appears indirectly in the bearing area of the head, A_h as well as through the factor k_p. The factor k_p is given by Eq. (4.7).

$$k_p = \alpha_p \cdot \frac{k_a \cdot k_A}{k_2} \text{ [–]} \tag{4.7}$$

In Eq. (4.7), the shoulder width appears indirectly in the expression for k_a (see Eq. (4.8)) and k_A (see Eq. (4.9)).

$$k_a = \sqrt{5/a} \geq 1 \tag{4.8}$$

$$k_A = 0{,}5 \cdot \sqrt{d^2 + m \cdot (d_h^2 - d_s{}^2)} - 0{,}5 \cdot d_h \tag{4.9}$$

Thus, based on Eq. (4.5) through Eq. (4.9), a significant dependence of the component P on the parameter, a, should be expected. No value of the shoulder width is recommended in the design manual, however, considering the normal range of shoulder widths that may be encountered in practice, in this study, the shoulder width is varied between 0.25 mm to 4.0 mm. Fig. 4.6 summarizes the influence of shoulder width on the stiffness of anchorage. As expected, a very high sensitivity of the secant stiffness is obtained on the shoulder width, a, especially at lower displacements. However, since the bolt dimensions are known with quite high accuracy while performing the analysis, the estimated stiffness values are not expected to vary significantly from its real value due to shoulder width.

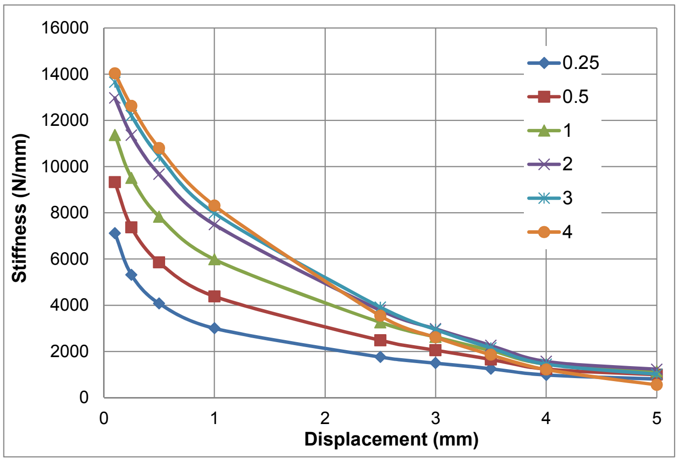

Fig. 4.6: Influence of shoulder width, a, on stiffness of anchorage

4.2.8 Sensitivity to pressing relation m

Pressing relation, m, appears in the equation for evaluating stiffness for component 'P' (see Eq. (4.9)). The value of this factor may not be known exactly and a value of '9' is currently recommended in the design manual. The parameter variation from in the range of 7 to 12 displays little sensitivity of stiffness on this parameter (see Fig. 4.7). Therefore, a value of 9 is reasonable.

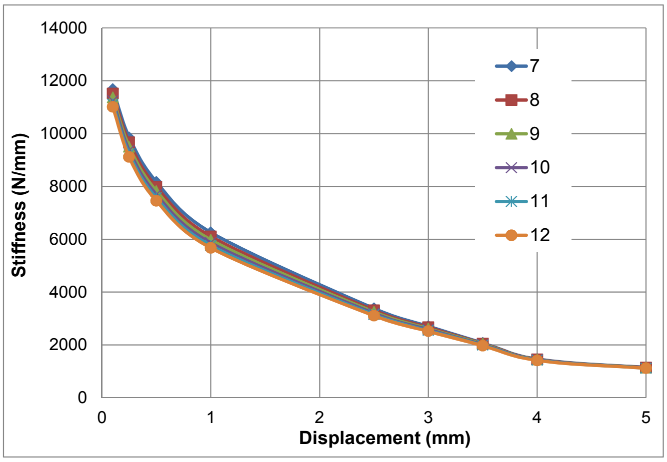

Fig. 4.7: Influence of pressing relation, m on stiffness of anchorage

4.2.9 Sensitivity to design bond strength f_{bd}

For the case of anchorage with supplementary reinforcement, the design bond strength of stirrups, f_{bd} influences the stiffness of the anchorage system. The failure load for the reinforcement due to bond is given by Eq. (4.4). The value of the design bond strength is directly dependent on the concrete strength, f_{ck}. No particular value of the design bond strength is recommended in the design manual. For the grades of concrete considered in this study (f_{ck} = 25 – 65 MPa), the typical value of the design bond strength may vary approximately between 2 to 5 MPa. In this work, the influence of the design bond strength on the stiffness is evaluated for a range of 0 to 5 MPa. It is observed that the stiffness of the anchorage is not affected by the bond strength at low displacements as shown in Fig. 4.8. Though at higher displacement levels, the estimated stiffness value depends on the f_{bd} value, the variation is within reasonable range that can be accounted for through material safety factor.

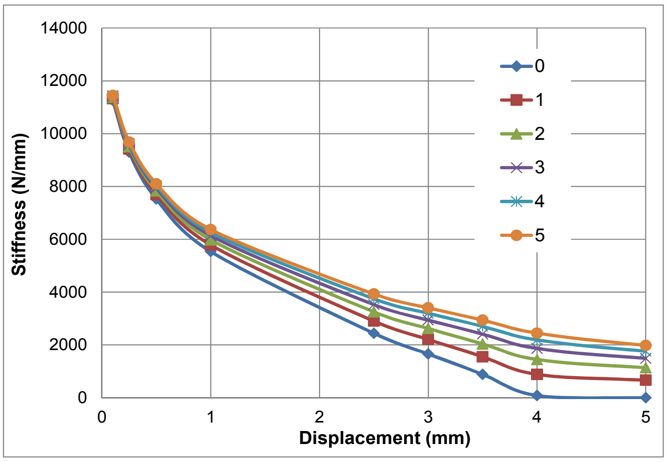

Fig. 4.8: Influence of design bond strength, f_{bd} on stiffness of anchorage

4.2.10 Sensitivity to diameter of supplementary reinforcement $d_{s,re}$

The diameter of supplementary reinforcement, $d_{s,re}$ influences the components RS and RB. The failure load corresponding to bond failure of stirrups is given by Eq. (4.4), while the failure load corresponding to the yielding of stirrups in tension is given by Eq. (4.10).

$$N_{Rd,s,re} = A_{s,re} \cdot f_{yd,re} = n_{re} \cdot \pi \cdot \left(\frac{d_{s,re}^2}{4}\right) \cdot f_{yd,re} \text{ [N]} \quad (4.10)$$

The load-displacement relationship of the anchorage corresponding to the failure of supplementary reinforcement is given by Eq. (4.11).

$$\delta_{Rd,s,re} = \frac{2N_{Rd,re}^2}{\alpha_s \cdot f_{ck} \cdot d_{s,nom}^4 \cdot n_{re}^2} \text{ [mm]} \quad (4.11)$$

In Eq. (4.11), $N_{Rd,re}$ is equal to the minimum of $N_{Rd,b,re}$ and $N_{Rd,s,re}$ (minimum of steel failure and bond failure load of supplementary reinforcement). No particular value of the diameter is recommended for stirrups in the design manual. Considering the normal range of diameters used in practice, the results of the parametric study performed on the anchorage by varying the stirrup diameter in the range of 6 mm to 20 mm are displayed in Fig. 4.9. It can be observed that the stiffness of the anchorage is insensitive to the diameter of supplementary reinforcement at low displacement levels but the variation slightly increases at higher displacement levels. Nevertheless, the diameter of the stirrups is also generally known with good accuracy and therefore the stiffness of the anchorage system can be reasonably accurately estimated.

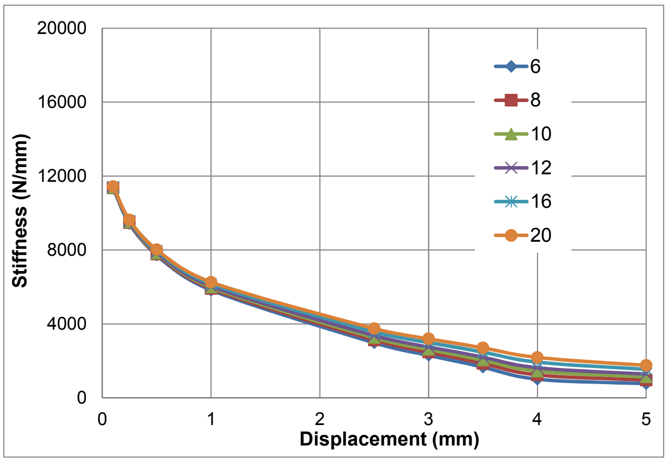

Fig. 4.9: Influence of diameter of supplementary reinforcement, $d_{s,re}$ on stiffness of anchorage

4.2.11 Sensitivity to descending anchor stiffness due to concrete, $k_{p,de}$

The stiffness of the descending branch, $k_{p,de}$ in case of pullout failure of the stud (component P) depends on the failure mode. If the supplementary reinforcement fails by yielding ($N_{Rd,s,re} < N_{Rd,p}$) the recommended value of $k_{p,de}$ is -10^4 N/mm² (negative due to descending branch). In this parametric study, the value of $k_{p,de}$ is varied between -5000 to -20,000 N/mm². As shown in Fig. 4.10, the stiffness of the anchorage system is insensitive to this parameter and therefore the value of -10000 can be used with sufficient accuracy.

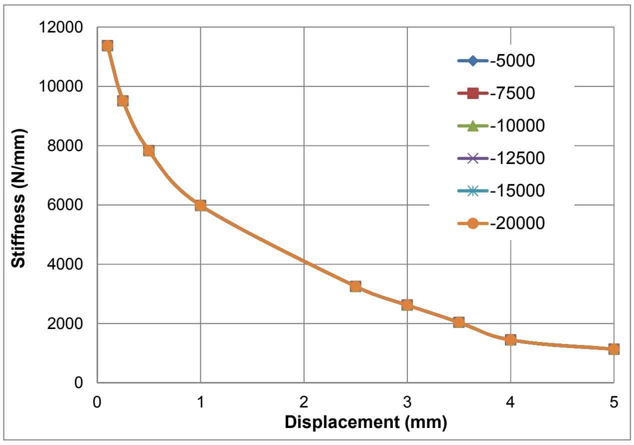

Fig. 4.10: Influence of descending anchor stiffness due to concrete, $k_{c,de}$ on stiffness of anchorage

4.2.12 Summary of sensitivity of anchorage stiffness to various parameters

In this study, the sensitivity of the stiffness of an anchorage with supplementary reinforcement towards different parameters is investigated. Table 5.2.2 summarizes the statistical information on the sensitivity to various parameters studied in this chapter. The table gives the values of secant stiffness (kN/mm) corresponding to peak load obtained for various values of parameters governing the stiffness of anchorage system. The values of the stiffness are first arranged in an ascending order in the table followed by the mean and coefficient of variation.

The stiffness of the anchorage is found to be most sensitive to the shoulder width 'a', followed by the embedment depth, 'h_{ef}'. However, both these parameters are known quite accurately during design, therefore the stiffness can be reasonably accurately determined. The next biggest variation comes through the concrete strength with a reasonable coefficient of variation of 20%. For the given range of concrete strength that can be expected in practice from the same concrete mix, the sensitivity to concrete strength can be considered through material safety factor. The stiffness is sensitive to the parameter, α_c only in the mid-range of displacement (see Figure 5.2.3), while the initial stiffness and the stiffness at large displacements are practically independent of this parameter. The variation in stiffness due to α_c can also be considered through material safety factor. The stiffness is found to be practically insensitive to other parameters listed in Tab. 4.2.

Tab. 4.2: Statistical information on parameter study

	f_{ck}	**a**	**$k_{p,de}$**	**m**	**α_c**	**f_{bd}**	**h_{ef}**	**$d_{s,re}$**
Min	3,29	1,49	3,3	3,48	2,88	3,5	4,5	3,3
	3,704	2,29	3,3	3,38	3,01	3,4	4	3,3
	3,96	3,29	3,3	3,3	3,3	3,3	3,3	3,3
	4,64	4,21	3,3	3,22	3,54	3,2	2,87	3,3
	4,95	5,1	3,3	3,15	3,78	3,1	2,56	3,2
Max	5,66	5,32	3,3	3,1	4,29	3,06	2	3,1
Mean	**4,367**	**3,617**	**3,300**	**3,272**	**3,467**	**3,260**	**3,205**	**3,250**
Stabw	**0,878**	**1,539**	**0,000**	**0,143**	**0,522**	**0,172**	**0,927**	**0,084**
Var Koeff	**20%**	**43%**	**0%**	**4%**	**15%**	**5%**	**29%**	**3%**

4.3 Parameter study on simple steel-to-concrete joints

4.3.1 General

The following parameter study is carried out in order to describe the influence by varying different input factors of the simple joint. With the variation of different parameters the load bearing capacity and the rotational stiffness of the whole joint can be influenced to a high extend. The optimization of the simple joint will be aimed to achieve on one hand maximum strength with minimum costs and on the other hand a ductile behaviour of the whole joint. For the concrete component ductility exists if the load can be transferred at the cracked level to other components such as stirrups, as a certain amount of deformation occurs at the maximum level of load. Furthermore the parameter study will demonstrate a range of validity and will point out the possible increase in loading of the joint by changing different parameters.

4.3.2 Validation of the model

Within the INFASO project a design approach based on the component method has been developed for the simple steel-to-concrete joints [12]. Thereby the joint is subdivided into its different components and the deformations can be calculated as each of the component is represented by a spring. The calculation of the load carrying capacity mainly consists of the following procedure:

1. Evaluation of the decisive tension component.
2. Verification of the influence of the compression zone on the tension component.
3. Calculation of the shear resistance of the joint out of the moment equilibrium, see Fig. 4.11.
4. Verification of interaction conditions.

In the Design Manual I "Design of steel-to-concrete joints" [13] this approach is described in more detail based on a flowchart and a worked example. In order to determine the moment-rotation curve of the joint, the deformation of the single components have to be calculated. Therefore load-deformation curves of the single steel and concrete components have been developed. A parameter study on the concrete components and a detailed investigation on the unknown factors of the concrete components can be found in the previous chapter. Fig. 4.11 shows the mechanical model and a simplified joint model if the tensional and the compression components are assembled in one spring.

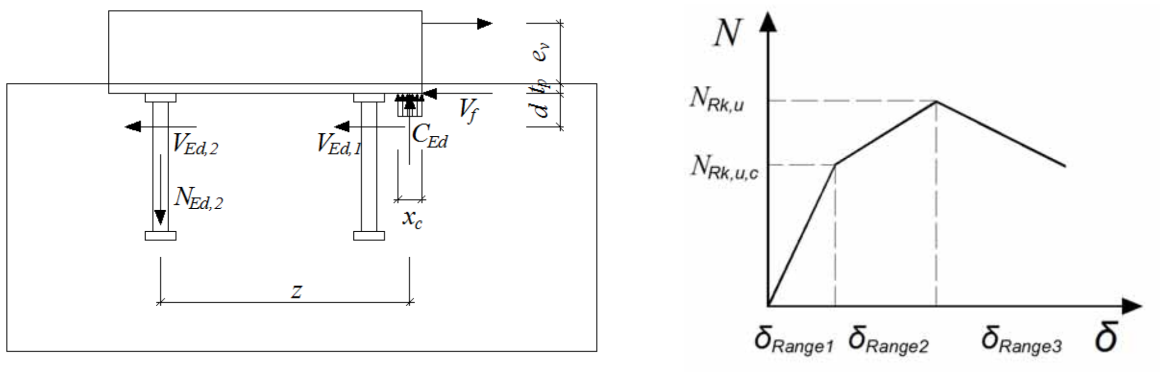

Fig. 4.11: Analytic model of the simple steel-to-concrete joint (left), load-deformation of the tensional component if supplementary reinforcement can be activated in best case (right)

The deformation of the tensional component can be determined in three ranges (see Fig. 4.11). In the first range the deformations can be calculated according to [12] with Eq. (4.12). For this the deformation due to pull-out failure (see Eq. (4.5)) and the deformation due to elongation of the shaft of the headed stud are added.

$$\delta_{\text{Range1}} = \delta_{\text{Rk,p,1}} + \delta_{\text{Rk,s1}} \tag{4.12}$$

With:

$\delta_{\text{Rd,p,1}}$ Deformation due to pull-out failure;

$\delta_{\text{Rd,s1}}$ Deformation due to yielding of the headed stud.

At the end of the first range first cracks might develop from the head of the headed stud into the direction of the concrete surface. If the load carrying capacity at concrete cone failure is reached, the supplementary reinforcement can be activated. In this case the deformations can be calculated up to the ultimate load with Eq. (4.13).

$$\delta_{Range2} = \delta_{Rk,p,2} + \delta_{Rk,s1} + \delta_{Rk,re} \tag{4.13}$$

With:

$\delta_{Rk,p,1}$ Deformation due to pull-out failure;
$\delta_{Rk,s1}$ Deformation due to yielding of the headed stud;
$\delta_{Rk,re}$ Deformation of the supplementary reinforcement in interaction with concrete cone failure.

The deformations in the third range depend on the failure mode of the ultimate load. If yielding of the supplementary reinforcement occurs, a ductile behaviour can be observed in the third range. The deformations in the third range can be calculated with Eq. (4.14).

$$\delta_{Range3} = \delta_{Range2}\left(N_{Rk,re}\right) + \frac{N - N_{Rk,re}}{k_{c,de}} + k \tag{4.14}$$

With:

$k_{c,de}$	Stiffness of the descending branch see Eq. (4.2);
$k = \frac{N_u - N}{10000}$	If yielding of the supplementary reinforcement occurs;
$k = 0$	If the failure mode concrete failure and anchorage failure of the stirrups occurs;
$N_{Rk,re}$	Characteristic load carrying capacity of the supplementary reinforcement in interaction with concrete cone failure;
N_u	Ultimate load carrying capacity.

It has to be considered, that the supplementary reinforcement can only be activated in the optimum case. As the failure modes like, pull-out failure of the headed studs, concrete cone failure between the supplementary reinforcement and steel failure of the headed stud can also occur, scenario distinctions have to be made in all ranges. Within the following parameter study this issue will be highlighted and explained. The rotation of the joint can be determined with Eq. (4.15) according to the spring model of Fig. 4.12.

$$\Phi_j = \frac{\delta_t - \delta_c}{z} \tag{4.15}$$

With:

δ_t Deformation of the tensional component;
δ_c Deformation of the compression component according to Design Manual I "Design of steel-to-concrete joints" [13] Eq. (3.75).

For the calculation of the full moment-rotation curve of the joint the interaction conditions for steel failure (see Eq. (4.16)) and for concrete failure (see Eq. (4.17)) have to be considered as tension forces and shear forces are acting simultaneously on the simple steel-to-concrete joint.

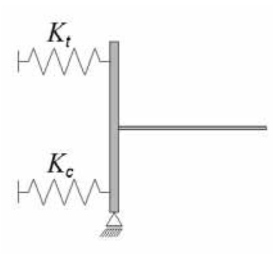

Fig. 4.12: Spring model

Steel failure
$$\left(\frac{N}{N_{Rk,u,s}}\right)^2 + \left(\frac{V}{V_{Rk,u,s}}\right)^2 \leq 1 \tag{4.16}$$

Concrete failure
$$\left(\frac{N}{N_{Rk,u}}\right)^{3/2} + \left(\frac{V}{V_{Rk,cp}}\right)^{3/2} \leq 1 \tag{4.17}$$

With:

$N_{Rk,u,s}/V_{Rk,u,s}$ Characteristic load carrying capacity due to steel-failure of the headed stud;
$N_{Rk,u}/V_{Rk,cp}$ Characteristic load carrying capacity due to concrete failure modes.

In Fig. 4.13 the validation of the model is shown for the different test specimens [12]. In this figures the moment-rotation curves are compared with the calculated curves according to the developed mechanical joint model. It can be seen, that the model curves fit well to the test curves.

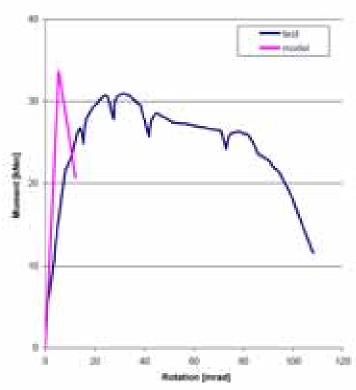

Moment-rotation-curve for test B1-BS

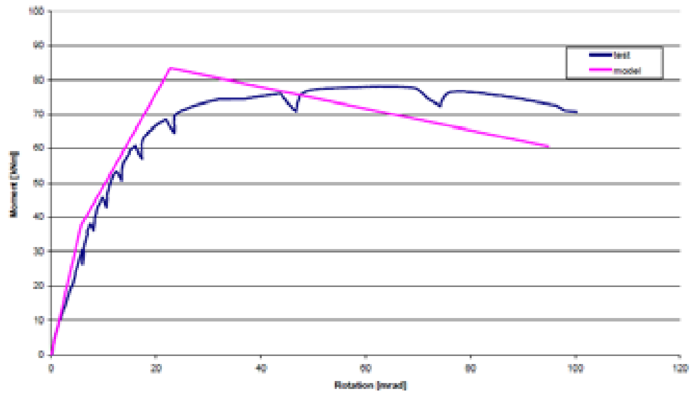

Moment-rotation-curve for test B1-B-R

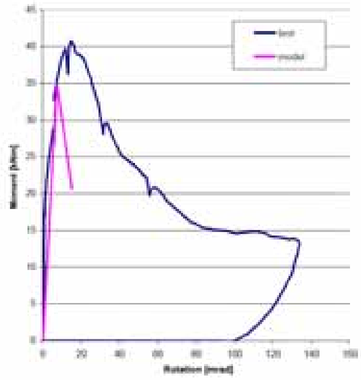

Moment-rotation-curve for test R1-C

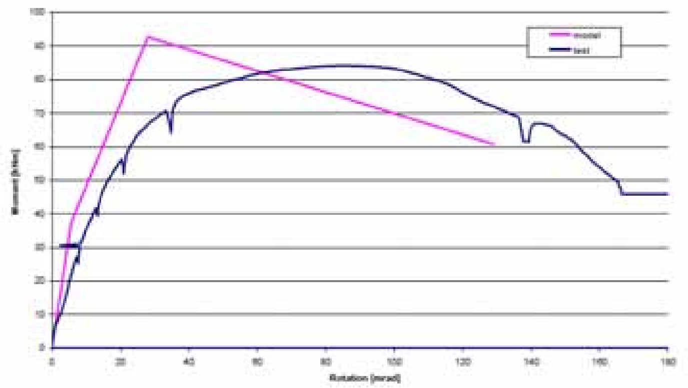

Moment-rotation-curve for test B2-C-R

Fig. 4.13: Validation of the INFASO model without supplementary reinforcement (left), with supplementary reinforcement (right)

Within the first section the moment-rotational behaviour of the joint is described up to concrete cone failure. Test specimens without additional reinforcement reach their ultimate resistance up to this point. If additional reinforcement is placed next to the stirrups, the load carrying capacity of the tensional component can be increased (see 2nd range for B1-B-R and B2-C-R in Fig. 4.13). In these cases the additional reinforcement is activated and the ultimate load can be increased. In the following parameter study configurations will be shown, where the supplementary reinforcement can be activated and a ductile failure mode can be obtained.

4.3.3 **Sensitivity study of major parameters**

4.3.3.1 General

Based on the worked example on simple joints of Design Manual I "Design of steel-to-concrete joints" [13] the different parameters were defined and varied in particular in the following. The worked example is used thereby as reference version. Safety factors weren`t considered in this parameter study. Furthermore the absolute terms in the equations for pull-out failure and concrete cone failure were assumed as 12 and 15.5 to reproduce the real load-carrying capacity. Values for application may be taken from the relevant European Technical Specification of the specific headed studs.

4.3.3.2 Overview of the major parameters

The load-carrying capacity and the rotational stiffness depends on different parameters and boundary conditions. The examined parameters are listed in Table 4.1.

Tab. 4.3: Overview of the examined parameters and their influence on the model

Parameter	Influence	Remarks and brief description	Chapter
Effective height	++	Influences the ultimate load carrying capacity as well as the load carrying capacity of the concrete cone failure $N_{Rk,c}$	4.3.3.3
Eccentricity	++	Can have high influence on the moment resistance of the joint within high utilization factors of the interaction equations	4.3.3.5
Diameter headed studs	+++	High influence on the ductility of the joint.	4.3.3.3
Diameter stirrups	++	Diameter of the stirrups can increase the overall load-carrying capacity	4.3.3.6
Number of stirrups	++	If the number of stirrups is increases brittle failure modes can be avoided.	4.3.3.6
Concrete strength	+++	Concrete strength has influence on all concrete components	4.3.3.7

4.3.3.3 Effective height

The effective height (see Fig. 4.4) can either be varied by changing the thickness of the anchor plate, the overall length of the headed stud or the head height of the anchor. In this study only the anchor length has been modified as this factor has the biggest influence on the final result, see Tab. 4.4.

Tab. 4.4: Analyzed effective heights

Parameter	Case 1	Case 2	Reference version	Case 3	Case 4
Anchor length [mm]	50	100	150	200	250
Effective height [mm]	65	115	165	215	265

Fig. 4.14 shows the load-displacement curve of the tensile component. The desired behaviour of the simple joint can be monitored, if an effective height of 165 mm is used. By selecting this effective height all three sections δ_{Range1}, δ_{Range2} and δ_{Range3} in Fig. 4.14 are clearly evident. By the end of the first section δ_{Range1} the ultimate load of the concrete cone failure without considering supplementary reinforcement $N_{Rk,c}$ = 190 kN is reached for the reference version (see Tab. 4.4). By further increase of the load, the hanger reinforcement is activated and the smallest resistance of steel yielding of the stirrups $N_{Rk,re,1}$, anchorage failure of the stirrups $N_{Rk,re,2}$ or the small concrete cone failure $N_{Rk,cs}$ can be decisive. In the third range δ_{Range3} the inclination of the load-displacement-curve depends whether brittle failure modes like concrete cone failure or anchorage failure or steel failure becomes crucial. According to Fig. 4.14 ductile behaviour occurs if longer headed studs are used. The headed stud is yielding before other failure modes can be recognized. Fig. 4.14 indicates that the selection of longer headed studs does not increase the load carrying capacity of the tensional component of the joint. In this cases steel failure of the headed studs becomes the decisive failure mode. If headed studs with smaller effective heights are used, brittle failure modes might occur. For effective height of 115 mm concrete cone failure between the supplementary reinforcement with approx. $N_{Rk,cs}$ = 250 kN is decisive and for an effective height of 65 mm with approx. $N_{Rk,cs}$ = 105 kN is the governing failure mode. In Fig. 4.15 the moment-rotation curve by varying the effective length of the headed stud is shown. By changing the effective height the rotational behavior of the joint can be influenced less as if the diameter of the heads stud is changed. Changes of the diameter of the headed stud have higher influence on the stiffness EA of this component (see Eq.(4.12)).

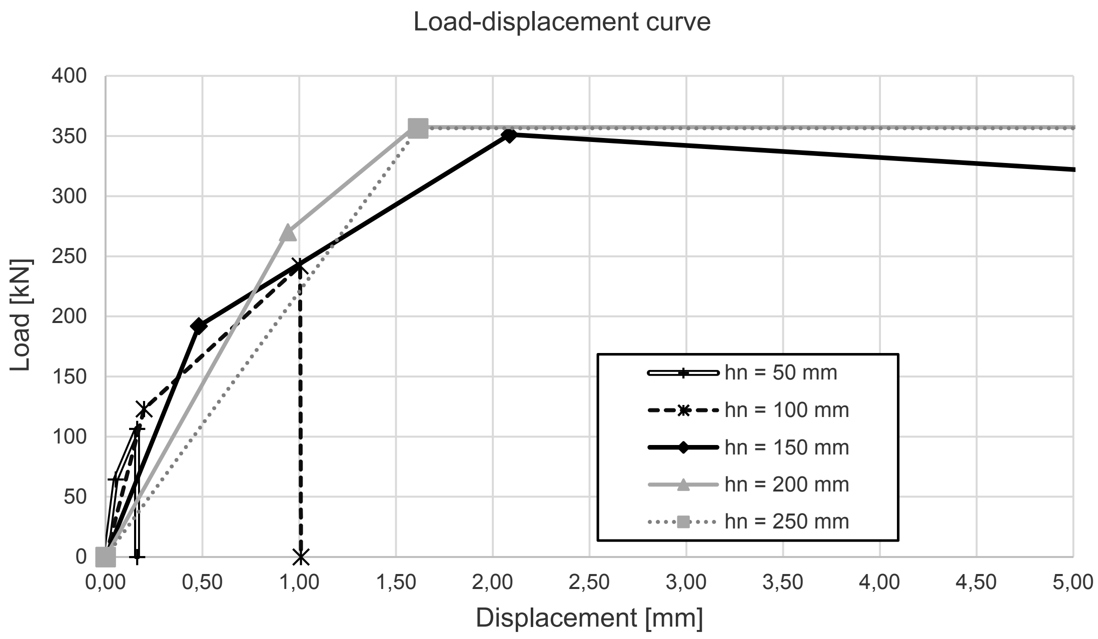

Fig. 4.14: Load-displacement curve of the tensional component for variation of the effective height

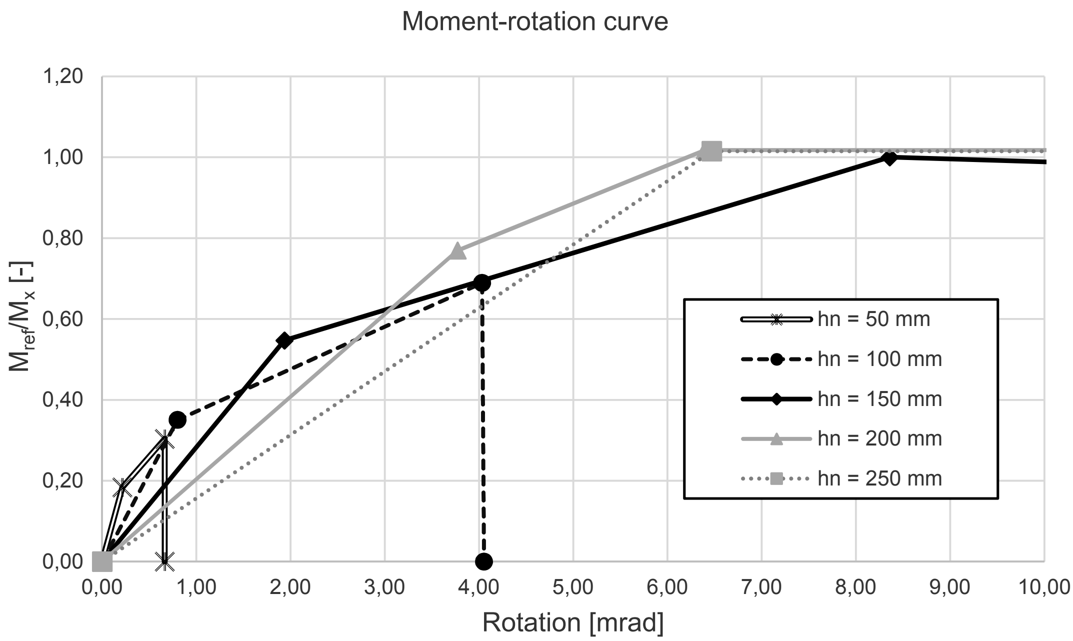

Fig. 4.15: Moment-rotation curve for variation of the effective height

4.3.3.4 Diameter of the headed studs

In Fig. 4.16 the load-displacement curves of the tensional component for different diameters of the headed stud is shown. The diameters of the headed studs are varied according to Tab. 4.5. By using a diameter of 22 mm in the reference version the supplementary reinforcement can be activated. This can be seen in Fig. 4.16 as the load can be increased from approx. $N_{Rk,u,c}$ = 190 kN up to $N_{Rk,u}$ = 350 kN (for definition see Fig. 4.11, right). The overall load carrying capacity cannot be increased by selecting even a higher diameter of the headed stud. As yielding of the supplementary reinforcement becomes the decisive component with $N_{Rk,re,1}$ = 350 kN a larger diameter is not more advantageous. If the diameter is reduced, the increase in loading due to the supplementary reinforcement cannot be taken into account fully. In this case a diameter of 16 mm is too small as the load level of concrete cone failure, $N_{Rk,c}$ = 190 kN, cannot be reached. In Fig. 4.17 the moment-rotation curves of this simple steel-to-concrete joint by varying the diameter of the headed stud are shown. The variation of the diameter has also an influence on the interaction equations of the joint. Steel failure might become the decisive interaction equation.

Tab. 4.5: Diameter of the headed studs

Parameter	Case 1	Case 2	Case 3	Reference version	Case 4
Diameter headed studs [mm]	13	16	19	22	25

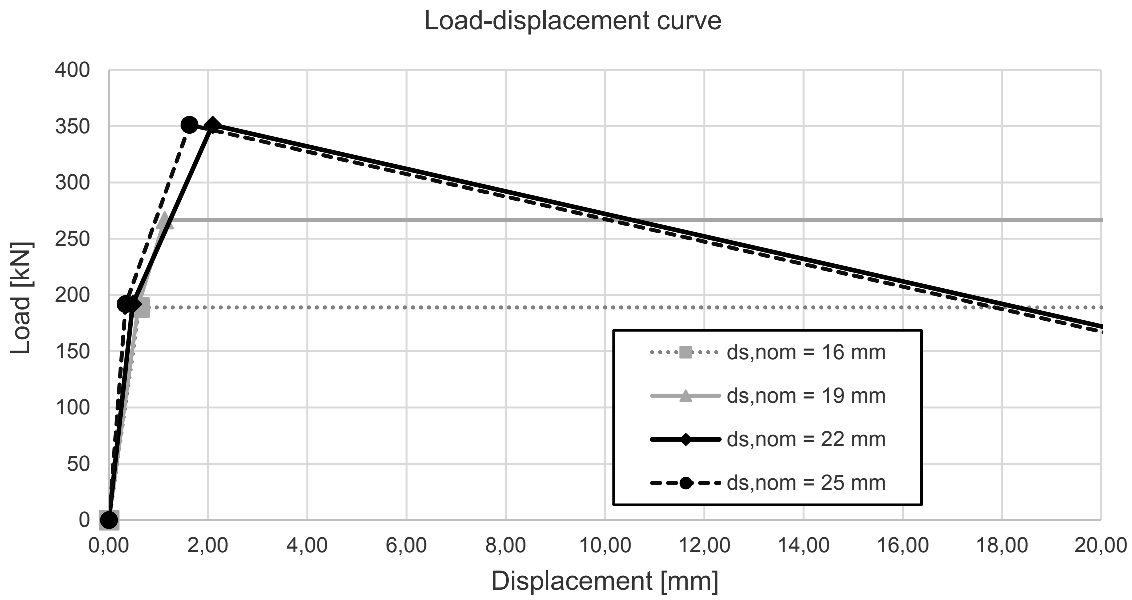

Fig. 4.16: Load-displacement curve of the tensional component for variation of the diameter of the headed studs

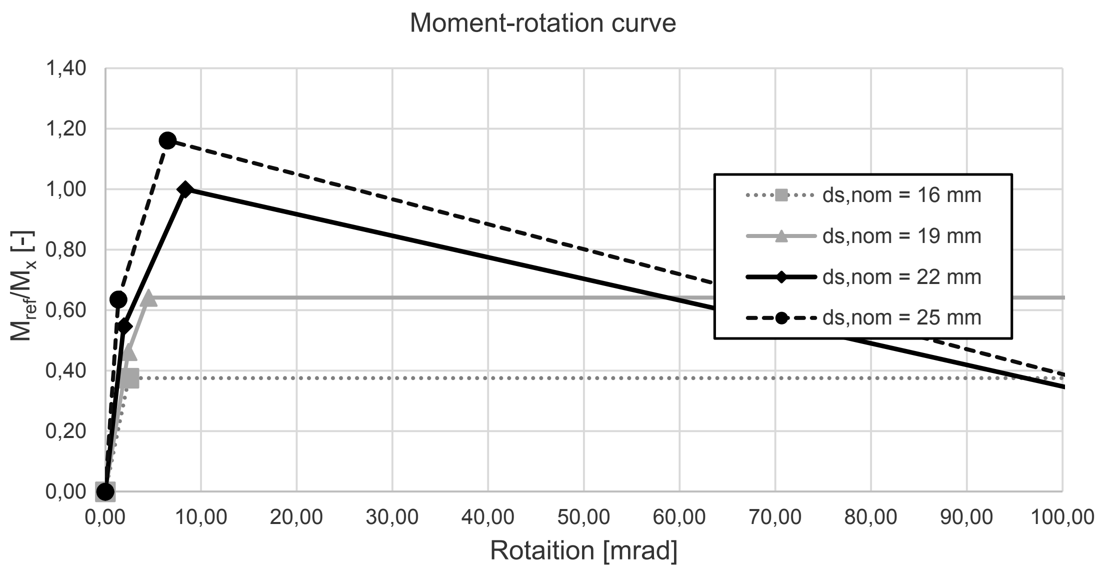

Fig. 4.17: Moment-rotation curve of the simple steel-to-concrete joint for variation of the diameter of the headed studs

4.3.3.5 Eccentricity

According to Tab. 4.6 five different cases are considered in order to determine the influence of the eccentricity on the rotational behavior of the joint. Originally there shouldn`t be any effect to the load-carrying capacity of the simple joint since there is no direct relation between the eccentricity and the tensile component. But changes in the eccentricity have influence on the overall load-carrying capacity. As interaction equations (see Eq. (4.16) to (4.17)) have to be considered, increases of the eccentricity can have an influence on the moment resistance of the joint. Either steel failure or concrete failure can be decisive. If joints are designed with higher eccentricities, increases of the tensional components of the joint have to be considered. By varying the eccentricity in this example the interaction equation is not overstepped as the resistances due to friction also increases due to higher normal forces in the joint (see Fig. 4.19). As the normal forces are getting larger the load capacity of the friction component rises and the shear resistance of the headed studs is exceeded. Smaller shear forces are transferred to the second anchor row and possible normal forces can be raised in this row. The particular application must be investigated therefore on case-by-case basis.

Tab. 4.6: Analyzed eccentricities

Parameter	Case 1	Case 2	Reference version	Case 3	Case 4
Eccentricity [mm]	50	75	100	200	250

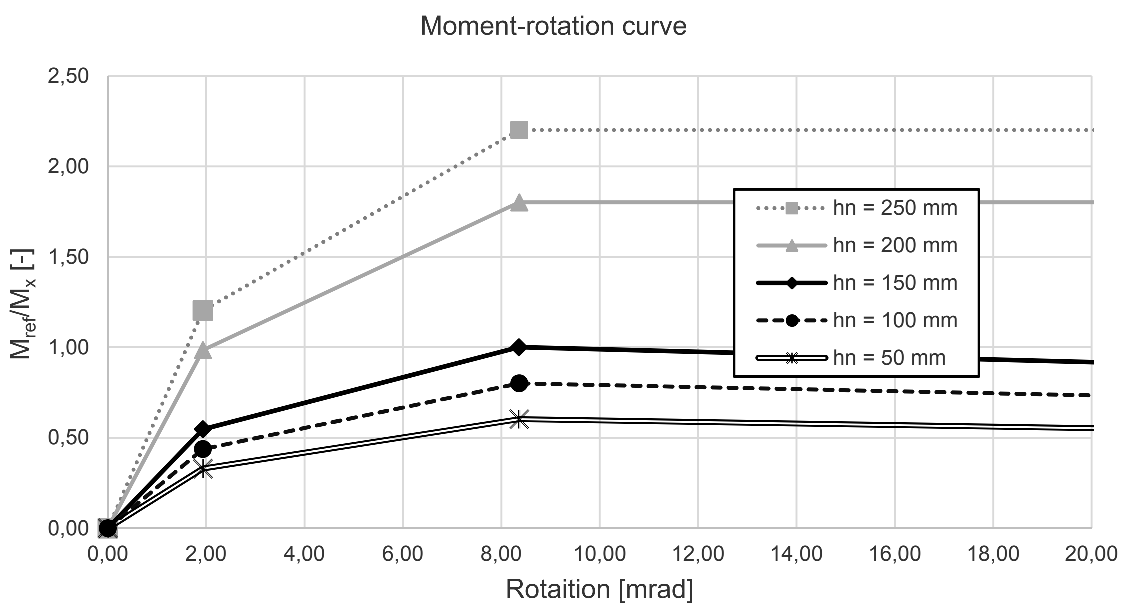

Fig. 4.18: Moment-rotation curve for variation of the eccentricity

4.3.3.6 Diameter and number of the stirrups

The parameters of the diameter and the number of stirrups have been changed according to Tab. 4.7. If the load carrying capacity of concrete cone failure is reached, further load increases depend on the supplementary reinforcement. Two different failure modes have to be considered if the supplementary reinforcement can be activated. Bond failure according to Chapter 4.2.9 or yielding of the supplementary reinforcement might occur. By increasing the diameter of the stirrup the ultimate resistance of the tensile component can only be increased slightly (see Fig. 4.19). By increasing the diameter of the headed stud, steel failure of the headed studs becomes the decisive component with approx. $N_{Rk,s}$ = 350 kN. As this is the crucial component increases in the diameter of the supplementary reinforcement are not more advantageous. In a further parameter study the number of stirrups has been varied. If the number of stirrups is reduced brittle failure modes might occur, as the surface area of the supplementary reinforcement is reduced (see Fig. 4.20).

Tab. 4.7: Analyzed diameter of stirrups and analyzed number of stirrups

Parameter	Case 1	Reference version	Case 2	Case 3	Case 4
Diameter of stirrups [mm]	6	8	10	12	14

Parameter	Case 1	Case 2	Reference version
Number of stirrups [mm]	1	2	4

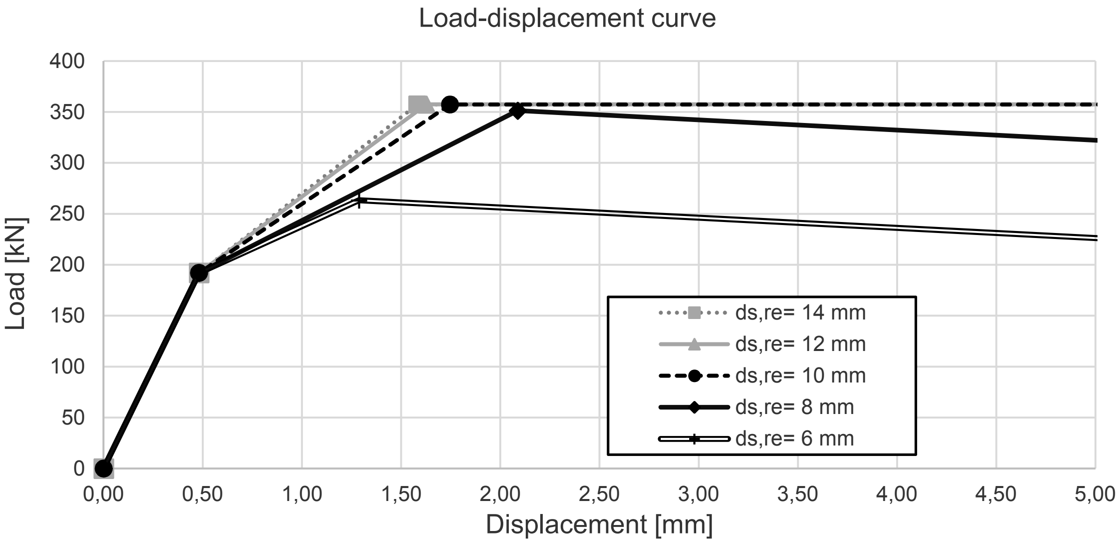

Fig. 4.19: Load-displacement curve for variation of the diameter of the supplementary reinforcement

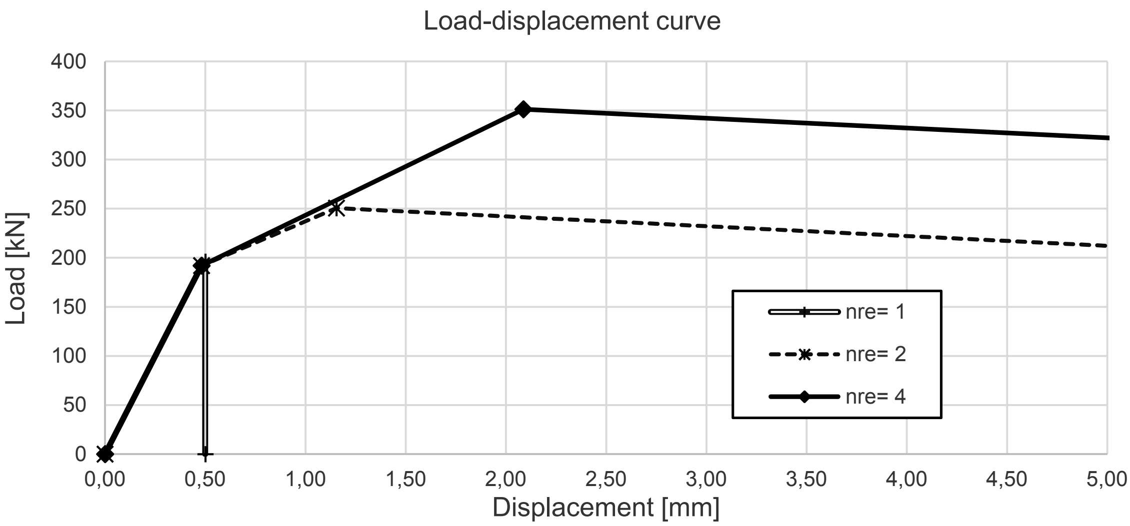

Fig. 4.20: Load-displacement curve for variation of the number of stirrups

4.3.3.7 Concrete strength

The concrete strength has an influence on all components and therefore a high influence on the load-deformation behavior of the tensile components. The issue of the scattering of this parameter is described in Chapter 4.2.4. In this parameter study this component is varied according to Tab. 4.8. If the concrete strength is reduced the load carrying capacity of the concrete component without considering the additional reinforcement (see Eq. (4.1)) decreases. The supplementary reinforcement cannot be activated fully in two cases as (Case 1 and Case 2) as pull-out failure is the decisive component $N_{Rk,p}$ = 280 kN (Case 1) in this cases.

Tab. 4.8: Variation of concrete strength

Parameter	Case 1	Case 2	Reference version	Case 3	Case 4
Concrete strength [N/mm²]	C20/25	C25/30	C30/37	C35/45	C40/50

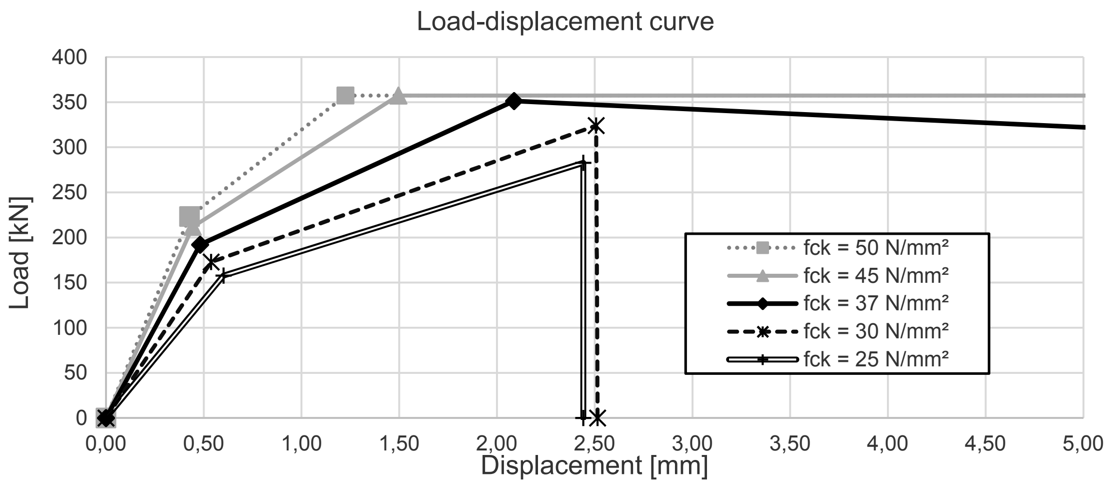

Fig. 4.21: Load-displacement curve for variation of the concrete strength

4.3.4 Limits of the model and recommendations

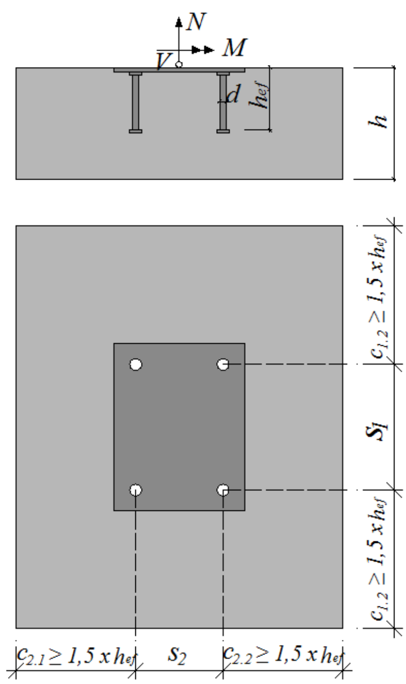

4.3.4.1 General

Fig. 4.22: Required edge-distances

In the parameter study above the sensitivity of simple steel-to-concrete joints to changes of different parameters is shown. The overall influence on the load-carrying capacity of the tensile components or the moment-rotation curve of the whole joint depends strongly on the design, e.g. geometry, size of anchors etc., of the simple steel-to-concrete joints in particular. Brittle failure modes have to be prevented within case by case studies where the different parameters are changed carefully. A very helpful tool in the design process of the joint can be the use of the design program for "Rigid anchor plate with headed studs – simple joint" (see Chapter 2.3). With the help of this program the failure modes of the specific anchor plate can be determined. By varying the above mentioned parameters ductile behavior of this joint can be achieved. Nevertheless limitations have to be made, if the newly developed INFASO-components are considered. These limitations are described in the following.

4.3.4.2 Edge distances

Within the INFASO project [11] a calculation approach for the tensile concrete components has been developed. Tests with loading perpendicular toward a free edge under shear with consideration of the positive contribution of the supplementary reinforcement have not yet been made. The additional reinforcement can only be taken into account, if the geometric limitations in Fig. 4.22 are taken into consideration. These limitations ensure that there are no edge effects which might lead to different failure modes. Further information will be given in Ožbolt [19]. Furthermore conservative calculation approaches for the calculation of the shear resistance due to pry-out failure have to be made, as the calculation of the resistance due to pry-out failure is based on the tensile resistance of the concrete components without considering the additional reinforcement. In future further tests have to be done for this failure mode.

4.3.4.3 Number of headed studs

In the INFASO project [11] tests on anchor plates of simple steel-to-concrete connections with dispositions of 2x3 and 2x2 of the headed studs have been made. Limitations for anchor plates with a larger number of headed studs are given in CEN/TS 1992-4-1 [1]. Anchor plates with more than nine headed studs are not covered by this standard. If the number of headed studs is increased, according to the tests of the INFASO project [11] further considerations have to be made, if the supplementary reinforcement is taken into account..

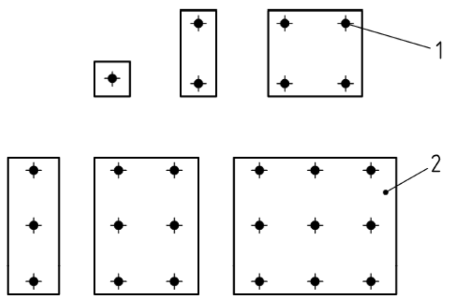

Fig. 4.23: Number of headed studs according to CEN/TS 1992-4-1 [1]

4.3.4.4 Concrete strength

A relatively low concrete strength of C20/25 [7] has been used for all test specimens to achieve concrete failure modes as lower bound of all failure mechanism. The developed INFASO models [11] are only valid for normal-strength concrete and should not be transferred to high-strength concrete.

4.3.4.5 Number of stirrups

The model of the tensile components has been developed in the INFASO project [11] for one stud row. This model is based on tests of headed studs under pure tension, where supplementary reinforcement is considered. In the test specimens with consideration of supplementary reinforcement two stirrups have been placed next to the headed stud. In total four legs have been considered within the concrete cone of one headed stud. The model of this tensile component has been implemented in the model of the simple joint, where the tensional forces have to be considered in the second row of headed studs (see Fig. 4.11). The model of this simple steel-to-concrete joint has been validated with good agreement against the test results (see Fig. 4.13) with the exact constellation of supplementary reinforcement as in the component tests under pure tension.

If the new INFASO design approach [11] is transferred to anchor plates with more than two stud rows, the load distribution among the supplementary reinforcement has to be considered in special. If the model is assigned for two stud rows under tension, calculation approaches are given in [16]. If the supplementary reinforcement is placed next to the headed studs according to Fig. 4.24 the concrete cone can be subdivided into the intermediate part with normal concrete break-out and the right side and left side part where the factor ψ_{supp} is considered. The failure load of this component can be calculated with Eq. (4.18):

$$N_{u,max} = \psi_{supp} \cdot \frac{A_{c,N,1}}{A_{c,N,total}} \cdot N_{u,c} + \frac{A_{c,N,2}}{A_{c,N,total}} \cdot N_{u,c} + \psi_{supp} \cdot \frac{A_{c,N,3}}{A_{c,N,total}} \cdot N_{u,c} \qquad (4.18)$$

Further investigations no the subject of edge effects, number of stirrups (see [19] and [14]) and number of heads studs (see [15])are on the way but not yet in a status to be implemented in Eurocodes.

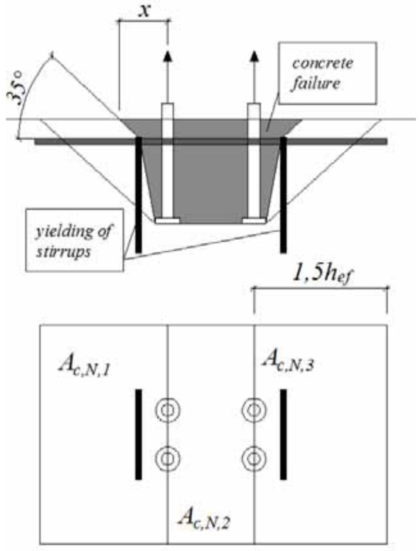

Fig. 4.24: Design approach for more than one headed stud under tension

4.4 Parameter study on column bases

4.4.1 Validation of the model

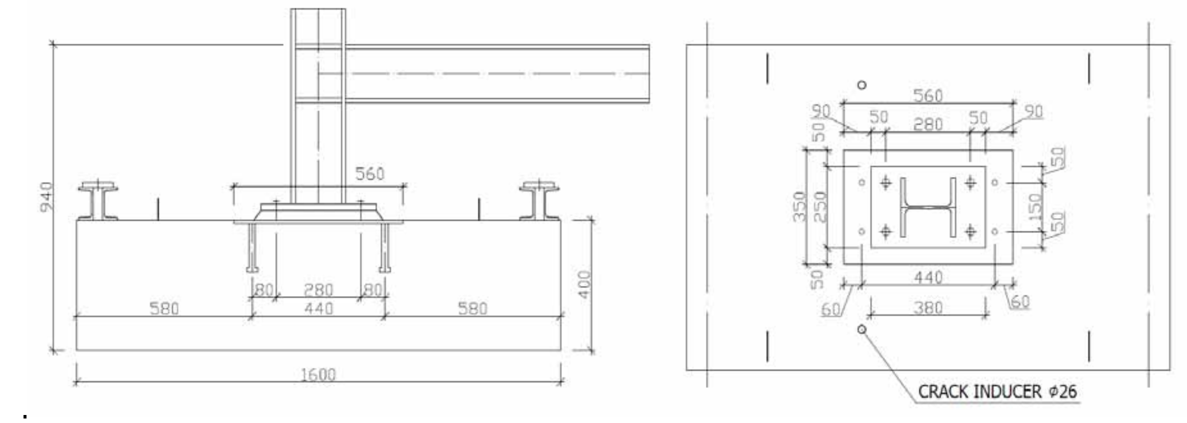

Fig. 4.25: Geometry of tests with column base with anchor plate

The analytical component based model of column base with anchor plate was validated on experiments prepared under the project, see Kuhlman et al. [12]. The specimen was consisted of two steel units, see Fig. 4.25. The thin steel anchor plate was t_{p1} = 10 mm with welded studs d = 22 mm, h = 150 mm and with threaded studs d = 24 mm, h = 100 mm. The thick steel base plate t_{p2} = 25 mm was design under the column HE180B, fillet weld a_w = 6 mm. The concrete block was made from reinforced concrete 1 600 x 1 000 x 400 mm, see Tab. 4.9 The test results were published in Ph.D. thesis of Žižka, J. [20]

Tab. 4.9: Geometric dimensions of the tests

Column		**Base plate**		**Anchor plate**	
HE180B	S355	250x380x25	S355	350x560x10	S235
f_{yk} = 355 MPa	f_{uk} = 510 MPa	f_{yk} = 355 MPa	f_{uk} = 510 MPa	$f_{y,exp}$ = 270.1 MPa	$f_{u,exp}$ = 421.3
Threaded studs		**Headed studs**		**Foundation (cracked)**	
d = 24 mm; h = 100 mm	S355	d = 22 mm; h = 150 mm	S355	1600x1000x400	C25/30
f_{yk} = 355 MPa	f_{uk} = 510 MPa	$f_{y,exp}$ = 444.8 MPa	$f_{u,exp}$ = 542.1	f_{ck} = 25 MPa	$f_{ck,c}$ = 30 MPa

The analytical model is described in Design Manual I "Design of steel-to-concrete joints" [13]. For the calculation were taken the measured values of material properties of steel. In the experiments S2-0, S2-5, and S2-30 varies the thickness of the grout, form 0 mm, 5 mm and 30 mm. The experimental moment rotational curves are summarized in Fig. 4.26.

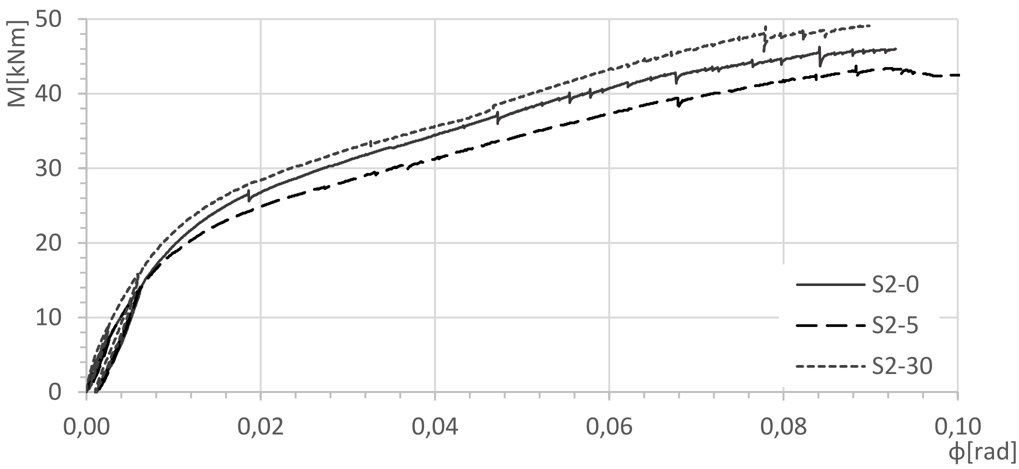

Fig. 4.26: Moment-rotation curves of three experiments with different position of headed and threaded studs

The differences of experimental results are reported to be due to changes of lever arm during the loading at large deformations, see Fig. 4.27. The vertical deformations were measured at points 1-11, the horizontal ones in 12 and 13, see Fig. 4.27. Results of each experiments were recalculated based on the measured actual acting force, see Fig. 4.28 to Fig. 4.30. The eccentricity is recalculated to the column axes. The comparison of the calculated and measured initial stiffness $S_{j,ini}$ shows a good agreement. The difference is in between a range of 5 %. The elastic-plastic stage is affected to the material properties and the development of cracks in concrete block. The modelling respects the engineering level of accuracy in prediction of resistance.

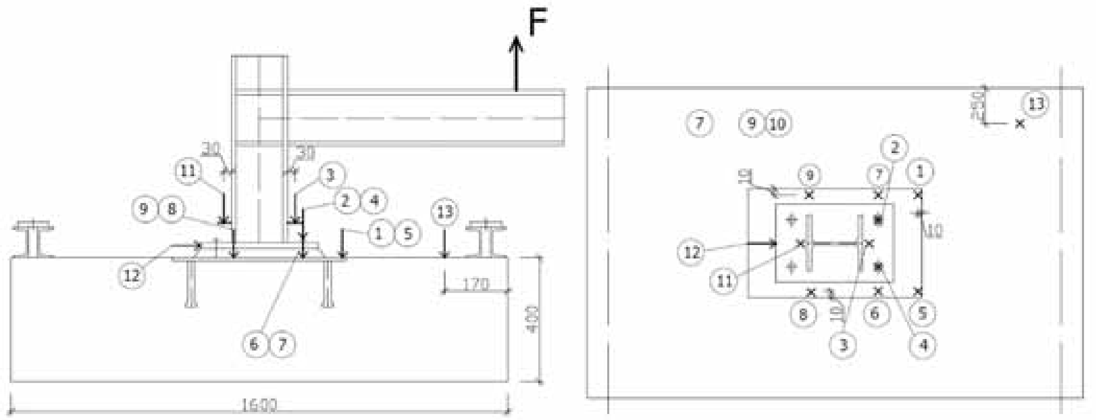

Fig. 4.27: Measured values during the tests

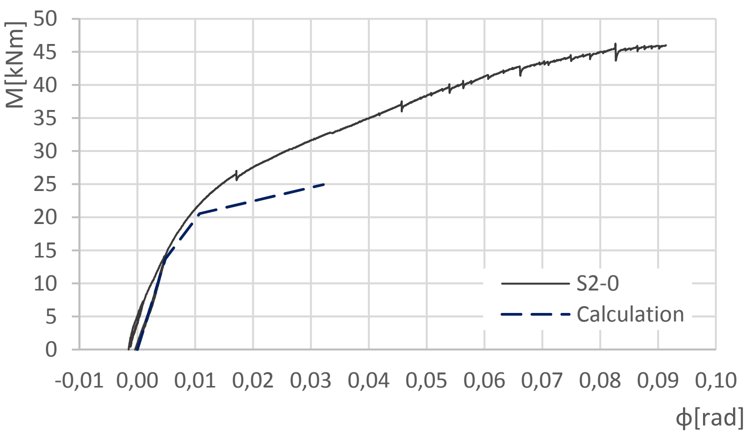

Fig. 4.28: Comparison of predicted and measured moment rotational relation for experiment S2-0, eccentricity 495 mm

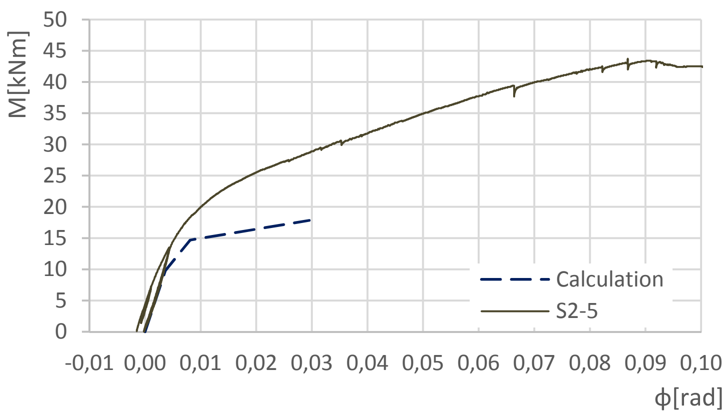

Fig. 4.29: Comparison of predicted and measured moment rotational relation for experiment S2-5, eccentricity 354 mm

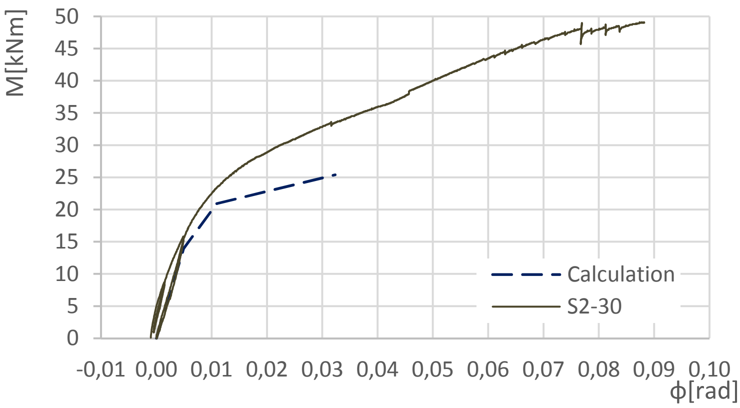

Fig. 4.30: Comparison of predicted and measured moment rotational relation for experiment S2-30, eccentricity 504 mm

4.4.2 Sensitivity study of major parameters

The bending resistance of the base plate with anchor plate is assembled from the tensile and compression resistance of its components. The additional component is the anchor plate in bending and in tension. The procedure for evaluation of the resistance is the same in all connections loaded by bending moment and normal force. The influence of parameters like the base plate thickness, the anchor plate thickness, and the distance between the headed and threaded studs is studied. The study is prepared for column of cross section HE180B, for all plates and cross sections of steel S355 (if not mentioned for all plates and cross sections S235), concrete C25/30, threaded studs M 24, steel S355, and headed studs M22, steel S355. In each normal force moment interaction diagram are marked the important points e. g. the resistance in tension, in maximal bending, in pure bending, and in maximal compression. The Fig. 4.31 and Fig. 4.32 demonstrate the influence of the base plate thickness t_{p2} for steel S355 and S235.

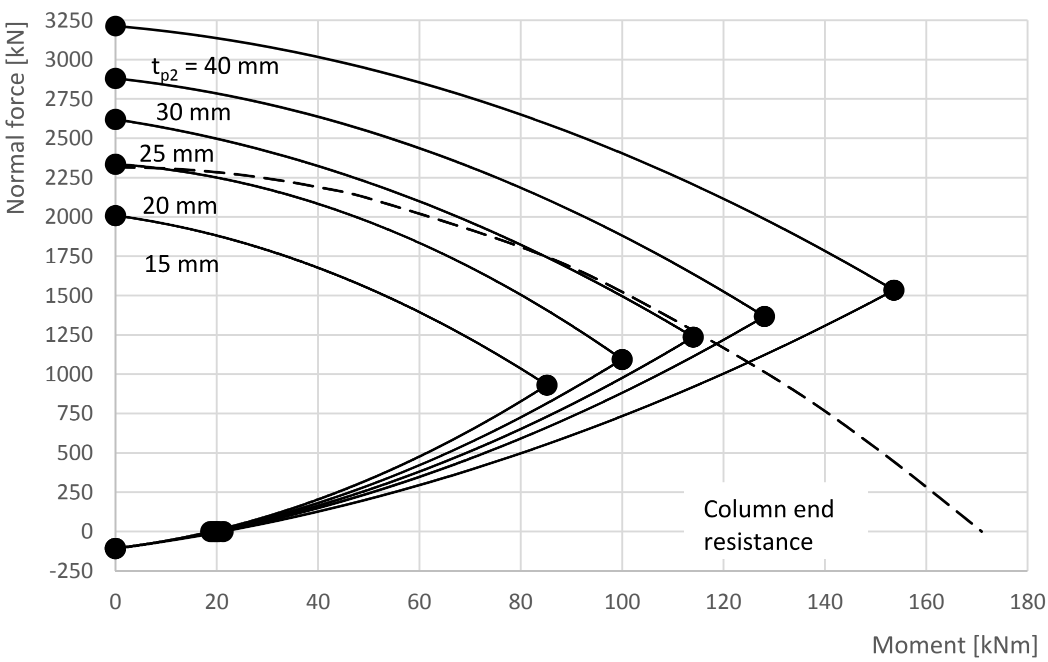

Fig. 4.31: Moment – normal force interaction diagram for different base plate thickness t_{p2} and steel S355

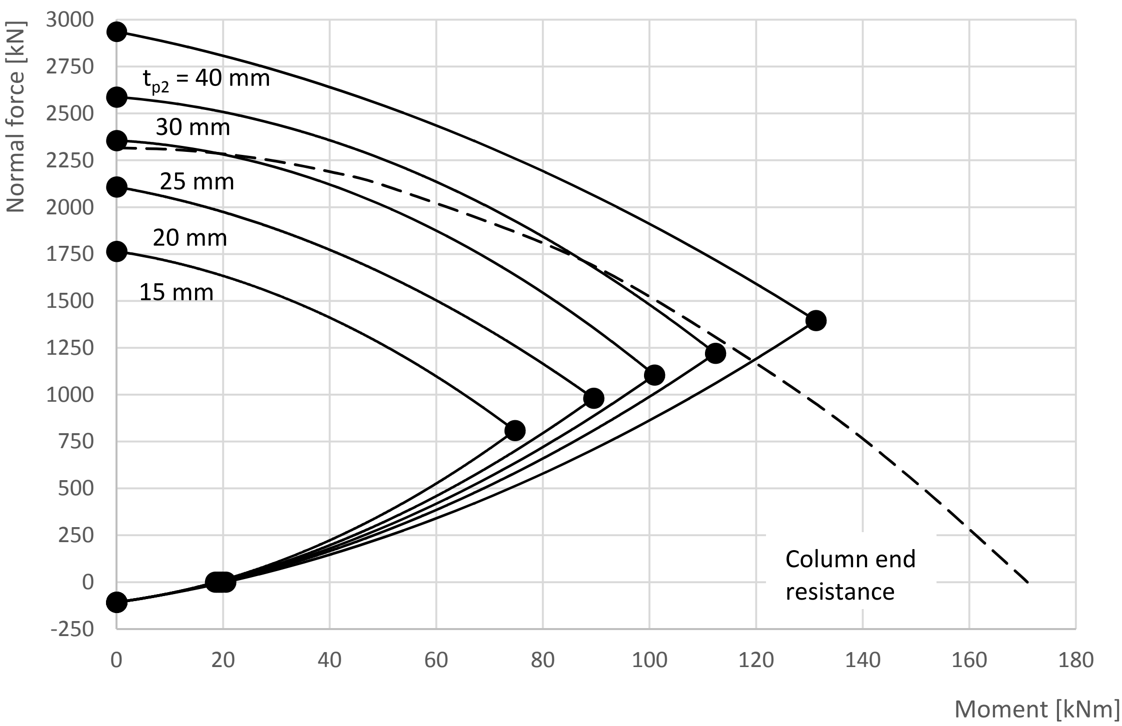

Fig. 4.32: Moment – normal force interaction diagram for different base plate thickness t_{p2} and steel S235

The parameter study of the anchor plate thickness t_{p1} is influenced by the interaction of acting developed forces in headed studs in shear and in tension. The selected value of effective height of the headed stud is included for each anchor plate thickness. Fig. 4.33 to Fig. 4.36 show the influence of the anchor plate thickness to the column base resistance for two material properties. For headed studs with the effective height 150 mm, only the anchor plate with thickness 10 mm is not affected by the headed stud's resistance.

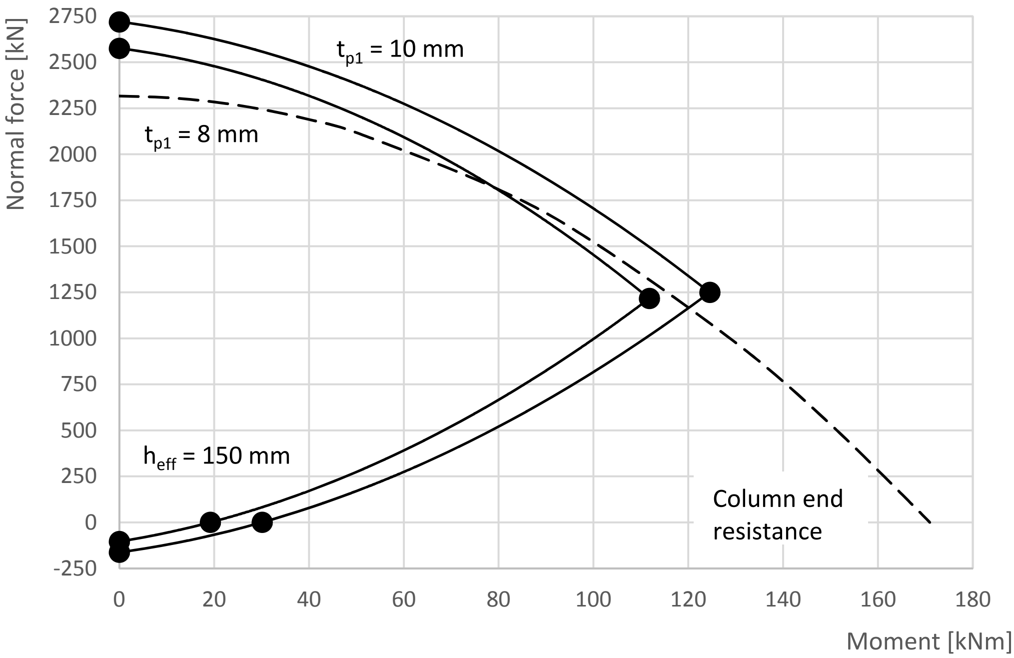

Fig. 4.33: Moment – normal force interaction diagram for different anchor plate thickness t_{p1}, for the anchor plate steel S355, and the headed stud length h_{eff} = 150 mm

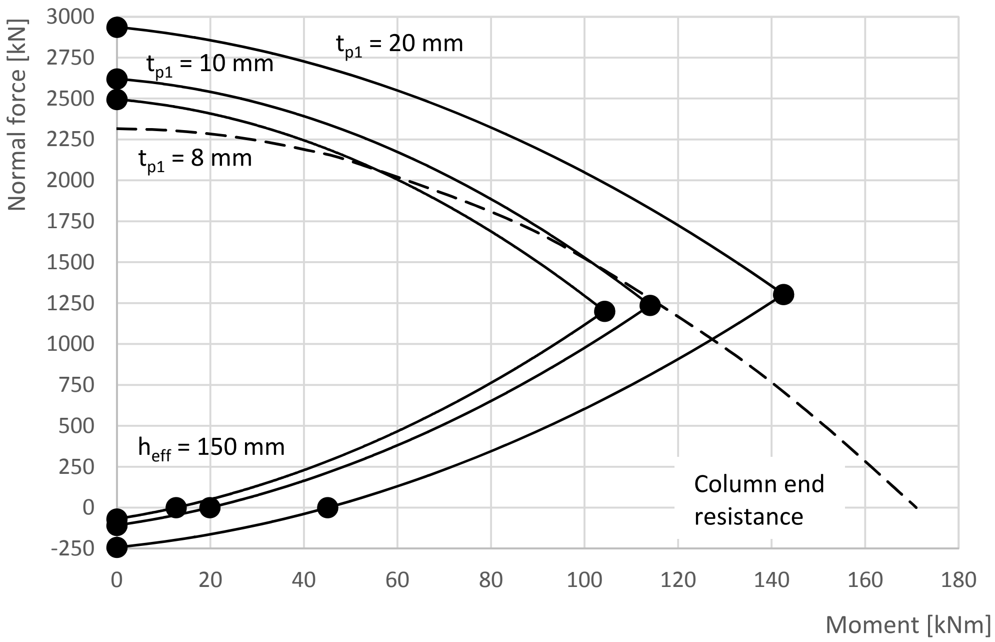

Fig. 4.34: Moment – normal force interaction diagram for different anchor plate thickness t_{p1}, for the anchor plate steel S235, and the headed stud length h_{eff} = 150 mm

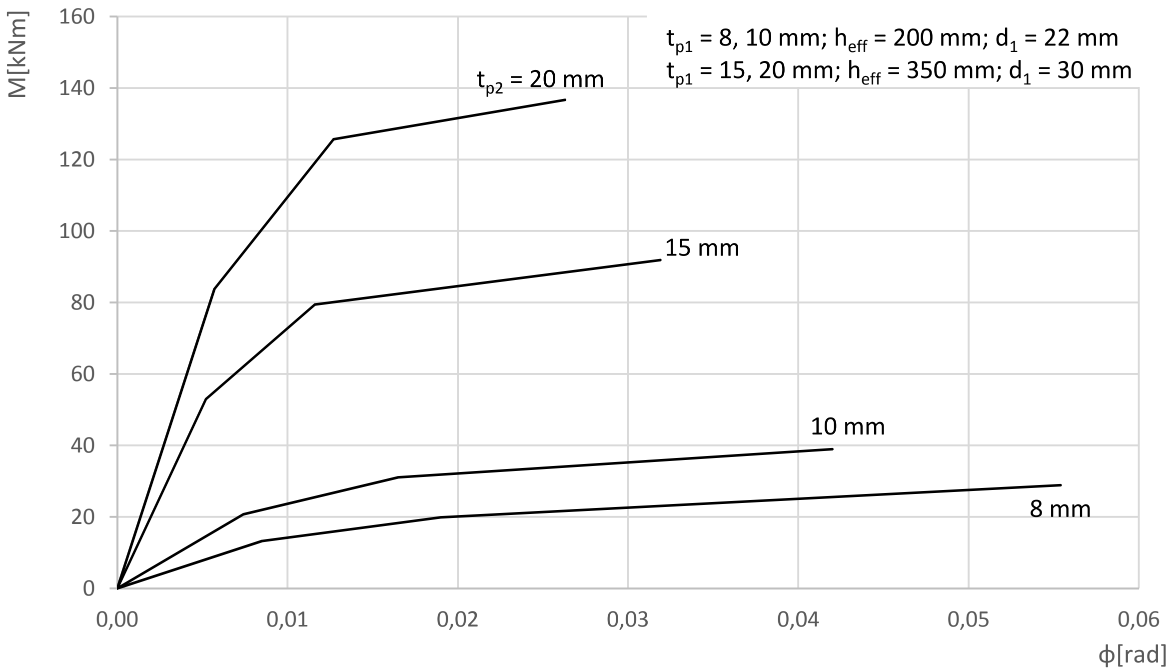

Fig. 4.35: Moment – rotation diagram for different anchor plate thickness t_{p1}, for the anchor plate steel S355, and the headed stud lengths h_{eff} = 200 mm and 350 mm

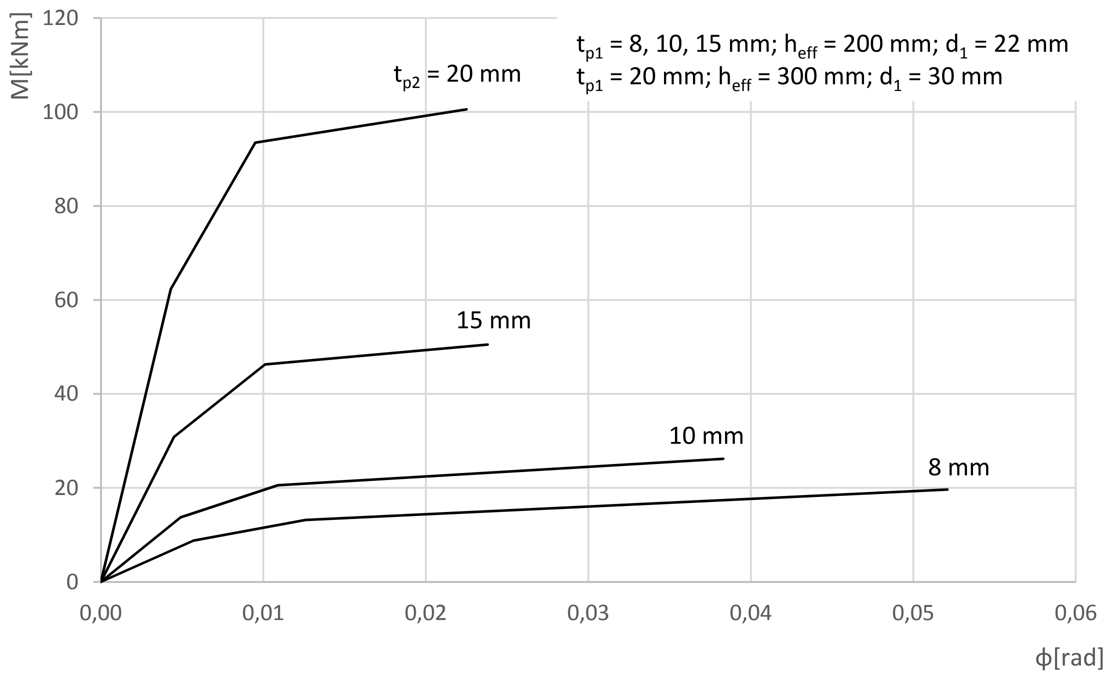

Fig. 4.36: Moment – rotation interaction diagram for different anchor plate thickness t_{p1}, for the anchor plate steel S235, and the headed stud lengths h_{eff} = 200 mm and 300 mm

The influence of the effective length of the headed stud 200 and 350 mm, for steel S355, the plate thickness 25 mm is summarized in a moment – normal force interaction diagram in Fig. 4.37 and Fig. 4.38.

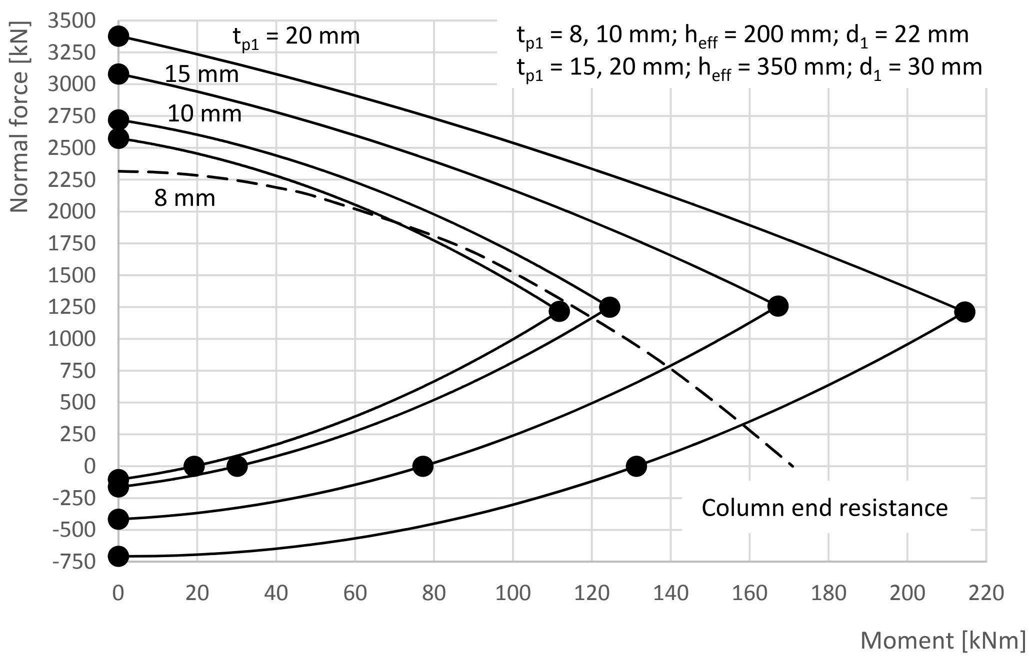

Fig. 4.37: Moment – normal force interaction diagram for different anchor plate thickness t_{p1}, for the anchor plate steel S355, and the headed stud lengths h_{eff} = 200 mm and 350 mm

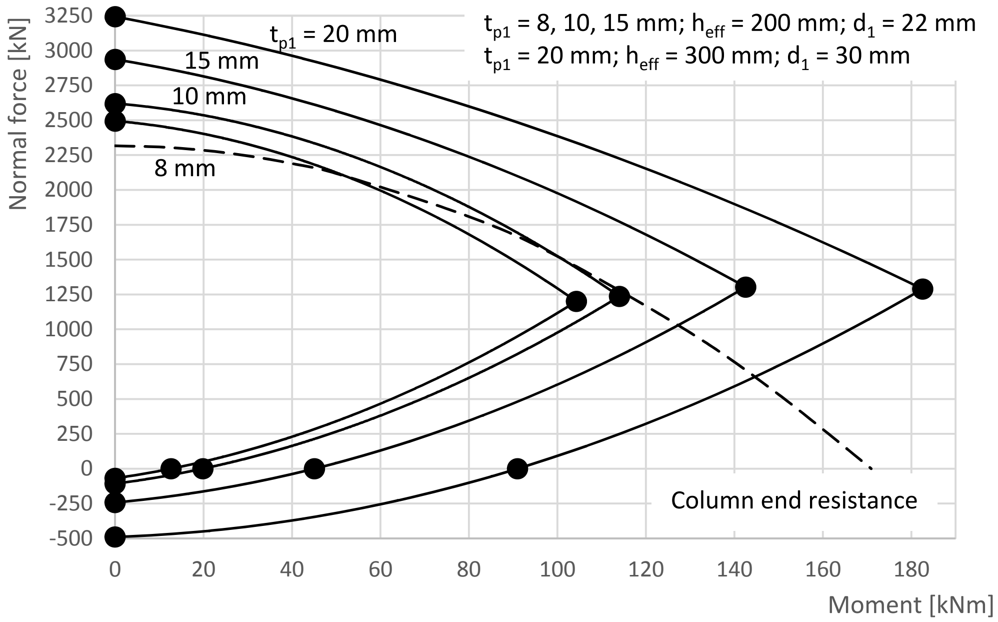

Fig. 4.38: Moment – normal force interaction diagram for different anchor plate thickness t_{p1}, for the anchor plate steel S235, and the headed stud lengths h_{eff} = 200 mm and 300 mm

Different distance between the headed and threaded studs of the anchor plates and their influence on the moment resistance are shown in Fig. 4.39 to Fig. 4.42 for the anchor plate thickness 10 mm, base plate thickness 25 mm, and steels S355 and S235. The pure bending resistance decreases till the distance between the headed and threaded studs 200 mm, where the base plate resistance is changed.

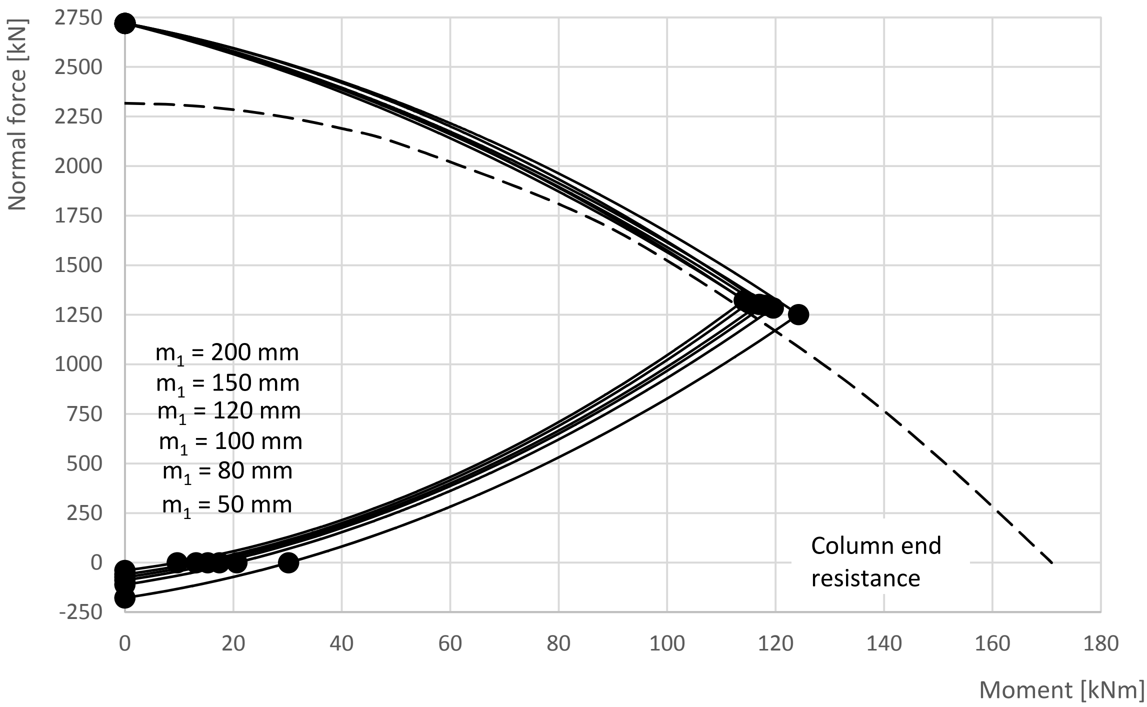

Fig. 4.39: Moment – normal force interaction diagram for different distances between the headed and threaded studs m_1, for the anchor plate steel S355

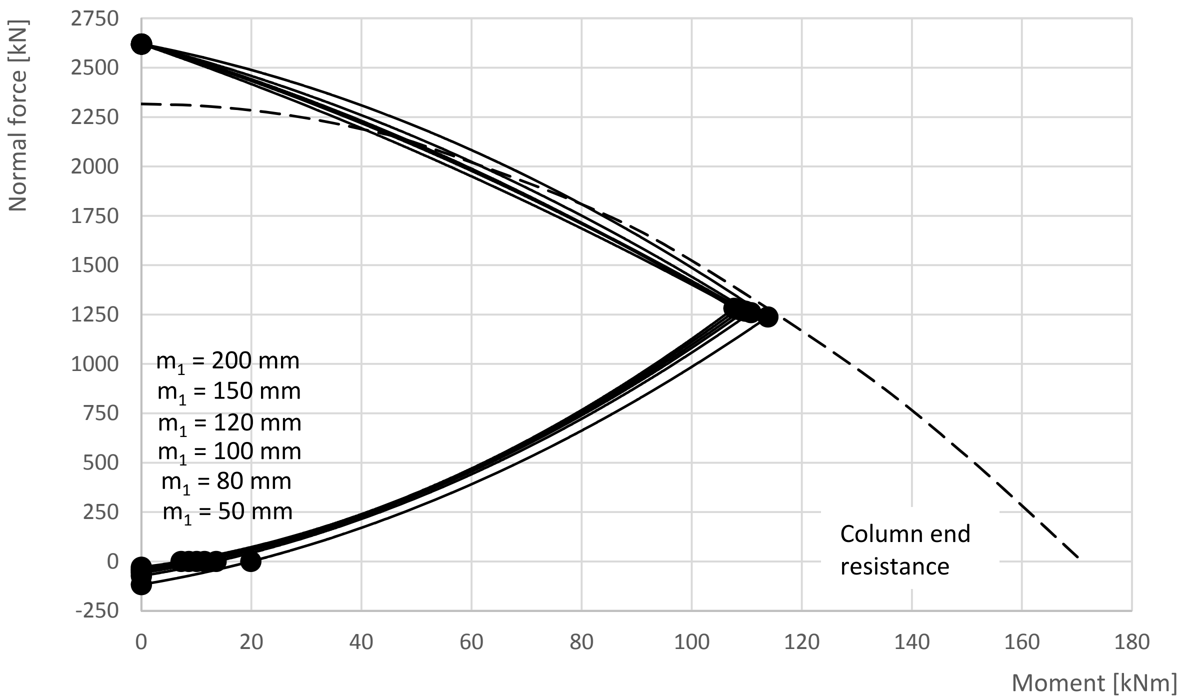

Fig. 4.40: Moment – normal force interaction diagram for different distances between the headed and threaded studs m_1, for the anchor plate steel S235

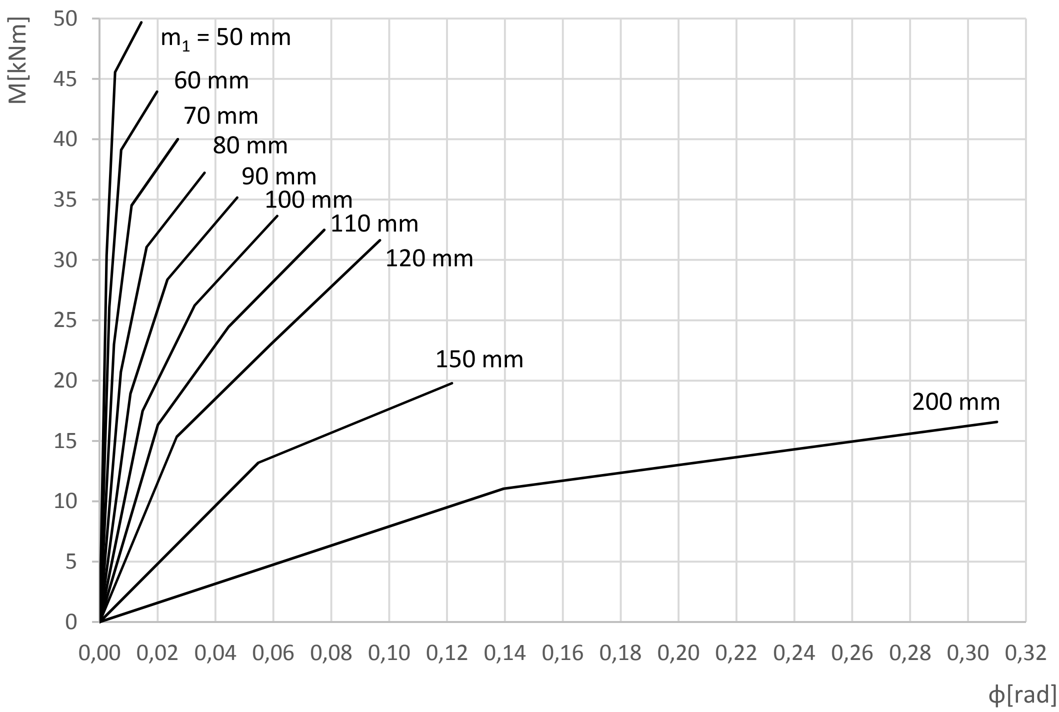

Fig. 4.41: Moment – rotation diagram for different distances between the headed and threaded studs m_1, for the anchor plate steel S355

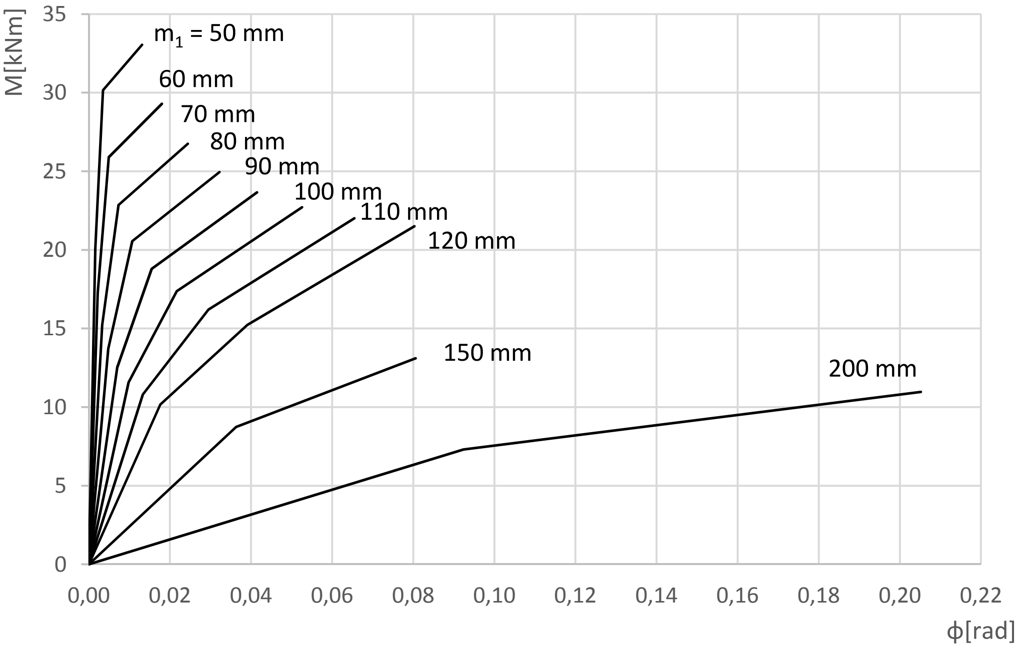

Fig. 4.42: Moment – rotation diagram for different distances between the headed and threaded studs m_1, for the anchor plate steel S235

4.4.3 Limits of the model

The analytical design model by component based method of a base plate with an anchor plate offers freedom in selection of material properties and geometries of the threaded and headed studs, the base and anchor plates and the concrete foundation. The limits follows the recommended values in Chapter 2.2. Information about positioning of holes for bolts and rivets is given in EN 1993-1-8 [9]. The symbols used are summarized in Fig. 4.43. These limits may be interpreted for a base plate with an anchor plate in terms of

$$p_2 = \min(2.5\ d_{20}) \tag{4.19}$$

$$e_{b2} = \min(1.2\ d_{20}) \tag{4.20}$$

$$m_2 = \min(1.2\ d_{20} + a_w\sqrt{2}) \tag{4.21}$$

$$e_{a2} = \min(1.2\ d_{20}) \tag{4.22}$$

$$e_{a1} = \min(1.2\ d_{10}) \tag{4.23}$$

With:

p_2 is distance between the threaded studs
d_{10} is diameters of headed stud including weld to the anchor plate
d_{20} is diameters of threaded stud including weld to the anchor plate
e_{b1} is the edge distance the headed stud
e_{b2} is the edge distance the threaded stud
m_2 is distance between the threaded stud and column cross section

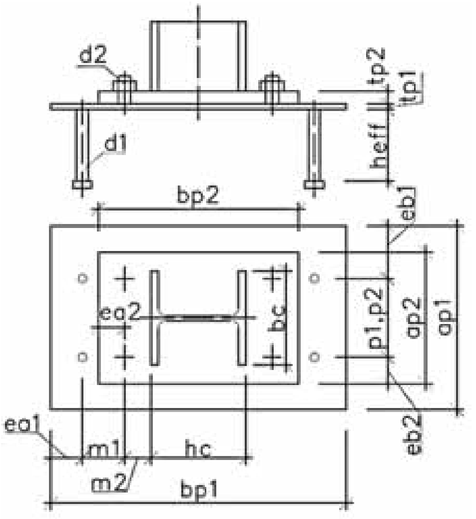

Fig. 4.43: Scheme of base plate with anchor plate

The presented model was validated/verified in limited range of geometry and materials S235 to S355 for:

t_{p1} = 6 to 20 mm

d_1 = 20 to 40 mm

d_2 = min d_1

h_{eff} = min 150 mm

where
t_{p1} is thickness of the anchor plate
t_{p2} is thickness of the base plate
d_1 is diameters of headed stud
d_2 is diameters of threaded stud
h_{eff} is the effective height of the headed stud

For very thin anchor plates t_{p1} < 6 mm and huge headed and threaded studs d_1 > 40 mm too rough simplification of changes in the geometry in the model might occur. The prediction of the tensile resistance of the component anchor plate in bending and in tension should be modelled by iteration, which is described in Žižka, J. [20].

For ductile behaviour of the base plate with anchor plate it is necessary to avoid a brittle failure of the concrete components. The concrete cone failure without or with reinforcement, the pull-out failure of headed studs, the pry-out failure of headed stud, and its interaction. The steel failure of the threaded stud in tension is unacceptable brittle for design of steel structures. In column bases it is approved, that the failure of the anchor bolts is for predominantly static loading of column bases ductile enough. The headed studs with embedded length of at least 8 d_1 may be expected to present ductile behaviour. The deformation capacity of headed studs with shorter embedded length in the reinforced concrete block should be checked by presented method in Design Manual I "Design of steel-to-concrete joints" [13].

Under serviceability limit state the elastic plastic behaviour without any membrane actions is expected in connections. Column bases with base plate and anchor plate develop the plastic hinge mechanism and the anchor plate due to a tensile bar. This behaviour is ductile but creates large deformations. Hence this method is recommended to limit the serviceability limit state by the creation of the full plastic mechanism only.

4.4.4 Recommendation for design values

The column base with base plate in pure compression is not limited by the size of the concrete block for a_c = min 3 a_{p2} and b_c = min 3 b_{p2}. Full resistance of the steel part may be developed, where a_c and b_c is the concrete width/length, and a_{p2} and b_{p2} is the base plate width/length.

The resistance of column base with anchor plate in pure bending is mostly limited by interaction of tension and shear of headed studs be creating the tensile bar behaviour of the anchor plate. The longer headed studs of higher diameter and better material properties of stirrups allows the development of this ductile behaviour. The contribution of the tensile resistance of the component the anchor plate in bending and in tension is expected $t_1 \leq$ max 0,5 t_2, where t_1 is the anchor plate thickness and t_2 is the base plate thickness. For typical column cross sections recommended sizes of the column base with anchor plate are summarized in Tab. 4.10. to Tab. 4.15. The table is prepared for all plates and cross sections of steel S355, concrete C25/30, threaded studs M 24, steel S355, and headed studs M22 of effective length h_{eff} =200 mm, steel S355. Stirrups have diameter Ø 8 mm, steel B500A, 4 legs for stud. The influence of the weld size on tension part resistance is not taken into account.

The distance between the threaded and headed studs m_1 is expected in one direction along the base plate only. For distances in both direction the real distance m_1 should be taken into account. The threaded and headed stud´s deviation from the specified location is expected in the calculations as 6 mm. The stud deviation is taken into consideration reducing the lever arm as:

$m_1 = \pm 4$ mm
$m_2 = \pm 2$ mm

Due to loading of the of column base with plastic mechanism in the anchor plate internal vertical and horizontal forces in the headed studs from changed geometry have to be considered. In the presented tables this is dissipated till 20 % of the horizontal resistance of headed studs. The remaining 80 % may carry the acting external shear forces. The symbols used are summarized in Fig. 4.43. By utilization of tables the linear transition for different normal force / bending moment ratio is recommended. The geometry of the column base is defined by following values:

a_{p2} is width of the base plate
d_1 is diameters of threaded stud
d_2 is diameters of headed stud
e_{b1} is the edge distance the threaded stud
e_{b2} is the edge distance the headed stud
m_1 is distance between the threaded and headed studs
m_2 is distance between the threaded stud and column cross section
p_1 is distance between the threaded studs
p_2 is distance between the headed studs
t_{p2} is thickness of the base plate
t_{p1} is thickness of the anchor plate

Tabularized are values for:

$M_{N=0,pl}$ is the bending design resistance of column base under poor bending for SLS, under plastic bending of the anchor plate, see Fig. 4.44.

$M_{N=0,mem}$ is the bending design resistance of column base under poor bending for ULS, the anchor plate acts as anchor plate

M_1 is the specific design bending resistance of column base for acting normal force N_1 for effective cross section under one flange in compression only

$M_{2,}$ is the maximal design bending resistance of column base for acting normal force N_2 for one-half of effective cross section is in compression

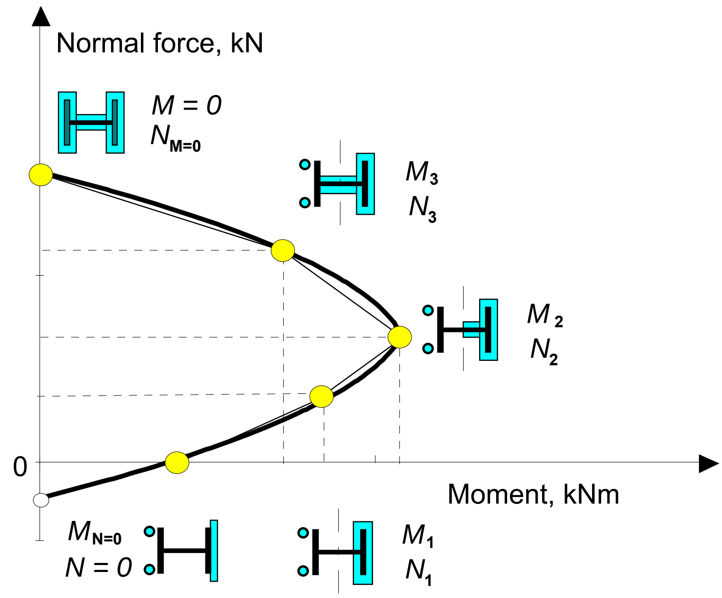

Fig. 4.44: Tabulated points at the moment –normal force interaction diagram in Tab. 4.10. to Tab. 4.15

M_3 is the specific design bending resistance of column base for acting normal force N_3 for effective cross section under the column web and one flange in compression

$N_{M=0}$ is the design compression resistance of column base under poor compression

The column bases are classified based on its relative stiffness compared to the column stiffness in the terms of column length. Shorter columns with this column base may be design with a rigid connection in bending.

The tables contain the limiting length of columns for the rigid column bases for frames where $L_{cb} = 8\ E\ I_c\ /\ S_{j.ini}$ and for other frames as $L_{co} = 25\ E\ I_c\ /\ S_{j.ini}$.

Tab. 4.10: Recommended geometry of the column base with anchor plate, its design resistances, stiffness and limiting length for HE160B

HE160B	Column	Base plate	Anchor plate	Threaded studs	Headed studs	Stirrups
	a_{wf} = 6 mm S355	**P25** - 200 x 360 S355	P(**t_{p1}**) - 240 x **(380 + 2m_1)** S355	Ø 24 mm S355	Ø 22 mm S355	Ø 8 mm
	Foundation	e_{a2} = 50 mm p_2 = 100 mm	e_{a1} = 60 mm p_1 = 100 mm		h_{eff} = 200 mm	B500A
	700 x 1200 x 850 C20/25	e_{b2} = 50 mm m_2 = 50 mm	e_{b1} = 70 mm			4 legs for stud

Varying		Resistance / Stiffness / Limiting length																				
m_1	t_{p1}	$M_{N=0,pl}$	$S_{j,ini,pl}$	$M_{N=0,mem}$	L_{cb}	L_{co}	M_1	N_1	$S_{j,ini}$	L_{cb}	L_{co}	M_2	N_2	$S_{j,ini}$	L_{cb}	L_{co}	M_3	N_3	$S_{j,ini}$	L_{cb}	L_{co}	$N_{M=0}$
[mm]	[mm]	[kNm]	[kNm/rad]	[kNm]	[m]	[m]	[kNm]	[kN]	[kNm/rad]	[m]	[m]	[kNm]	[kN]	[kNm/rad]	[m]	[m]	[kNm]	[kN]	[kNm/rad]	[m]	[m]	[kN]
	10	53	15133	-	2.8	8.6	95	700	13939	3.0	9.4	95	700	13939	3.0	9.4	95	700	13939	3.0	9.4	1804
0	12	54	15045	-	2.8	8.7	100	742	13826	3.0	9.5	100	742	13826	3.0	9.5	100	742	13826	3.0	9.5	1887
	15	55	14913	-	2.8	8.8	108	806	13669	3.1	9.6	108	806	13669	3.1	9.6	108	806	13669	3.1	9.6	1926
	10	31	6380	34	6.6	20.5	86	767	6301	6.6	20.8	86	767	6301	6.6	20.8	86	767	6301	6.6	20.8	1804
50	12	45	8683	48	4.8	15.1	98	756	8093	5.2	16.2	98	756	8093	5.2	16.2	98	756	8093	5.2	16.2	1887
	15	65	10958	65	3.8	11.9	114	756	9917	4.2	13.2	114	756	9917	4.2	13.2	114	756	9917	4.2	13.2	1926
	10	24	494	29	84.8	265.0	84	784	536	78.1	244.2	84	784	536	78.1	244.2	84	784	536	78.1	244.2	1804
100	12	35	950	39	44.1	137.7	94	785	930	45.0	140.7	94	785	930	45.0	140.7	94	785	930	45.0	140.7	1887
	15	54	1953	58	21.4	67.0	112	775	1780	23.5	73.5	112	775	1780	23.5	73.5	112	775	1780	23.5	73.5	1926

HE160B	Column	Base plate	Anchor plate	Threaded studs	Headed studs	Stirrups
	a_{wf} = 6 mm S355	**P30** - 200 x 360 S355	P(**t_{p1}**) - 240 x **(380 + 2m_1)** S355	Ø 24 mm S355	Ø 22 mm S355	Ø 8 mm
	Foundation	e_{a2} = 50 mm p_2 = 100 mm	e_{a1} = 60 mm p_1 = 100 mm		h_{eff} = 200 mm	B500A
	700 x 1200 x 850 C20/25	e_{b2} = 50 mm m_2 = 50 mm	e_{b1} = 70 mm			4 legs for stud

Varying		Resistance / Stiffness / Limiting length																				
m_1	t_{p1}	$M_{N=0,pl}$	$S_{j,ini,pl}$	$M_{N=0,mem}$	L_{cb}	L_{co}	M_1	N_1	$S_{j,ini}$	L_{cb}	L_{co}	M_2	N_2	$S_{j,ini}$	L_{cb}	L_{co}	M_3	N_3	$S_{j,ini}$	L_{cb}	L_{co}	$N_{M=0}$
[mm]	[mm]	[kNm]	[kNm/rad]	[kNm]	[m]	[m]	[kNm]	[kN]	[kNm/rad]	[m]	[m]	[kNm]	[kN]	[kNm/rad]	[m]	[m]	[kNm]	[kN]	[kNm/rad]	[m]	[m]	[kN]
	10	55	16445	-	2.5	8.0	105	762	15214	2.8	8.6	105	762	15214	2.8	8.6	105	762	15214	2.8	8.6	1926
0	12	56	16338	-	2.6	8.0	110	805	15090	2.8	8.7	110	805	15090	2.8	8.7	110	805	15090	2.8	8.7	1926
	15	57	16177	-	2.6	8.1	119	871	14916	2.8	8.8	119	871	14916	2.8	8.8	119	871	14916	2.8	8.8	1926
	10	33	6623	36	6.3	19.8	96	830	6616	6.3	19.8	96	830	6616	6.3	19.8	96	830	6616	6.3	19.8	1926
50	12	47	9103	49	4.6	14.4	108	820	8540	4.9	15.3	108	820	8540	4.9	15.3	108	820	8540	4.9	15.3	1926
	15	67	11589	67	3.6	11.3	125	822	10519	4.0	12.4	125	822	10519	4.0	12.4	125	822	10519	4.0	12.4	1926
	10	25	493	30	84.9	265.4	94	847	544	76.9	240.3	94	847	544	76.9	240.3	94	847	544	76.9	240.3	1926
100	12	36	952	41	44.0	137.4	105	850	943	44.4	138.7	105	850	943	44.4	138.7	105	850	943	44.4	138.7	1926
	15	56	1968	60	21.3	66.5	123	841	1803	23.2	72.6	123	841	1803	23.2	72.6	123	841	1803	23.2	72.6	1926

Tab. 4.11: Recommended geometry of the column base with anchor plate, its design resistances, stiffness and limiting length for HE180B

HE180B	Column	Base plate	Anchor plate	Threaded studs	Headed studs	Stirrups
	a_{wf} = 6 mm S355	**P25** - 220 x 380 S355	P(**t_{p1}**) - 260 x (**400 + 2m_1**) S355	M24 S355	Ø 22 mm S355	Ø 8 mm
	Foundation	e_{a2} = 50 mm p_2 = 100 mm	e_{a1} = 60 mm p_1 = 100 mm		h_{eff} = 200 mm	B500A
	800 x 1200 x 850 C25/30	e_{b2} = 60 mm m_2 = 50 mm	e_{b1} = 80 mm			4 legs for stud

Varying		**Resistance / Stiffness / Limiting length**																				
m_1 [mm]	t_{p1} [mm]	$M_{N=0,pl}$ [kNm]	$S_{j,ini,pl}$ [kNm/rad]	$M_{N=0,mem}$ [kNm]	L_{cb} [m]	L_{co} [m]	M_1 [kNm]	N_1 [kN]	$S_{j,ini}$ [kNm/rad]	L_{cb} [m]	L_{co} [m]	M_2 [kNm]	N_2 [kN]	$S_{j,ini}$ [kNm/rad]	L_{cb} [m]	L_{co} [m]	M_3 [kNm]	N_3 [kN]	$S_{j,ini}$ [kNm/rad]	L_{cb} [m]	L_{co} [m]	$N_{M=0}$ [kN]
	10	63	18604	-	3.5	10.8	127	942	16566	3.9	12.1	127	989	16342	3.9	12.3	127	1036	16088	4.0	12.5	2316
0	12	63	18493	-	3.5	10.9	134	1023	16299	3.9	12.3	134	1054	16160	4.0	12.4	134	1085	16009	4.0	12.6	2316
	15	65	18325	-	3.5	11.0	145	1148	15925	4.0	12.6	145	1151	15911	4.0	12.6	145	1154	15897	4.0	12.7	2316
	10	36	8107	39	7.9	24.8	117	1022	7795	8.3	25.8	117	1069	7668	8.4	26.2	116	1116	7522	8.6	26.7	2316
50	12	52	10958	55	5.9	18.4	131	1046	9795	6.6	20.5	131	1077	9701	6.6	20.7	131	1107	9600	6.7	21.0	2316
	15	74	13710	74	4.7	14.7	149	1114	11642	5.5	17.3	149	1117	11631	5.5	17.3	149	1120	11620	5.5	17.3	2316
	10	27	659	33	97.6	305.1	114	1042	697	92.3	288.4	114	1089	685	94.0	293.8	113	1135	670	96.1	300.3	2316
100	12	40	1269	45	50.7	158.5	126	1080	1190	54.1	169.0	127	1110	1177	54.7	171.0	126	1141	1162	55.4	173.1	2316
	15	62	2600	66	24.8	77.4	148	1123	2222	29.0	90.5	148	1126	2220	29.0	90.6	148	1129	2217	29.0	90.7	2316

HE180B	Column	Base plate	Anchor plate	Threaded studs	Headed studs	Stirrups
	a_{wf} = 6 mm S355	**P30** - 220 x 380 S355	P(**t_{p1}**) - 260 x (**400 + 2m_1**) S355	M24 S355	Ø 22 mm S355	Ø 8 mm
	Foundation	e_{a2} = 50 mm p_2 = 100 mm	e_{a1} = 60 mm p_1 = 100 mm		h_{eff} = 200 mm	B500A
	800 x 1200 x 850 C25/30	e_{b2} = 60 mm m_2 = 50 mm	e_{b1} = 80 mm			4 legs for stud

Varying		**Resistance / Stiffness / Limiting length**																				
m_1 [mm]	t_{p1} [mm]	$M_{N=0,pl}$ [kNm]	$S_{j,ini,pl}$ [kNm/rad]	$M_{N=0,mem}$ [kNm]	L_{cb} [m]	L_{co} [m]	M_1 [kNm]	N_1 [kN]	$S_{j,ini}$ [kNm/rad]	L_{cb} [m]	L_{co} [m]	M_2 [kNm]	N_2 [kN]	$S_{j,ini}$ [kNm/rad]	L_{cb} [m]	L_{co} [m]	M_3 [kNm]	N_3 [kN]	$S_{j,ini}$ [kNm/rad]	L_{cb} [m]	L_{co} [m]	$N_{M=0}$ [kN]
	10	65	20062	-	3.2	10.0	140	1093	17608	3.7	11.4	140	1096	17593	3.7	11.4	140	1099	17577	3.7	11.4	2316
0	12	66	19928	-	3.2	10.1	147	1150	17448	3.7	11.5	147	1150	17448	3.7	11.5	147	1150	17448	3.7	11.5	2316
	15	67	19728	-	3.3	10.2	158	1231	17255	3.7	11.7	158	1231	17255	3.7	11.7	158	1231	17255	3.7	11.7	2316
	10	37	8401	40	7.7	23.9	129	1173	7984	8.1	25.2	129	1177	7976	8.1	25.2	129	1180	7967	8.1	25.2	2316
50	12	54	11456	56	5.6	17.6	144	1174	10173	6.3	19.8	144	1174	10173	6.3	19.8	144	1174	10173	6.3	19.8	2316
	15	77	14458	77	4.5	13.9	163	1197	12328	5.2	16.3	163	1197	12328	5.2	16.3	163	1197	12328	5.2	16.3	2316
	10	28	659	34	97.7	305.3	126	1193	691	93.2	291.3	126	1196	690	93.3	291.6	126	1200	689	93.4	292.0	2316
100	12	41	1272	46	50.6	158.1	139	1208	1188	54.2	169.2	139	1208	1188	54.2	169.2	139	1208	1188	54.2	169.2	2316
	15	64	2621	68	24.6	76.7	161	1208	2254	28.6	89.2	161	1208	2254	28.6	89.2	161	1208	2254	28.6	89.2	2316

Tab. 4.12: Recommended geometry of the column base with anchor plate, its design resistances, stiffness and limiting length for HE200B

HE200B	Column	Base plate	Anchor plate	Threaded studs	Headed studs	Stirrups
	a_{wf} = 6 mm S355	**P25** - 240 x 400 S355	P(**t_{p1}**) - 280 x (**420 + 2m_1**) S355	M24 S355	Ø 22 mm S355	Ø 8 mm
	Foundation	e_{a2} = 50 mm p_2 = 120 mm	e_{a1} = 60 mm p_1 = 120 mm		h_{eff} = 200 mm	B500A
	800 x 1300 x 900 C25/30	e_{b2} = 60 mm m_2 = 50 mm	e_{b1} = 80 mm			4 legs for stud

Varying		**Resistance / Stiffness / Limiting length**																				
m_1	t_{p1}	$M_{N=0,pl}$	$S_{j,ini,pl}$	$M_{N=0,mem}$	L_{cb}	L_{co}	M_1	N_1	$S_{j,ini}$	L_{cb}	L_{co}	M_2	N_2	$S_{j,ini}$	L_{cb}	L_{co}	M_3	N_3	$S_{j,ini}$	L_{cb}	L_{co}	$N_{M=0}$
[mm]	[mm]	[kNm]	[kNm/rad]	[kNm]	[m]	[m]	[kNm]	[kN]	[kNm/rad]	[m]	[m]	[kNm]	[kN]	[kNm/rad]	[m]	[m]	[kNm]	[kN]	[kNm/rad]	[m]	[m]	[kN]
	10	69	22107	-	2.9	9.1	152	1041	19735	3.3	10.2	152	1131	19257	3.3	10.4	148	1220	18664	3.4	10.8	2725
0	12	70	21967	-	2.9	9.2	160	1127	19423	3.3	10.4	160	1203	19043	3.4	10.6	157	1279	18588	3.5	10.8	2772
	15	71	21758	-	3.0	9.2	172	1260	18985	3.4	10.6	172	1311	18748	3.4	10.7	171	1363	18483	3.5	10.9	2772
	10	38	9400	42	6.8	21.4	139	1131	9302	6.9	21.6	139	1219	9036	7.1	22.3	135	1308	8696	7.4	23.1	2725
50	12	55	12865	58	5.0	15.6	155	1160	11676	5.5	17.2	155	1235	11421	5.6	17.6	153	1310	11117	5.8	18.1	2772
	15	80	16297	80	3.9	12.3	176	1232	13907	4.6	14.5	176	1284	13721	4.7	14.7	175	1335	13514	4.8	14.9	2772
	10	29	756	35	85.1	266.0	135	1152	837	76.9	240.3	136	1240	810	79.4	248.2	132	1328	776	82.9	259.1	2725
100	12	42	1472	47	43.7	136.6	150	1195	1424	45.2	141.2	150	1270	1389	46.3	144.8	148	1344	1346	47.8	149.4	2772
	15	66	3058	70	21.0	65.8	174	1248	2651	24.3	75.9	174	1298	2612	24.6	77.0	173	1349	2567	25.1	78.3	2772

HE200B	Column	Base plate	Anchor plate	Threaded studs	Headed studs	Stirrups
	a_{wf} = 6 mm S355	**P30** - 240 x 400 S355	P(**t_{p1}**) - 280 x (**420 + 2m_1**) S355	M24 S355	Ø 22 mm S355	Ø 8 mm
	Foundation	e_{a2} = 50 mm p_2 = 120 mm	e_{a1} = 60 mm p_1 = 120 mm		h_{eff} = 200 mm	B500A
	800 x 1300 x 900 C25/30	e_{b2} = 60 mm m_2 = 50 mm	e_{b1} = 80 mm			4 legs for stud

Varying		**Resistance / Stiffness / Limiting length**																				
m_1	t_{p1}	$M_{N=0,pl}$	$S_{j,ini,pl}$	$M_{N=0,mem}$	L_{cb}	L_{co}	M_1	N_1	$S_{j,ini}$	L_{cb}	L_{co}	M_2	N_2	$S_{j,ini}$	L_{cb}	L_{co}	M_3	N_3	$S_{j,ini}$	L_{cb}	L_{co}	$N_{M=0}$
[mm]	[mm]	[kNm]	[kNm/rad]	[kNm]	[m]	[m]	[kNm]	[kN]	[kNm/rad]	[m]	[m]	[kNm]	[kN]	[kNm/rad]	[m]	[m]	[kNm]	[kN]	[kNm/rad]	[m]	[m]	[kN]
	10	71	23682	-	2.7	8.5	167	1205	20840	3.1	9.7	167	1256	20579	3.1	9.8	166	1307	20286	3.2	9.9	2772
0	12	72	23518	-	2.7	8.6	175	1293	20524	3.1	9.8	175	1326	20367	3.2	9.9	174	1359	20198	3.2	10.0	2772
	15	74	23274	-	2.8	8.6	187	1430	20077	3.2	10.0	187	1431	20071	3.2	10.0	187	1432	20066	3.2	10.0	2772
	10	39	9709	43	6.6	20.7	154	1294	9508	6.8	21.2	154	1345	9366	6.9	21.5	153	1396	9206	7.0	21.8	2772
50	12	57	13398	60	4.8	15.0	170	1326	12005	5.4	16.8	170	1358	11901	5.4	16.9	170	1391	11790	5.5	17.1	2772
	15	82	17112	82	3.8	11.8	192	1402	14392	4.5	14.0	192	1403	14388	4.5	14.0	192	1404	14384	4.5	14.0	2772
	10	30	756	35	85.2	266.2	151	1315	830	77.6	242.4	151	1366	816	78.9	246.5	150	1416	800	80.4	251.3	2772
100	12	43	1476	48	43.6	136.3	165	1361	1412	45.6	142.4	165	1393	1398	46.0	143.8	165	1425	1383	46.5	145.4	2772
	15	67	3081	72	20.9	65.3	189	1418	2633	24.4	76.4	189	1419	2633	24.4	76.4	189	1420	2632	24.5	76.4	2772

Tab. 4.13: Recommended geometry of the column base with anchor plate, its design resistances, stiffness and limiting length for HE220B

HE220B	Column	Base plate	Anchor plate	Threaded studs	Headed studs	Stirrups
	a_{wf} = 6 mm S355	**P25** - 260 x 420 S355	P(**t_{p1}**) - 300 x (**440 + 2m_1**) S355	M24 S355	Ø 22 mm S355	Ø 8 mm
	Foundation	e_{a2} = 50 mm p_2 = 120 mm	e_{a1} = 60 mm p_1 = 120 mm		h_{eff} = 200 mm	B500A
	900 x 1400 x 1000 C25/30	e_{b2} = 70 mm m_2 = 50 mm	e_{b1} = 90 mm			4 legs for stud

Varying		Resistance / Stiffness / Limiting length																				
m_1 [mm]	t_{p1} [mm]	$M_{N=0,pl}$ [kNm]	$S_{j,ini,pl}$ [kNm/rad]	$M_{N=0,mem}$ [kNm]	L_{cb} [m]	L_{co} [m]	M_1 [kNm]	N_1 [kN]	$S_{j,ini}$ [kNm/rad]	L_{cb} [m]	L_{co} [m]	M_2 [kNm]	N_2 [kN]	$S_{j,ini}$ [kNm/rad]	L_{cb} [m]	L_{co} [m]	M_3 [kNm]	N_3 [kN]	$S_{j,ini}$ [kNm/rad]	L_{cb} [m]	L_{co} [m]	$N_{M=0}$ [kN]
0	10	74	25718	-	2.5	7.8	177	1149	23107	2.8	8.7	177	1411	21614	3.0	9.3	162	1672	19614	3.3	10.3	3232
	12	75	25547	-	2.5	7.9	186	1240	22751	2.8	8.8	186	1470	21509	3.0	9.4	175	1700	19909	3.2	10.1	3232
	15	76	25291	-	2.5	8.0	201	1380	22250	2.9	9.0	201	1560	21351	3.0	9.4	194	1740	20258	3.2	9.9	3232
50	10	41	10735	44	6.0	18.7	161	1221	10963	5.9	18.3	161	1468	10175	6.3	19.8	148	1714	9108	7.1	22.1	3220
	12	59	14863	62	4.3	13.5	179	1256	13750	4.7	14.6	179	1470	12962	5.0	15.5	169	1685	11958	5.4	16.8	3232
	15	85	19056	85	3.4	10.6	203	1331	16407	3.9	12.3	203	1498	15742	4.1	12.8	197	1665	14953	4.3	13.5	3232
100	10	30	855	36	75.3	235.3	157	1243	992	64.9	202.8	158	1489	913	70.5	220.3	145	1734	807	79.7	249.1	3220
	12	44	1683	49	38.3	119.5	173	1291	1685	38.2	119.4	173	1506	1575	40.9	127.7	164	1719	1437	44.8	140.0	3232
	15	69	3539	74	18.2	56.8	199	1352	3128	20.6	64.3	200	1517	2987	21.5	67.3	194	1681	2821	22.8	71.3	3232

HE220B	Column	Base plate	Anchor plate	Threaded studs	Headed studs	Stirrups
	a_{wf} = 6 mm S355	**P30** - 260 x 420 S355	P(**t_{p1}**) - 300 x (**440 + 2m_1**) S355	M24 S355	Ø 22 mm S355	Ø 8 mm
	Foundation	e_{a2} = 50 mm p_2 = 120 mm	e_{a1} = 60 mm p_1 = 120 mm		h_{eff} = 200 mm	B500A
	900 x 1400 x 1000 C25/30	e_{b2} = 70 mm m_2 = 50 mm	e_{b1} = 90 mm			4 legs for stud

Varying		Resistance / Stiffness / Limiting length																				
m_1 [mm]	t_{p1} [mm]	$M_{N=0,pl}$ [kNm]	$S_{j,ini,pl}$ [kNm/rad]	$M_{N=0,mem}$ [kNm]	L_{cb} [m]	L_{co} [m]	M_1 [kNm]	N_1 [kN]	$S_{j,ini}$ [kNm/rad]	L_{cb} [m]	L_{co} [m]	M_2 [kNm]	N_2 [kN]	$S_{j,ini}$ [kNm/rad]	L_{cb} [m]	L_{co} [m]	M_3 [kNm]	N_3 [kN]	$S_{j,ini}$ [kNm/rad]	L_{cb} [m]	L_{co} [m]	$N_{M=0}$ [kN]
0	10	76	27392	-	2.3	7.3	195	1325	24272	2.7	8.3	195	1498	23316	2.8	8.6	188	1672	22155	2.9	9.1	3232
	12	77	27194	-	2.4	7.4	204	1418	23913	2.7	8.4	204	1559	23178	2.8	8.7	200	1700	22319	2.9	9.0	3232
	15	78	26901	-	2.4	7.5	219	1562	23405	2.7	8.6	219	1651	22973	2.8	8.8	217	1740	22498	2.9	8.9	3232
50	10	42	11057	45	5.8	18.2	179	1395	11184	5.8	18.0	179	1555	10702	6.0	18.8	173	1716	10113	6.4	19.9	3232
	12	60	15426	63	4.2	13.0	197	1432	14102	4.6	14.3	197	1559	13658	4.7	14.7	193	1687	13145	4.9	15.3	3232
	15	88	19931	88	3.2	10.1	221	1511	16924	3.8	11.9	221	1588	16630	3.9	12.1	220	1665	16312	3.9	12.3	3232
100	10	31	854	37	75.4	235.5	175	1417	984	65.4	204.4	175	1577	937	68.7	214.6	170	1736	880	73.1	228.5	3232
	12	45	1686	51	38.2	119.3	191	1468	1672	38.5	120.3	191	1595	1612	39.9	124.8	188	1721	1543	41.7	130.3	3232
	15	71	3563	75	18.1	56.5	218	1532	3108	20.7	64.7	218	1608	3048	21.1	66.0	217	1684	2983	21.6	67.4	3232

Tab. 4.14: Recommended geometry of the column base with anchor plate, its design resistances, stiffness and limiting length for HE240B

HE240B	**Column**	**Base plate**	**Anchor plate**	**Threaded studs**	**Headed studs**	**Stirrups**
	a_{wf} = 6 mm S355	**P25** - 280 x 440 S355	P(**t_{p1}**) - 320 x **(460 + 2m_1)** S355	M24 S355	Ø 22 mm S355	Ø 8 mm
	Foundation	e_{a2} = 50 mm p_2 = 140 mm	e_{a1} = 60 mm p_1 = 140 mm		h_{eff} = 200 mm	B500A
	900 x 1400 x 1000 C25/30	e_{b2} = 70 mm m_2 = 50 mm	e_{b1} = 90 mm			4 legs for stud

Varying		**Resistance / Stiffness / Limiting length**																				
m_1 [mm]	t_{p1} [mm]	$M_{N=0,pl}$ [kNm]	$S_{j,ini,pl}$ [kNm/rad]	$M_{N=0,mem}$ [kNm]	L_{cb} [m]	L_{co} [m]	M_1 [kNm]	N_1 [kN]	$S_{j,ini}$ [kNm/rad]	L_{cb} [m]	L_{co} [m]	M_2 [kNm]	N_2 [kN]	$S_{j,ini}$ [kNm/rad]	L_{cb} [m]	L_{co} [m]	M_3 [kNm]	N_3 [kN]	$S_{j,ini}$ [kNm/rad]	L_{cb} [m]	L_{co} [m]	$N_{M=0}$ [kN]
0	10	81	29714	-	2.2	6.8	206	1251	26832	2.4	7.5	206	1426	25704	2.5	7.8	193	1601	24068	2.7	8.4	3328
	12	82	29509	-	2.2	6.8	216	1347	26425	2.4	7.6	216	1513	25420	2.5	7.9	205	1679	24010	2.7	8.4	3502
	15	83	29205	-	2.2	6.9	233	1495	25853	2.5	7.8	233	1643	25031	2.6	8.0	225	1791	23934	2.7	8.4	3763
50	10	43	12106	47	5.3	16.6	183	1292	12783	5.0	15.7	183	1448	12204	5.3	16.5	172	1605	11359	5.7	17.7	3176
	12	62	16942	65	3.8	11.9	202	1329	16025	4.0	12.6	202	1476	15408	4.2	13.1	193	1621	14560	4.4	13.8	3341
	15	91	21975	91	2.9	9.2	229	1407	19151	3.4	10.5	229	1535	18567	3.5	10.8	222	1663	17821	3.6	11.3	3588
100	10	32	955	38	67.4	210.7	179	1314	1162	55.4	173.1	179	1470	1104	58.3	182.2	168	1626	1019	63.1	197.3	3176
	12	46	1898	52	33.9	106.0	196	1366	1971	32.7	102.0	196	1512	1886	34.1	106.7	187	1657	1768	36.4	113.8	3341
	15	73	4040	78	15.9	49.8	224	1433	3653	17.6	55.1	225	1559	3529	18.2	57.0	219	1685	3372	19.1	59.6	3588

HE240B	**Column**	**Base plate**	**Anchor plate**	**Threaded studs**	**Headed studs**	**Stirrups**
	a_{wf} = 6 mm S355	**P30** - 280 x 440 S355	P(**t_{p1}**) - 320 x **(460 + 2m_1)** S355	M24 S355	Ø 22 mm S355	Ø 8 mm
	Foundation	e_{a2} = 50 mm p_2 = 140 mm	e_{a1} = 60 mm p_1 = 140 mm		h_{eff} = 200 mm	B500A
	900 x 1400 x 1000 C25/30	e_{b2} = 70 mm m_2 = 50 mm	e_{b1} = 90 mm			4 legs for stud

Varying		**Resistance / Stiffness / Limiting length**																				
m_1 [mm]	t_{p1} [mm]	$M_{N=0,pl}$ [kNm]	$S_{j,ini,pl}$ [kNm/rad]	$M_{N=0,mem}$ [kNm]	L_{cb} [m]	L_{co} [m]	M_1 [kNm]	N_1 [kN]	$S_{j,ini}$ [kNm/rad]	L_{cb} [m]	L_{co} [m]	M_2 [kNm]	N_2 [kN]	$S_{j,ini}$ [kNm/rad]	L_{cb} [m]	L_{co} [m]	M_3 [kNm]	N_3 [kN]	$S_{j,ini}$ [kNm/rad]	L_{cb} [m]	L_{co} [m]	$N_{M=0}$ [kN]
0	10	83	31486	-	2.0	6.4	227	1439	28047	2.3	7.2	227	1587	27147	2.4	7.4	218	1735	25948	2.5	7.8	3651
	12	84	31253	-	2.1	6.4	238	1538	27640	2.3	7.3	238	1672	26870	2.4	7.5	231	1806	25880	2.5	7.8	3763
	15	86	30907	-	2.1	6.5	254	1690	27062	2.4	7.4	254	1799	26484	2.4	7.6	251	1908	25779	2.5	7.8	3763
50	10	44	12436	48	5.2	16.2	203	1473	13017	4.9	15.5	203	1601	12582	5.1	16.0	197	1728	12007	5.4	16.8	3481
	12	64	17530	67	3.7	11.5	223	1514	16396	3.9	12.3	223	1626	15954	4.0	12.6	218	1738	15401	4.2	13.1	3641
	15	93	22905	93	2.8	8.8	250	1594	19694	3.3	10.2	250	1681	19320	3.3	10.4	247	1769	18885	3.4	10.7	3763
100	10	33	954	39	67.5	210.9	199	1496	1153	55.8	174.4	199	1623	1111	57.9	181.0	193	1750	1055	61.0	190.6	3481
	12	47	1901	53	33.9	105.8	216	1550	1957	32.9	102.8	217	1662	1897	33.9	106.0	212	1774	1823	35.3	110.3	3641
	15	74	4064	79	15.8	49.5	245	1621	3631	17.7	55.4	246	1706	3554	18.1	56.6	243	1792	3465	18.6	58.0	3763

Tab. 4.15: Recommended geometry of the column base with anchor plate, its design resistances, stiffness and limiting length for HE260B

HE260B		**Column**			**Base plate**					**Anchor plate**					**Threaded studs**			**Headed studs**			**Stirrups**	
		a_{wf} = 6 mm		S355	**P25** - 300 x 460				S355	P(**t_{p1}**) - 340 x **(480 + 2m_1)**				S355	M24		S355	Ø 22 mm		S355	Ø 8 mm	
		Foundation			e_{a2} = 50 mm		p_2 = 140 mm			e_{a1} = 60 mm		p_1 = 140 mm						h_{eff} = 200 mm			B500A	
		100 x 1500 x 1050		C25/30	e_{b2} = 80 mm		m_2 = 50 mm			e_{b1} = 100 mm											4 legs for stud	
Varying		**Resistance / Stiffness / Limiting length**																				
m_1	t_{p1}	$M_{N=0,pl}$	$S_{j,ini,pl}$	$M_{N=0,mem}$	L_{cb}	L_{co}	M_1	N_1	$S_{j,ini}$	L_{cb}	L_{co}	M_2	N_2	$S_{j,ini}$	L_{cb}	L_{co}	M_3	N_3	$S_{j,ini}$	L_{cb}	L_{co}	$N_{M=0}$
[mm]	[mm]	[kNm]	[kNm/rad]	[kNm]	[m]	[m]	[kNm]	[kN]	[kNm/rad]	[m]	[m]	[kNm]	[kN]	[kNm/rad]	[m]	[m]	[kNm]	[kN]	[kNm/rad]	[m]	[m]	[kN]
	10	86	33765	-	1.9	6.0	235	1355	30797	2.1	6.5	235	1576	29258	2.2	6.9	215	1796	26868	2.4	7.5	3627
0	12	87	33523	-	1.9	6.0	247	1457	30340	2.1	6.6	247	1670	28938	2.2	7.0	229	1883	26826	2.4	7.5	3816
	15	88	33164	-	1.9	6.1	266	1613	29698	2.2	6.8	266	1811	28498	2.3	7.1	251	2010	26774	2.4	7.5	4099
	10	45	13518	49	4.8	14.9	204	1346	14783	4.4	13.6	204	1531	14019	4.6	14.3	189	1716	12847	5.0	15.7	3339
50	12	66	19111	69	3.4	10.5	225	1386	18528	3.5	10.9	225	1563	17694	3.6	11.4	212	1738	16489	3.9	12.2	3511
	15	97	25071	97	2.6	8.0	255	1465	22170	2.9	9.1	255	1625	21346	3.0	9.4	244	1786	20242	3.2	9.9	3769
	10	34	1057	40	60.9	190.4	200	1369	1350	47.7	149.0	200	1554	1273	50.5	157.9	185	1738	1156	55.7	174.0	3339
100	12	48	2120	55	30.4	94.9	218	1424	2287	28.1	87.9	219	1600	2172	29.6	92.6	206	1774	2005	32.1	100.3	3511
	15	76	4563	81	14.1	44.1	249	1495	4232	15.2	47.5	250	1654	4059	15.9	49.6	240	1811	3827	16.8	52.6	3769

HE260B		**Column**			**Base plate**					**Anchor plate**					**Threaded studs**			**Headed studs**			**Stirrups**	
		a_{wf} = 6 mm		S355	**P30** - 300 x 460				S355	P(**t_{p1}**) - 340 x **(480 + 2m_1)**				S355	M24		S355	Ø 22 mm		S355	Ø 8 mm	
		Foundation			e_{a2} = 50 mm		p_2 = 140 mm			e_{a1} = 60 mm		p_1 = 140 mm						h_{eff} = 200 mm			B500A	
		100 x 1500 x 1050		C25/30	e_{b2} = 80 mm		m_2 = 50 mm			e_{b1} = 100 mm											4 legs for stud	
Varying		**Resistance / Stiffness / Limiting length**																				
m_1	t_{p1}	$M_{N=0,pl}$	$S_{j,ini,pl}$	$M_{N=0,mem}$	L_{cb}	L_{co}	M_1	N_1	$S_{j,ini}$	L_{cb}	L_{co}	M_2	N_2	$S_{j,ini}$	L_{cb}	L_{co}	M_3	N_3	$S_{j,ini}$	L_{cb}	L_{co}	$N_{M=0}$
[mm]	[mm]	[kNm]	[kNm/rad]	[kNm]	[m]	[m]	[kNm]	[kN]	[kNm/rad]	[m]	[m]	[kNm]	[kN]	[kNm/rad]	[m]	[m]	[kNm]	[kN]	[kNm/rad]	[m]	[m]	[kN]
	10	88	35615	-	1.8	5.6	259	1556	32062	2.0	6.3	259	1755	30753	2.1	6.5	245	1954	28875	2.2	7.0	3987
0	12	89	35342	-	1.8	5.7	272	1660	31606	2.0	6.4	272	1847	30442	2.1	6.6	260	2035	28824	2.2	7.0	4171
	15	90	34940	-	1.8	5.8	291	1820	30960	2.1	6.5	291	1986	30008	2.1	6.7	282	2152	28750	2.2	7.0	4203
	10	46	13855	50	4.6	14.5	227	1534	15027	4.3	13.4	227	1694	14420	4.5	13.9	217	1854	13571	4.7	14.8	3665
50	12	67	19720	71	3.3	10.2	248	1577	18914	3.4	10.6	248	1724	18271	3.5	11.0	240	1870	17420	3.7	11.5	3832
	15	99	26050	99	2.5	7.7	278	1659	22735	2.8	8.8	278	1782	22141	2.9	9.1	273	1906	21409	3.0	9.4	4083
	10	34	1056	41	61.0	190.5	223	1557	1340	48.0	150.0	223	1717	1281	50.2	157.0	213	1876	1198	53.7	167.8	3665
100	12	50	2123	56	30.3	94.8	242	1615	2271	28.3	88.6	242	1761	2185	29.5	92.0	234	1906	2071	31.1	97.1	3832
	15	78	4588	83	14.0	43.8	273	1689	4207	15.3	47.8	273	1811	4086	15.8	49.2	268	1933	3936	16.4	51.1	4083

4.5 Parameter study on composite joints

4.5.1 General

Composite joint behaviour depends on the characteristics of several active components. The hogging moment capacity can be calculated with the hypothesis of failure of the weakest of them, while the total displacement (and relative rotation) can be found considering the contribution of all of them. The following basic components are identified in Design Manual I "Design of steel-to-concrete joints" [13]: i) longitudinal steel reinforcement in the slab; ii) slip of the composite beam; ii) beam web and flange; iv) steel contact plate; v) components activated in the anchor plate connection; vi) the joint link. Among them, the longitudinal steel reinforcement transfers the tension force; the others contribute to the transmission of the compression force. Failure that depends on the steel reinforcement behaviour is ductile, while failure of concrete components is brittle and should be avoided. The aim of this investigation is to evaluate the failure mechanism of the joint in order to ensure a ductile failure. For this reason, a parametric study followed by sensitivity analysis is carried out, taking into account the variation of some parameters that determine the behaviour of basic components.

4.5.2 Parameters Studied and methodology followed

The attention is mainly focused on the behaviour of steel reinforcement and the joint link. The force in the reinforcement is a function of the steel grade and of bars layout. The first aspect concerns the yield strength (f_{syk}), the coefficient between the ultimate and yield strength (k) and ductility ($\varepsilon_{s,u}$).The second one is characterized by number and diameter of bars and number of layers. In the analysis three values of f_{syk}, four values of k, three $\varepsilon_{s,u}$ values and four reinforcement layouts are considered. The possibility of development of the strut&tie mechanism in the concrete panel depends on the angle θ. This geometrical quantity is calculated through the ratio between the sum of beam height and slab thickness on the thickness of the wall. In the analysis, six beam profiles, four wall thickness t_{wall} and three slab thickness s_{slab} are considered. Wall concrete properties, i.e. the characteristic compressive cylinder ($f_{ck,cyl}$) and cubic ($f_{ck,cube}$) strength, and secant modulus of elasticity (E_{cm}), affect as well the joint link behaviour. In the analysis five concrete grades for wall are considered. The sensitivity analysis compared by 51840 combinations. Tab. 4.16 summarizes the parameters considered for the parameter study.

Tab. 4.16: Parameters considered for parameter study

Element	Parameter					
Reinforcement	Yield strength					
	f_{syk}[MPa]	400	500	600		
	Coefficient f_u/f_{syk}					
	k [-]	1.05	1.15	1.25	1.35	
	Ductility					
	$\varepsilon_{s,u}$ [‰]	25	50	75		
	Bar layout					
		Case A	Case B	Case C	Case D	
	N layers [-]	1	1	1	2	
	N bars [-]	6	6	6	6	
	Diameter bars [mm]	12	14	16	16	
Slab	Thickness					
	t_{slab} [mm]	120	160	200		
Wall	Thickness					
	t_{wall} [mm]	160	200	240	300	
	Concrete grade					
	$f_{ck,cyl}$[MPa]	20	30	40	50	60
	$f_{ck,cube}$[MPa]	25	37	50	60	75
	E_{cm}[MPa]	30	33	35	37	39
Beam	Profile					
	IPE 240	IPE 270	IPE 300	IPE 330	IPE 360	IPE 400

4.5.3 Failure Mechanism

Considering the simultaneous variation of all parameters, the most common failure type is the joint link (34149 cases of 51840, 65.87%); only in 14493 cases (27.96) a slab reinforcement failure occurs; in few cases (3198, 6.17%) the failure depends on the behaviour of beam. Fig. 4.45 summarizes found failure types in the sensitivity analysis.

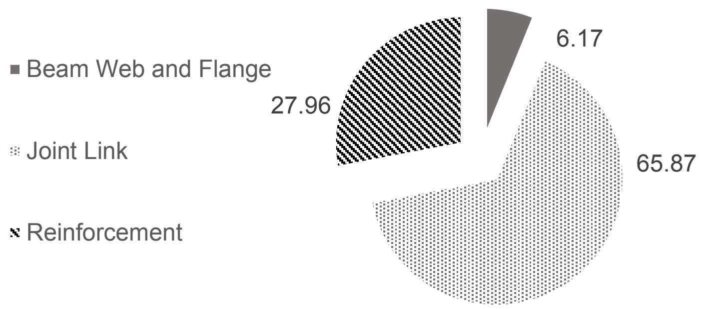

Fig. 4.45: Failure type

4.5.4 Valorization of slab reinforcement properties

The role of slab reinforcement layout is studied, taking into account four bars configurations, according to Tab. 4.16. Fig. 4.46 illustrates the influence. Increasing the reinforcement area, incidence of joint link failure grows significantly, while reinforcement failure decreases. The trend is reversed considering the reinforcements on two layers (Case D). Beam failure is almost absent for low values of steel area, but it assumes a quite relevant rate in Case D.

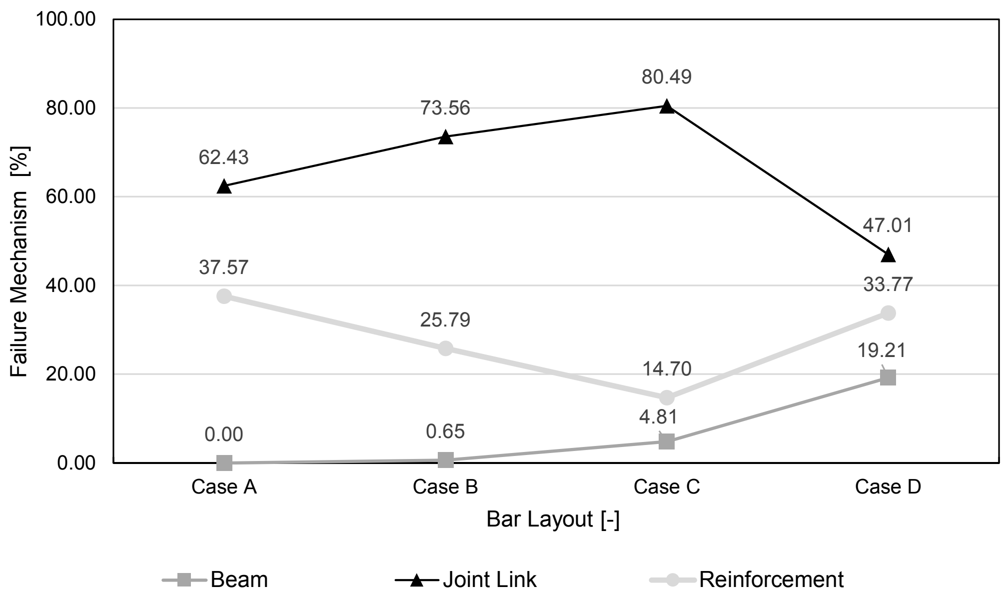

Fig. 4.46: Influence of rebar layout

As expected, one of the most influential parameter is the steel grade (see Fig. 4.47).Here, increasing the yield strength, the percentage of joint link failure switches from 49.65 to 75.67, while cases with ductile failure decrease. Variation of ductility of the bar does not lead to changes in failure type distribution.

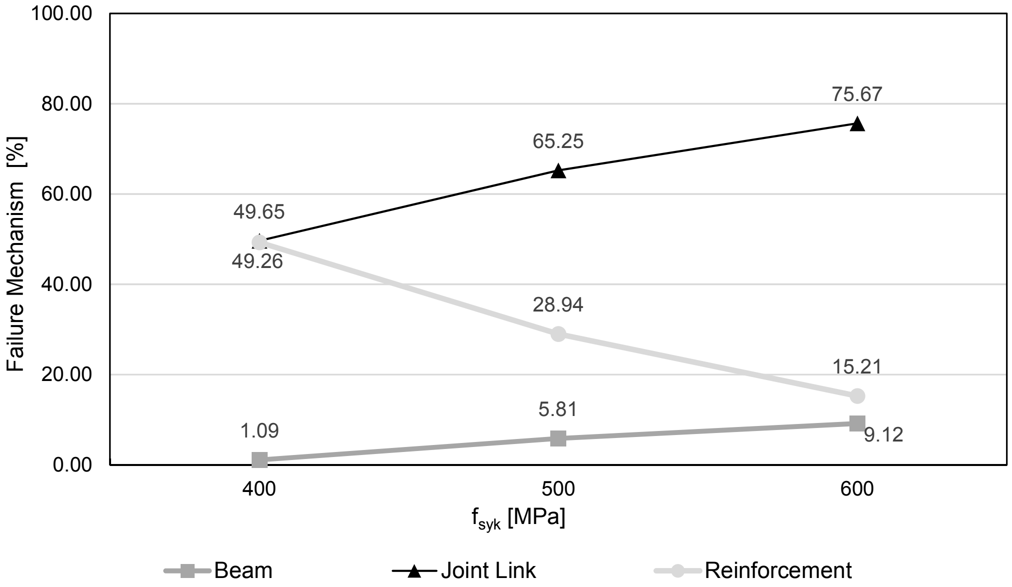

Fig. 4.47: Influence of yield strength of slab reinforcement

The coefficient k influence is highlighted in Fig. 4.48. Increasing k, joint link failures number rises, while cases of reinforcement failure are approximately halved.

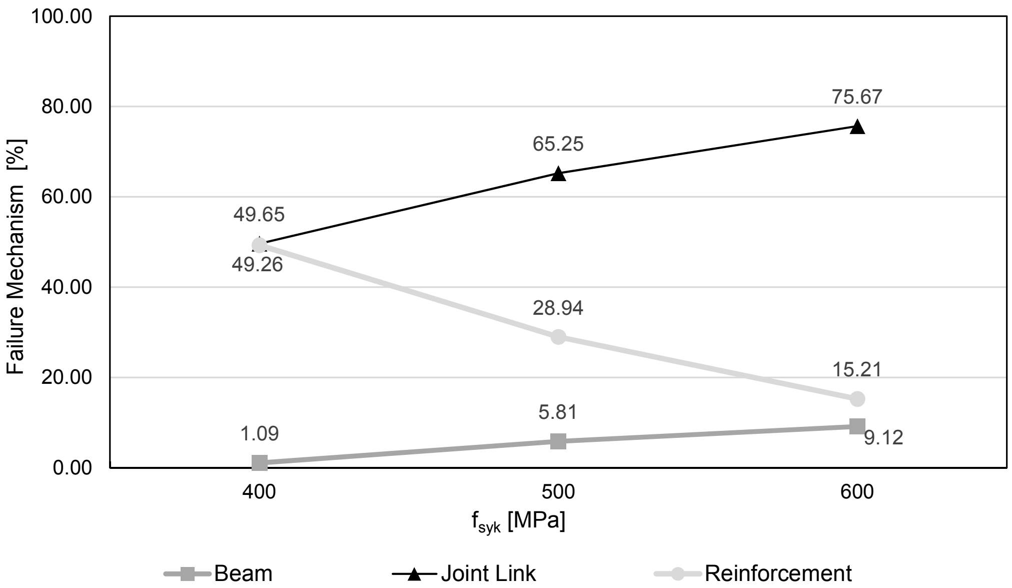

Fig. 4.48: Influence of coefficient k

The interaction between the yield and ultimate strength is evaluated in Fig. 4.49. A change of the main failure type is visible for yield strength equal to 400MPa. While the joint link is crucial for high values of k (61% of failures), the longitudinal reinforcement becomes the most important component for a lower value of k (57% of failures). The number of cases with joint link failure grows significantly (+20%) with increasing k for a steel with a low value of yield strength (f_{syk}= 400 MPa). The same trend is visible for a steel with greater yield strength (f_{syk} =600 MPa), but the increase is lower (10%).

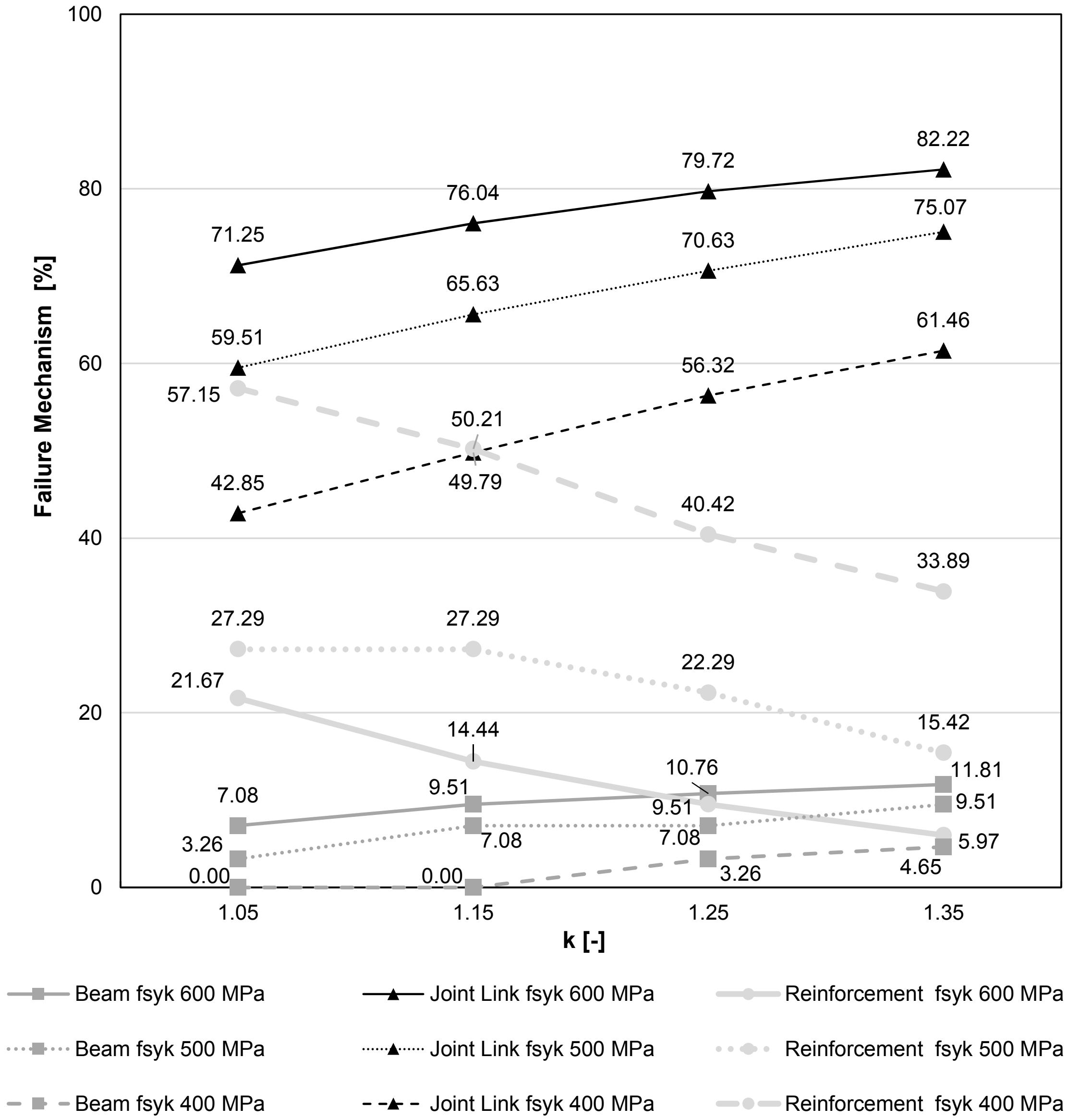

Fig. 4.49: Interaction between yield and ultimate strength

4.5.5 Variation of angle θ

In order to assess the role of the angle theta, the influence of the individual parameters (t_{wall}, t_{slab} and h_{beam}) is studied. In addition, the total height (slab + beam) has been considered. The main parameter that affects the development of the failure mechanism is the wall thickness. For a thickness of 160 mm in 93.45% of cases the failure occurs in the concrete panel. The number of cases of brittle failure drops to 76.04 for a thickness of 200 mm (Fig. 4.50). The ductile failure becomes the main type of failure only for a thickness of 300 mm.

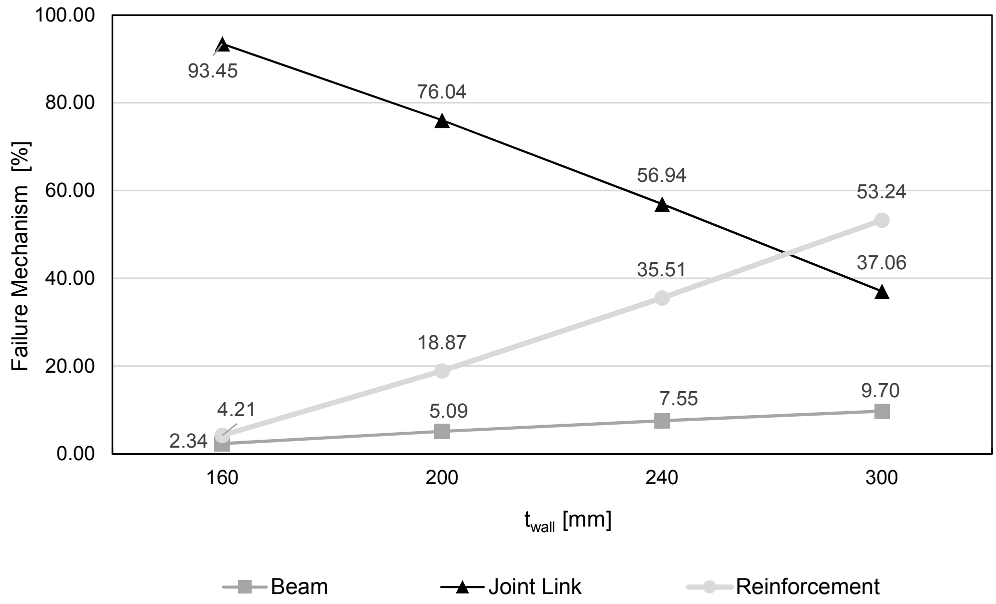

Fig. 4.50: Influence of t_{wall}

The influence of the slab thickness is shown in Fig. 4.51. For the three values considered (120, 160, 200), structural failure happens in the concrete panel in most of the cases (variation between 55.09% and 67.34%). The percentage of beam failure does not vary appreciably. The increase in the height of the beam determines a clear trend, as seen in Fig. 4.52. For a height of 240 mm, in about 50% of cases the failure happens for the concrete panel. Here, the number of cases with beam failure is not negligible (22%). With the increase of the height, the possibility of a failure in the beam decreases significantly, increasing sharply the percentage of the failure in the concrete panel. The consideration of the total height (slab + beam) leads to a less clear trend for low values (Fig. 4.53).

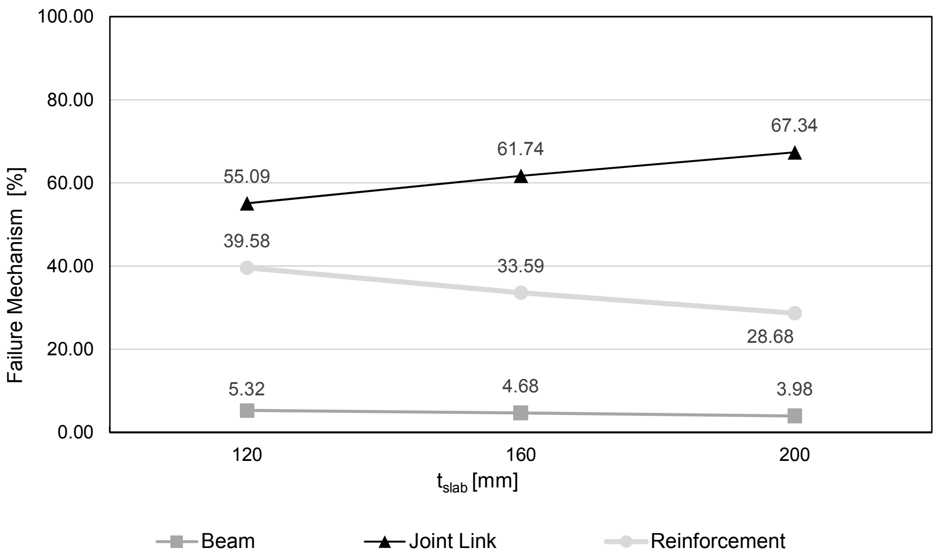

Fig. 4.51: Influence of t_{slab}

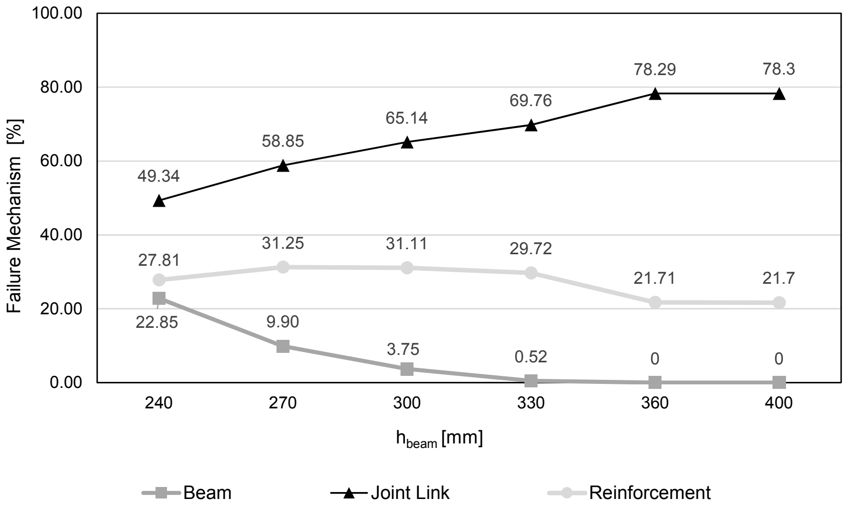

Fig. 4.52: Influence of h_{beam}

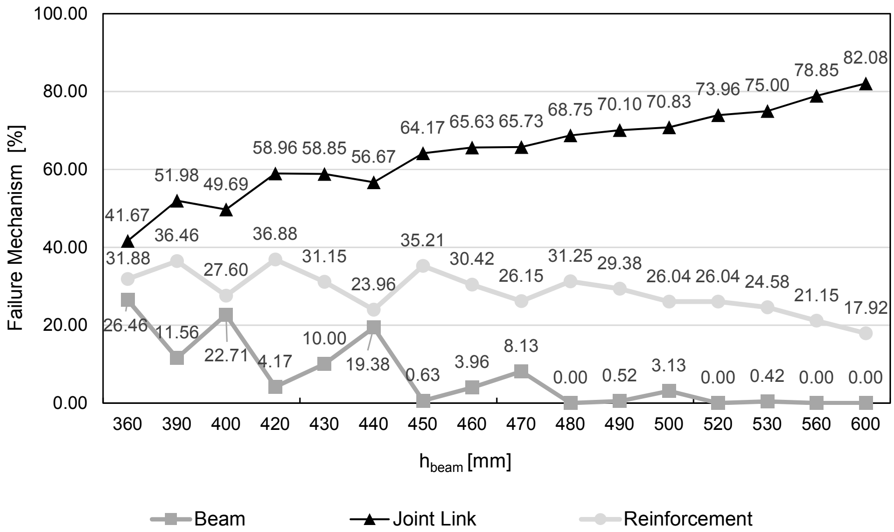

Fig. 4.53: Influence of total height

Initial beam failure peaks (26.46%, 22.7% and 19.38%) are due to the presence of IPE240. However, joint link represents always the main failure type and the possibility of brittle crisis doubles, moving from a height of 360 mm (41.67%) to 600 mm (82.08).

4.5.6 Variation of wall concrete grade

The concrete grade is an important parameter. Fig. 4.54 shows the variation of number of case for each mechanism failure type. For concrete grade C20/25, joint link behaviour represents the limit condition in almost all of the cases (97.25%). The variation is evident. This percentage drops to 36.86 % for concrete C60/75. Brittle failure is the most probable event for $f_{ck,wall}$ is smaller than 40MPa.

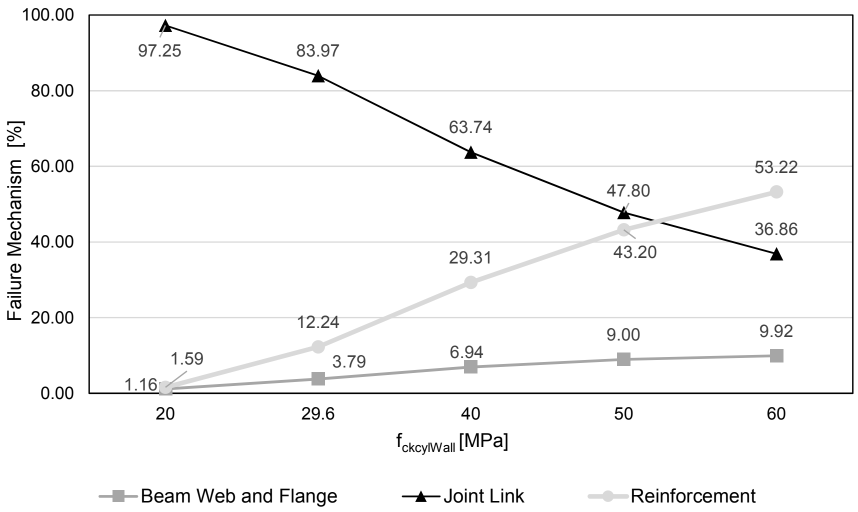

Fig. 4.54: Influence of wall concrete grade

4.5.7 Interaction between wall thickness and concrete grade

The interaction between geometrical properties and material of the wall is studied. For a thickness of 160 mm, joint link determines the failure for all types of concrete considered (Fig. 4.54).

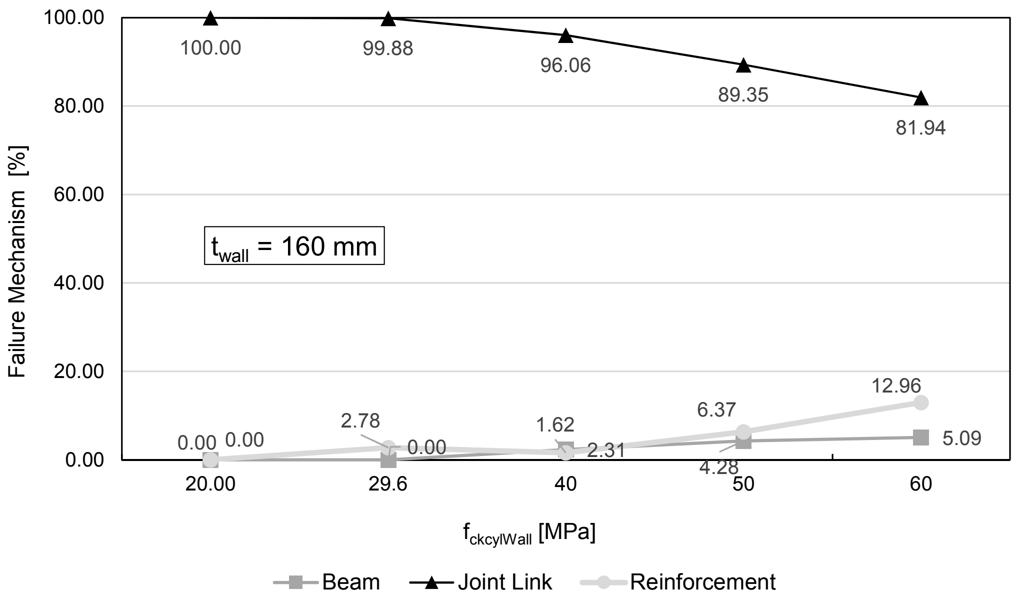

Fig. 4.55: Influence of wall concrete grade for t_{wall} = 160 mm

The percentage drops from 100% (C20/25) to 81.94% (C60/75). The decrease in the percentage of brittle failure is more pronounced for a thickness of 200 mm (Fig. 4.56). In this case for C60/75, ductile failure is more probable than a brittle failure (44.68%).

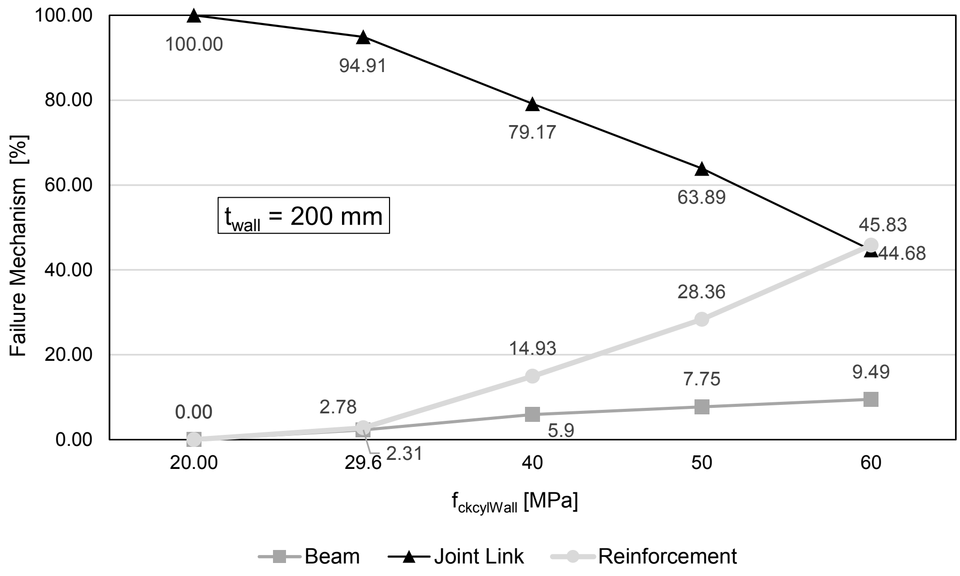

Fig. 4.56: Influence of wall concrete grade for t_{wall} = 200 mm

With a wall thickness of 240mm (Fig. 4.57), the increase of reinforcement failure is evident. It represents 0.96% of the cases for $f_{ck,Wall}$ equal to 20 MPa and becomes 70.37 % when $f_{ck,Wall}$ is 60 MPa. Reduction of joint link failures is noteworthy. From 97.92% (C20/25) to 17.59% (C60/75). Considering a wall thickness of 300 mm (Fig. 4.58), the inversion of most probable failure type (from brittle to ductile) occurs for concrete grade C40/50. A strong change in the trend is visible between C20/25 and C40/50, where brittle failure switches from 91.09 to 25.54 and reinforcement failure switches from 5.44 to 64.12. After this, the change is less marked.

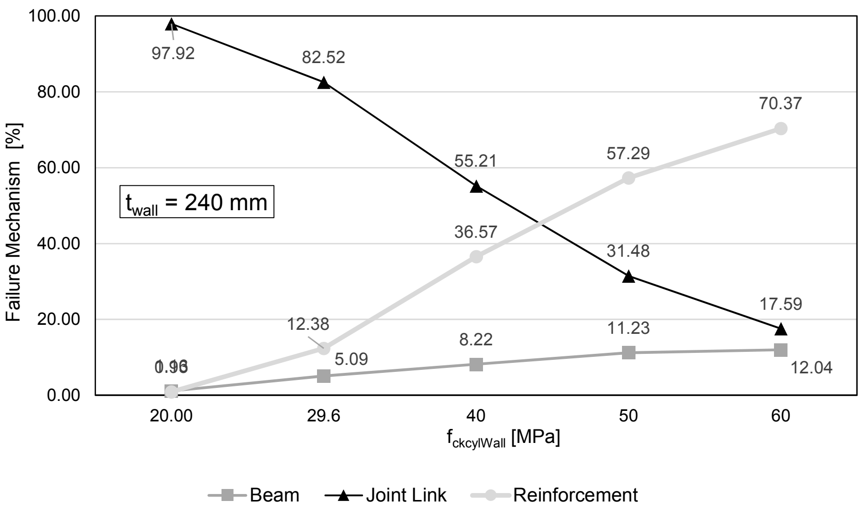

Fig. 4.57: Influence of wall concrete grade for t_{wall} = 240 mm

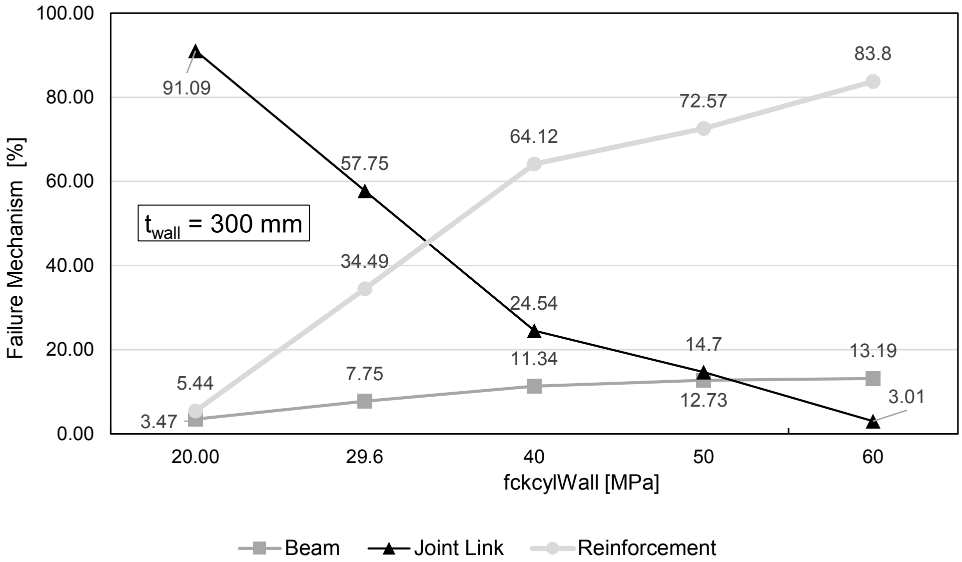

Fig. 4.58: Influence of wall concrete grade for t_{wall} = 300 mm

4.5.8 Summary, Predesign charts for ductile behaviour

The above sensitivity analysis shows the main parameters that affect the failure mode:

Yield strength: cases with brittle failure rises from 49.65% (for f_{syk} = 400 MPa) to 75.67% (for f_{syk} = 600 MPa).

Wall thickness: the concrete panel failure occurs in 93.45% of cases for a thickness of 160mm and in 37.06% for a thickness of 300 m.

Total height of the composite beam: for the lowest value (360mm) a ductile failure happens in 59.33% cases, while for the highest height, 19.72% of cases show this failure.

Concrete grade: for C20/25, there are 97.25% cases of brittle behaviour, and this percentage drops to 36.86 % for concrete C60/75.

For these considerations, a pre design chart (Fig. 4.59, Fig. 4.60 and Fig. 4.61) can be a useful tool in order to lead to a ductile failure. Here, the wall thickness (on the ordinate) is related to the concrete grade (on the abscissa). Separation curves between ductile (top-right) and brittle (bottom-left) failure can be built for nine steel grades (3 f_{syk} and 3 k). To take into account the total height of the composite beam, three charts are drawn: Fig. 4.59 represents the pre design chart for a total height between 360mm and 440mm; Fig. 4.60 refers to a range between 440mm and 520mm; finally Fig. 4.61 concerns the behaviour for a total height between 520mm and 600mm. In these figures, black lines refer to f_{syk} = 400 MPa, dark grey to f_{syk} = 500 MPa and light grey f_{syk} = 600 MPa; solid lines refer to k = 1.05, dash lines to k = 1.15, long dash lines to k = 1.25, dash-dot-dot lines to k = 1.35. Curves stretches found for regression are shown dotted.

For example, for a total height of 390mm, a wall thickness of 160mm and a concrete characteristic compressive cylinder equal to 50 MPa, the steel yield strength that ensure a ductile behaviour is equal to 400MPa with a k = 1.05, according to Fig. 4.59.

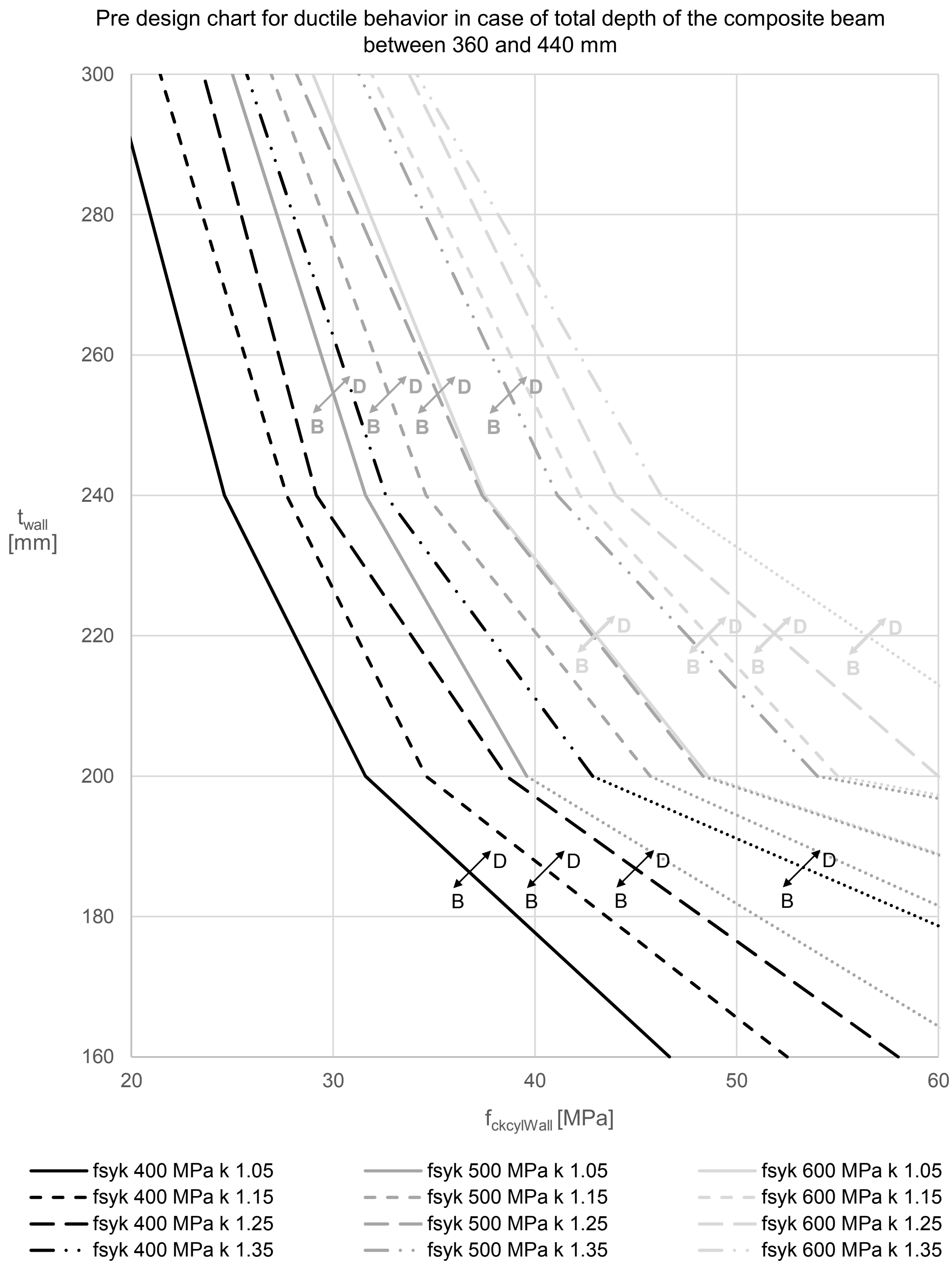

Fig. 4.59: Pre design chart for ductile behaviour in case of total depth of the composite beam between 360 and 440 mm

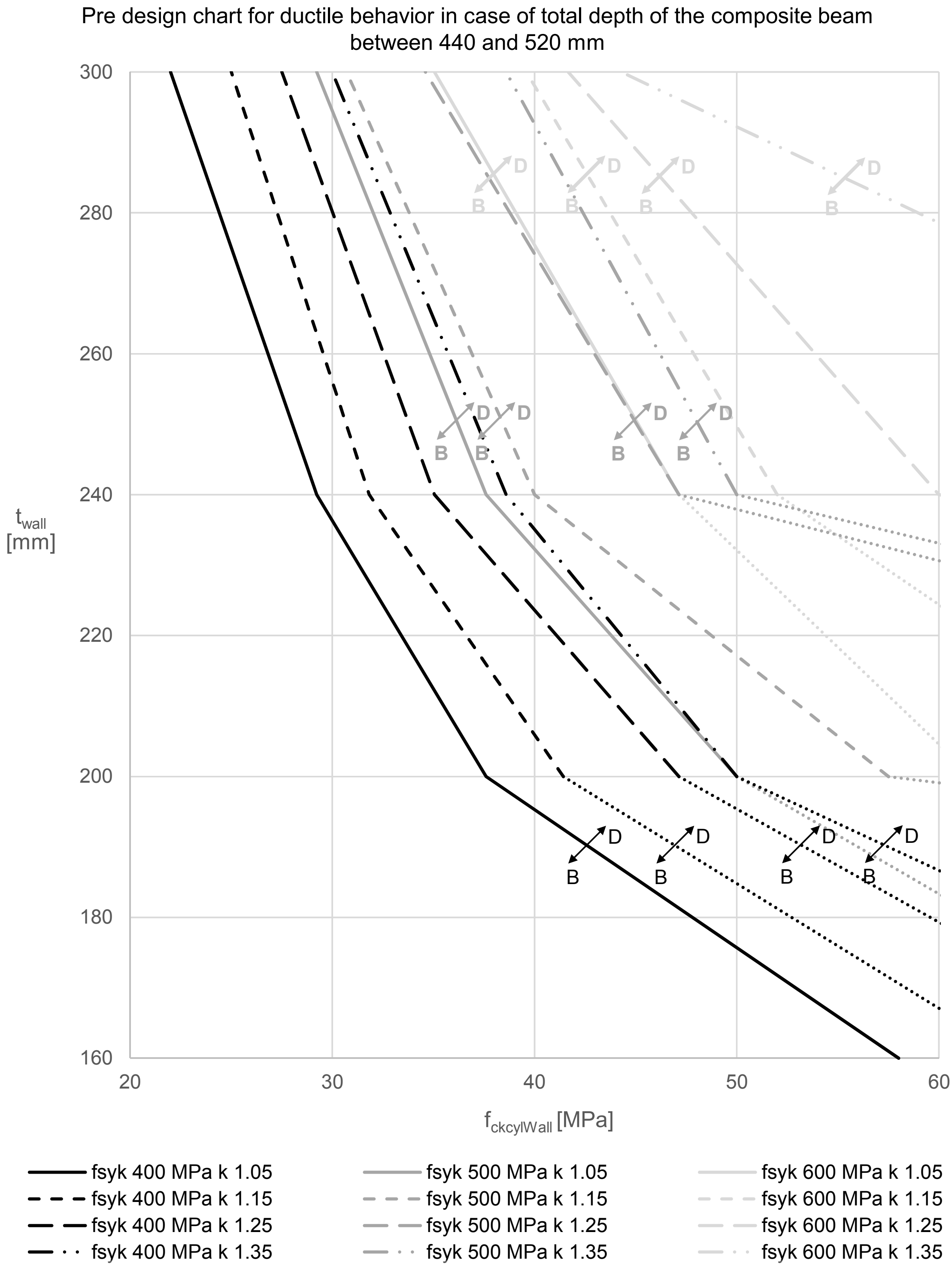

Fig. 4.60: Pre design chart for ductile behaviour in case of total depth of the composite beam between 440 and 520 mm

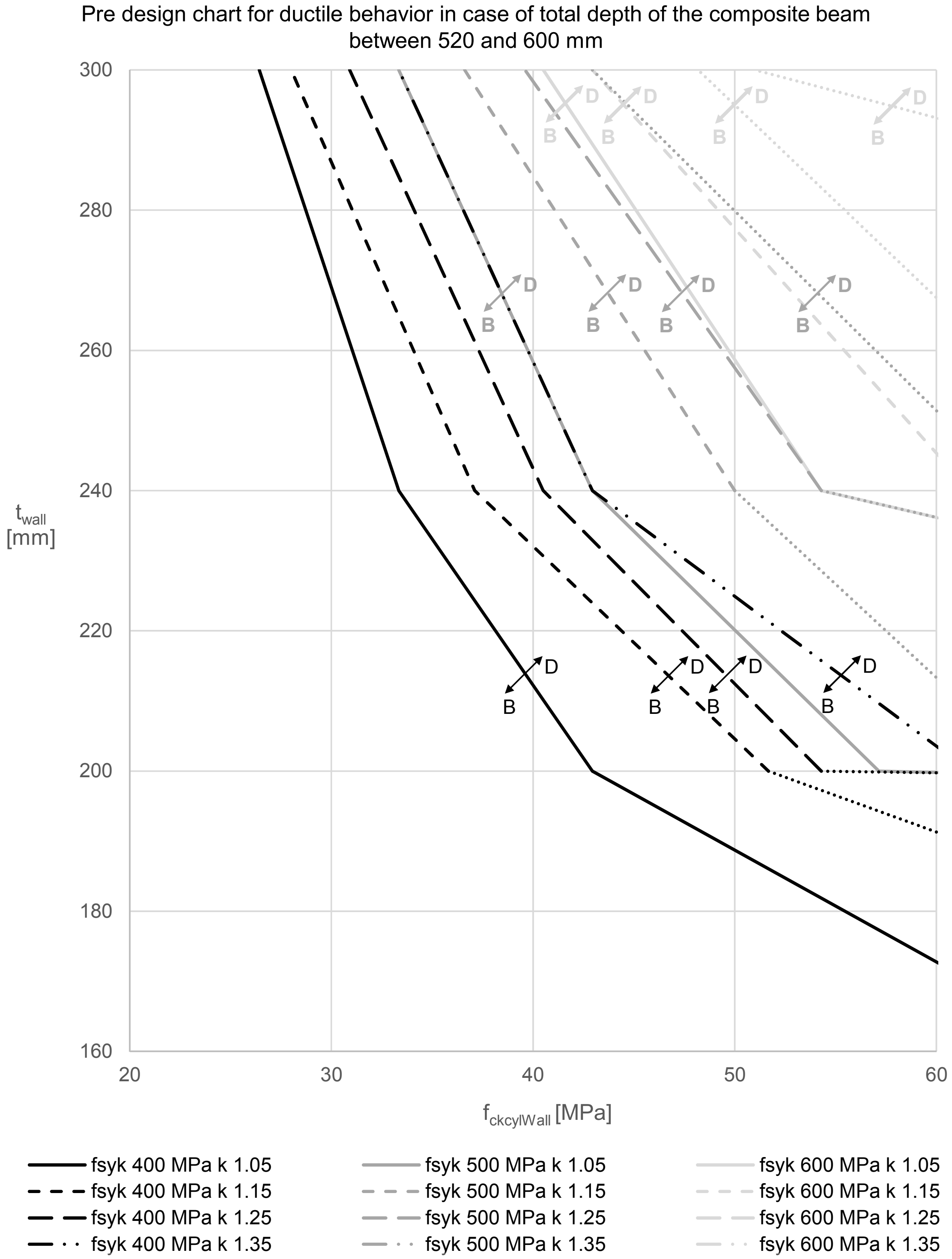

Fig. 4.61: Pre design chart for ductile behaviour in case of total depth of the composite beam between 520 and 600 mm

5 Summary

This Design Manual II is based on the Design Manual I "Design of steel-to-concrete joints" [13] which summarizes the reached knowledge in the RFCS Project RFSR-CT-2007-00051 New market Chances for Steel Structures by Innovative Fastening Solutions between Steel and Concrete (INFASO) [12].

Within the INFASO project design programs were developed for three different steel-to-concrete joints. This programs have been revised and updated within INFASO+. In this design manual background information about this design programs is given and the application of the programs is explained in detail (see Chapter 2). This includes following design programs:

- Restrained connection of composite beams (Version 2.0) [21]
- Slim anchor plates with headed studs - bending joints (Version 2.0) [22]
- Rigid anchor plate with headed studs – simple joint (Version 2.0) [23]

Furthermore the transferability of the results to real life is shown within realistic design examples taken from practice where the newly developed design rules are applied (see Chapter 3). In the worked examples common solutions for steel-to-concrete connections are compared with the innovative developed solutions. These connections are compared in terms of calculation approaches, handling, tolerances and behavior under fire conditions. Parameter studies of the components and analytic model of the three different steel-to-concrete joints show the influence of each parameter. Furthermore recommendations for design values and limits of the model are given (see Chapter 4).

The material was prepared in cooperation of two teams of researchers one targeting on fastening technique modelling and other focusing to steel joints design from the Institute of Structural Design and Institute of Construction Materials, University Stuttgart, Department of Steel and Timber structures, Czech Technical University in Prague and practitioners Gabinete de Informática e Projecto Assistido Computador Lda., Coimbra, Goldbeck West GmbH, Bielefeld, stahl+verbundbau GmbH, Dreieich and European Convention for Constructional Steelwork, Bruxelles.

6 References

Standards and guidelines

[1] CEN/TS 1992-4-1, Design of fastenings for use in concrete – Part 4-1, General, CEN, Brussels, 2009.

[2] CEN/TS 1992-4-2, Design of fastenings for use in concrete – Part 4-2, Headed fasteners Technical Specification, CEN, Brussels, 2009.

[3] DIN 488-1, Reinforcing steels – Part 1: Grades, properties, marking, CEN, Brussels, 2009.

[4] DIN EN 10025-1, Designation systems for steels – Part 1: Steel names, CEN, Brussels, 2005.

[5] EN1991-1-1, Eurocode 1: Actions on structures, Part 1.1, General actions, Densities, self-weight, imposed load for buildings, CEN, Brussels, 2002.

[6] EN1991-1-7, Eurocode 1: Actions on structures, Part 1.7, General actions, Accidental actions, CEN, Brussels, 2006.

[7] EN1992-1-1, Eurocode 2, Design of concrete structures, Part 1-7, General actions - Accidental actions, CEN, Brussels, 2004.

[8] EN1993-1-1, Eurocode 3, Design of steel structures, Part 1-1, General rules and rules for buildings, CEN, Brussels, 2010.

[9] EN1993-1-8, Eurocode 3, Design of steel structures, Part 1-8, Design of joints, CEN, Brussels, 2006.

[10] EN1994-1-1, Eurocode 4, Design of composite steel and concrete structures, Part 1-1, General rules and rules for buildings, CEN, 2010.

[11] Abaquus 6.11: *Theory Manual and Users Manuals*, Dassault Systemes Simulia Corp., 2011.

Textbooks and publications

[12] KUHLMANN, U.; WALD, F.; DA SILVA, L et al: New Market Chances for Steel Structures by Innovative Fastening Solutions between Steel and Concrete, INFASO Publishable Report, Project No. RFSR-CT-2007-00051, Research Fund for Coal and Steel, European Comission, 2011.

[13] KUHLMANN, U.; WALD, F.; DA SILVA, L et al: Valorisation of Knowledge for Innovative Fastening Solutions between Steel and Concrete, INFASO+ Design Manual 1, Project No. RFSR-CT-2012-00022, Research Fund for Coal and Steel, European Comission, 2013.

[14] KUHLMANN, U,; OŽBOLT, A.: Verbesserung der Tragfähigkeit von Ankerplatten mit angeschweißten Kopfbolzen in stabförmigen Stahlbetonbauteilen. Schlussbericht, Forschungsvorhaben Aif/IGF-Nr. 17028 über den Deutschen Ausschuss für Stahlbau (DASt), 2013.

[15] KURZ, W.; KUHLMANN, U: Große Ankerplatten mit Kopfbolzen für hochbeanspruchte Konstruktionen im Industrie- und Anlagenbau, Forschungsvorhaben Aif/IGF-Nr. 17654 über den Deutschen Ausschuss für Stahlbau (DASt), geplant 2015.

[16] INFASO-IWB-09: Determination of the Failure Load and Load-Displacement. Behaviour of the Joints with Supplementary Reinforcement under Tension Load, internal project document, RFSR-CT-2007-00051, 2010.

[17] INFASO-KE-50: Component Model for Pinned Steel to Concrete Joints, internal project document, RFSR-CT-2007-00051, 2010.

[18] KRÄTZIG, W.; Tragwerke 2 – Theorie und Berechnungsmethoden statisch unbestimmter Stabtragwerke. 1. Auflage. Heidelberg: Springer-Verlag, 1990.

[19] OŽBOLT, A.: Bemessung von Kopfbolzenverankerungen in bewehrten Betonbauteilen, Dissertation, Institut für Konstruktion und Entwurf, Universität Stuttgart, Veröffentlichung, geplant 2015.

[20] ŽIŽKA, J.: Component method for column base with embedded plate, Ph.D. thesis, ČVUT, Prague 2012.

Software

[21] VAN KANN, J.: Restrained connection of composite beams (Version 2.0), (http://www.uni-stuttgart.de/ke/forschung/INFASOplus/index.html)

[22] KRIMPMANN, M.: Slim anchor plates with headed studs – bending joints (Version 2.0), (http://www.uni-stuttgart.de/ke/forschung/INFASOplus/index.html)

[23] KRIMPMANN, M.: Slim anchor plates with headed studs – simple joints (Version 2.0), (http://www.uni-stuttgart.de/ke/forschung/INFASOplus/index.html)

[24] KRASTA – Stabstatik für betriebsfestigkeitsrelevante und bewegte Strukturen, KÜHNE BSB GmbH Fördertechnik & Stahlbau.